# Exploring Novel Stratified Therapeutic Targets in B- Cell Chronic Lymphocytic Leukaemia

Thesis submitted for the degree of

Doctor of Philosophy

University of Leicester

(2017)

By

Ghalia M A Shelmani

(MSc Biomedical Sciences Research, University of Bristol)

Department of Molecular and Cell Biology

**Ghalia M A Shelmani**

# Exploring Novel Stratified Therapeutic targets in B- Cell Chronic Lymphocytic Leukaemia

## Abstract

Chronic lymphocytic leukaemia (CLL) is a heterogeneous B-cell malignancy with multiple genetic abnormalities, which have been used to stratify patient's treatments and prognosis. For instance, genetic alterations have been identified in CLL patients, such as SF3B1, Notch1, TP53, and Myd88, and they have been related to prediction of progression and survival. Moreover, mitogen activated protein kinase (MAPK) signalling is crucial in the pathogenesis of a number of cancers, and it has also showed increased expression in a large subset of CLL patients. In this project, we investigated the sensitivity of five leukaemic cell lines to 22 targeted inhibitors. We found that cells with V600EBRAF mutations showed greater sensitivity to MAPK inhibition, while cells with K601NBRAF mutations were more resistant. Wild type BRAF CLL cells showed varied sensitivity to 16 different inhibitors but not to MAPK inhibitors. Combination of a MAPK inhibitor (Sorafenib) and CUDC-907 (CDK/HDAC inhibitor) showed strong synergism in CLL cells at nanomolar concentration, suggesting a potential therapeutic application of blocking both pathways simultaneously. BRAF exon 15 mutations had low frequencies in our cohort (1.052%), but we also found Notch1 mutations (14.81%), Myd88 (1.35%) and SF3B1 (16.21%, 20.8% of which were first-time reports of non-coding regions). Notch1 mutants were more resistant to pladienolide B and more sensitive to MK-0752. On the other hand Myd88 mutants were more sensitive to IRAK1/4 inhibitors. In conclusion, our results showed that therapies for CLL can be stratified based on *in vitro* information of drug sensitivity in relation to mutations present in the cells and suggest that inhibiting the MAPK pathway could be an effective approach in combination therapies. These preclinical data could be applied in CLL management in the near future.

*Dedicated to the loving memory of my father*
*(1944-1984)*

## Acknowledgments

I have worked with a great number of people whose contribution to the research and the making of this thesis deserve special mention. It is a pleasure to convey my gratitude to them all in this humble acknowledgment.

Firstly, I would like to record my gratitude to Dr Salvador Macip and Professor Martin Dyer for their supervision, advice, and guidance of this research as well as providing extraordinary experiences throughout the work.

I would like to thank my committee members Dr Ildiko Gyory and to Professor Catrin Pritchard for their guidance and support for the duration of this project, thanks to Dr Sandrine Jayne for her help with patients and normal volunteers samples provision, Dr Meike Vogler for kindly providing CalcuSyn software for my combination analysis. Dr Tamihiro Kamata for helping with SIG-M5 cells culture.

I must also acknowledge Professor Ian Eperon and Justine Dacanay for assistance with SF3B1 nested PCR.

I would also like to sincerely thank Mrs Christine Stephens for her team work with SF3B1 DNA sequencing, Angie Anifalaje for team work in cell lines Western analysis.

I would like to thank all members of MOCAA lab Victoria Smith, Antonella Tabasso, Akang Ekpenyong-Akiba, Konstantinos Polymeros, Dr Gabriella Kocsis-Fodor, Dr Yixiang Chen, and Sandra Germano, and all previous PhD and undergraduate students.

I would like to thank Dr Kayoko Tanaka, Professor Shaun Cowley, Dr Kees Straatman, Dr Sally Prigent and Dr Sue Shackleton for their advice and support. I would like to thank Dr Emma Kelsall, Dr Lyndsey Wright, Dr Richard Kelly, Grace Hudson, and Clair Barnes for motivating and assisting me during my lab work.

I would also like to thank everyone who contributed over the course of four years of my research at department of Molecular and Cell Biology, and to all Henry Wellcome Building staff that made me feel welcome and in particular for the nice friendly atmosphere they provided in this department, special thanks to Chris Gott, Jon Tillotson-Roberts, and Karen monger.

I am so grateful to the Libyan Ministry of Higher Education and Scientific Research, and to KKLF Key Kendall Leukaemia Fund for all their support over the years. To my friends Sandra Travide, Sara Lord, Enas Belrween, Arwa Bukhari, Kathy Dunn, and Wahiba Kaddah, thank you so much for your support, encouragement and understanding. Very special thanks to all my family members for giving me much-needed support throughout my study.

Heartfelt thanks to my husband Akram for his faith in me and encouragement to begin my PhD; you have been non-judgmental and instrumental in instilling confidence in me. You have always been there for me, during the good and bad times. I truly thank you for standing by my side. I feel that through this experience, we discovered a lot about life, strengthened our commitment and determination to each other, and learned to live life to the fullest. To my lovely kids Mohammed, Jury, and AbdulMalek, this PhD would not have happened without your unconditional love and support. Finally, words cannot express how grateful I am - Thank you, Mother, who had the arduous task of raising ten children by herself following the untimely death of my father. Nothing would be done without you, and your prayers for me were what sustained me thus far.

# Table of Contents

# List of Tables

# List of Figures

## List of abbreviations

AIC Autoimmune cytopenias

AICD Activation-Induced Cell Death

AID Activation Induced Deaminase

AIF Apoptosis-Inducing Factor

AIHA Autoimmune Haemolytic Anaemia

ALL Acute Lymphoblastic Leukaemia

AML Acute Myeloid Leukaemia

AMP Adenosine monophosphate

APAF-1 Apoptotic Protease Activating Factor 1

APCs Antigen Presenting Cells

APRIL a proliferation-inducing ligand

ATM Ataxia Telangiectasia Mutated

ATP Adenosine triphosphate

ATR Ataxia Telangiectasia Mutated and RAD3-related

BAFF B-cell activating factor

BAFFR BAFF receptor

BAG6 BCL2-associated athanogene 6

BCL B-cell Lymphoma

BCL2 B-cell lymphoma 2

BCMA B-cell maturation antigen

BCR B cell receptor

bFGF basic fibroblast growth factor

BIRC3 baculoviral IAP repeat containing 3

BMSC bone marrow stromal cell

bp Base pairs

BSA Bovine serum albumin

BTK Bruton's Tyrosine Kinase

CCL C-C motif ligand

CCL Chemokine (C-C motif) Ligand

CCND1 Cyclin D1

CCND3 Cyclin D3

CD Cluster of Differentiation

CD40L CD40 ligand

CDKN1A Cyclin-Dependent Kinase Inhibitor 1A

CDKs Cyclin-Dependent Kinases

CLL Chronic Lymphocytic Leukaemia

CML Chronic Myelogenous Leukaemia

CpG ODN Cytosine Guanine motif rich - Oligodeoxynucleotide

CR Complete Remission

CSR Class Switch Recombination

CT Comparative Threshold

CTLA-4 cytotoxic T-lymphocyte-associated protein 4

CXCL Chemokine (C-X-C motif) Ligand

CXCL C-X-C motif ligand

CXCR C-X-C motif receptor

CXR4 Chemokine Receptor Type 4

DCs Dendritic Cells

DLBCL Diffuse Large B-Cell Lymphomas

DMSO Dimethylsulphoxide

DNA Deoxyribonucleic acid

dNTP Deoxyribunucleotyde triphosphate

DTT Dithiothreitol

ECL Enhanced chemiluminescence

EDTA Ethylene diamine tetraacetic acid

ER Endoplasmic reticulum

ERK extracellular signal-regulated kinase

ET-1 endothelin 1

ETAR endothelin subtype A receptor

F Female

FBS Foetal Bovine Serum

FC Fludarabine and Cyclophosphamide

FCR Fludarabine, Cyclophosphamide and Rituximab

FDC follicular dendritic cell

FDCs Follicular Dendritic Cells

FISH Fluorescence In Situ Hybridization

FN fibronectin

GC Germinal Centre

HCL Hairy Cell Leukaemia

HLA-G human leukocyte antigen G

HMGB1 high mobility group box 1

HSCs Hematopoietic Stem Cells

IAP Inhibitor of Apoptosis

ICAM1 Intercellular Adhesion Molecule 1

IF Immunofluorescence

Ig Immunoglobulin

IGHV Immunoglobulin Heavy Chain Variable Region Genes

IL Interleukin

ITAM immunoreceptor tyrosine-based activation motif

JAK Janus Kinase

kDa Kilo Dalton

LPS lipopolysaccharide

LTαβ lymphotoxin alpha beta

LTβR lymphotoxin beta receptor

M Male

mAb Monoclonal Antibody

MAPK Mitogen activated protein kinase

MBL Monoclonal B-Cell Lymphocytosis

MCL1 Myeloid Cell Leukaemia 1

MCL1 myeloid cell leukemia 1

M-CLL mutated IGHV-gene carrying CLL

Mdm2 Mouse Double Minute 2 homologue

MDS Myelodyspastic Syndrome

mg Milligram

min Minutes

MiR MicroRNA

mL Millilitre

mM Millimolar

MMP9 Matrix Metallopeptidase 9

mRNA Messenger ribonucleic acid

MYD88 myeloid differentiation primary response

MZ Marginal Zone

MZL Marginal Zone Lymphoma

N- Amino

NAC N-acetylcysteine

NAD nicotinamide adenine dinucleotide

NAMPT nicotinamide phosphorybosiltransferase

NF-κB Nuclear Factor Kappa-light-Chain-Enhancer of Activated B Cells

ng Nanogram

NKp30 natural killer cell p30-related protein

NLC nurselike cells

nM Nanomolar

NRP1 neuropilin-1

NT-L Non-transfected Mouse L-cells

PB Peripheral Blood

PBMC Peripheral Blood Mononuclear Cell

PBS Phosphate buffered saline

PCR Polymerase chain reaction

PD-1 programmed cell death protein 1

PDGF platelet-derived growth factor

PD-L1 PD-1 ligand

PI3K phosphoinositide-3-kinase

PIM proviral integration site for moloney murine leukemia virus

PKC protein kinase C

PLC-γ2 phospholipase C gamma 2

PR Partial Remission

PVDF Polyvinylidene difluoride

RAGE receptor for advanced glycation end-product

RNA Ribonucleic acid

ROS Reactive oxygen species

RPMI Roswell Park Memorial Institute Medium

RS Richter's Syndrome

RT Room temperature

SD Standard deviation

SDF-1 stromal cell derived factor 1

SDS Sodium dodecyl sulphate

SDS-PAGE Sodium dodecyl sulphate polyacrylamide gel electrophoresis

sec Seconds

SF3B1 Splicing Factor 3B, Subunit 1

SH2 Src homology 2

SHIP1/2 SH2 domain containing inositol 5-phosphatases 1/2

SHM Somatic Hypermutation

SHP1 SH2 domain containing protein tyrosine phosphatase-1

sIg surface immunoglobulin

STAT Signal Transducer and Activator of Transcription

STAT-3 signal transducer and activator of transcription 3

SYK spleen tyrosine kinase

TACI transmembrane activator and calcium modulator and cyclophilin ligand interactor

TAM tumour associated macrophage

TBP TATA-Binding Protein

TBS Tris-buffered saline

TD T-cell-Dependent

TEMED N,N,N,N,-tetramethylethylenediamine

TI T-cell-Independent

TLR toll like receptor

TNF Tumour necrosis factor

TNFR TNF receptor

Tris Tris(hydroxymethyl)aminomethane

U-CLL unmutated IGHV-gene carrying CLL

UV Ultraviolet

VCAM-1 vascular cell-adhesion molecule-1

VEGF vascular endothelial growth factor

VLA-4 very late antigen-4

ZAP70 Zeta-Chain-Associated Protein Kinase 70

µg Microgram

µl Microlitre

µM Micromolar

# Chapter 1 Introduction

## 1.1 Cancer

Cancer in humans has been described as a multistep process that starts with genetic alterations that are needed to transform the normal human cells into malignant cells (Hanahan and Weinberg, 2000). The ten capabilities of cancer cells are known as hallmarks of cancer (figure 1.1). First is that most cancer cells has the ability to sustain their own growth by a number of mechanisms for example; autocrine proliferative stimulation, in which cancer cells produce growth factor ligands to which the cancer cell itself responds by expressing the cognate receptors, or by disrupting (inhibiting) negative feedback mechanism of growth signals, while normal cells and tissues are regulating their proliferation through the production and attenuation of growth signals. The second hallmark of cancer is evading growth suppressors by several mechanisms for example; by disrupting p53-RB (retinoblastoma protein) axis which is important for regulation of cell-cycle progression. The third is resisting cell death, for example; evasion of apoptosis by upregulation of anti-apoptotic proteins. The fourth is immortal replicative ability, which is explained as unlimited replication for example; alteration in telomerase function. The fifth is angiogenesis induction via aberrant angiogenesis signals as producing more blood vessels and branching surrounding the tumour. The sixth is metastasis and invasion abilities, for example; adherent junctions formation with adjacent cells. The seventh is avoiding immune destruction for example, cancer cells secrete immunosuppressive factors to immobilise infiltrating cytotoxic T lymphocytes and natural killer (NK) cells. The eighth is tumour promoting inflammation, for example; reactive oxygen species, which are mutagenic are produced by inflammatory cells increasing cancer cells genetic evolution and enhancing tumourigenesis. The ninth is deregulation of cellular energetics by cancer cells ability to reprogram or modify cellular metabolism to support tumour proliferation. The tenth is genome instability and mutation by several mechanisms for example, acquired inactivation of tumour suppressor genes through epigenetic mechanisms of DNA methylation and histone modifications (Hanahan and Weinberg, 2011).

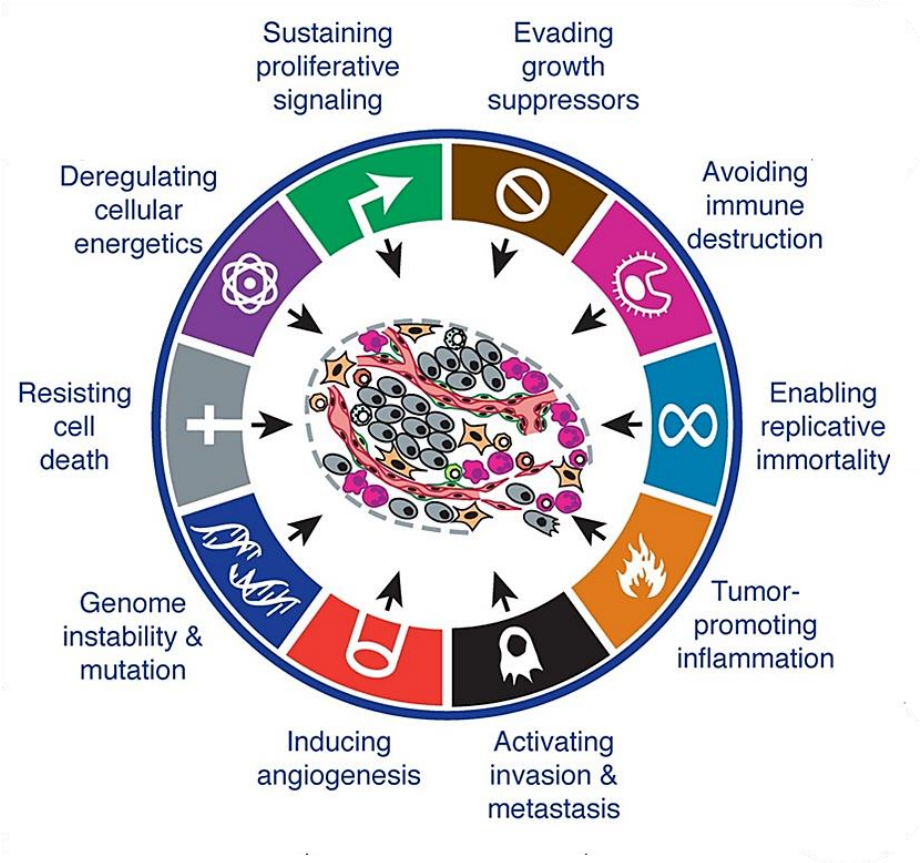


**Figure 1.1 Hallmarks of cancer and therapeutic targeting. Adapted from (Hanahan and Weinberg, 2011).**

### 1.1.1 B-cell malignancies

B-cells development play an important role in B-cell malignancy occurrence. Pro-B-cells are driven by interluekin-7 receptors (IL-7R) signalling (Rickert, 2013). Rearrangement of Immunoglobulin heavy chain variable V, diversity D, and joining J gene parts causes IgM heavy chain expression that pairs with substitutive light chain for pre-B-cell receptor formation. IL-7R and pre-BCR work together for inducing the proliferation of large active pre-B-cells. At this point chromosomal translocations or mutations can give rise to B-cell-derived acute lymphocytic leukaemia B-ALL (figure 1.2). Immature B-cells that gets into lymph node or spleen from bone marrow will develop into different subsets of B-cell such as marginal zone B-cells, germinal centre B-cells and follicular B-cells and this is regulated through different microenvironmental stimuli. Mature B-cells in lymph node follicles could develop into unmutated B-CLL or mantle cell lymphoma (MCL). Mature B-cells in secondary lymphoid tissue germinal centre could give rise to splenic marginal zone lymphoma (SMZL) or mucosa associated lymphoid tissue lymphoma (MALT). B-cell non-Hodgkin lymphoma (B-NHL) types such as DLBCL, Burkitt's lymphoma, and

follicular lymphoma. Mutations of immunoglobulin heavy chain V gene is an indicator of mutated B-CLL and multiple myeloma (figure 1.2).

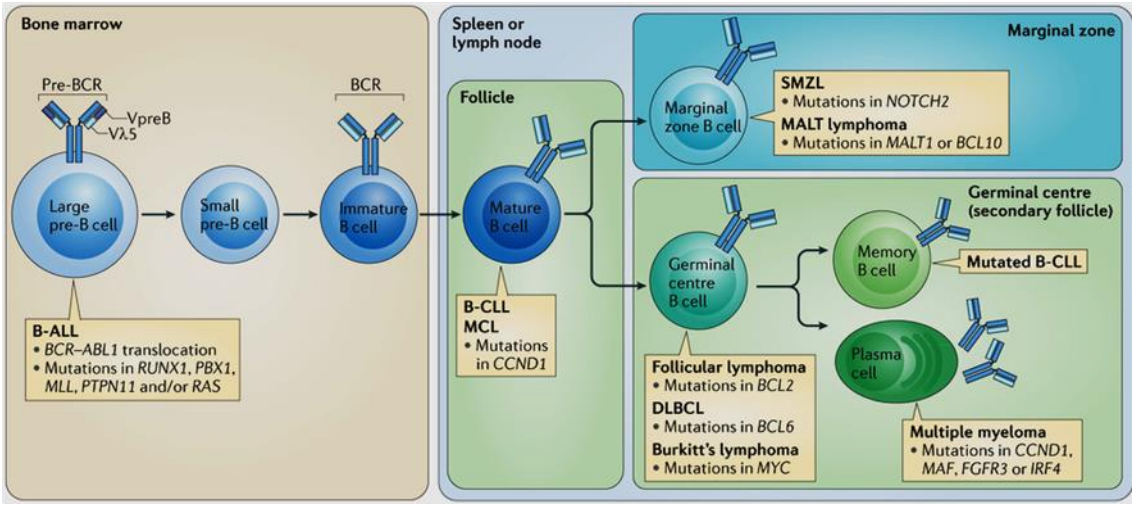


**Figure 1.2 B-cell malignancies happen in different stages of B-cell development.**

Adapted from (Rickert, 2013).

### 1.1.2 Chronic lymphocytic leukaemia

Chronic lymphocytic leukaemia (CLL) is a blood cancer that causes accumulation of mature B-lymphocytes. Basically, white blood cells accumulate in the blood, and lymph nodes, leading to anaemia, and multiple infections, and it might lead to death if the disease course becomes aggressive. CLL mostly affects western countries. CLL can be an indolent type of disease, or can be aggressive, and could transform into Richter Syndrome, which is very aggressive type of blood cancer. In addition, the progression of CLL patients is affected by several types of mutations in different genes.

#### 1.1.2.1 Aetiology and Epidemiology of CLL

There are 8,600 cases of leukaemia diagnosed in the UK each year, and 3,200 of these cases are CLL. CLL is more common in men than women; commonly in 60 years old people, and rare in people under 40 years old (*http://www.cancerresearchuk.org/about-cancer/type/cll/about/chronic-lymphocytic-leukaemia-risks-and-causes*). CLL cells in the blood seem to be primarily resting lymphocytes in G0, whereas in the lymphoid tissue there are aggregates of various sizes where leukaemia cells proliferate. Some patients have high rates of leukaemia cell turnover: 0.1–1% of their entire leukaemia cell

population is produced each day. As such growth kinetics can be observed in patients who have pretty stable disease, the high growth rate detected is probably balanced by a high rate of spontaneous apoptosis (Zhang and Kipps, 2014).

In the UK, CLL accounts for 1% of all new cancer cases, and 37% of all leukaemia types combined (2014) (*http://www.cancerresearchuk.org/health-professional/cancer-statistics/statistics-by-cancer-type/leukaemia-cll/incidence#ref-0).* In 2014, there were 3,515 new cases of CLL. 63% in males and 37% in females, providing a male: - female ratio of around 17:10. There are 7 new CLL cases of males and 4 females for every 100,000 in the UK. CLL incidence is related to age, with the uppermost incidence rates being in older people. In 2012-2014, each year on average more than 4 in 10 (43%) cases were diagnosed in 75 years age and over. Incidence rates increase suddenly from around age 45-49 years, with the maximum rates in the 85-89 years in males and the 90+ years in females. Incidence rates are higher for males than for females aged 15-19 and aged 40-44 and over, and this gap is widest at the age of 85-89 years as can be seen in (figure 1.3) from year 2012-2014.

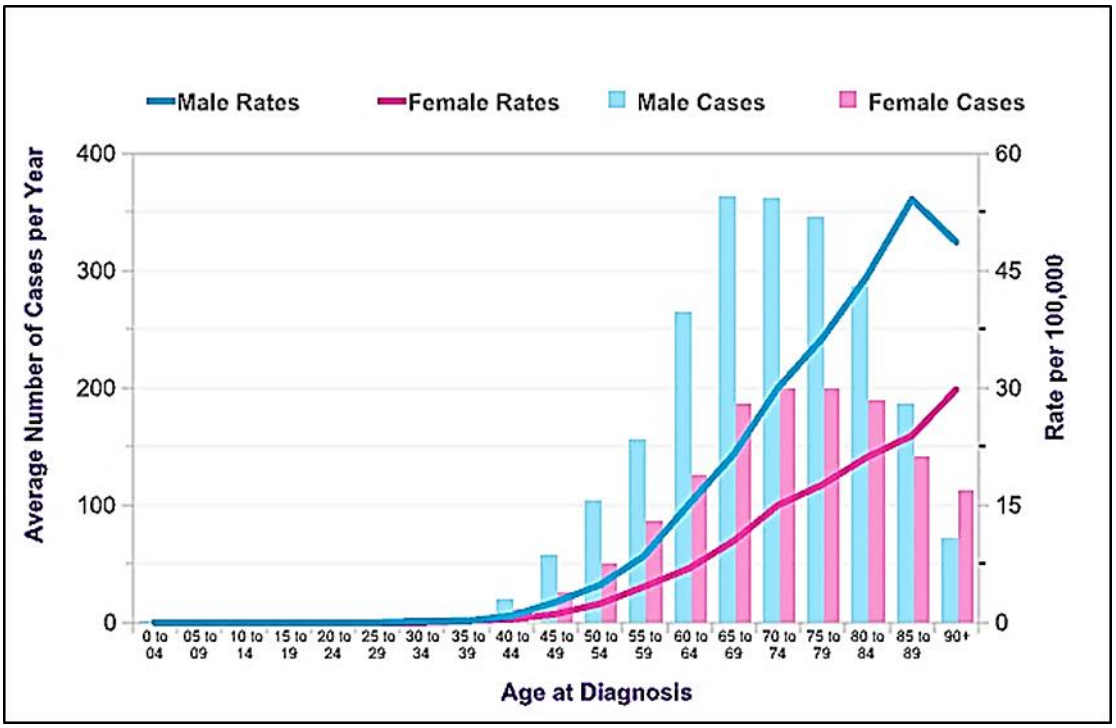


**Figure 1.3 Incidence of CLL in the UK per year.**

Average number of new cases per year and age-specific incidence rates, UK, 2012-2014. (*http://www.cancerresearchuk.org/health-professional/cancer-statistics/statistics-by-cancer-type/leukaemia-cll/incidence#heading-One*).

Different to most other B cell lymphoproliferative disorders, there is a strong evidence of genetic predisposition to CLL. The aetiology of CLL is generally unidentified, however, a familial component to CLL has been described, with approximately 10% of CLL patients reporting a familial history of CLL and a 30-fold increase in the risk of CLL in first-degree relatives of patients (Houlston, Catovsky and Yuille, 2002; Yuille *et al*, 2000; Capalbo *et al*, 2000). The identification of a CLL-associated marker in healthy relatives of patients with familial CLL may provide an alternate marker of inherited predisposition, helping in the detection of gene mutations impact (Rawstron *et al*, 2002). First-degree relatives of CLL patients have approximately 8.5-fold elevated risk of developing CLL (Cerhan and Slager, 2015). A germ line loss-of-function mutation in shelterin genes occur in a subset of families with CLL. By whole-exome sequencing of 66 CLL families, 4 families were found to have loss-of-function mutations in protection of telomeres1 (*POT1*) (Speedy *et al*, 2016).

Remarkably, there are geographic and racial variations noticed, with higher incidences of CLL 20-30 times more common in Europe, North America, and Australia than in India, Japan, and China (Sgambati, Linet and Devesa, 2001). CLL is very rare in China and Korea and almost absent in Japan. The Japanese emigrants maintained the low incident rate and their progeny, thus excluding an environmental modifier of such genetic predisposition (Weiss, 1979).

#### 1.1.2.2 Diagnosis and prognostic factors

CLL is a leukaemic lymphocytic lymphoma that can be differentiated from small lymphocytic lymphoma (SLL) by its leukaemic appearance (Müller-Hermelink *et al*, 2001). To prove that it is CLL and not some other lymphoproliferative disease (such as hairy cell leukaemia, or marginal zone lymphoma, splenic marginal zone lymphoma with circulating villous lymphocytes, leukaemic manifestations of mantle cell lymphoma, or follicular lymphoma), it is vital to assess the blood count, blood smear, and the immune phenotype of the circulating lymphoid cells (Melo *et al*, 1987; Hallek *et al*, 2008b). The diagnosis of CLL requires the presence of more than $5x10^9$ B-lymphocytes/L (5000/µL) in the peripheral blood. Flow cytometry is needed to confirm the clonality of circulating B-lymphocytes. Typically, leukaemic cells are small, mature lymphocytes with a narrow border of cytoplasm and a dense nucleus lacking apparent nucleoli and having partially aggregated chromatin, ‘Smudge cells’ or burst cells are also characteristic on blood

smears. These cells may be found mixed with larger or atypical cells, cleaved cells, or pro-lymphocytes, which may consist of up to 55% of the blood lymphocytes. Any lymphocytes that are found in excess of this percentage will support the diagnosis of prolymphocytic leukaemia (Hallek *et al*, 2008b). Either CLL or SLL could be assumed in healthy adults who have a total increase in the clonal B-lymphocytes, but SLL as "monoclonal B-lymphocytosis", MBL diagnosis can be assumed in patients who have less than $5x10^9$/L B-lymphocytes in the blood; in the absence of lymphadenopathy or organomegaly or other symptoms that are associated with CLL (Marti *et al*, 2005).

CLL cells co-express the T-cell antigen CD5 and B-cell surface antigens CD19, CD20, and CD23. The levels of surface immunoglobulin, CD20, and CD79b are classically low in comparison to those found on normal B cells (Hallek *et al*, 2008b). In comparison to B-prolymphocytic leukaemia (B-PLL) cells which do not express CD5 in half of the cases, and characteristically express high levels of CD20 and surface Ig (Catovsky *et al*, 2001). In addition, cells of mantle cell lymphoma, generally do not express CD23, but instead they express B-cell surface antigens and CD5 (Hallek *et al*, 2008b). CLL cells are characteristically negative for FMC7 expression distinguished from PLL cells which commonly express FMC7 (Ghia, Ferreri and Caligaris-Cappio, 2007).

In around 70–80% of CLL cases diagnosis are made following a routine blood test, or in a patient showing vague or non-specific symptoms. Distinctive symptoms presented consist of: weakness and fatigue due to haemolysis or marrow infiltration, loss of weight, recurrent fever, enlarged lymph nodes and spleen or liver causing pain in the abdomen (Oscier *et al*, 2004). CLL is incurable and it is a slow developing disease that may last several years under control with treatment. Around 70% of men; and almost 75% of women will survive their leukaemia for 5 years or more after being diagnosed. Younger patients (15-64 years) tend to do better, with more than 80% surviving for 5 years or more after diagnosis, while in 65 years old is 60% only (*http://www.cancerresearchuk.org/about-cancer/chronic-lymphocytic-leukaemia-cll/survival*). The incidence of second malignancies is high in both treated and untreated CLL patients (Oscier *et al*, 2004).

CLL is traditionally staged into two widely accepted methods: - the Rai system (Rai *et al*, 1975), and the Binet system (Binet *et al*, 1981). Both systems describe three prognostic groups with clinical outcomes. These two staging systems are simple, inexpensive, and merely depend on a physical examination and standard laboratory tests; they do not

require ultrasound, computed tomography, or magnetic resonance imaging (Hallek *et al*, 2008a). The modified Rai staging system defines:

A) Low-risk disease as patients who have lymphocytosis with leukaemia cells in the peripheral blood and/or marrow (lymphoid cells >30%, former Rai stage 0).

B) Intermediate risk disease with lymphocytosis, and lymphadenopathy formerly considered Rai Stage I or Stage II).

C) High-risk disease includes patients with disease-related anaemia (as defined by a haemoglobin level less than 11 g/dL, formerly Stage III) or thrombocytopenia (as defined by a platelet count of less than 100 x $10^9$/L, formerly Stage IV) (Rai *et al*, 1975; Hallek, 2015).

The Binet staging system is based on the number of involved areas, as defined by the presence of enlarged lymph nodes of more than one cm in diameter or organomegaly, and on whether there is anaemia or thrombocytopenia.

Binet stages are defined as follows:

A) Haemoglobin Hb≥10 g/dL and platelets ≥ 100 x $10^9$/L and up to two sites involved.

B) Haemoglobin ≥ 10 g/dL and platelets ≥100 x $10^9$/L and organomegaly more than two sites involved.

C) All patients who have Hb of less than 10 g/dL and/or a platelet count of less than 10 x $10^9$/L, regardless of organomegaly (Binet *et al*, 1981; Hallek, 2015).

More than 25 % of patients with indolent disease (stage A or stage 0) die of causes related to CLL; in 40 % the disease progresses to advanced stages and 50% eventually require treatment. Neither the Rai nor the Binet staging system assists physicians to predict which patients in the good prognosis group will eventually have progressive disease (Dighiero and Binet, 2000).

Most of CLL patients will have reduction in normal immunoglobulin (Ig) levels (IgG, M and A) during the course of their disease, mostly IgG3 and IgG4. There will be rise in the severity with duration and stage of the CLL, with ~70% of patients developing hypogammaglobulinemia within 7 years of diagnosis (Dearden, 2008). In addition, hypogammaglobulinemia is present in one-quarter of newly diagnosed CLL patients (Parikh *et al*, 2015). Hypogammaglobulinemia in B-CLL might be due to dysfunction of

non-clonal CD5-negative B-cells. This inhibition of normal CD5- negative B-cells could also clarify the typical inability of B-CLL to respond to new antigenic challenges, as Ly1-B-cells (the murine counterpart of human CD5 B-cells) are supposed to be incapable of responding to exogenous antigens (Dighiero, 2003; Hardy and Hayakawa, 1986).

Infection susceptibility in CLL patients can be associated with immunological defects related to the disease, such as hypogammaglobulinemia, or T-cell, natural killer-cell and innate immunity dysfunctions (Visentin *et al*, 2015).

Recurrent infections and morbidity are related to hypogammaglobulinemia in CLL patients, however, no significance has been found between hypogammaglobulinemia and infection in 47 CLL study cohort (Atilla *et al*, 2016). CLL disease course could be complicated by autoimmune cytopenias (AIC) in 10–25% of cases during the disease course. It occurs mostly when CLL is clinically active (Hamblin, 2006; Moreno *et al*, 2010; Rogers *et al*, 2016). The most common AIC observed is autoimmune haemolytic anaemia (AIHA), followed by immune thrombocytopenia (ITP). Rarely observed are pure red cell aplasia (PRCA) and autoimmune granulocytopenia (AIG). AIC as a secondary complication of CLL requires treatment with immunosuppressive agents, which adds to morbidity, and sometimes mortality experienced by CLL patients. AIC are also in some cases caused by treatment with standard therapies, particularly chemotherapeutic agents such as fludarabine (Myint *et al*, 1995; Weiss *et al*, 1998; Rogers *et al*, 2016).

Richter syndrome (RS) is one of the complications that accompany CLL. RS transformation occurs in 2-10% of CLL patients throughout their disease course; at a rate of 0.5% to 1% per year (Lortholary *et al*, 1964). RS is the transformation of CLL into a very aggressive lymphoma, mostly diffuse large B-cell lymphoma (DLBCL) (Parikh, Kay and Shanafelt, 2014). Studies have reported that median time to occurrence of RS is 1.8 to 5 years (Rossi *et al*, 2008; Parikh, Kay and Shanafelt, 2014). Epstein-Barr virus (EBV) was identified in 13% of RS samples of (CLL/SLL) (Tsimberidou *et al*, 2006). RS transformed patients will have poor prognosis and lower survival rates (Parikh, Kay and Shanafelt, 2014).

### 1.1.2.3 Cell of Origin

The main trigger that causes CLL is still unknown, unlike other cancers that are caused by defined genetic mutations or alterations, viruses, radiations or carcinogens. However, it has been suggested that epigenetic silencing of Patched (PTCH), which is a tumour suppressive gene, is a mechanism contributing to CLL tumourigenesis (Schmidt-Wolf *et al*, 2016). In addition, it has been proposed that genetic variations associated with both Longer Telomere Length LTL also increase CLL risk (Ojha *et al*, 2016). Recently, common genetic variations that influence CLL risk at 33 loci have been established. These loci mark genes that contribute to inter-connecting pathways that are vital to B-cell development (Law, P J et al, 2017). These latest discoveries might help to find mutations of origin of CLL patients that could help in early diagnosis and therapy.

Technologic developments helped in improving the finding of the CLL cells origin, however, they did not provide a conclusive evidence. Functional similarities between splenic marginal zone B-cells and CLL led to the proposal that CLL is derived from the marginal zone (Chiorazzi and Ferrarini, 2011). In bone marrow, when precursor B-cells effectively rearrange Ig heavy and light chain genes and at early B-cells development stages, cells that express a functional and non-autoreactive BCR differentiate into mature naïve B-cells that leave the bone marrow, while B-cells that fail to express BCR will go through apoptosis (Küppers, 2005).

The origin of CLL is still controversial. Many suggestions support the fact that the very early genetic and epigenetic alterations occur in pluripotent haematopoietic stem cells (HSCs) that lead to CLL. Experiments in mice revealed that HSCs CLL cells engrafted effectively into immunodeficient mice and resulted in clonal B-cell lympho-proliferations *in vivo*, which indicate that genetic and epigenetic lesions in HSCs patient cells lead to monoclonal B-cell lymphocytosis (Kikushige *et al*, 2011; Fabbri and Dalla-Favera, 2016) (figure 1.4).

CLL HSCs may acquire genetic and epigenetic lesions of unknown nature, and as a result of antigenic stimulation that might lead to selection and expansion of mature B-cells in oligo-clonal populations. Gene expression profiling indicated that MCLL and UCLL are similar to memory B-cells (Klein *et al*, 2001). Immunoglobulin heavy chain variable region-unmutated (IGHV)-UCLL appears to rise from pre-germinal centre CD5+CD27– B-cells that might be derived from naïve or a separate lineage of precursor B-cells

(Forconi *et al*, 2010). On the other hand, (IGHV)-MCLL appears to originate from post-germinal centre CD5+CD27+ memory B-cells, which are transcriptionally the same as memory B-cells and are almost certainly to be derived from CD5+CD27– memory B-cells that have experienced the germinal centre reaction. Expression of specific cell surface markers helped to identify that CLL derived from mature B-lymphocytes. Expression of CD23, CD19, the weak expression of CD20 and the weak expression of cell surface membrane immunoglobulins (Igs) with CD5 antigen make CLL cells distinct from other B-cell derived cancers (Fabbri and Dalla-Favera, 2016). UCLL and MCLL differ in their clinical course, with UCLL as a poor prognosis (Hamblin *et al*, 1999; Damle *et al*, 1999) and most of RS transformation are from UCLL (Jain and O'Brien, 2012; Rossi *et al*, 2013b; Rossi *et al*, 2013a).

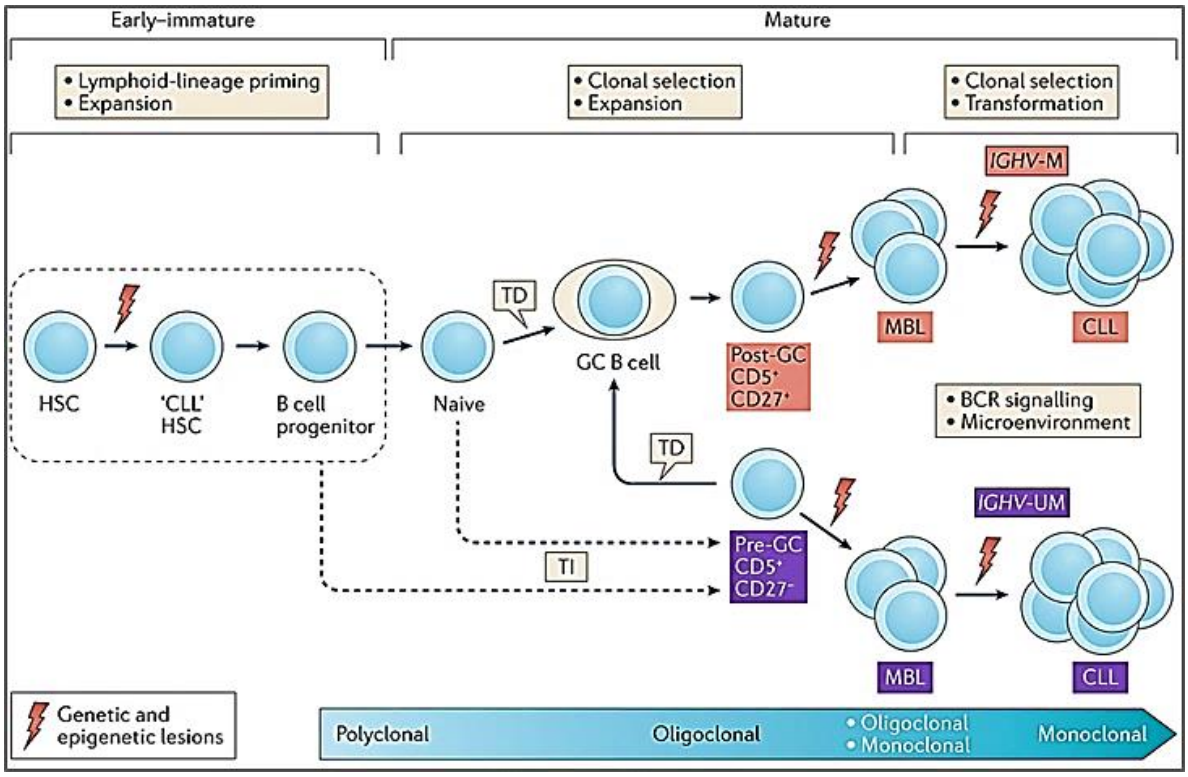


**Figure 1.4 Cell of origin of CLL.**

TD, T cell-dependent antigen; TI, T cell-independent antigen; MBL monoclonal B-cell Lymphocytosis; IGHV Immunoglobulin heavy chain variable region; UM unmutated; M mutated; GC germinal centre (Fabbri and Dalla-Favera, 2016).

### 1.1.2.4 Biology of CLL

Malignant CLL cells classically evade apoptosis *in vivo*, however, in culture they die spontaneously by apoptosis. Around over 99% of circulating CLL cells are arrested in the G0/G1 phase of the cell cycle. Hence their accumulation *in vivo* seems to arise because of apoptosis inhibition instead of increased proliferation (Gamberale *et al*, 2001; Hamblin and Oscier, 1997; Robertson and Plunkett, 1993). It has been shown that signals from accessory leukocytes can inhibit CLL cells apoptosis via a Bcl-2 dependent pathway (Gamberale *et al*, 2001). It has been reported that using deuterated water showed that leukaemic cells of each patient had a distinct and significant birth rate, ranging from 0.1% to more than 1.0% of the entire clone per day. An association between disease activity and progression and birth rates numbers seems to happen. Patients who had leukaemic cells birth rates more than 0.35% per day were more likely to show active or to develop progressive disease than others with lower leukaemic cells birth rates. Therefore, CLL is not a result just from accumulation of long-lived lymphocytes, but of dynamic cells that proliferate and die (Messmer *et al*, 2005).

Immunohistochemical study of 30 lymph nodes of CLL patients revealed the existence of 'Proliferation centres' or pseudofollicles, which enclose proliferating CLL cells dispersed with follicular dendritic cells, and T-lymphocytes (Schmid and Isaacson, 1994). Spleen, lymph nodes, and bone marrow would be expected to encompass pseudofollicles where CLL cells proliferate, and peripheral blood circulating CLL cells, where cells travel to undergo apoptosis. Divergent levels of proliferation of CLL cells has been identified using *in vitro* co-culture models of CLL cells protected from spontaneous and drug induced apoptosis by soluble ligands of CD-40, IL-4, IL-2, and co-culture of CLL cells with mouse fibroblast L-cells (NTL) and/ or human bone marrow derived mesenchymal stem cells (MSC), and or combination of CD-40, IL-4 and co-culture systems (Willimott *et al*, 2007).

CLL cells from poor prognosis cases had better survival than cells from indolent cases. Therefore, the heterogeneity is not only in apoptosis resistance, but also with progression of the disease (Plander *et al*, 2009). In short, apoptosis tendency of CLL cells *in vitro* was reduced using different co-culture systems and helped in explanation and understanding of the disease process. CLL cells travel to lymph nodes to proliferate and then travel back

to peripheral blood to accumulate and this makes CLL malignancy complicated and heterogeneous.

#### 1.1.2.5 The microenvironment of CLL

The previous data underscore the importance of the microenvironment in the disease course of CLL, since the stromal cells layer further augmented CLL drug resistance (Ranheim and Kipps, 1993; Burger *et al*, 2000; Kurtova *et al*, 2009; Lagneaux *et al*, 1998). CLL cells interact with the microenvironment and this play a vital role in CLL pathogenesis (ten Hacken and Burger, 2016). Secretion of chemokines secretion induce survival, proliferation, and drug-resistance signals in CLL (Caligaris-Cappio, 2003). Moreover, a cross talk between Bcl-2 family proteins and Proviral integration site of murine leukaemia viral kinases (Pim) family proteins provides a pro-inflammatory microenvironment that supports CLL cell maintenance and survival (Chen, Balakrishnan and Gandhi, 2010). CLL specifically deregulate genes in nurse like cells (NLCs) that play a role in immune-competency (Bhattacharya *et al*, 2011).

Bone marrow and secondary lymph organs have distinctive microenvironments for lymphocyte maturation and differentiation. Lymphopoiesis a process that occur in the marrow, leads to generation of B-cells with functional antigen (Ag) receptors B-cell receptors (BCRs), after mature B-cells migrate to secondary lymph organs. There, they are exposed to antigens within germinal centres, and interact with CD4+ T cells for antigen recognition and with follicular dendritic cells (FDCs) for necessary quality control after affinity maturation (Burger and Gribben, 2014).

The CLL microenvironment involves components such as bone marrow stromal cells (BMSC), mesenchymal stromal cells (MSCs), monocytes derived nurse like cells (NLCs), natural killer cells (NK) and T cells (figure 1.5). The communication within the CLL microenvironment is achieved by different adhesion molecules and chemokine receptors and ligands including tumour necrosis family (TNF), BCR, and Toll like receptors TLR. The contact between CLL cells and NLCs is established by chemokine receptors and BCR get activated in CLL after co-culture with NLCs.

There are several pro-survival pathways in the CLL microenvironment (figure 1.5). A proliferation-inducing ligand with B-cell maturation antigen (APRIL-BCMA), TNF family receptors with transmembrane activator and calcium modulator and cyclophilin

ligand interactor (TACI), B-cell activating factor (BAFF-BAFF-R) TNF family members, CD38-CD31 axis activate genetic pathways in CLL cells leading to proliferation, extracellular secretion of nicotinamide phosphoribosyl transferase (NAMPT) by CLL cells upon BCR, TLR, and NF-κB activation and is associated with immunosuppressive IL-10, tumour promoting IL- 6, and IL-8 cytokines. CLL cells secrete High-mobility group protein B-1- (HMGB-1) interactions with receptor for advanced glycation end products (RAGE) promotes NLCs differentiation. NLCs secrete CXCL12 and CXCL13 to attract CLL cells by binding to CXCR4, CXCR5 receptors respectively. BCR activation induces CCL3, CCL4 chemokines secretion that in turn recruits T-cells and monocytes. CD40-CD40L axis for CLL cells survival and proliferation. Programmed cell death protein-1 (PD-1) and PD-1Ligand which are expressed on T cells surface, helping immune evasion of CLL cells from T-cell cytotoxicity. CLL cells soluble BCL2-associated athanogene 6 (BAG6) secretion and low expression of NK-P30 and soluble BAFF secretion by NK cells will reduce NK-cytotoxicity. Adhesion molecules of Very Late Antigen-4 and its receptor fibronectin/vascular cell adhesion molecule-1 (VLA4-FN/VCAM-1) and CXCR4-CXCL12 mediate adhesion of CLL cells to BMSCs. CXCR5-CXCL13 and lymphotoxin-αβ-lymphotoxin-β receptors (LTαβ–LTβR) axis mediates cross-talk between FDCs for positioning CLL cells within lymph follicles, endothelin-1-endothelin subtype A receptor (ET-1-ETAR) axis for endothelial cells interaction to promote drug resistance and survival (ten Hacken and Burger, 2016).

There are several key pathways mediating the crosstalk within the microenvironment will be highlighted in this section.

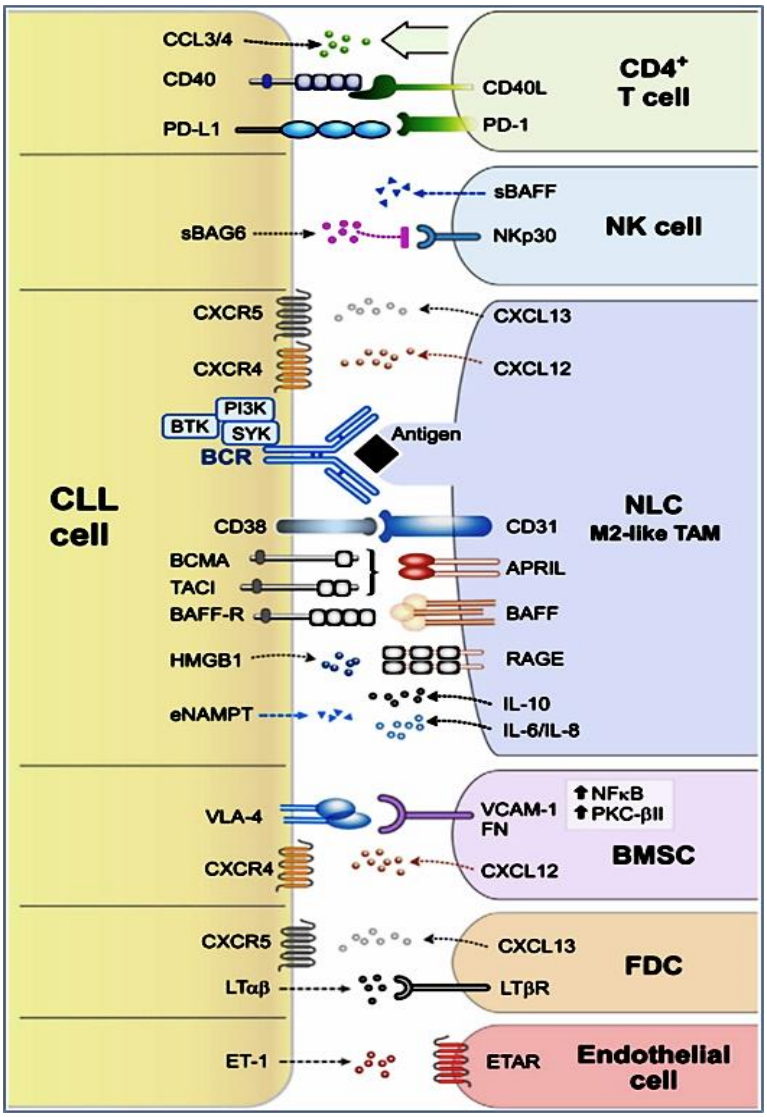


**Figure 1.5 Summary of cellular and molecular components of CLL microenvironment.**

Adapted from (ten Hacken and Burger, 2016).

#### 1.1.2.5.1 Bone Marrow Stromal Cells, Mesenchymal Stromal Cells, and Nurse Like Cells

In the bone marrow, stromal "feeder" cells maintain hematopoietic stem cells in particular 'niches' alongside the marrow vasculature (vascular niche) or to the endosteum (osteoblast niche) (Sugiyama *et al*, 2006; Burger and Gribben, 2014). The high affinity of CLL cells for stromal cells was demonstrated by the *in vitro* phenomenon named 'pseudo-emperipolesis'. Pseudo-emperipolesis describes the fraction of CLL cells that migrate spontaneously underneath BMSCs cells within few hours of co-culture. The

activation is bidirectional, as CLL and BMSCs cells both get activated (Burger and Gribben, 2014; Burger, Burger and Kipps, 1999).

NLCs symbolise a significant part of the CLL microenvironment (figure 1.5). NLCs originate from monocytes. Gene expression profile analysis of CLL cells after CLL-NLC co-culture showed that NLCs activate the BCR and NF-κB signalling in CLL cells (Burger *et al*, 2009). They also induce chemotaxis and secrete C-X-C motif chemokines, CXCL12 or stromal-derived factor-1 (SDF-1), CXCL13, TNF family members BAFF, and APRIL (Nishio *et al*, 2005). NLCs express calreticulin and vimentin antigens that activate BCR on CLL cells (Binder *et al*, 2010), NLCs also express CD31 which interacts with CD38 (Deaglio *et al*, 2010). CD31/CD38 interactions are followed by activation of genetic programs related to proliferation responses, migration and homing of CLL cells, HMGB-1 which induces differentiation of NLCs via the activation of RAGE and TLR9 pathway (Jia *et al*, 2014). CLL cells protected from apoptosis *in vitro* by monocyte-derived soluble CD14 that activates NF-κB (Seiffert *et al*, 2010).

Mesenchymal stromal cells, such as BMSCs, function as feeder layers for normal haematopoietic progenitor cells and are important for normal bone marrow structure (ten Hacken and Burger, 2016). MSCs are usually found in secondary lymphatic tissues of CLL patients where they secrete chemokines to regulate migration and survival of CLL cells (Burger *et al*, 2009). They also protect CLL cells from drug-induced apoptosis (Lagneaux *et al*, 1998). It has been found that BMSCs result in upregulation of CD38 and ZAP-70, which are aggressive disease markers in CLL cells, also down regulate CXCR4 receptors, which results in the continuing presence of residual disease after treatment (Purroy *et al*, 2015).

BMSCs have been shown to down regulate CD20 expression, which contributes to rituximab resistance (Marquez *et al*, 2015). They also increased aerobic glycolysis and glucose uptake, with activation of NOTCH signalling and its transcriptional target c-myc inducing drug-resistance (Jitschin *et al*, 2015).

MSCs express VLA-4 (α4β1)/ vascular cell adhesion molecule-1 (VCAM-1) (Pittenger *et al*, 1999). Binding of (Integrin α4β1) and VLA-4 which is an integrin dimer composed of CD49d and CD29 to VCAM-1 or to the extracellular matrix component FN saves CLL cells from spontaneous apoptosis and fludarabine stimulated apoptosis, because of induction of the BCL-2 anti-apoptotic protein (delaFuente *et al*, 2002; Lagneaux *et al*,

1998). Equally bidirectional activation occurs between CLL cells and MSCs via activation of protein kinase CβII (PKCβII) and NF-κB pathway in stromal cells (Lutzny *et al*, 2013).

#### 1.1.2.5.2 Endothelial and Dendritic cells

Endothelial cells and FDCs are essential for CLL cells tissue homing and survival (Badoux *et al*, 2011b; Maffei *et al*, 2014; Maffei *et al*, 2012). CLL cells bind to β1 and β2 integrins, BAFF, and APRIL, on the surface of microvascular endothelial cells (Cols *et al*, 2012), and also ET-1 (figure 1.5). They get together with EATR on endothelial cells to promote survival and drug resistance, which can be blocked by EATR inhibition by BQ-123 (Maffei *et al*, 2014; Maffei *et al*, 2012). FDCs protect CLL from apoptosis *in vitro* through direct cell-cell contact in CD44-dependent mechanism in CLL cells followed by upregulation of anti-apoptotic protein myeloid cell leukaemia-1 (MCL-1) (Pedersen *et al*, 2002). The CXCR5-CXCL13 axis and LTβR/LTαβ signalling between CLL cells and FDCs are very vital for CLL homing within lymphatic follicles, and also for progression of leukaemia *in vivo* in CLL mouse model EμTCL1 (the mouse model created by exogenous expression of the human *TCL1* gene under the control of the IGHV promoter and IGH enhancer (*Eμ*) *in vivo*, which results in the clonal expansion of $CD5^{+}IgM^{+}$ B cells) (Heinig *et al*, 2014).

#### 1.1.2.5.3 T-cells and Natural killer cells

There has been a lot of efforts to identify the role of T cells in CLL, and it has been agreed that T cells compartments are abnormally high in CLL, and there is an increase in T cells population in peripheral blood (PB) (Riches and Gribben, 2013). This increase is due to CD8+ T cells increase so that the ratio of CD4+/CD8+ is decreased in comparison to bone marrow and lymph nodes where numbers of CD4+ increase. The mechanism underlining these fluctuations is uncertain, though there are suggestions of increased susceptibility to Fas-mediated apoptosis of CD4+ T cells in PB. Other reports suggested that the change of circulating T cells numbers is related to disease prognosis. It has been reported that reversed CD4+/CD8+ ratio is due to rise of CD8+PD-1+ replicative senescence

phenotype in CLL patients at early stage and is linked to more aggressive clinical disease and shorter time to treatment (Nunes *et al*, 2012). However, it has been shown that high relative CD8+ counts CLL patients show an indolent clinical course and longer survival probability (Gonzalez-Rodriguez *et al*, 2010).

It is essential for B-cells to interact with T cells through the CD40 cell surface receptor that belongs to TNF-R family on CLL cells, and CD40-Ligand on T cells, for antigen presentation and normal B-cell immune responses (Van Kooten and Banchereau, 2000). It has been shown that for CLL cells, CD40-CD40L is important for decreasing spontaneous and drug-stimulated apoptosis; and increasing anti-apoptotic protein MCL-1 and Bcl-$X_L$ increase in CLL cells (Choudhary *et al*, 2015; Kitada *et al*, 1999a). CLL patients have impaired T cell immune synapse formation due to defective actin polymerisation. Improved synapse function was attained after treatment with immunomodulating agent lenalidomide (Ramsay *et al*, 2008). In addition, a novel evasion mechanism was identified in CLL cells, which misuse multiple co-inhibitory ligand-receptor signalling to cause T-cell-F-actin synapse dysfunction and inhibit effector function in both formerly healthy allogeneic and autologous patient T-cell populations, by inhibiting Rho-GTPases RhoA, Rac1, and Cdc42, key regulators of T-cell synapse actin dynamics (Ramsay *et al*, 2012). CLL-derived CMV-specific CD8 (+) T cells exhibit lower expression of exhaustion markers (inhibitory molecules CD160, CD244 and PD1) and are intact functionally (te Raa *et al*, 2014), which means that changes in the T-cell compartment in CLL are possibly very heterogeneous. In the Eμ-TCL1 mouse model for CLL, antibody blockade of PD-L1 re-established CD8 T-cell cytotoxicity and immune synapse formation and normalized T-cell cytokines and proliferation *ex vivo* and *in vivo* (McClanahan *et al*, 2015). It has been reported that T cells from patients with CLL have increased expression of CTLA-4 (CD152) with unfavourable diagnosis and unmutated IGHV status UCLL, and anti-CD152 monoclonal anti-body may be a therapeutic potential to increase the immune response against autologous leukaemia cells (Motta *et al*, 2005).

Natural killer (NK) cells are a key component of the anti-tumour immune response (figure 1.5). In CLL, the NK cytotoxicity is compromised and several studies revealed some of the possible mechanisms for that. Low expression levels of natural killer cell p30-related protein (NKP30), and natural killer group 2-member D (NKG2D), which reduce NK cytotoxicity, and decrease NK cells responses to BAG6, has been described in CLL

patients (Hilpert *et al*, 2012; Reiners *et al*, 2013). The cytolysis that induced by NK cells is inhibited through the presence of human leukocyte antigen G (HLA-G) molecules, which block trans-endothelial migration of NK cells in CLL microenvironment, as part of 'tolerogenic conditions' in CLL microenvironment (Rizzo *et al*, 2014). Furthermore, rituximab (anti-CD20) synergistically increased CLL cells clearance mediated by NK cells in NSG mice (Veuillen *et al*, 2012). However, it has been reported that (NK-cell-derived BAFF) involvement in the impaired CLL cells susceptibility to direct and rituximab-induced NK-cell reactivity, suggests combining other monoclonal anti-bodies (mAbs) with rituximab such as Obinutuzumab, Ofatumumab or BAFF blocking agent as belimumab more efficient therapy for CLL (Wild *et al*, 2015).

#### 1.1.2.5.4 BCR

Initial sIg binding in normal B-cells leads to the 'Signalosome' formation. The 'signalosome' is a complex of kinases and scaffold proteins found at the plasma membrane at sites of sIg activation. Phosphorylation of tyrosine (based activation motif) in the C-terminal end of BCR-associated IgαCD79A and Ig βCD79B by LYN Src-family kinase stimulates the formation of the signalosome, and this will act as a specific site to recruit tyrosine kinase SYK via tandem Src homology2 (SH2) domain by SRC-family kinase phosphorylation and auto-phosphorylation. The signal is then amplified by association of SYK with adaptor molecule B-cell linker protein (BLNK) and its downstream signalling component, the Brurton's tyrosin kinase (BTK); and phospholipase Cγ2 (PLCγ2) (Stevenson *et al*, 2011). LYN dependent phosphorylation of the CD19 cytoplasmic domain recruits the P85 subunit of phosphoinositide 3-kinase (PI3K). Downstream signalling will lead to NF-κB and nuclear factor of activated T cells (NFAT) pathways activation, MAPK (RAF/MEK/ERK) and P38 kinase pathways that eventually lead to proliferation, survival and migration.

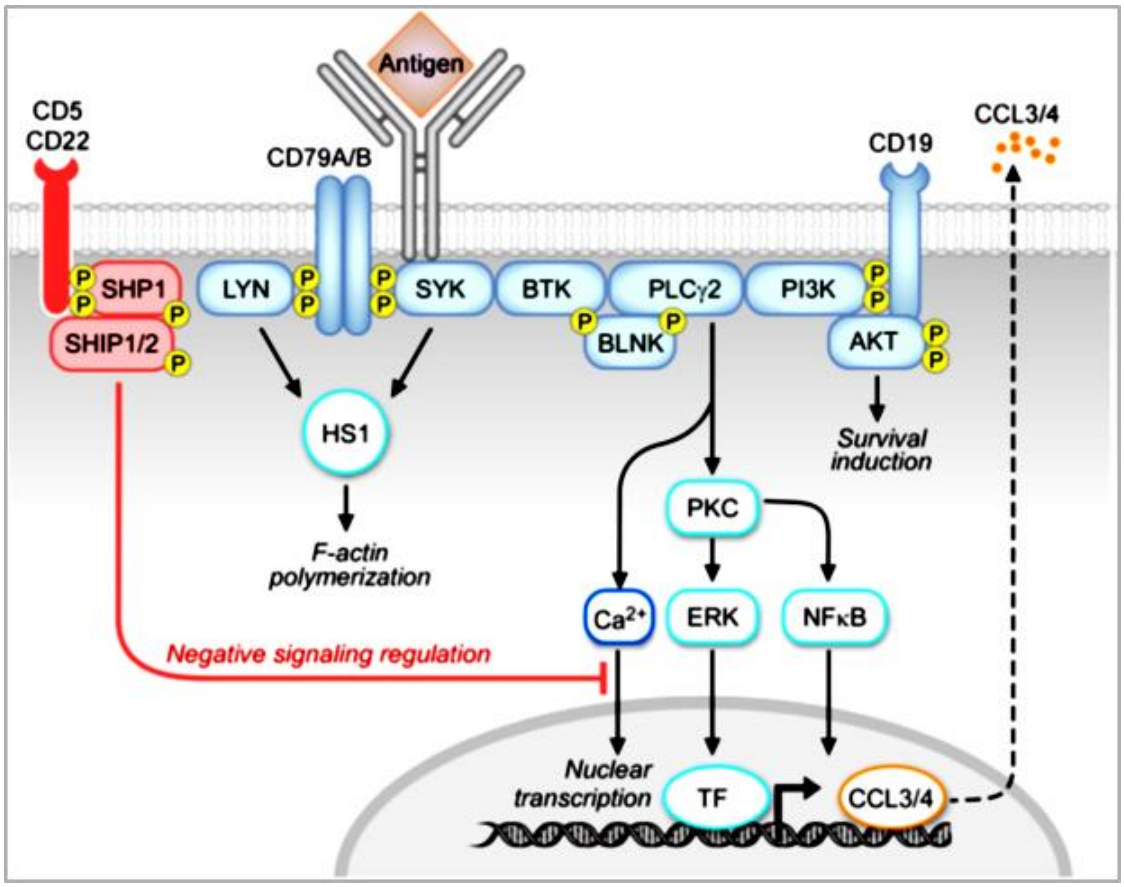


**Figure 1.6 illustration of BCR signalling in B-cells.**

Adapted from (ten Hacken and Burger, 2016).

There are also negative regulation of BCR signalling in B-cells, CD5, CD22, CD72, and FcγRIIB, are essential in controlling BCR signalling duration and intensity, as can be seen in (figure 1.6). The inhibition motif that resides in these receptors, phosphorylated by LYN when BCR activated, leading to recruitment of inhibitory phosphatases, such as SH2 domain containing protein tyrosine phosphatase-1 (SHP1) and SH2 domain containing inositol 5-phosphatases 1/2 (SHIP1/2), which will eventually reduce BCR signalling (ten Hacken and Burger, 2016; Stevenson *et al*, 2011). Therefore, LYN both positively and negatively regulates BCR signalling transduction.

Noticeably, CLL cells response to BCR activation is heterogeneous. A subset of CLL seems not responsive to antigen engagement. sIgM levels are generally but variably decreased in CLL compared with normal naive B-cells, and this occurs specifically in M-CLL, which could be attributed to strong down-modulation that lead to no responses to sIgM. Remarkably, one subset of CLL seems to constitutively express phosphorylated extracellular-signal regulated kinase (P-ERK), and increased transactivation nuclear

factor of activated T cells (NFAT), with absence of AKT activation and unresponsiveness to sIg ligation. Also it is characterised by low levels of surface immunoglobulin M and impairment of calcium mobilisation after *in vitro* BCR engagement; which presents a human model of anergic B-cells (Muzio *et al*, 2008; Apollonio *et al*, 2013).

Since CLL is a mature B-lymphocytes disease, cells express IgM, and IgD on their surfaces, with low affinity and autoreactive BCR expression of U-CLL B-cells, while M-CLL B-cells tend to express high affinity mono-reactive BCR for certain pathogens (Haerzschel *et al*, 2016).

CLL cells has been reported to show autonomous BCR activation independent of antigen binding (Dühren-von Marcus *et al*, 2012). Consistent with this, targeting BCR in CLL provided promising results, SYK inhibitors (entospletinib and R406) attained a complete Mcl-1 down-regulation, due to SYK inhibitors capability to stop BCR-inhibition to the main negative Mcl-1 regulator (GSK-3)(Bojarczuk *et al*, 2016). Ibrutinib, which is a BTK inhibitor, exerts its action via irreversible binding to specific cysteine residue in the kinase domain of BTK to halt its enzymatic activity. In addition, secretion of CCL3 and CCL4 chemokines that are dependent on BCR activation is down-regulated in plasma concentration of CLL patients getting treatment. Ibrutinib also caused a transient early lymphocytosis in the TCL1 CLL mouse model and inhibited CLL progression (Ponader *et al*, 2012; Burger and Montserrat, 2013).

#### 1.1.2.5.5 TLR and TNF family proteins

TLR consists of 5 adaptor proteins: - myeloid differentiation primary response gene-88 (MyD88), MyD88-adaptor like protein (MAL), Toll/interleukin-1-receptor (TIR) domain containing adaptor protein-inducing interferon-β (TRIF), TRIF related adaptor molecule (TRAM) and sterile-α and armadillo motif containing protein (SARM) (figure 1.7). They link to downstream signalling, which eventually leads to NF-κB and some members of interferon (IFN) family members (IRF) activation. It has been reported in CLL cells that ligation of (TLR9, and TLR7) cause CD38 expression which is associated with poor prognosis (Rozkova *et al*, 2010). In addition, in CLL (TLR2, TLR1, and TLR6) ligands activation with bacterial lipopeptides protect from apoptosis by activation of NF-κB pathway (Muzio *et al*, 2008).

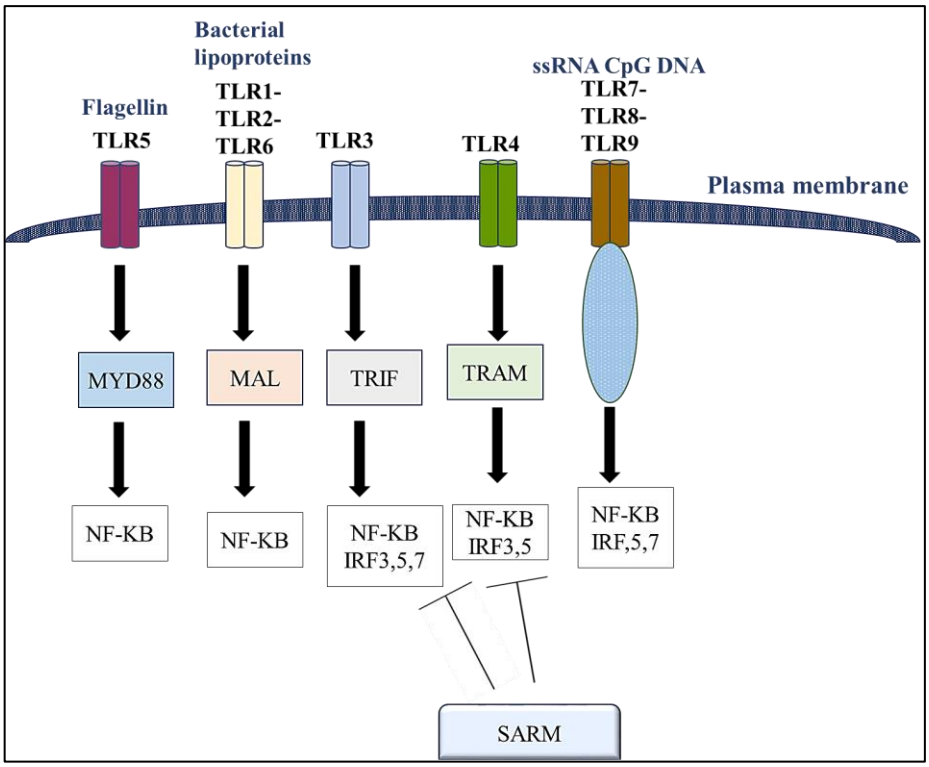


**Figure 1.7 Illustration of five adaptor proteins of TLR signalling.**

(Wang *et al*, 2014b).

It has been reported that CLL cells response to TLR7-agonists ligation is decreased through IL-6 that present in CLL microenvironment. Hence, IL-6 works as tumour suppressor through activating (mir-19a and mir-17) to induce tolerance state for TLR7-agonists (Li *et al*, 2015a). In 2014 p.L265P mutations in Myd88 has been identified in younger CLL patients of M-CLL category (Martinez-Trillos *et al*, 2014).

The TNF family plays a very important role in CLL survival. CD40L-CD40 (CD154) are members of this family that transduce the survival signals from T-cells to B-CLL cells. Other factors that have been shown to have effect on CLL survival and proliferation are APRIL, and BAFF (van Attekum *et al*, 2016). Both APRIL and BAFF have high binding affinity to TACI, and BCMA. Several cancers growth has been shown to be mediated by APRIL. Therefore, serum APRIL levels are related to poor prognosis and CLL survival (Planelles *et al*, 2007). APRIL expression in CLL cells appears to be more prognostic than BAFF and increased levels of APRIL are correlated with Rai stage (Bojarska-Junak *et al*, 2009). Moreover, BAFF and APRIL protect CLL cells from drug-induced and spontaneous apoptosis (Kern *et al*, 2004). In addition, CD40/CD154 expressing T-cells

in CLL tumour microenvironment or B-CLL cells have been shown to be linked to NF-κB activation and CLL survival *in vitro* (Furman *et al*, 2000).

Many studies have shown that CD40 in combination with IL-4 or IL-21cytokines protects CLL cells from apoptosis and enhances their survival (Buske *et al*, 1997; Kitada *et al*, 1999b; Willimott *et al*, 2007; Ahearne *et al*, 2013; Pascutti *et al*, 2013). Lately, it has been discovered that BAFF is an important signalling in CLL cells as it induces IL-10 production by CLL cells in EμTCL1-Tg mouse model molecules, and in normal B-cells. This action is facilitated through TACI receptors, suggesting that if TACI is targeted for IL-10 inhibition this might restore suppressed immunity in CLL (Saulep-Easton *et al*, 2016). Recently, it has been reported that microRNAs are regulating the TNF/TNFR superfamily in CLL, miR-15a, miR181, miR-29a, and miR-223a targeting FBXW7, Bcl2, Bcl6, DDX3X, and IL-10RA (Srivastava, Tsongalis and Kaur, 2016).

CD4+ T-cells express CD40L and stimulate B-CLL cells in proliferation centres. CD40 is a member of TNF superfamily and after stimulation it exerts its action in CLL cells through TNF receptor associated factors (TRAFs) domain in cytoplasm in CD40 receptors and leads to proliferation, differentiation, antibody isotype switching, humoral memory response and B-cell survival (Elgueta *et al*, 2009).

Without CD40-CD40L stimulation, a complex between cellular inhibitors of apoptosis-1 and -2 (cIAP1/2) is formed in CLL cells. The complex interacts with TRAF2, TRAF3 and then with NF-κB inducing kinase (NIK) causing NIK degradation and antagonising non-canonical NF-κB pathway leading to apoptosis.

CD40-CD40L stimulation in CLL cells enhances cells ability to adhere to hyaluronan through CD44, which restricts CLL cells mobility by CCL21 and the disruption of this activation could release CLL cells from their protective environment, which has a therapeutic potential (Girbl *et al*, 2013). (CD40-IL4R) stimulation induces TACI and BCMA expression in leukaemic cells, BCMA expression is related to poor prognosis in UCLL patients (Ferrer *et al*, 2014).

Recently, CD40/IL-4 stimulated CLL cells were shown to release extracellular vesicles with miRNAs to CD4+T-cells in their microenvironment, which increases immune synapse formation, interaction in tumour microenvironment and augment their migration (Smallwood *et al*, 2016). In addition, the expression of IgM, CD79b, and BCR signalling was restored in CLL cells with IL-4; and that is strongly marked in UCLL more than

MCLL cells (Guo *et al*, 2016). High IL-4R expression is associated with increase in STAT6, and sIgM expression in CLL cells, and it also protects them from PI3K and BTK inhibition (Aguilar-Hernandez *et al*, 2016).

#### 1.1.2.5.6 CLL cell Trafficking and Homing to Microenvironment

High endothelia vessels (HEV) are important for CLL cell relocation to lymph nodes (LN) through a CD62L L-selectin dependent adhesion process that helps rolling, sticking and crawling of CLL cells *in vivo* (Lafouresse *et al*, 2015). Chemokines and their receptors are also important factors in CLL migration. A high level of L-selectin has been observed in CLL patients with increased number of circulating CLL cells, while the opposite was seen in patients with less circulating CLL cells. In addition, in trafficking of normal B-cells through LN egress, in which cells depend on sphingoine-1 phosphate receptor (S1PR), S1PR expression found to be low in poor prognostic CLL (Caligaris-Cappio, 2015). CLL migration to and from proliferation centre plays important role in drug resistance, proliferation, and disease progression.

Chemokine CXCL12 (SDF-1) is secreted in CLL microenvironment by BMSCs and NLCs. CD38 and CXCR4 signalling synergise together on CLL cells surface to enhance chemo-taxis to CXCL12.

Expression of VLA-4 integrin was linked to poor outcomes in CLL patients (ten Hacken and Burger, 2016). Integrins are adhesion molecules important for CLL adhesion, trans-endothelial migration, growth, and function. CD49d/VLA-4 is essential for CLL cells to be retained in their microenvironment; blocking VLA-4 *in vivo* lead to inhibition of CLL trafficking to bone marrow (Davids and Burger, 2012). VLA-4/CD49d, zeta chain associated protein kinase-70 (ZAP-70) and cluster of differentiation38 (CD38) expressing CLL cells display more chemotaxis toward CXCL12. CXCL13 works through CXCR5 and attracts CLL cells to their microenvironment.

CCL3 and CCL4 are CC motif ligands secreted by CLL cells that engages monocytes, macrophages and T-cells to CLL tissue sites to enhance their interactions, and they are secreted after CLL BCR stimulation *in vitro* (Bystry *et al*, 2001). High CCL3, CCL4 plasma levels are linked to poor prognosis (Sivina *et al*, 2011).

*In vitro*, CXCR4 activation is linked to survival and stimulation of ERK, and STAT-3. High levels of CXCR4 in CLL cells are linked to poor prognosis and jeopardy of infiltration to lymphoid organs (Calissano *et al*, 2009).

CCL19 and CCL21 chemokines are secreted by stromal cells to attract CLL cells though CCR7. CCR7 expression is high in CLL cell surfaces. Studies suggested that ZAP-70 increases CCR7 expression via ERK1/2 and enhances CLL cell migration (Calpe *et al*, 2011).

VCAM-1, (α4β7) and the β2 integrins leukocyte function antigen-1LFA-1 (αLβ2) and intracellular adhesion molecule-1 (ICAM), are among integrins that establish CLL cells trafficking to LN (Hartmann *et al*, 2009). Matrix metalloproteinase-9 (MMP-9) is produced by CLL cells to induce their migration and also to protect malignant cells from apoptosis by LYN/STAT3 activation and Mcl-1 stimulation (Redondo-Muñoz *et al*, 2010), and induced CLL resistance to treatment of fludarabine and arsenic trioxide cytotoxic drugs by upregulating Blc-2 family of anti-apoptotic proteins *in vitro* (Amigo-Jiménez *et al*, 2014).

#### 1.1.2.5.7 *In vitro* modelling of the CLL proliferative microenvironment

When culturing CLL cells *in vitro* they will undergo spontaneous apoptosis, since they lack survival signals that they have in their microenvironment. CD40L-CD40 and IL-4 were shown to be effective in saving CLL cells from apoptosis *in vitro* (Grdisa, 2003). CLL cells express high levels of cyclin D and p27 cyclin-dependent inhibitor. Survival antigen presentation and proliferation of normal B-cells depends on CD40 signals. In addition, (CD40-CD40L) or IL-4 delayed onset of apoptosis in leukaemia cells after treatment with fludarabine.

STAT6 phosphorylation was higher in CLL cells than normal B-cells when both were stimulated by IL-4 (Bhattacharya *et al*, 2015). Survivin was found to be the only inhibitor of apoptosis protein (IAP) to be expressed by CLL cells up on stimulation with CD40L *in vitro*. On the other hand, *In vivo* in lymph nodes and bone marrow samples, survivin was found to be in proliferating cells in proliferation centres (Granziero *et al*, 2001).

*In vitro* spontaneous apoptosis is reversely controlled by levels of constitutive STAT3 and NF-κB activation *in vivo* (Liu *et al*, 2016). *In vitro* cultured and CD40 stimulated CLL cells showed P50, P65, and c-Rel NF-κB activation and survival, while using CD154-mAb caused apoptosis (Furman *et al*, 2000). Another study shows that Rel-A of NF-κB is related to CLL cells survival *in vitro* (Hewamana *et al*, 2008).

#### 1.1.2.6 Pro-and Anti-Apoptosis signals in CLL

CLL cells have been known to have defects in apoptosis, and are known to be quiescent in peripheral blood. Their inability to start apoptosis might be due to a survival signal overload. Excessive constitutive survival signals activation in proliferation centres lead to increase in Bcl-2, IAP and Mcl-1 expression in CLL cells. Other signalling pathways were linked to anti-apoptotic signals in CLL such as BCR activation via PI3K inducing Mcl-1 expression (Billard, 2014). Increased Bcl-2/Bax ratio is found in CLL cells, which supports cells survival (Packham and Stevenson, 2005). Studies have shown that PB cells of all CLL patients, no matter cytogenetic abnormality or stage of disease, undergo spontaneous apoptosis.

A linear correlation was found between PB B-lymphocyte count and increased spontaneous apoptosis with the decrease in intracellular STAT3 (Uri *et al*, 2012). In addition, p53 alterations are linked to defective apoptosis in CLL (Billard, 2014). P53 impaired function has been reported in CLL, such as missense mutations in TP53, which are partially resistant to irradiations, TP53 deletions, nonsense mutations and bi-allelic mutations, which are resistant completely to irradiation (Marinelli *et al*, 2013). Approximately 8-18% of CLL patients have TP53 associated with 17p13 deletion and ataxia telangiectasia (ATM) associated with 11q22.3 deletion mutations and would need early treatment (te Raa *et al*, 2015). ATM mutations will lead to p53 impaired function. However, CLL cells with defective TP53 are more aggressive and CLL cells with defective ATM are related to long clinical course. Both biallelic mutation and deletion in ATM will lead to impairment in p53 response.

Defects in TP53 can now be detected by functional assays *in vitro* (Pozzo *et al*, 2013b) and by next-generation sequencing (NGS), as they will affect the duration of responses to tyrosine kinases inhibitors in CLL patients. They account approximately for 5-10% of

patients at diagnosis and in refractory disease they could be 40-50% in frequency (te Raa and Kater, 2016).

#### 1.1.2.7 Genetic alterations and their prognostic values in CLL

Genetic abnormalities in CLL play an important role in the pathogenesis process (figure 1.8). Some genetic aberrations will define the treatment plan for CLL patients, such as TP53 mutations/deletions. Others will give prognostic values, such as IGHV mutational status, trisomy12, 17p13 deletions, and other genetic defects that affect CLL patients. Approximately, 80% of CLL patients have chromosomal abnormalities. Fluorescence in situ hybridization (FISH) and, conventional G-banding cytogenetics (CGC) helped in identification of karyotyping and chromosomal translocations. In addition, NGS recently has facilitated the detection of important genetic mutations such as TP53, SF3B1, BIRC3 and NOTCH1 (Puiggros, Blanco and Espinet, 2014).

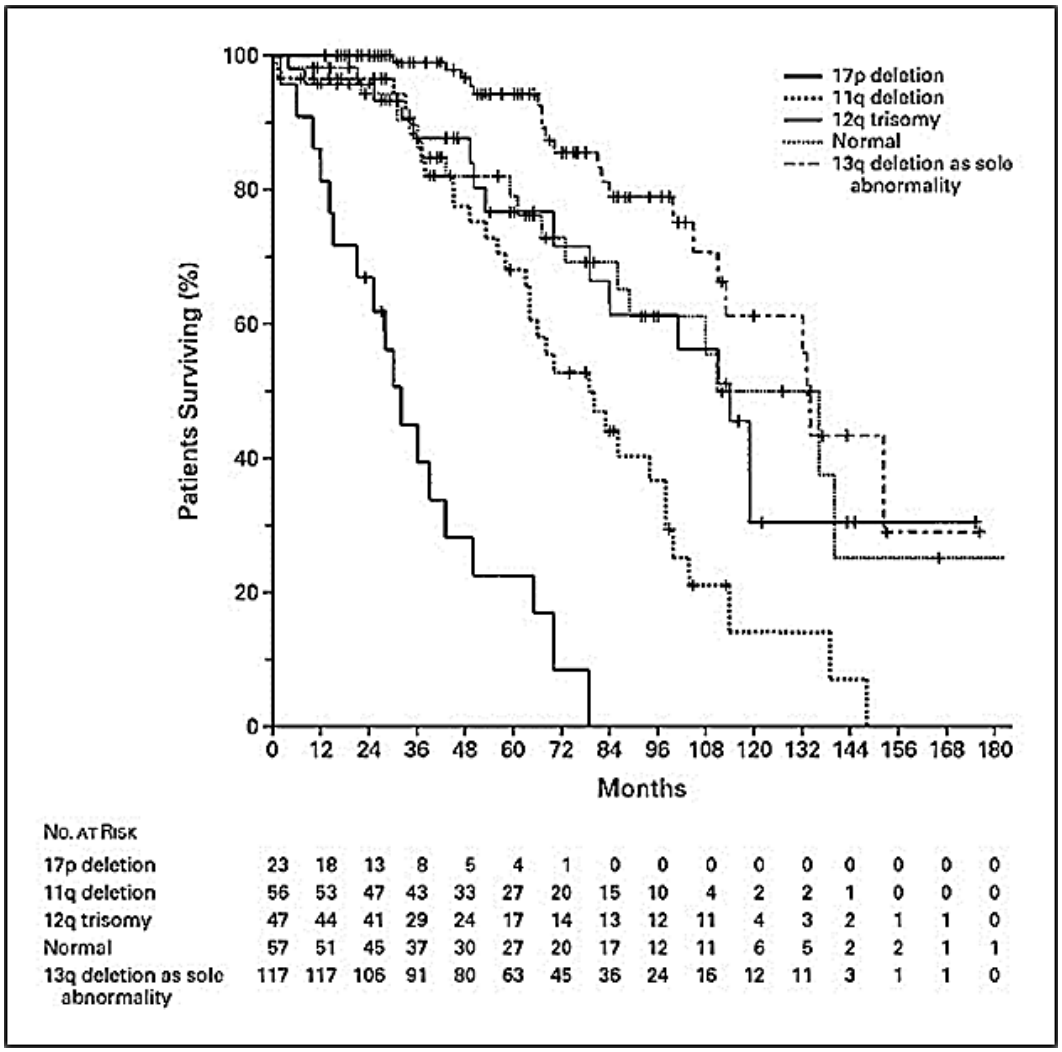


**Figure 1.8 Kaplan-Meier curves of hierarchy of 5 classes of genetic aberrations in CLL.**

Survival probability from date of diagnosis, adapted from (Dohner *et al*, 2000).

### 1.1.2.7.1 13q14 deletions

Mostly detected by FISH (fluorescence in situ hybridisation), this group of patients are considered as indolent CLL with good prognosis. Biallelic deletion in 13q was reported in 30% of CLL patients with 13q deletions (Puiggros, Blanco and Espinet, 2014). 13q14 is associated with low ZAP-70 expression and MCLL. MicroRNAs, miR-15a/miR-16-1 cluster is located within the deleted region of 13q14 gene, are negative regulators of Bcl-2 expression. Also *DLEU7*, which is identified as a tumour suppressor gene, that inhibiting NF-κB and NFAT is located in minimal deleted region (MDR) of 13q14 gene (Palamarchuk *et al*, 2010). Therefore, miR15a/miR16-1 inhibition causes Bcl-2 and, Mcl-1 constitutive activation, which plays an important role in CLL pathogenesis (Pekarsky and Croce, 2015).

#### 1.1.2.7.2 Trisomy 12

This is the third most common chromosomal aberration in CLL (RW.ERROR - Unable to find reference:doc:59524aa9e4b00ccedc489817). Mainly detected by FISH, trisomy 12 affects nearly 10-20% of CLL patients. The cytogenetic abnormality is considered as medium risk group of CLL. In addition, it is associated with increased MDM2, P27 and CDK4 expression, since they that are located in same chromosome. Remarkably, the cytogenetic abnormality accounts for 50-90% in RS transformed CLL patients, have higher CD38+, thrombocytopenia, and second cancer development (Strati *et al*, 2015; Puiggros, Blanco and Espinet, 2014).

As monoclonal B- cell lymphocytosis (MBL) seems to be the early stage of CLL, recently trisomy 12 has been found among MBL patients that have different phenotype from non-trisomy 12 MBL, indicating similarity with CLL (Sorigue, Maluquer and Junca, 2017). Trisomy 12 CLL showed increased HH hedgehog signalling expression, which is associated with many cancers such as brain, skin and prostate; and can be targeted in this CLL subset of patients (Decker *et al*, 2012). Trisomy 12 CLL cells have overexpression of integrin signalling molecules CD11a-CD18 (LFA-1), CD49d-CD29 (VLA-4), CD38, CD323, integrin subunit beta7 (ITGB7), CD11b-CD18 (Mac-1) integrins, while NOTCH1 trisomy 12 cases had CD11b, CD11a, and CD18 under expressed (Riches *et al*, 2014). Preferentially, NOTCH1 mutations appear to happen in CLL patients of trisomy 12 as the only genetic lesion associated with poor outcomes (Del Giudice *et al,* 2012). Rituximab (anti-CD20 mAb) have had shown better results with trisomy 12 CLL patients as they are characterised by significant expression of CD20 in comparison to other CLL subsets (Tam *et al*, 2008).

#### 1.1.2.7.3 17p13 deletion

This is the highest risk group among CLL cytogenetic abnormalities, with shortest overall survival (OS) and progression free survival (PFS). 17p deletion can be detected in CLL patients at diagnosis between 3-8% of cases, however, can be also acquired in refractory CLL after chemotherapy. 17p deletion/ TP53 mutations/deletions do not respond to CLL standard therapy such as fludarabine and cyclophosphamide (FC) or fludarabine, cyclophosphamide, and rituximab (FCR). TP53 gene mutations/deletions might be

concomitant with 17 p deletion, and can be detected in 75% of 17p deletion cases, with remarkable low occurrence of TP53 mutations in cases lacking 17p deletion, and clinical heterogeneity has been shown among 17p deletion CLL cases (Tam *et al*, 2008; Puiggros, Blanco and Espinet, 2014).

#### 1.1.2.7.4 11q23 deletion

5-20% of CLL patients harbour these cytogenetic abnormalities. 11q22-11q23 is were ATM lies. Large deletion cases will be associated with ATM gene loss. 11q deletions are associated with UCLL, poor outcomes and lymphadenopathy, and could be associated with BIRC3 deletion/mutations but has no relation to disease progression. So far no 11q homozygous deletion has been detected (Puiggros, Blanco and Espinet, 2014). ATM mutations not BIRC3 were linked to poor clinical outcomes and survival among CLL patients (Rose-Zerilli *et al*, 2014).

#### 1.1.2.7.5 Other Mutations and chromosome translocations

Chromosomal translocations can be balanced when they result in no gain or loss of genetic materials, and non-balanced when they result in genetic material loss or unequal exchange of chromosomal materials. Translocations in CLL are reported in 13q, 14q, 18q, 17q, 17p, 2p, 1p, 11q, and 5q (Baliakas *et al*, 2014). BCL3 gene rearrangement at 19q13 t(14;19)(q32;q13) was found in CLL cases, however, it is a rare event in CLL (Stilgenbauer *et al*, 2002; Nguyen-Khac *et al*, 2011).

Identification of translocations of the Bcl2 gene rearranged at the 5' end analogous to the immunoglobulin light chain gene resulting in translocation t(18;22)(q21.3;q11) that disrupt the promoter region of Bcl2 in CLL (Dyer *et al*, 1994).

In recent years mutations in CLL that helped in prediction of progression and survival rates among CLL patients have been uncovered, such as Notch1 activation mutations that appeared as an indication of high risk to RS transformation and short survival (Rodríguez *et al*, 2015). TLR protein Myd88 gain of function mutations, TLR2, and MAPK1 mutations associated with M-CLL. A component of U2 spliceosome SF3B1, ATM, BIRC3, POT1, FBXW7, XPO1, DDX3X, U2AF2, and TP53 mutations linked to chemo refractoriness and U-CLL.

All above mentioned mutations was were discovered using NGS and whole exome sequencing (WES). These mutations have helped in prediction of disease progression and survival rates. Some mutations were more abundant in U-CLL while others were more abundant in M-CLL cases, which helped in the stratification of the disease. Recently, circulating tumour DNA (ctDNA) serial analysis using low-coverage whole-genome sequencing (LC-WGS) and WES detected ctDNA in samples of refractory /relapsed CLL patients as an emerging biomarker for CLL molecular disease monitoring (Yeh *et al*, 2017).

#### 1.1.2.8 Molecular abnormalities in CLL and their implications

Recently, the molecular genetics of chronic lymphocytic leukemia knowledge has increased significantly. Next generation sequencing technologies identified genomic alterations in CLL such as Notch1 (mostly frameshift deletion c.7541_7542 delCT), SF3B1 (mostly K700E) that have been associated with short time to survival. Clinical implications of these molecular abnormalities have been currently established as Notch1 mutations linked to Richter syndrome transformation, and SF3B1 mutations linked to short PFS after treatment (Foà *et al*, 2013; Rossi *et al*, 2013a). Myd88 mutations (mainly L265P) have been found to be prevalent in mutated IGHV gene and young age CLL patients and are linked to better prognosis (Rossi and Gaidano, 2016). In addition, MAPK appeared as an upregulated pathway in CLL cells (Shukla, Shukla and Joshi, 2017), and BRAF mutations reported to be in low frequency among patients (Jebaraj *et al*, 2013).

##### 1.1.2.8.1 BRAF mutations in CLL

Considering the inhibition of MAPK signalling as a therapeutic approach in CLL, 3.7% of CLL show BRAF mutations (Damm *et al*, 2014). Other clustered genetic mutations have been found in the kinase domain activation part (Landau *et al*, 2015). Using an Allele-specific (AS)-PCR technique, BRAFV600E was identified in CLL patients; in a very low frequency in one CLL of (n=128) screened CLL samples (Langabeer *et al*, 2012), and using direct Sanger-sequencing method, 2.8% of BRAF mutations were detected in a CLL patient's cohort (Jebaraj *et al*, 2013).

### 1.1.2.8.2 SF3B1 mutations in CLL

In 2011 it was reported that SF3B1 mutations occur in 9.7% of untreated CLL patients with unmutated IGHV, poor prognosis, and elevated β2 microglobulin (Quesada *et al*, 2011; Wang *et al*, 2011). SF3B1 mutations occur as a subclonal event, therefore, they are proposed to be a promoter for CLL progression rather than initiators of the disease. Most common SF3B1 mutations in CLL are K700E, which emerge from an A 2098 G transition on the sense strand, encoded by exons 14 to 16, and accounts for up to 50% of reported cases in CLL (Wan and Wu, 2013) (figure 1.9). SF3B1 mutations have been detected in fludarabine refractory CLL patients (Rossi *et al*, 2011).

As a component of the splicing machinery, SF3B1mutation in CLL might lead to generation of alternative spliced transcripts, premature stop codons transcripts, and truncated proteins (Wang *et al*, 2016; Alsafadi *et al*, 2016).

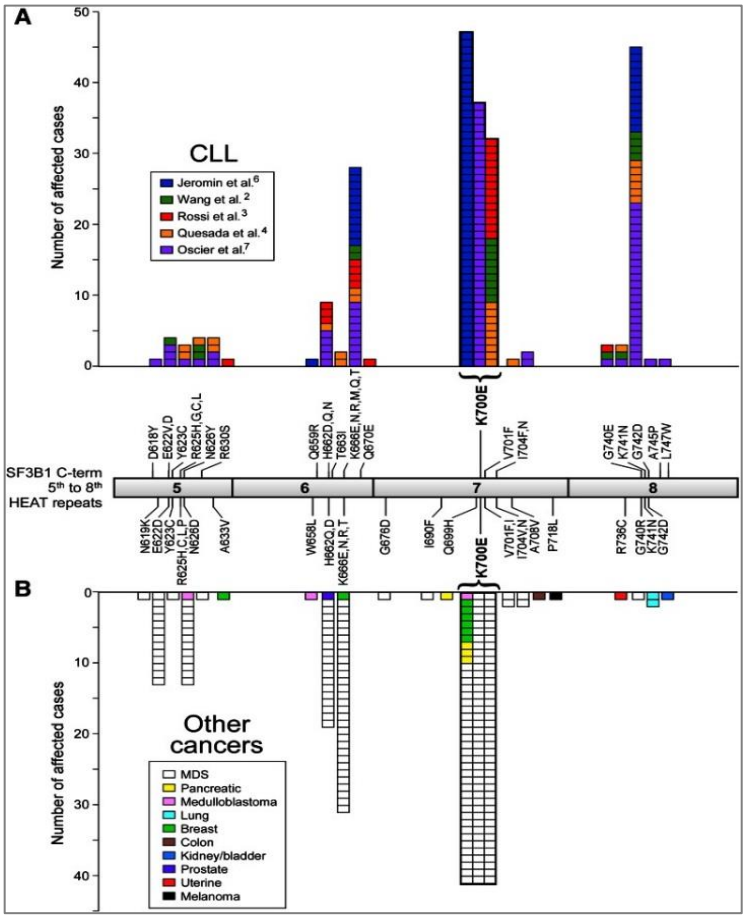


**Figure 1.9 SF3B1 mutations in CLL.**

C-terminal domain (HEAT repeats) where recurrent mutations in SF3B1, 5 CLL reported studies with frequencies of mutations in CLL are indicated in **A**. Other cancers SF3B1 mutations reported from COSMIC indicated in **B**. This figure adapted from (Wan and Wu, 2013).

Transcriptome analysis of CLL samples revealed that SF3B1 mutations cause changes in splicing and gene expression that results in increase in NOTCH signalling via altered splicing of DVL2, and modulate DNA damage response by upregulation of KLF8, which is linked to carcinogenic transformation (Wang *et al*, 2016). Adult mice with heterozygous mutations of SF3B1 developed macrocytic anaemia, and showed faults in haematopoietic stem cells auto-renewal (Wang *et al*, 2014a). Spliceosome dysfunctions in zebra fish impacted haematopoiesis detrimentally, yet cell type sensitivity counts on which component of splicing machinery affected. SF3B1 mutant zebra fish showed that SF3B1 is crucial for hematopoietic cells development and differentiation and that is unconnected to Notch signalling for proper specification of hematopoietic stem cells (De La Garza *et al*, 2016). A recent report showed that cryptic 3'splice sites are sequestered within secondary structures of RNA and inaccessible to normal splicing catalysis in wild-type cells, but the SF3B1K700E mutant overcomes this constraint, making cryptic 3' splice sites accessible for spliceosome complexes (Kesarwani *et al*, 2017).

#### 1.1.2.8.3 NOTCH1 mutations in CLL

NGS has revealed Notch1 frameshift mutations mainly in U-CLL cases (Puente *et al*, 2011), and these mutations mainly occur in RS and chemorefractory CLL cases and predict poor outcomes (Fabbri *et al*, 2011). Notch1 mutation was found to be concurrent with trisomy 12 cases. c.7541_7542delCT (p.P2514fs*) exon 34 at chromosome 9 is the most common mutation, being nearly 80% of all Notch1 mutations in CLL (figure 1.10) (Bilous *et al*, 2016; RW.ERROR - Unable to find reference:doc:59524aa9e4b00ccedc489817; Rossi *et al*, 2012; Del Giudice *et al*, 2012).

In a large unselected CLL study, Notch1 mutation frequency was 12.1% and was associated with shorter time to treatment (Weissmann *et al*, 2013). It has been found that Notch1 mutations were more frequent in advanced and treated CLL patients (Baliakas *et al*, 2015a), and are associated with decrease survival among Notch mutated CLL patients (Willander *et al*, 2013). In addition, Notch1 mutated CLL patients were found to be resistant to fludarabine treatment, and Notch1 mutations are enriched with in RS transformed patients (Hernandez, Galvez and Zweidler-McKay, 2014).

c.7541_7542delCT 2-bp deletion leads to truncated PEST domain's C-terminal, consequently, a constitutively active protein will be accumulated and the pathway deregulated. C-terminal is important in regulation of Notch1 degradation through turnover by the ubiquitin-proteasome complex. As a result, constitutively active Notch1 will cause apoptosis resistance and greater survival in CLL cells (Bilous *et al*, 2016).

The intracellular part of the Notch protein found overexpressed in the cytoplasm and nuclei of mutated CLL cases with Notch1 mutations compared to unmutated, and it is suggested to activate the NF-κB pathway (Xu *et al*, 2015). Notch1 c.7541_7542delCT mutations of PEST domain in CLL are associated with overexpression of mRNA of c-Myc, which may be linked to increased survival and proliferation of the U-CLL cells subset of patients (D'Avola *et al*, 2016).

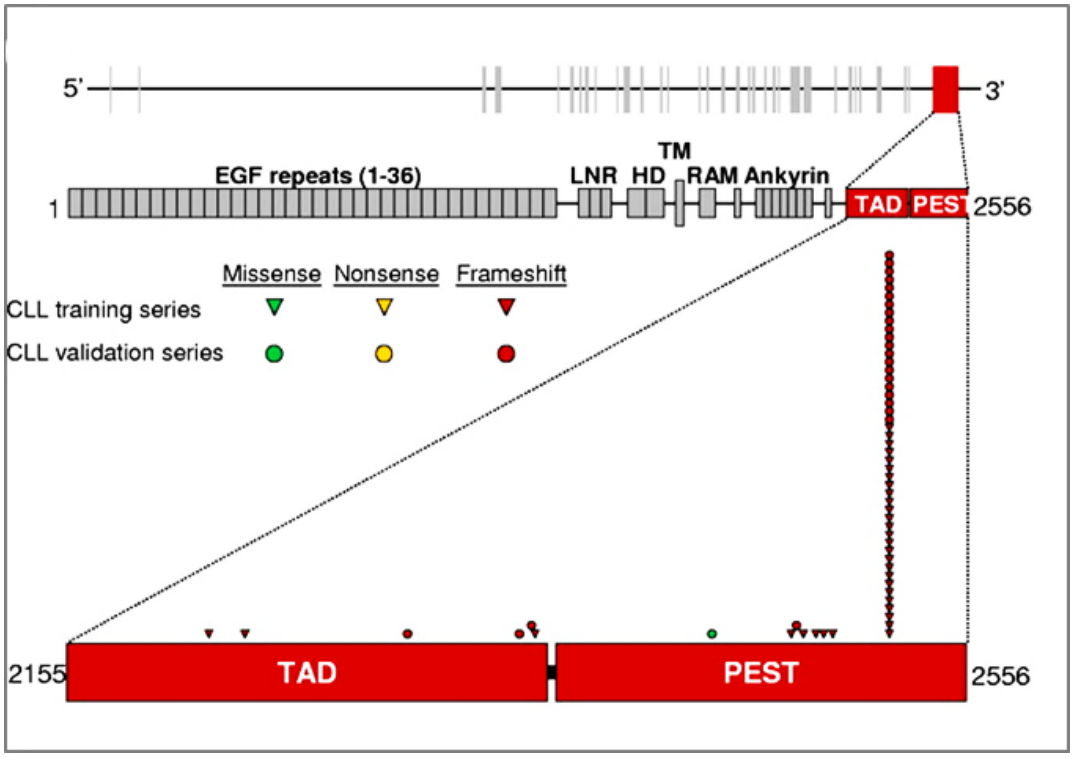


**Figure 1.10 Notch1 mutations in CLL cases.**

Most of NOTCH1 mutations in CLL are in the PEST domain, and are frameshift CT 2-bp deletion c.7541_7542delCT at exon 34 (Rossi *et al*, 2012).

#### 1.1.2.8.4 MYD88 mutations in CLL

In 2011, 2.9% of Myd88 8 p.L265P mutations were reported in CLL using WES. TLR mutations in CLL promote survival and protect from spontaneous apoptosis. CLL patients with Myd88 mutations are younger than wild type, and are M-CLL subtype (Puente *et al*, 2011; Martinez-Trillos *et al*, 2014). Myd88 L265P mutations high frequency in LPL were suggested to be used as a differential diagnosis from MZL and CLL/SLL (Insuasti-Beltran *et al*, 2015). In a collaborative multicentre study, 2% of CLL cases had Myd88 mutations and 90% of them carried the hot spot p.L265P, which was exclusive to M-CLL, low occurrence of TP53, Notch and SF3B1 mutations, with frequent isolated 13q deletion, similar young age at diagnosis, and was more in males (Baliakas *et al*, 2015b). In another recent report of (Martínez-Trillos *et al*, 2016), they found that 70% of MYD88 mutations in their series are p.L265P, but no differences in patient's age, mutational status and clinical stages, were similar to previous reports (Baliakas *et al*, 2015b). Recently, a study of mutation frequency in subsets of CLL patients according to mutational status of stereotyped B-cell receptor immunoglobulins, Myd88 mutations was absent or rare in all subsets (Sutton *et al*, 2016).

### 1.1.2.9 Current therapeutic approaches in CLL

CLL is a heterogeneous disease and its treatment would depend on many factors such as IGHV mutational status, TP53 mutational status, and 17p deletions. CLL patients might not need treatment at diagnosis, but after prognostic markers are checked (for instance, FISH, IGHV, ZAP-70, CD38, and β2-microglobulin), they will guide to treatment strategies.

Chemoimmunotherapy is one of the standard first line treatments in CLL. Monoclonal antibodies (mAb) have already been developed, such as anti-CD20 ofatumumab and obinutuzumab. Also, lenalidomide, which is an immunomodulatory drug, idelalisib, which is a phosphatidylinositol-3kinase inhibitor (PI3K), Ibrutinib, which is a Bruton kinase inhibitor (BTK), and Bcl-2 inhibitor Venetoclax (ABT-199) have been tested in CLL (figure 1.11). It has been reported that 17p deletion patients are the difficult subgroup of CLL to treat and that they have no benefit from chemoimmunotherapy (FCR)

, as their response is very low, so they should be offered new targeted therapy such as Ibrutinib, irrespective of age (Jain and O'Brien, 2015).

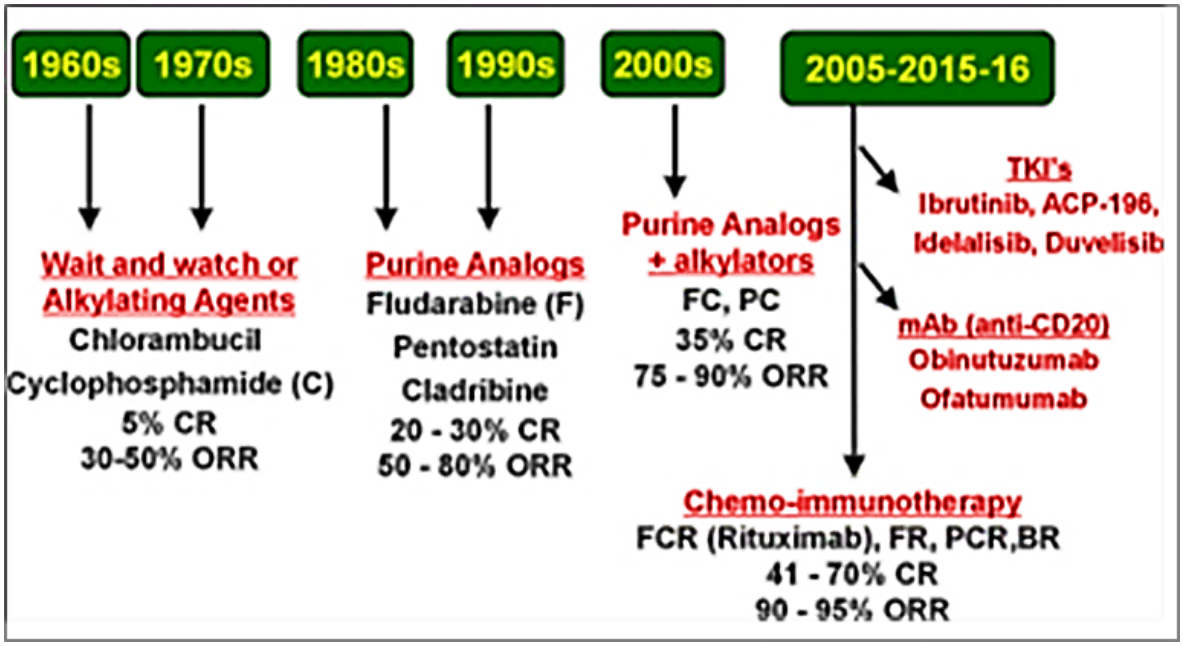


**Figure 1.11 Progression in CLL treatment during 1950s to 2016.**

CR complete response, ORR overall response rate, FC fludarabine rituximab, PC pentostatin and cyclophosphamide, FR fludarabine and rituximab, PCR pentostatin, cyclophosphamide and rituximab, BR bendamustin and rituximab. Adapted from (Rai and Jain, 2016).

#### 1.1.2.9.1 Alkylating agents, chemoimmunotherapy, and monoclonal antibodies, single agent therapy and combinations

Single agent treatment with Chlorambucil, cyclophosphamide, lenalidomide, fludarabine and bendamustin has been reported in many clinical trials. A combination of fludarabine, cyclophosphamide, and rituximab (FCR), fludarabine and pentostatin, fludarabine and cyclophosphamide (FC), or caldribine and cyclophosphamide (CC), have been used till late 2000s. Single agent therapy with fludarabine or bendamustine exhibited major improvement over chlorambucil in randomized trials (Rai and Jain, 2016).

Bendamustin-rituximab (BR) in a recent study was a suitable alternate first frontline therapy to fit and elderly CLL patients (Gentile *et al*, 2016).

PFS and ORR have been improved using FC and CC over using single agent treatment. Rituximab (anti-CD20) was first used in the 1990s and showed improved responses in high doses. In 2005, it was combined with FCR and showed better results for M-CLL

over U-CLL patients. OS of M-CLL with this combinational therapy reached 87% (Rai and Jain, 2016).

Significant severe infections of older CLL patients treated with FCR in comparison to BR has been reported (Eichhorst *et al*, 2014). CLL patients with 17p deletion and TP53 aberrations have lower responses to FCR with less PFS, for which it is recommended for them to use kinase inhibitors and rituximab as a front-line and relapse therapy (Eichhorst *et al*, 2015).

After success with anti-CD20 rituximab, other mAb, such as oftaumumab, and anti-CD52 alemtuzumab, have been used as frontline therapy. Oftaumumab has been combined with FC (O-FC) and with cyclophosphamide and pentostatin and showed equal efficacy to FCR (Rai and Jain, 2016). In a randomized study, it was reported that CLL patients with co-morbidities, their outcomes were improved after using a combination of anti-CD20 and chlorambucil (Goede *et al*, 2014). Alemtuzumab (anti-CD52) has been tested in combination with FCR (A-FCR) in 17p deletion/TP53 aberrations, and showed increase on overall response, but major toxicities have limited the trial (Rai and Jain, 2016).

#### 1.1.2.9.2 Stem cell transplantation

Allogeneic haematopoietic stem cell transplantation (allo-HSCT) is recommended for high risk CLL patients with refractoriness and shorter responses to treatment (less than 2 years). 50 % of those patients would have a permanent MRD (minimal residual disease) after transplantation (Dreger *et al*, 2014). Allo-HSCT is recommended for CLL patients that reached remission with Bcl-2 antagonists and kinase inhibitors, harbouring 17pdeletion/TP53 aberrations or early relapsed patients from chemoimmunotherapy. However, the criteria that should be considered to allo-SCT are matched donor availability, patient's age, co-existing disease, and their responses to therapy (Eichhorst *et al*, 2015).

Patients who relapsed after allo-HSCT would be rescued by lymphocyte donor infusion or immunosuppressant exclusion. However, complications such as acute and chronic graft versus host disease (GVHD) would accounts for mortality among allo-grafted patients affecting around 15-30% during first 2 years post-transplantation (Dreger *et al*, 2014).

## 1.2 MAPK signalling

MAPK pathway was shown to be constitutively active in a subset of CLL patients (Muzio *et al*, 2008). In addition, BRAF mutations have been linked to a number of cancers such as hairy cell leukemia and melanoma. Therefore, we aimed to investigate targeting MAPK signalling in CLL cells using (RAF/MEK/ERK) inhibitors, and using available cell lines of JVM3 (B-PLL) (BRAFK601N), MEC-1(B-CLL), HC-1 and ESKOL (HCL), and SIG-M5 (AML) (BRAFV600E), considering the inhibition of MAPK signalling as a therapeutic approach in CLL.

Mitogen activated protein kinase (MAPK) signalling regulates cell responses to microenviromental alterations. This pathway plays a vital role in growth and proliferation of cells, as well as in pathogenesis and initiation of several tumours. The main MAPK cascade comprises of RAS, which is attached to the plasma membrane and attached to small guanine nucleotide binding protein. Up on ligand binding (growth factor) to tyrosine kinase receptors, the receptor tyrosine kinase get activated, leading to receptor autophosphorylation on multiple tyrosine residues. Then, signaling proteins with Src homology 2 (SH2) domains binds to these tyrosine-phosphorylated residues, initiating multiple signaling cascades. One of these SH2 domain proteins, Grb2, exists in the cytoplasm in a preformed complex with a second protein son of sevenless (SOS), which can catalyse GTP/GDP exchange of RAS. RAS activated through guanine nucleotide exchange factor (GEF) SOS, which will exchange GDP to GTP in RAS. Active RAS will recruit RAF to the membrane and activates it. RAF will phosphorylate and activate MEK1/2, MEK1/2 will phosphorylate and activate ERK1/2, which will be translocated to the nucleus to activate several transcription factors to enhance cell survival and proliferation. The complexity of this cascade is in the isoforms of each protein. RASs are KRAS, NRAS, and HRAS. RAFs are ARAF, BRAF, and CRAF. MEKs and ERKs are MEK1, ERK1, and MEK2, ERK2. These genes encode for equally functional proteins. BRAF activation will lead to CRAF phosphorylation and activation and that will phosphorylate and activate MEK1/2 (figure 1.12). The high mutation profile of BRAF in human cancer indicated the main role of BRAF than CRAF or ARAF in the signalling cascade (Pratilas and Solit, 2010; Cseh, Doma and Baccarini, 2014; Machnicki and Stoklosa, 2014; Heidorn *et al*, 2010). Furthermore, BRAF is distinctive from ARAF and CRAF kinases, which needed additional N-phosphorylation at their kinase domain for

complete activation process. BRAF will be recruited by RAS, phosphorylated, and activated, indicating its dominant role in this signalling pathway (Cantwell-Dorris, O'Leary and Sheils, 2011).

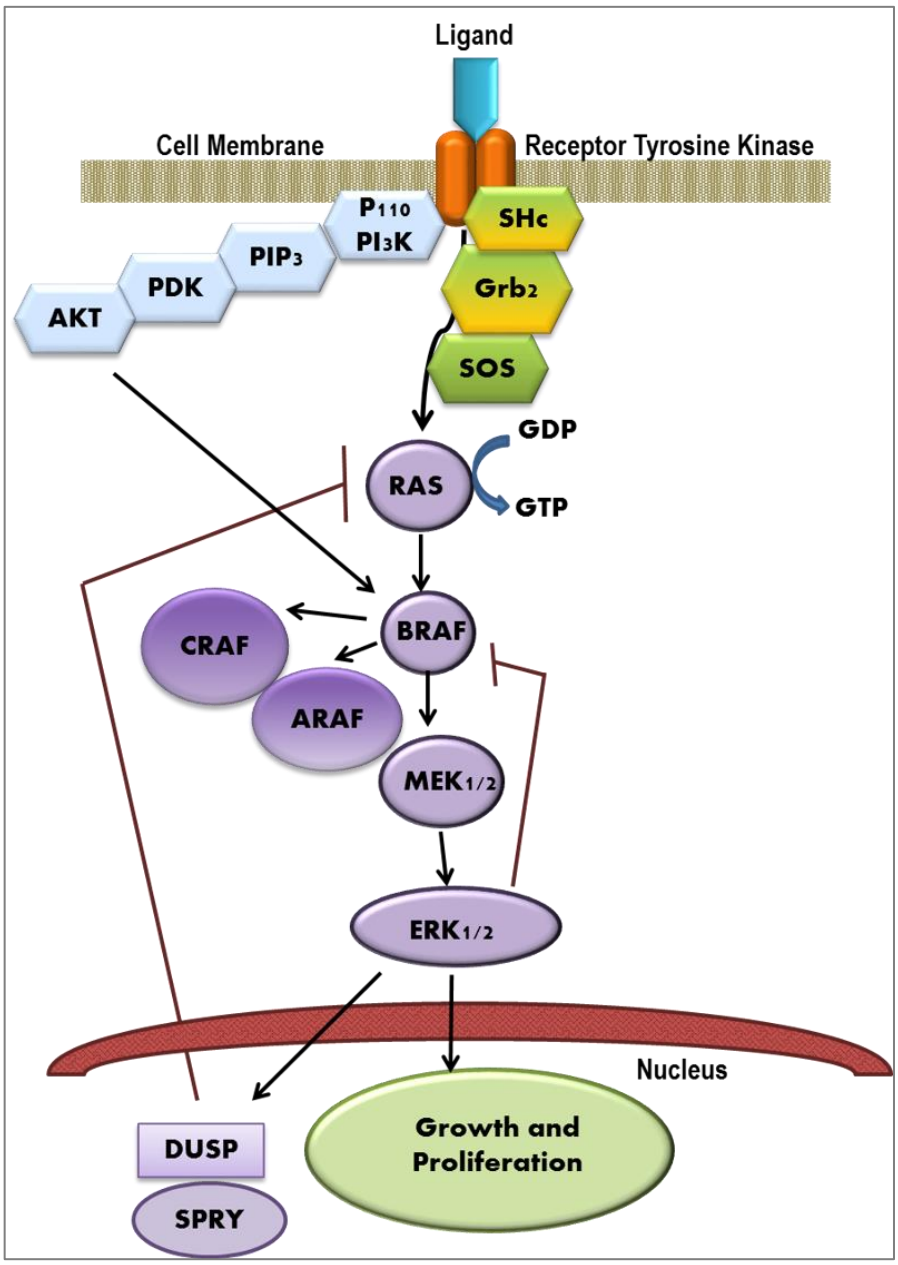


**Figure 1.12 RAS/RAF/MEK1/2/ERK1/2 signalling.**

Phosphorylated ERK1/2, DUSP Dual-specificity phosphatases and SPRY form a negative feedback loop to regulate MAPK pathway under normal biological conditions (Heidorn *et al*, 2010).

### 1.2.1 BRAF

All RAF kinases are able to bind to RAS and activate downstream MAPK signalling, and homo- and hetero-dimerization between RAF (BRAF-BRAF), (CRAF-BRAF) kinases under normal activation of MAPK signalling is essential. Phosphorylated and active ERK1/2 will disrupt RAS-RAF interactions, and RAF kinases dimerization as a negative feedback loop mechanism (Freeman, Ritt and Morrison, 2013). RAS binds directly to RBD and forms secondary interactions independent of GTP status of RAS with cysteine rich domain (CRD) (figure 1.13). This interaction will recruit RAF kinase to the membrane. The ability of RAF binding to RAS is regulated by some adaptor scaffolding protein (14-3-3 binding site) in CR2. S338 is conserved in all RAFS, but in BRAF S445 is also conserved and constitutively phosphorylated, unlike other RAFs, and that results in BRAF only requires recruitment by RAS to be activated (Wellbrock, Karasarides and Marais, 2004).

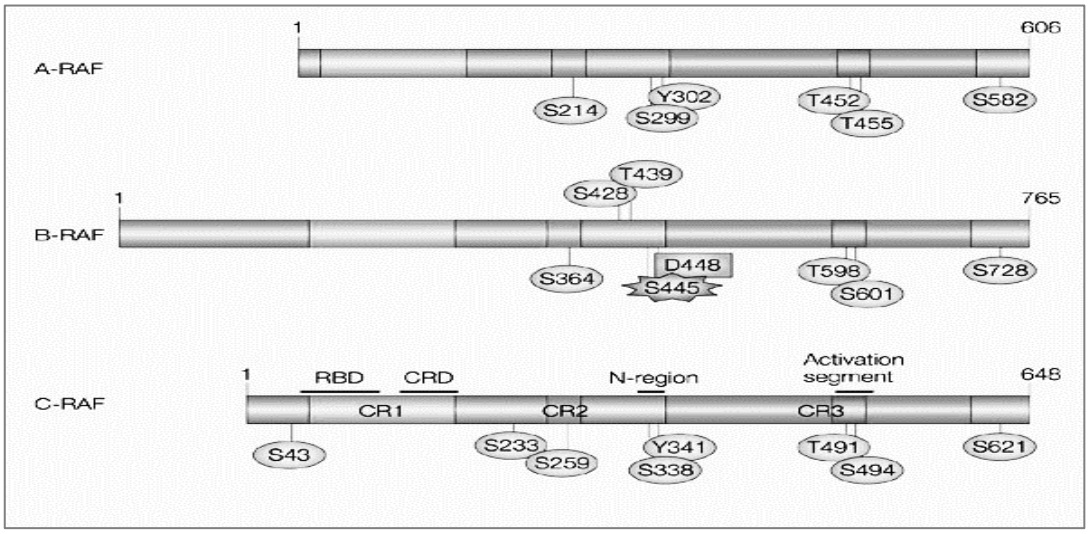


**Figure 1.13 RAF kinases structure and domains.**

Three conserved regions in RAF kinases, highlighted amino acids show phosphorylation sites required for activation. CR1 is the RAS binding domain RBD, and cysteine rich domain CRD both required for plasma membrane recruitment, CR2 contains 14-3-3 binding sites, CR3 is the catalytic domain; and the negative charge regulatory region N-region. S338 is conserved in all RAFs, S299 in ARAF and S445 in BRAF, it is constitutively phosphorylated in BRAF. C-RAF is 72–74 kDa; ARAF is 68 kDa, and BRAF is subjected to alternative splicing, has a variety of proteins that range from 75 to 100 kDa. Adapted from (Wellbrock, Karasarides and Marais, 2004).

### 1.2.2 BRAF mutations in cancer

RAF kinases haves been associated with cancer since their discovery in 1983. They were considered both main drivers of several cancers and a target for therapeutic potential. BRAF is mutated in approximately 8% of all tumours (Holderfield *et al*, 2014). More than 90% of all detected BRAF mutations are the BRAFV600E mutation, which is a thymine to adenosine transversion at nucleotide 1,799. This will result in valine substituted by glutamic acid at 600 in exon 15 in the translated protein (Cantwell-Dorris, O'Leary and Sheils, 2011). The substitution of Valine for a larger, negative glutamic acid destabilizes the interactions between the kinase domain and the P loop (Wan *et al*, 2004). This destabilisation of interactions mimics the phosphorylation of activation loops required for activation. The kinase will then be constitutively active, causing constant MAPK signal transduction. This increases cell growth and upregulates proteins involved in angiogenesis (VEGF) and metastasis (IL-8) (Ascierto *et al*, 2012).

BRAFV600E mutations prompting BRAF to be constitutively active are the most common driver mutation in nearly 40-50% of melanoma patients (Banzi *et al*, 2016), 60% of thyroid cancers, 10% of colorectal carcinoma, all cases of hairy cell leukaemia, and 6% of lung cancers (Holderfield *et al*, 2014). BRAF mutations are the most extensively studied and targeted, as they are drivers of several tumours and they are crucial in MAPK signalling.

### 1.2.3 BRAF as targeted therapy and mechanisms of resistance

ATP-competitive RAF kinase inhibitors were developed in early 2000, and sorafenib was the first Pan-RAF inhibitor that entered clinical trials. Due to similarity between ATP-kinases, several other targets of sorafenib were identified, such as VEGFR-2, KIT and, PDGFR-β. Vemurafenib and dabrafenib were developed with more selectivity over the mutant constitutively active enzyme conformation of BRAFV600E (figure 1.14), while sorafenib lacks this selectivity as it binds preferably to the inactive conformation. It has been reported that all three inhibitors mentioned are poor inhibitors to BRAF wild type and also cause paradoxical activation of MAPK signalling in wild type cells (Holderfield *et al*, 2014).

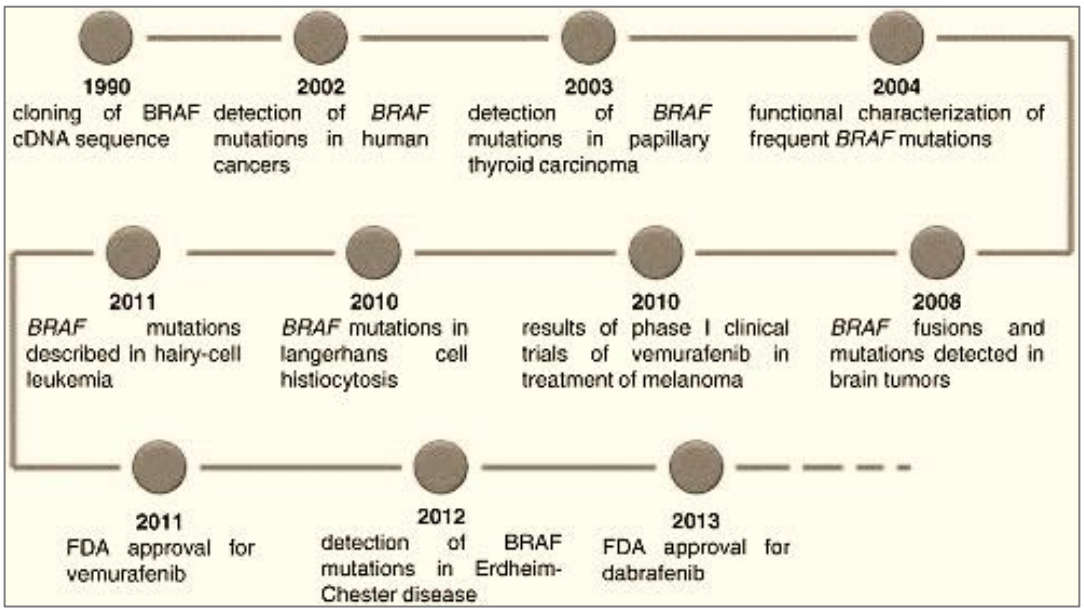


**Figure 1.14 BRAF inhibitors history.**

Adapted from (Machnicki and Stoklosa, 2014).

In melanoma patients, vemurafenib showed similar efficacy and toxicity in BRAFV600E and BRAFV600K mutated patients. Dabrafenib showed good tolerability in melanoma patients with brain metastasis. Similar toxicities have been reported with both dabrafenib and vemurafenib, such as skin toxicity and fever. In addition, BRAF inhibitors in combination with MEK1/2 inhibitors in melanoma patients showed improved response rate and PFS in comparison to monotherapy (Banzi *et al*, 2016).

One of the primary causes of resistance to BRAF V600E inhibitors was the loss of negative feedback loop to tyrosine kinase receptors-EGFR signalling, and the upregulation of PI3K pathway in metastatic colorectal and thyroid cancers, while in melanoma cells levels of EGFR are low. Therefore, the cellular milieu in which BAF inhibitors have been targeted is determining its efficacy and the mechanism of resistance. In addition to that, a melanoma cell culture model has shown increase in levels of CRAF as a resistant mechanism to BRAF inhibition, and serine/threonine MAP3K8 COT activates MEK in presence of BRAF inhibition (Holderfield *et al*, 2014). COT kinase activity was concomitant with BRAFV600E resistance in tissues from relapsed melanoma patients after RAF or MEK inhibitor treatment (Johannessen *et al*, 2010).

Receptor tyrosine kinases overexpression has been involved in BRAF inhibitor resistance, such as EGFR, PDGFRβ, and IGF1R. BRAF inhibitor resistance mechanisms is mediated by the overexpression of tumour derived factors such as NRG, EGF, and IGF1.It has been found that chemokine CCL2 is elevated in plasma of melanoma patients after treatment with vemurafenib and overexpressed in vemurafenib resistant melanoma cell lines (Vergani *et al*, 2016). Melanoma cells also will express splice variants of BRAF that will be resistant to vemurafenib, this process can be interrupted by interfering with pre-mRNA splicing. This suggests a slow development of BRAF inhibition resistance in melanoma (Salton *et al*, 2015)

Melanoma MAPK inhibitor resistant cells showed different glutamine metabolism. These cells have significantly greater sensitivity to glutamine deficiency than MAPK inhibitor responsive melanoma cells (Hernandez-Davies *et al*, 2015). Vemurafenib has been used for hairy cell leukaemia patients in relapse and refractory cases, in phase II trial one patient acquired KRAS mutation as a resistant mechanism (Falini, Martelli and Tiacci, 2016). In a previous study in our lab, a purine analogue-refractory hairy cell leukaemia patient with biallelic BRAFV600E mutation was treated with vemurafenib 240mg twice daily, resulted in a decrease in BRAF activity 75% in day 1 and 90% in day 8 of treatment, however, this had no effect on the phosphorylation of ERK1/2 nor MEK1/2 suggesting an alternative signalling pathway that could be targeted along with BRAF (Samuel, Macip and Dyer, 2014).

## 1.3 Spliceosome complexes and SF3B1

Splicing of messenger RNA is crucial and a major stage in regulation of genes expression and RNA maturation of all human mRNAs. In eukaryotes, splicing at selective sites will lead to diverse protein products (isoforms) that come from a single gene. Small nuclear ribonucleoprotein particles (snRNPs) in the nucleus are important to remove introns (non-coding sequences) and join the flanking exons (coding sequences) together (figure 1.15). Spliceosomes consist of five snRNPs: U1, U2, U4, U5, and U6. The 5′ splice site is located at the intron start of pre-mRNA. The 3′splice site is located at the end of the intron and the adenosine A (branch point) is usually located upstream of the 3’ splicing site, about 15 to 50 nucleotides (Matera and Wang, 2014). SF3B1 is a subunit of U2 snRNP, which is involved in early stages of splicing. SF3B1 mediates the U2snRNP recruitment

to the branch point by interacting with U2FA and both sides of branch point intronic RNA (Dvinge *et al*, 2016; Cazzola, Rossi and Malcovati, 2013).

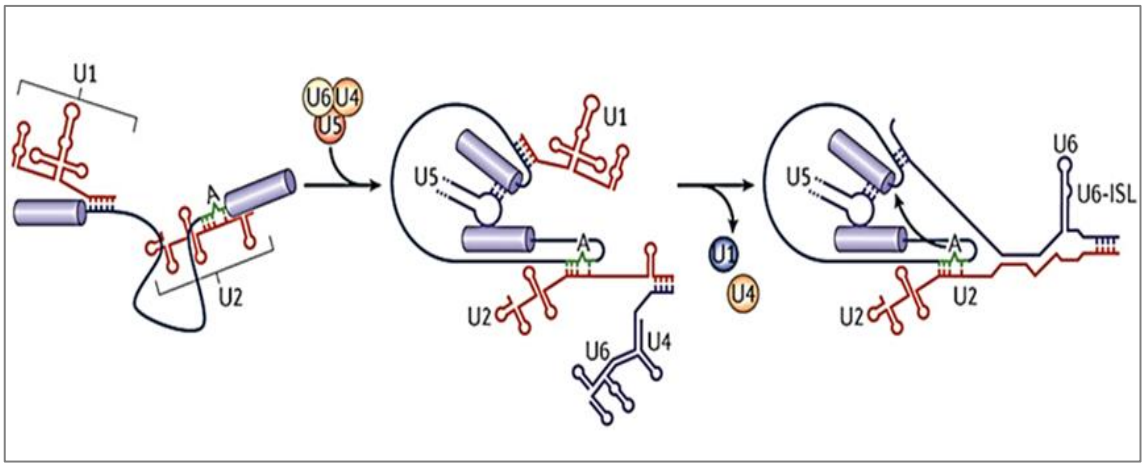


**Figure 1.15 Illustration of spliceosome assembly.**

Coding exons (purple) and non-coding introns (lines). U2 dependent spliceosome is the major one, with U2-snRNP for branching site recognition. Adenosine (A) is the branching point, U4–U6 join U2 and a new base pairs between U2 and U6, and between U5 and exonic sequences near the 5′splicing site is formed. U4 separates from U6 to expose the 5′ end of U6, which then base pairs with the 5′splicing site to dislodge U1. Base pairing interactions between U6 and U2, alongside the 5′splicing site and branch-point A is the first catalytic step of splicing. The central region of U6 forms an intramolecular stem loop ISL, which is crucial for splicing catalysis. Adapted from (Matera and Wang, 2014).

### 1.3.1 SF3B1and spliceosome components mutations in cancer

In some cases, tumour suppressor genes have miss-splicing, owing to mutation near splicing sites, which contributes to the emergence of cancers. Somatic mutations in genes that code splicing proteins was related to cancer development and tumour suppression (figure 1.16). SF3B1, serine and arginine rich splicing factor 2 (SRSF2), and U2 small nuclear RNA auxiliary factor 2 (U2AF2) are suggested to be proto-oncogenes, because they are highly subjected to miss-sense mutations that would result in gain or alteration of function. SF3B1 is mutated in CLL, uveal melanoma, pancreatic cancer, myelodysplastic syndromes, and breast cancer. However, the most common uveal melanoma mutation in SF3B1 is R625, and it is less common in haematological cancers (Dvinge *et al*, 2016). Using WES, SF3B1 somatic mutations were identified in 2010 in myelodysplastic syndrome MDS patients, which is a group of heterogeneous diseases affecting hematopoietic stem cells. SF3B1 mutations were identified in 30% of MDS patients, clustered at exons 12-16 of the SF3B1 gene (Cazzola, Rossi and Malcovati, 2013). In CLL, SF3B1 mutations are linked to poor outcomes, but in myelodysplasia and

uveal melanoma are linked to improved favoured prognosis. SF3B1 is using cryptic 3' splice sites 10–30 bp upstream of canonical 3' splice sites and this happens dominantly in cancers were hot spot mutations of SF3B1 are occurring (DeBoever *et al*, 2015).

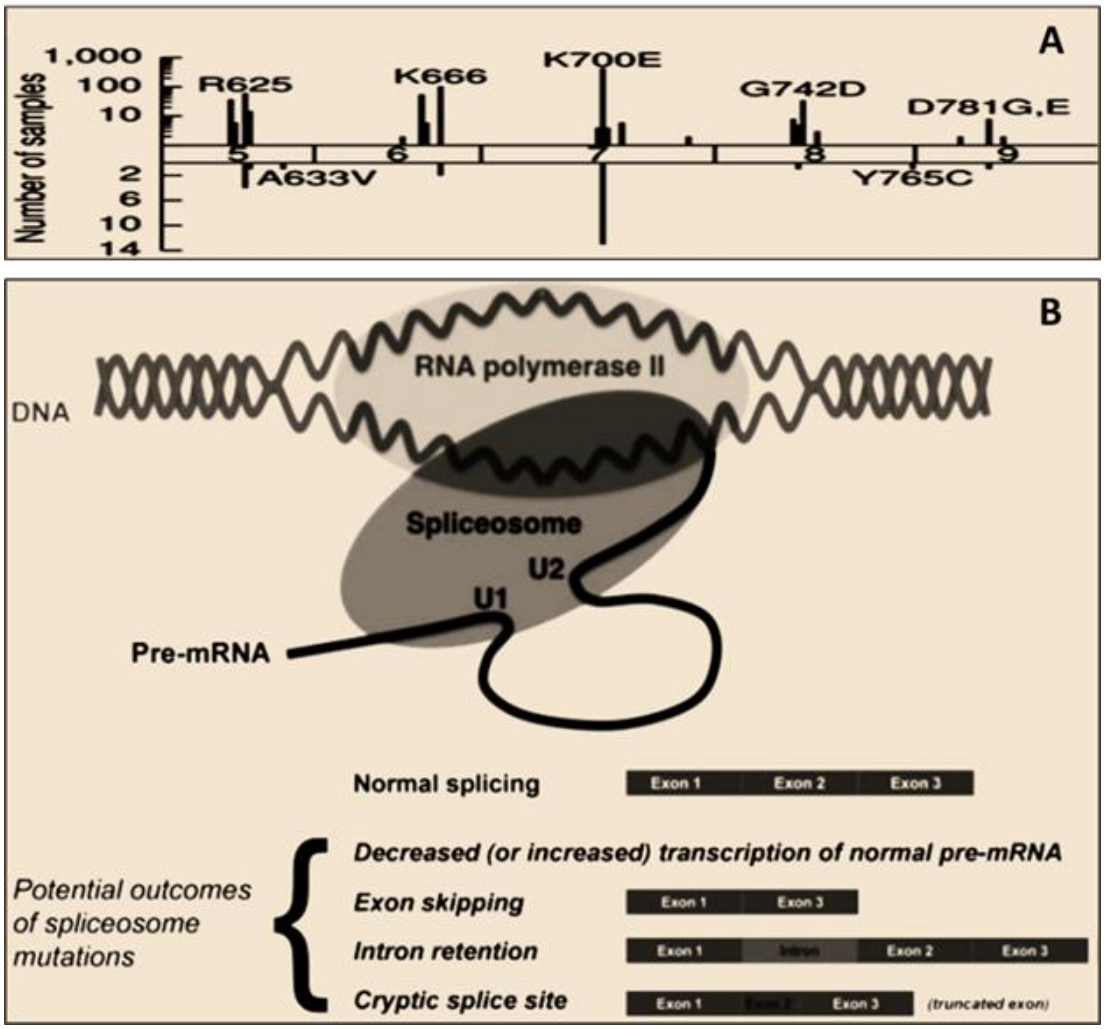


**Figure 1.16 SF3B1 hot spot mutations and potential results of spliceosomes mutations.**

Hot spot mutations that linked to cryptic splice site, upper axis in COSMIC, lower axis shows breast cancer samples used in the study adapted from (DeBoever *et al*, 2015) **A**. Possible consequences of spliceosome mutations, adapted from (Cazzola, Rossi and Malcovati, 2013) **B**.

### 1.3.2 Targeting SF3B1 as a therapeutic approach

Modulating the splicing machinery could be a target in cancer therapy by inhibiting spliceosome assembly at branch points of pre-mRNA. Synthetic inhibitors of splicing with great stability and activity were created, comprising of spliceostatin A, sudemycins,

E7107, and meayamycin. SF3B1 was found to be a target protein for pladienolide suggesting the latter could be a promising anticancer drug (Kotake *et al*, 2007). A phase I clinical trial with E7107 in solid tumour patients in 2014 was discontinued due to loss of vision (that was experienced by 2 patients out of 26), and dose limited toxicities affected others (Hong *et al*, 2014). Pladienolide is a natural macrolide extracted from Streptomyces platensis, it binds to the SF3b complex and inhibits splicing of mRNA. However, it has been reported that SF3B1 R1074 mutated cells confer resistance to pladienolide by impairing its ability to bind and inhibit the SF3B complex (Yokoi *et al*, 2011).

In a study, meayamycin was reported to be potently and specifically inhibiting the growth of lung cancer cells and multi-drug resistant cancer cells in picomolar concentrations *in vitro*, however, it was less effective in inhibiting normal lung cells growth (Brian *et al*, 2009). Since spliceostatin A, meayamycin, and pladienolide are targeting SF3B complex, a recent study has found that these agents cause a massive accumulation of non-spliced pre-mRNAs in the nucleus in human cell lines, and a small fraction are exported to the cytoplasm and degraded by nonsense-mediated mRNA decay independent of exon junction complex facilitation. This implies that these immature transcripts are not detected and removed instantly by surveillance mechanisms of the cell (Carvalho *et al*, 2017). In another study, the treatment of serine/arginine-rich splicing factor2 (srsf2) mutated mouse model representing AML and MDS with spliceosome inhibitor E7107 reduced leukaemia burden, and elongated the survival more selectively in mutated srsf2 leukaemia mice, but not wild type srsf2 leukaemia mice (Lee *et al*, 2016).

SF3B1 mutant breast cancer cells showed selective sensitivity to spliceostatin A, and breast cancer cells with SF3B1 K700E mutation were associated with consistent differential splicing pattern (Maguire *et al*, 2015). Another study showed that inhibition of spliceosome in Myc-dependent tumours, among them breast and B-cells cancers, impairs its growth and metastasis (Hsu *et al*, 2015). Spliceosome inhibitors suggested to be not only binding to and preventing the assembly of spliceosomes complexes, but also interfering with conformational changes in SF3B1(figure 1.17) (Effenberger *et al*, 2016). SF3B1 primary human M-CLL cells showed more sensitivity to sudemycin D1, which is a synthetic analogue to pladienolide B, and went through apoptosis in a dose dependent pattern *in vitro*, in contrast to U-CLL cells (Saez, Walter and Graubert, 2016).

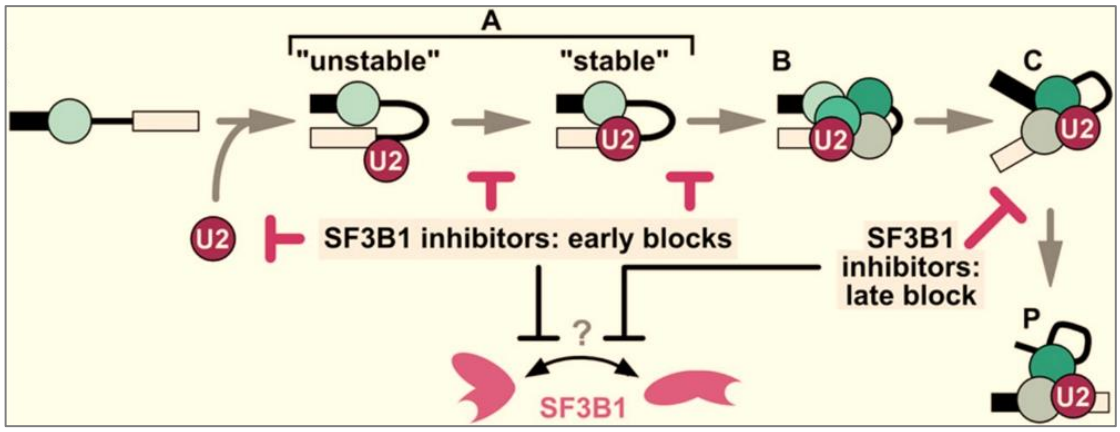


**Figure 1.17 Proposed model of spliceosome inhibitors mechanism.**

SF3B1 inhibitors are interfering with a conformational change in SF3B1 and disturb the spliceosome assembly at several stages. Adapted from (Effenberger *et al*, 2016).

## 1.4 NOTCH1 signalling cascade

Causing a ‘notched' wing phenotype in Drosophila as a result of a partial loss of function was the original discovery of Notch cascade. The canonical Notch signalling is a highly conserved pathway and is essential for cell development, homeostasis, proliferation, differentiation, and fate regulation. Notch receptors are transmembrane proteins expressed on the cell surface membrane, and in different combination in cells, and activated up on ligand binding. Four Notch receptors in mammals are Notch1, Notch2, Notch3, and Notch4 (figure 1.18). Notch receptors have 29 to 36 epidermal growth factor repeats that are essential for ligand binding, followed by three Lin Notch repeats (LNR), a heterodimerization domain (HD), followed by RBPJ-associated molecule domain (RAM), six Ankyrin repeats (ANK), transactivation domain (TAD), and (Pro-Glu-Ser-Thr) sequence (PEST) that regulates intracellular domain of the notch protein (NICD)degradation (Andersson and Lendahl, 2014; Osborne and Minter, 2007).

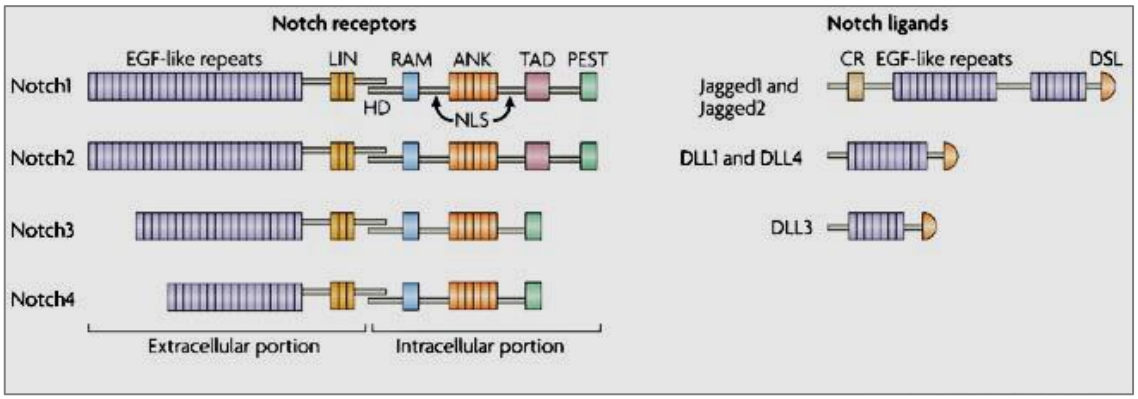


**Figure 1.18 Illustration of mammalian Notch receptors with their domains.**

Non covalent adherent of HD links extracellular and intracellular transmembrane domains, adapted from (Osborne and Minter, 2007).

Five ligands type-I transmembrane proteins with epidermal growth factor EGF-like repeats in their extracellular domain bind to Notch receptors. They are: serrate-like jagged-1 (JAG1), JAG2, delta like ligand1 (DLL1), DLL2 and DLL4. After binding of extracellular domain of Notch receptors which contains EGF-like repeats to jagged or delta ligands, Notch receptors cleaved by a member of a disintegrin and extracellular matrix metalloprotease family (ADAM10), or ADAM17, resulting in generation of a Notch extracellular truncation (NEXT) that is a substrate for γ-secretase complex. The latter cleavage generates NICD, consequently, NICD is released, and translocated to the nucleus. This translocation results in formation of multimeric transcriptional factors complexes with transcription factors CSL (CBF1/Suppressor of Hairless/LAG-1, also known as RBPJ, C-promoter-binding factor CBF-1 in human), and Mastermind-like protein (MAML) in the nucleus. Notch targets are helix–loop–helix factors of the hairy and enhancer of split (Hes) and Hes-related repressor protein (Hey) families. These targets will facilitate Notch signalling, determining cell fate, cell proliferation, cell differentiation or apoptosis through regulating cyclinD1, c-Myc, P27, P21, survivin, and the NF-κB pathway (figure 1.19) (Sethi and Kang, 2011; Yuan *et al*, 2015).

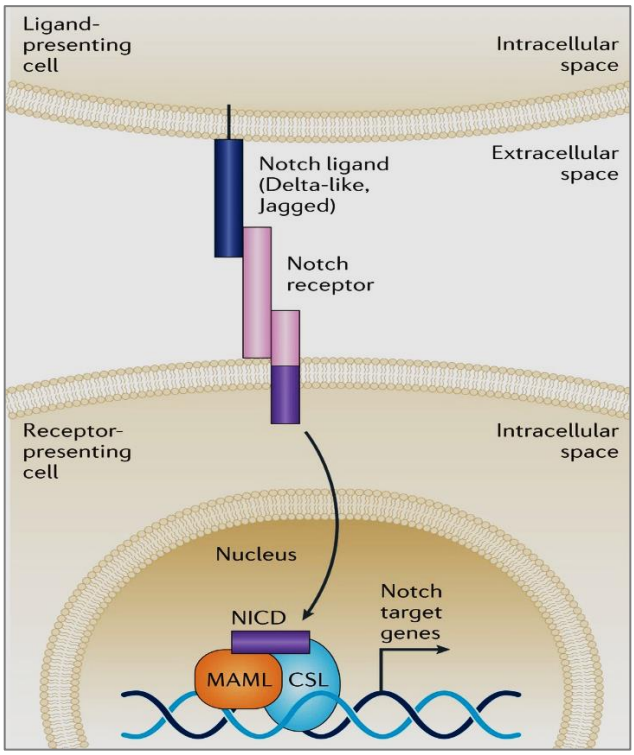


**Figure 1.19 Notch signalling cascade.**

Ligand binding promotes the cleavage of NICD, which translocated to the nucleus to exert its action of cell proliferation, differentiation, or apoptosis, adapted from (Andersson and Lendahl, 2014).

### 1.4.1 NOTCH1 mutations in cancer

Notch signalling is deregulated in many cancers, such as T-cell leukaemia, prostate cancer, breast cancer, lung cancer, and colorectal cancer. Notch signalling has been implicated in cancer progression through activation mutations in the upstream region of the PEST domain that leads to inhibition of PEST function, as a negative regulator of Notch cascade. Notch1 was related to increased metastasis in lung cancers through tumour angiogenesis alterations, by interaction with VEGF-A (Yuan *et al*, 2015).

50% of T- cell acute lymphoblastic leukaemia has activations mutations in Notch1 (Weng *et al*, 2004). Notch inactivation promotes bladder cancer and increases the disease invasiveness. Loss of function mutations of Notch1 and Notch2 have been detected in human bladder tumours (Maraver *et al*, 2015). Notch signalling was found to be upregulated in pancreatic cancer stem cells compartment and to be crucial in their maintenance and function (Abel *et al*, 2014). Overexpression of Notch1 in colon cancer tissue in contrast to normal one has been detected. Furthermore, Notch1 activation in colorectal cancer cell lines promoted epithelia to mesenchymal transition and self-

renewal and differentiation, which is linked to poor prognosis and recurrence in colon cancer patients (Fender *et al*, 2015). In breast cancer, overexpression of Notch1 and Jagged1are associated with poor prognosis. The negative regulator of Notch signalling, Numb, was down regulated in high grade patients. Because all this, it has been suggested that Notch might play a role in initiation of breast cancer (Brennan and Clarke, 2013).

### 1.4.2 Targeting NOTCH1as a therapeutic approach

Gamma-secretase inhibitors (GSIs) are small molecules, monoclonal antibodies, or peptides fragments that have been suggested to inhibit Notch signalling (figure 1.20). As active Notch half-life is only short, long time inhibition might not be a possible option, but intermittent inhibition would be a better technique as a therapeutic approach (Rizzo *et al*, 2008). Although Notch signalling promotes cancer when overexpressed in some cell types, it has different effects in squamous epithelia, skin and vasculature as a tumour suppressor. Therefore, different methodologies for Notch inhibition are needed.

MK-0752 inhibitor to Notch cleavage; was made to inhibit amyloid-β cleavage for Alzheimer patients. However, using GSI in Alzheimer patients caused skin cancers with poor cognitive performance rates among patients. A clinical trial in 2006 in T-ALL patients showed reduction in mediastinal mass after 28 days with MK-0752. However, the cancer progressed after that (Andersson and Lendahl, 2014). DLL4 monoclonal antibody demcizumab was tested in clinical trials in non-small-cell lung cancer, ovarian, fallopian, and peritoneal cancer, pancreatic cancer and colorectal cancer, but they resulted in liver endothelial cells changes and cancers in vasculature.

Phase I clinical trial of MK-0752 for solid cancer patients, showed promising effects of stable disease over a year in 10 patients with advanced glioma, and complete response in 1 anaplastic astrocytoma patient, but it has no effect on breast cancer and colon cancer patients (Krop *et al*, 2012). A combination of fludarabine and PF-03084014 overcame NF-κB activation mediated by fludarabine and downregulated invasiveness and angiogenesis of Notch mutated CLL primary cells (Lopez-Guerra *et al*, 2015). MK-0752 in combination with chemotherapy docetaxel suggested to be having a combining effect in reducing breast cancer stem cells in breast cancer patients in a phase IB clinical trial and in preclinical tumour graft samples (Schott *et al*, 2013).

Gamma secretase inhibitors have been shown to induce apoptosis in CLL cells by increasing ER stress and inhibiting Notch signalling (Rosati *et al*, 2013). GSI-1 was shown to induce P53-independent apoptosis in CLL cells by blocking the proteasome and upregulating NOXA (Hallaert *et al*, 2007). Recently, using DAPT, which is a GSI, to inhibit Notch signalling in mucosal mast cells (MMCs) has been suggested to be possibly a useful approach to reduce food-allergy induced by MMCs hyperplasia (Honjo *et al*, 2017).

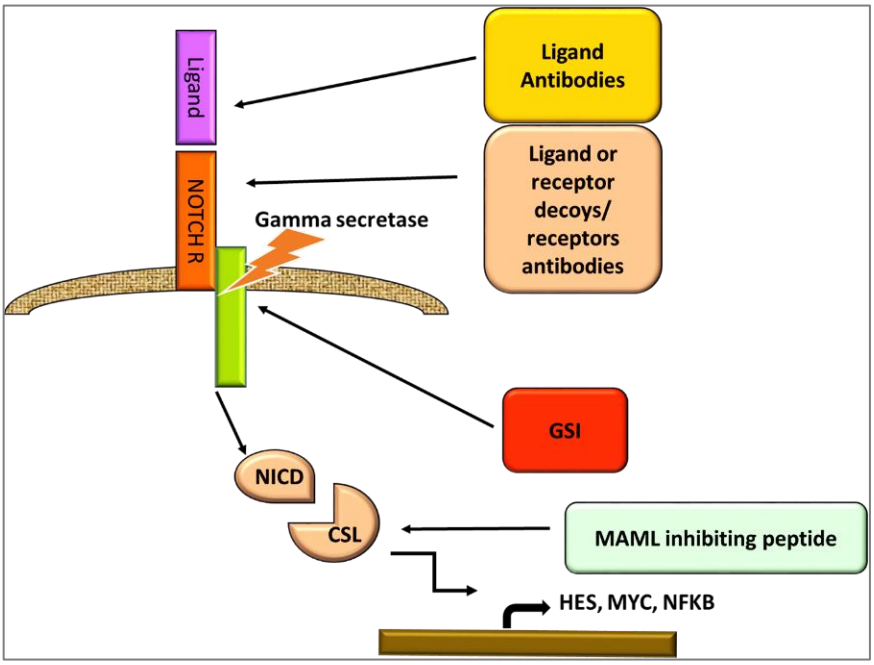


**Figure 1.20 Targeting Notch signalling.**

GSI, monoclonal antibodies, peptides and proteins fragments, or decoys (Honjo *et al*, 2017).

## 1.5 MYD88 and TLR signalling

TLRs are a family of transmembrane receptors recognizing patterns of microbes and play an important role in infection host defence responses, tissue repair, and tissue inflammation responses to injury (Rakoff-Nahoum and Medzhitov, 2009). Gram negative bacteria recognition receptor are TLR4, TLR3 activated by double stranded RNA, TLR7, and TLR8 by single stranded. Bacteria flagellin activates TLR5 and bacterial lipoproteins activate TLR2, TLR6, and TLR1. TLR11 is activated by a profilin-like molecule. TLR9 is activated by unmethylated CpG that present in DNA (figure 1.21). TLRs stimulation

initiate activate NFκβ, MAPK, Jun N-terminal kinases JNK, p38 and ERK kinases, PI3K, and interferon regulatory factors (IRF3, 5, 7) pathways. All TLRs and IL-1 receptor family members pass the signal over to MyD88, except for TLR3.

Myd88 is made up of two functional domains: the N-terminal death domain (DD) and a C-terminal Toll/IL-1 receptor homology (TIR) domain (figure 1.21). Myd88 is a cytosolic adaptor molecule in Toll-like receptor TLR signalling. Following TLR or IL-R activation, MYD88 is recruited as a homodimer that complexes with IL-1 receptor-associated kinase 4 (IRAK4). It then activates IRAK1 and IRAK2. IRAK1 activates TNF6, leading to phosphorylation of IκBα and NF-κB pathway activation (Xu *et al*, 2013).

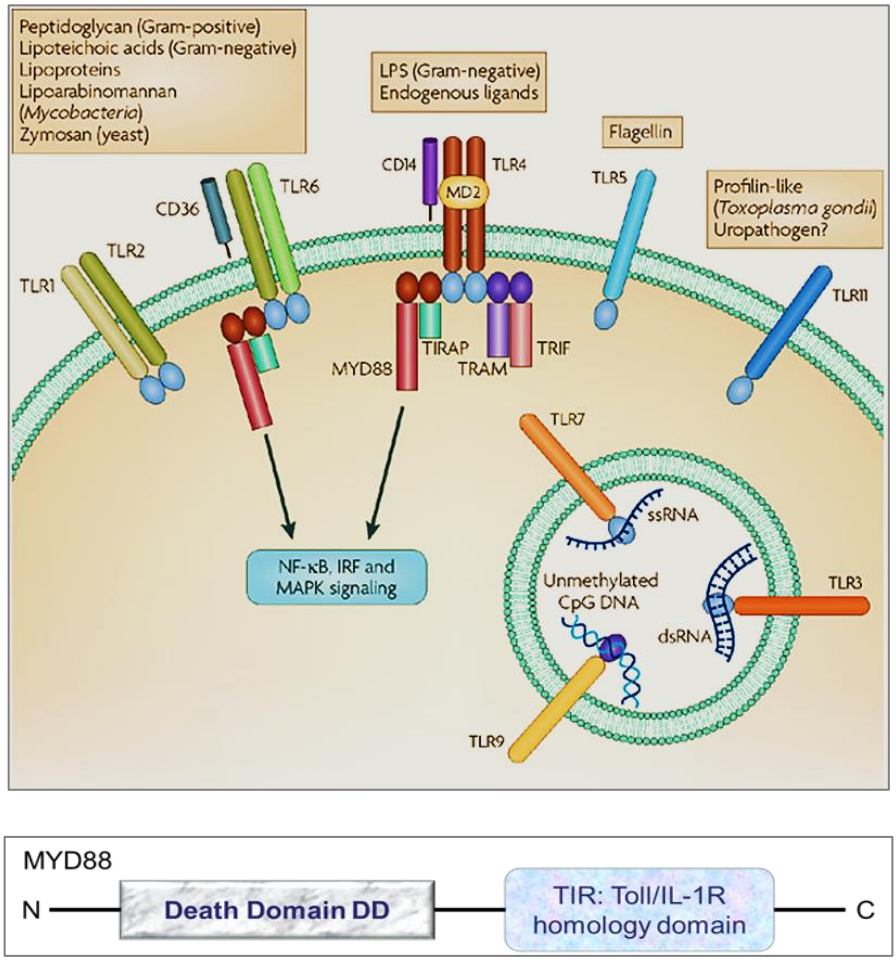


**Figure 1.21 TLR receptor signalling.**

Function of TLR in recognising microbial patterns, and regulating innate and adaptive immune responses. Adapted from: (Rakoff-Nahoum and Medzhitov, 2009).TIRAP also known as Mal (TIR domain-containing adaptor protein), TRAM (TRIF-related adaptor molecule), TRIF (TIR domain-containing adaptor inducing IFN-β), TIR (Toll/Interleukin-1 receptor homology). Lower diagram illustrates Myd88 main domains.

### 1.5.1 MYD88 mutations in cancer

Myd88 was found to be essential in diethyl-nitrosamine induced hepatocellular cancers, and it is a positive regulator to skin and connective tissues chemically-induced cancers (Rakoff-Nahoum and Medzhitov, 2009). Myd88 p.L265P T to C transversion in exon 5 is a gain of function mutation. It was found in approximately 93-97% of Waldenström macroglobulinemia (WM) patients using whole-genome and/or Sanger sequencing (figure 1.22) (Xu *et al*, 2013; Treon, Xu and Hunter, 2015).

Cancer growth is mediated by MYD88 mutations through IRAK and BTK to activate NF-κB signalling (Treon, Xu and Hunter, 2015; Poulain *et al*, 2013).

WM is an IgM-secreting lymphoplasmacytic lymphoma were Myd88 alterations are very common, mainly p.L265P, amongst patients with a positive family history of WM. p.L265P mutations were present in 100% of the patients. *In vitro*, an inhibitor of dimerization of Myd88 decreased IκBα and NF-κB (P65) phosphorylation in WM cell lines with L265P mutation (Treon *et al*, 2012). Myd88 p.L265P is a crucial determinant of survival in WM patients (Treon *et al*, 2014). Myd88 p.L265P mutation was reported in 29% of activated B-cell–like diffuse B-cell lymphomas (ABC-DLBCL), though it is rare in other DLBCL types (Ngo *et al*, 2011), suggesting that Myd88-IRAK signalling is important in ABC-DLBCL cancers survival and progression. Hot spot p.L265P promotes cancer survival by the assembly of signalling complex of IRAK1 and IRAK4, leading to IRAK4 kinase activation, IRAK1 phosphorylation, and NF-κB activation (Rhyasen and Starczynowski, 2015). In WM patients, Myd88 homozygous mutations p.L265P are associated with CXCR4 activation mutations and respond better to Ibrutinib BTK inhibitor treatment (Treon *et al*, 2016).

### 1.5.2 Targeting MYD88 as a therapeutic approach

Small-molecule inhibitors of IRAK-family kinases have already been generated (figure 1.22) (Powers *et al*, 2006; Wang *et al*, 2006; Buckley *et al*, 2008). A natural product, ginsenoside Rb1 (its metabolite compound k), has been discovered as IRAK1, NF-κB, IKK-β, JNK, ERK and p-38 kinases inhibitor in inflammatory diseases (Joh *et al*, 2011). IRAK4 inhibitor ND-2158 did not reduce wild type Myd88 DLBCL cell lines viability,

but reduced viability of Myd88 mutated ABC-DLBCL cell line, suggesting its efficacy against activated Myd88 signalling. Furthermore, a combination of SYK, PI3Kdelta, or BTK signalling inhibitors with ND-2158 promoted its efficacy in ABC-DLBCL cells, which implies that BCR and Myd88 signalling co-inhibition will reduce the proliferation of ABC-DLBCL cancer (Chaudhary *et al*, 2013). Inhibiting IRAK1 induced apoptosis and blocked cell cycle in MDS cells *in vitro*. In MDS-derived patient cells, combination of IRAK 1 inhibitor with Bcl2 inhibitor ABT-263 results in joint cytotoxicity (Rhyasen *et al*, 2013). IRAK1 and IRAK4 RNA gene expression levels appeared lower in CLL patients than normal B-cells, but Myd88 expression levels were higher in CLL samples, and there were no differences in BTK levels between wild type and p.L265P mutated CLL cases. IRAK inhibitors showed equal activity among both wild type and mutant CLL cells, and ibrutinib showed less effect in p.L265p mutant CLL cells *in vitro* (Tesar *et al*, 2013). IRAK4 inhibitors could be used in treatment for B-cell lymphoma and inflammatory disease patients in combination with BCR inhibitors or Bcl2 inhibitors (Kelly *et al*, 2015). In murine mammary carcinoma, inhibiting Myd88 dependent signalling not only significantly reduces cancer growth, but also promotes MMP9 and IL-1β overexpression, and leads to cancer progression (Higgins *et al*, 2016). In hepatocellular carcinoma cells IRAK1was reported to be crucial for protection from apoptosis and for cancer proliferation, and in that context, inhibiting IRAK1 could be a potential target for treatment (Li *et al*, 2016)

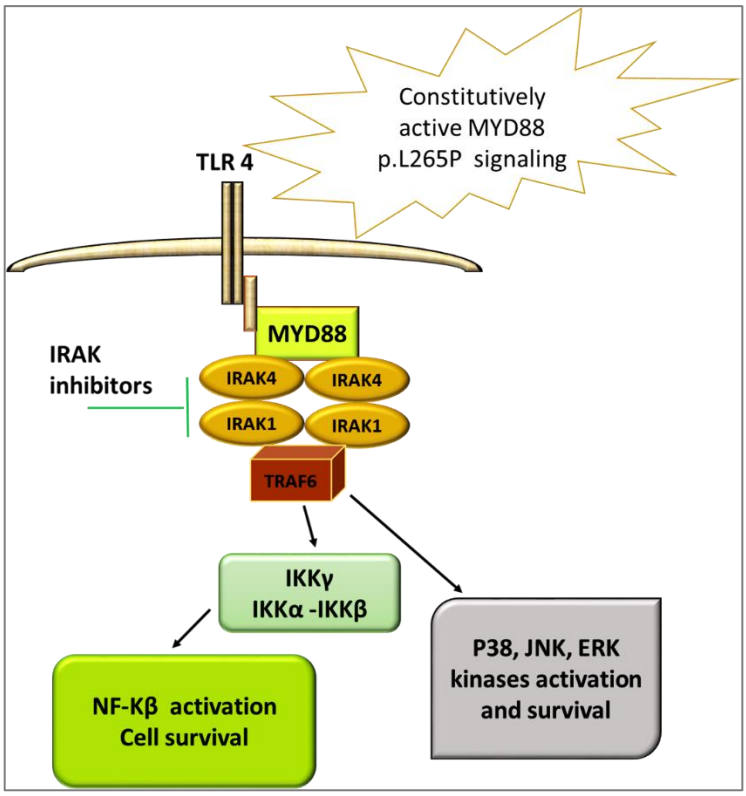


**Figure 1.22 Myd88 gain of function mutations and IRAK1/4 inhibition.**

(Li et al, 2016)

## 1.6 The need for new therapeutic strategies: Stratification and personalized medicine

The National Cancer Institute NCI dictionary for cancer terms, describes personalized medicine as 'a form of medicine that uses information about a person's genes, proteins, and environment to prevent, diagnose, and treat disease' (*https://www.cancer.gov/publications/dictionaries/cancer-terms*). It can also be named 'precision medicine', 'genomic medicine', 'stratified medicine', or 'sequential medicine'. For development of personalized medicine different professionals need to be involved, including molecular biologists, pharmacologists, clinicians, and epidemiologists (Montserrat, Bauman and Delgado, 2016).

The idea of personalized CLL treatment is needed in the new era of kinase selective inhibitors development and advances in gene mutations detection, though the cost-effectiveness of this approach has yet to be determined. To improve the efficacy of CLL treatment and to minimise using same treatment for such a heterogeneous disease, patient classification and stratification according to their mutational status and drug responses is

needed. Using *in vitro* techniques mimicking tumour microenvironment to elucidate the response of patient primary malignant cells to selected inhibitors and apply this *in vivo* to the same patients based on his age, gender, co-existing conditions, genetic aberrations, epigenetic information, and prognostic markers would be a novel future technique to consider for cancer patients in general, with advanced treatment and diagnostic approaches nowadays (figure 1.23).

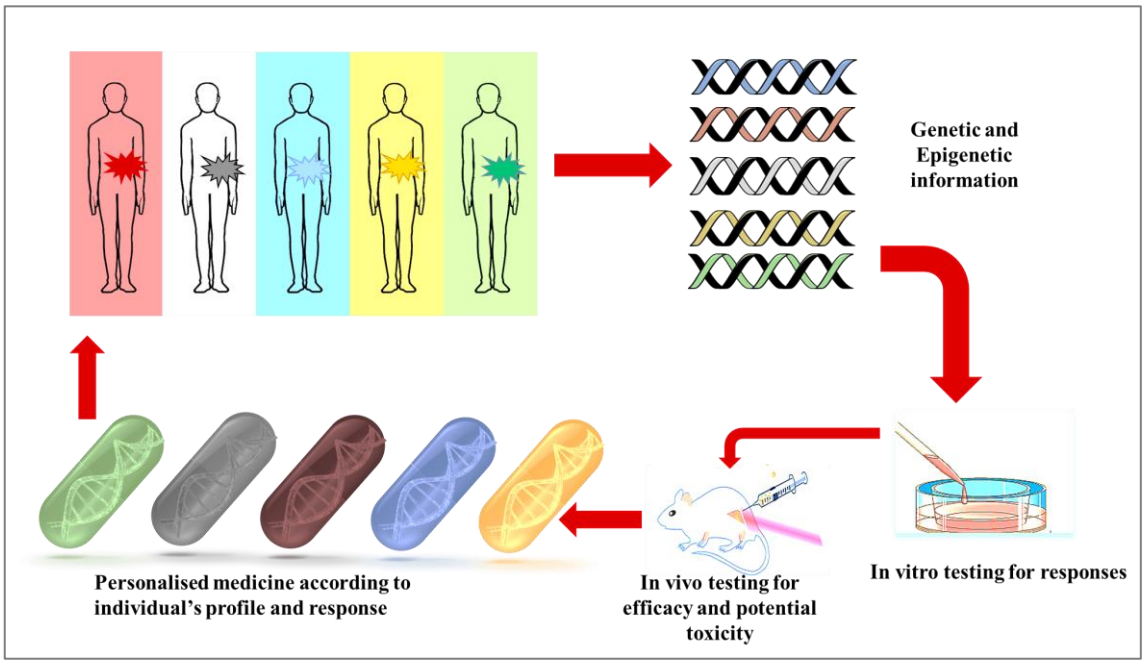


**Figure 1.23 Personalized stratified medicine approach.**

A study using PBMCs isolated from CLL patients, found out that cells that did not respond *in vitro* to combinational therapy have no response *in vivo*, which has given an indication of expected response and sensitivity to anti-cancer agents (Rogalińska *et al*, 2015; Rogalińska *et al*, 2017). Another comprehensive index has been developed in CLL as personalised treatment approach (Pflug *et al*, 2014). However, there are still barriers to personalized therapy. For instance, pharmaceutical companies who prefer to profit from one drug big sale rather than making small profits from different therapeutic agents, the long time needed for development of new therapeutic agents, and for efficacy and safety testing, the physician preference of using old standard therapy approaches, the subset of cancer patients who have low response to therapy or are resistant, and long months of ineffective treatments (Rogalińska and Kiliańska, 2015). Furthermore, it is of

importance to have *in vitro* assays that mimic cancer microenvironment, and it is vital to determine the least toxic combinations of these drugs (Dyer *et al*, 2013).

One of the limiting factors is the heterogeneity in one cancer, which means the single sample taken from the patient is a clone that does not represent all cells. Therefore, there might be other active molecular pathways that will confer resistance to that targeted therapy, and in addition, targeted treatment might enhance appearance of resistant clones to that treatment, and disease progression. Also, targeting molecular pathways might affect normal cells and may be associated with toxicities. On the other hand, responses of BRAFV600E mutated melanoma to vemurafenib, and HER2 positive breast cancer to trastuzumab provides successful examples of driver gene targeting, but the rise of resistant clones has limited the clinical success (Tannock and Hickman, 2016). In short, a framework should be established for precision medicine strategy that enable patients to receive treatment designed for them and achieve better responses.

## 1.7 Aims and objectives

Treatment of CLL is based on chemotherapy and monoclonal antibodies combination. Recently, specific inhibitors such as ibrutinib, and venetoclax have been added to the therapeutic tools. In addition, combination therapy provides a better way to target more than one vital signalling in cancer cells. Thus, stratification of CLL patients has become important.

In this project my aims were:

- To assess the sensitivity of five different leukaemia cell lines to 22 specific inhibitors, and to determine their IC50. Also, to assess the effect of same inhibitors on primary CLL cells viability alone or in combination. The final goal is to propose novel drug sensitivities that could inform future clinical trials in B-cell malignancies.
- To look for potential stratification factors in CLL:
    - To determine the frequency of BRAF exon 15 mutated CLL patients in our cohort and to study their sensitivity to MAPK inhibitors, alone or in combination treatments.
    - To determine the frequency of NOTCH1 exon 34 mutations, SF3B1 exon 14-15 mutations, and MYD88 exon 5 mutations in our cohort and study their sensitivity to different specific inhibitors.

# Chapter 2 Materials and Methods

## 2.1 Cell culture

Different human malignant B cell lines were used in this project. Cell lines were provided kindly by Professor Martin Dyer's Lab. Details can be seen in table 2.1.

| Cell Line's Name | Origin/Species | Mutations | Culture Medium |
|---|---|---|---|
| **JVM-3 (B-PLL)** | Chronic B-Cell Leukaemia established from the peripheral blood of 73 years old man with B-Prolymphocytic Leukaemia (PLL) at diagnosis; cell line was established by EBV-transformation during treatment with phorbol ester TPA; cells express mRNA of the proto-oncogenes BCL2 and BCL3. (DSMZ-ACC 18) | 766 mutations (importantly, BRAF K601N c.1803A>T Substitution-missense**).** were reported in COSMIC - Cell Lines Project (*https://cansar.icr.ac.uk/cansar/cell-lines/JVM-3/mutations/)* | 90% RPMI-1640 (Gibco) supplemented with 10% FBS, 2mM L-glutamine, 50U/ml penicillin and 50µg/ml streptomycin. |
| **MEC-1 (B-CLL)** | Chronic B-cell Leukaemia established in 1993 from the peripheral blood of a 61-year-old Caucasian man with chronic B cell leukaemia (B-CLL in pro-lymphocytoid transformation to B-PLL); serial sister cell line of MEC-2 (DSMZ-ACC 500) | $TP53^{mut/del}$ ,17p deletion (Pozzo *et al*, 2013c) | 90% Iscove's MDM supplemented with 10% FBS, 2mM L-glutamine, 50U/ml penicillin and 50µg/ml streptomycin. |

| | | | |
|---|---|---|---|
| **ESKOL (B-HCL)** | A B-lymphoblastoid cell line established from peripheral blood of HCL 69-year-old white male composed of differentiated cells resembling hairy-cell leukaemia (Harvey *et al*, 1991). | No mutations reported. | 80% RPMI-1640 (Gibco) supplemented with 20% FBS, 2mM L-glutamine, 50U/ml penicillin and 50µg/ml streptomycin. |
| **HC-1 (B-HCL)** | Spontaneously immortalized peripheral blood leukocytes from a 56-year-old white man with hairy cell leukaemia (HCL) at diagnosis; cells were described to grow in soft agar, to be tumourigenic in irradiated nude mice and to be negative for the HCL-associated mutation BRAF V600E (DSMZ-ACC 301) | 457 mutations were reported in COSMIC-Cell Lines Project (*https://cansar.icr.ac.uk/cansar/cell-lines/HC-1/)* | 80% RPMI-1640 (Gibco) supplemented with 20% FBS, 2mM L-glutamine, 50U/ml penicillin and 50µg/ml streptomycin. |
| **SIG-M5 (AML)** | Established in 1995 from the bone marrow of a 63-year-old man with acute myeloid leukaemia of monocytic origin (AML FAB M5a) at diagnosis. (DSMZ-468) | Vitally, BRAF (V600E) mutation. 505 mutations reported (*https://cansar.icr.ac.uk/cansar/cell-lines/SIG-M5/mutations/)* | 80% Iscove's MDM supplemented with 20% FBS, 2mM L-glutamine, 50U/ml penicillin and 50µg/ml streptomycin. |

**Table 2.1 Cell lines origins, known mutations, and culture medium requirements.**

### 2.1.1 Cell Lines Culture and maintenance

All cell lines were cultured in flasks of different sizes (Corning® 25cm2, 75cm2, and 175cm2), to allow cells to grow and expand consistently with the recommended maximum cell density (MEC-1=1X$10^6$ cells/ml, JVM-3=1-1.5x$10^6$ cells/ml, ESKOL=1-1.5X$10^6$ cells/ml, HC-1=1-1.5X$10^6$ cells/ml, SIG-M5= 1X$10^6$ cells/ml).To maintain cells viability, medium was regularly added to the growing suspension cells. If cell number was less than needed, cells were centrifuged, and pellets resuspended in the required volume.

Cell lines were passaged when they reached confluency, roughly every 2-3days. Cell lines were maintained at 37°C and 5% CO2 incubator (Thermo-Electron Corporation).

### 2.1.2 Cryopreservation of cell lines

Cell lines were counted using counting slides, Trypan Blue Sigma® and TC20™ automated Cell Counter BIO-RAD®. 10µl of cell suspension and 10µl of trypan Blue were mixed and immediately pipetted into counting slides. Total viable cell count and % were calculated by inserting the slides into Bio-Rad automated cell counter. After counting, cells were centrifuged at 250 x g for 5 minutes and media were discarded. Cell pellets were resuspended in the recommended cell density (2-4X$10^7$cells/ml) in freezing media. Freezing media was prepared with 90%FBS and 10% DMSO (Dimethyl Sulphoxide-Sigma®). Cells suspensions were aliquoted 1ml per cryovial (Cryovials-Corning®) of required cell density and placed in a (NALGENE®) freezing container to achieve a -1ºC /minute of cooling in -80 ºC overnight for cell suspension. Next day, cells were stored in a liquid nitrogen tank in labelled boxes for future usage. When cells needed for culture, frozen cells were thawed under room temperature, then cells were slowly and gently added to pre-warmed 9ml of culture media of the corresponding cell line, then centrifuged and the cells pellet were resuspended in desired density in small flasks (25cm2).

## 2.2 Peripheral Blood Mononuclear Cells (PBMCs) Isolation

Peripheral blood mononuclear cells (PBMCs) were isolated from whole blood using density separation. 20 to 30ml of whole blood was taken from CLL patients into heparinised test- tubes by qualified staff at the Leicester Royal Infirmary. Sterile PBS solution (HBSS) and Histopaque 1077 (Sigma Aldrich) density medium were allowed to equilibrate to room temperature prior to use. Heparinised blood was diluted 1:1 v/v with sterile PBS. 25 to 30 ml of diluted blood was carefully layered onto 15 ml of Histopaque density medium in 50ml falcon tubes. The samples were separated by centrifugation (5810 R centrifuge Eppendorf) at 400 x g for 30 min at room temperature without any brakes. The layer of PBMCs in the interphase between the serum and Histopaque were carefully aspirated using a Pasteur pipette. The cells were washed in 30ml of RPMI 1640 media, by centrifuging at 250 x g for 10 min at room temperature. The supernatant was

discarded and the cells were resuspended in RPMI-1640 supplemented with 10% FBS, 2mM L-glutamine, 50U/ml penicillin and 50µg/ml streptomycin. Concentration of cells was determined using counting slides, Trypan Blue Sigma® and TC20™ automated Cell Counter BIO-RAD® as mentioned above.

### 2.2.1 CD19+ selection using magnetic beads

Isolated PBMC's of normal volunteers were resuspended in 5mL MACS buffer (Miltenyi Biotec, USA), composed of PBS supplemented with 0.5% BSA) and 2µM EDTA (Sigma, USA), and then washed by centrifugation for 10 min, 4°C at 450g. 80µL of MACS buffer and 20µL of CD19 microbeads (Miltenyi Biotec, USA) were added for every $10^7$ cells and incubated on ice for 15 min. Following incubation, 10mL of MACS buffer was added to the mixture and the cells were centrifuged at 450 x g for 7 min at 4°C. Excess fluid was removed, and 0.5mL of MACS buffer was added to enable the re-suspension of the cells by gentle tapping of the tube. The MACS column (Miltenyi Biotec, USA) was washed with 0.5mL of MACS buffer and the cell suspension was carefully pushed through followed by three washes using each time 0.5mL of MAC buffer. Cells were suspended in 1mL of RPMI-1640. The purity of the CD19+ve cells was ascertained by staining with PE-Cy5-conjugated mouse anti-human CD19 mAb (BD biosciences, USA) and analysed by flow cytometry with a BD FACS Canto II using BD DIVA FAC Suite software (Becton Dickinson Immunocytometry Systems, USA). This was found to be 95% or greater for each selection.

### 2.2.2 Cryopreservation of primary cells

CLL primary cells were counted, centrifuged at 250 x g for 5 minutes, then resuspended in freezing media 90%DMSO and 10%FBS. Cells were resuspended in freezing media with cell's density between 1-4X$10^7$cells/ml/cryovial. Cells were stored and thawed as mentioned in cryopreservation of cell lines 2.1.2.

### 2.2.3 Co-culture System

Primary CLL cells were maintained in vitro by co-culturing on a feeder layer of irradiated non- transfected mouse fibroblast L-cells (NT-L) and L-cells stably transfected with

human CD40 ligand (CD154L). Both cell lines were maintained in RPMI-1640 supplemented with 10% FBS, 2mM L-glutamine, 50U/ml penicillin and 50µg/ml streptomycin at 37°C in a humidified atmosphere containing 5% CO2. The cells were passaged every 3 to 4 days, when the cell density approached confluency. To passage a confluent cell culture T75 flask of cells, the old medium was aspirated and the cells carefully washed once with 5ml of sterile PBS to remove any residual media. The adherent cells were detached by adding 2ml of 0.25% Trypsin-EDTA (GIBCO®), and incubated at 37°C for 3 – 5 min until the cells started to detach. The cell suspension was collected with 8ml of media supplemented with 10% FCS into sterile falcon tubes and centrifuged at 200 x g for 3 min. The cells were then re-cultured at a 1 to 10 dilution.

Prior to co-culture, the fibroblasts were irradiated to prevent proliferation whilst in co-culture. The NT-L and CD154L(CD40-L) cells were grown to near confluency, detached using trypsin and harvested by centrifugation in a sterile falcon tube after washing in complete media. The cell suspension was irradiated to 35Gy using a Pantak industrial X-ray machine (Pantak, Connecticut, USA; 250 kV constant potential, HLV 1.5 mm Cu) delivering acute X-rays at 2.85Gy/min. The cell concentration was determined using the Bio-Rad cell counter and seeded onto six wells plates at a density of 5 x $10^5$ cells/well in 2ml of complete media. The irradiated fibroblasts allowed to adhere to the cell culture plates overnight. The following day, the media was removed and cells suspended containing 3-4x$10^6$ cells in 2ml complete media supplemented with 10ng/ml IL4. CLL cells were harvested by detaching them from the feeder layer by gentle pipetting to minimise contamination.

### 2.2.4 Soluble Ligands Stimulation System (sCD154 and IL4)

The recombinant human CD154 ligand (CD40L purchased from R&D systems), was expressed as a homo-trimer (trimeric protein) with a six-His tag. Crosslinking using an anti-Histidine monoclonal antibody, also purchased from (R&D systems), served as the ‘enhancer’, allowing receptor clustering and much stronger stimulation to B-cells. 2-12ng/ml of CD40 ligand was added in the presence of 1µg/ml of cross- linking antibody. CLL cells were cultured in complete media supplemented with 10ng/ml CD154 mixed with a 0.5µg/ml anti-histidine monoclonal antibody ‘enhancer ‘and 10ng/ml IL-4. CLL cells were cultured at a density of 2-4 x $10^6$ cells/ml in 2ml/well of a six wells plate for different times.

## 2.3 Western Blotting

### 2.3.1 Whole lysate extraction

Whole cell lysate was extracted from cell lines, or primary cells (1-3x$10^6$cells/ml) using lysis buffer Cell Signalling Technology® (CST, no.9803). Cell lysis buffer (10x) was prepared fresh as following:

| |
|---|
| **50µl phosphatase inhibitor cocktail 2(Sigma®)** |
| **50µl AEBSF(Calbiochem)** |
| **500µl 10x lysis buffer (Cell Signalling Technology®)** |
| **up to 5000µl dd$H_2O$** |

**Table 2.2 Lysis Buffer preparation.**

Cell pellets were collected by centrifugation at 200 x g for 5 minutes, then were washed from media by adding 1ml 1xPBS and centrifuged again. Fresh cells pellets were put on ice and resuspended in 5x lysis buffer of cell pellet's volume (if cell pellet volume was 10µl then 50µl lysis buffer is added), phosphatase inhibitor cocktail, and AEBSF, all added fresh at ice cold 4°C. Cell suspensions were homogenised by passing it through 25G gauge needle 10-15 times, and then, were incubated on ice for 20-30 minutes. Cell-lysis buffer suspension was centrifuged for 20 minutes at maximum speed centrifuge (16,000 x g). The supernatant (cell lysate) was carefully collected into a new labelled tube, and cell pellet were discarded. At this point protein samples can be stored at -20°C. Bradford reagent (Thermo-Scientific) was used to determine total protein concentration of each sample. A Spectrophotometer, and Bovine Serum Albumin (BSA) were used at concentrations from 0-20mg/ml. 1ml of Bradford reagent mixed with each 1µl protein sample. The absorbance was read at 595nm and standard curve was created to calculate protein concentration in each sample.

### 2.3.2 SDS-Gel Electrophoresis

Typically, 30-50µg of total protein from each sample were mixed with 1/4$^{th}$ the volume of 4x SDS loading buffer (see table 2.3), and was denatured by boiling the samples at 95°C for 5 mins. Proteins were separated by sodium dodecyl sulphate polyacrylamide gel electrophoresis (SDS-PAGE) on a 4 – 12% SDS-gel SDS (table 2.4), and 1x running

buffer was used. Samples were run alongside Precision Plus Protein™ standards (BioRad) at 100V in a BioRad® electrophoresis machine. Gels were transferred to Amersham® nitrocellulose membrane using 1X transfer buffer with 20% methanol using a wet transfer system at 350 mA (milliampere) for 1hr. The membranes were blocked with 5% BSA in 1xPBS-Tween 0.1% on a shaker, which ensured gentle even rocking. Then, washed with 1xPBS-Tween 0.1% for 10 mins three times at room temperature. Then, membranes were incubated with the primary antibody solutions overnight at 4°C on a shaker. Primary antibody solutions were made in blocking solutions at the dilutions indicated in table 2.5. Membranes were then washed three times in 1xPBS-Tween 0.1% for 10 mins and incubated with the secondary antibody solution for 1hr at room temperature on a shaker and covered from light. Membranes were washed as mentioned previously and protected from light. A final wash with 1xPBS for 15 minutes before proteins were detected using the LiCOR-Odyssey infrared imaging system, LiCOR IRDye™ conjugated secondary antibodies were used.

4X SDS Protein Sample Buffer:

| **Final concentration:** |
|---|
| **40% Glycerol** |
| **240 mM Tris-HCl pH 6.8** |
| **8% SDS** |
| **0.04% Bromophenol blue** |
| **20% β-Mercatoethanol** |
| **dd$H_2O$** |

**Table 2.3 4x sample buffer preparation**

| **Resolving SDS-Gel** | **4% (8ml)** | **6%(8ml)** | **10%(8ml)** | **12%(8ml)** |
|---|---|---|---|---|
| **$H_2O$** | 5ml | 4.6ml | 3.8 | 3.4ml |
| **1.5 M TRIS-HCl pH 8.8** | 2ml | 2ml | 2ml | 2ml |
| **40% Acrylamide** | 0.8ml | 1.2ml | 2ml | 2.4ml |
| **10% SDS** | 80µl | 80µl | 80µl | 80µl |
| **10%APS** | 80µl | 80µl | 80µl | 80µl |
| **TEMED** | 8µl | 8µl | 8µl | 8µl |

| Stacking Gel | 4% (5ml) | 6% (5ml) |
|---|---|---|
| **$H_2O$** | 3.1ml | 2.9ml |
| **0.5 M TRIS-HCl pH 6.8** | 1.25ml | 1.25ml |
| **40% Acrylamide** | 0.5ml | 0.75ml |
| **10% SDS** | 50µl | 50µl |
| **10%APS** | 50µl | 50µl |
| **TEMED** | 5µl | 5µl |

**Table 2.4 SDS-resolving and stacking gel preparation.**

### 2.3.3 Antibodies used

| Antibody , Source | Specificity /Sensitivity | Dilution | Supplier |
|---|---|---|---|
| **P-ERK (Rabbit)** | Phospho-p44/42 MAPK (Erk1/2) (Thr202/Tyr204) The antibody does not cross-react with the corresponding phosphorylated residues of either JNK/SAPK or p38 MAP Kinase, and does not cross-react with non-phosphorylated Erk1/2. | 1:1000 | CELL SIGNALLING TECHNOLOGY® #9101 |
| **P-MEK (Rabbit)** | Phospho-MEK1/2 Antibody detects endogenous levels of MEK1/2 only when activated by phosphorylation at Ser217/221. This antibody does not cross-react with related kinases including activated SEK (MKK4), MKK3 or MKK6. | 1:1000 | CELL SIGNALLING TECHNOLOGY® #9121 |
| **P-BRAF (Rabbit)** | Phospho-B-Raf (Ser445) Antibody detects endogenous levels of B-Raf when phosphorylated at serine 445. | 1:1000 | CELL SIGNALLING TECHNOLOGY® #2696 |
| **P-AKT (Rabbit)** | Rabbit mAb, detects endogenous levels of Akt only when phosphorylated at Ser473. | 1:1000 | CELL SIGNALLING TECHNOLOGY® #4060 |

| | | | |
|---|---|---|---|
| **NFKB-P65 (Rabbit)** | Detects nuclear factor kappa-Beta P65. | 1:1000 | Santa Cruz Biotechnology® C-20 |
| **BCL-XL (Rabbit)** | Epitope corresponds to amino acids 126-188 mapping at the C-terminus of Bcl-$x_{L.}$ | 1:1000 | Santa Cruz Biotechnology® sc-7195 |
| **MCL-1 (Rabbit)** | Epitope corresponding to amino acids 1-260 mapping at the N-terminus of Mcl-1 of human origin. | 1:1000 | Santa Cruz Biotechnology® SC-20679 |
| **PARP (Rabbit)** | Detects endogenous levels of full length PARP1 (116 kDa), as well as the large fragment (89 kDa) of PARP1 resulting from caspase cleavage. | 1:1000 | CELL SIGNALLING TECHNOLOGY® #9542 |
| **B-Actin (Rabbit)** | Detects Beta-Actin | 1:10,000 | Abcam #Ab8227 |

**Table 2.5 Primary antibodies used.**

## 2.4 MTS Viability assay for cell lines and primary cells.

The Cell-Titer96®$AQ_{ueous}$Promega® One Solution Cell Proliferation Assay is a colorimetric method for determining the number of viable cells in proliferation, cytotoxicity or chemo-sensitivity assays. The Reagent contains a tetrazolium compound [3-(4,5-dimethylthiazol-2-yl)-5-(3-carboxymethoxyphenyl)-2-(4-sulfophenyl)-2H-tetrazolium, inner salt; MTS] and an electron coupling reagent (phenazine ethosulfate; PES). PES has enhanced chemical stability to form a stable solution. MTS relies on mitochondrial reductases to convert the tetrazolium to formazan, a purple coloured product. The quantity of formazan product, as measured by the amount of 490nm absorbance using a plate reader, is directly proportional to the number of living cells (metabolically active) in the sample (figure 2.1).

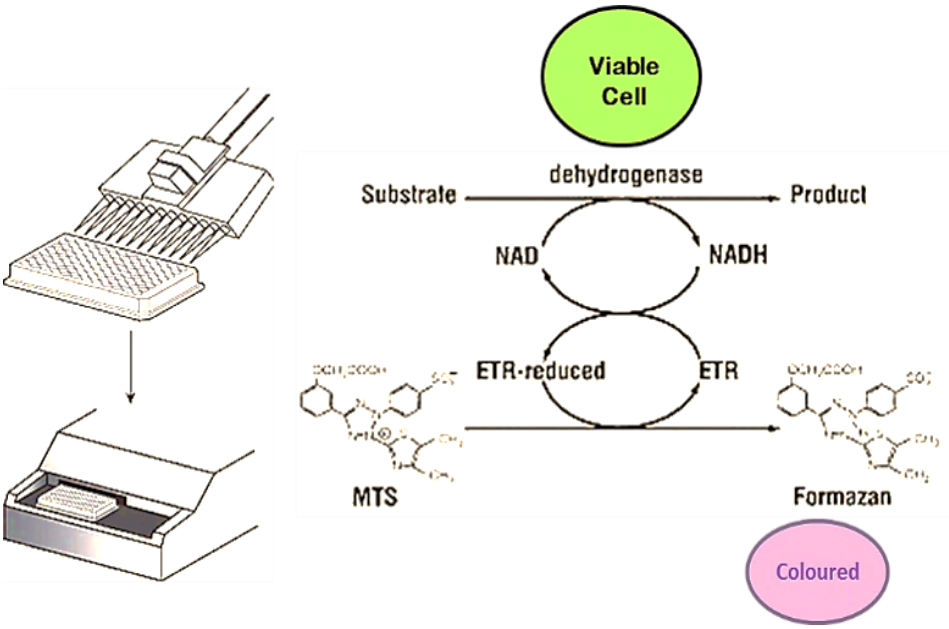


**Figure 2.1 MTS viability assay principal.**

Reduction reaction in viable cells will lead to coloured product, if cells are apoptotic or growth arrested the colour would be less or none.

### 2.4.1 Counting and seeding cells in 96 wells plates for MTS

Cells were pipetted gently up and down for approximately 10 times to break up clusters. The cells were counted as mentioned above (2.1.2 Cryopreservation of cell lines). 10ml of cell suspension (1.0 x $10^6$ cells /ml) was needed to seed 96 well culture plates to achieve 5.0 x$10^4$ cells/50 µl/well of 96 wells (clear flat transparent, (Corning™) Fisher-Scientific. Cells were spun at 200 x g for 3 minutes in 50ml falcon tubes, supernatant removed and cell lines were resuspended in 10ml of appropriate medium. Primary cells were stimulated with soluble ligands (sCD40L, IL-4, Anti-HisTag) and then counted and seeded into the assay plates.

Example of counting cells:

$$volume\ of\ resuspension\ to\ add\ to\ 10\ ml = \left({Concentration\ (Want)}/{Concentration\ (Have)\ x\ Total\ vol.}\right) \times 10$$

Cells were seeded in 96 wells plate in triplicate per each single concentration of each inhibitor (five concentrations were used for each inhibitor), and triplicate or four wells

for control untreated cells (control untreated, control untreated with DMSO). 96 wells plate in figure 2.2 shows 4 cell lines plate with one inhibitor, wells 2, 3,4,5,6 are representing the five concentrations triplicate.

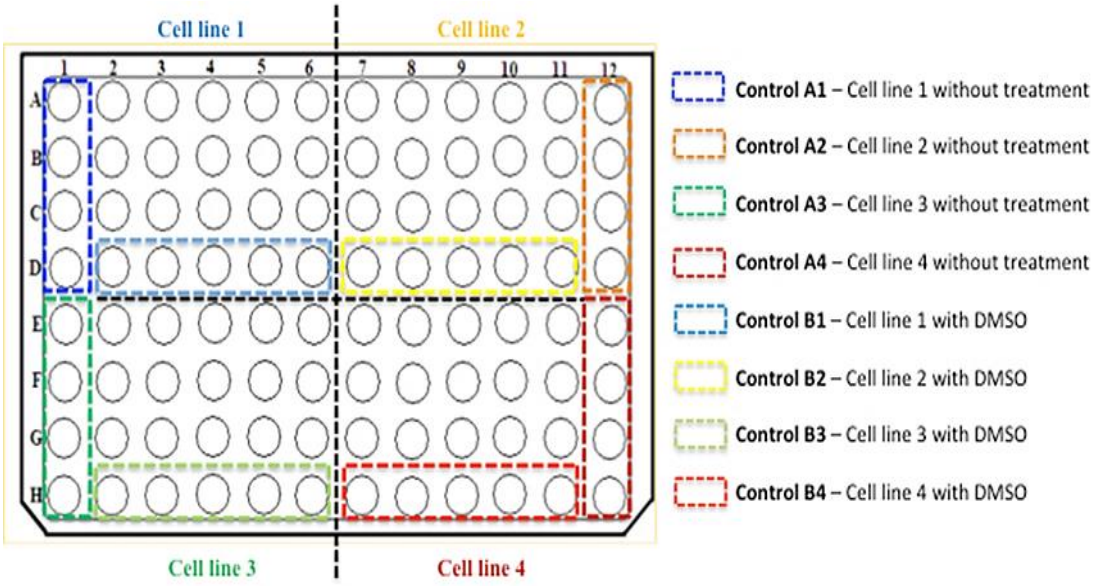


**Figure 2.2 Seeding of 50 µl of cell suspension to 96 wells cell culture plate for MTS assay.**

## 2.4.2 Diluting inhibitors for MTS assay

Inhibitors were purchased and prepared before dilution according to this example:

Drug preparation (ex: Ibrutinib, 10 mg):

$$Volume\ (ml) = (Mass\ (mg)/M.W.)/(Concentration\ (mM)) \times 1000$$

$$Volume\ (lm) = \frac{(10\ (mg)/440.5)}{20\ (mM)} \times 1000 = 1.135ml\ of\ DMSO$$

Firstly, inhibitors were serially diluted in DMSO to five concentrations labelled as 10mM, 1mM, 0.1mM, 0.01mM and 0.001mM. Inhibitors were mixed well, then 3µl of them were added to other five labelled Eppendorf tubes with 1497µl appropriate media (RPMI is an example in figure 2.3). From each tube, 50µl of inhibitor-diluted media were added to each correspondent well in assay plates (figure 2.4). Plates were incubated at 37°C for 12, or 24, or 48 hours in a humidified, 5% CO2 atmosphere.

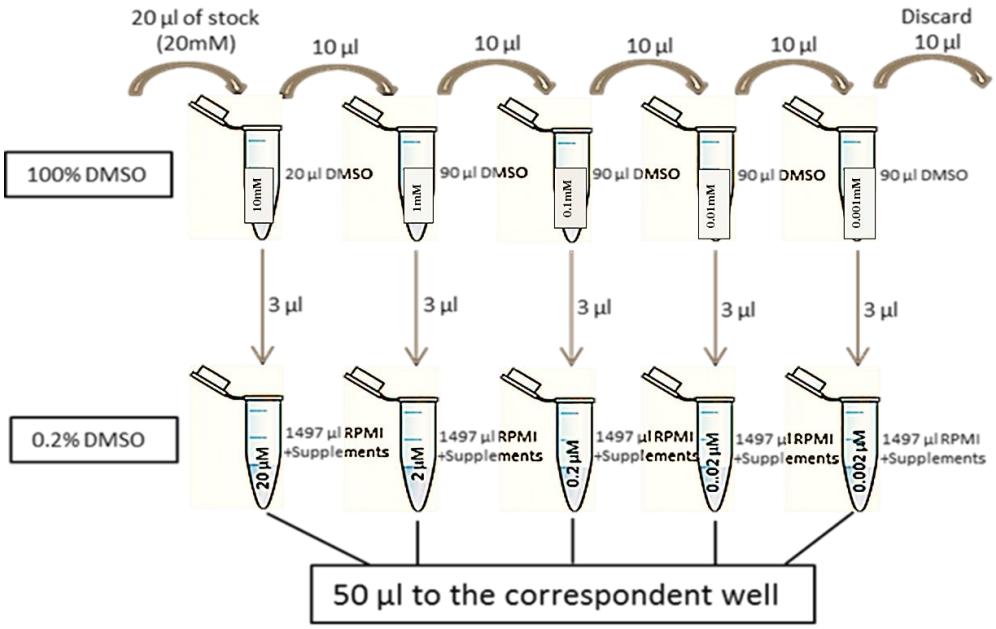


**Figure 2.3 Serial dilution of inhibitors.**

Dilution of different inhibitors with DMSO to achieve 5 concentrations of each inhibitor/well, then further diluted with media to achieve 0.1% DMSO in each well in the assay plates.

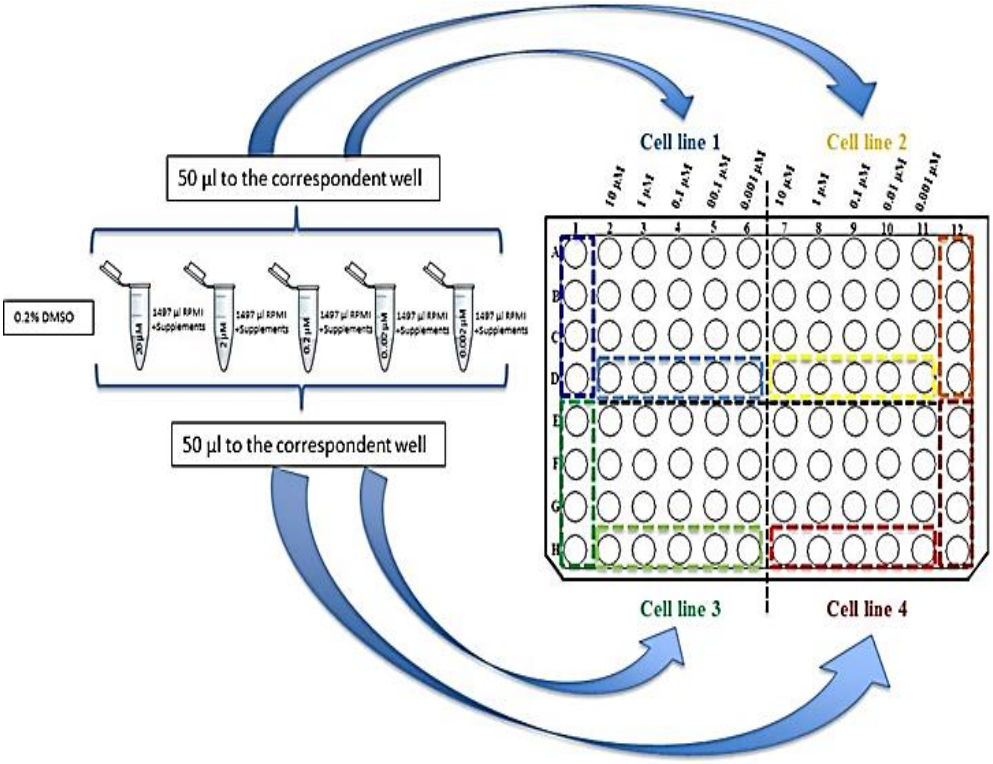


**Figure 2.4 MTS assay plate preparation.**

Adding media-diluted inhibitors (1497µl media+3µl DMSO inhibitor), 50µl to each well cell suspension of 50µl, to a final volume of 100µl/well in the assay plates to achieve 0.1% DMSO in each well in the assay plates.

After 48hrs, CellTiter96®$AQ_{ueous}$ One Solution Reagent was thawed from -20C freezer, approximately 90 minutes at room temperature or 10 minutes in a water bath at 37ºC. Assay plates were removed from incubator, and 20µl of CellTiter 96® $AQ_{ueous}$ One Solution reagent was added to each assay well, incubated for 2-4 hours in a humidified, 5% CO2 atmosphere. Absorbance was recorded at 490nm using a plate reader TECAN (Infinite® F50 with Magellan™ software). Background control with 100µl media were prepared on same plates instead of cell line 4 or primary cells 4 and incubated with same conditions and time, and read by plate reader at the same time. The average 490 nm absorbance from the "no cells" control wells was subtracted from all other absorbance values to yield corrected absorbance.

### 2.4.3 Combination of Drugs using MTS Assay for Cell Lines and Primary Cells

Firstly, 20µl of 100% DMSO were added to first labelled eppendorf tube (10mM), and 90µl were added to other four labelled tubes (1, 0.1, 0.01, 0.001 mM) (figure 2.5). Then, 996µl of appropriate media were added to other five labelled Eppendorf tubes.

Secondly, 0.4% DMSO solution was prepared to use as a control for cells without treatment; for that, 4µl of DMSO was added to 996µl of the appropriate medium and mixed. Then, 20µl of Drug 1 stock was added (20mM) to the first Eppendorf tube that was labelled at the beginning (10mM) with 20µl DMSO, mixed and10µl of the solution transferred to the next tube (1mM). Serial dilutions performed as with one drug viability assay. 4µl from the selected tube transferred to the tube with the appropriate medium for Drug 1. Same was done to Drug2. Plate section 3 and 4 were used for background absorbance and for testing single inhibitors at the same plate. Drugs in combination were added (25µl of each Drug1 and Drug2/well) to 50µl of cells suspension. In single drugs treatment testing; at same assay plates, 25µl of each drug were added with 25µl of media and DMSO control/well to 50µl cell suspension. For untreated cells (control DMSO media), 50µl was added. Plates were incubated and absorbance were read as mentioned previously.

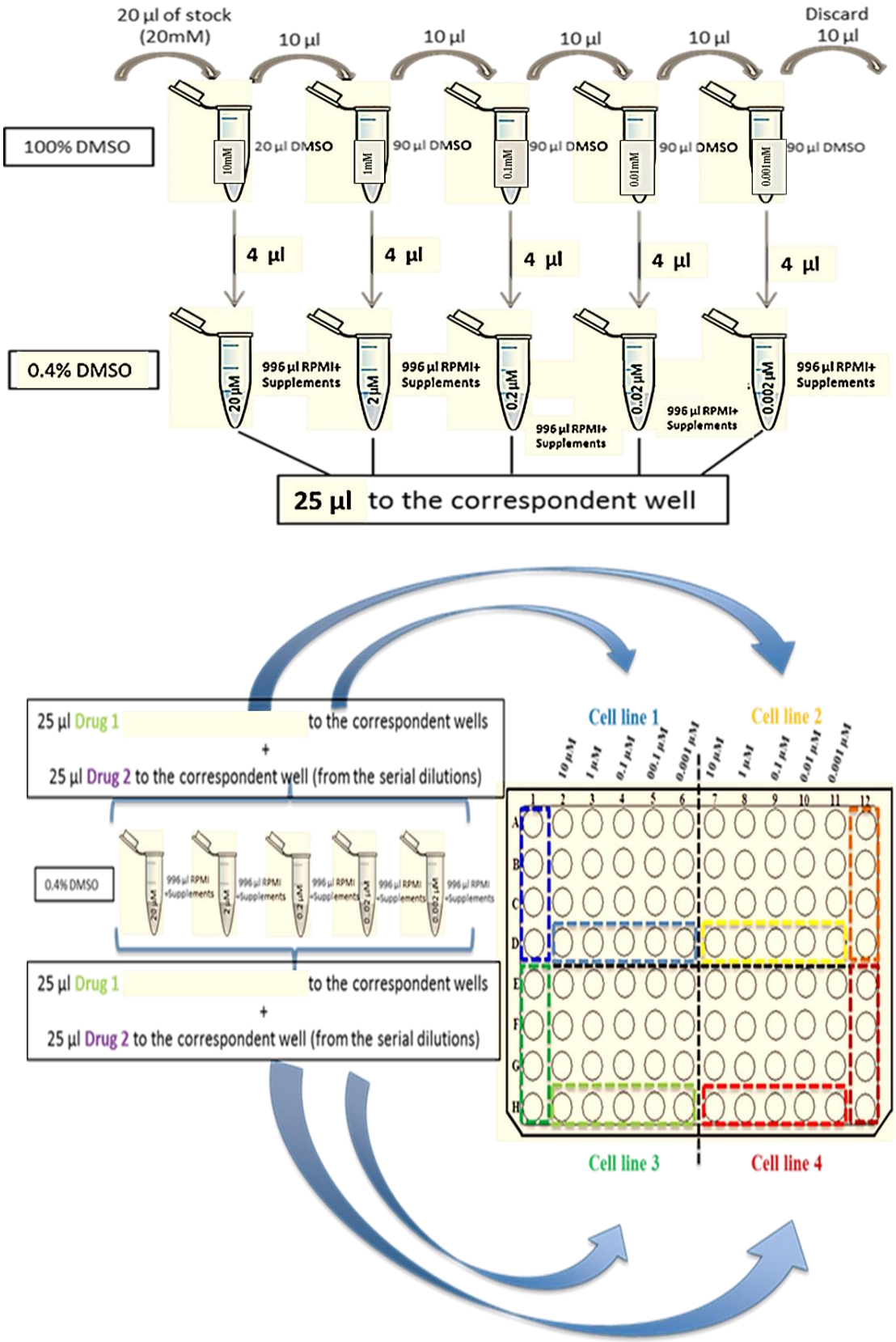


**Figure 2.5 Combination assay plate.**

25µl of both drugs added to make 50µl, plus 50µl cell suspension in media totally 100µl/well final volume, for testing single drugs at same plate 25µl drug plus 25µl DMSO media, plus 50µl cells suspension; and also for background (no cells –media only) would be done at same plate.

### 2.4.4 Combination analysis and Combination Index using CalcuSyn

CalcuSyn software (Biosoft® USA) was used to analyse combination therapy results and to establish a possible synergism between two inhibitors. Combination Index (CI) was calculated and used as an indication of synergy.

| Range of CI | Description |
|---|---|
| **< 0.1** | Very strong synergism |
| **0.1 – 0.3** | Strong synergism |
| **0.3 – 0.7** | Synergism |
| **0.7 – 0.85** | Moderate synergism |
| **0.85 – 0.9** | Slight synergism |
| **0.90 – 1.1** | Nearly additive |
| **1.1 – 1.2** | Slight antagonism |
| **1.2 – 1.45** | Moderate antagonism |
| **1.45 – 3.3** | Antagonism |
| **3.3 – 10** | Strong antagonism |
| **>10** | Very strong antagonism |

**Table 2.6 Table showing recommended interpretations of CI values.**

## 2.5 Genotyping (Sanger Sequencing) for cell lines and primary cells.

### 2.5.1 DNA Extraction from primary cells and cell lines

Cells-media suspension was spun in a falcon tube at 200 x g for 5 minutes, supernatant was removed and pellet was resuspended in 1ml of sterile 1xPBS in 1.5ml Eppendorf tube, and mixed thoroughly. Cell suspension spun at 300 x g for 5 minutes and this step was repeated one more time. The cell pellet was stored at -80°C, until it is ready to be used by (Qiagen DNeasy®Blood & Tissue Kit (250). Cells were allowed to thaw, then resuspended in 200µl 1xPBS. 20µl proteinase K was added, and 200µl Buffer AL (without added ethanol) were added and mixed thoroughly by vortexing, and incubated at 56°C for 10 minutes. 200µl ethanol (96-100%) was added to the sample, and mixed thoroughly by vortexing, the mixture was pipetted into the DNeasy Mini spin column and placed in a 2ml sterile collection tube. Then, centrifuged at ≥6000 x g for 1minute, flow-through was discarded with collection tube. DNeasy Mini spin column was placed in a

new 2ml collection tube 500µl Buffer AW1 was added, and centrifuged for 1minute at ≥6000 x g, flow-through and collection tube were discarded. DNeasy Mini spin column was placed in a new 2ml collection tube. 500µl Buffer AW2 added, and centrifuged for 3minutes at ≥20,000 x g to dry the DNeasy membrane, to make sure no residual ethanol is left. DNeasy Mini spin column placed in a clean sterile1.5 ml or 2.0 ml microcentrifuge tube and 200µl Buffer AE pipetted directly onto the DNeasy membrane, incubated at room temperature for 1minute, and then centrifuged for 1minute at ≥6000 x g to elute genomic DNA (figure 2.6). Purified DNA was diluted in ultrapure water, 1µl of a sample was placed on Sub Microliter Cell (Sample Compression Technology) and Lid10/1mm was placed over the sample to allow for samples quantification (>50ng/µl).

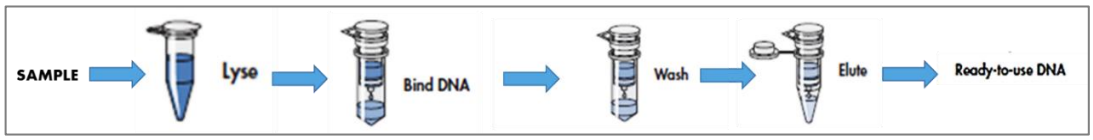


**Figure 2.6 Genomic DNA extraction illustration by DNeasy® Blood & Tissue Kit (250).**

## 2.5.2 PCR Reaction

Master Mix using (Extensor Hi-Fidelity PCR Master Mix-Thermo Scientific®) was prepared for the PCR as follows:

| | For 1 PCR: | for 10 PCRs |
|---|---|---|
| Ultrapure water: | 8.5µl | 85µl |
| Extensor mix (2X): | 12.5µl | 125µl |
| Forward primer (10 µM): | 1.0 µl | 10µl |
| Reverse primer (10 µM): | 1.0 µl | 10µl |

A total of above 23µl primers, water and Master Mix were aliquoted into each PCR tube. Then, 2µl DNA sample (50 ng/µl) was added to each corresponding tube, and lid was closed.

Samples were placed in PCR machine and run according to the following programme:

94°C 5 min

94°C 15 sec
60°C 30 sec
68°C 30 sec
} 35 cycles

68°C 5 min

4°C ∞

Samples were then run on (1-1.5%) agarose gel. Picture was taken by (Gel Doc™ XR System-Bio-Rad®) UV radiation transilluminator, to ensure exon amplification.

### 2.5.3 Agarose gel electrophoresis

Preparing 1xTBE:

To prepare 10x TBE using a magnetic stirrer, 108g of Tris (Fisher) and 55 g of Boric Acid (Fisher) were dissolved in 800ml of distilled water. 40ml of 0.5M EDTA pH 8.0 was added, the volume then adjusted to 1000 ml and stored at room temperature. For each experiment, in a 1000ml flask, 100ml of 10x TBE were diluted in 900ml of distilled water to prepare 1xTBE solution.

1% agarose gels were prepared, by adding 0.4g agarose (Fisher) to 40ml 1xTBE, and was put in a microwave until agarose gel was dissolved completely, which takes about 1minute at full power. The agarose gel was allowed to cool to ~55ºC, which could felt still warm. 0.7µl Ethidium Bromide was added and mixed well. Cassettes were placed in the holder and combs were attached. Agarose gel was poured while still warm and let to set ~ 30minutes-1hour. Then, the cassette was placed in the agarose gel tank; the gel tank (Fisher) was filled with1xTBE solution. 5µl of 100 bp DNA ladder (PCR ranger 100 bp DNA –Generon) was loaded into the first well. 8-10µl of the sample was loaded into next wells, and run at 100 volts for ~30 minutes. The gel was visualised using gel dock (Gel Doc™ XR System-Bio-Rad®) UV radiation transilluminator for gel electrophoresis results.

### 2.5.4 DNA Clean up and DNA sequencing

An equal volume of SureClean plus (BIOLINE) was added to DNA PCR sample and mixed thoroughly by vortexing. Samples were incubated at room temperature for 10mins, then centrifuged at 13000 x g for 10mins and supernatant discarded by aspirating carefully. 100µl of 70% ethanol was added and vortexed, samples were centrifuged at 13000g for 10mins and supernatant discarded by aspirating carefully. All ethanol was removed completely and samples allowed to air dry for 10mins. DNA was resuspended in 20µl of ddH2O. DNA quantification was performed using Nano-Photometer P300 (IMPLEN). The technique uses the concentration to absorbance relationship (Lambert-Beer Law) A=e ×c ×d where: A= absorbance; e=the substance specific coefficient; c= the concentration of the absorbing sample; d=optical path length (cm). (It is well established that a solution of double stranded DNA in a 10mm path length cell with an optical density of 1.0 has a concentration of 50µg/ml). Nano-Photometer determines the sample's absorbance at 260nm along with the above information to determine DNA concentration (ng/µl). Purified PCR products diluted in ultrapure water were used to quantify DNA in each sample. 1µl of a sample was placed on Sub Microliter Cell (Sample Compression Technology) and Lid10/1mm was placed over the sample. After quantification, samples (>50ng/µl) were sent using online order form for submission to (GENEWIZ UK DNA sequencing).

## 2.6 Primers

All primers were supplied by Sigma-Aldrich.

### 2.6.1 Primers for BRAF

Primers used to amplify BRAF exon 15 are 5'>3' Forward primer 5'TGCTTGCTCTGATAGGAAAATG3' and 5'>3' Reverse primer was 5'AGCATCTCAGGGCCAAAAAT3', these primers covers hotspot p.V600E mutation, the predominant mutation in the BRAF gene, involving thymidine to adenosine substitution at nucleotide 1,799, and accounting for more than 90% of the detected mutations in BARF (Davies *et al*, 2002), 4HCL (BRAFV600E) samples were used as a positive control.

### 2.6.2 Primers for NOTCH1

Exon 34 of Notch1 gene was amplified by sequencing a known hotspot region (around 1,500bp) for Notch1 mutations found in B- cell malignancies. Exon 34 Notch1 were TAD and PEST domains of hot spot mutations were sequenced using: 5'>3' Forward primers 5'ATGGCTACCTGTCAGACGTG3' and 5'>3' Reverse primer 5' TCTCCTGGGGCAGAATAGTG3', was used for TAD domain, and 5'>3' Forward primer 5' GAGCTTCCTGAGTGGAGAGC3' and 5'>3' Reverse primer 5'GAGCTTCCTGAGTGGAGAGC 3' for PEST domain. These amplifications cover the whole PEST domain and most of the TAD domain and include 97% of NOTCH1 mutations previously described in CLL (Villamor *et al*, 2013).

### 2.6.3 Primers for SF3B1

To cover K700E hotspot mutation between exons 14-16 SF3B1, the SF3B1 primers used were Intron 13 5'>3' Forward primer 5'CCAACTCATGACTGTCCTTTC3' intron 15 5'>3' Reverse primer 5'GCCTTCAAGAAAGCAGCCAAACC3'.

### 2.6.4 Primers for MYD88

Exon 5 of MYD88 was amplified using 5'>3 Forward primer 5'TGCCAGGGGTACTTAGATGG3', and 5'>3 Reverse primer used 5'GAAGTTGGCATCTCCAGGAA3' to cover MYD88 L265P (Martínez-Trillos *et al*, 2016).

## 2.7 Patient Samples

Peripheral blood samples were obtained from patients diagnosed with Chronic Lymphocytic Leukaemia following an approval from the Local Research Ethics Committee and the Research and Development Office of the University Hospitals of Leicester NHS Trust (UHL09723). A total of 359 samples of patients were used in this project and were categorised into two individual sets. BRAF mutation set included 190 randomly treated and untreated samples of selected patients from the database plus (4 classical HCL (positive control), and 10 of other leukaemia and lymphoma samples). (SF3B1, MYD88, and NOTCH1) sets included 148 plus (7 leukaemia and lymphoma samples) all CLL cohort were treated. Patient information of gender, age at diagnosis,

IGHV mutational status, cytogenetic abnormalities and treatment were provided by Dr Sandrine Jayne.

## 2.8 SF3B1 intron mutation testing

5 samples of intron mutations, 1 sample 6bp and 3 samples 8bp from splicing site, were tested for potential effects of intron mutations on splicing exons products. In addition, one control unmutated was selected.

### 2.8.1 RNA extraction

RNA was extracted according to Direct-zol™ RNA Kits figure 2.7. First for each of 6 samples cell suspension 3x volume of TRI reagent® was added and mixed thoroughly for 5 minutes. Then samples were centrifuged at 10,000-16,000 x g for 30 seconds. Then supernatants were transferred into clean RNase-free tubes. Equal volume of ethanol (95-100%) was added to each sample and mixed thoroughly. Then mixtures were transferred into Zymo-Spin™I IC Column in a collection tube, and the flow through was discarded. 400µl of Direct-zol™ RNA Prewash was added to the column and centrifuged at 10,000-16,000 x g for 30 seconds, and the flow through was discarded. This step was repeated. 700µl of RNA Wash Buffer was added to column and centrifuged at 10,000-16,000 x g for 2minutes ensuring complete removal of the wash buffer. Columns were transferred to clean RNase-free tubes and RNA was eluted by adding 20-50µl of DNase-RNase-free water directly to the column matrix and centrifuged at 10,000-16,000 x g for 30seconds (figure 2.7).


**Figure 2.7 Illustrates Direct-zol™ RNA extraction.**

RNA quantification was performed using Nano-Photometer P300 (IMPLEN). 1µl of a sample was placed on Sub Microliter Cell (Sample Compression Technology) and Lid10/1mm was placed over the sample. Samples were then read.

### 2.8.2 Reverse transcription

For reverse transcription reaction, 2µg of RNA extract was mixed with 1µg of random hexamers (Promega), then made up to 15µl with TE.1 buffer (10mM Tris 1mM EDTA; pH 8.0). Then, samples were heated to 70°C for 15mins (Denaturation of the RNA template, by heating the RNA in the absence of reaction buffer and enzyme prior to cDNA synthesis to remove secondary structure that may impede full length cDNA synthesis). After that, samples were allowed to cool down on ice for 10 minutes.

Master Mix was made according to the following (figure 2.8):

<u>For one Reaction:</u>

5 µl 5xM-MLV Reverse Transcriptase (RT) Buffer (Promega)

1 µl of M-MLV Reverse Transcriptase (RT) (Promega)

1.2 µl mix containing 10mM (dATP, dCTP, dGTP, dTTP (Promega- Fisher BioReagents))

0.5 µl RNaseOut (Invitrogen™)

6 µl Water

Master mix was divided into two groups: (+RT, and -RT)

<u>For + RT tube:</u>

0.5 x 1 µl M-MLV RT were added.

<u>For - RT tube:</u>

0.5 x 1 µl Water were added.

7.5µl of RNA extract was added to 17.3µl of + RT. The remaining 7.5µl of RNA extract was added to 17.3µl of – RT, and samples were incubated at 37°C for 1 hour.

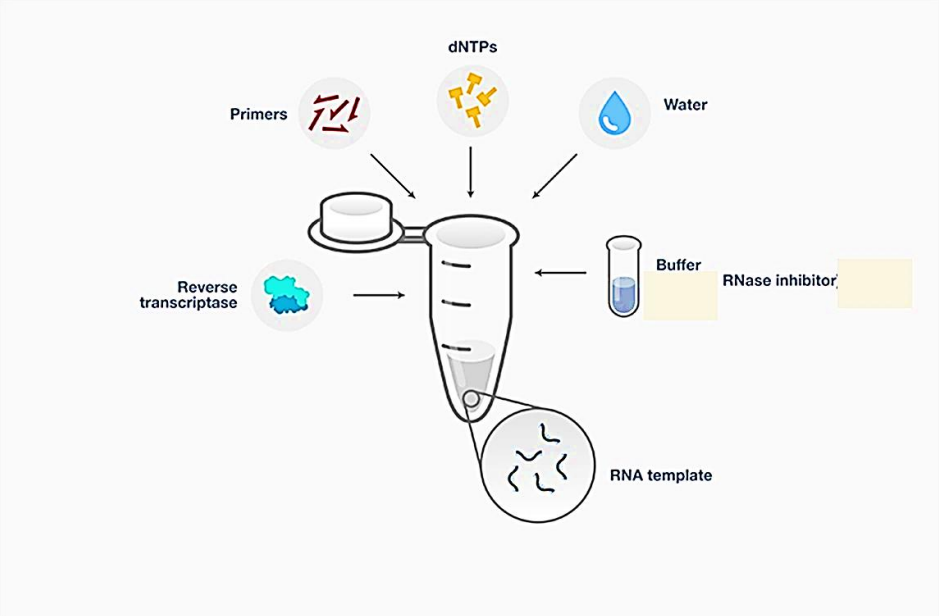


**Figure 2.8 Illustration of reverse transcription of RNA.**

### 2.8.3 PCR amplification

100 ng/µl of the reverse transcribed RNA template (cDNA) was used for amplification.

Master Mix was made as following for one Reaction:

0.4 µl 10mM dNTP mix

2 µl REDTaq® PCR Buffer (Sigma Aldrich)

1 µl SF3B1 Forward primer (10µM)

1 µl SF3B1 Reverse primer (10µM)

14.1 µl Water

0.5 µl REDTaq® DNA polymerase (Sigma Aldrich)

19 µl of above Master mix was added to 1µl of cDNA template (+/- RT), and 19µl of master mix was added to 1µl of water (negative control).

PCR amplification was carried out as following:

| | | | |
|---|---|---|---|
| Preheating | 94°C | 2 min | |
| Denaturation | 94°C | 1 min | 20-25 cycles |
| Annealing | 60°C | 30 sec | |
| Extension | 72°C | 1min | |
| Final extension | 72°C | 5 min | |

To analyse samples, 1.5% agarose gel electrophoresis were performed as mentioned in section (2.5.3).

## 2.8.4 Nested PCR

The target DNA undergoes the first run of polymerase chain reaction with the first set of primers, shown in red (figure 2.9). The product from the first reaction undergoes a second run with the second set of primers, shown in blue.

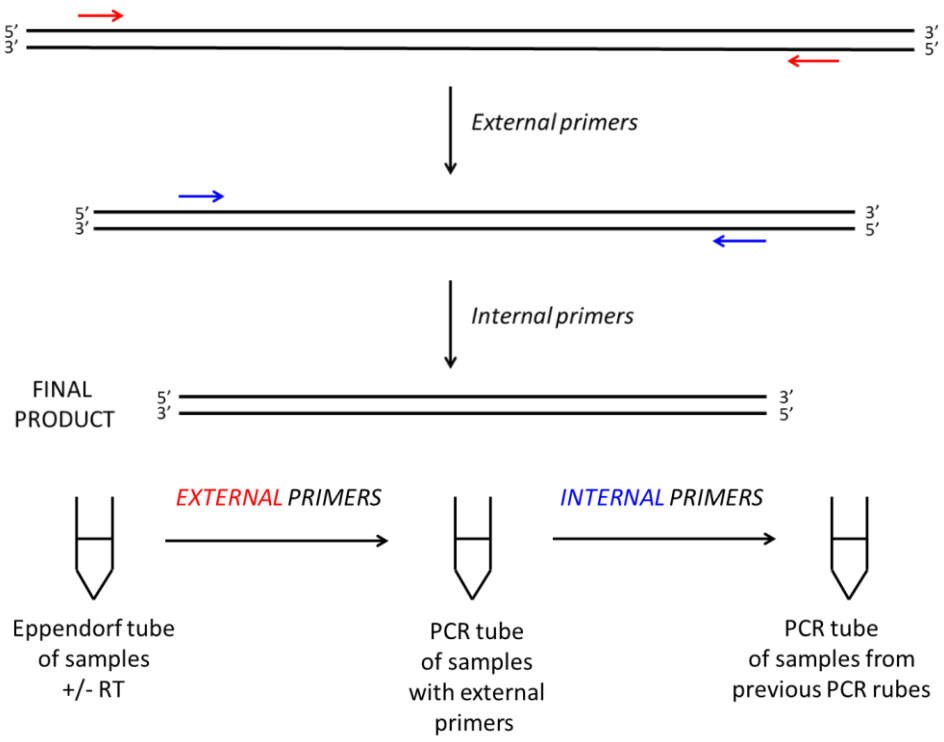


**Figure 2.9 nested PCR illustration.**

PCR with external primers was done according to 2.8.3.

External primers covered SF3B1 exons14-15 region used and were:

Forward primer: 5'TGGCAAGCGAGACACTGGTA3'

Reverse primer: 5'GCCAAAGCACTGATGGTCCGAA3'

Then external primers amplification was confirmed by agarose gel electrophoresis as in section (2.5.3).

Internal primers were then used for nested PCR:

SF3B1 forward: 5'CTTATGGGCTGTGCCATCTTG 3'

SF3B1 reverse: 5'GGTCCGAACTTTCTGCTGCT 3'

Amplified product of external primers were used as a DNA template (1µl) and all other master mix compounds added as same as mentioned above in 2.8.3 PCR amplification. Internal primers were used as following:

| | | | |
|---|---|---|---|
| Preheating | 94°C | 2 min. | |
| Denaturation | 94°C | 1 min | 35-45 cycles |
| Annealing | 55°C | 30 sec | |
| Extension | 72°C | 1 min | |
| Final extension | 72°C | 5 min. | |

To analyse samples, 1.5% agarose gel electrophoresis were performed (2.5.3). Nested PCR samples were purified as mentioned in DNA clean up protocol (2.5.4). Purified PCR products diluted in ultrapure water were used to quantify DNA in each sample. 1µl of a sample was placed on Sub Microliter Cell (Sample Compression Technology) and Lid10/1mm was placed over the sample. After quantification, samples (>50ng/µl) were sent using online order form for submission to GENEWIZ UK DNA sequencing.

## 2.9 Mycoplasma testing for cell lines

The MycoAlert™ PLUS Assay is a selective biochemical test that utilizes certain mycoplasmal enzymes activity. The presence of these enzymes provides a rapid screening

procedure, allowing sensitive detection of contaminating mycoplasma in a test sample. The viable mycoplasma are lysed and the enzymes react with the MycoAlert™ PLUS Substrate, catalysing the conversion of ADP to ATP.

By measuring the level of ATP in a sample both before and after the addition of the MycoAlert™ PLUS Substrate, a ratio can be obtained which is indicative of the presence or absence of mycoplasma. If mycoplasma enzymes are not present, Read B shows no increase over Read A. If mycoplasma was present, reaction of mycoplasmal enzymes with the MycoAlert™ PLUS Substrate leads to elevated ATP levels and an increase in Read B. This increase in ATP can be detected using the following bioluminescent reaction:

$$ATP + Luciferin + O2 \rightarrow luciferase\ \&\ Mg2+ \rightarrow Oxyluciferin + AMP + PPi + CO2 + Light$$

The emitted light intensity is linearly related to the ATP concentration and was measured using a luminometer. The assay was conducted at room temperature (18°C-22°C), the optimal temperature for luciferase activity.

First, supernatant of suspension cell culture was collected, then cell supernatant was spun at 200 x g for 5 minutes to remove any remaining cells. For optimal assay performance, supernatant was tested as soon as possible after collection, or stored immediately after collection at -80°C; and then thawed and equilibrated to room temperature, then tested.

100µl of sample was transferred into a luminometer tube, then 100µl of MycoAlert™ PLUS Reagent was added to each sample. After 5 minutes tubes were placed in the luminometer and initiate reading (Reading A). Then, 100µl of MycoAlert™ PLUS Substrate was added to each sample. After 10 minutes the tube was placed back again in the luminometer to get (Reading B). The ratio was calculated as:

Ratio = Reading B/Reading A.

A MycoAlert™ positive control, and (100µl of MycoAlert™ PLUS Assay Buffer or deionized water) as a negative control were also read with samples.

Ratio Interpretation:

< 1 Negative for mycoplasma.

1 - 1.2 Borderline: Quarantine cells and re-test in 24-48 hours.

> 1.2 Mycoplasma contamination.

Mycoplasma testing was performed every 6 months for all cell lines that were used in this project. All cell lines were free of mycoplasma when experiments were performed with them.

## 2.10 List of all used inhibitors:

| | Inhibitor | Supplier | Target |
|---|---|---|---|
| 1. | Vemurafenib,PLX4032, RG7204 (Zelboraf ®) | Stratech | BRAF wild-type and BRAF V600E inhibitor |
| 2. | Dabrafenib, GSK2118436 (Tafinlar®) | Stratech | BRAFV600E selective inhibitor |
| 3. | Sorafenib, BAY 43-9006 (Nexavar ®) | Stratech | VEGFRII, PDGFRβ and pan-RAF inhibitor. |
| 4. | RAF265, CHIR-265 | Stratech | Pan-RAF inhibitor. |
| 5. | C-RAF inhibitor (475958 Millipore) | Millipore | CRAF inhibitor. |
| 6. | Selumetinib, AZD6244 | Stratech | MEK1/2, phosphorylated ERK1/2 inhibitor. |
| 7. | Trametinib,GSK1120212 (Mekinist®) | Stratech | MEK1/2 inhibitor. |
| 8. | PD0325901 (Licensed by Pfizer feb-2015) | Stratech | MEK inhibitor. |
| 9. | UO126- EtOH | Stratech | MEK1/2 inhibitor. |
| 10. | Idasanutlin, RG-7388 | Stratech | MDM2 antagonist. |
| 11. | Idelalisib, CAL-101, GS-1101(Zydelig®) | Stratech | PI3K p110δ inhibitor. |
| 12. | Entospletinib, GS-9973 | Stratech | Syk inhibitor. |
| 13. | MG-132 | Stratech | Proteasome inhibitor. |
| 14. | BX-912 | Stratech | PDK1 (PDK1-AKT) inhibitor. |
| 15. | VER- 155008 | Stratech | Hsp70 inhibitor. |
| 16. | Dinaciclib, SCH727965 | Stratech | CDK1,2,5,9 inhibitor. |
| 17. | Axitinib, AG 013736 (Inlyta ®) | Stratech | VEGFRII, VEGFRIII, PDGFRβ inhibitor. |
| 18. | Fedratinib, SAR302503, TG101348 | Stratech | JAK/STAT JAK2 inhibitor. |
| 19. | IMD-0354 | Stratech | IKKβ inhibitor. |
| 20. | CUDC-907 | Stratech | PI3K and HDAC inhibitor. |
| 21. | Ibrutinib, PCI-32765 (IMBRUVICA®) | Stratech | BTK inhibitor. |
| 22. | Fludarabine (Fludara ®) | Cayman | Purine analogue, inhibits DNA synthesis. |
| 23. | Dactolisib (BEZ235, NVP-BEZ235) | Stratech | Dual PI3K and mTOR inhibitor. |
| 24. | PF- 04691502 | Stratech | Dual PI3K and mTOR inhibitor. |

| | | |
|---|---|---|
| 25. Sotrastaurin (AEB071) | Stratech | Protein kinase C inhibitor. |
| 26. IRAK1/4 inhibitor | Sigma | Interleukin-1 receptor associated kinases 1/4 inhibitor. |
| 27. MK-0752 | Cayman | Gamma-secretase inhibitor. |
| 28. Pladienolide B | Santa Cruz | SF3B1 inhibitor. |

## 2.11 Statistical analysis

Statistical data analysis and diagrams of all figures in this project were performed by myself using Microsoft excel and Graph-Pad software © UAS programmes. Using student t-test for P-value, non-linear regression analysis for IC50 calculation, grouped XY column, and box plots, for cell viability testing, clustering and Venn diagrams for mutation analysis.

# Chapter 3 Screening test of sensitivity of B-cell lines to inhibitors of the MAPK cascade and other survival signalling pathways

**Introduction:**

BCR activation in stimulated CLL leads to Syk and Lyn activation. This will stimulate intracellular signals that activate NF-κB, RAF/MEK/ERK, and AKT/mTOR, and STAT/JAK signalling, leading to increases in Bcl-XL, Mcl-1, and XIAP expression, which eventually causes proliferation and survival (Herishanu *et al*, 2013). Most CLL patient samples showed constitutively active MAPK signalling, which suggest its significance in survival of malignant cells (Muzio *et al*, 2008). Moreover, CLL microenvironment recapitulation *in vitro* resulted in increased MAPK signalling activity, suggesting its implication in CLL pathogenesis and responses to treatment (Best *et al*, 2013). In the microenvironment of 'proliferation centres', CLL cells receive growth signals through BCR receptors, T-cells chemokines of CD40-Ligand, IL-4, and PD-1 ligand, TLR, cytokines of MSCs and NLCs. In turn, the RAF/MEK/ERK cascade will be activated, along with other survival proliferation pathways such as NF-κB, PI3K/P-AKT. This will amplify the survival signals in CLL cells and will render them more resistant to treatments.

## 3.1 BRAF/MEK/ERK MAPK cascade is highly expressed in CLL cells, especially after modelling CLL microenvironment.

Our first aim was to test whether inhibition of RAF/MEK/ERK could have a therapeutic relevance in CLL. In this experiment, I used primary cells and compared their P-BRAF/P-MEK/P-ERK expressions to normal B-cells from normal healthy volunteers (table 3.1). Cells were either grown with culture media only (RPMI+10%FBS) unstimulated, or grown with CD40L/IL-4 soluble ligands to mimic CLL microenvironment stimulation for 48 hours. We assessed survival and the activation of signalling pathways using Western blotting. As can be seen in figure 3.1 P-ERK was significantly high in stimulated

malignant CLL cells, which is an indicator of MAPK pathway activation. In addition, phosphorylated AKT and NF-κB are highly expressed in stimulated malignant CLL cells.

P-ERK promotes growth, NF-κB activates anti-apoptotic and survival signals, and PI3K triggers MAPK cascade as well as NF-κB signals. Consequently, CLL cells proliferate as they receive signals from their microenvironment. That suggests the MAPK cascade, along with other survival signalling, are involved in CLL cell growth and disease progression.

| Code | Age at diagnosis | IGHV | Gender | Cytogenetic abnormalities |
|---|---|---|---|---|
| **BOH** | 73 | U | F | 13q14 deletion 99% Trisomy 12 |
| **BHA** | 76 | U | M | Deletion of p53 (95%) and a (partial trisomy 12 (94%) |
| **BNS** | 61 | M | M | Heterozygous 13q-deletion (66%) |
| **AA** | n.d | n.d | n.d | n.d |
| **AC** | n.d | n.d | n.d | n.d |
| **AU** | n.d | n.d | n.d | n.d |

**Table 3.1 The information of CLL patients and normal volunteers used in this experiment.**

AA, AC, AU: normal healthy volunteers, n.d not done, U: unmutated, M: mutated.

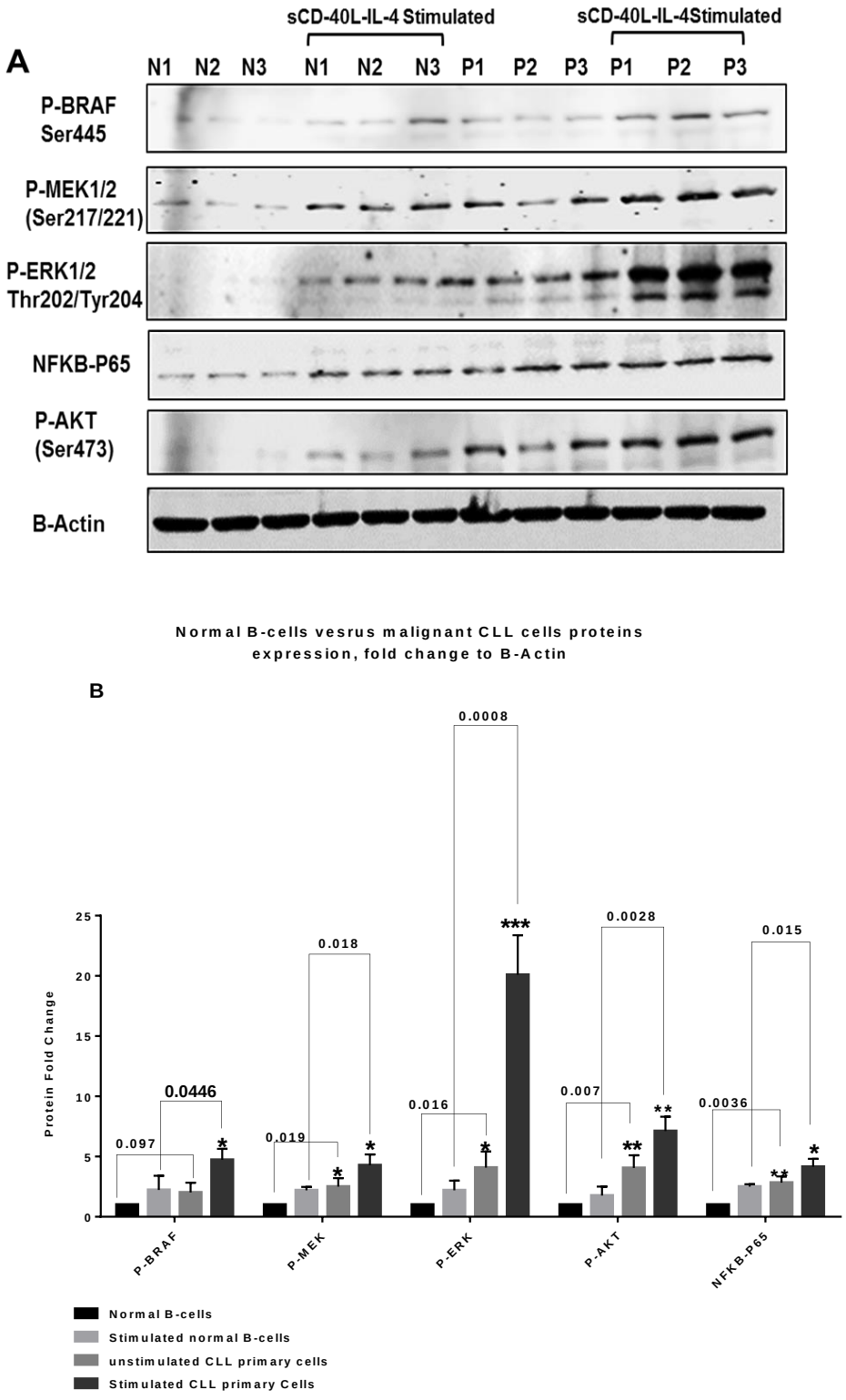


**Figure 3.1 Proliferation signalling with or without stimulation with (soluble CD40-Ligand/IL-4) system.**

Levels of P-BRAF (Ser445), P-MEK1/2 (Ser217/221), P-ERK1/2 (Thr202/Tyr204), P-AKT (Ser473) for PI3K signalling, and NF-κB (C-terminus of NF-κB P65) are shown before and after stimulation. **A)** N1, N2, N3 normal B-cells, P1, P2, P3 are CLL cells. Malignant and healthy human B-cells were placed in RPMI+10%FBS media; then cells pellets were collected, or stimulated with sCD40-L/IL-4 for 48 hours, then cells pellets were collected. **B**) Figure shows mean (Fold Change to B-Actin) of three samples (unstimulated normal cells normalised to 1), and standard deviation from two Western blots. Significantly different ($P < 0.05$) indicated by a star (*) was calculated using student t-test (Graph Pad Prism).

Unstimulated cells are not representative of the malignant subset that needs to be targeted, which is the one that contributes to disease progression and treatment resistance in patients. They have no significant expression of survival signals as can be seen in figure 3.1. Proliferation pathways are essential for malignant B-cells proliferation and may play a role in protecting malignant cells from spontaneous and drug-induced apoptosis. In addition, this protective milieu possibly contributes to minimal residual disease (MRD) and relapse after treatments.

## 3.2 Screening B-cell lines show different sensitivity to inhibitors and significant viability reduction after 48 hours treatment.

Next we used different leukaemia cell lines to assess their sensitivity to MAKP inhibition as a novel therapeutic target in CLL.

Five B-cell lines (MEC-1 CLL cell line, JVM-3 B-PLL B-prolymphocytic leukaemia cell line with BRAFK601N mutation, HC-1 and ESKOL HCL hairy cell leukaemia cell lines but they lack BRAFV600E mutation, which is a signature of all HCL cases, and SIG-M5 AML acute monoblastic leukaemia cell line BRAFV600E mutated) used in this this experiment (see materials and methods for cell of origin and mutations) (table 3.2).

To evaluate the sensitivity of these five cell lines to 22 inhibitors, among them MAPK inhibitors, cells were grown in cultures. They were tested using inhibitors at five different concentrations (10, 1, 0.1, 0.01, 0.001 μM) with the aim of calculating the IC50 (concentration that inhibits cell viability by 50%) for each inhibitor. For practical purposes, only concentrations that reached values below 50% were considered to have a significant effect on cell survival. Also, they were tested for three different times in order to check the suitable time for cell viability inhibition: 12hours, 24 hours, and 48 hours after treatment. Table 3.3 below shows the inhibitors that used and their targets. All cell lines were tested for Mycoplasma (see materials and methods) and all were confirmed negative before proceeding into our experiment.

| Cell line | Media |
|---|---|
| JVM-3 (B-PLL) BRAFK601N | 90% RPMI 1640 + 10% FBS |
| ESKOL (HCL) | 80% RPMI-1640 + 20% FBS |
| HC-1 (HCL) | 80% RPMI-1640 + 20% FBS |
| SIG-M5 (AML) | 80% Iscove's MDM+20%FBS |
| MEC-1 (B-CLL) | 90% Iscove's MDM+20%FBS |

**Table 3.2 Cell lines media.**

Each cell line used in each experiment was grown and treated in its specific media.

| Inhibitor | Target |
|---|---|
| **Vemurafenib,PLX4032, RG7204 (Zelboraf ®)** | Inhibits BRAFV600E and wild-type BRAF, also inhibits several non-RAF kinases. |
| **Dabrafenib, GSK2118436 (Tafinlar®)** | Mutant BRAFV600 specific inhibitor. |
| **Sorafenib, BAY 43-9006 (Nexavar ®)** | Sorafenib a multikinase inhibitor of CRAF, BRAF, VEGFRII, it inhibits both wild type and V600E mutant BRAF, VEGFRII (Flk-1), VEGFRIII, PDGFRβ, Flt3, and c-Kit. |
| **RAF265, CHIR-265** | RAF265 inhibits CRAF, wild type BRAF and mutant BRAFV600E and shows inhibition on VEGFR II phosphorylation. |
| **C-RAF inhibitor (475958 Millipore)** | A cell-permeable pyrazoloimidazole phenyl urea derivative that acts as a selective type II inhibitor of CRAF. |
| **Selumetinib, AZD6244** | Selective MEK1 inhibitor, also inhibits ERK1/2 phosphorylation. |
| **Trametinib,GSK1120212 (Mekinist®)** | Specific MEK1/2 inhibitor. |
| **PD0325901 (Licensed by Pfizer feb-2015)** | MEK 1/2 inhibitor. |

| | |
|---|---|
| **UO126- EtOH** | Selective inhibitor of MEK1/2. |
| **Idasanutlin, RG-7388** | MDM2 antagonist, selective p53-MDM2 inhibitor. |
| **Idelalisib, CAL-101, GS-1101 (Zydelig®)** | A selective PI3K class p110δ inhibitor. |
| **Entospletinib, GS-9973** | Selective Syk inhibitor. |
| **MG-132** | A peptide aldehyde (Z-Leu-Leu-Leu-al), 26S proteasome inhibitor. |
| **BX-912** | A specific PDK1 inhibitor, blocks PDK1/AKT signalling. |
| **VER- 155008** | Adenosine-derived inhibitor of Heat Shock Protein 70 (Hsp70). |
| **Dinaciclib, SCH727965** | CDK inhibitor for CDK2, CDK5, CDK1 and CDK9. |
| **Axitinib, AG 013736 (Inlyta ®)** | A multi-target inhibitor of VEGFRI, VEGFRII, VEGFRIII, PDGFRβ and c-Kit. |
| **Fedratinib, SAR302503, TG101348** | A selective inhibitor of JAK2. |
| **IMD-0354** | IKKβ inhibitor and blocks IκBα phosphorylation in NF-κB pathway. |
| **CUDC-907** | A dual PI3K and HDAC inhibitor for PI3Kα and HDAC1/2/3/10. It inhibits PI3K isoforms such as PI3Kβ, PI3Kγ, PI3Kδ, PI3KαH1047R and PI3KαE545K. |
| **Ibrutinib, PCI-32765 (IMBRUVICA®)** | A highly selective Brutons tyrosine kinase BTK inhibitor. |
| **Fludarabine (Fludara ®)** | A purine analogue and a chemotherapy, inhibits DNA synthesis by interfering with ribonucleotide reductase and DNA polymerase alpha. It is a STAT1 inhibitor. |

**Table 3.3 Inhibitors used in screening sensitivity of cell lines using MTS viability assay.**

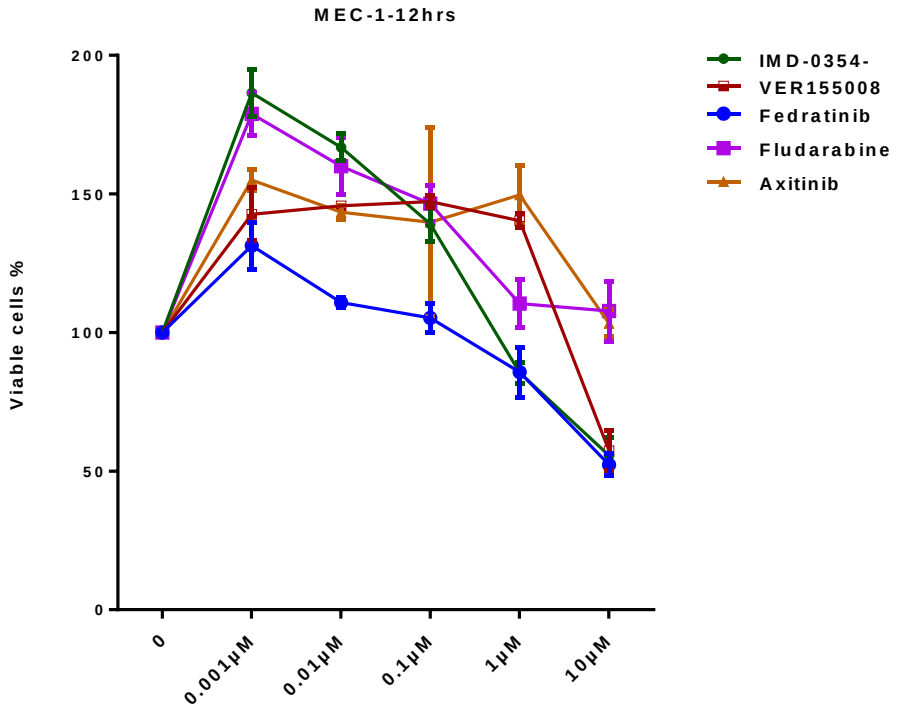
MEC-1-12hrs
Viable cells %
200
150
100
50
0
0
0.001μM
0.01μM
0.1μM
1μM
10μM
IMD-0354-
VER155008
Fedratinib
Fludarabine
Axitinib

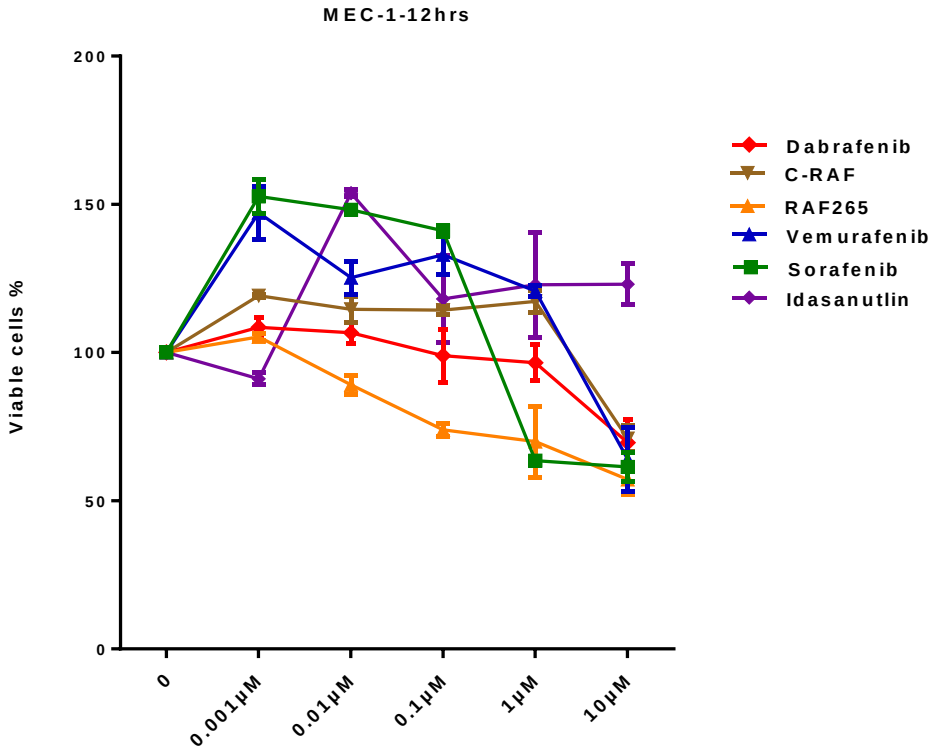
MEC-1-12hrs
Viable cells %
200
150
100
50
0
0
0.001μM
0.01μM
0.1μM
1μM
10μM
Dabrafenib
C-RAF
RAF265
Vemurafenib
Sorafenib
Idasanutlin

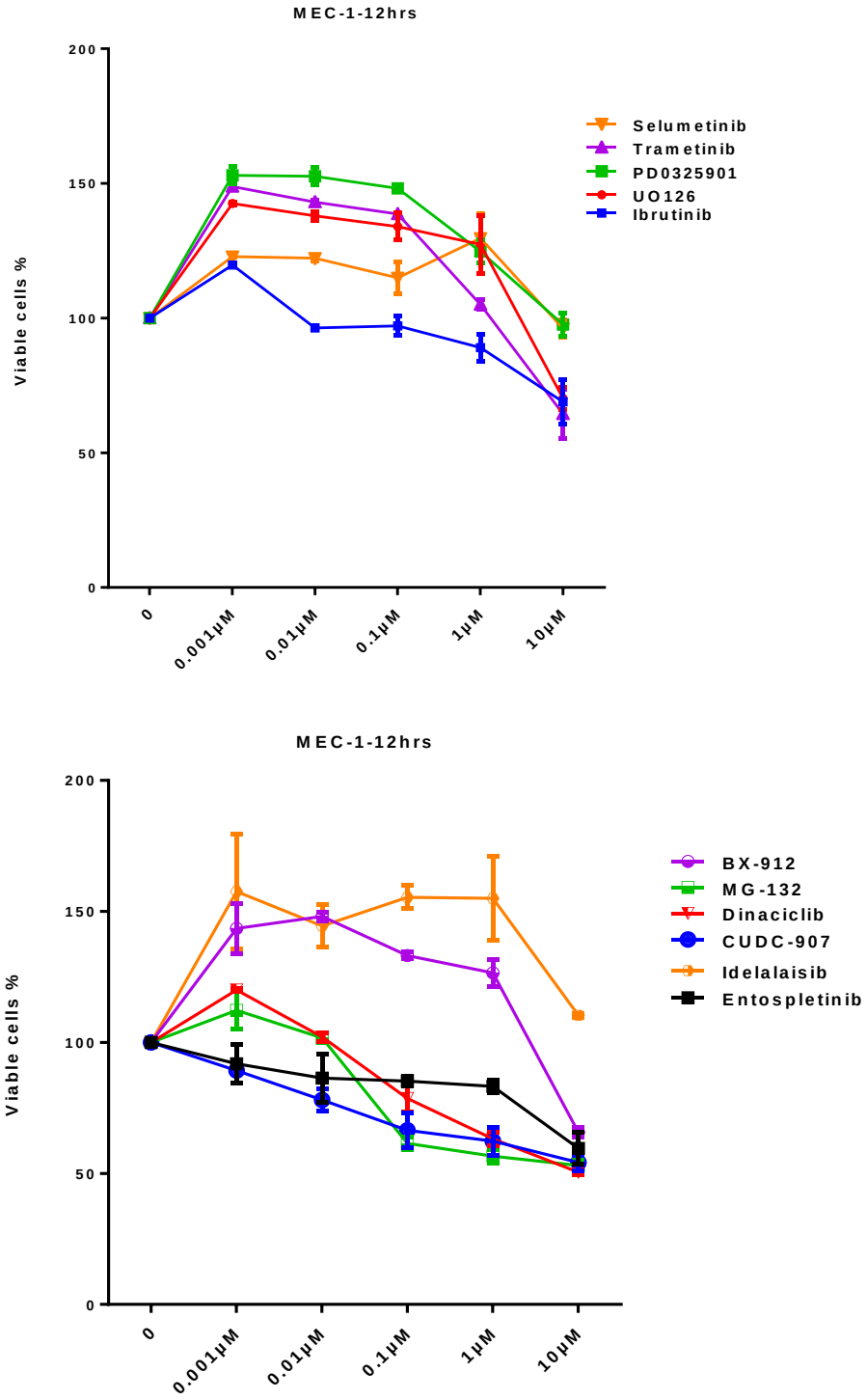


**Figure 3.2 MEC-1 CLL cell line treatment for 12 hours viability assay.**

Cells were counted, plated, treated for 12 hours, then MTS reagent were added, after 2-4hours in incubator at 5%CO2 and 37°C , plates were read using plate reader. Concentrations of each inhibitor were 10, 1, 0.1, 0.01, 0.001µM respectively. Y axis shows percentage of viable cells to DMSO control, which was normalised to 100%. X axis shows concentration of inhibitors. Each concentration presented in mean and standard deviation of two biological duplicates and two or three technical triplicates readings per inhibitor.

MEC-1 shows no important sensitivity (<50%) at 12hours treatment to any of the 22 inhibitors, as can be seen in figure 3.2. this might be due to insufficient time of treatment.

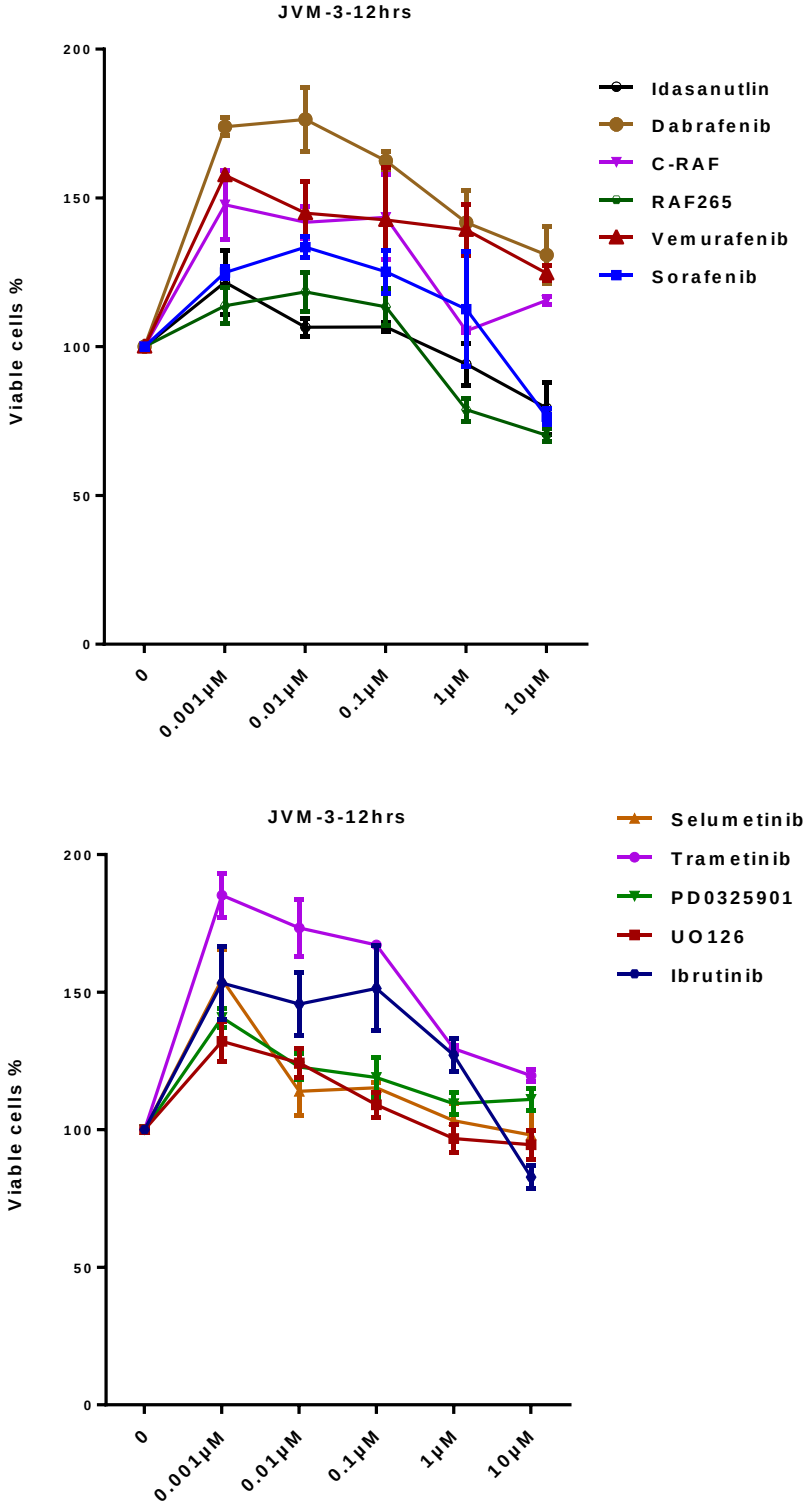

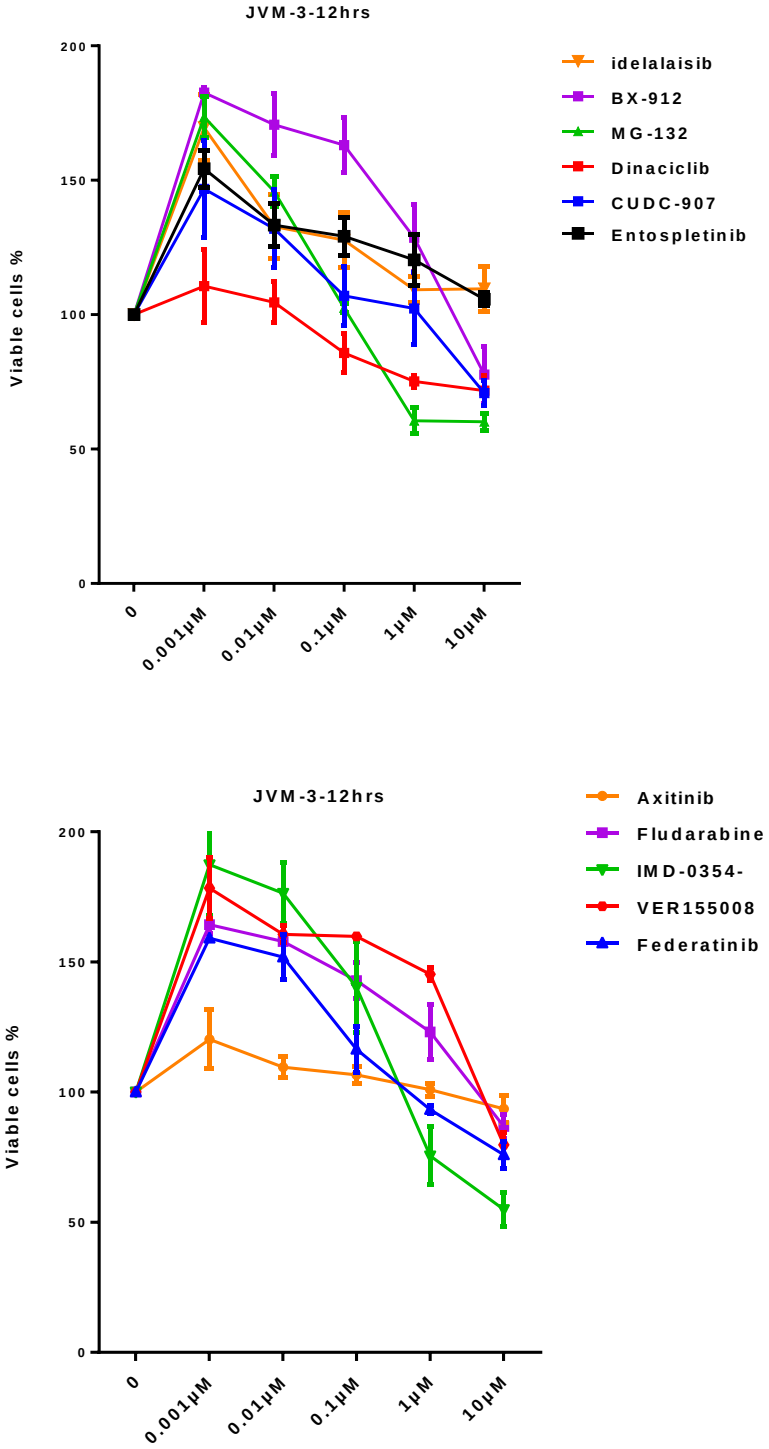


**Figure 3.3 JVM-3 B-PLL (BARFK601N) cell line treatment for 12 hours viability assay.**

Cells were counted, plated, treated for 12 hours, then MTS reagent were added, after 2-4hours in incubator at 5%CO2 and 37°C , plates were read using plate reader. Concentrations of each inhibitor were 10, 1, 0.1, 0.01, 0.001µM respectively. Y axis shows percentage of viable cells to DMSO control, which was normalised to 100%. X axis shows concentration of inhibitors. Each concentration presented in mean and standard deviation of two biological duplicates and two or three technical triplicates readings per inhibitor.

JVM-3 shows no important sensitivity at 12 hours treatment. Most of cells viability was more than the control DMSO viability, which might be due to that treatment for such short time and low concentrations promoting growth of cells for unknown reasons.

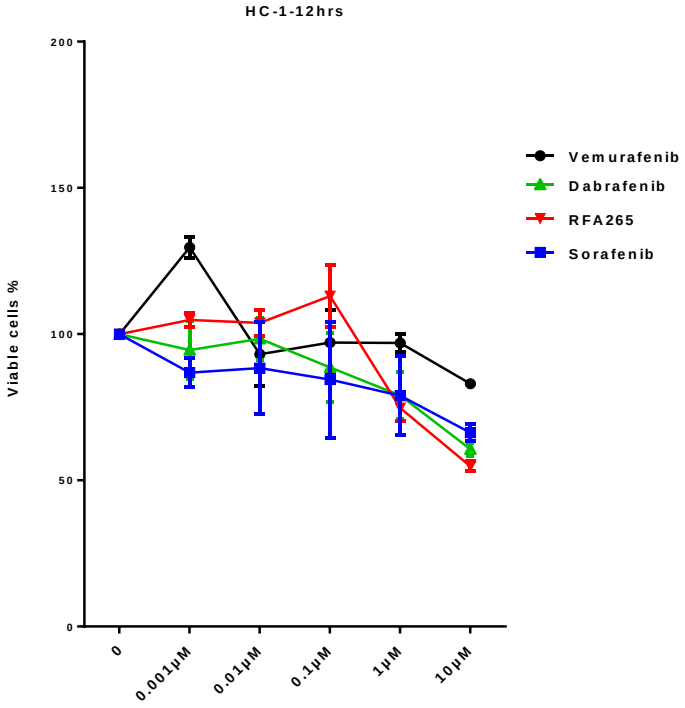


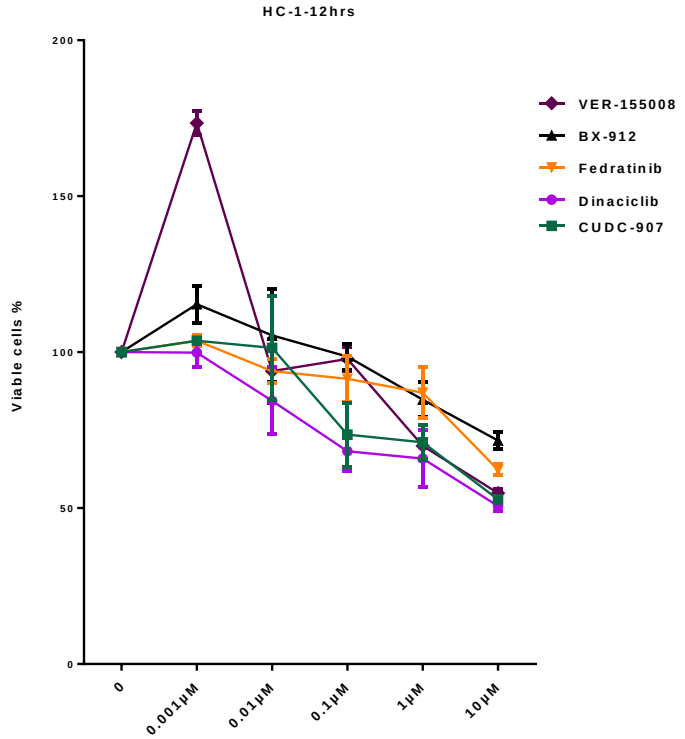

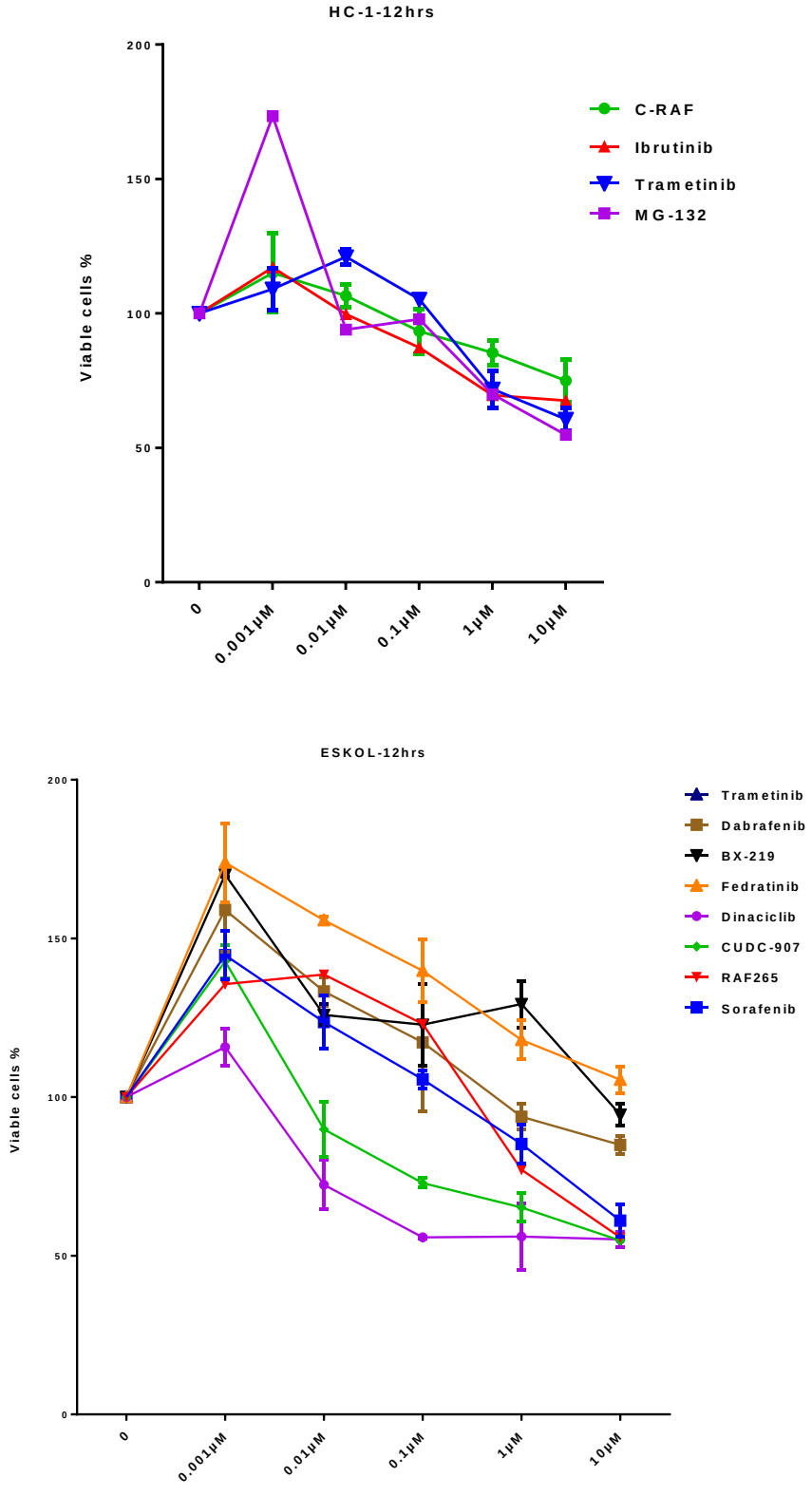


**Figure 3.4 HC-1 (HCL) cell line, and ESKOL cell line treatment for 12 hours viability assay.**

Cells were counted, plated, treated for 12 hours, then MTS reagent were added, after 2-4hours in incubator at 5%CO2 and 37°C , plates were read using plate reader. Concentrations of each inhibitor were 10, 1, 0.1, 0.01, 0.001µM respectively. Y axis shows percentage of viable cells to DMSO control, which was normalised to 100%. X axis shows concentration of inhibitors. Each concentration presented in mean and standard deviation of two biological duplicates and two or three technical triplicates readings per inhibitor.

HC-1 showed no sensitivity at 12 hours treatment to any of the 13 inhibitors tested. In addition, I used only 8 inhibitors for the ESKOL cell line. For technical reasons, fewer inhibitors were used for HC-1 and ESKOL cell lines.

In summary, 12 hours treatment showed no significant decrease in cells viability. Higher concentrations showed reduction in survival, although none reached the IC50. Some cells showed viability more than the control 100% in low concentrations of inhibitors that is either because inhibitors alter cells metabolism rate at short times and lower concentrations, therefore more formazan is produced, or perhaps owing to that inhibitors enhance cells growth at lower concentrations and shorter times. The SIG-M5 cell line was not tested for 12 hours, but were tested at 24 hours.

We next tested the same inhibitors 24 hours after treatment.

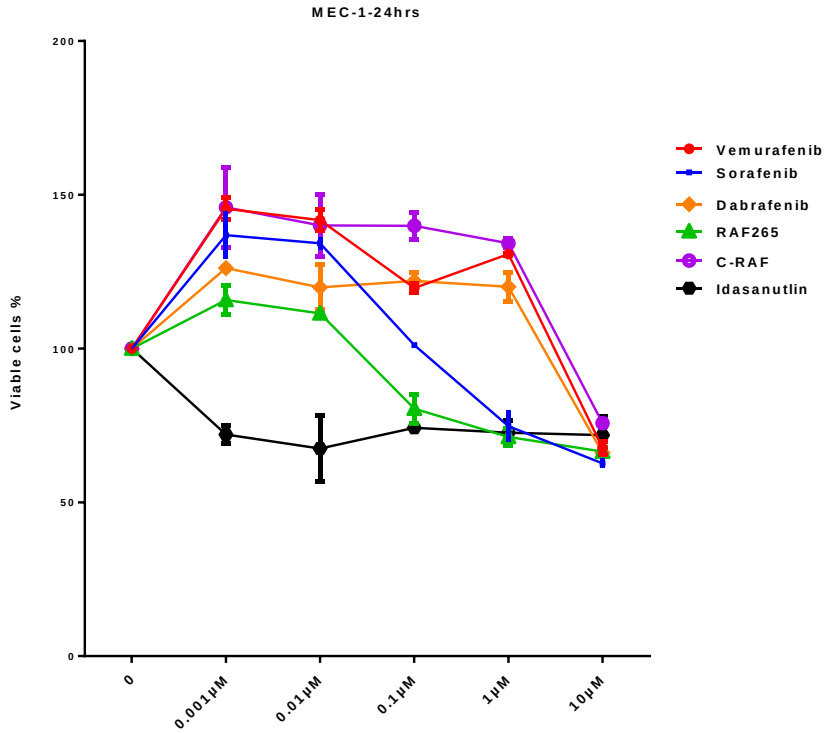

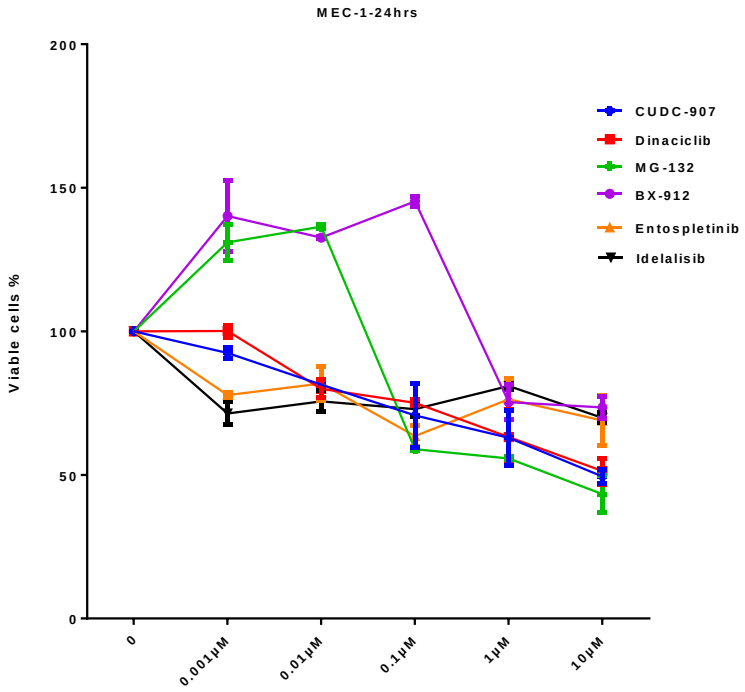
MEC-1-24hrs
Viable cells %
200
150
100
50
0
0
0.001μM
0.01μM
0.1μM
1μM
10μM
CUDC-907
Dinaciclib
MG-132
BX-912
Entospletinib
Idelalisib

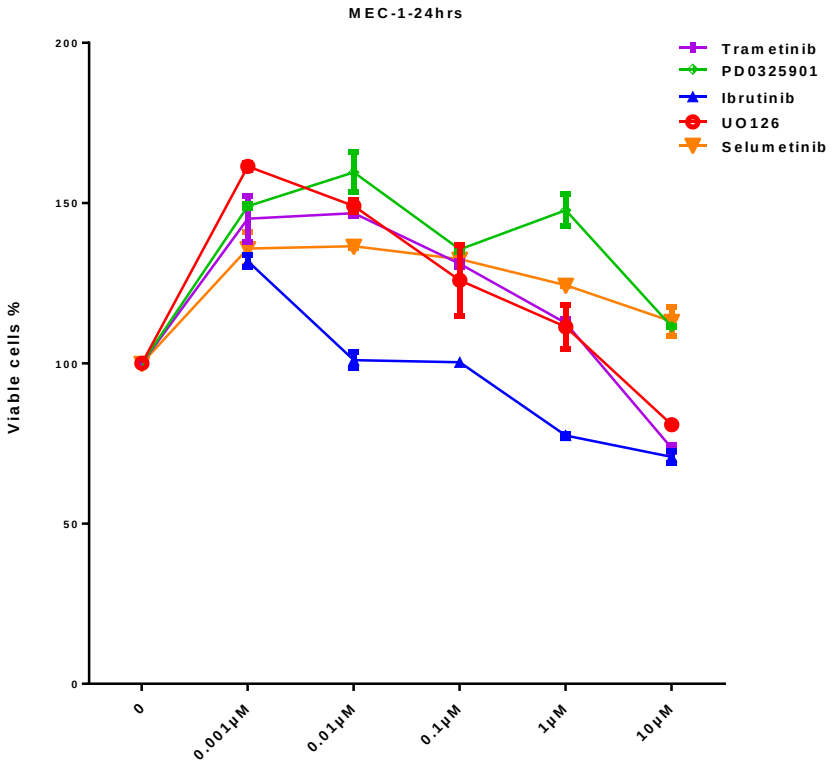
MEC-1-24hrs
Viable cells %
200
150
100
50
0
0
0.001μM
0.01μM
0.1μM
1μM
10μM
Trametinib
PD0325901
Ibrutinib
UO126
Selumetinib

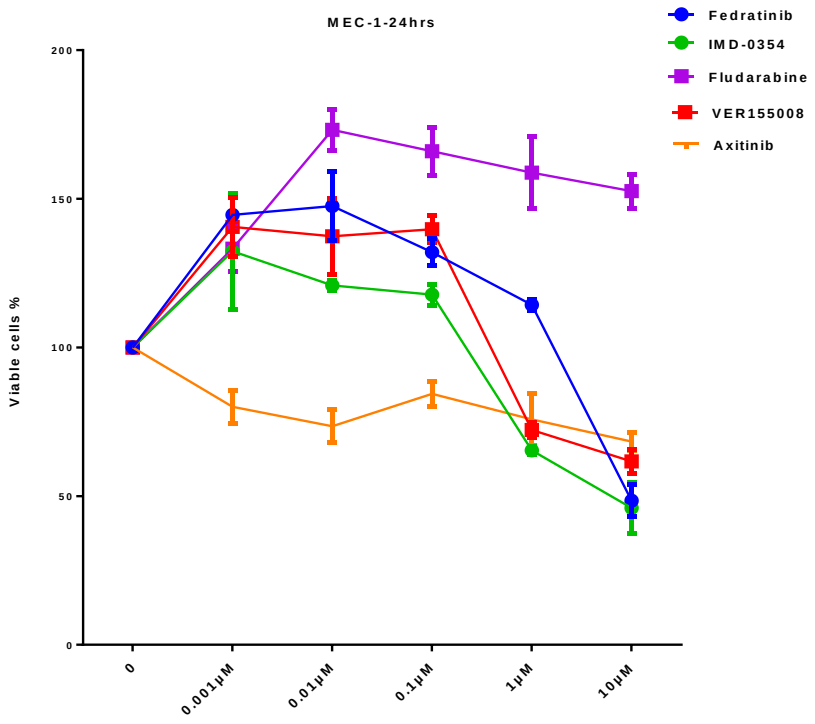


**Figure 3.5 MEC-1 CLL cell line treatment for 24 hours viability assay**

Cells were counted, plated, treated for 24 hours, then MTS reagent were added, after 2-4hours in incubator at 5%CO2 and 37°C , plates were read using plate reader. Concentrations of each inhibitor were 10, 1, 0.1, 0.01, 0.001µM respectively. Y axis shows percentage of viable cells to DMSO control, which was normalised to 100%. X axis shows concentration of inhibitors. Each concentration presented in mean and standard deviation of two biological duplicates and two or three technical triplicates readings per inhibitor.

MEC-1 still showed no sensitivity to most of the 22 inhibitors after 24 hours. However, some inhibitors (CUDC-907, IMD-0354, MG-132, and Fedratinib) showed viability reductions under 50% in high concentrations, such as 10µM.

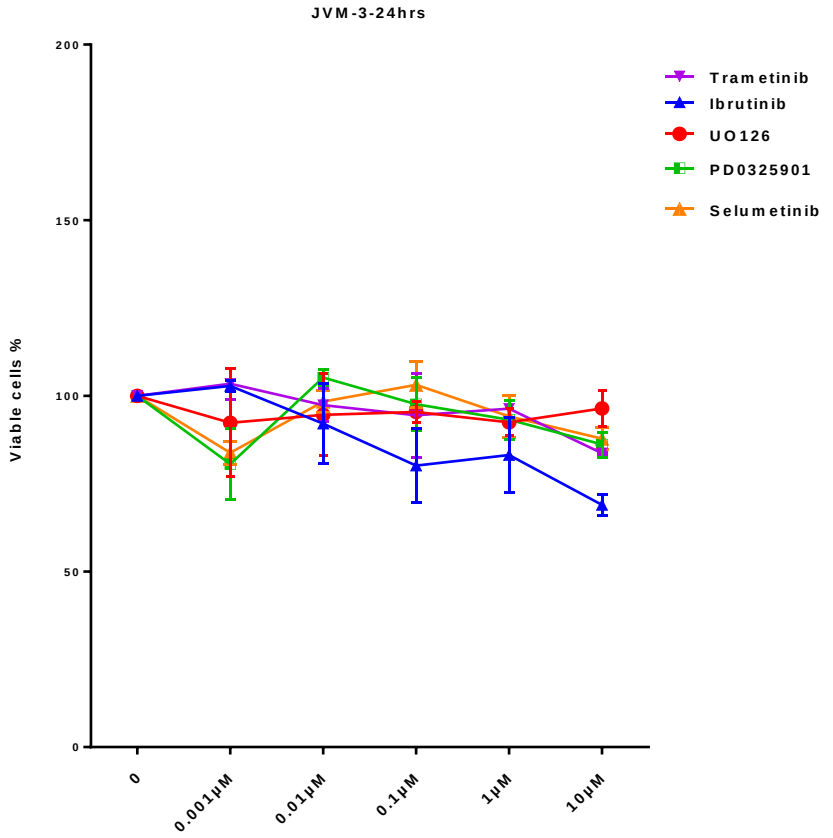
JVM-3-24hrs
Viable cells %
200
150
100
50
0
0
0.001μM
0.01μM
0.1μM
1μM
10μM
Trametinib
Ibrutinib
UO126
PD0325901
Selumetinib

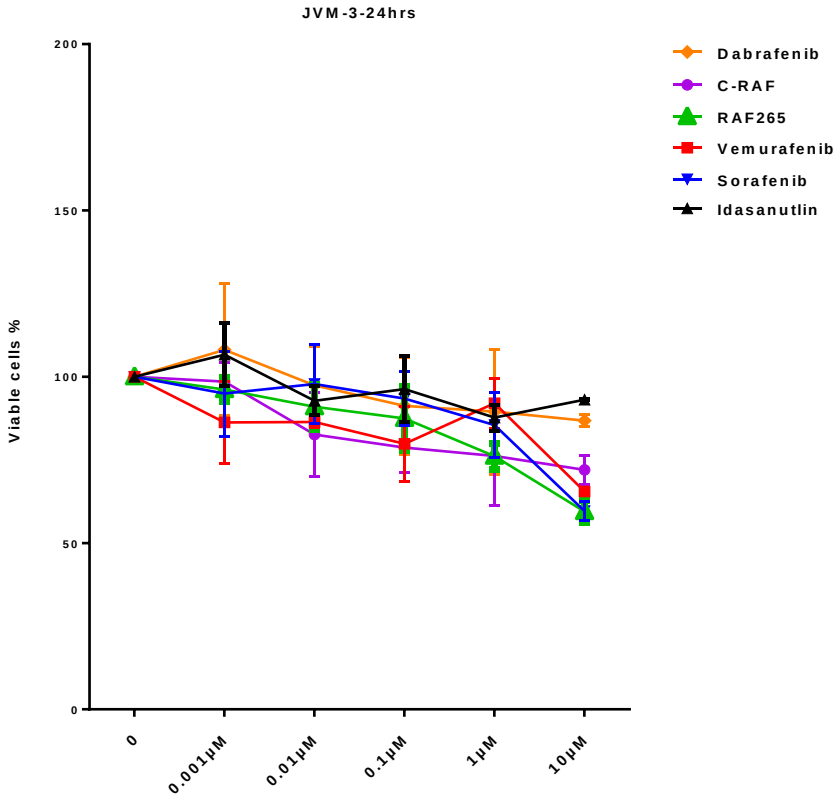
JVM-3-24hrs
Viable cells %
200
150
100
50
0
0
0.001μM
0.01μM
0.1μM
1μM
10μM
Dabrafenib
C-RAF
RAF265
Vemurafenib
Sorafenib
Idasanutlin

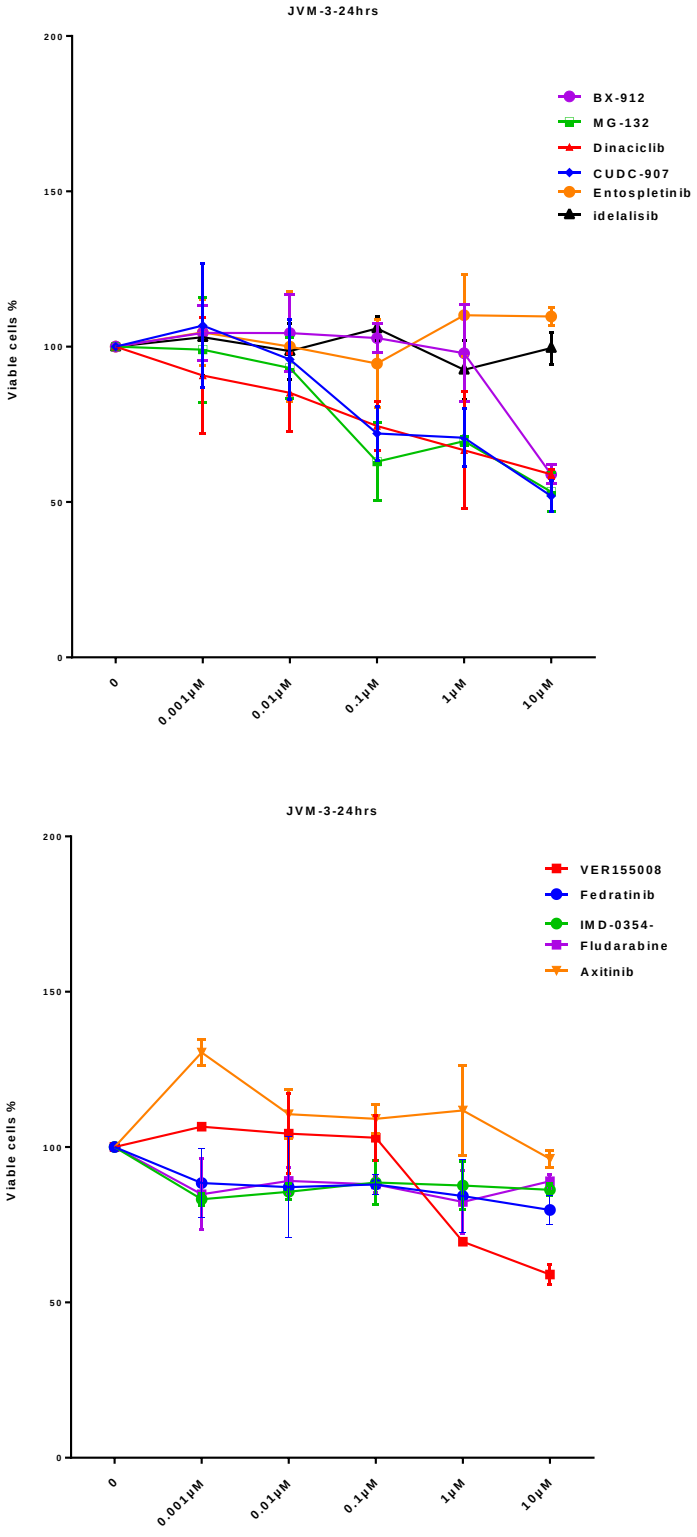


**Figure 3.6 JVM-3 B-PLL cell line treatment for 24 hours viability assay.**

Cells were counted, plated, treated for 24 hours, then MTS reagent were added, after 2-4hours in incubator at 5%CO2 and 37°C , plates were read using plate reader. Concentrations of each inhibitor were 10, 1, 0.1, 0.01, 0.001µM respectively. Y axis shows percentage of viable cells to DMSO control, which was normalised to 100%. X axis shows concentration of inhibitors. Each concentration presented in mean and standard deviation of two biological duplicates and two or three technical triplicates readings per inhibitor.

JVM-3 had no sensitivity to any of 22 inhibitors at 24 hours, which implies that more time of treatment is needed for this cell line to check its sensitivity to all of inhibitors.

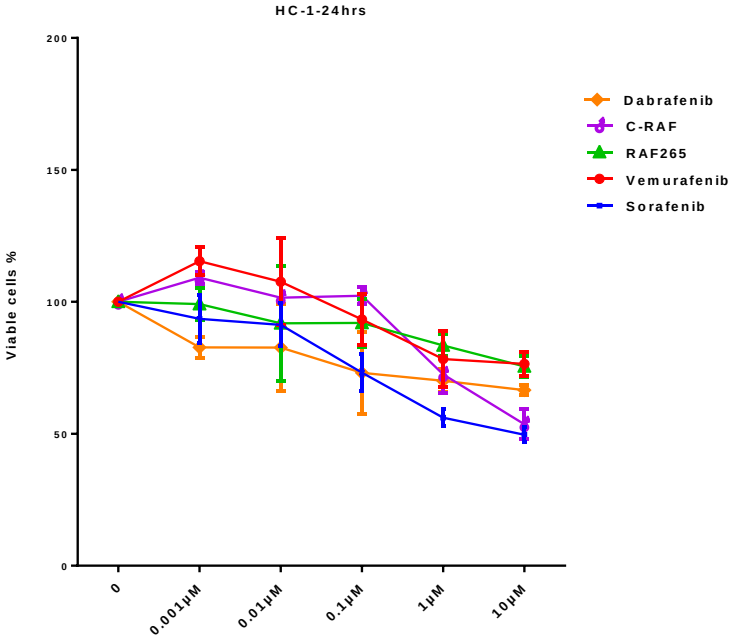


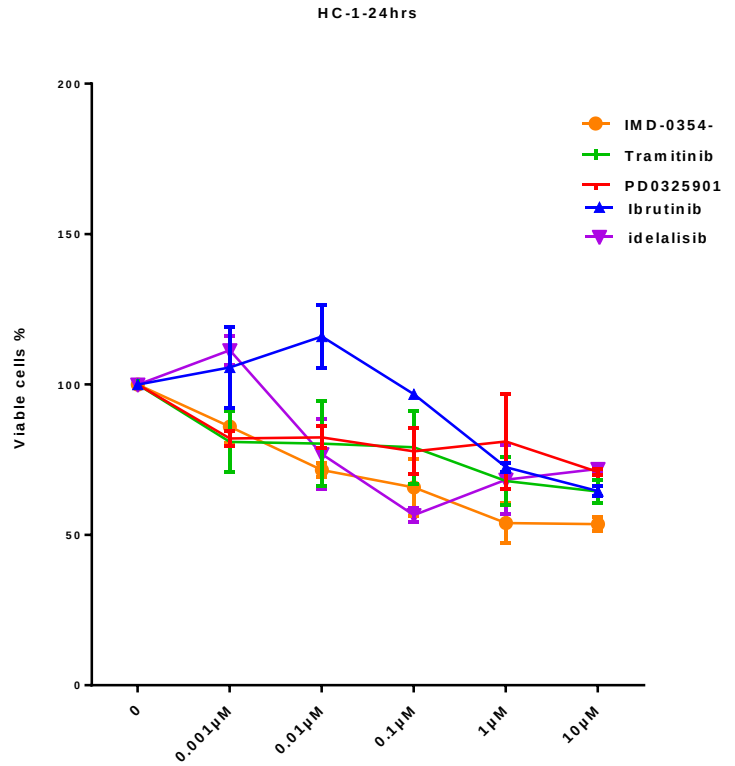

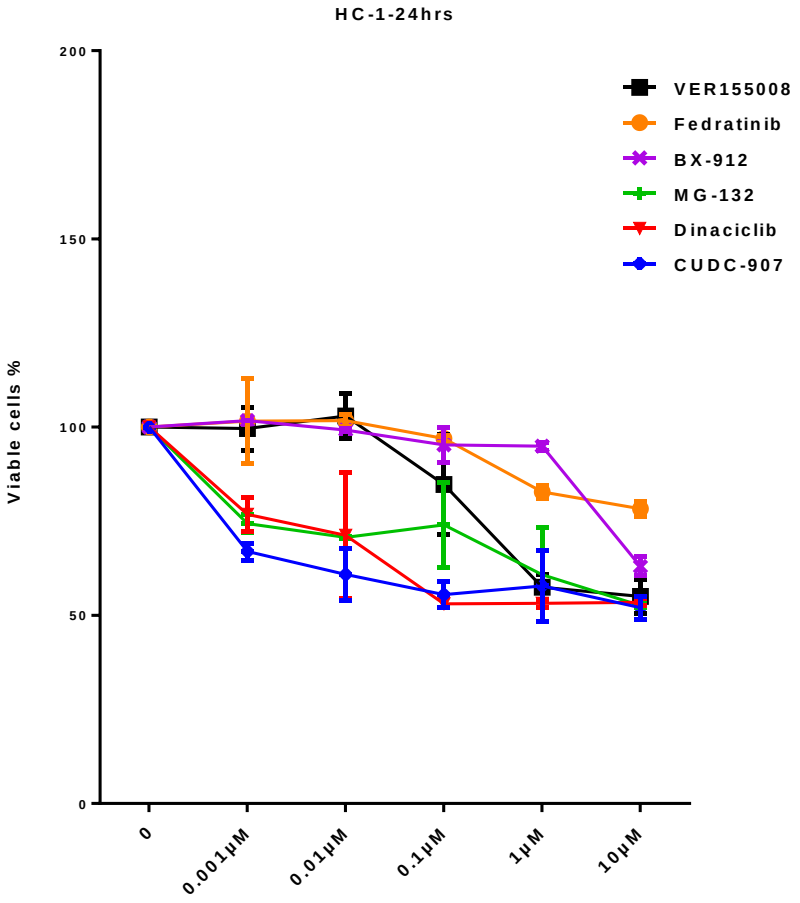


**Figure 3.7 HC-1 HCL cell line treatment for 24 hours viability assay.**

Cells were counted, plated, treated for 24 hours, then MTS reagent were added, after 2-4hours in incubator at 5%CO2 and 37°C , plates were read using plate reader. Concentrations of each inhibitor were 10, 1, 0.1, 0.01, 0.001µM respectively. Y axis shows percentage of viable cells to DMSO control, which was normalised to 100%. X axis shows concentration of inhibitors. Each concentration presented in mean and standard deviation of two biological duplicates and two or three technical triplicates readings per inhibitor.

HC-1 also shows viability over 50% in 24 hours treatment. Therefore, more treatment time is needed for this cell line as well.

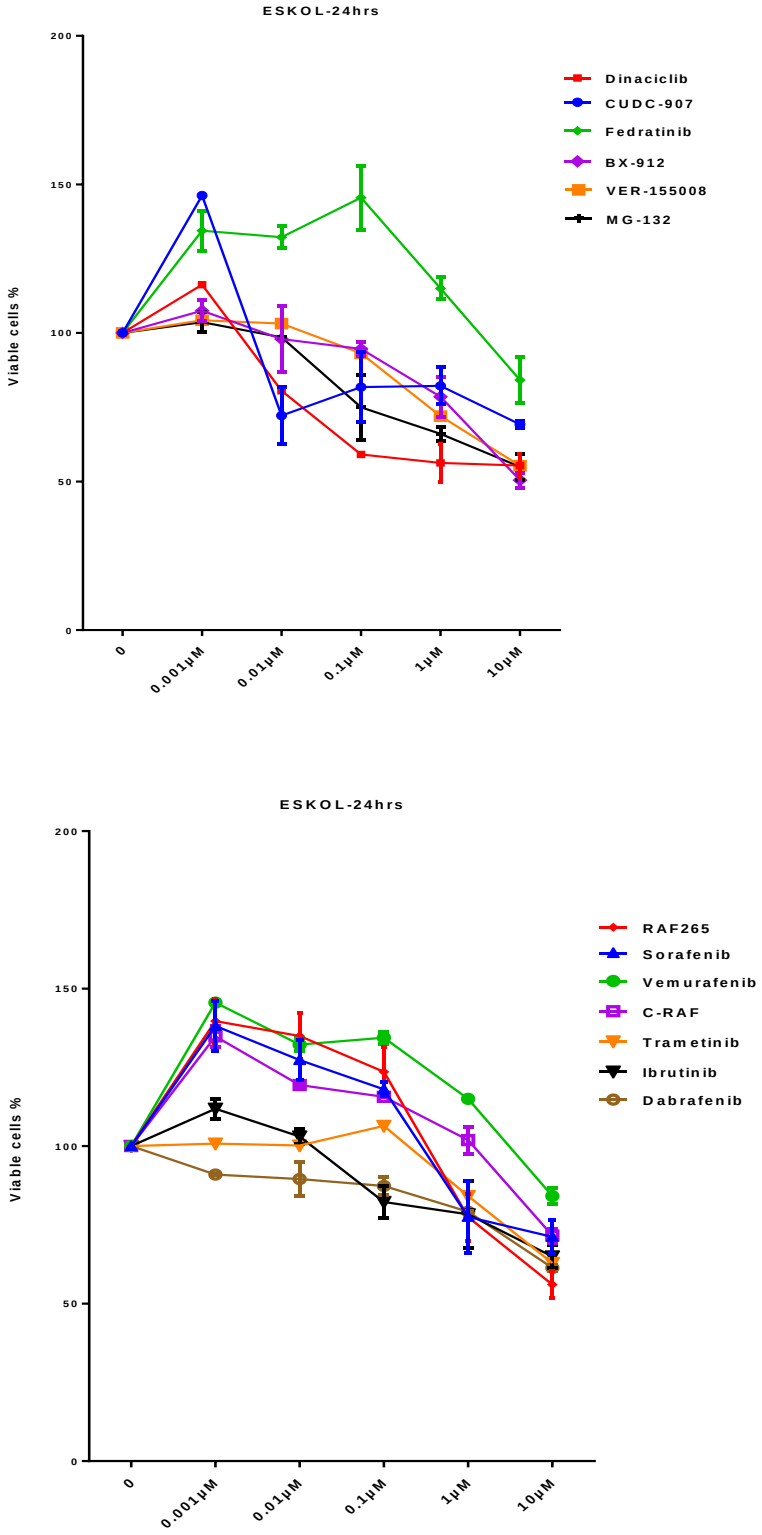


**Figure 3.8 ESKOL HCL cell line treatment for 24 hours viability assay**.

Cells were counted, plated, treated for 24 hours, then MTS reagent were added, after 2-4hours in incubator at 5%CO2 and 37°C , plates were read using plate reader. Concentrations of each inhibitor were 10, 1, 0.1, 0.01, 0.001µM respectively. Y axis shows percentage of viable cells to DMSO control, which was normalised to 100%. X axis shows concentration of inhibitors. Each concentration presented in mean and standard deviation of two biological duplicates and two or three technical triplicates readings per inhibitor.

The ESKOL cell line was screened for 24 hours with 13 inhibitors, and viability was not reduced under 50%.

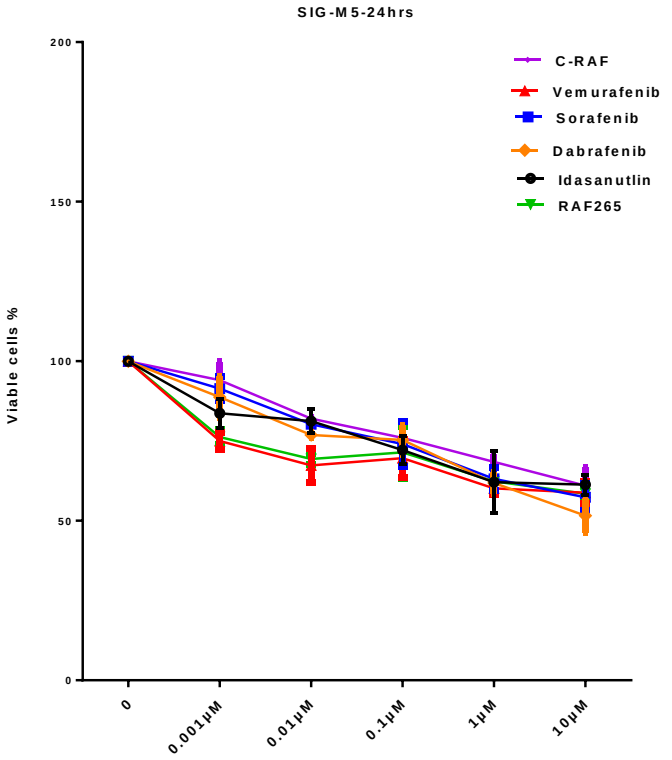


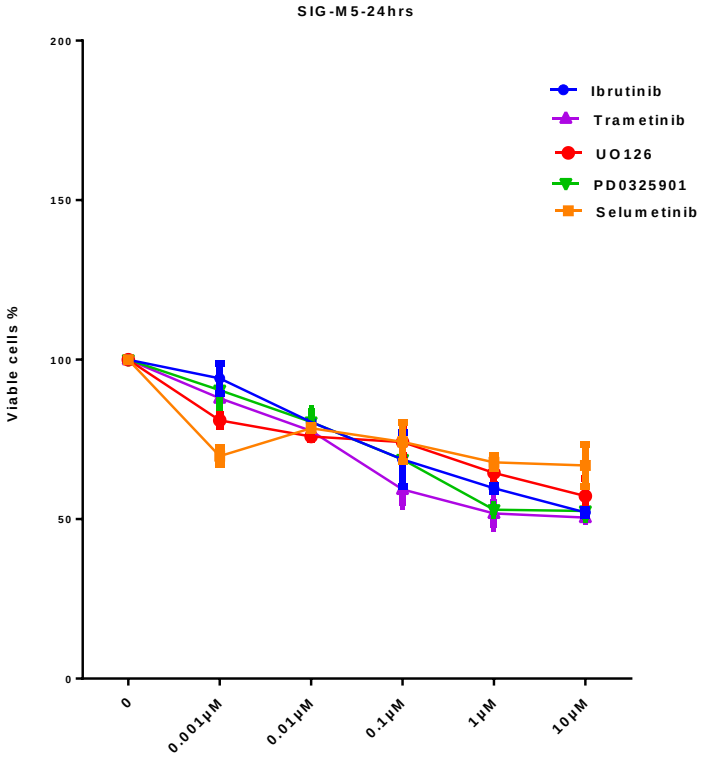

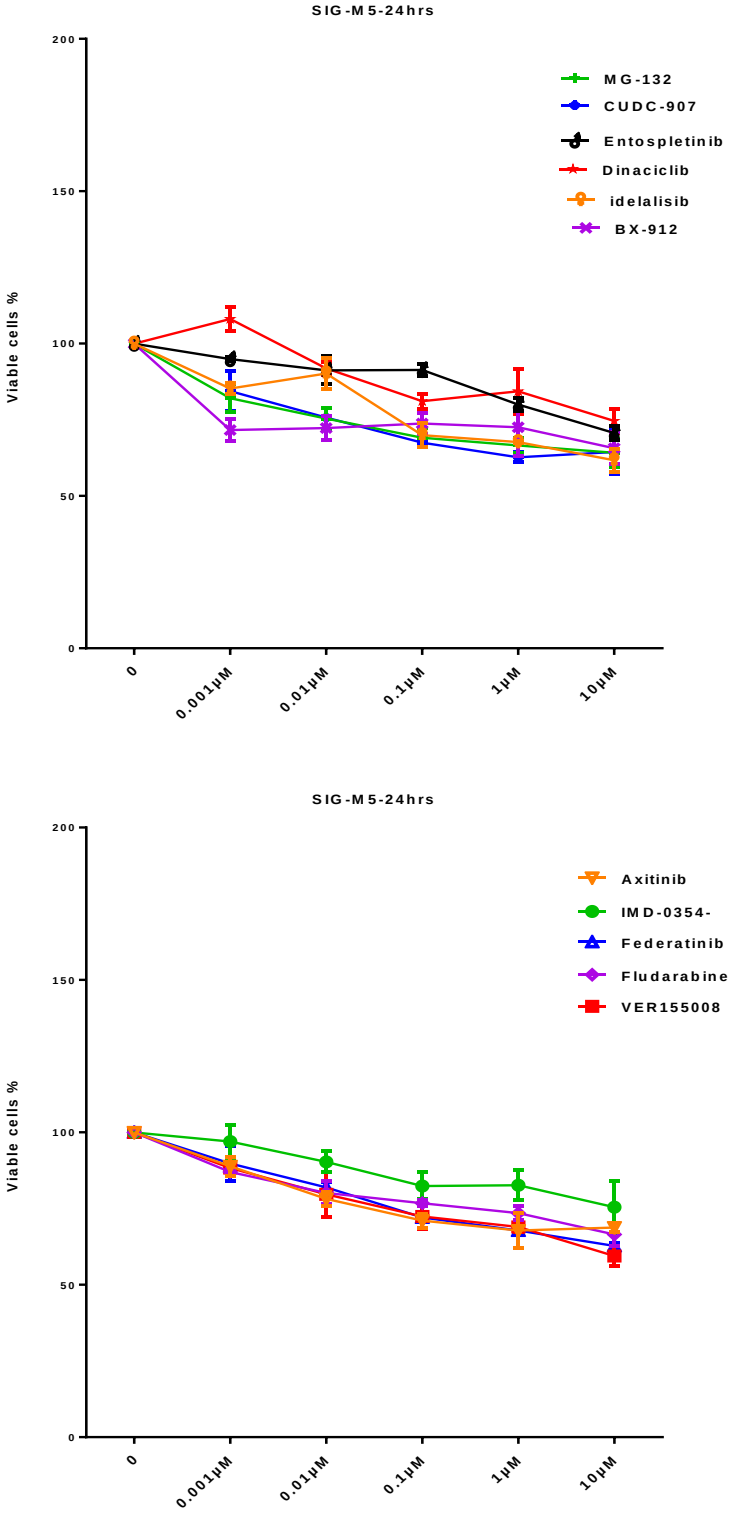


**Figure 3.9 SIG-M5 AML cell line treatment for 24 hours viability assay.**

Cells were counted, plated, treated for 24 hours, then MTS reagent were added, after 2-4hours in incubator at 5%CO2 and 37°C , plates were read using plate reader. Concentrations of each inhibitor were 10, 1, 0.1, 0.01, 0.001µM respectively. Y axis shows percentage of viable cells to DMSO control, which was normalised to 100%. X axis shows concentration of inhibitors. Each concentration presented in mean and standard deviation of two biological duplicates and two or three technical triplicates readings per inhibitor.

SIG-M5 did not show any sensitivity to 24 hours treatment either.

In summary, all five cell lines showed no sensitivity below 50% survival to any of the drugs tested at 24 hours. Only MEC-1 showed decrease in viability below 50% at 10μM of the following inhibitors: - 46% IMD-0354, 49.4% CUDC-907, 48% Fedratinib, and 43% MG-132. MG-132 is a proteasome inhibitor, consequently it is effective in short times. CUDC- 907 is a dual HDAC, and PI3K inhibitor, Fedratinib is JAK/STAT and IMD-0354 is NF-κB inhibitor. They are potent inhibitors at high concentrations in short times. JVM-3 and SIG-M5 showed no major decrease in viability to all 22 inhibitors, yet no major increase in viability at lower inhibitor concentrations except (JVM-3 with 1nM axitinib, VER-155008). ESKOL and, HC-1 showed no notable decrease either to 13 or 16 inhibitors that were tested correspondingly.

We next tested the same inhibitors after 48 hours of treatment.

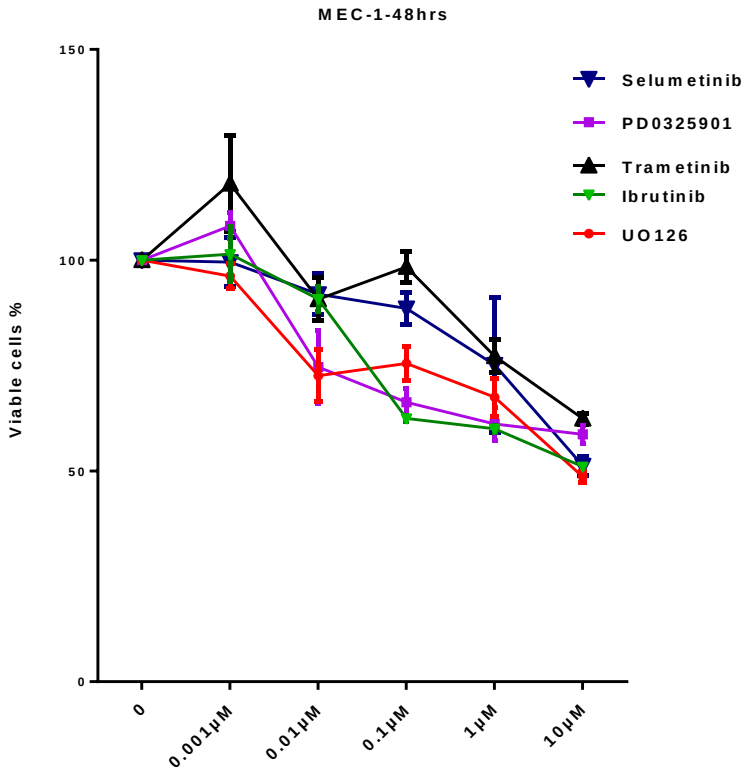


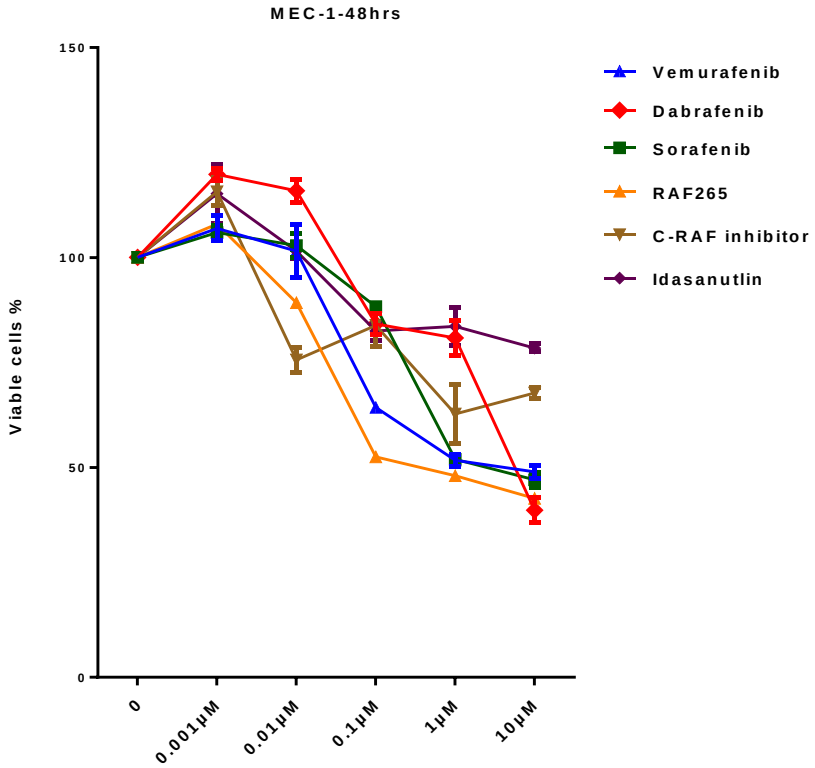

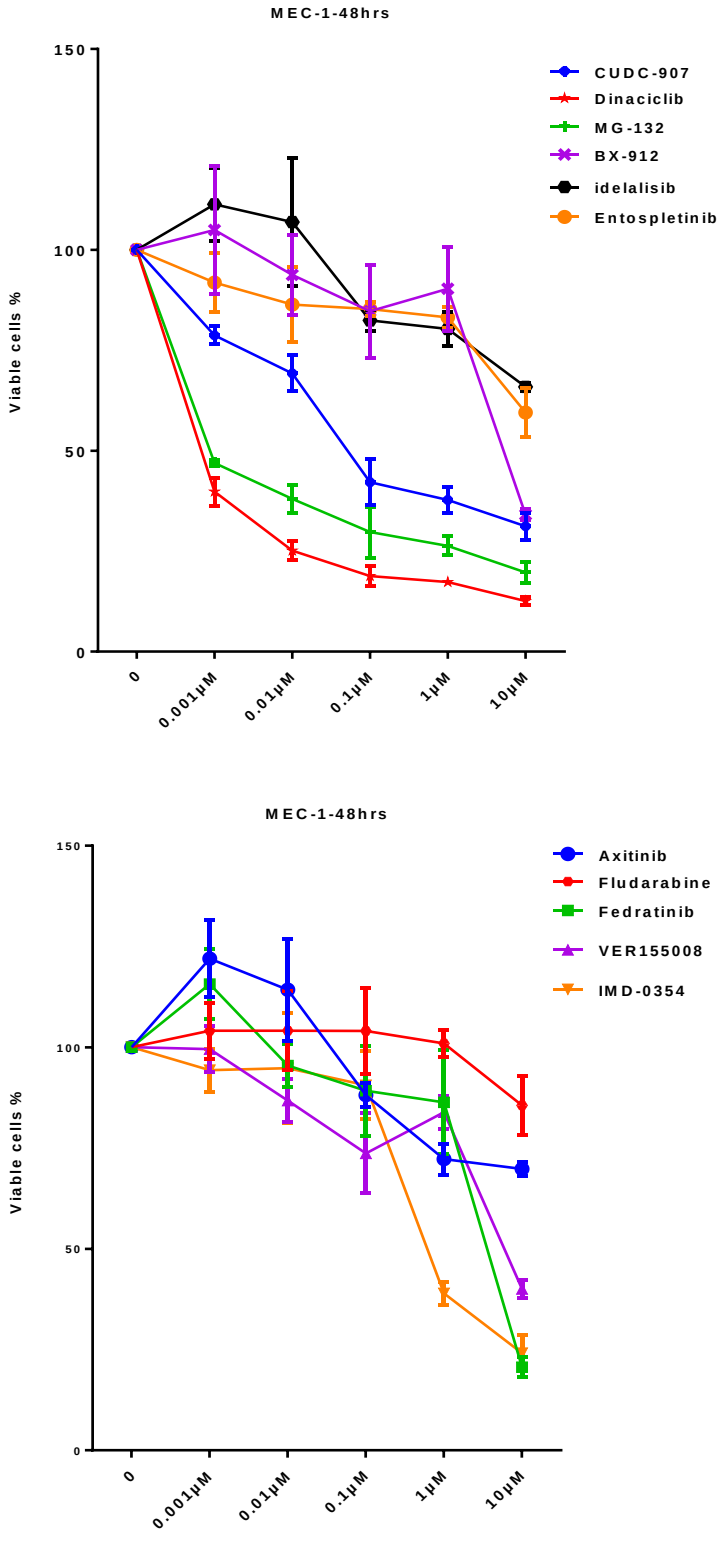


**Figure 3.10 MEC-1 CLL cell line treatment for 48 hours viability assay.**

Cells were counted, plated, treated for 48 hours, then MTS reagent were added, after 2-4hours in incubator at 5%CO2 and 37°C , plates were read using plate reader. Concentrations of each inhibitor were 10, 1, 0.1, 0.01, 0.001µM respectively. Y axis shows percentage of viable cells to DMSO control, which was normalised to 100%. X axis shows concentration of inhibitors. Each concentration presented in mean and standard deviation of two biological duplicates and two or three technical triplicates readings per inhibitor.

MEC-1 showed sensitivity to most of 22 inhibitors when treated for 48 hours, especially at high concentrations. MEK1/2 inhibitors PD0325901, selumetinib, and trametinib showed insignificant reduction in MEC-1 cells viability, except for UO126 at 10µM. Among RAF/BRAF inhibitors at 10µM concentration, dabrafenib inhibits cells viability to 39%, sorafenib to 47%, vemurafenib to 48.9%, and RAF265 to 42%.

Ineffective viability inhibition was noticed with CRAF inhibitor, ibrutinib, axitinib, idelalisib, entospletinib, fludarabine and idasanutlin.

Effective viability inhibition was achieved by Dinaciclib, and MG-132 at all five concentrations. In addition, at 10µM, BX-912, fedratinib, and VER-155008 showed decrease in viability to 34%, 20%, and 40% respectively. At 10, 1, and 0.1µM, CUDC-907, and at 10, 1µM IMD-0354 showed less than 50% reduction in cells viability. In short, MEC-1 cell line showed sensitivity not only to higher concentrations of inhibitors, but also to lower concentrations of CDK inhibitor dinaciclib, and proteasome inhibitor MG-132.

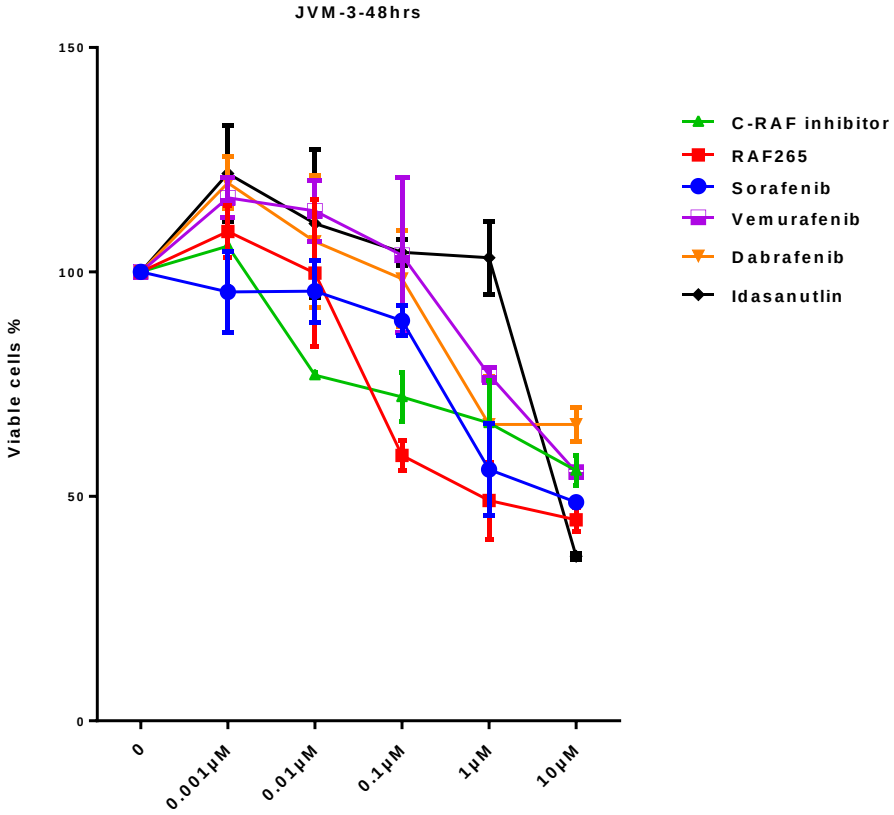
JVM-3-48hrs
Viable cells %
150
100
50
0
0
0.001μM
0.01μM
0.1μM
1μM
10μM
C-RAF inhibitor
RAF265
Sorafenib
Vemurafenib
Dabrafenib
Idasanutlin

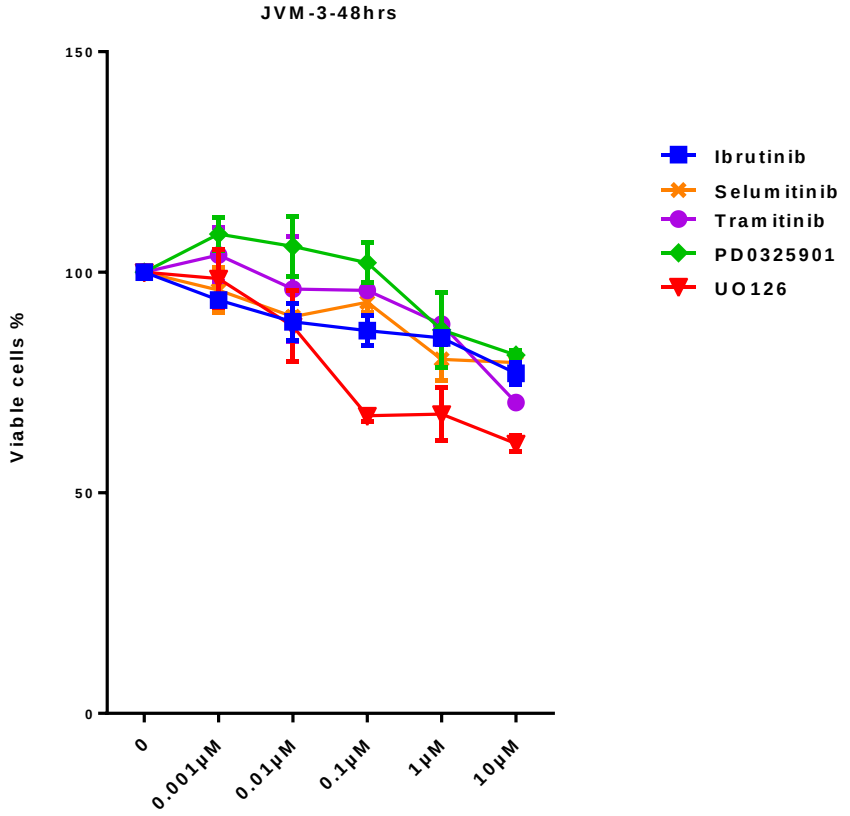
JVM-3-48hrs
Viable cells %
150
100
50
0
0
0.001μM
0.01μM
0.1μM
1μM
10μM
Ibrutinib
Selumitinib
Tramitinib
PD0325901
UO126

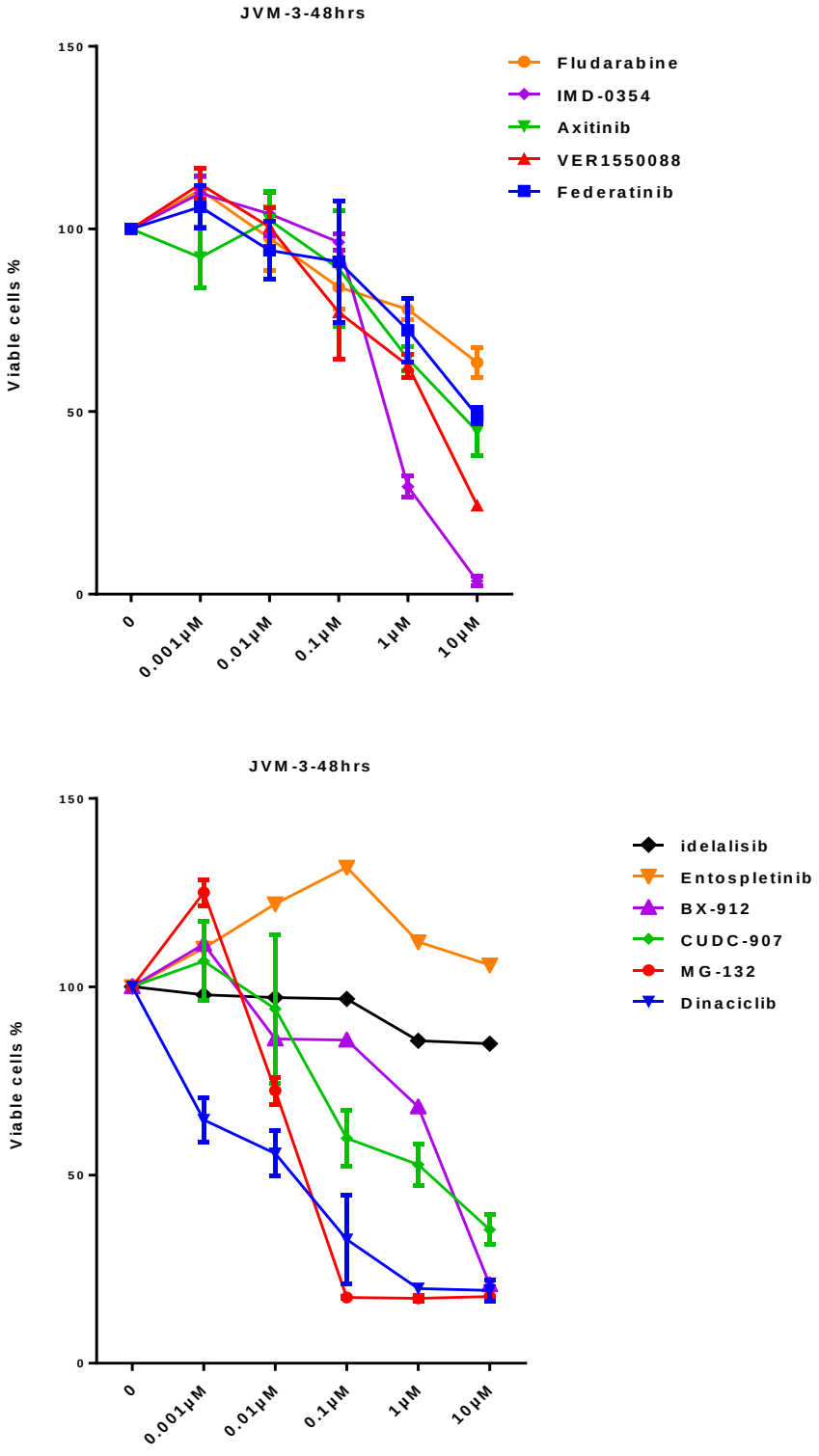


**Figure 3.11 JVM3 B-PLL cell line treatment for 48 hours viability assay.**

Cells were counted, plated, treated for 48 hours, then MTS reagent were added, after 2-4hours in incubator at 5%CO2 and 37°C , plates were read using plate reader. Concentrations of each inhibitor were 10, 1, 0.1, 0.01, 0.001µM respectively. Y axis shows percentage of viable cells to DMSO control, which was normalised to 100%. X axis shows concentration of inhibitors. Each concentration presented in mean and standard deviation of two biological duplicates and two or three technical triplicates readings per inhibitor.

The JVM-3 cell line showed no sensitivity to MAPK inhibition, except for RAF265 (44.7%) and sorafenib (48.9%) at 10µM only. Dinaciclib and MG-132 at 10, 1, 0.1µM, IMD-0354 at 10, and 1µM were reducing cells viability <50%.

At 10µM concentration, viability of cells was reduced to 35% (CUDC-907), 20.8% (BX-912), 48.9% (fedratinib), 24% (VER-155008), 36.5% (idasanutlin), and 44.5% (axitinib). Ineffective viability inhibition was noticed with ibrutinib, vemurafenib, CRAF inhibitor, UO126, PD0325901, trametinib, selumetinib, dabrafenib, idelalisib, entospletinib, and fludarabine.

To sum up, JVM-3 showed sensitivity to CDK inhibitor dinaciclib, and proteasome inhibitor MG-132 even at low concentrations, but most of inhibitors were effective in reducing cells viability at 10µM, which is above physiologically relevant levels.

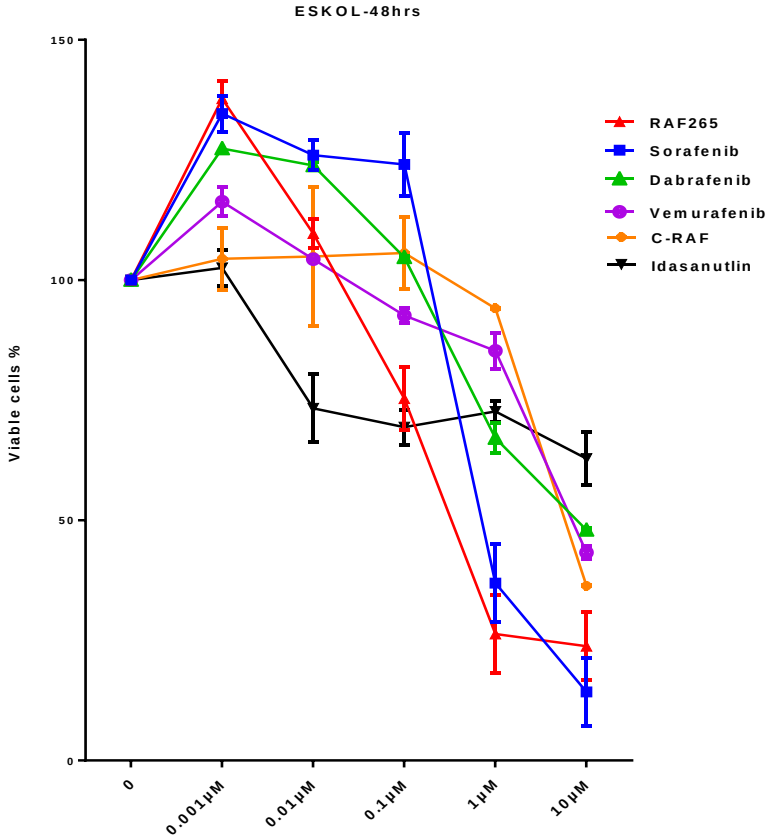

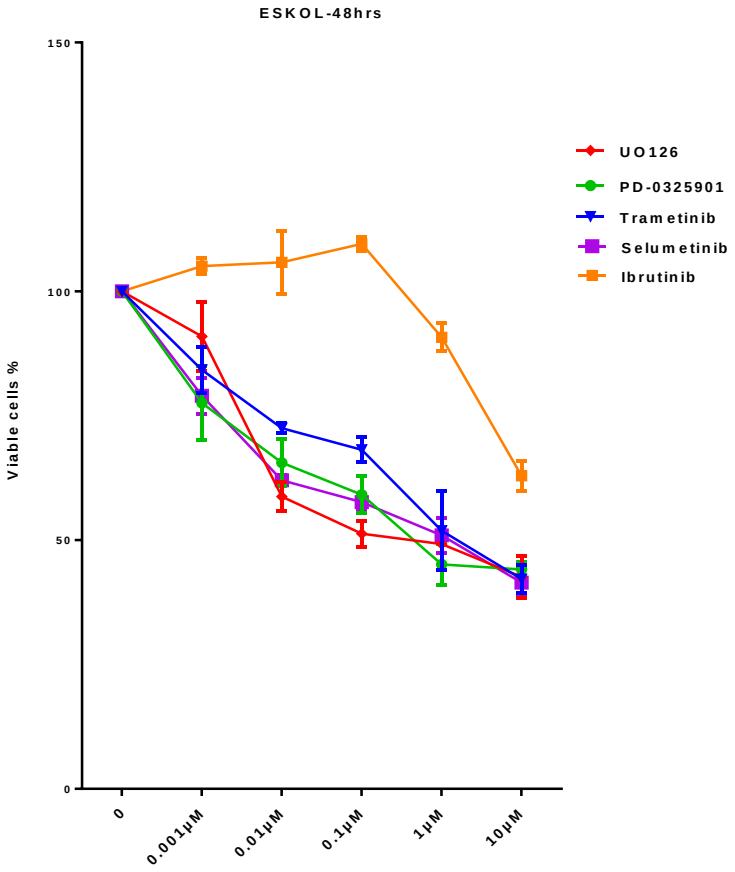
ESKOL-48hrs
Viable cells %
150
100
50
0
0
0.001µM
0.01µM
0.1µM
1µM
10µM
UO126
PD-0325901
Trametinib
Selumetinib
Ibrutinib

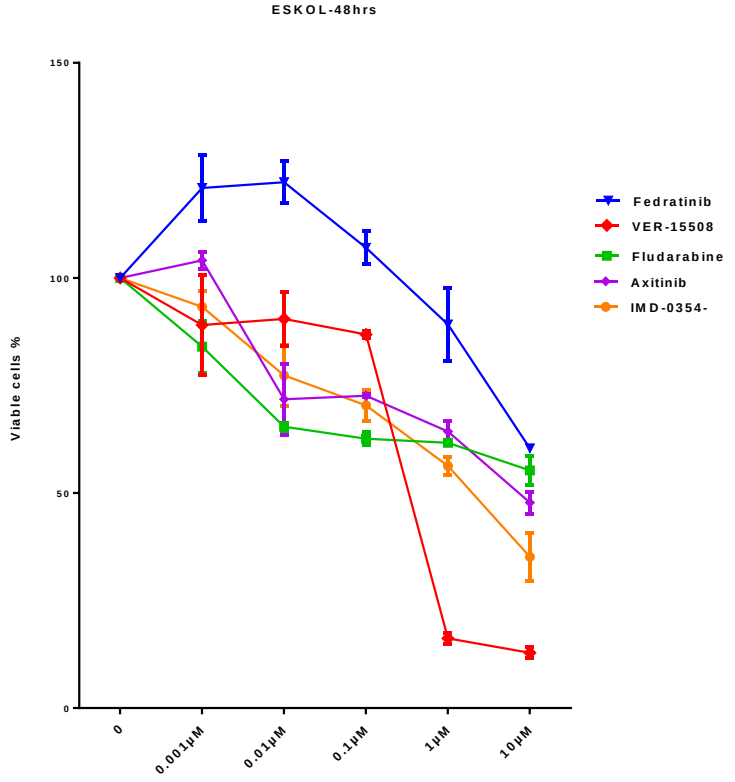
ESKOL-48hrs
Viable cells %
150
100
50
0
0
0.001µM
0.01µM
0.1µM
1µM
10µM
Fedratinib
VER-15508
Fludarabine
Axitinib
IMD-0354-

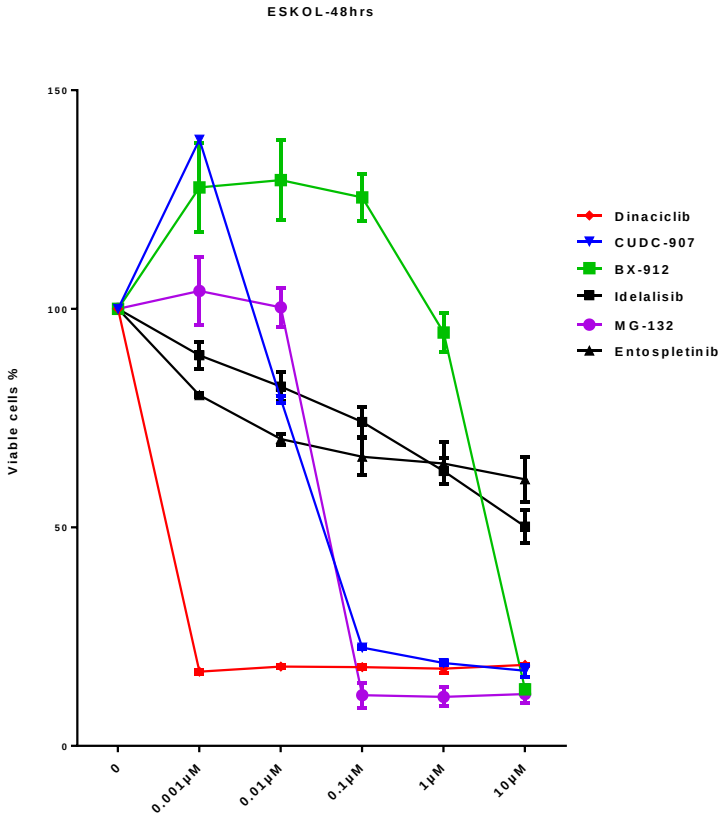


**Figure 3.12 ESKOL HCL cell line treatment for 48 hours viability assay.**

Cells were counted, plated, treated for 48 hours, then MTS reagent were added, after 2-4hours in incubator at 5%CO2 and 37°C , plates were read using plate reader. Concentrations of each inhibitor were 10, 1, 0.1, 0.01, 0.001µM respectively. Y axis shows percentage of viable cells to DMSO control, which was normalised to 100%. X axis shows concentration of inhibitors. Each concentration presented in mean and standard deviation of two biological duplicates and two or three technical triplicates readings per inhibitor.

ESKOL viability after 48 hours treatment was reduced to less than 20% with all five dinaciclib concentrations. At 10, 1, 0.1µM concentrations the viability of ESKOL cells was 17%, 18%, 22% with CUDC-907, and reduced sharply to 11.8%, 11.2%, 11.6% with MG-132. At 10, and 1µM concentrations, viability was reduced to 14%, and 36% with sorafenib, 23%, and 26% with RAF265, 12%, and 16% with VER-155008, 42.2%, 49% with UO126, and to 44%, and 45% with PD0325901, respectively.

At 10µM the following reduced ESKOL cells viability: BX-912 to 12.9%, dabrafenib to 48%, trametinib to 42%, vemurafenib to 43%, CRAF inhibitor to 36%, selumetinib to 41.4%, axitinib to 47.7%, and IMD-0354 to 35%.

Ineffective viability inhibition was noticed with fedratinib, ibrutinib, fludarabine, entospletinib, idelalisib, and idasanutlin. In brief, ESKOL cells showed great sensitivity to dinaciclib, MG-132, and CUDC-907. In addition, viabilities of ESKOL cells were reduced significantly with high concentrations of sorafenib, RAF265, BX-912, CRAF inhibitor and VER-155008.

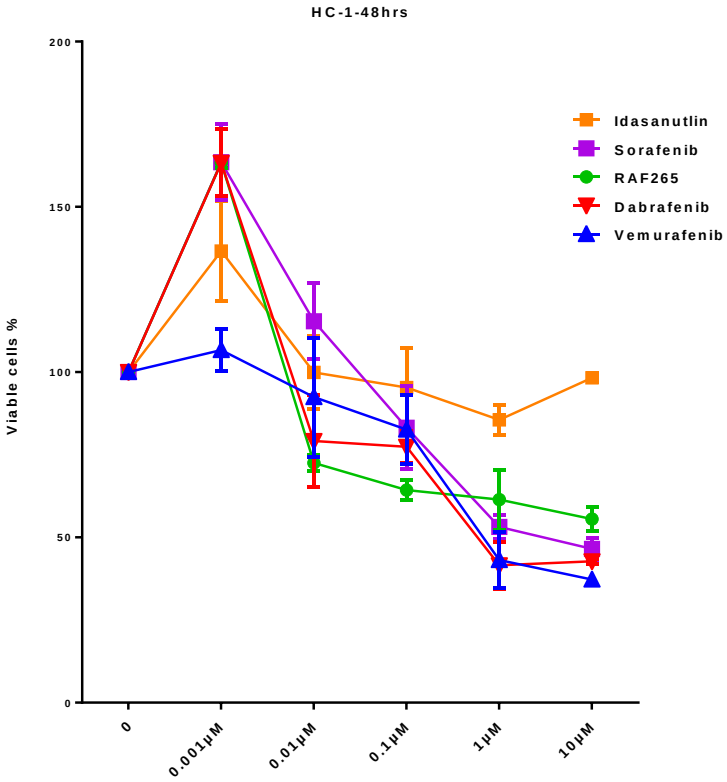
HC-1-48hrs
Viable cells %
200
150
100
50
0
0
0.001μM
0.01μM
0.1μM
1μM
10μM
Idasanutlin
Sorafenib
RAF265
Dabrafenib
Vemurafenib

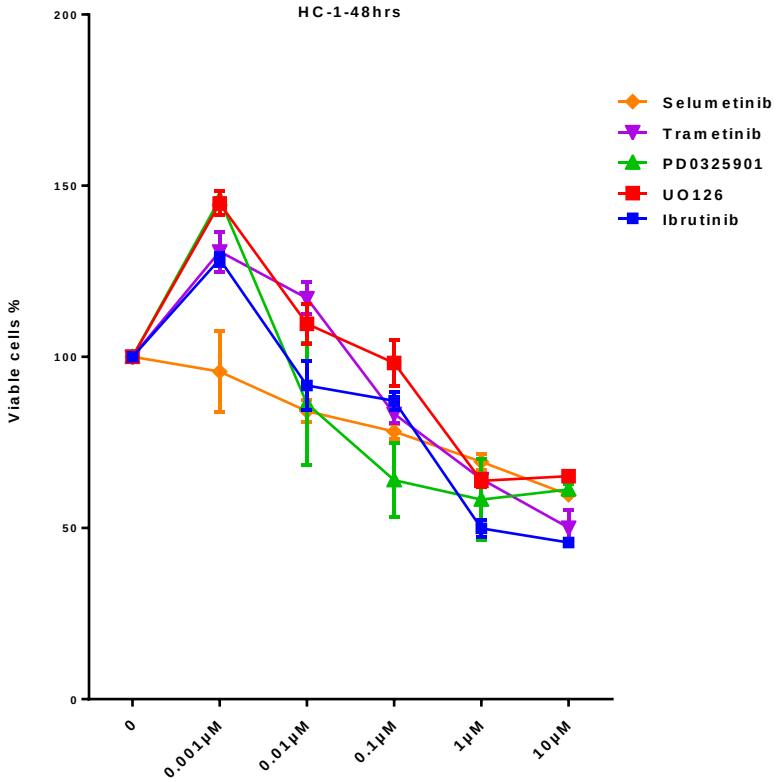
HC-1-48hrs
Viable cells %
200
150
100
50
0
0
0.001μM
0.01μM
0.1μM
1μM
10μM
Selumetinib
Trametinib
PD0325901
UO126
Ibrutinib

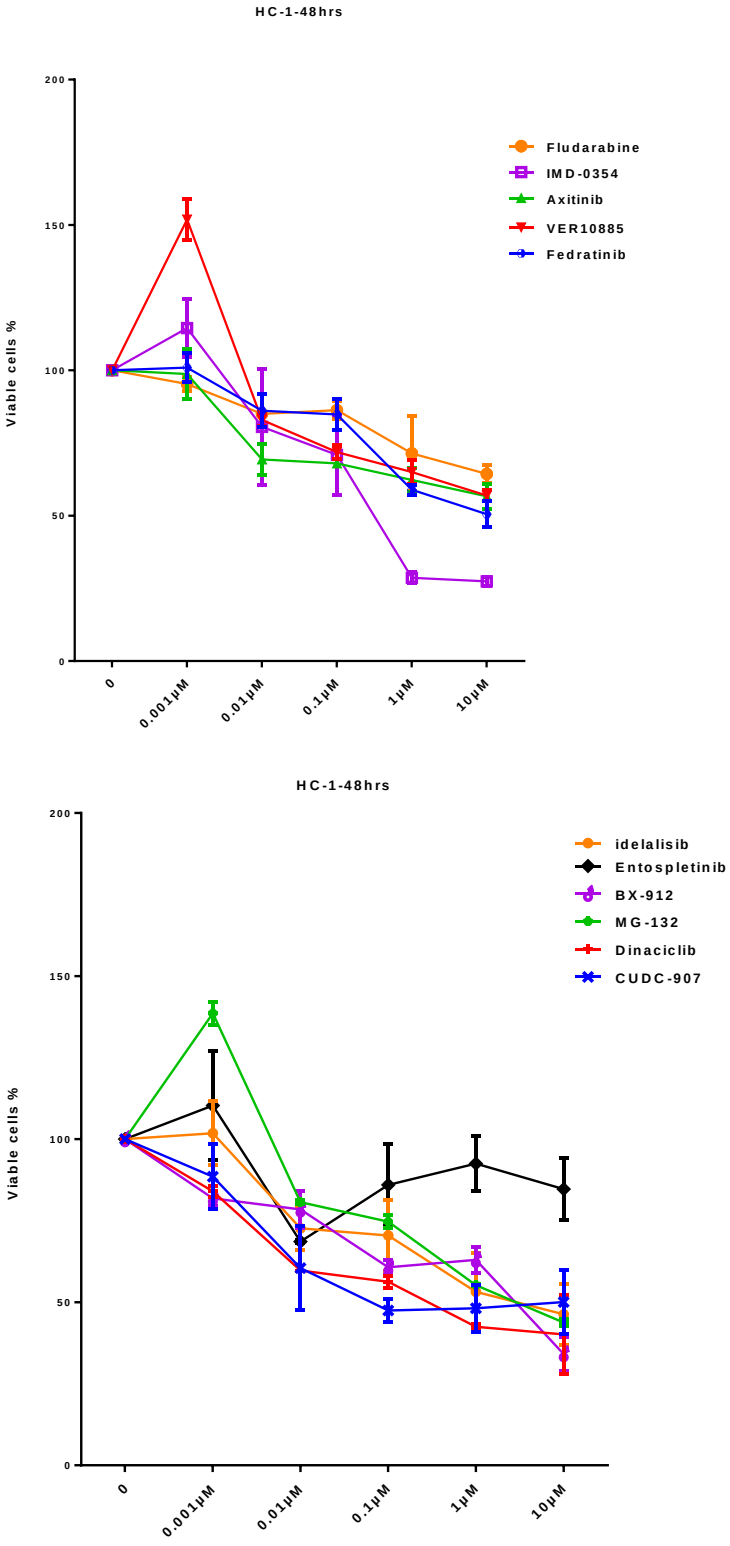


**Figure 3.13 HC-1 HCL cell line treatment for 48 hours viability assay.**

Cells were counted, plated, treated for 48 hours, then MTS reagent were added, after 2-4hours in incubator at 5%CO2 and 37°C , plates were read using plate reader. Concentrations of each inhibitor were 10, 1, 0.1, 0.01, 0.001µM respectively. Y axis shows percentage of viable cells to DMSO control, which was normalised to 100%. X axis shows concentration of inhibitors. Each concentration presented in mean and standard deviation of two biological duplicates and two or three technical triplicates readings per inhibitor.

HC-1 viability was reduced at 10 and 1µM of the following: vemurafenib (37% and 43%), dabrafenib (42% and 41%), ibrutinib (45% and 49.8%), CRAF inhibitor (39% and 41.6%), IMD-0354 (27.39% and 28.6%), and dinaciclib (40% and 42.1%).

Also at 10µM: sorafenib (46.5%), MG-132 (34.1%), BX-912 (34%), and idelalisib (46.2%). Ineffective viability inhibition with RAF265, UO126, PD0325901, trametinib, selumetinib, CUDC-907, VER-155008, fedratinib, entospletinib, idasanutlin, axitinib, and fludarabine.

In short, HC-1 response was different from ESKOL cells, though both are HCL cell lines. HC-1 cells viability were mostly reduced by inhibitors at higher concentration and with IMD-0354.

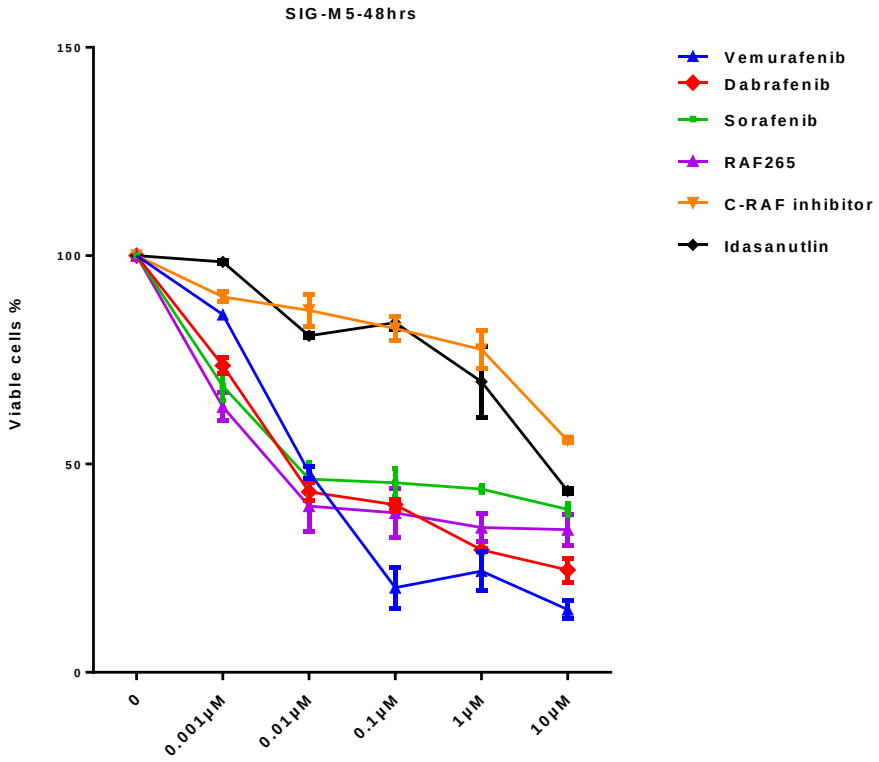

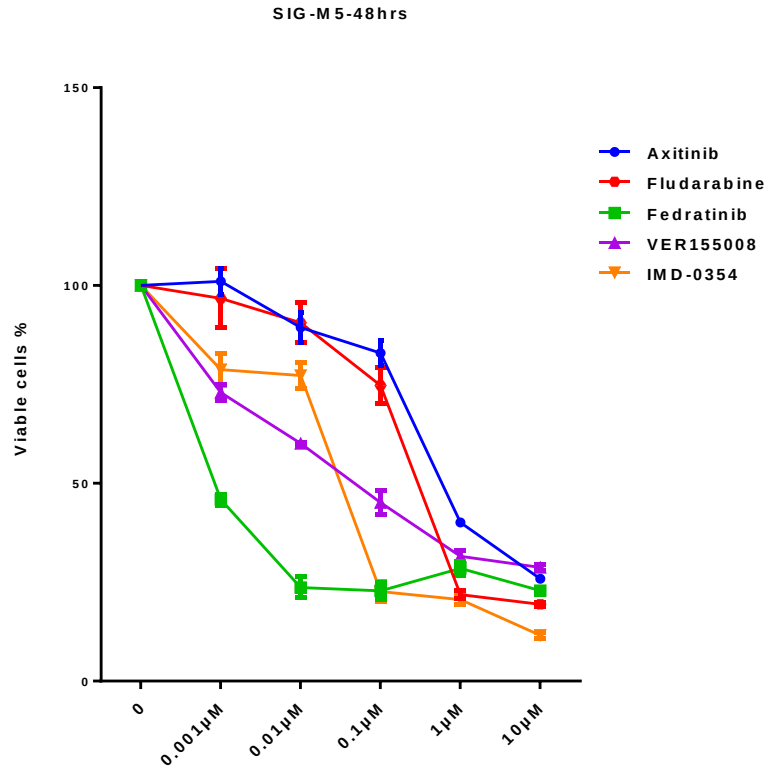
SIG-M5-48hrs
Viable cells %
150
100
50
0
0
0.001µM
0.01µM
0.1µM
1µM
10µM
Axitinib
Fludarabine
Fedratinib
VER155008
IMD-0354

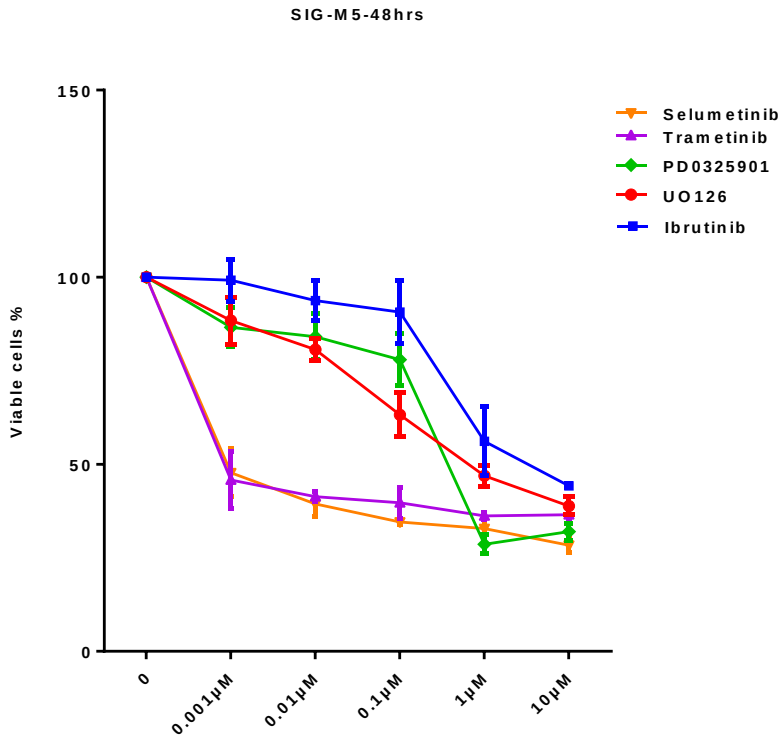
SIG-M5-48hrs
Viable cells %
150
100
50
0
0
0.001µM
0.01µM
0.1µM
1µM
10µM
Selumetinib
Trametinib
PD0325901
UO126
Ibrutinib

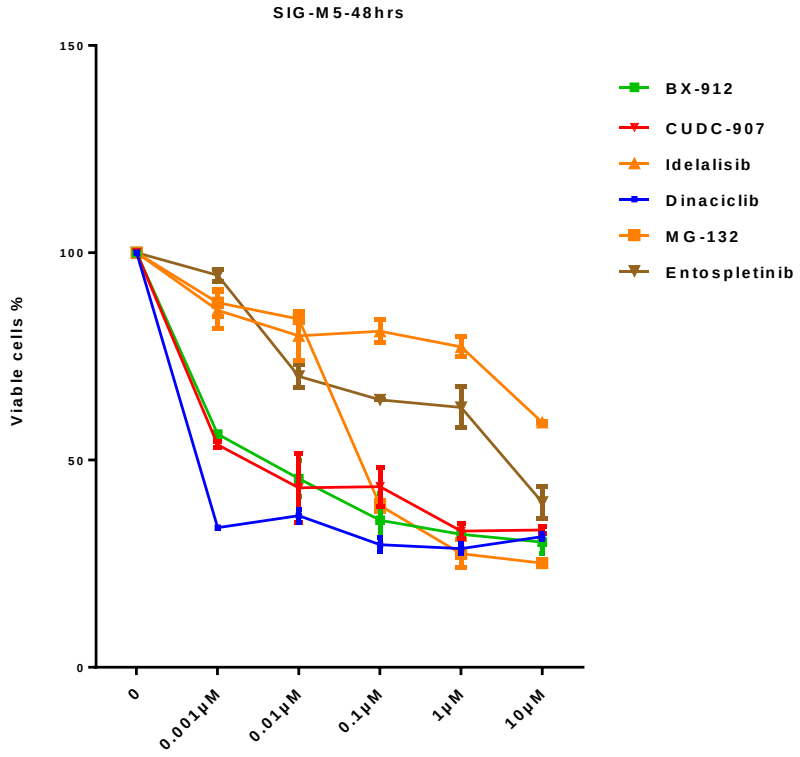


**Figure 3.14 SIG-M5 AML cell line treatment for 48 hours viability assay.**

Cells were counted, plated, treated for 48 hours, then MTS reagent were added, after 2-4hours in incubator at 5%CO2 and 37°C , plates were read using plate reader. Concentrations of each inhibitor were 10, 1, 0.1, 0.01, 0.001µM respectively. Y axis shows percentage of viable cells to DMSO control, which was normalised to 100%. X axis shows concentration of inhibitors. Each concentration presented in mean and standard deviation of two biological duplicates and two or three technical triplicates readings per inhibitor.

SIG-M5 were strongly sensitive to all dinaciclib concentrations, with viability less than 35%. To 4 concentrations out of 5, SIG-M5 cells viability was reduced to less than 50% with CUDC-907, BX-912, fedratinib, trametinib, selumetinib, dabrafenib, vemurafenib, sorafenib, and RAF265. To 3 out of 5 concentrations SIG-M5 viability reached less than 50% cell viability with MG-132, VER-155008, and IMD-0354. To 2 concentrations out of 5 were effective in reducing the viability of SIG-M5 cells with UO126, PD0325901, axitinib, and fludarabine. At 10µM, viability decreased under 50% with ibrutinib, entospletinib, and idasanutlin. Ineffective inhibition of viability was noticed with CRAF inhibitor, and idelalisib. To sum up, SIG-M5 cells were sensitive to MAPK inhibition up to 0.01µM and cells viability was reduced under 50% by, vemurafenib, dabrafenib, trametinib, selumetinib, RAF265 and sorafenib.

To summarize all the data so far, we can say that the five B-cell lines tested showed different sensitivity to 22 selected inhibitors. Cell lines that showed sensitivity (<50% viability) to all five dinaciclib concentrations were MEC-1, ESKOL and SIG-M5. Proteasome inhibitor MG-132 were was effective at decreasing cell viability of ESKOL, SIG-M5, JVM-3 and MEC-1, though all 5 concentrations of MG-132 were strongly inhibiting MEC-1 cells viability below half. Remarkably, SIG-M5 were effectively inhibited by MAPK inhibitors: 4 out of 5 concentrations of dabrafenib, vemurafenib, selumetinib, trametinib, sorafenib and RAF265. HC-1 were inhibited by the highest concentrations (10, 1μM) with dabrafenib, vemurafenib and CRAF inhibitor, whereas, ESKOL with sorafenib, RAF265, PD0325901, and UO126.

Responses to other inhibitors were heterogeneous and incomparable. Importantly, MEC-1, showed no reduction in viability to idasanutlin (MDM2-p53 inhibitor), however, JVM-3 showed inhibition at 10μM. We predicted that MEC-1 might not be affected by idasanutlin, as they are p53 mutated while, JVM-3 is p53 wild type and was reduced by high concentration of idasanutlin. SIG-M5 also reduced less than 50% with high concentration of idasanutlin.

HC-1, ESKOL cell lines did not show any reduction of viability with idasanutlin and their p53 mutational status is not yet identified. None of the cell lines showed significant decrease in viability with fludarabine and entospletinib except for SIG-M5. All cell lines showed different sensitivity to concentrations of CUDC-907 and VER-155008 except for HC-1 cells which did not show any sensitivity. All cell lines showed no great sensitivity to idelalisib PI3Kδ inhibitor except HC-1 at high concentration. HC-1 and SIG-M5 showed significant reduction of viable cells to high concentration of ibrutinib but not JVM-3, MEC-1, and ESKOL. In summary, cell lines responses to inhibitors were not similar or as we predicted. For example, JVM-3 cell line is BRAFK601N mutated and showed no great sensitivity to MAPK inhibition, in contrast to SIG-M5 BRAFV600E, which showed great sensitivity to MAPK inhibitors.

## 3.3 Calculation of IC50

Using the percentage of viable cells obtained in the MTS assays, we calculated the percentage of inhibition of viability of each inhibitor, by applying this equation:

$$\left(\frac{number\ of\ viable\ cells\ of\ treated}{number\ of\ viable\ cells\ of\ control} \times 100\right) - 100 = \%\ of\ inhibition.$$

Subsequently, IC50 (50% the inhibitory concentration of drug after 48 hours treatment) were calculated using Prism non-linear regression analysis (Graph Pad Software©, USA) (figure 3.15). Since the concentrations used ranged from 10 to 0.001µM, we could maximally calculate IC50 up to 10µM. However, we can estimate IC50 of drugs which their inhibiting capabilities are over 10µM by drawing a line to the 50% line (figure 3.15). All IC50s above 10µM were estimated this way.

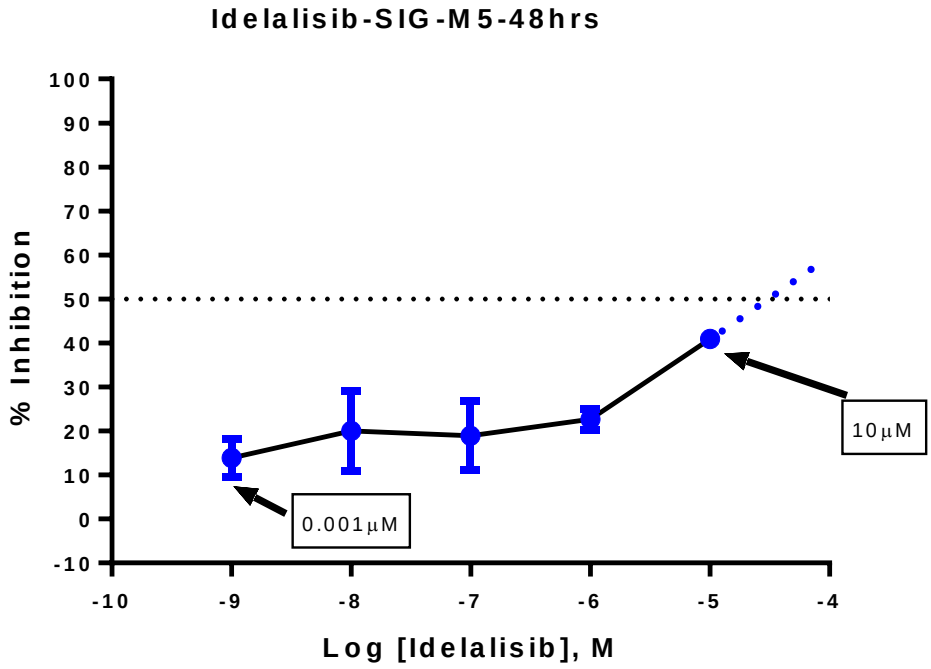


**Figure 3.15 IC50 non-linear regression analysis using Graph Pad prism.**

Percentage of inhibition % was calculated from MTS assay viability data, and then using prism, IC50 were calculated. X axis indicates log of drug concentrations, Y axis indicates inhibition of viability (%). Each dot in the line indicated inhibitor concentrations (10, 1, 0.1, 0.01, 0.001µM). Error bars indicate SD between readings.

IC50 were calculate for all 5 cell lines with all inhibitors, as can be seen in (figure 3.16). Strikingly, mutated BRAF JVM-3 needed higher concentration of vemurafenib, and dabrafenib than wild type BRAF MEC-1 cell line. SIG-M5 was the most sensitive, especially with MAPK inhibitors IC50 at nano-molar concentrations (0.009, 0.006, 0.007, and 0.003µM for vemurafenib, dabrafenib, sorafenib, and RAF265 respectively). In addition, MEK1/2 inhibitors trametinib, selumetinib, and dinaciclib achieved less than 1nm IC50 in this cell.

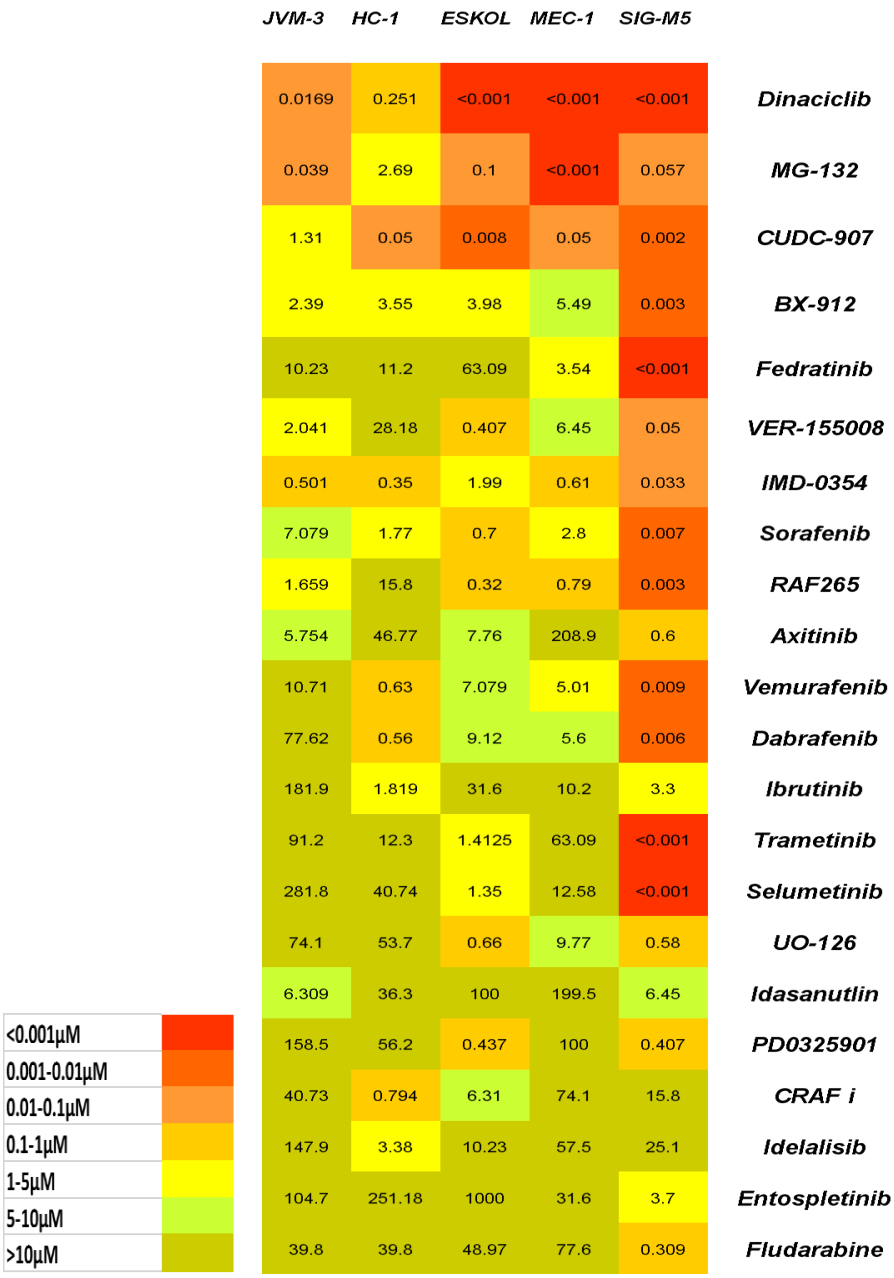


**Figure 3.16 IC50 of SIG-M5, ESKOL, HC-1, JVM-3, and MEC-1(heat map of five cell lines with 22 inhibitors).**

In order to validate our data, we compared it to the available IC50 on Genomics of Drug Sensitivity in Cancer web site (*http://www.cancerrxgene.org/).* As can be seen in table 3.4, similarities between our data and the web site were low. Sorafenib and BX-912 in MEC-1 were close. Also, vemurafenib in JVM-3 and Idelalisib in HC-1.

| *Drugs* | MEC-1 LAB | MEC-1 www.cancerrxgene.org/ | JVM-3-LAB | JVM-3 www.cancerrxgene.org/ | HC-1 LAB | HC-1 www.cancerrxgene.org/ | SIG-M5 LAB | SIG-M5 www.cancerrxgene.org/ |
|---|---|---|---|---|---|---|---|---|
| *Sorafenib* | 2.8µM | 4.55µM | 7.08µM | 15.8µM | 1.78µM | 13.5µM | 0.007µM | 1.94µM |
| *Selumitinib* | 12.58µM | 22.3µM | 281.8µM | 10.1µM | 40.7µM | 5.08µM | <0.001µM | ND |
| *Tramitinib* | 63.09 µM | 1.16µM | 91.2µM | 0.374µM | 12.3µM | 0.972µM | <0.001µM | ND |
| *CAL101 (Idelalisib)* | 57.5µM | 1.39µM | 147.9µM | 279µM | 3.38 µM | 2.7µM | 25.1µM | 4.25µM |
| *Dabrafenib* | 5.6µM | 31.1µM | 77.6µM | 3.41µM | 0.56µM | 12.9µM | 0.006µM | ND |
| *MG-132* | <0.001µM | 0.339µM | 0.039µM | 2.29µM | 2.69µM | 0.299µM | 0.057µM | 0.359µM |
| *Axitinib* | 208.9µM | 26µM | 5.7µM | 1.19µM | 46.77µM | 10.9µM | 0.6µM | ND |
| *PD-0326901* | 100uM | 0.99µM | 158.5µM | 0.301µM | 56.2µM | 0.61µM | 0.4µM | ND |
| *PLX-4720 (Vemurafenib)* | 5µM | 23.6µM | 10.7µM | 9.57µM | 0.63µM | 26.8µM | 0.009µM | ND |
| *BX-912* | 5.49µM | 5.5µM | 2.39µM | 29µM | 3.55µM | 19.3µM | 0.003µM | 0.396µM |

**Table 3.4 Comparison of our lab results to http://www.cancerrxgene.org/.**

Our data show the different sensitivity of malignant B-cell lines to drugs. SIG-M5 could be inhibited by nanomolar concentrations of MAPK inhibitors while JVM-3 needed more than 10µM for most of MAPK inhibitors, which might be due to differences in the effects of BRAF mutations. Generally, the results were heterogeneous, as viability curves showed before. The fact that our data differs from that already available might be due to technical issues. 72 hours of treatment followed by fluorescence-based cell viability assay was the method that used in the Genomic of Drug Sensitivity in cancer project while we

used MTS viability assay following 48 hours drug treatment. Therefore, confirmation with other methods and treatment times would be ideal.

## 3.4 Different responses of signalling pathways to MAPK inhibitors.

Protein expression of proteins in the MAPK cascade could be used as an indicator of cells sensitivity to inhibitors. Western blotting was used to test cells signalling activity in three different treatment times. We looked at the MAPK cascade, PI3K, and NF-κB as well as PARP cleavage which is observed at the final stage of apoptosis.

Five cell lines (JVM-3, MEC-1, SIG-M5, ESKOL, and HC-1) were grown to confluency, treated with IC50 concentrations of inhibitors (as per table 3.5), for three different times (12 hours, 24 hours, and 48 hours).

We checked P-p44/42 (ERK1/2) (Thr202/Tyr204), P-MEK1/2 (Ser217/221) and, P-BRAF (Ser445) for MAPK signalling activity. Also, we looked at protein expression of NF-κB P65, P-AKT (Ser473), both associated with survival, and cleaved PARP which indicates apoptosis.

| *Inhibitor* | *MEC-1* | *ESKOL* | *HC-1* | *SIG-M5* | *JVM-3* |
|---|---|---|---|---|---|
| *Vemurafenib* | 5.01μM | 7.07μM | 0.63μM | 0.009μM | 10.7μM |
| *Dabrafenib* | 5.6μM | 9.12μM | 0.56μM | 0.006μM | 77.6μM |
| *Sorafenib* | 2.8μM | 0.7μM | 1.77μM | 0.007μM | 7.07μM |
| *Trametinib* | 63.09μM | 1.4μM | 12.3μM | 0.001μM | 91.2μM |

**Table 3.5 IC50 concentration for five cell lines for western blotting treatment.**

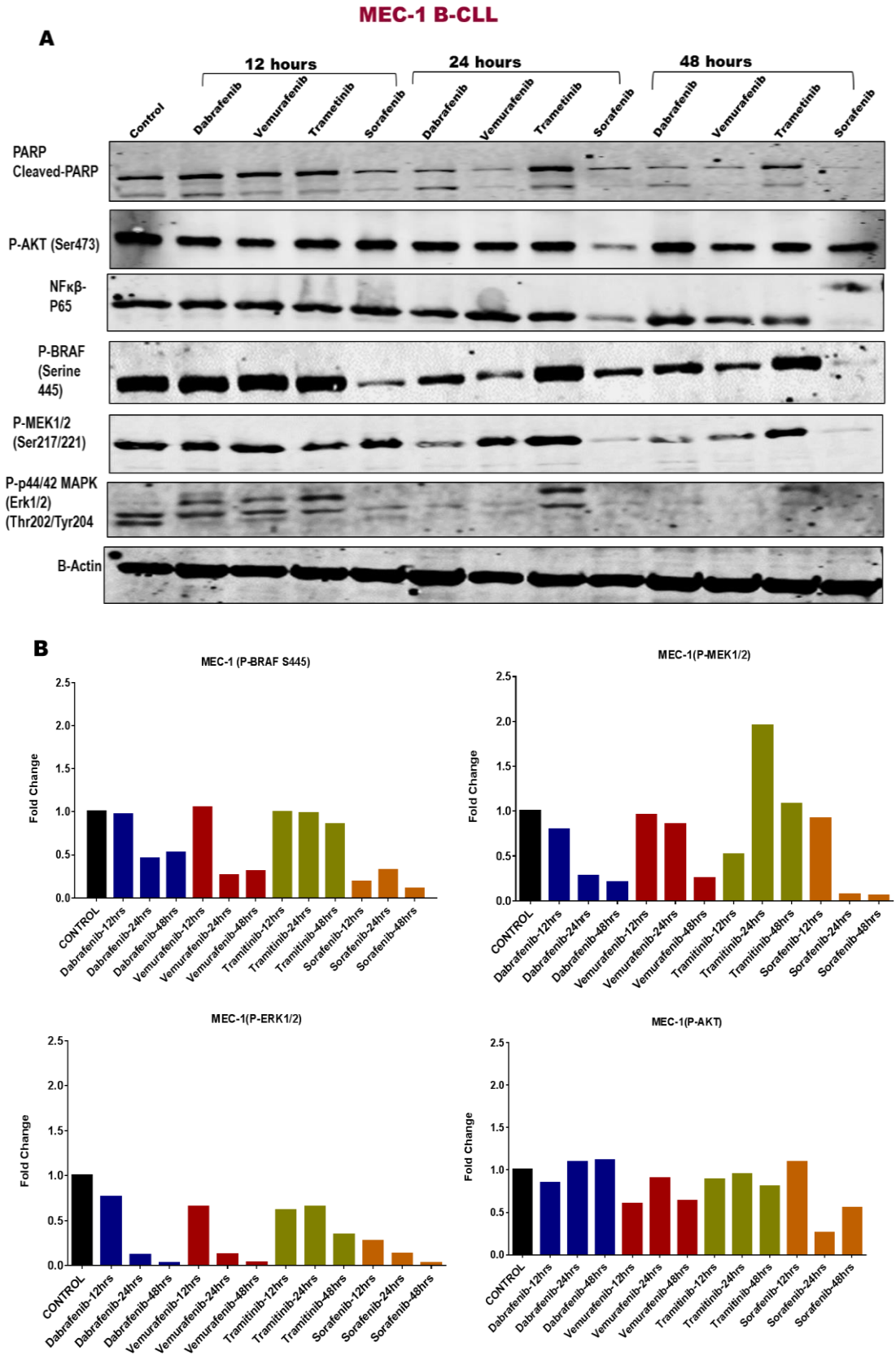
MEC-1 B-CLL
A
12 hours
24 hours
48 hours
Control
Dabrafenib
Vemurafenib
Trametinib
Sorafenib
PARP
Cleaved-PARP
P-AKT (Ser473)
NFκβ-P65
P-BRAF (Serine 445)
P-MEK1/2 (Ser217/221)
P-p44/42 MAPK (Erk1/2) (Thr202/Tyr204
B-Actin
B
MEC-1 (P-BRAF S445)
MEC-1(P-MEK1/2)
MEC-1(P-ERK1/2)
MEC-1(P-AKT)
Fold Change
CONTROL
Dabrafenib-12hrs
Dabrafenib-24hrs
Dabrafenib-48hrs
Vemurafenib-12hrs
Vemurafenib-24hrs
Vemurafenib-48hrs
Tramitinib-12hrs
Tramitinib-24hrs
Tramitinib-48hrs
Sorafenib-12hrs
Sorafenib-24hrs
Sorafenib-48hrs

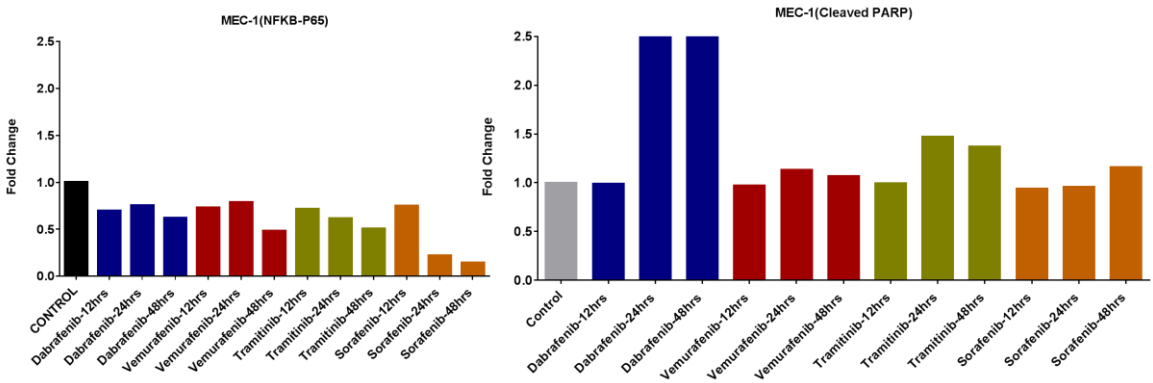


**Figure 3.17 MEC-1 cell line.**

MEC-1 cells were grown to confluency, treated for three different times (12, 24, 48 hours), with IC50 concentrations of vemurafenib 5µM, sorafenib 2.8 µM, trametinib 63 µM, and dabrafenib 5.6µM. B-Actin is the loading control. **A** Western blotting bands in 10% gel. **B** Calculations of proteins fold change to B-actin, comparing FC treated to control (normalised to 1) protein expression. MEC-1 Western blotting were done in one experiment, though some antibodies were repeated more than two times to confirm the result.

MEC-1 had a remarkable response to sorafenib, which reduced strongly MAPK proteins activity that related to its lowest IC50 concentration. With sorafenib in 12hours treatment time, MAPK P-BRAF, P-MEK and, P-ERK proteins expression appears to be slightly reduced with very slight reduction in P-MEK, but no effect on NF-κB P65, and P-AKT. After 24 hours it seems to reduce MAPK cascade proteins, with reduction in P-AKT and NF-κBP65 protein. In both times PARP is undergoing cleavage, which might indicate that cells are undergoing apoptosis. At 48 hours, all proteins were decreased significantly, except P-AKT which is slightly increasing after being decreased in 24 hours. Notably, PARP cleaved fragments seems to be degraded with increase in time, that may be due to very unstable cleaved fragments are degraded further in the cell with time.

Dabrafenib and vemurafenib both in 12 hours appears to have a slight effect on MAPK, P-AKT, and NF-κB P65 protein expression, though PARP begins to cleave with vemurafenib. At 24 hours both seemed to lower P-ERK expression, with no considerable effect on P-AKT, or NF-κB P65, and PARP seems to be undergoing cleavage which might means that cells are undergoing apoptosis. In 48 hours, dabrafenib and vemurafenib, seem to entirely reduce P-ERK, and slightly P-AKT, NF-κB P65, with PARP cleavage and degradation.

Trametinib at 12 hours has trivial effect on most proteins expressions, and significant increase in P-MEK in 24 hours. In 48 hours caused a slight reduction in P-ERK and NF-κB P65.

To sum up, 48 hours seems to be the time were inhibitors exert most of their action on protein signalling and PARP cleavage (figure 3.17). In consistent with our MTS results, trametinib did not show effective viability inhibition in MEC-1 cells (48hrs), we noted that from proteins expression in Western blotting that it slightly reduced P-ERK, and NF-κBP65 only after 48 hours. Sorafenib has effectively reduced MEC-1 cells viability in MTS assay (48hrs), and also significantly reduced most of protein expression of MAPK cascade, and NF-κBP65 at 48 hours.

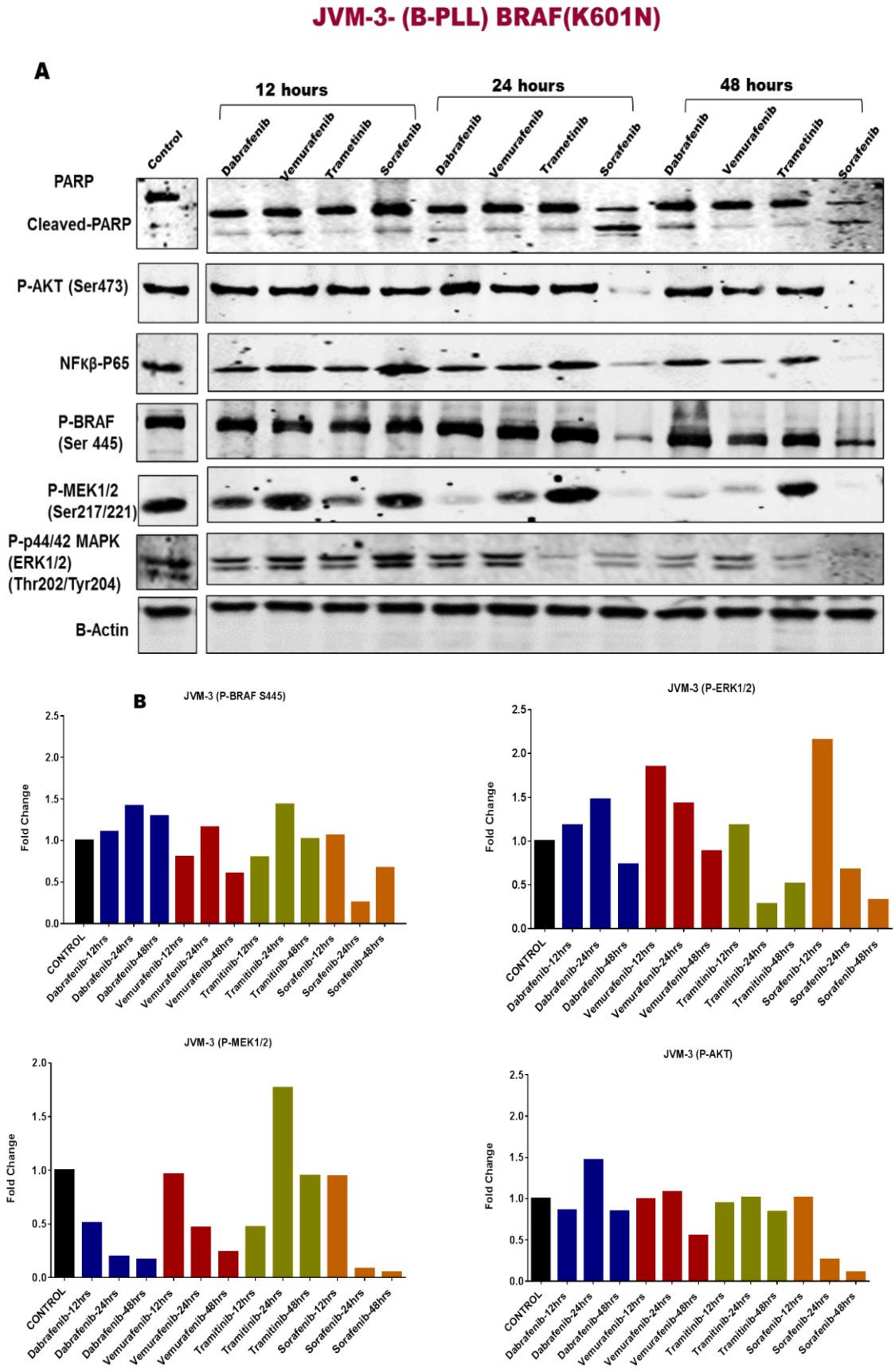
JVM-3- (B-PLL) BRAF(K601N)
A
12 hours
24 hours
48 hours
Control
Dabrafenib
Vemurafenib
Trametinib
Sorafenib
PARP
Cleaved-PARP
P-AKT (Ser473)
NFκβ-P65
P-BRAF (Ser 445)
P-MEK1/2 (Ser217/221)
P-p44/42 MAPK (ERK1/2) (Thr202/Tyr204)
B-Actin
B
JVM-3 (P-BRAF S445)
JVM-3 (P-ERK1/2)
JVM-3 (P-MEK1/2)
JVM-3 (P-AKT)
Fold Change
CONTROL
Dabrafenib-12hrs
Dabrafenib-24hrs
Dabrafenib-48hrs
Vemurafenib-12hrs
Vemurafenib-24hrs
Vemurafenib-48hrs
Tramitinib-12hrs
Tramitinib-24hrs
Tramitinib-48hrs
Sorafenib-12hrs
Sorafenib-24hrs
Sorafenib-48hrs

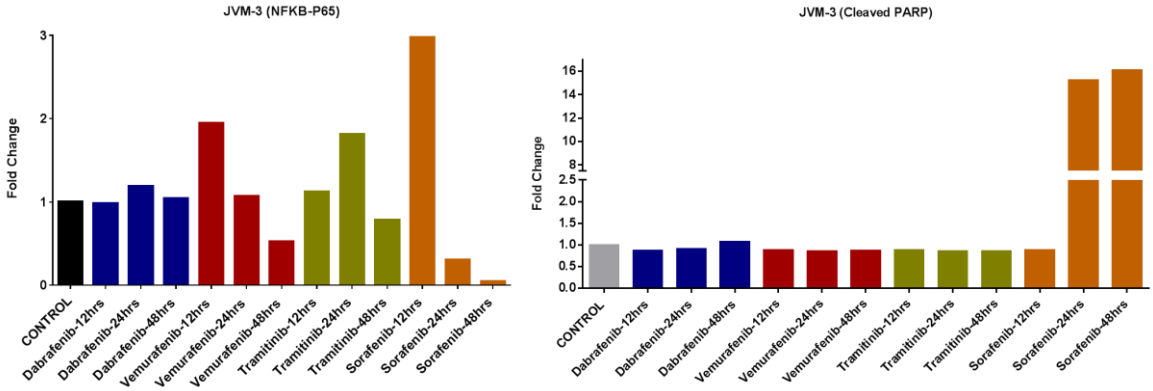


**Figure 3.18 JVM-3 cell line.**

JVM-3 cells were grown to confluency, treated for three different times (12, 24, 48 hours), with IC50 concentrations of vemurafenib 10.7µM, sorafenib 7.07µM, trametinib 91µM, and dabrafenib 77µM. B-Actin is the loading control. **A** Western blotting bands in 10% gel. **B** Calculations of proteins fold change to B-actin, comparing FC treated to control (normalised to 1) protein expression. JVM-3 Western blotting were done in one experiment, though some antibodies were repeated more than two times to confirm the result.

We expected JVM-3 to show more responsiveness to MAPK inhibition, due to its BRAF mutation, compared with MEC-1, which is BRAF wild type. However, with sorafenib treatment, JVM-3 showed PARP cleavage at 24 hours, suggesting that it starts to undergo apoptosis. P-BRAF was significantly reduced at 24 hours and then, was increased slightly at 48 hours where more PARP cleavage was seen with sorafenib at 48 hours.

Dabrafenib and vemurafenib had mostly their effects at 48 hours, P-ERK and P-MEK seem to be reduced to some extent without significant PARP-cleavage, which is related to our MTS assay results of JVM-3 viability with dabrafenib, and vemurafenib.

Trametinib seems to have slight effect on MAPK cascade proteins mostly at 48 hours, yet no significant PARP cleavage, as in MTS assay JVM-3 showed no sensitivity to trametinib.

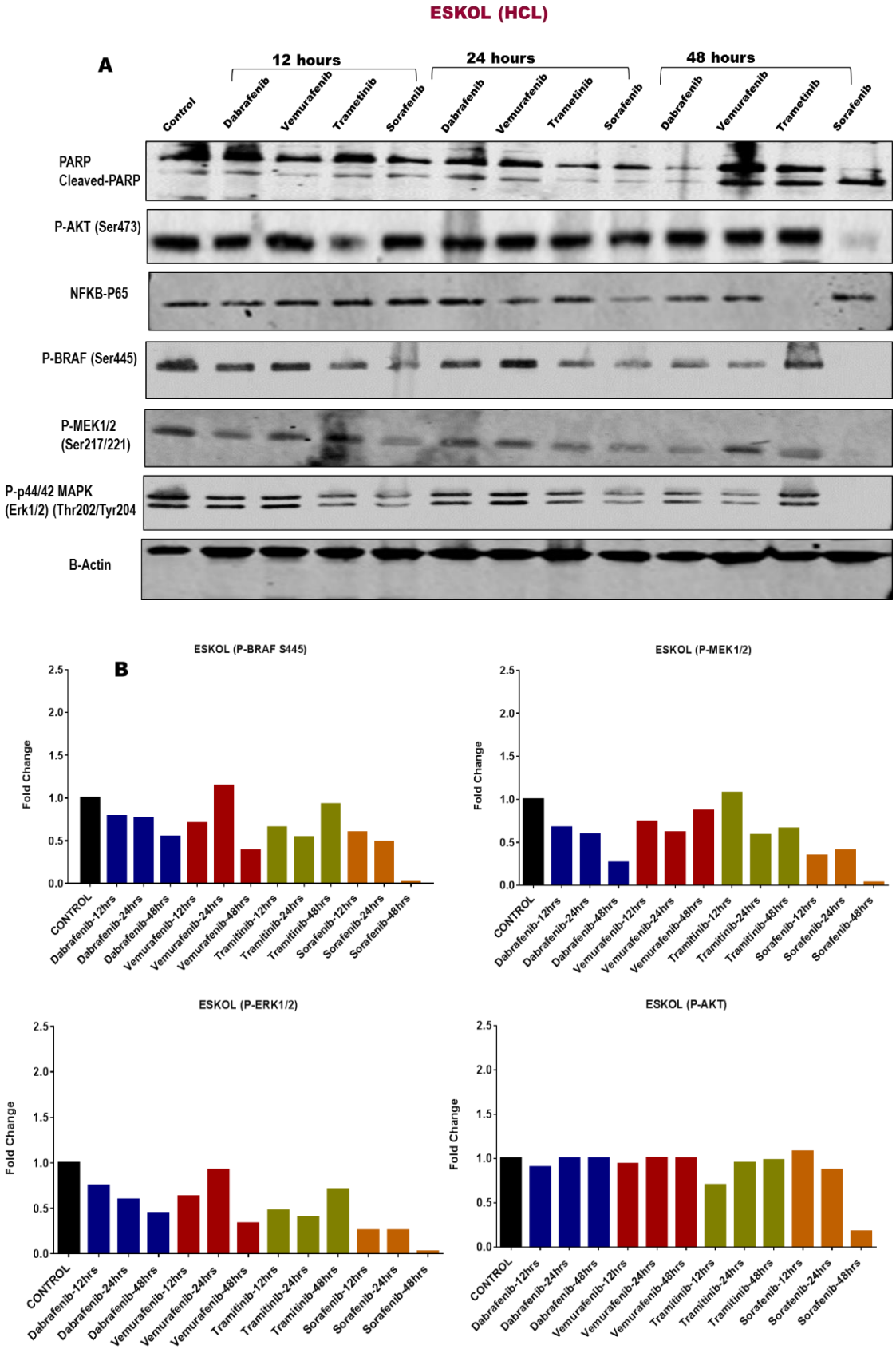
ESKOL (HCL)
A
12 hours
24 hours
48 hours
Control
Dabrafenib
Vemurafenib
Trametinib
Sorafenib
PARP
Cleaved-PARP
P-AKT (Ser473)
NFKB-P65
P-BRAF (Ser445)
P-MEK1/2
(Ser217/221)
P-p44/42 MAPK
(Erk1/2) (Thr202/Tyr204
B-Actin
B
ESKOL (P-BRAF S445)
ESKOL (P-MEK1/2)
ESKOL (P-ERK1/2)
ESKOL (P-AKT)
Fold Change
CONTROL
Dabrafenib-12hrs
Dabrafenib-24hrs
Dabrafenib-48hrs
Vemurafenib-12hrs
Vemurafenib-24hrs
Vemurafenib-48hrs
Tramitinib-12hrs
Tramitinib-24hrs
Tramitinib-48hrs
Sorafenib-12hrs
Sorafenib-24hrs
Sorafenib-48hrs

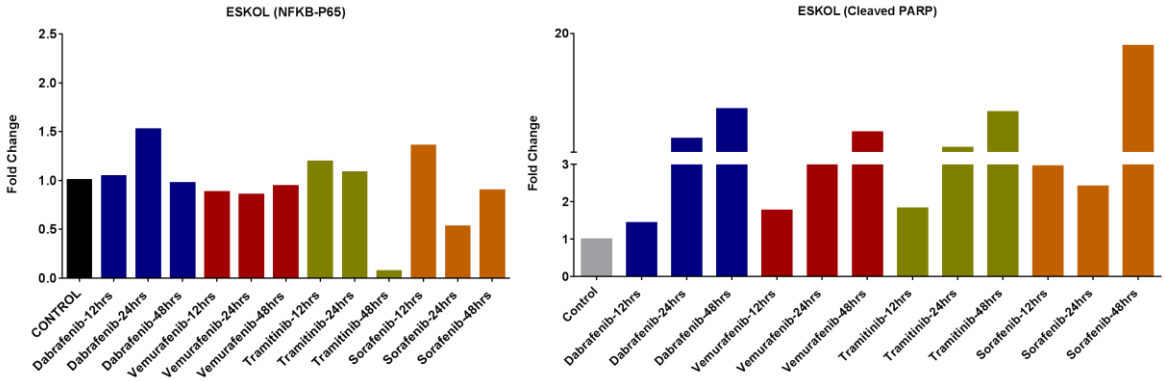


**Figure 3.19 ESKOL cell line.**

ESKOL cells were grown to confluency, treated for three different times (12, 24, 48 hours), with IC50 concentrations of vemurafenib 7µM, sorafenib 0.7µM, trametinib 1.4µM, and dabrafenib 9.12µM. B-Actin is the loading control. **A** Western blotting bands in 10% gel. **B** Calculations of proteins fold change to B-actin, comparing FC treated to control (normalised to 1) protein expression. ESKOL Western blotting were done in one single experiment, though some antibodies were repeated more than two times to confirm the result.

ESKOL is hairy cell leukaemia cell line but lacks BRAF V600E mutations. Sorafenib, which had the lowest IC50 (0.7µM), showed most of its influences on MAPK and other proteins expression at 48 hours. All proteins were reduced substantially, and PARP was completely, though NF-κBP65 is still slightly expressed.

Vemurafenib and dabrafenib cleaved PARP and reduced P-ERK and other proteins expression radically at 48 hours as well, though PARP cleavage seems to start at 24 hours. Both dabrafenib and vemurafenib affected cells viability effectively at slightly high concentrations in MTS assay results.

Trametinib also cleaved PARP and switched off NF-κB P65 expression at 48 hours, with slight reduction in MAPK cascade proteins.

Most of inhibitors seems to have no great influence on P-AKT except for sorafenib at 48 hours. NF-κβ P65 was mostly reduced by trametinib at 48 hours.

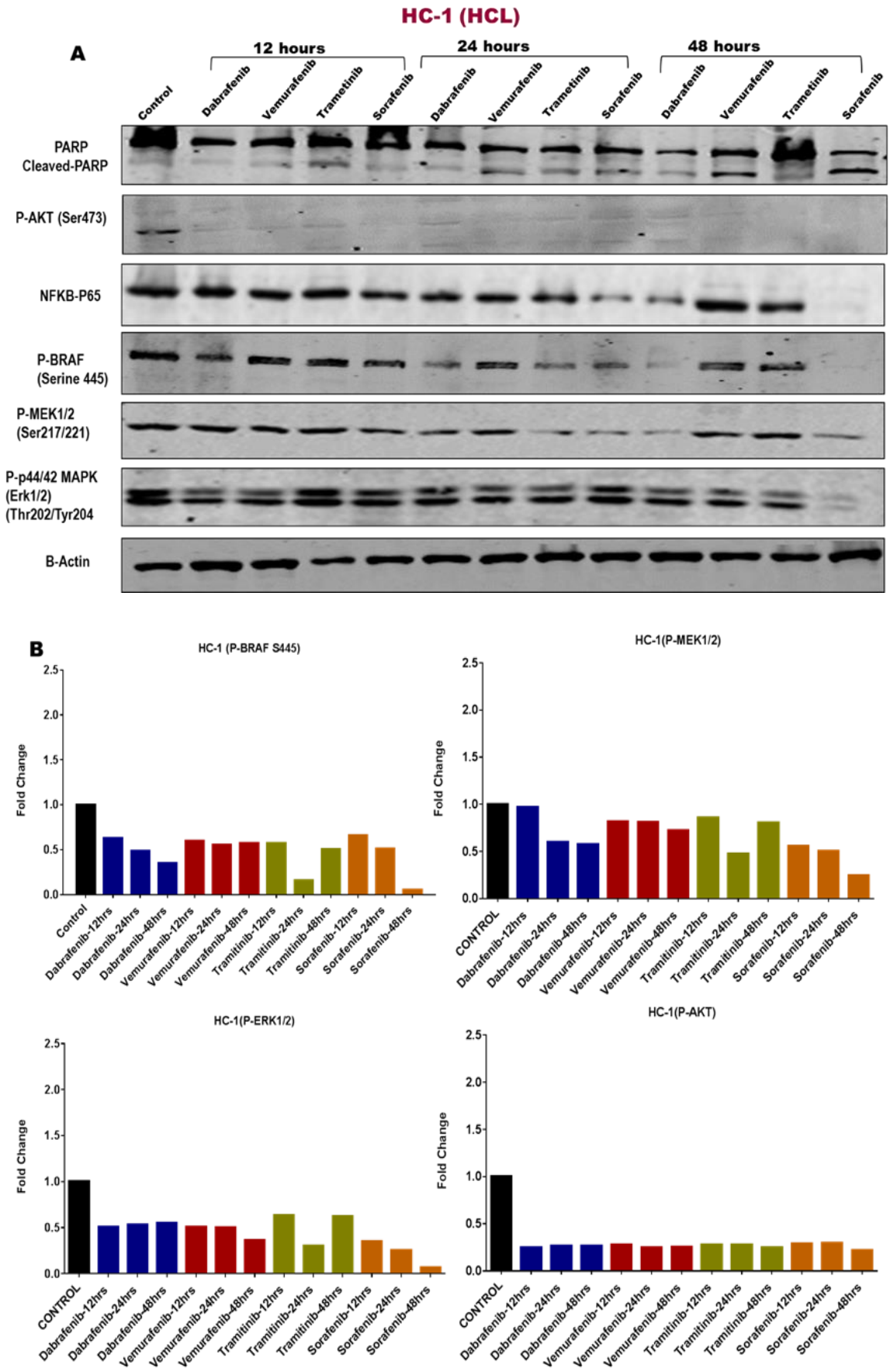
HC-1 (HCL)
A
12 hours
24 hours
48 hours
Control
Dabrafenib
Vemurafenib
Trametinib
Sorafenib
PARP
Cleaved-PARP
P-AKT (Ser473)
NFKB-P65
P-BRAF
(Serine 445)
P-MEK1/2
(Ser217/221)
P-p44/42 MAPK
(Erk1/2)
(Thr202/Tyr204
B-Actin
B
HC-1 (P-BRAF S445)
HC-1(P-MEK1/2)
HC-1(P-ERK1/2)
HC-1(P-AKT)
Fold Change
CONTROL
Dabrafenib-12hrs
Dabrafenib-24hrs
Dabrafenib-48hrs
Vemurafenib-12hrs
Vemurafenib-24hrs
Vemurafenib-48hrs
Tramitinib-12hrs
Tramitinib-24hrs
Tramitinib-48hrs
Sorafenib-12hrs
Sorafenib-24hrs
Sorafenib-48hrs

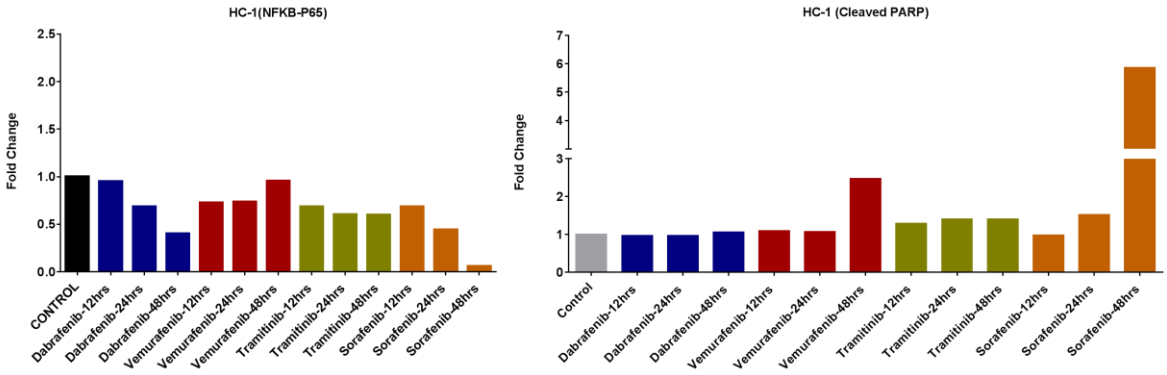


**Figure 3.20 HC-1 cell line.**

HC-1 cells were grown to confluency, treated for three different times (12, 24, 48 hours), with IC50 concentrations of vemurafenib 0.63µM, sorafenib 1.77µM, trametinib 12.3µM, and dabrafenib 0.56µM. B-Actin is the loading control. **A** Western blotting bands in 10% gel. **B** Calculations of proteins fold change to B-actin, comparing FC treated to control (normalised to 1) protein expression. HC-1 Western blotting were done in one single experiment, though some antibodies were repeated more than two times to confirm the result.

The origin of HC-1 as well as ESKOL is still debatable, because they both lack BRAFV600E mutation. Sorafenib has the most PARP cleavage at 48 hours with significant inhibition of mostly all proteins tested, in our MTS assay these cells showed sensitivity to sorafenib as well.

Vemurafenib lead to cleave PARP at 48 hours with no significant effect on MAPK or NF-κB P65, but complete inhibition of P-AKT. Dabrafenib, with the lowest IC50 (0.56µM), showed slight PARP cleavage, with considerable decrease in MAPK cascade, NF-κB P65, and P-AKT proteins expression.

Trametinib seems to have minor effect on proteins expression at 48 hours with minimal PARP cleavage. Remarkably, P-AKT expression was switched off with all inhibitors starting from 12 hours, suggesting the sensitivity of this cell line is linked to this pathway.

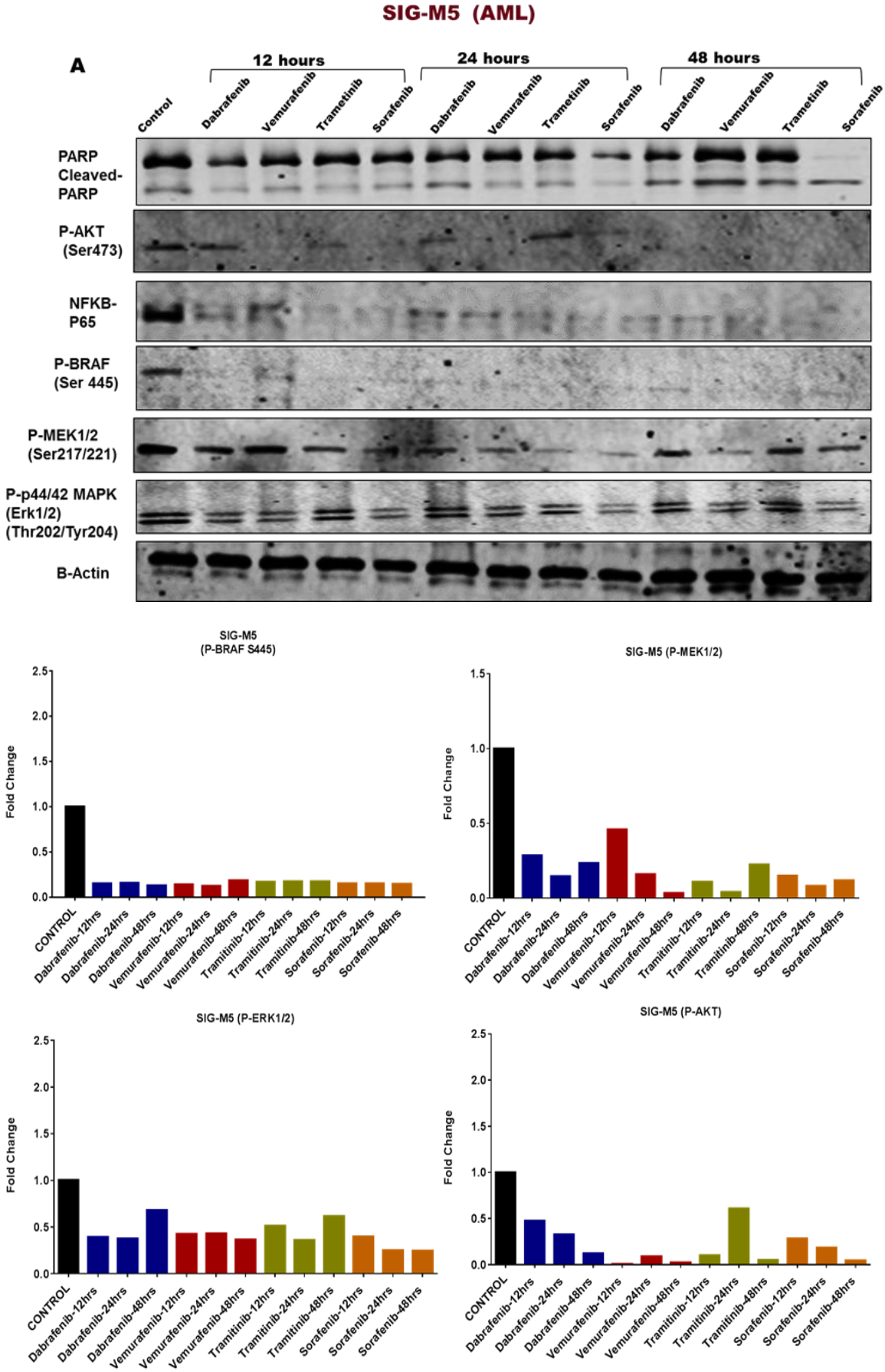
SIG-M5 (AML)
A
12 hours
24 hours
48 hours
Control
Dabrafenib
Vemurafenib
Trametinib
Sorafenib
PARP
Cleaved-PARP
P-AKT (Ser473)
NFKB-P65
P-BRAF (Ser 445)
P-MEK1/2 (Ser217/221)
P-p44/42 MAPK (Erk1/2) (Thr202/Tyr204)
B-Actin
SIG-M5 (P-BRAF S445)
SIG-M5 (P-MEK1/2)
SIG-M5 (P-ERK1/2)
SIG-M5 (P-AKT)
Fold Change
CONTROL
Dabrafenib-12hrs
Dabrafenib-24hrs
Dabrafenib-48hrs
Vemurafenib-12hrs
Vemurafenib-24hrs
Vemurafenib-48hrs
Tramitinib-12hrs
Tramitinib-24hrs
Tramitinib-48hrs
Sorafenib-12hrs
Sorafenib-24hrs
Sorafenib-48hrs

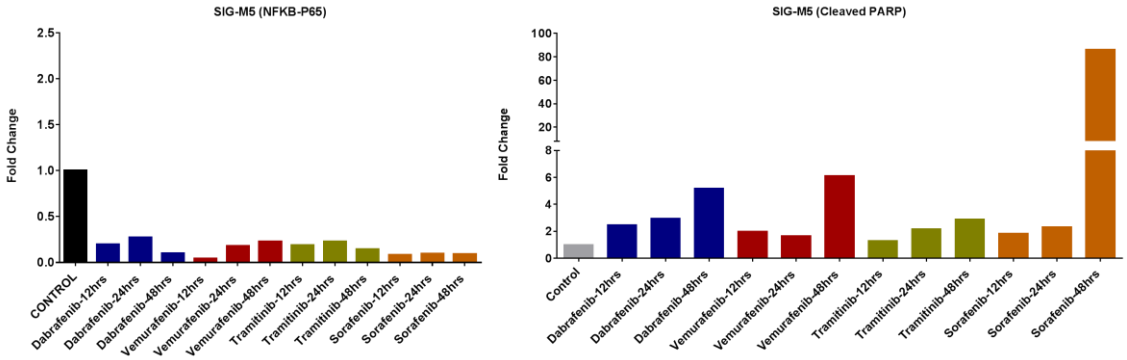


**Figure 3.21 SIG-M5 cell line.**

SIG-M5 cells were grown to confluency, treated for three different times (12, 24, 48 hours), with IC50 concentrations of vemurafenib 0.009µM, sorafenib 0.007µM, trametinib 0.001µM, and dabrafenib 0.006µM. B-Actin is the loading control. **A** Western blotting bands in 10% gel. **B** Calculations of proteins fold change to B-actin, comparing FC treated to control (normalised to 1) protein expression. SIG-M5 Western blotting were done in one single experiment, though some antibodies were repeated more than two times to confirm the result.

SIG-M5 cell line showed great sensitivity to MAPK inhibition in MTS assay. Of note it is a BRAFV600E mutated cell line. Dabrafenib, and vemurafenib are selective BRAFV60E inhibitors, though vemurafenib has some effects on BRAF wild type. Strikingly, all P-BRAF, P-AKT and NF-κB P65 seems to be diminished as early as 12hours. P-ERK, and P-MEK also seem to be decreased as well.

Heat map of all five cell lines (figure 3.22) with all protein fold changes after 48 hours treatment time. As we have seen most of reduction of proteins expression and PARP cleavage at this time. It was of interest to look at the extent of inhibition of cross talk between pathways. In general, some inhibitors were effective, although not all to the same extent. To sum-up, in 48 hours SIG-M5 had the highest PARP cleavage with sorafenib and dabrafenib. Our MTS assay data showed SIG-M5 was the most sensitive cell line to MAPK inhibition with IC50 in nanomolar concentrations, and our Western blotting data confirmed this with most protein expression reduction (blue colour). ESKOL and SIG-M5 had highest cleaved PARP with vemurafenib. ESKOL has the highest PARP cleavage with trametinib. Notably, HC-1 showed significant decrease in P-AKT with all inhibitors and slight reduction in other protein expression. JVM-3 showed resistance to MAPK inhibitors in MTS assay data with IC50 >10µM of vemurafenib, dabrafenib, and trametinib, and showed less protein expression inhibition and PARP cleavage in Western blotting except with sorafenib. Sorafenib treatment had most PARP cleavage in all cell lines as the most effective inhibitor of proteins expression.

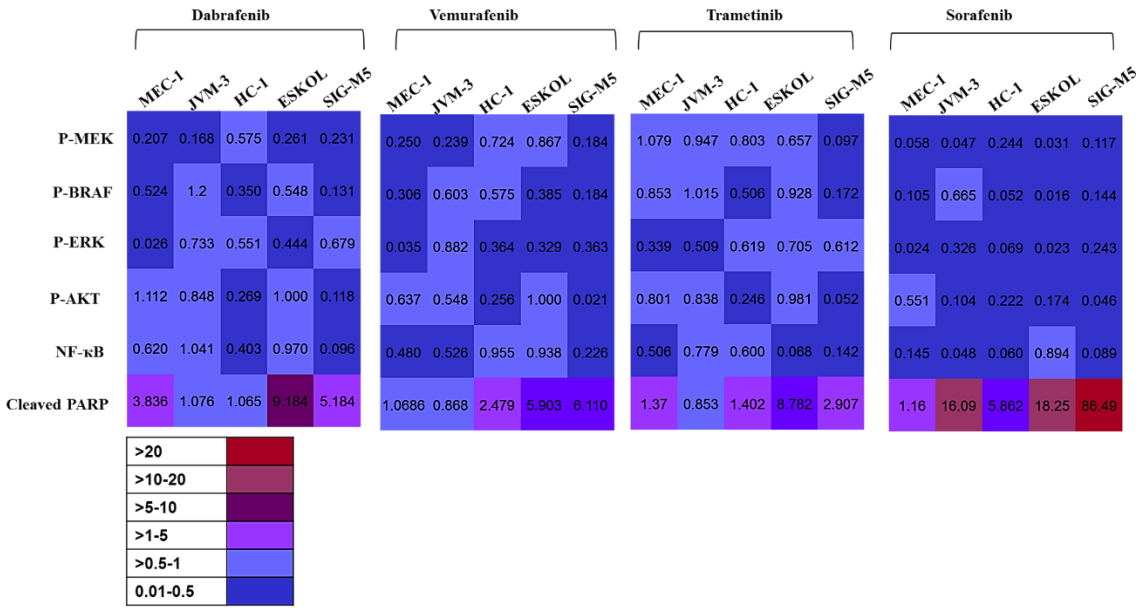


**Figure 3.22 Fold change of protein expressions after treatment of five cell lines with four MAPK inhibitors for 48 hours.**

Heat map of fold change of proteins to B-Actin, and treated to control (control was normalised to 1) for all cell lines. FC (0.01-0.5) means protein expression in treated cells decreased to half and less than half of control cells. FC > (0.5-1) indicates proteins that expressed more than half control cells or equal. FC>1 to 5 means proteins expressed more than control, but in the PARP cleavage FC >1 or more means more PARP cleavage (apoptosis).

## 3.5 Discussion

Microenvironment stimulation of CLL cells is initiated by many factors such as stromal cells, T cells cytokines, BCR receptors, and other cytokines. One of the stimulatory effects that CLL cells receive in lymph nodes is CD40-Ligand and cytokine IL-4 activation that is performed through T cells in proliferation centres (Crassini *et al*, 2017; Herman and Wiestner, 2016). CLL cells cultured with sCD40-L-IL-4 stimulation significantly express more P-ERK than unstimulated normal B-cells (figure 3.1), consistent with the fact that MAPK has been shown to be constitutively active in a subset of CLL patients (Muzio *et al*, 2008). This suggests that MAPK signalling is essential for CLL cells proliferation.

We aimed to investigate the response of B-leukaemic cells to BRAF/MEK/ERK inhibitors. Our experimental design involved other inhibitors and fludarabine, which is a chemotherapy that used in CLL treatment. 12, and 24 hours treatment of all five cell lines (figures 3.2-3.9) showed no significant decrease in cell viability. This was expected as 12 hours treatments might show little effect on protein phosphorylation or apoptosis induction using techniques such as Western blotting. However, MEC-1 showed decrease

in viability than 50% with 10μM of the following: IMD-0354 (an IKK-β inhibitor), CUDC-907 (a dual PI3K and HDAC inhibitor), fedratinib (a JAK2 inhibitor), and MG132 (a proteasome inhibitor). 48 hours treatment (figures 3.10-3.14) showed some decrease in viability for most of 22 inhibitors. This indicates that this seems to be the suitable time of treatment that influencing B-cells proliferation and viability. MAPK signalling inhibitors showed different efficacies among cell lines.

MAPK inhibitors showed different efficacies among five cell lines. MEC-1 cell line showed reduced viability with high concentrations of 10μM UO126 (MEK1/2 inhibitor), dabrafenib (BRAF V600E inhibitor), sorafenib (pan-RAF inhibitor), vemurafenib (BRAFV600E inhibitor), and RAF265 (pan-RAF inhibitor) (figure 3.10). JVM-3 cell line with BRAF mutation (K601N), which was expected to display more sensitivity to MAPK inhibitors showed no sensitivity to MAPK inhibition, except for RAF265 and sorafenib at 10μM only (figure 3.11).

ESKOL and HC-1 are both hairy cell leukaemia, yet, both cell lines displayed different responses to MAPK inhibitors. ESKOL was sensitive to sorafenib, RAF265, UO126, PD0325901, dabrafenib, trametinib, vemurafenib, CRAF inhibitor, and selumetinib (figure 3.12). While HC-1 was sensitive to vemurafenib, dabrafenib, sorafenib, and CRAF inhibitor (figure 3.13). SIG-M5 mutated with BRAFV600E was sensitive to all MAPK signalling inhibitors and in nanomolar concentrations to most of them (figure 3.14).

SIG-M5 (BRAFV600E mutated) showed additional sensitivity and IC50 values in nanomolar concentrations, to MEK1/2 inhibition (trametinib and selumetinib), and RAF inhibitors (dabrafenib, sorafenib, RAF265, and vemurafenib), while JVM-3 showed less sensitivity with high IC50 values (figure 3.16). It seems that p.BRAFV600E activation mutation are most sensitive cells to MAPK inhibitors, which may be due to that this mutation is essential for cancer proliferation. Surprisingly, JVM-3 with BRAFK601N activation mutation, has less sensitivity to MAPK inhibitors than MEC-1 wild type BRAF cells. Important finding that confirms our results is that published by Yao *et al*, 2015. They found that BRAFV600E mutant are activated monomers, while all other BRAF activating mutations mutants function as RAS-independent dimers with high level of phosphorylated MEK. Therefore, RAF inhibitors will efficiently supress mutants monomers of BRAFV600E but not dimers of other activating BRAF mutations.

Potent inhibitors according to our IC50 values were dinaciclib, MG-132, and CUD-907. Dinaciclib showed potent inhibition of cell viability in less than 1nM in ESKOL, MEC-1 and SIG-M5 cells. It was shown by our lab that dinaciclib induced apoptosis through the activation of caspases 8 and 9, and this occurs independent of microenvironment activation, or IGHV mutation status (Chen *et al*, 2016). We also have found that dinacilcib blocks anti-apoptotic proteins of Bcl2 family in CLL cells. MG-132 showed efficacy in ESKOL, SIG-M5, JVM-3 and MEC-1 cells (figure 3.16). Specifically in MEC-1 cells (IC50 was less than 1nM). It has been described that proteasome inhibitor MG132 induces the intrinsic pathway of apoptosis and NOXA protein expression in CLL cells (Baou *et al*, 2010).

MEC-1, ESKOL, SIG-M5 and HC-1 showed high sensitivity to CUDC-907 (a dual PI3K and HDAC inhibitor) in low concentrations (figure 3.16). However, moderate sensitivity was noticed in JVM-3. Another PI3K inhibitor is idelalisib. *In vitro* sensitivity to idelalisib was not significant, most cells needed more than 10μM with the exception of HC-1 (figure 3.16). Idelalisib (Zydelig®) was approved for CLL treatment in 2014 in relapsed CLL patients, and had substantial clinical activity in patients with relapsed or refractory CLL. It is a selective potent inhibitor of PI3Kδ, and it has been approved in a combination with rituximab for the treatment of relapsed and refractory CLL. PI3K has four catalytic isoforms (p110 α, β, γ, and δ) where PI3Kδ is highly expressed in malignant CLL cells and lymphoid cells. BCR signalling activation in B- CLL cells is facilitated through delta isoform of PI3K (PI3Kδ) activation (Furman *et al,* 2014). Most adverse events that occur with idelalisib treatment are fatigue, nausea, diarrhoea, skin rash, and pyrexia however, hepatotoxicity was one of main reason of idelalisib discontinual in clinical trials (Falchi *et al,* 2016).

Another kinase inhibitor used was entospletinib, which is a Syk inhibitor. Syk is a cytoplasmic protein tyrosine kinase that is highly expressed in haematological cells. Up on BCR activation, Syk transduce signals of cellular proliferation, differentiation, and adhesion, which is very important signals in malignant B-cells in proliferation centres. In a multicentre, phase 2 study (#NCT01799889) including 41 relapsed or refractory CLL patients the progression free survival (PFS) rate at 24 weeks in CLL patients reached 70.1%; toxicities include neutropenia, pyrexia, and pneumonia (Sharman *et al*, 2015). Entospletinib was well tolerated with significant clinical activity in a phase 1b/2 study (#NCT02343939) were it has been used as a single agent treatment and in combination

with chemotherapy in AML patients (Walker *et al*, 2016). In our *in vitro* results entospletinib IC50 value was higher than 10µM in all cells except SIG-M5 cells (figure 3.16), suggesting limited use in monotherapies.

Ibrutinib inhibits BTK by binding covalently and irreversibly to cysteine-481 in the adenosine-tri-phosphate binding domain of BTK (Wodarz *et al*, 2014). Ibrutinib response in CLL patients has been described to be improving gradually with treatment duration. Death rate of CLL cells is 2.7% per day in the lymph node, and a number of cells will be driven to exit lymph nodes into circulation. It is very likely that ibrutinib interferes with adhesion, migration, and egression. In addition, it has been noticed that cells with high IgM and CXCR4 expression are more subjected to ibrutinib induced cell death (Wodarz *et al*, 2014; Forconi, 2015). *In vitro* anti-proliferative effects of ibrutinib on CLL cells has been shown to be potentiated when combined with dexamethasone (Manzoni *et al*, 2016). Our results show that the most sensitive cell line to ibrutinib was HC-1 with IC50 (1.8 µM), then SIG-M5 (3.3 µM), MEC-1 (10.12 µM), ESKOL and JVM-3 IC50 were above 10µM. Our results showed no specificity.

Idasanutlin (MDM2 antagonist) showed moderate efficacy in JVM-3 and SIG-M5 (figure 3.16). Conversely, MEC-1 showed resistant to idasanutlin (IC50 199.5µM). This may be attributed to the fact that MEC-1 have both 17p deletion and TP53 mutation (Pozzo *et al*, 2013a). Idasanutlin has shown substantial clinical activity in pre-clinical studies in acute myeloid leukaemia AML (Higgins *et al*, 2014). MDM2 helps in p53 degradation and ubiquitination, therefore, certain cancers would have higher levels of MDM2 that to suppress p53 activity (Reis *et al*, 2016). Most CLL patients have wild type p53, which suggests that this drug could potentially be useful, probably in combinations.

Fludarabine is used in CLL and has been reported as a successful treatment with acceptable side effects (Keating *et al*, 1989). It is the most effective purine analogue in CLL treatment (Ricci *et al*, 2009). Fludarabine, cyclophosphamide, and rituximab (FCR) chemoimmunotherapy has been reported as effective and well tolerated combination therapy for relapsed or refractory CLL patients (Badoux *et al*, 2011a). However, our results show that fludarabine IC50 was more than 10µM in all cell lines except SIG-M5 0.3µM (figure 3.16), which suggests a low specificity.

In table 3.4 we compared our results to The Genomics of Drug Sensitivity in Cancer Project, which is a multicentre project funded by Wellcome trust. For MEC-1 the IC50

value of BX-912 was very close. BX-912 is PDK-1 inhibitor, mantle cell lymphoma cell lines showed high sensitivity to BX-912 and sensitive cells showed great G2 arrest and PDK1 inhibition (Hutter *et al*, 2013). Vemurafenib IC50 of JVM-3 cells was also close. Idelalisib IC50 value of HC-1 and sorafenib IC50 value for MEC-1 cells was not vastly different from the project IC50 values. In general, the other IC50 values were different from the project and that is may be attributed to the fact that they used different method (72 hours treatment followed by Fluorescent based cell viability assay). While we treated cells for 48 hours followed by MTS cell viability assay. Confirmation of our results using different method is needed. After the MTS cell viability assay of five leukaemic cell lines, we used Western blotting analysis with four MAPK inhibitors (dabrafenib, vemurafenib, trametinib and sorafenib) in same three different times 12, 24, and 48 hours.

Firstly, at 48 hours most of proteins/signalling are inhibited and PARP is cleaved the most as can be seen from figures 3.17-3.21, which is similar to our observation in MTS cell viability assay results of cell lines. Secondly, sorafenib seems to be the most effective inhibitor among used in Western blotting. Sorafenib showed low to moderate IC50 values among five cell lines in MTS cell viability assay (figure 3.16). Considerably, greatest inhibition of proteins were noticed more with sorafenib among four MAPK inhibitors (figure 3.22). Sorafenib found to be effective in inhibiting the proliferation of all thyroid carcinoma cell lines, regardless their BRAF mutation status (Broecker-Preuss *et al*, 2015).

Remarkably, trametinib did not decrease but increased P-MEK1/2 in 48 hours in MEC-1, and JVM-3. It did not cause significant reduction in P-MEK1/2 in ESKOL, and HC-1 in 48 hours, and it reduced P-MEK1/2 in SIG-M5 after 48 hours treatment. Trametinib as is a MEK1/2 inhibitor developed to overcome the paradoxical MAPK activation that caused by CRAF transactivation after treatment with BRAFV600E inhibitors vemurafenib and dabrafenib (Heuck *et al*, 2016). Finally, SIG-M5 showed inhibition of most of proteins phosphorylation with all four MAPK inhibitors (figure 3.22), which was observed previously in our MTS cell viability assay as SIG-M5 was very sensitive to MAPK inhibition. Our next aim is to evaluate primary CLL cells response to similar inhibitors and to stratify the sensitivity of cells according to their BRAF exon 15 mutational status.

# Chapter 4 BRAF mutated CLL primary cells showed more sensitivity to MAPK inhibition.

In recent years, new targeted drugs have been approved for CLL such as Idelalisib (PI3K kinase inhibitor), Ibrutinib (Irreversible inhibitor of BTK), obinutuzumab (anti-CD20 mAb), and ABT-199 (Bcl-2 inhibitor) (Guièze and Wu, 2015). These drugs are now being used, alone or in combination, as an alternative to classic chemotherapy to overcome resistance to treatment and relapse.

In order to investigate potential novel therapies for CLL, we studied the responses of CLL primary cells (after stimulation or not with sCD40-IL4 to mimic microenvironment of CLL cells) to inhibitors of MAPK cascade and other inhibitors. We investigated cell survival and measured signalling activity using Western blotting.

Cells from five different patients have been used in these experiments. They have different IGHV mutational status and different cytogenetics to allow us to see if these parameters do affect cells responses. Cells were stimulated with sCD-40-L/IL-4 system for ~24 hours priors to treatment. MTS assays in 96 well plates were performed, after treatment for 48 hours with (10, 1, 0.1, 0.01, 0.001μM) of 16 inhibitors (in table 4.1).

| Inhibitor | Target |
|---|---|
| Dinaciclib | A potent CDK inhibitor for CDK1, 2 9 and 5. |
| CUDC-907 | A dual PI3K and HDAC inhibitor. |
| MG-132 | 26S proteasome inhibitor. |
| BX-912 | A specific PDK1 inhibitor, blocks PDK1/AKT signalling. |
| Fedratinib | A selective inhibitor of JAK2 (JAK/STAT). |
| VER-155008 | Inhibitor of Heat Shock Protein 70 (Hsp70). |
| Sorafenib, BAY 43-9006 (Nexavar ®) | A multikinase inhibitor, it inhibits both wild type and V600E mutant BRAF, CRAF, VEGFRII (Flk-1), VEGFRIII, PDGFRβ, Flt3, and c-Kit. |
| RAF265 /CHIR-265 | RAF265 inhibits CRAF, wild type BRAF and mutant BRAFV600E |
| Dabrafenib GSK2118436 (Tafinlar®) | Mutant BRAFV600 specific inhibitor. |
| Vemurafenib, PLX4032, RG7204 (Zelboraf ®) | Inhibits BRAFV600E and wild-type BRAF. |

| | |
|---|---|
| Ibrutinib, PCI-32765 (IMBRUVICA®) | A selective BTK inhibitor. |
| Trametinib, GSK1120212 (Mekinist®) | A specific MEK1/2 inhibitor. |
| PD0325901 (Licensed by Pfizer feb-2015) | MEK1/2 inhibitor. |
| Selumetinib, AZD6244 | MEK1/2 inhibitor, also inhibits ERK1/2 phosphorylation. |
| C-RAF inhibitor (475958 Millipore) | A selective type II inhibitor of CRAF. |
| UO126- EtOH | A selective inhibitor of MEK1/2. |

**Table 4.1 Inhibitors used in this experiment (16) to screen responses of 5 primary CLL cells.**

Proliferation signalling were targeted in 5 CLL primary cells using different inhibitors that are demonstrated in figure 4.1. RAF kinase, MEK/ERK, JAK/STAT, PI3K and HDAC, proteasome, heat shock protein, CDKs, BTK and PDK1 inhibitors. Dinaciclib, CUDC-907, and MG-132 were potent inhibitors. VER-155008, BX-912, fedratinib, sorafenib, RAF265, and ibrutinib were of moderate efficacy.

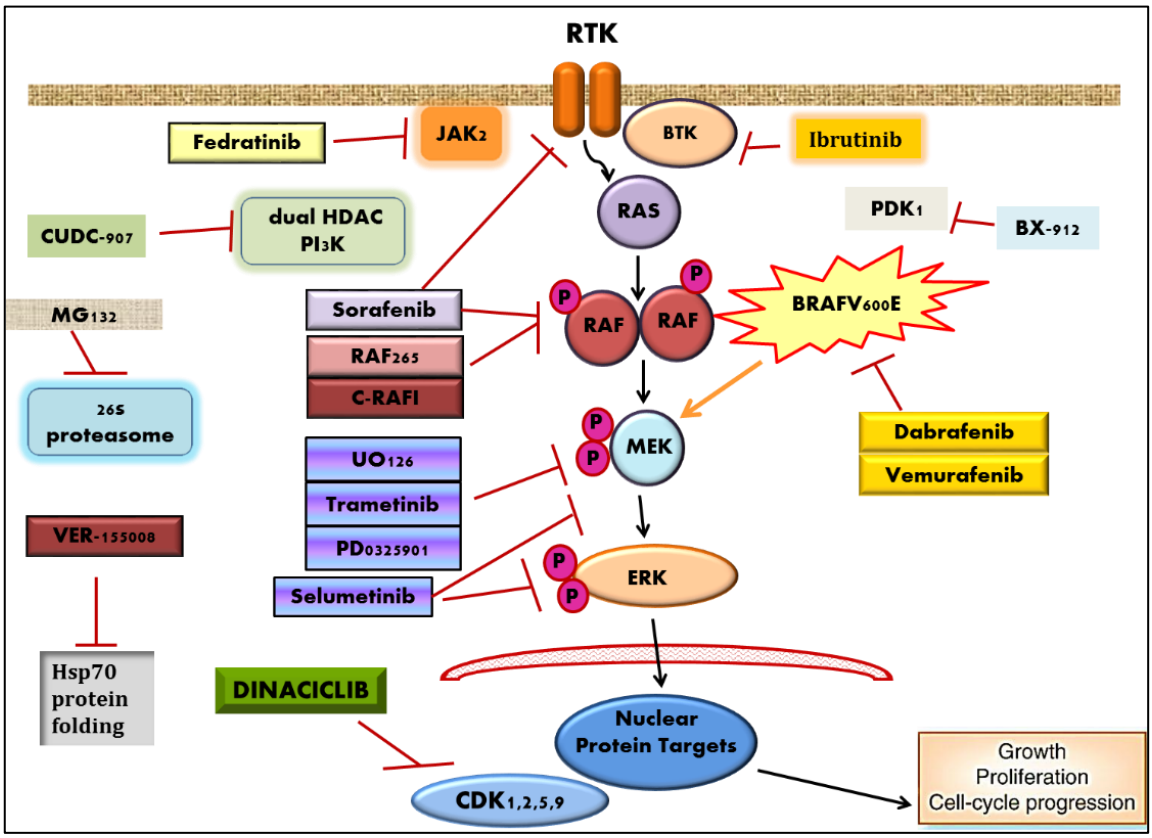


**Figure 4.1 Inhibitors that have been used in sensitivity screening of primary CLL cells.**

The figure shows mainly different inhibitors of MAPK and other anticancer inhibitors which target other signalling.

## 4.1 Primary cells have variable sensitivity to the inhibitors tested.

We first tested the viability of primary CLL cells after being exposed to different targeted inhibitors. Patient information is shown in table 4.2.

| Patient number | IGHV | Gender | Cytogenetics |
|---|---|---|---|
| **P65** | M | M | A clone with heterozygous deletion in 13q14 (89%) |
| **P29** | No band | F | Normal |
| **P38** | U | F | BCL3 break (62%), trisomy 12 83% |
| **P70** | M | M | An IGH-BCL2-fusion (95%) and a (partial) trisomy 12 (8%) |
| **P137** | U | M | n.d |

**Table 4.2 Available information of patients, including mutations and cytogenetic abnormalities.**

n.d stands for not done.

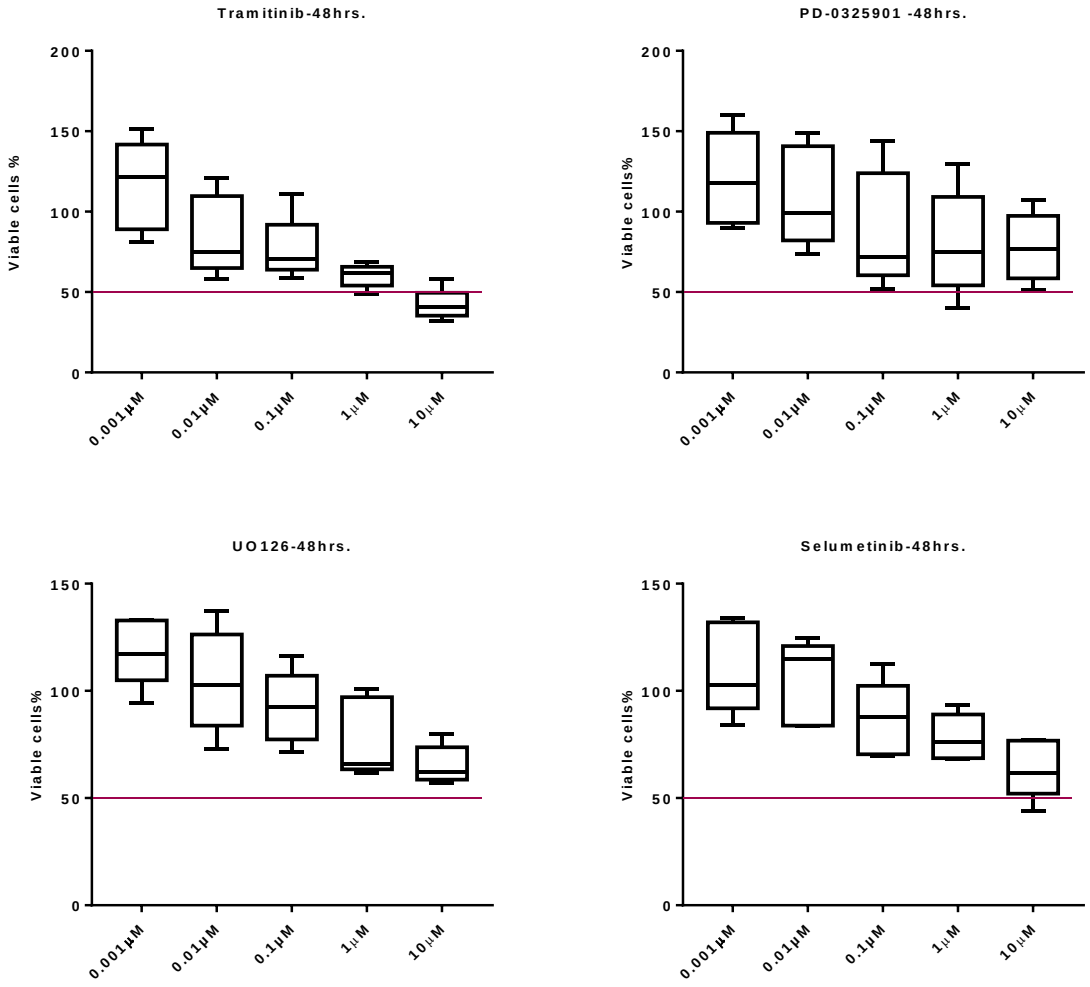


**Figure 4.2 MEK1/2 inhibitors efficacy in primary CLL cells.**

Box plot figure, each box represents (CLL viable primary cells percentage n=5) after 48 hours treatment with MEK1/2 inhibitors. The middle line represents the mean of n=5 viable cells %. Error bars represent SD between n=5 viable cells %. Primary cells were stimulated with (sCD40L-IL4) for 24hrs, then cells were plated in 96 wells plates, treated for 48 hours with 5 concentrations (10, 1, 0.1, 0.01, 0.001µM) of each inhibitor and in technical triplicate per concentration. After treatment MTS cell viability assay reagent was added, and plate were incubated for 2-4 hours in 5% CO2 37°C and then read using plate reader.

MEK1/2 inhibitors (Selumetinib, PD-0325901, and UO126) did not reduce cell viability below 50%. However, high concentrations of trametinib (10µM) substantially reduced viability of all primary CLL cells.

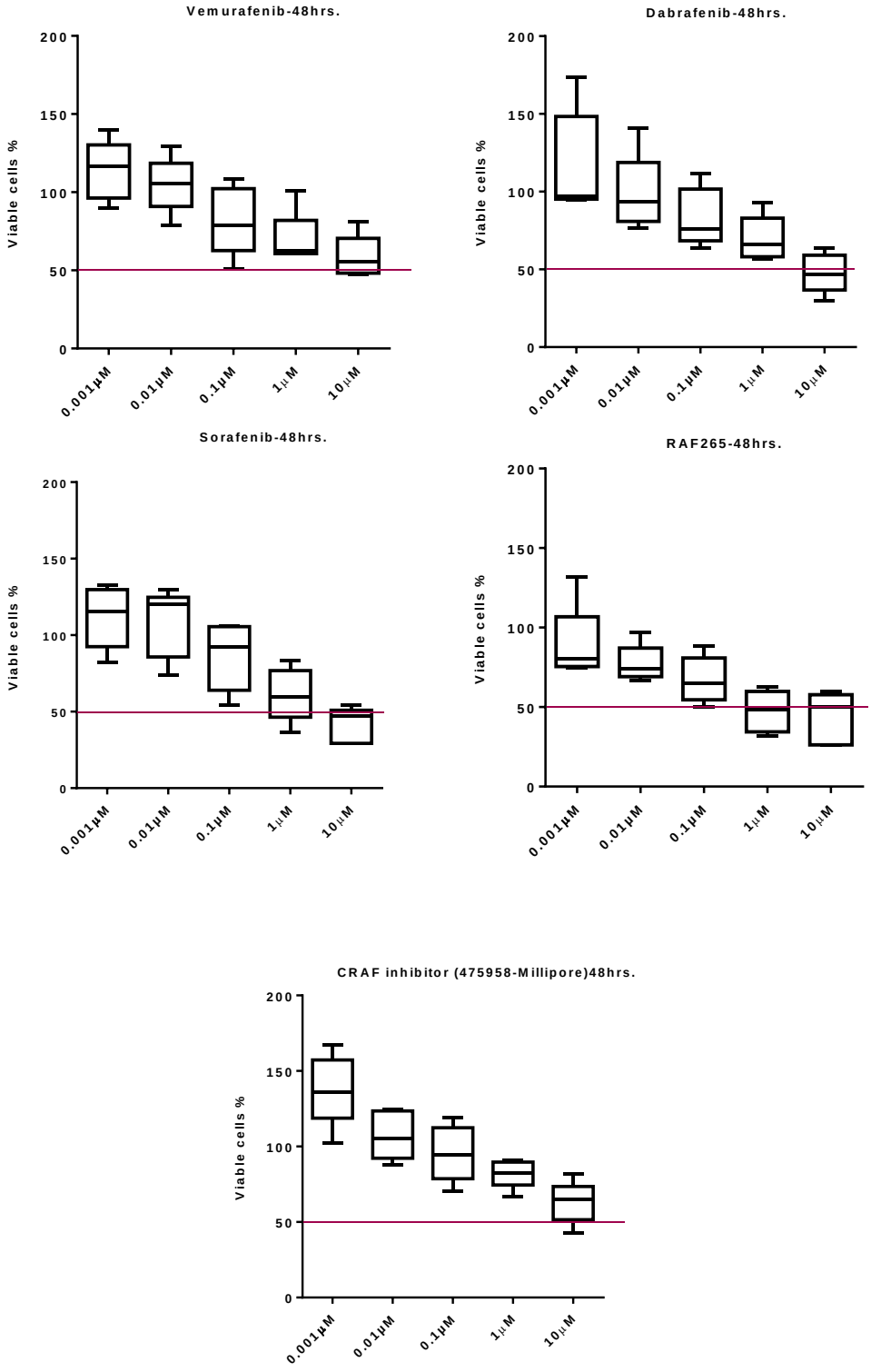


**Figure 4.3 RAF kinase inhibitors efficacy in primary CLL cells.**

Box plot figure, each box represents (CLL viable primary cells percentage n=5) after 48 hours treatment with RAF inhibitors. The middle line represents the mean of n=5 viable cells %. Error bars represent SD between n=5 viable cells %. Primary cells were stimulated with (sCD40L-IL4) for 24hrs, then cells were plated in 96 wells plates, treated for 48 hours with 5 concentrations (10, 1, 0.1, 0.01, 0.001µM) of each inhibitor and in technical triplicate per concentration. After treatment MTS cell viability assay reagent was added, and plate were incubated for 2-4 hours in 5% CO2 37°C and then read using plate reader.

RAF inhibitors (sorafenib and RAF265) showed substantial efficacy, decreasing viable cells percentage under 50% in high concentrations of 10µM, and partly at 1µM. vemurafenib significantly reduced cells viability only at 10µM in 2 patients, and dabrafenib in 3 out of 5 patients. C-RAF inhibitor showed no efficacy in reducing viable cells.

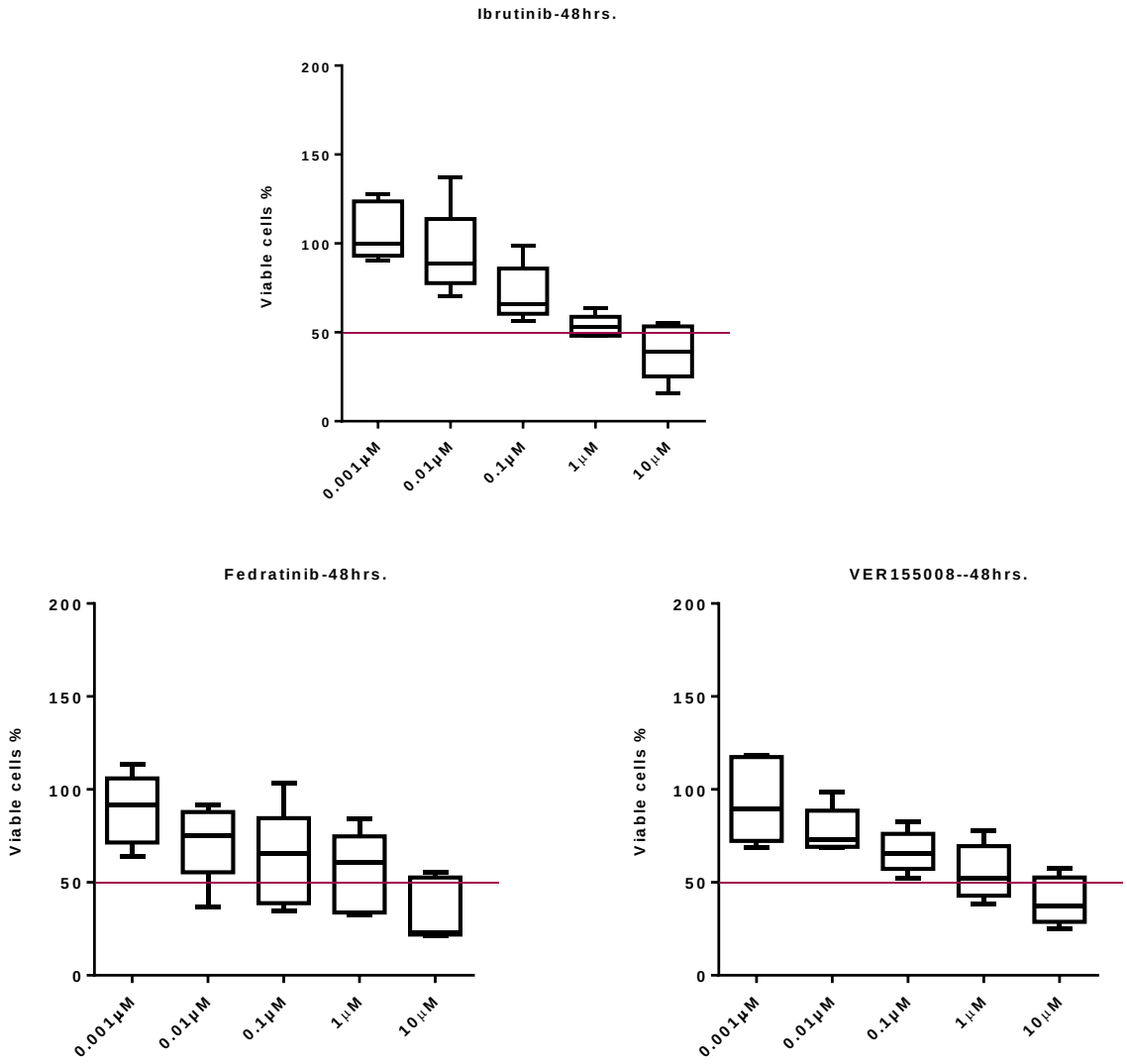


**Figure 4.4 Ibrutinib BTK kinase inhibitor, heat shock protein inhibitor VER-155008, and fedratinib JAK2 inhibitor efficacy in primary CLL cells.**

Box plot figure, each box represents (CLL viable primary cells percentage n=5) after 48 hours treatment with different inhibitors. The middle line represents the mean of n=5 viable cells %. Error bars represent SD between n=5 viable cells %. Primary cells were stimulated with (sCD40L-IL4) for 24hrs, then cells were plated in 96 wells plates, treated for 48 hours with 5 concentrations (10, 1, 0.1, 0.01, 0.001µM) of each inhibitor and in technical triplicate per concentration. After treatment MTS cell viability assay reagent was added, and plate were incubated for 2-4 hours in 5% CO2 37°C and then read using plate reader.

High concentration of ibrutinib reduced viable primary CLL cells under 50%, VER-155008 and fedratinib decreased CLL cell viability at 10μM, and to some extent, at 1μM.

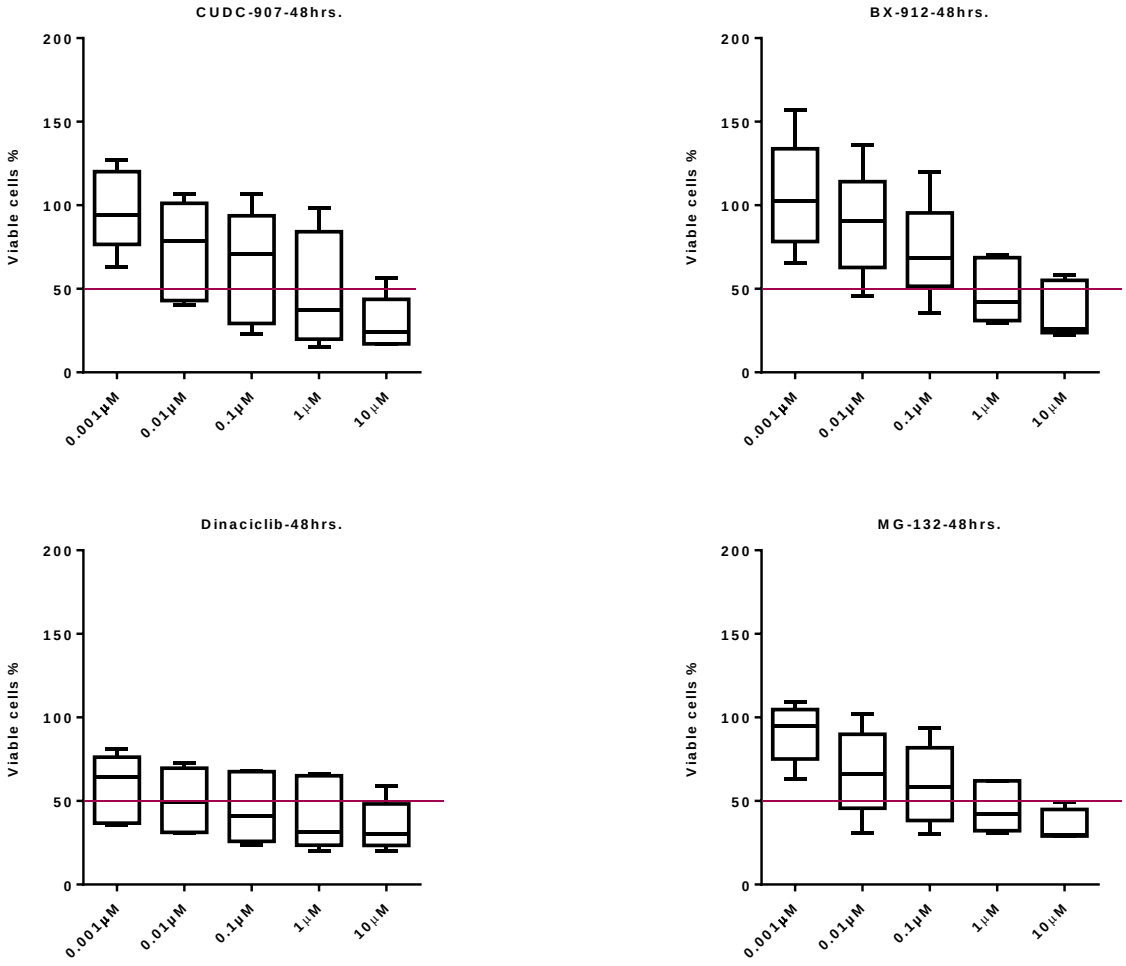


**Figure 4.5 CUDC-907 dual HDAC and PI3K inhibitor, BX-912 PDK1 inhibitor, dinaciclib CDK inhibitor, and MG-132 heat shock protein inhibitor efficacy in primary CLL cells.**

Box plot figure, each box represents (CLL viable primary cells percentage n=5) after 48 hours treatment with different inhibitors. The middle line represents the mean of n=5 viable cells %. Error bars represent SD between n=5 viable cells %. Primary cells were stimulated with (sCD40L-IL4) for 24hrs, then cells were plated in 96 wells plates, treated for 48 hours with 5 concentrations (10, 1, 0.1, 0.01, 0.001μM) of each inhibitor and in technical triplicate per concentration. After treatment MTS cell viability assay reagent was added, and plate were incubated for 2-4 hours in 5% CO2 37°C and then read using plate reader.

Dinaciclib showed apparent inhibitory effect on viable cells, even at low concentrations. CUDC-907 907 and MG-132 also showed viable cell inhibition under 50% in 2 out of 5 patients. MG-132 achieved it in 1 out of 5 CLL cells. BX-912 also reached IC50 at a physiologically relevant concentrations in nanomolars. These four drugs were the most potent of all tested.

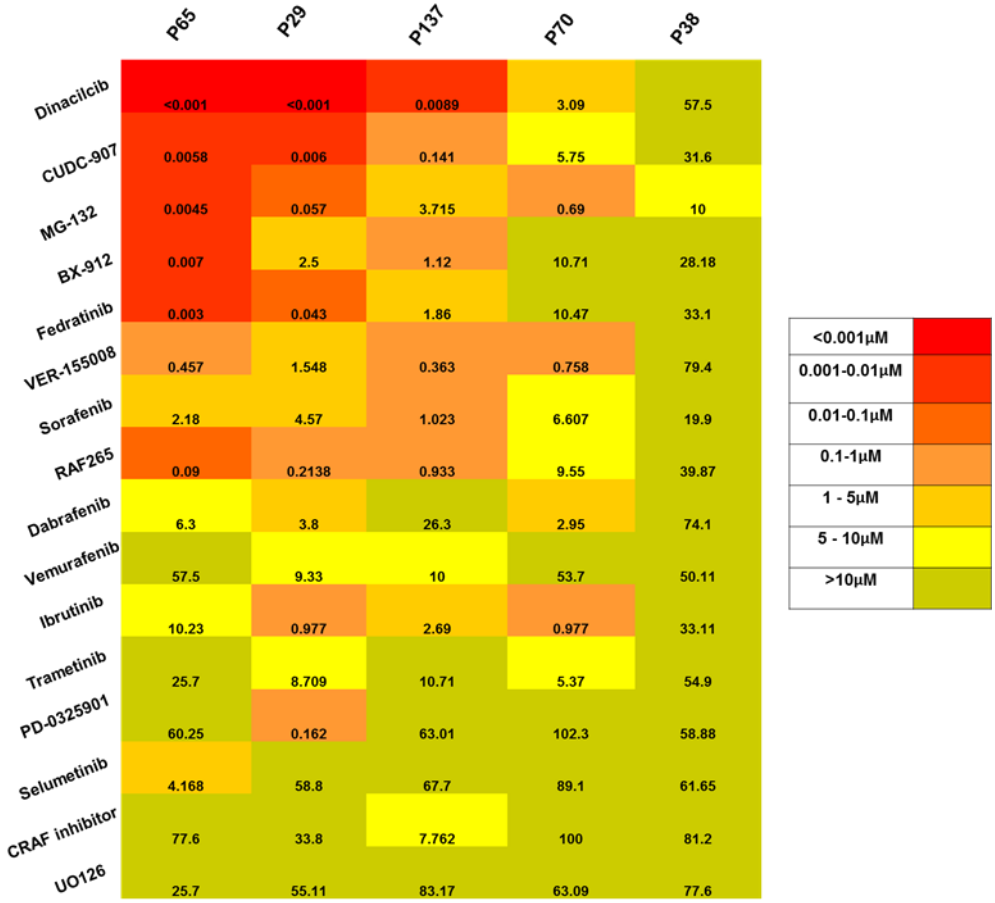


**Figure 4.6 IC50 heat map for all n=5 CLL cells to 16 different inhibitors.**

Each number indicated is IC50 value in µM concentrations. IC50 values were calculated using prism, IC50 values more than 10µM were estimated from the curve.

Figure 4.6 shows a heat map of each inhibitor used (IC50). P65 cells appear to be considerably sensitive to dinaciclib, CUDC-907, MG-132, BX-912, and fedratinib. In addition, has moderate IC50 value to RAF inhibitors (dabrafenib, sorafenib, RAF265), to VER155008, and to selumetinib. P65 is mutated (IGHV) and has 13q deletion, which are linked to favourable prognosis (table 4.2). Conversely, P38 cells displayed consistently higher IC50 values. P38 is unmutated (IGHV), which is linked to poor prognosis and short time to treatment, and has trisomy 12, which might be associated with NOTCH1 mutations. P137, P29, and P65 are sensitive to dinaciclib in nanomolar concentrations.

P29 has no cytogenetic abnormalities. P137 is unmutated, which has poor outcomes, but its response is different from P38. P137 has a moderate response to inhibitors in comparison to the IC50 of P38. P70 is mutated but had an IC50 above what expected to dinaciclib, CUDC-907, and MG-132, may be due to partial trisomy 12. Of note, the IC50 value of sorafenib are not drastically different for P29, P65, P137 and P70. However, P38

needed up to 19.9μM to reach 50% inhibition of viable cells. In conclusion, the response of CLL cells to the 16 inhibitors was highly patient dependent. We could potentially predict the responses of CLL cells according to their U or M IGHV status, and to their cytogenetic abnormalities, which endorses stratification of patients and the precision medicine principles.

## 4.2 Relationship between pathway inhibition and cell viability in CLL.

We aim in this experiment to look at MAPK inhibitors effect on the expression of P-BRAF, P-MEK, P-ERK, NF-κB P65, P-AKT and PARP cleavage after treatment of all 5 CLL cells that we tested with MTS assay previously. Due to lack of material, I was able to do Western blotting with only 2 out of five primary CLL cells. Treatments were done for 24 hours and 10μM of each inhibitor. P38 is U-CLL, while P65 is M-CLL, and their cells were used as representative of the two categories of CLL.

As can be seen in figure 4.7, most of the protein inhibition in patient P38 occurred in unstimulated cells, while we used stimulated cells in MTS assay and therefore, we could not see any sensitivity to inhibition with CD40L-IL-4 stimulation.

PARP was cleaved in unstimulated cells of P38 with sorafenib 10μM and ERK phosphorylation was reduced compared to control cells. Other inhibitors did not produce any significant PARP cleavage, possibly because of their high IC50 values. NF-κB P65, which enhances anti-apoptotic signals, were significantly higher in stimulated CLL cells, which enhance anti-apoptotic signals, and AKT was less phosphorylated in unstimulated treated cells. That demonstrates the protective effects of the CLL microenvironment, as expected. Surprisingly, MEK phosphorylation was increased more than in control cells after treatment with trametinib which was unexpected. Also, phosphorylated BRAF seems to be not significantly affected by treatment but slightly reduced in unstimulated cells. Vemurafenib decreased phosphorylated ERK but has no major effect on PARP cleavage in unstimulated cells. Consistent with our MTS results, IC50 values of P38 of trametinib, dabrafenib, vemurafenib, and sorafenib were higher than 10μM, and PARP cleavage was not observed in stimulated cells.

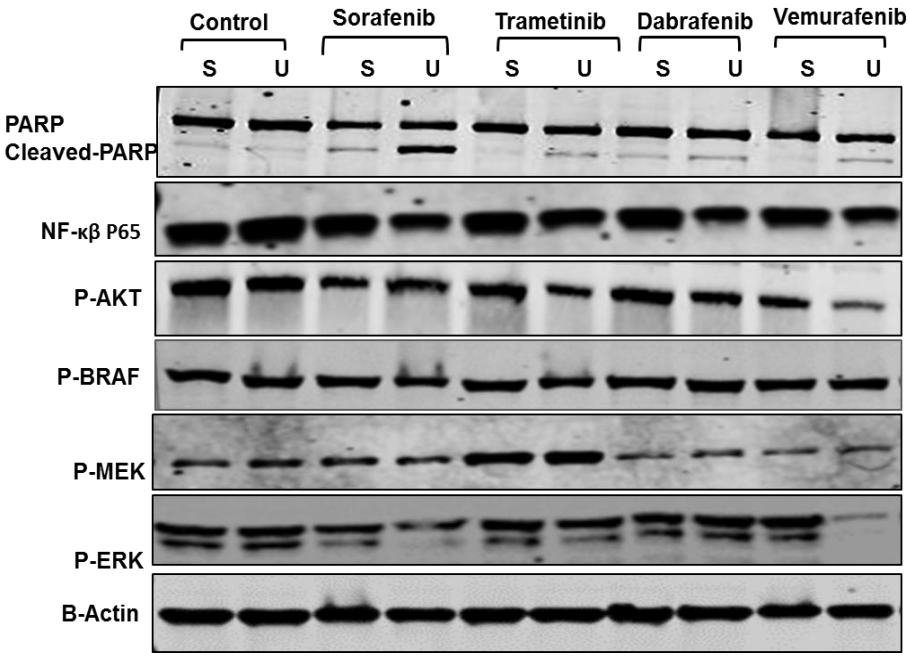


**Figure 4.7 Western blotting of primary cells P38 treated with inhibitors for 24 hours.**

Primary cells were plated in 6 well plates, stimulated with sCD40-L and IL-4 for ~24 hours (S) or unstimulated (U), then treated with inhibitors (diluted in media for DMSO ~0.1-0.2%). DMSO ~0.1-0.2% was added to untreated control cells as well, cells pellets were collected, and Western blotting analysis was performed loading 30-50µg protein/well in 10% SDS-gel. Antibodies for NF-κB P65, P-AKT S473, P-BRAF S445, P-ERK T202, Y204, P-MEK S217, S221, and PARP and cleaved PARP were used. Sorafenib, dabrafenib, trametinib, and vemuarfenib all in 10µM concentration.

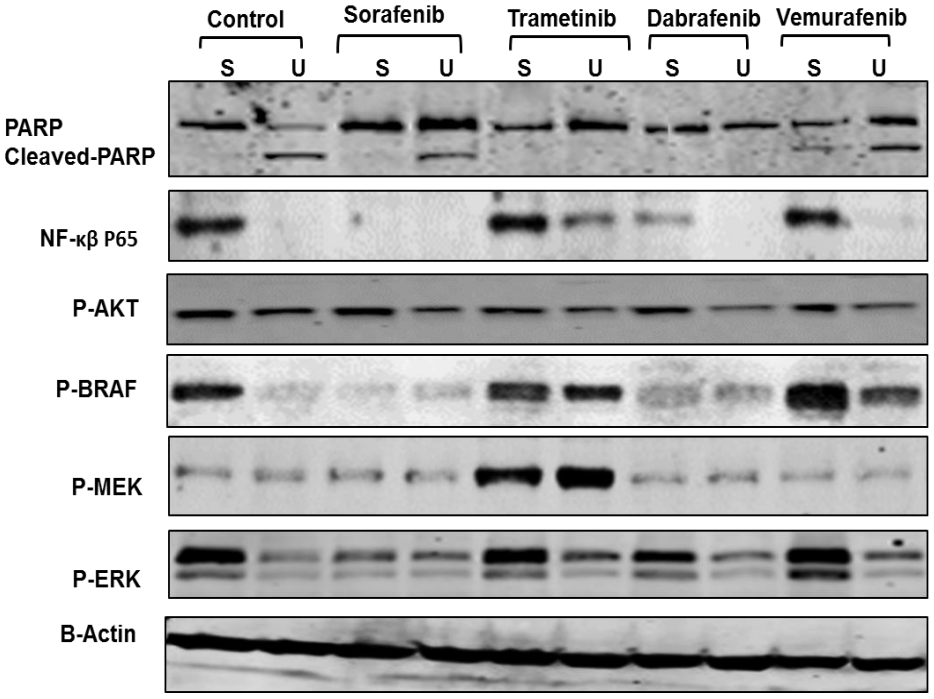


**Figure 4.8 Western blotting of primary cells P65 treated with inhibitors for 24 hours.**

Primary cells were plated in 6 well plates, stimulated with sCD40-L and IL-4 for ~24 hours (S) or unstimulated (U), then treated with inhibitors (diluted in media for DMSO ~0.1-0.2%). DMSO ~0.1-0.2% was added to untreated control cells as well, cells pellets were collected, and Western blotting analysis was performed loading 30-50µg protein/well in 10% SDS-gel. Antibodies for NF-κB P65, P-AKT S473, P-BRAF S445, P-ERK T202, Y204, P-MEK S217, S221, and PARP and cleaved PARP were used. Sorafenib, dabrafenib, trametinib, and vemuarfenib all in 10µM concentration.

P65 belongs to better prognosis category. As can be seen in figure 4.8 PARP cleavage in unstimulated cells, even in control cells, implies that these cells have spontaneous apoptotic tendency if not stimulated. PARP was considerably cleaved in unstimulated cells with sorafenib, and was significantly cleaved with vemurafenib, indicating that cells are undergoing apoptosis. Remarkably, NF-κB P65, P-BRAF, P-MEK, and P-ERK were slightly observed in control unstimulated cells, and were inhibited by sorafenib in both stimulated and unstimulated cells. This was also the case, with dabrafenib and vemurafenib treatment of unstimulated cells. Of note, MEK was more phosphorylated in trametinib treated cells than control cells. Phosphorylated AKT was low in all unstimulated cells. Our MTS IC50 value were low for sorafenib, which is comply with our observation were sorafenib inhibited mostly all protein expression in stimulated cells except P-AKT with no PARP cleavage. Dabrafenib treatment resulted in decrease in P-MEK, P-BRAF, NF-κB and its IC50 value was moderate. Vemurafenib and trametinib have no significant effects in stimulated cells and their IC50 value was high in MTS assay results.

M-CLL samples showed apoptotic PARP cleavage and more sensitivity with Sorafenib treatment, even stimulated cells. This could be interesting to explore further. Sorafenib switched off proteins phosphorylation of MAPK, and NF-κB P65 in M-CLL (P65) but not in U-CLL (P38). It seems that NF-κB P65 inhibition and P-ERK reduction are linked to PARP cleavage in MCLL cells, and could be used as markers of cells sensitivity.

Trametinib increases MEK phosphorylation in both patients, and showed lower efficacy in both patients in MTS assay results. This protein is supposed to be a target of trametinib. Possibly MEK phosphorylation in the presence of MEK inhibitor could be the result of upstream RAF reactivation, as we can see no effect on P-BRAF.

Western blotting were confirmatory of the drug-sensitivity that we have observed with MTS assay, which is dependent on CLL cells prognostic cytogenetic abnormalities.

## 4.3 Combination treatments show promising results for CLL cells

Before starting treatment, clones of drug-resistant mutants occur in cancers in low levels. Single agent treatment will give the chance of cells to develop resistant clones, and by the time of change to a second line single agent treatment, the probability of getting resistant clones to the second agent as well is higher. Ending up with double resistant clones to both single agents (Komarova and Boland, 2013). However, combination drugs of two single agents together at the beginning of treatment will increase treatment efficiency (Figure.4.9). Combination therapy might help to reduce drug resistant evolution and decrease toxicities of high dose of single agents. Preclinical studies plays a main role in developing such drug combinations, which might be applicable to certain patients of certain disease. However, there are limitations in the animal models of certain diseases. Also, the drugs that could work in an animal might not show same efficacy in a human. These are of disadvantages that could happen throughout research for suitable combination therapies (He *et al*, 2016).

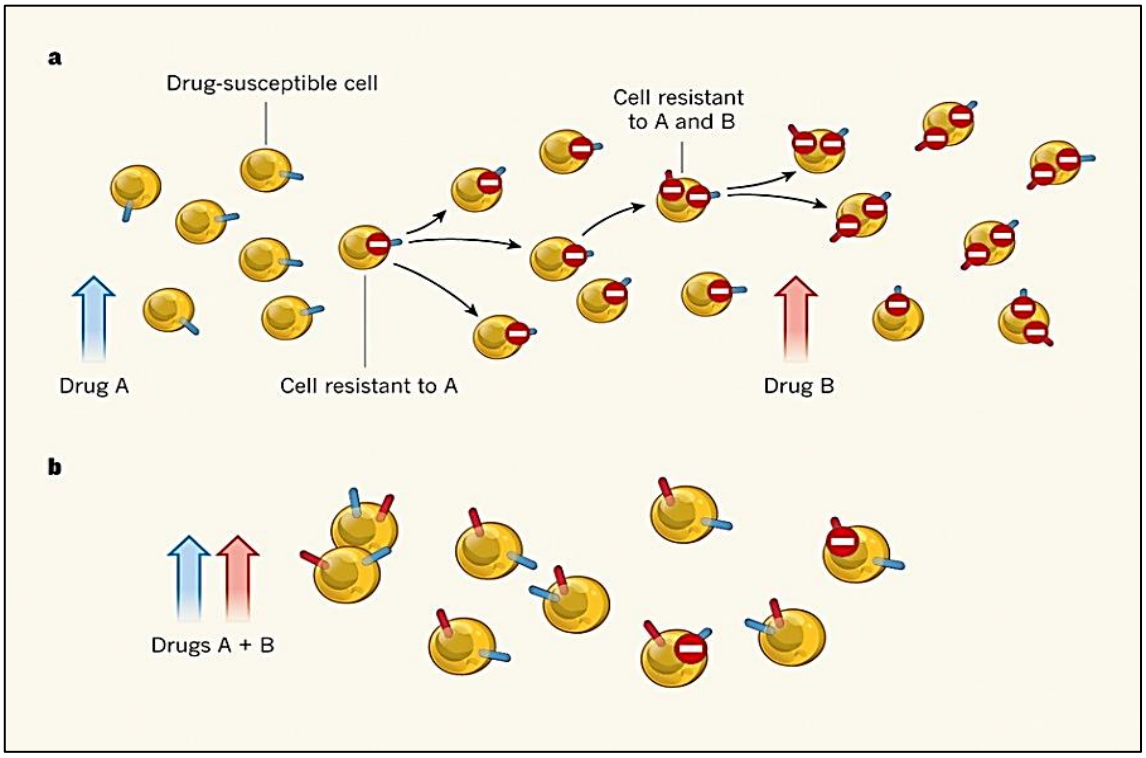


**Figure 4.9 Single agent treatment versus combination treatment.**

**A**) Treatment with single agent A will lead to resistant clones to drug A, as well as treatment with drug B as single agent will result in clones resistant to B. ending with two clones resistant to A and B. **B**) treatment with both (A+B) will result in resistance to either one of them and sensitive to the other, thus increase the chance of effective treatment. This figure was adapted from (Komarova and Boland, 2013).

We aimed to find potential combination therapies for CLL primary cells. (Sorafenib and CUDC-907) were chosen among other possible combination treatment according to IC50 previously calculated with MTS cell viability assay. CUDC-907 was chosen as a strong inhibitor with low IC50 concentration that might help to sensitize cells to the effect of sorafenib, which is a moderately effective inhibitor of cell viability, according to our previous results. Sorafenib was used in five concentrations (10, 1, 0.1, 0.01, 0.001µM), while CUDC-907 was fixed at three concentrations (0.01µM, 0.001µM, 0.0005µM). Cells were stimulated to mimic CLL microenvironment. 11 CLL primary cells were used in this study (Table 4.5).

| **Patient number** | **Age at diagnosis** | **IGHV M/U** | **Gender** | **Cytogenetic abnormalities** |
|---|---|---|---|---|
| P50 | 61 | M | M | Heterogeneous 13q deletion (66%) |
| P29 | | No band | F | Normal |
| P70 | 56 | M | M | Partial trisomy12 |
| P102 | 77 | U | M | Normal |
| P109 | 74 | U | M | Normal |
| P119 | 75 | U | M | |
| P121 | 72 | U | M | |
| P137 | | U | M | |
| P38 | | U | F | Trisomy 12 (83%) BCL3 breaks (62%) |
| P153 | | M | F | 13q deletion (79%) |
| P65 | | M | M | Heterozygous 13q14 deletion (89%) |

**Table 4.3 Available information of CLL patients used for combination testing. Empty boxes are either not done or not known.**

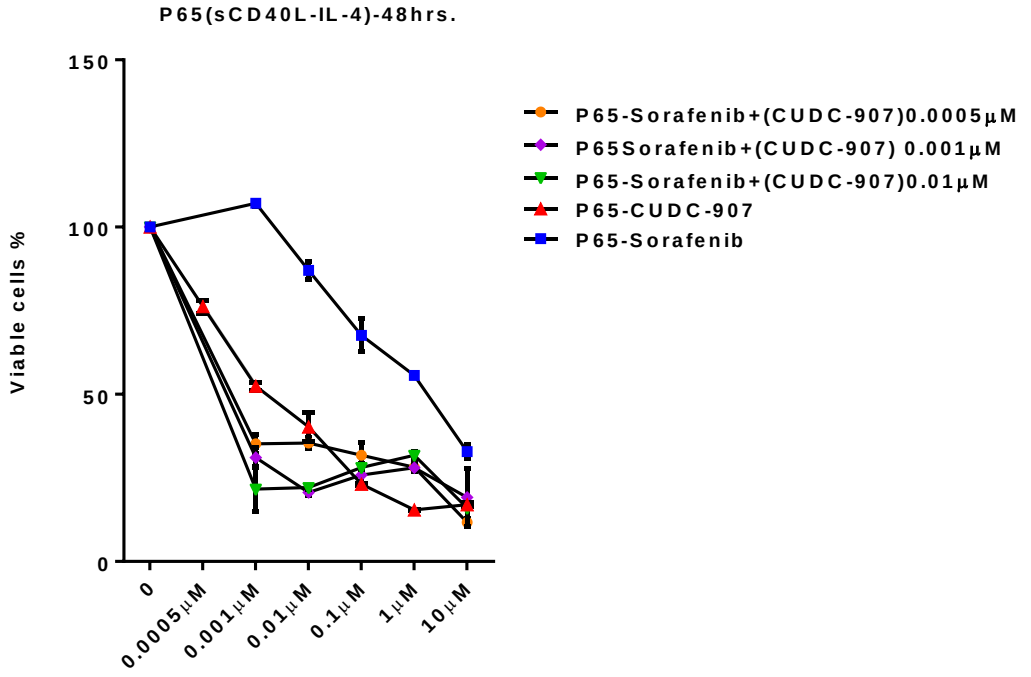
P65(sCD40L-IL-4)-48hrs.
Viable cells %
150
100
50
0
0
0.0005µM
0.001µM
0.01µM
0.1µM
1µM
10µM
P65-Sorafenib+(CUDC-907)0.0005µM
P65Sorafenib+(CUDC-907) 0.001µM
P65-Sorafenib+(CUDC-907)0.01µM
P65-CUDC-907
P65-Sorafenib

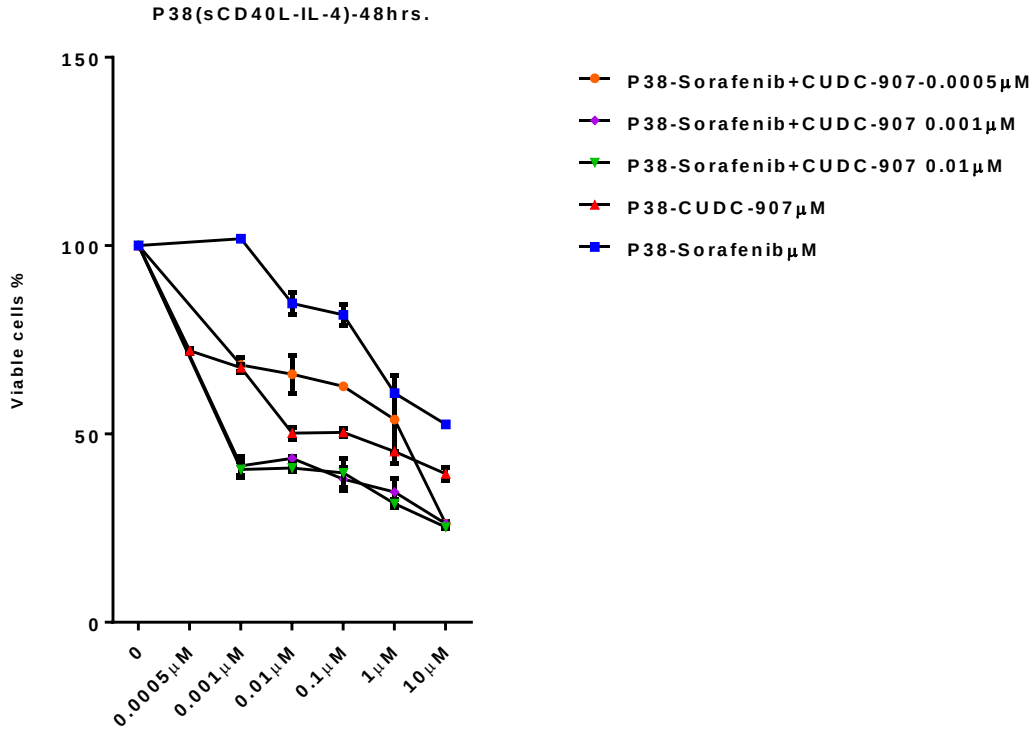
P38(sCD40L-IL-4)-48hrs.
Viable cells %
150
100
50
0
0
0.0005µM
0.001µM
0.01µM
0.1µM
1µM
10µM
P38-Sorafenib+CUDC-907-0.0005µM
P38-Sorafenib+CUDC-907 0.001µM
P38-Sorafenib+CUDC-907 0.01µM
P38-CUDC-907µM
P38-SorafenibµM

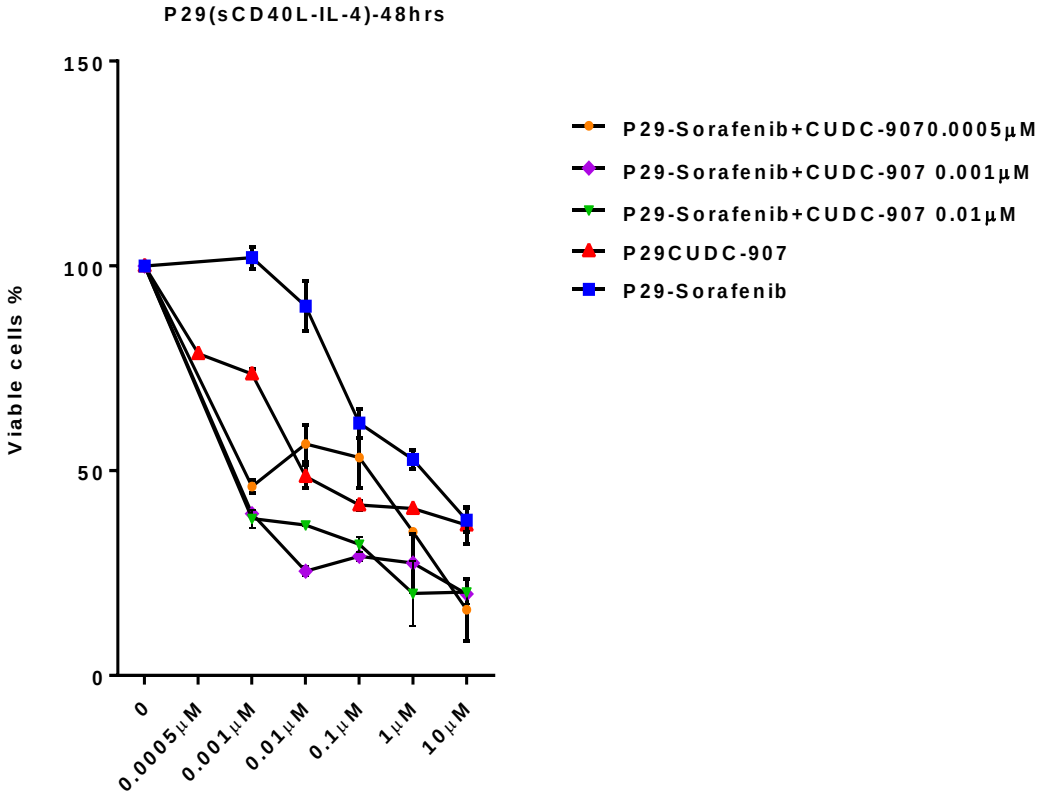
P29(sCD40L-IL-4)-48hrs
Viable cells %
150
100
50
0
0
0.0005µM
0.001µM
0.01µM
0.1µM
1µM
10µM
P29-Sorafenib+CUDC-9070.0005µM
P29-Sorafenib+CUDC-907 0.001µM
P29-Sorafenib+CUDC-907 0.01µM
P29CUDC-907
P29-Sorafenib

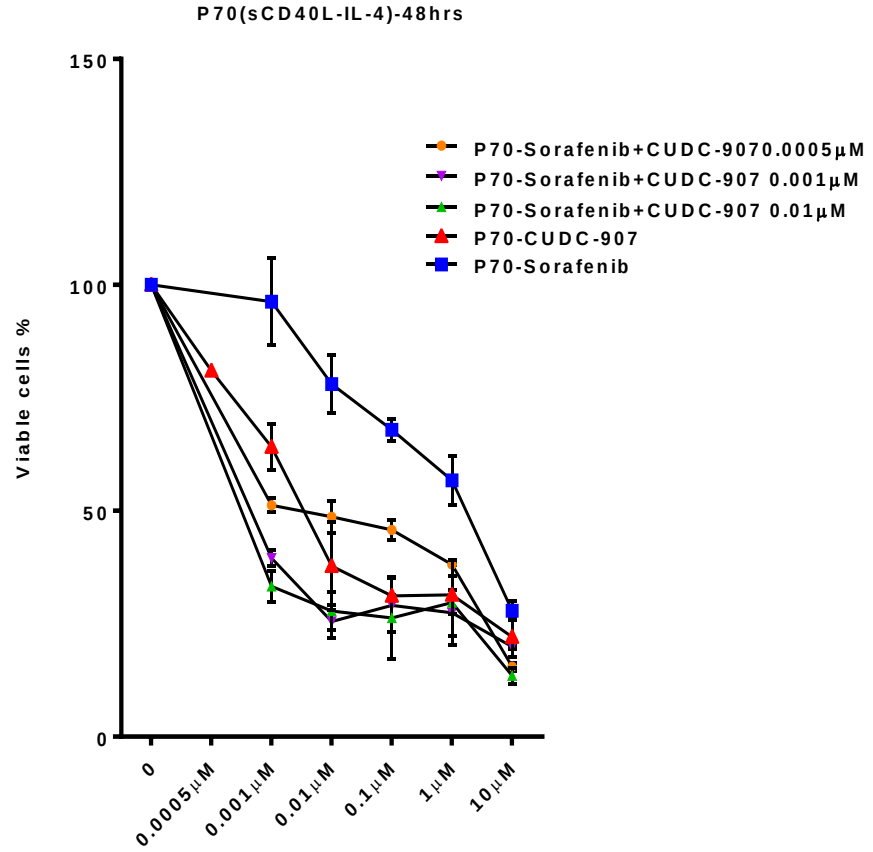
P70(sCD40L-IL-4)-48hrs
Viable cells %
150
100
50
0
0
0.0005µM
0.001µM
0.01µM
0.1µM
1µM
10µM
P70-Sorafenib+CUDC-9070.0005µM
P70-Sorafenib+CUDC-907 0.001µM
P70-Sorafenib+CUDC-907 0.01µM
P70-CUDC-907
P70-Sorafenib

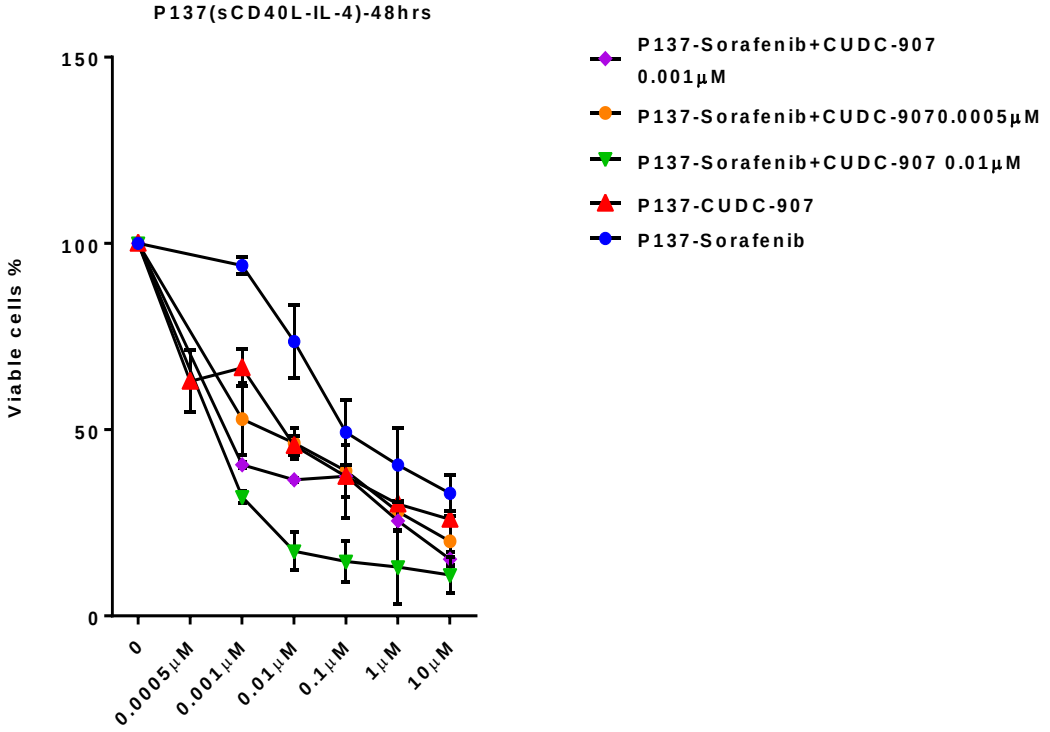
P137(sCD40L-IL-4)-48hrs
Viable cells %
150
100
50
0
0
0.0005µM
0.001µM
0.01µM
0.1µM
1µM
10µM
P137-Sorafenib+CUDC-907 0.001µM
P137-Sorafenib+CUDC-9070.0005µM
P137-Sorafenib+CUDC-907 0.01µM
P137-CUDC-907
P137-Sorafenib

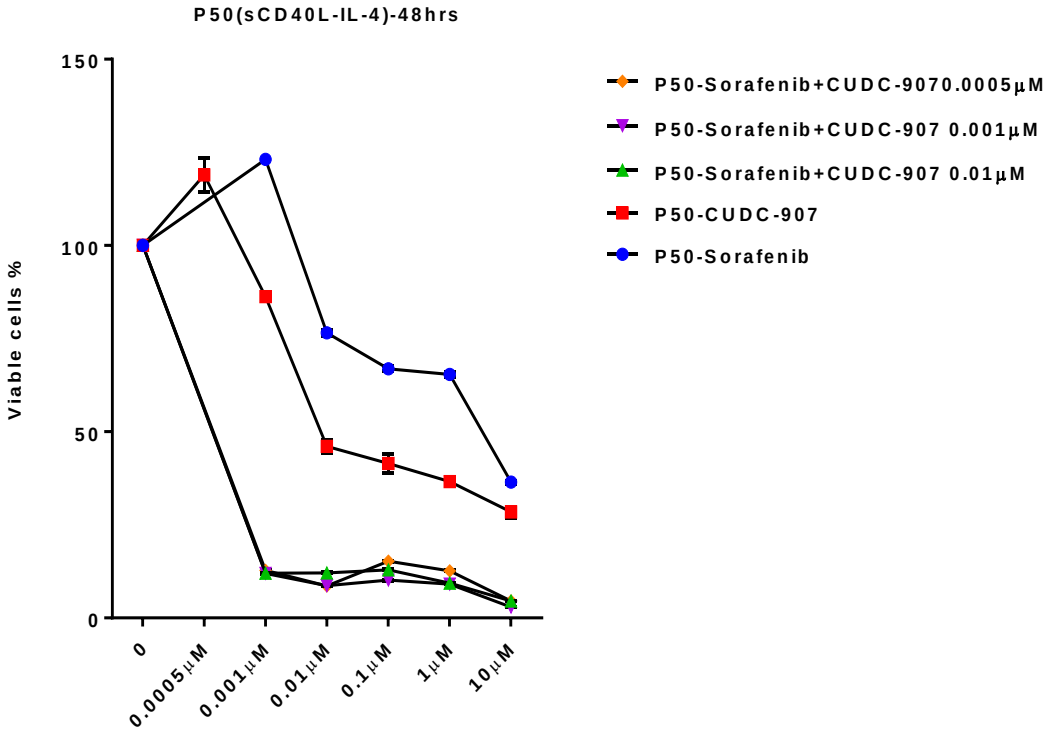
P50(sCD40L-IL-4)-48hrs
Viable cells %
150
100
50
0
0
0.0005µM
0.001µM
0.01µM
0.1µM
1µM
10µM
P50-Sorafenib+CUDC-9070.0005µM
P50-Sorafenib+CUDC-907 0.001µM
P50-Sorafenib+CUDC-907 0.01µM
P50-CUDC-907
P50-Sorafenib

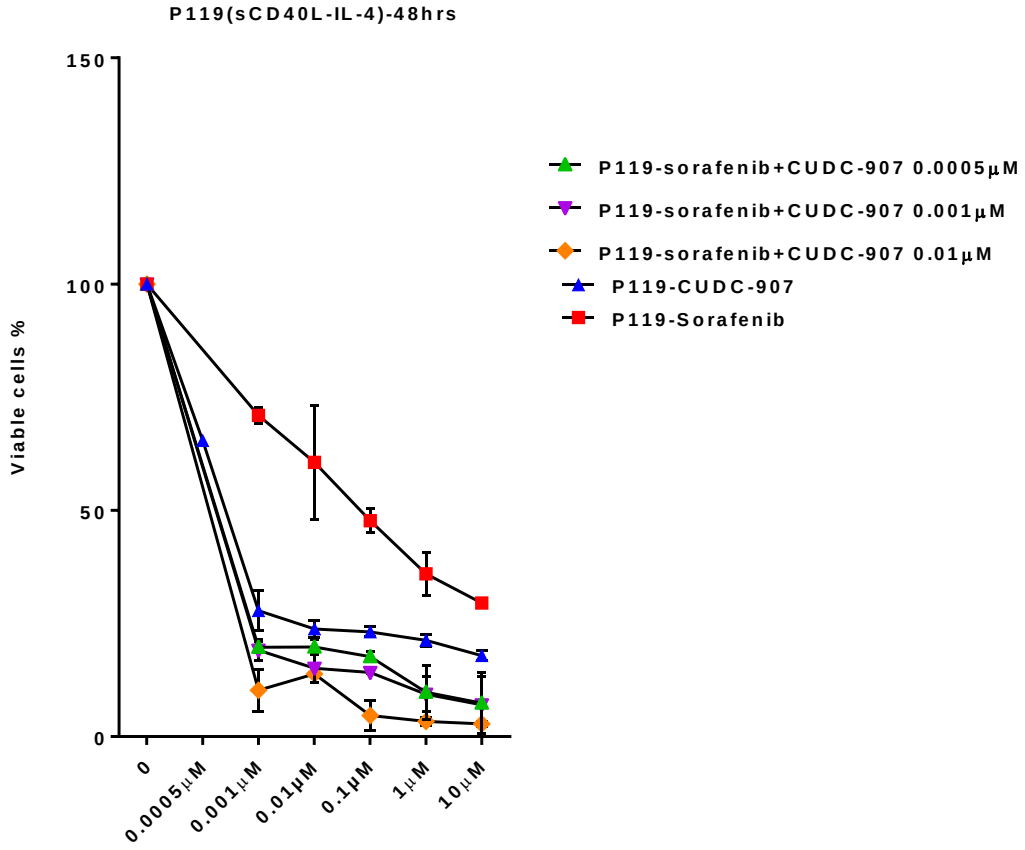
P119(sCD40L-IL-4)-48hrs
Viable cells %
150
100
50
0
0
0.0005μM
0.001μM
0.01μM
0.1μM
1μM
10μM
P119-sorafenib+CUDC-907 0.0005μM
P119-sorafenib+CUDC-907 0.001μM
P119-sorafenib+CUDC-907 0.01μM
P119-CUDC-907
P119-Sorafenib

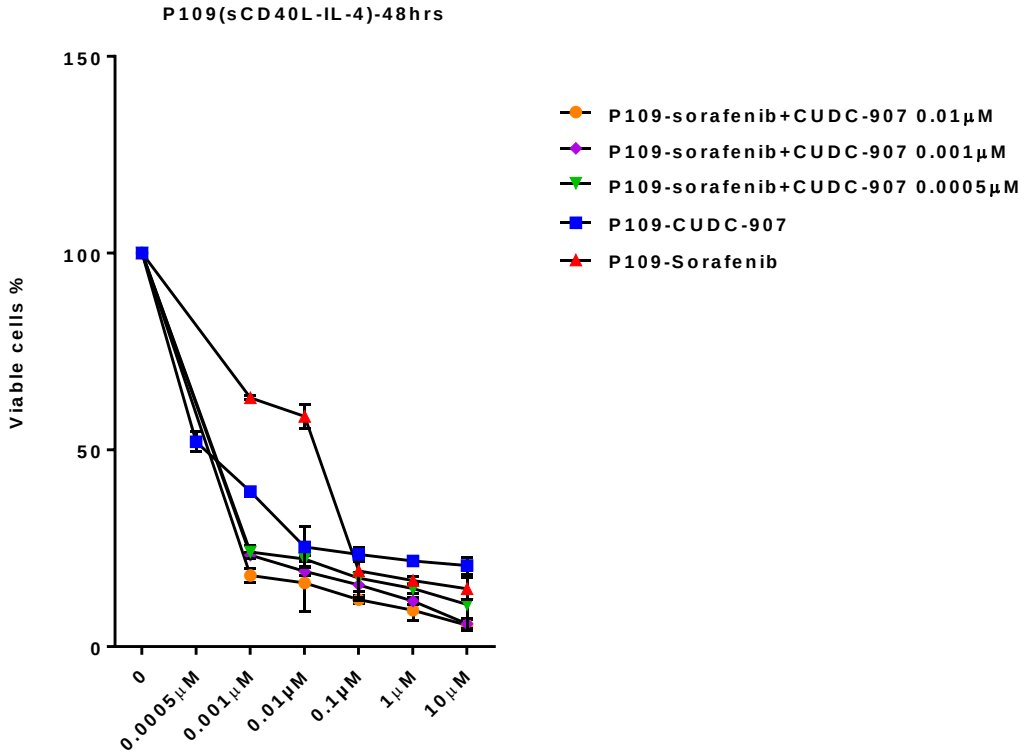
P109(sCD40L-IL-4)-48hrs
Viable cells %
150
100
50
0
0
0.0005μM
0.001μM
0.01μM
0.1μM
1μM
10μM
P109-sorafenib+CUDC-907 0.01μM
P109-sorafenib+CUDC-907 0.001μM
P109-sorafenib+CUDC-907 0.0005μM
P109-CUDC-907
P109-Sorafenib

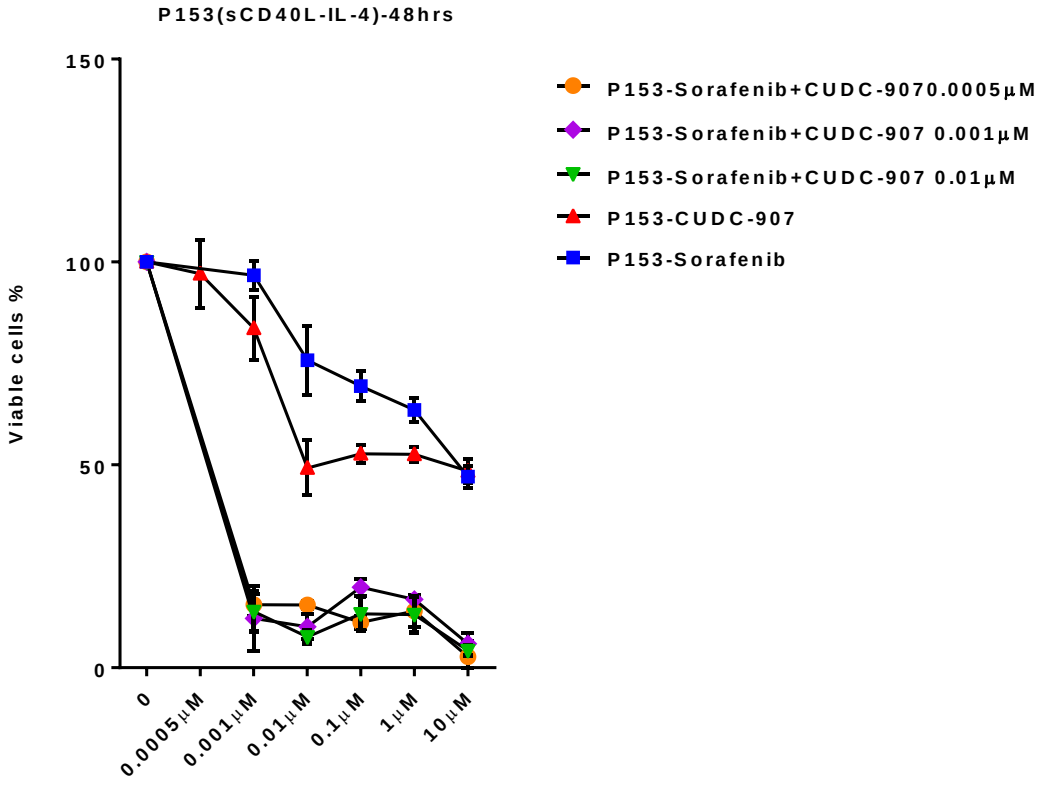
P153(sCD40L-IL-4)-48hrs
Viable cells %
150
100
50
0
0
0.0005µM
0.001µM
0.01µM
0.1µM
1µM
10µM
P153-Sorafenib+CUDC-9070.0005µM
P153-Sorafenib+CUDC-907 0.001µM
P153-Sorafenib+CUDC-907 0.01µM
P153-CUDC-907
P153-Sorafenib

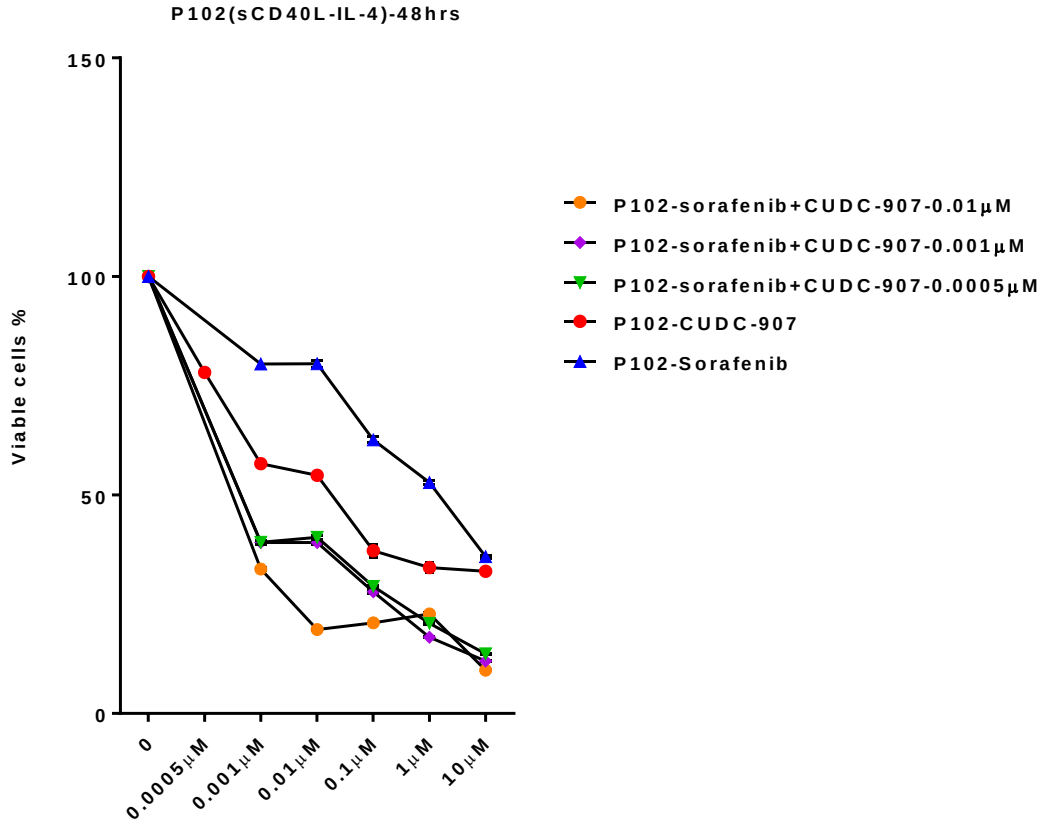
P102(sCD40L-IL-4)-48hrs
Viable cells %
150
100
50
0
0
0.0005µM
0.001µM
0.01µM
0.1µM
1µM
10µM
P102-sorafenib+CUDC-907-0.01µM
P102-sorafenib+CUDC-907-0.001µM
P102-sorafenib+CUDC-907-0.0005µM
P102-CUDC-907
P102-Sorafenib

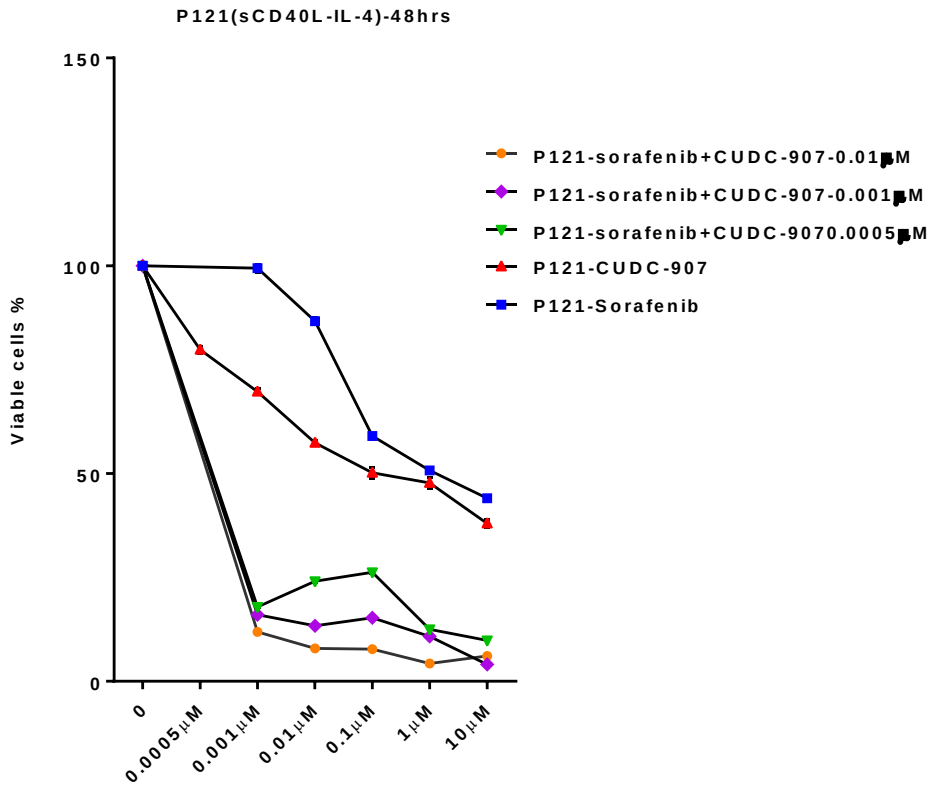


**Figure 4.10 MTS cell viability assay of combiantion treatment with sorafenib and CUDC-907 of 11 CLL patients.**

CLL cells were stimulated for 24 hours, counted, plated in 96 wells plates and, treated for 48 hours with CUDC-907 (0.01, 0.001, 0.0005µM) and sorafenib (10, 1, 0.1, 0.01, 0.001µM) together. Single agents testing on same plates was performed at five concentrations (10, 1, 0.1, 0.01, 0.001µM) of CUDC-907 and sorafenib. DMSO control was normalised to 100% of viable cells.

After performing MTS assay analysis (figure 4.10), combination indexes were calculated using CalcuSyn software for dose effect analysis. Table 4.4 shows the synergism and, antagonism CI combination index values. The results show very strong to strong synergism in all 11 CLL patients. That suggests this combination with 1nM and 0.5nM of CUDC-907 and different concentrations of sorafenib is very promising. Assessing its effects in *in vivo* models of CLL would be beneficial, specifically with only nanomolar concentrations of CUDC-907 that could be sensitizing cells to effects of sorafenib and inhibiting their viability.

| Range of CI Symbol Description | CalcuSyn description |
|---|---|
| <0.1 +++++ | Very strong synergism |
| 0.1-0.3 ++++ | Strong synergism |
| 0.3-0.7+++ | Synergism |
| 0.7-0.85++ | Moderate synergism |
| 0.85-0.90+ | Slight synergism |
| 0.90-1.10 ± | Nearly additive |
| 1.10-1.20 – | Slight antagonism |
| 1.20-1.45 – – | Moderate antagonism |

| Patients | CI (combination index) |
|---|---|
| P65 | 0.182 |
| P38 | 0.33 |
| P137 | 0.081 |
| P29 | 0.113 |
| P70 | 0.306 |
| P153 | 0.018 |
| P50 | 0.222 |
| P109 | 0.088 |
| P119 | 0.033 |
| P102 | 0.005 |
| P121 | 0.002 |

**Table 4.4 CI values according to CalcuSyn software. Under 0.1 is very strong synergism, over 0.9 is additive, and over 1 is antagonism.**

Combination treatment now is already been used in CLL, as monoclonal antibodies are being combined with chemotherapy and other agents. We have discovered that a combination of CUDC-907 in nanomolar concentrations and sorafenib was strongly synergistic in primary cells and it is encouraging that such a combination can be used in *in vivo* CLL models or in clinical trials in the future. We selected this combination from different other combinations, as this showed more viability inhibition. It would be interesting to test more agents for combination treatment based on this combination as a preliminary data.

## 4.4 Sanger sequencing for BRAF exon 15 mutations showed low frequency in CLL, and BRAF mutant CLL cells showed significant increased induction of the MAPK pathway.

BRAFV600E point mutation accounts for more than 90% of all BRAF mutations. However, it occurs at low frequencies in CLL (Langabeer *et al*, 2012). BRAF is mutated in approximately 8% of all cancers and in approximately 50% of melanoma cases (Holderfield *et al*, 2014). This mutation results in constitutive active BRAF that lead to constitutive activation of BRAF/MEK/ERK axis independently of RAS and thus to

cancer cell survival (Davies *et al*, 2002). It has been reported in a study that 1.5% CLL patients have BRAF V600E mutations, and 7% of Richter syndrome transformed CLL (Sellar *et al*, 2015). All of the above information suggests that BRAFV600E could be a target therapy for a small subset of CLL patients which might enhance stratified medicine protocol for such a heterogeneous disease.

I screened CLL primary cells for exon 15 BRAF mutation, to find out the frequency rate among our cohort. 190 CLL patients were sequenced for exon 15 BRAF mutations. Along with that, we screened 4 patients of classical hairy cell leukaemia as positive controls, (5 variant HCL, 2 marginal zone lymphoma, one follicular lymphoma, one T-cell lymphoma, and one T-cell-prolymphocytic leukaemia). Five cell lines were also screened (JVM-3, ESKOL, HC-1, MEC-1, and SIG-M5) to confirm their BRAF mutational status. Sanger sequencing was performed, by amplifying BRAF exon 15 gene in each sample, confirm the amplification on agarose gel and DNA was quantified, then samples were sent for sequencing, a text file received per sample from Genewiz-UK and the sequence was screened for mutations by myself.

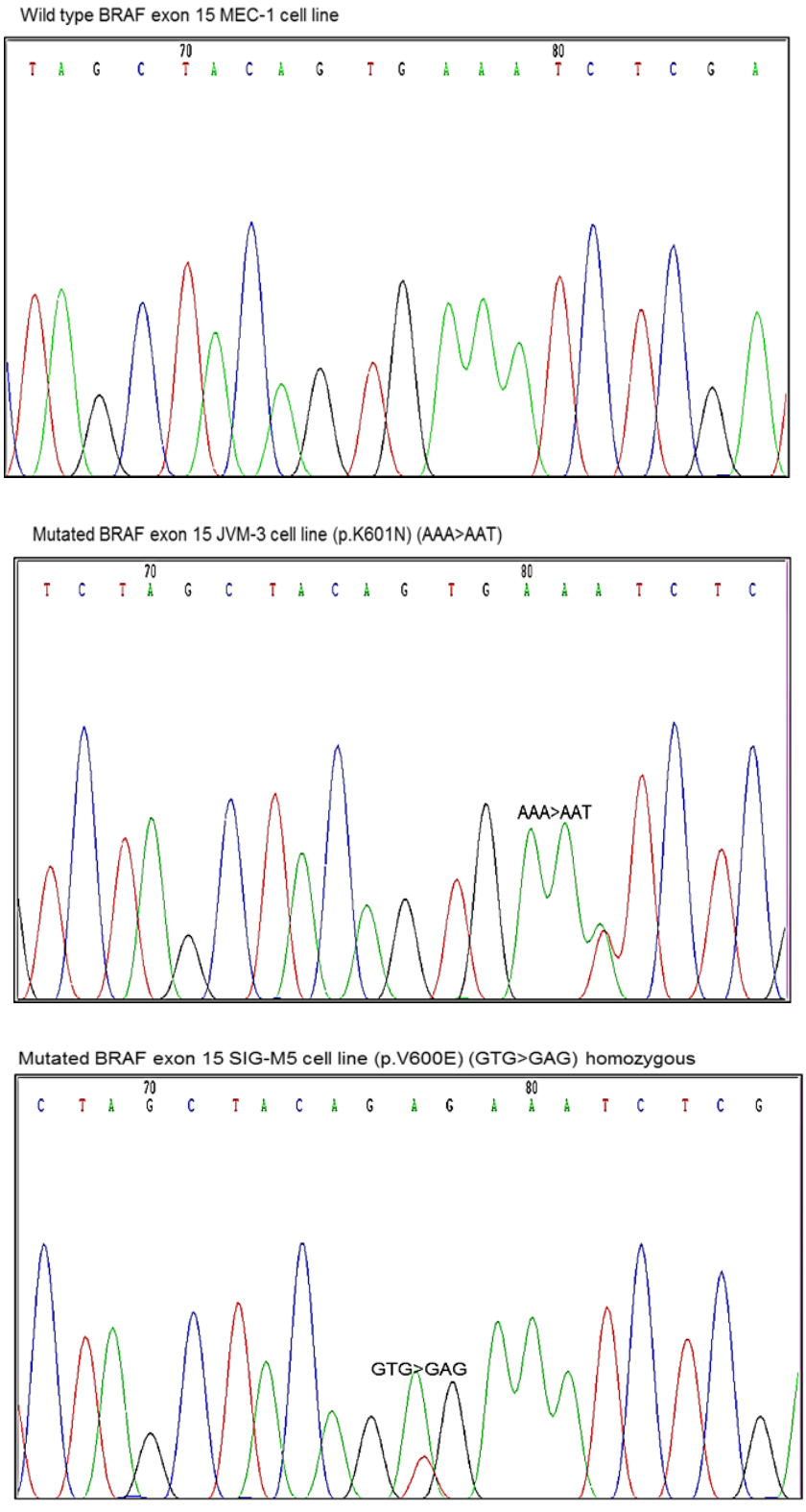


**Figure 4.11 BRAF gene exon 15 V600E mutation.**

Sanger sequencing results of MEC-1, JVM-3, and SIG-M5 cell lines. Chromatograms of SIG-M5 were positive for homozygous BRAFV600E mutation and JVM-3 positive for BRAFK601N mutation. MEC-1 is wild type for BRAF at exon 15. BRAF exon 15 were amplified using PCR and then sent to GENEWIZ-UK for sequencing, text files were received and were screened to identify mutated samples.

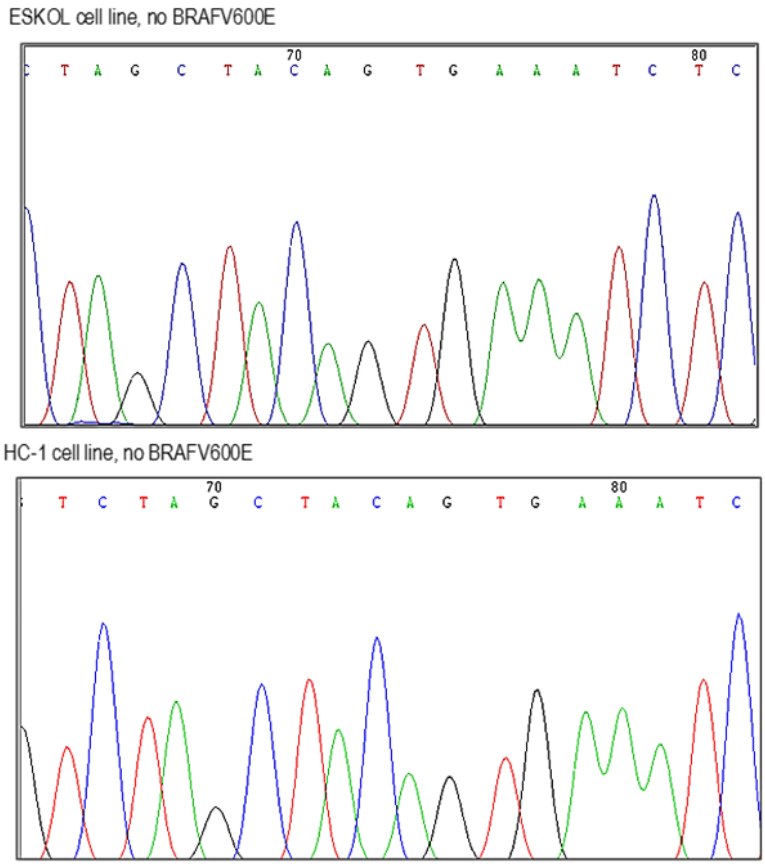


**Figure 4.12 BRAF gene exon 15 V600E mutation.**

Sanger sequencing results of HC-1 and ESKOL cell lines. In spite of these cell lines being originally from hairy cell leukaemia patients, they are BRAFV600E negative. BRAF exon 15 were amplified using PCR and then sent to GENEWIZ-UK for sequencing, text files were received and were screened to identify mutated samples.

As can be seen in figures 4.11 and 4.12, cell lines BRAF mutations were as expected. SIG-M5 BRAFV600E, JVM-3 K601N, MEC-1, ESKOL, and HC-1 were wild type. All classical hairy cell leukaemia patients harbour BRAFV600E mutations, however, ESKOL and HC-1 cells did not show this signature that is specific for them. We confirmed this with our Sanger sequencing results, and that has been reported before (Weston-Bell *et al*, 2013). As these cell lines lack this V600E mutation, they might not be representative of hairy cell leukaemia despite being found to express ANXA1,which is considered as the most specific tumour marker of hairy cell leukaemia and is absent in other B-cell lymphomas.

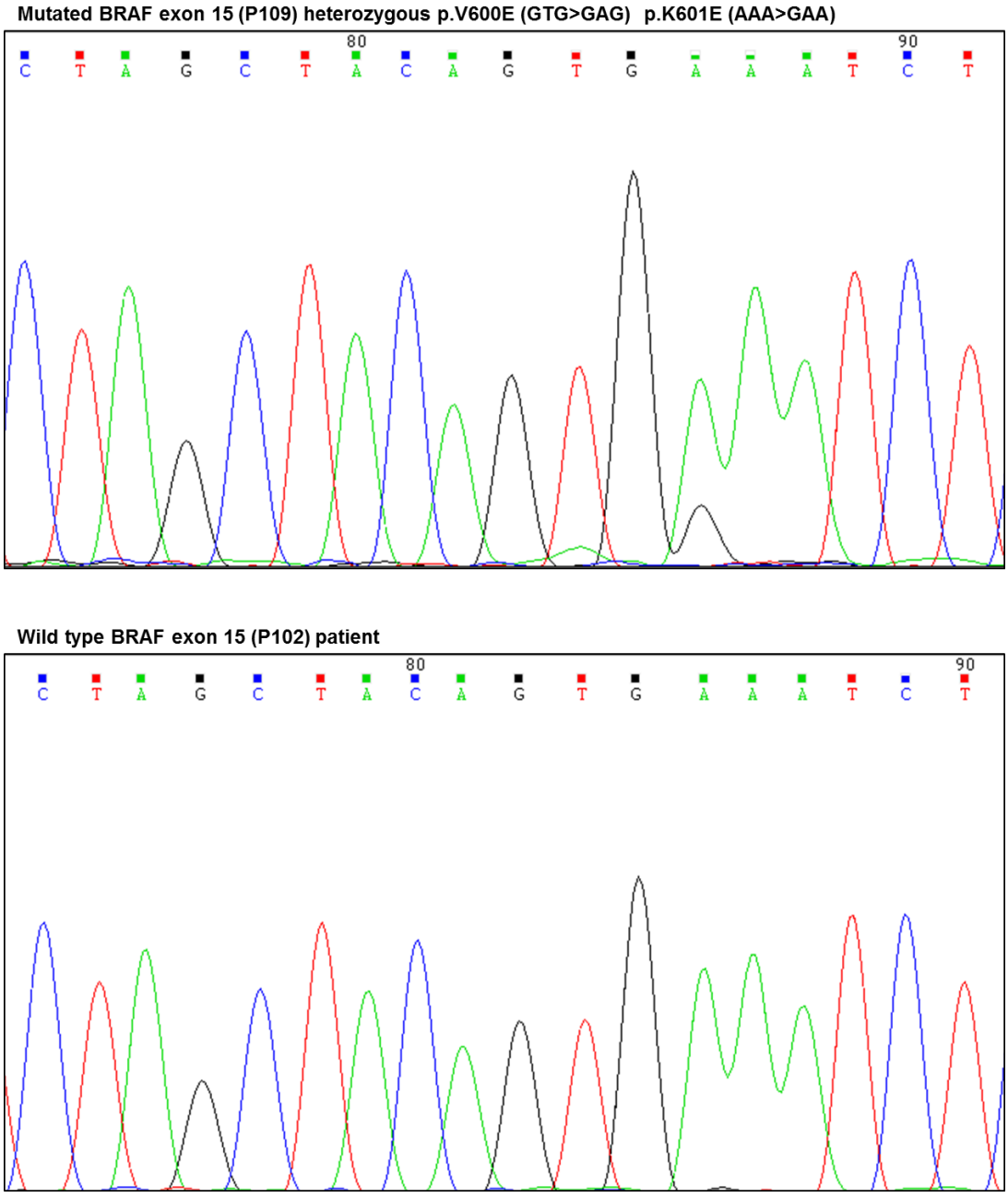


**Figure 4.13 BRAF gene exon 15 mutation.**

Sanger sequencing results of 190 CLL cohort. P109 has heterozygous mutation in p.V600E, and heterozygous p.K601E. CLL patient cells has been sequenced two separate times to confirm the results**.** BRAF exon 15 were amplified using PCR and then sent to GENEWIZ-UK for sequencing, text files were received and were screened to identify mutated samples.

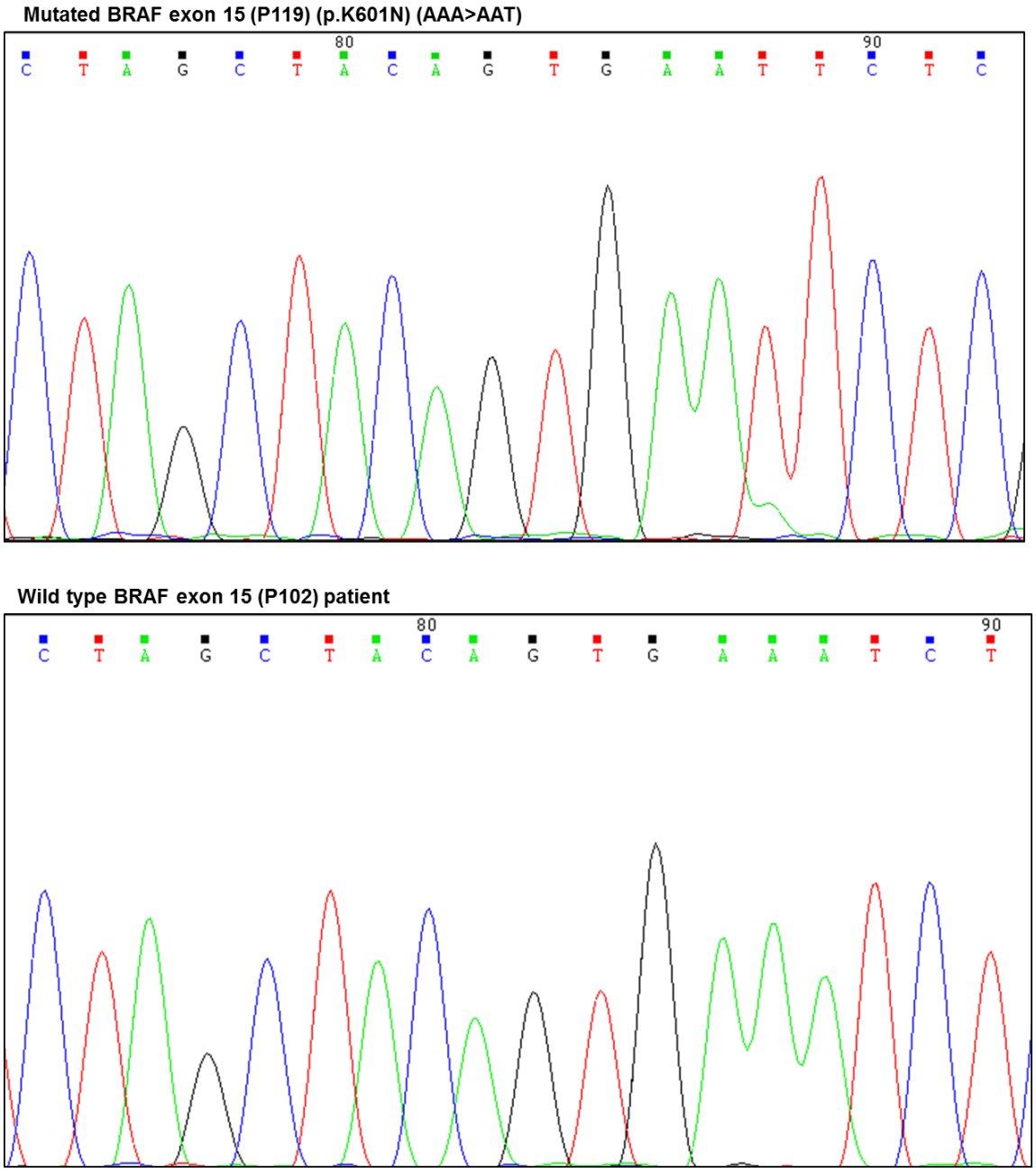


**Figure 4.14 BRAF gene exon 15 mutation.**

Sanger sequencing results of 190 CLL cohort. P119 has heterozygous mutation in p.K601N. CLL patient cells has been sequenced two separate times to confirm the results. BRAF exon 15 were amplified using PCR and then sent to GENEWIZ-UK for sequencing, text files were received and were screened to identify mutated samples.

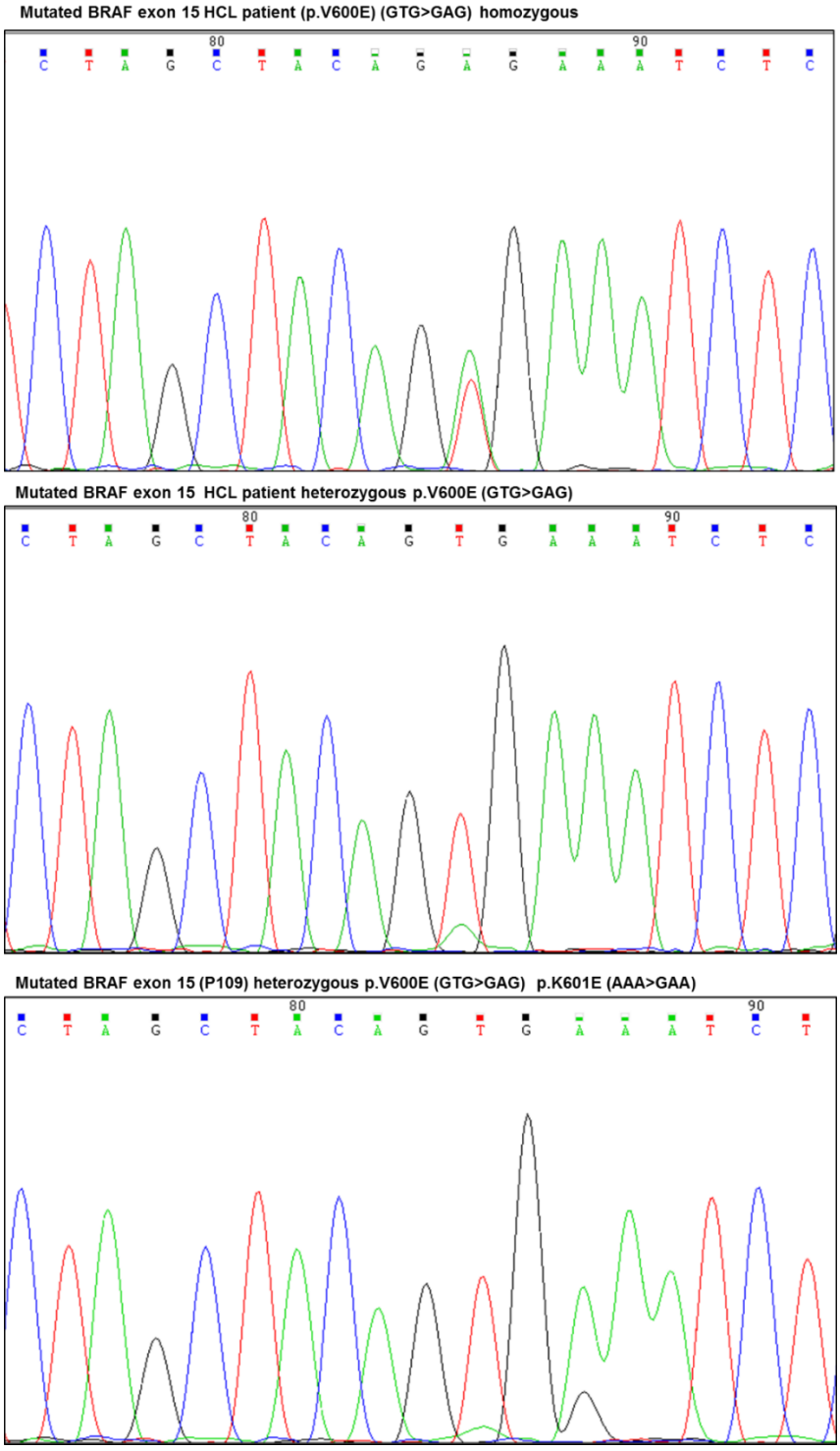


**Figure 4.15 Comparing our positive control HCL patients to P109 heterozygous BRAF V600E exon 15 mutation.**

P109 has heterozygous mutation in p.V600E, and heterozygous p.K601E, CLL patient cells has been sequenced two separate experiments to confirm the results. HCL patient cells in the top shows the peak of homozygous mutation, comparing to the second chromatogram of heterozygous HCL patient cells, with P109 cells heterozygous P.V600E. BRAF exon 15 were amplified using PCR and then sent to GENEWIZ-UK for sequencing, text files were received and were screened to identify mutated samples.

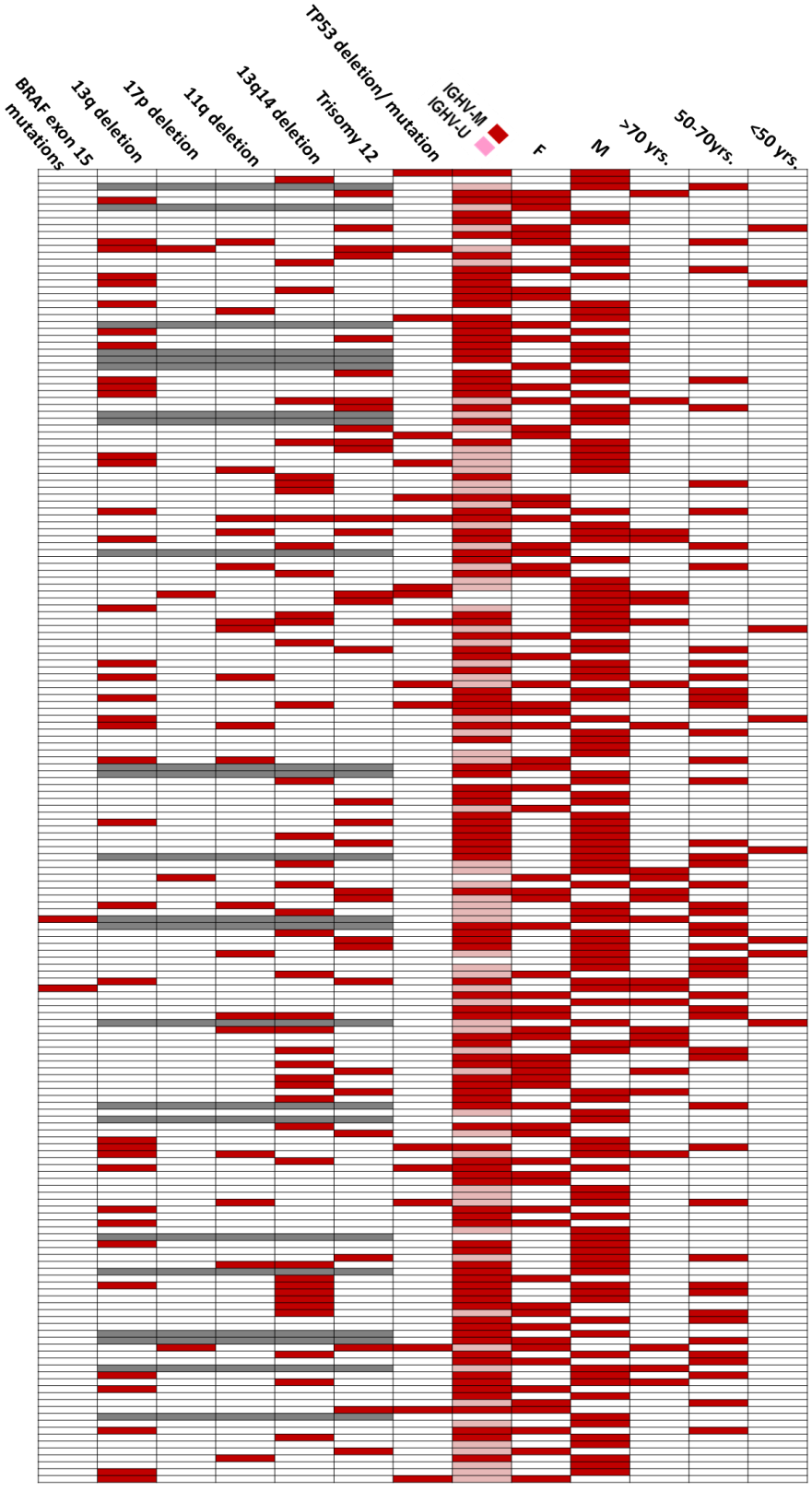


**Figure 4.16 Clustering diagram of cohort of 190 CLL for BRAF exon 15 mutations screening.**

This clustering diagram shows, age at diagnosis >50, 50-70, and >70 years, male/female. Pink squares are U-CLL, red squares are M-CLL, TP53 mutation/deletion, trisomy12, 13q14, 11q, 17p, and 13q deletions (cytogenetic abnormalities) and BRAF gene mutations at exon 15. Grey boxes are normal cytogenetics. (In all TP53 disruptions, cytogenetic abnormalities, IGHV status, gender, and age at diagnosis colourless boxes are not known). In BRAF exon 15 colourless boxes are unmutated.

The cohort of 190 CLL patients male to female ratio was 1:0.589, median age at diagnosis 65.2 years, M-CLL to U-CLL 1:0.59 (table 4.5).

| | | |
|---|---|---|
| <50yrs. age at diagnosis | 8 of 190 | 4.2% |
| 50-70yrs. age at diagnosis | 26 of 190 | 13.68% |
| >70yrs. age at diagnosis | 49 of 190 | 25.78% |
| IGHVM | 110 of 190 | 57.89% |
| IGHVU | 65 of 190 | 34% |
| M | 117 of 190 | 61.6% |
| F | 69 of 190 | 36% |
| TP53mutation/deletion | 18 of 190 | 9.5% |
| Trisomy 12 | 31 of 190 | 16% |
| 13q14 deletion | 40 of 190 | 21% |
| 11q deletion | 19 of 190 | 10% |
| 17p deletion | 4 of 190 | 2.1% |
| 13q deletion | 38 of 190 | 20% |
| BRAF exon 15 mutation | 2 of 190 | 1% |

**Table 4.5 Percentage of different cytogenetic abnormalities, age at diagnosis, gender, TP53 gene mutations, M and U IGHV status in our cohort of 190 CLL patients.**

As can be seen in figure 4.13 is the first BRAF mutated patient cells with two heterozygous mutations p.BRAFV600E, and p.BRAFK601E in exon 15.

The second mutated patient cells with homozygous p.BRAFK601N in figure 4.14. BRAF mutations (exon 15) in the190 CLL patients in Leicester-UK was 1.0526%.

Figure 4.15 shows distinction between HCL positive control cells of homozygous BRAFV600E point mutation, from P109 cells, and HCL cells with heterozygous BRAFV600E. P109 cells has two mutations in exon 15 BRAF gene (p.K601E and p.V600E) and both are heterozygous, which is indicating double heterozygous mutations in P-loop area that would increase the constitutive activity of BRAF gene.

These results have been confirmed in two separate experiments with these two patient CLL cells. According to the clustering diagram (figure 4.16), above there is no specific cytogenetic abnormality that is linked to BRAF mutations in exon 15. P109 was (normal)

with no detected cytogenetic abnormalities. Both P109, and P119 are unmutated IGHV gene, and age at diagnosis for P109 is 74yrs. and for P119 is 75yrs.

| Code | Diagnosis | Age at diagnosis | Gender | IGHV | BRAF exon15 mutations | FISH |
|---|---|---|---|---|---|---|
| SMJ | Hairy cell leukaemia | 66 | F | M | Heterozygous BRAF V600E | 3 copies for 5q23 in 73% of cells |
| PHN | Hairy cell leukaemia | | M | | Homozygous BRAF V600E | Normal |
| BIJ | Hairy cell leukaemia | | F | M | Heterozygous BRAF V600E | Normal |
| DJO | Hairy cell leukaemia | | M | M | Homozygous BRAF V600E | 7q-deletion (36%) and three copies of MPO in 17q22 (26%) |
| LDB | Variant Hairy cell leukaemia | 76 | M | M | WT | Normal |
| BDM | Variant Hairy cell leukaemia | 62 | F | M | WT | a heterozygous deletion in 11q22~23 (ATM and FDX-gene locus) |
| RES | Variant Hairy cell leukaemia | | F | M | WT | clone with heterozygous deletion of TP53 (21%) |
| BB | Variant Hairy cell leukaemia | 79 | F | U | WT | trisomy 3q |
| MAC | Variant Hairy cell leukaemia | | F | | WT | deletion in 14q. |
| SKK | T- cell Prolymphocytic leukaemia | | | | WT | |
| SJA | T-cell lymphoma | | F | | WT | |
| GJE | Marginal zone lymphoma | | F | U | WT | a loss of the CDK6 distal probe (95%). |
| OJA | Marginal zone lymphoma | | F | M | WT | heterozygous deletion in 7q31 |
| EWJ | Follicular lymphoma | | | M | WT | Normal |

**Table 4.6 BRAF exon 15 mutations in 14 samples of other B- and T-cell lymphomas.**

In this group of patients, 4 were positive controls for BRAFV600E of HCL origin, while others were to check if any of lymphoma/leukaemia patients could harbour such a mutation.

Table 4.6 shows BRAF exon 15 mutation testing results for other leukaemia/lymphoma samples. All classical HCL patients have BRAFV600E point mutation, but none of Variant-HCL, MZL, T-PLL, T-cell lymphoma, follicular lymphoma has BRAFexon15 mutations.

In short, our results confirm that BRAF mutations in exon15 are of low frequency in CLL patients. It appears to happen more often in U-CLL patients, older males and not related to any cytogenetic abnormalities. Cell lines such as ESKOL, and HC-1 are supposed to harbour BRAFV600E mutation but are negative for that hot spot mutation, which brings confusion about their origins and what they do represent, although specific tumour marker of classical HCL (ANXA1), which is differentiate classical HCL from other B-lymphomas has been reported to be positive in these cell lines.

## 4.5 BRAF mutant cell response to MAPK inhibitors.

We next assessed MAPK signalling activity in BRAF mutated CLL samples, and compared this with wild type CLL samples (age at diagnosis, and mutational status matched), in order to then assess and compare their sensitivity to BRAF inhibitors.

Using Western blotting analysis, we investigated BRAF/MEK/ERK proteins phosphorylation P-AKT for PI3K pathway, and NF-κB P65 with and without (sCD40L-IL-4) stimulation for 48 hours in P109 (M1) BRAFV600E, K601E heterozygous, P119 (M2) BRAFK601N, wild type P102 (P1), and wild type P121 (P2). We also used the MTS cell viability assay to assess cells sensitivity to MAPK inhibition after stimulation with (sCD40-L/-IL-4) to model the tumour microenvironment.

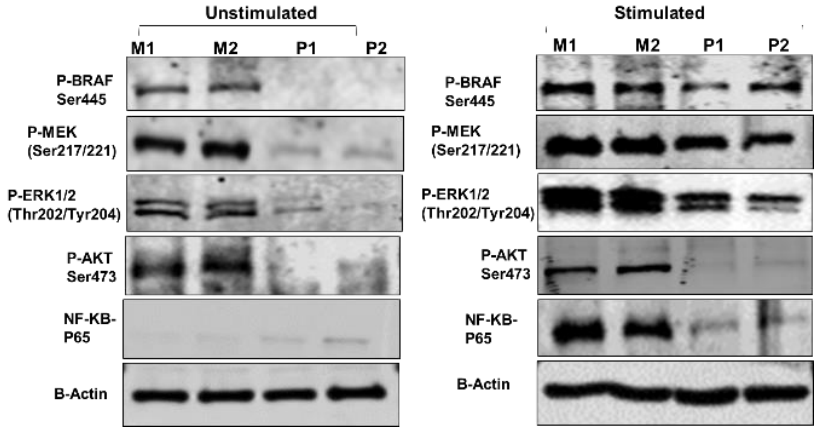


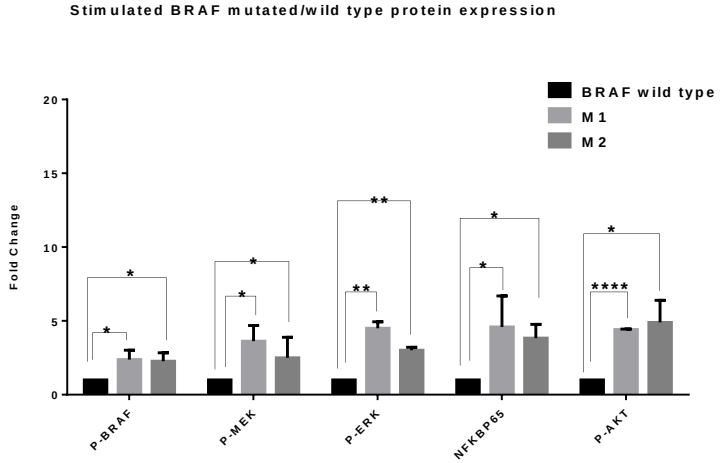


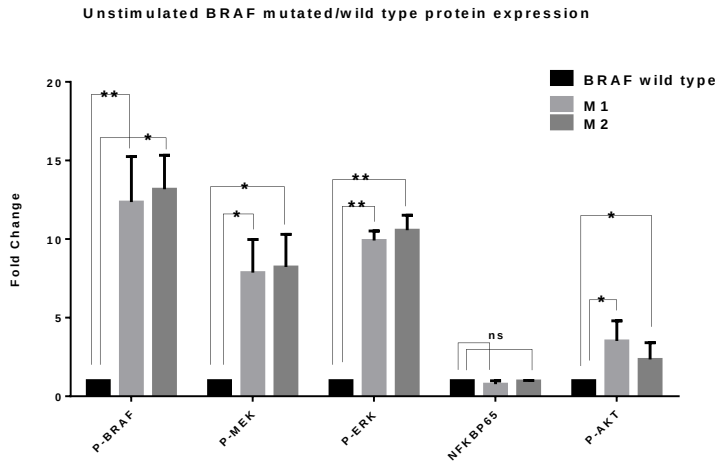


**Figure 4.17 Western blotting shows activation of MPAK pathway in BRAF mutated CLL samples.**

Western blotting analysis of whole cell lysate of two BRAF mutated CLL cells samples (30-50µg protein/well-in 10%SDS-gel) for MAPK and other survival pathways expression, in comparison with two BRAF wild type IGHV and age matched CLL samples. Western blotting were done in duplicates. CLL cells with and without stimulation (sCD40-IL-4). M1: BRAF V600E and K601E (P109), M2: BRAF K601N (P119), P1: BRAF wt (P102), P2: BRAF wt (P121). Fold change to B-Actin bar chart. Each bar is the mean of 2 western blots and standard deviation between them. BRAF wild type bar is the mean of two wild type cells (P1 and P2) fold change to B-Actin normalised to 1. M1 and M2 fold change to BRAF wild type value was calculated. Stars indicate P value <0.05 significant, ns non-significant. P-value stimulated: P-BRAF M1* 0.036, M2*0.0318, P-ERK M1**0.0027, M2**0.02, P-MEK M1*0.04, M2*0.027, P-AKT****M1<0.0001, M2*0.04 (student t-test)

Western blotting (figure 4.17) showed that the MAPK pathway is activated both in M1 and M2, compared to both wild type samples (BRAF wild type). P-ERK, which indicates MAPK signalling activity, were more significantly induced in mutated CLL cells, especially with stimulation of CD40-IL-4.

In addition, P-AKT was also more significantly induced in stimulated BRAF mutated CLL cells. NF-κB P65 was not showing any considerable changes in unstimulated BRAF mutated cells, but in stimulated CLL cells showed higher expression in mutated cells than BRAF wild type cells.

Next we tested sensitivity of BRAF mutants P109, and P119 to vemurafenib, dabrafenib, trametinib, and sorafenib, in comparison to wild type sensitivity using MTS cell viability assay. Wild type viable cells values were close, therefore we used the mean of both of wild type viable cells (figures 4.18-4.21).

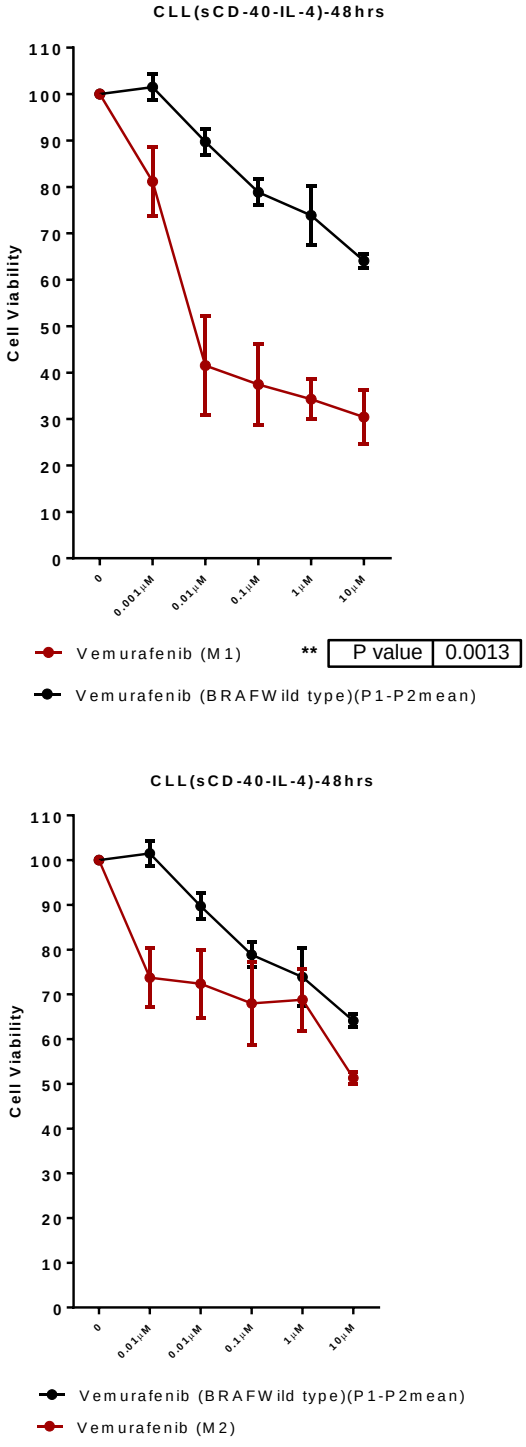


**Figure 4.18 MTS cell viability assay shows more sensitivity to Vemurafenib in BRAF mutated CLL samples.**

CLL cells were stimulated for 24 hours, plated in 96 well plates, and then treated with trametinib, sorafenib, vemurafenib and dabrafenib five concentrations (of 10,1 , 0.1, 0.01, 0.001 µM) for 48 hours. MTS reagent added and then results acquired using a plate reader. Each concentration is the mean and standard deviation of biological duplicates and technical triplicates. P value were calculated using student t-test (Graph-pad prism), for statistical significance of all five concentrations of mutated BRAF to wild type BRAF after treatment. BRAF wild type in black is the mean of two wild type CLL samples of P102 and P121 after treatment.

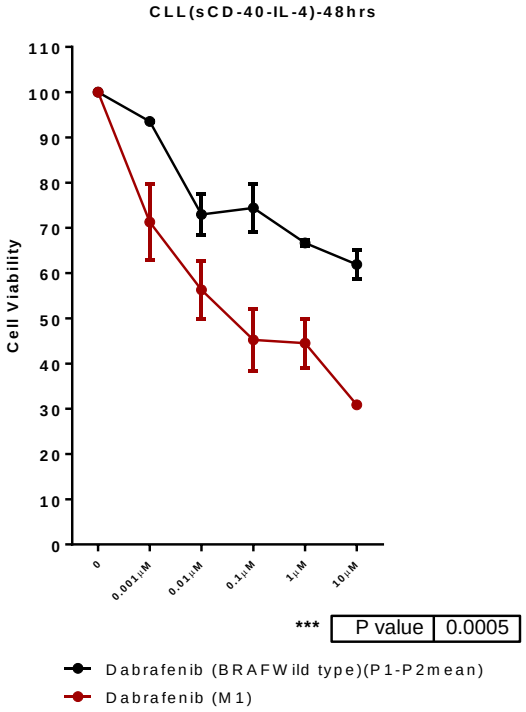


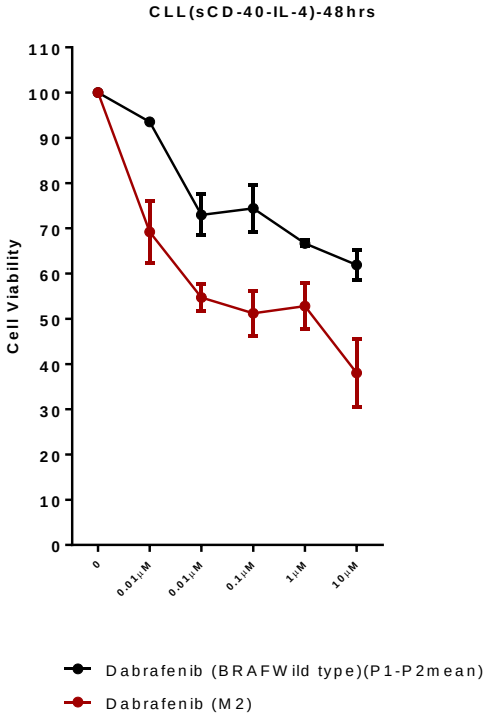


**Figure 4.19 MTS cell viability assay shows more sensitivity to dabrafenib in BRAF mutated CLL samples.**

CLL cells were stimulated for 24 hours, plated in 96 well plates, and then treated with trametinib, sorafenib, vemurafenib and dabrafenib five concentrations (of 10,1 , 0.1, 0.01, 0.001 µM) for 48 hours. MTS reagent added and then results acquired using a plate reader. Each concentration is the mean and standard deviation of biological duplicates and technical triplicates. P value were calculated using student t-test (Graph-pad prism), for statistical significance of all five concentrations of mutated BRAF to wild type BRAF after treatment. BRAF wild type in black is the mean of two wild type CLL samples of P102 and P121 after treatment.

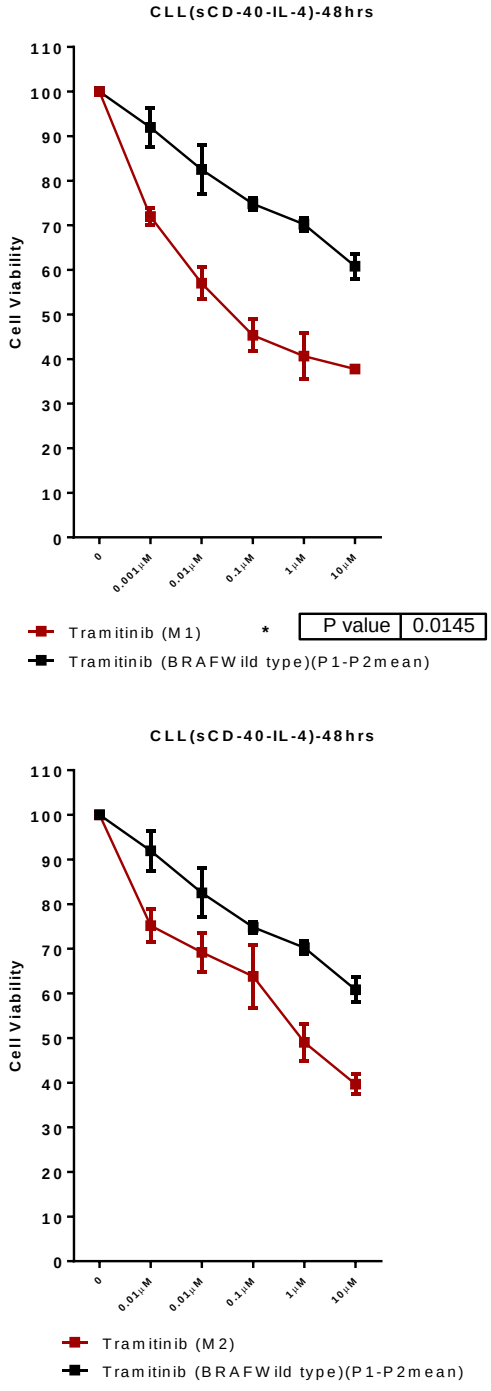


**Figure 4.20 MTS cell viability assay shows more sensitivity to trametinib in BRAF mutated CLL samples.**

CLL cells were stimulated for 24 hours, plated in 96 well plates, and then treated with trametinib, sorafenib, vemurafenib and dabrafenib five concentrations (of 10,1 , 0.1, 0.01, 0.001 µM) for 48 hours. MTS reagent added and then results acquired using a plate reader. Each concentration is the mean and standard deviation of biological duplicates and technical triplicates. P value were calculated using student t-test (Graph-pad prism), for statistical significance of all five concentrations of mutated BRAF to wild type BRAF after treatment. BRAF wild type in black is the mean of two wild type CLL samples of P102 and P121 after treatment.

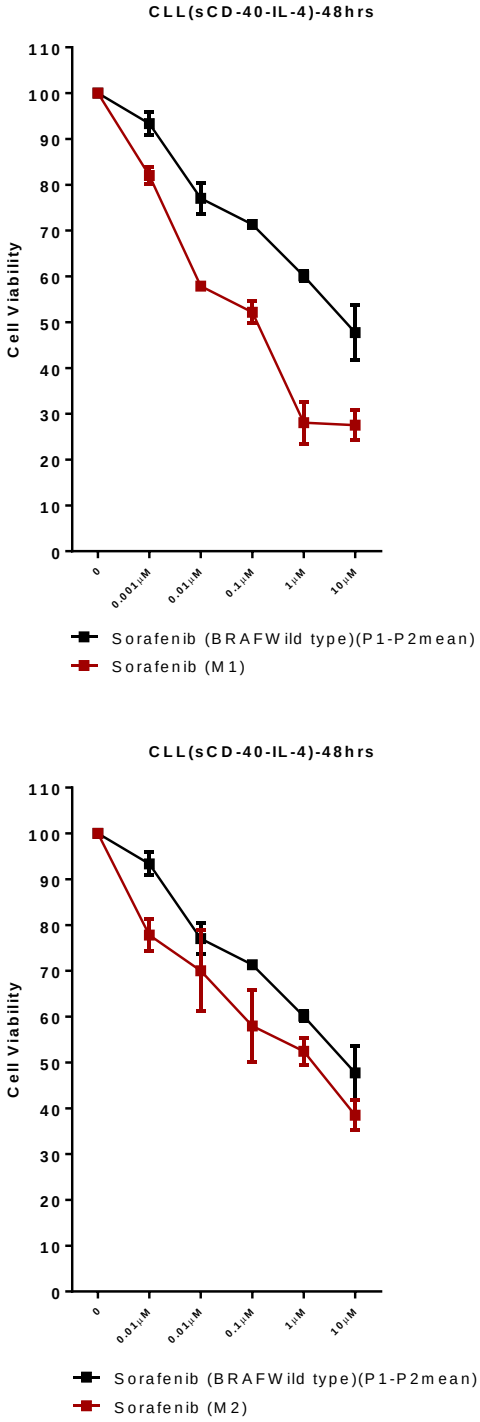


**Figure 4.21 MTS cell viability assay shows more sensitivity to sorafenib in BRAF mutated CLL samples.**

CLL cells were stimulated for 24 hours, plated in 96 well plates, and then treated with trametinib, sorafenib, vemurafenib and dabrafenib five concentrations (of 10,1 , 0.1, 0.01, 0.001 µM) for 48 hours. MTS reagent added and then results acquired using a plate reader. Each concentration is the mean and standard deviation of biological duplicates and technical triplicates. P value were calculated using student t-test (Graph-pad prism), for statistical significance of all five concentrations of mutated BRAF to wild type BRAF after treatment. BRAF wild type in black is the mean of two wild type CLL samples of P102 and P121 after treatment.

As can be seen in figure 4.18 MTS cell viability assay shows that M1 (heterozygous BRAFV600E, K601E) mutated CLL is significantly more sensitive to vemurafenib than wild type BRAF CLL cells (mean of two viable cells % P1and P2). While M2 (BRAFK601N) mutated CLL showed slight increase in sensitivity compared to BRAF wild type cells.

Dabrafenib efficacy appears to be similar between M1 and M2 in comparison to BRAF wild type cells (figure 4.19). Sorafenib inhibit cell viability greatly in M1 cells in contrast to BRAF wild type cells, though in M2 cells there is small difference in contrast to BRAF wild type cells (figure 4.21).

That merely displays that BRAFV600E in (BRAFV600E, K601E heterozygous) mutated cells is playing an important role in rendering cells more sensitive to RAF/MEK inhibitors. However, at high concentration of the four inhibitors that have been used, it seems that cell viability in BRAF mutated cells (M1 and M2) is significantly reduced compared to wild type cells.

In addition, previously with cell lines testing JVM-3 BRAFK601N mutant showed no sensitivity to MAPK inhibition, but SIG-M5 BRAFV600E showed greater sensitivity to nanomolar concentrations of MAPK inhibitors (table 3.5).

We next calculated IC50 using (Graph pad-Prism) of BRAF mutated and wild type cells to RAF/MEK inhibitors.

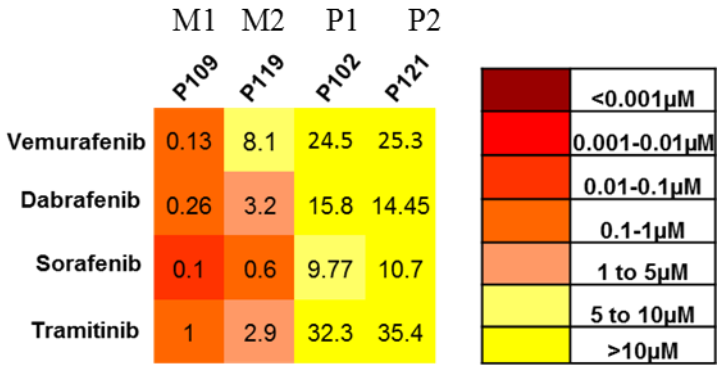


**Figure 4.22 IC50 diagram comparing two wild type CLL cells to two BRAF exon 15 mutated CLL cells.**

IC50 calculated using Graph Pad prism. IC50 values above 10µM were estimated.

As can be seen in figure 4.22, IC50 that (M1) P109 needs less concentrations to inhibit 50% of cells viability, which means they are more sensitive. Whereas, (M2) P119 needed more to reach 50% of inhibition of viable cells. In addition, BRAF wild type patients needed higher concentrations.

We next assessed MAPK, P-AKT, and NF-κB P65 protein expressions, and PARP cleavage after 24 hours treatment with 10µM of vemurafenib, sorafenib, trametinib and dabrafenib. Cells were stimulated with sCD40L/IL-4 for approximately 24 hours prior to treatment.

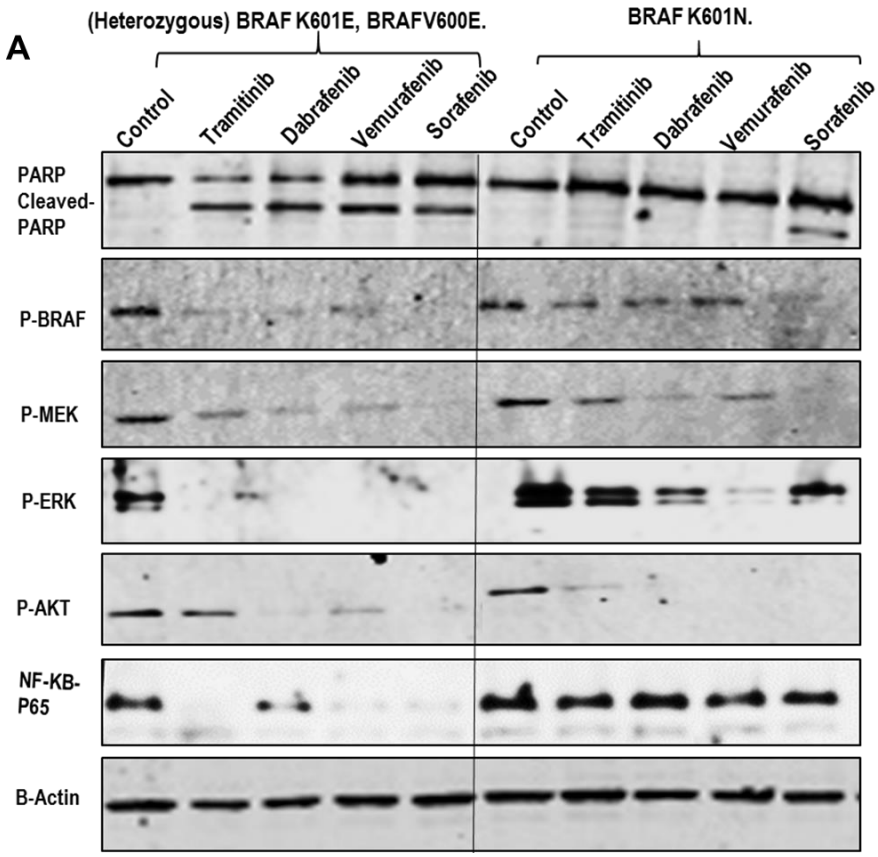


**Figure 4.23 Western blotting of BRAF mutant CLL cells.**

Cells were stimulated with sCD40L/-IL-4 for 24 hours, then treated with vemurafenib dabrafenib, sorafenib, trametinib 10µM each. Whole cell lysate were loaded 30-50µg protein/well in 10% SDS-gel.

As shown above in figure 4.23, that BRAF exon 15 mutated CLL cells showed great sensitivity to 10µM of each inhibitor. PARP was cleaved in P109, indicating that cells are undergoing apoptosis with all inhibitors. Phosphorylated BRAF was decreased along with MEK and ERK phosphorylation, which means complete block of the MAPK pathway. Phosphorylated AKT was reduced, except for a slight expression with trametinib. NF-κB P65 was also lowered after treatment.

P119 did not show significant PARP cleavage except with sorafenib. Phosphorylation of ERK was inhibited partially with sorafenib and significantly with vemurafenib, AKT phosphorylation was inhibited as well with all four inhibitors. However, NF-κB P65 expression was not affected after treatment. MEK and BRAF phosphorylation were considerably inhibited. P109 showed more apoptosis and less activity of MAPK and NF-κB P65 after treatment greater than P119. In MTS cell viability assay results (figure 4.21) P109 showed greater sensitivity and less IC50 values to these 4 inhibitors than P119 as well.

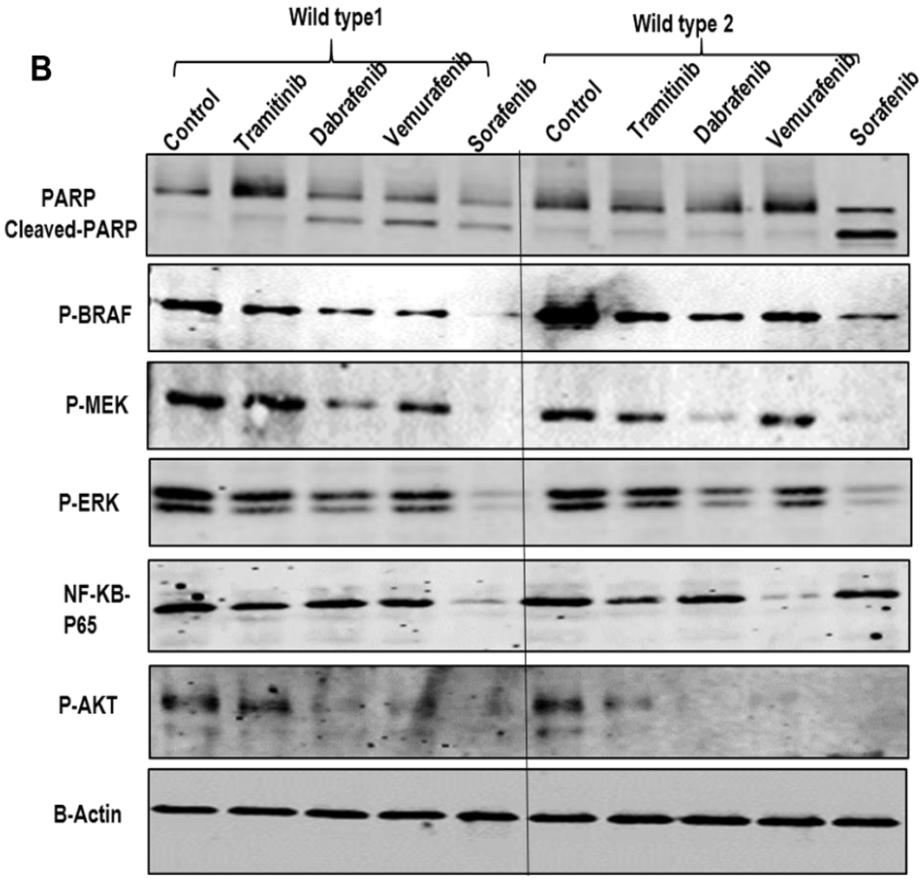


**Figure 4.24 Western blotting of BRAF wild type CLL cells.**

Cells were stimulated with sCD40L-IL-4 for 24 hours, then treated with vemurafenib dabrafenib, sorafenib, trametinib 10μM each. Whole cell lysate were loaded 30-50μg protein/well in 10% SDS-gel. WT1: P102 WT2: P121.

On the other hand, wild type BRAF CLL cells showed less sensitivity to MAPK inhibitors than BRAF mutant CLL cells. Sorafenib exert the most inhibition on both BRAF wild type CLL cells proteins phosphorylation and expression, and PARP was cleaved

significantly. Sorafenib reduced cell viability in wild type cells in MTS cell viability assay results (figure 4.21) and IC50 value for both patients was close to10μM (figure 4.22).

AKT phosphorylation was reduced significantly with vemurafenib, dabrafenib, and sorafenib. Interestingly, NF-κB P65 was reduced with sorafenib in P102 and reduced with vemurafenib treatment of in P121.

Our results strongly suggest that MAPK inhibitors could be used for treatment of BRAF mutant CLL patients, especially with the V600E point mutation that makes CLL cells more sensitive to treatment, even when we mimicked the microenvironment of proliferation centres. BRAF mutations in CLL increased MAPK activity and cells harbouring BRAFV600E are more sensitive to inhibition with MAPK inhibitors than other BRAF mutations. Finding patient with these mutations would help to target specifically for more selective treatment.

## 4.6 Discussion

MEK1/2 inhibitors have been used in cancer treatment and in clinical trials. Selumetinib has been described to have a modest anti-leukaemic activity as a single agent in advanced acute myelogenous leukaemia AML (Jain *et al*, 2014). Moreover, selumetinib enhanced dexamethasone toxicity by inhibiting mTORC1 signalling and autophagy induction in glucocorticoids-resistant B-cell acute lymphoblastic leukaemia (B-ALL) cells *(*Polak *et al*, 2015). It has been reported that PD-0325901 blocked ABT-737 (BH3-mimetic) induced Mcl-1 expression, and when PD-0325901 was combined with ABT-737 it worked as a potent synergistic combination that eradicated acute myeloid leukaemia derived cell lines (Konopleva *et al*, 2012). In addition, MEK1/2 inhibitor UO126 has decreased triple-negative breast cancer cell invasion, growth, and migration, and inhibits IL-8 (IL-8 is a metastatic breast cancer prognostic marker) (Kim *et al*, 2016). Trametinib was used in B-cell acute lymphoblastic leukaemia (B-ALL) cells as a single agent did not inhibit the growth of B-ALL cells, but trametinib synergized with BCL-2/BCL-XL family inhibitors and inhibited B-ALL cells proliferation and induced apoptosis (Korfi *et al*, 2016). In our hands, CLL cells showed no sensitivity to MEK1/2 inhibitors, except reduced cell viability at highest concentration of trametinib (figure 4.2).

Both dabrafenib and vemurafenib showed great clinical efficacy in treatment of melanoma patients with V600E mutations, though 15% of mutant BRAF melanoma

patients have intrinsically no sensitivity to V600E inhibitors treatment. Also, vemurafenib treatment of melanoma patients lead to acquired resistance developed by paradoxical activation of MAPK and led to development of other malignancies. Therefore, combination treatment regimen with MEK inhibitor trametinib has displayed significant clinical efficacy in V600E melanoma (Okimoto *et al*, 2016). Pan-RAF inhibitor sorafenib first developed in 2000 during development of CRAF inhibitor. Sorafenib is a very effective antitumour agent as it is a dual inhibitor of MAPK signalling and tyrosine kinase VEGFR/PDGFR. It has been proven clinically for liver, thyroid, and kidney cancers treatment, however, resistant developed in HCC hepatocellular carcinoma patients, and sorafenib-resistant cells showed upregulated AKT signalling with high levels of miR-21(He *et al*, 2015). Our experiments (figure 4.3) show that RAF inhibitors RAF265 and sorafenib showed modest efficacy, while BRAFV600E inhibitors dabrafenib and vemurafenib showed even less efficacy.

CRAF inhibitor (475958) is a cell permeable phenyl urea derivative one of the best compounds that showed effective anti-proliferative activity in A375P human and WM3629 melanoma cell lines(Yu *et al*, 2010). CRAF inhibitor showed no efficacy in reducing CLL cells viability (figure 4.3).

Ibrutinib showed low efficacy on CLL cells viability *in vitro*, however NF-κB and BCR signalling were substantially decreased and tumour proliferation was inhibited *in vivo* in ibrutinib-treated CLL patients (Niemann *et al*, 2016). In our findings (figure 4.4) ibrutinib has moderate IC50 values (figure 4.6), but in one particular patient (P38) showed resistance to ibrutinib.

VER-155008 and Fedratinib showed different IC50 values. One U-CLL with trisomy12 (P38) showed resistance to both of them. Other M-CLL with 13q14 deletion showed low to moderate IC50 values, (P65) showed lowest IC50 value of 3nM (figure 4.6). Therefore, the response appears to reflect the IGHV status and cytogenetic mutations of CLL cells.

In our cell lines, potent inhibitors were dinaciclib, MG132, and CUDC-907. Dinaciclib is a cyclin-dependent kinase inhibitor that was found to be clinically effective in relapsed/refractory and high risk 17p deletion CLL patients (Flynn *et al*, 2015). Proteasome inhibitor MG-132 has been shown to induce apoptosis in CLL cells via CD23 gene downregulation and Notch2 inhibition (Duechler *et al*, 2005). CUDC-907 induced apoptosis in cancer cells and disturbed their protective microenvironment in

haematological malignancies (Wang *et al*, 2013). P65 (M-CLL) showed lowest IC50 values in nanomolar to all of them. P70 is also M-CLL but with partial trisomy 12 showed higher IC50 values.

Western blotting results showed that P-ERK was slightly reduced and PARP was partially cleaved with sorafenib in unstimulated U-CLL (P38). But in (P65) M-CLL Sorafenib has inhibited MAPK phosphorylation in unstimulated and stimulated cells, cleaved PARP was more seen in unstimulated (figures 4.7, 4.8). P38 (U-CLL) with trisomy12, thus we suggest this as an explanation to its resistant in MTS assay results and in Western blotting results. The increased PARP cleavage that seen with unstimulated CLL cells represents the importance of microenvironment modelling in pre-clinical drug testing.

In both patients (P38 and P65) trametinib did not seem to inhibit, but increased MEK1/2 phosphorylation. Inhibiting MEK1/2 activity with MEK1/2 inhibitors and can lead to the paradoxical activation of ERK1/2 in cancer cells. This is due to interruption of the negative feedback loops in MAPK pathway. This observation was not seen when BRAFV600E is the driving oncogene, because BRAFV600E does not require an activating RAS signal and does not form heterodimers with CRAF that can lead to paradoxical MAPK activation (Poulikakos *et al*, 2010; Cox and Der, 2010). Some cancer cells exhibited intrinsic resistance to MEK1/2 inhibition as a result of PI3K pathway upregulation (Little *et al*, 2012; Balmanno *et al*, 2009). Hence, it appears that a combination of PI3K and MEK1/2 inhibitors is required to prevent resistance.

In primary cells, P65 CLL cells showed the most sensitive profile in heat map of IC50 (figure 4.6). This is may be attributed to the fact that it is a mutated IGHV (M-CLL) and had 13q14 cytogenetic abnormality, that is linked to favoured prognosis CLL patient. However, P38 cells (U-CLLTrsiomy12) were the most resistant cells to inhibitors even to strong inhibitors dinacilcib and CUDC-907. Trisomy 12 is linked to Notch1 mutations and poor outcomes (Del Giudice *et al*, 2012). P29 (IGHV not confirmed), and P137 (U-CLL but no trisomy 12 or p53 mutations) cells has moderate response, and P70 (M-CLL-partial trisomy 12) cells showed slight insensitivity to inhibitors.

Next our aim was to find a combination that could be used in CLL cells and show synergism. Sorafenib showed medium IC50 values among CLL primary cells and CUDC-907 showed low IC50 values as an effective inhibitor.

Combination therapy is not a new approach in cancer treatments, especially to overcome development of resistance in single agent regimes. The main goal of cancer therapy is to target two or more cancer stimulating or sustaining pathways, but the lack of specific drugs is an obstacle. Single agent treatment is still an option, yet, it is not efficient most of the time for cancer patients (Bayat *et al*, 2017). Combinations are effective way of treating diseases where complex molecular networks are involved in pathogenicity and drug resistance. They can overcome these difficulties and also increase the efficacy of drugs with decrease in dosage, which in turn will decrease side effects. Moreover, synergy is an important factor in combination, as compounds can be additive or antagonise each other's effect (He *et al*, 2016).

First combination therapy was suggested for acute leukaemia treatment in children and proved to be a success (Frei *et al*, 1965). Combination therapy for CLL is not a new approach. Chemoimmunotherapy is the standard first therapy for CLL. FCR (fludarabine, cyclophosphamide, and rituximab) has been used for CLL treatment with 95% overall rate response ORR. FC (Fludarabine and cyclophosphamide) FC was compared to FCR and in phase III (CLL8 trial) ORR was 80% compared to 90% with FCR. FCR works more effectively in younger IGHV mutated patients than FC (Fischer *et al*, 2016; Böttcher *et al*, 2012). Other combinations haves been used for CLL, treatment such as Chlorambucil and obinutuzumab or ofatumumab, and BR (bendamustine and rituximab) (Jain and O'Brien, 2015). Using ibrutinib for the first time in CLL treatment was unexpectedly successful, but the resistance to ibrutinib is a limitation. Therefore, it has been reported that preclinical combination studies of idelalisib and ibrutinib could be a potential synergistic combination for CLL and MCL mantle cell lymphoma (de Rooij *et al*, 2015).

In our preclinical testing we have used CUDC-907 (dual HDAC and PI3K inhibitor) combined with sorafenib (tyrosine kinase and pan-RAF inhibitor). CUDC-907 was used in different concentrations and in as low as 0.5nM and it still synergise with sorafenib to inhibit the growth of primary CLL cells. In our data, CUDC-907 is one of potent inhibitors (IC50 of ~6nM in two out of n=5 CLL samples), while sorafenib was of modest efficacy among our CLL cells (figure 4.6). Our findings showed that 6 CLL samples of 11 showed very strong synergism and the rest showed strong synergism between the two drugs (table 4.4). This indicates that potentially these two inhibitors could potentially be used for CLL

patients and that the nanomolar concentration of CUDC-907 possibly sensitises cells to sorafenib effects.

The next aim was to stratify CLL primary cells sensitivity to MAPK inhibitors according to their BRAF exon15 mutational status. Firstly, BRAF exon 15 mutations were as expected in cell lines (SIG-M5 BRAFV600E), (JVM-3 BRAFK601N), MEC-1 has no mutations, and finally HC-1 and ESKOL cell lines lack BRAFV600E mutation as has been previously reported (Tiacci *et al*, 2012).

According to our Sanger sequencing results P109 was heterozygous BRAFp.V600E and p.K601E (figure 4.13), and P119 has BRAFp.K601N mutations (figure 4.14). In our cohort of 190 CLL patients, BRAF exon 15 mutations were 1.052% (figures 4.13, 4.14), which is a very low frequency as has been reported previously. One BRAFV600E mutated patient of 140 CLL patients (Langabeer *et al,* 2012). BRAF exon 15 mutations have been detected in low frequency of 2.8% in CLL (Jebaraj *et al,* 2013). BRAF V600E counts for 50% of melanoma cases and in all cases of classical hairy cell leukaemia, and has been reported to be associated with Richter syndrome transformation in CLL patients (Sellar *et al,* 2015).

Among our cohort there was no specific cytogenetic abnormality associated with mutations in BRAF exon 15. The only common factor between two BRAF mutated patients was unmutated IGHV, P109 74yrs., P119 75yrs. age at diagnosis, and both were males (figure 4.16).

Using Western blotting to check MAPK signalling activity in mutated in comparison to wild type patients, it seems that both BRAF mutated CLL cells exhibit significant increased expression of BRAF/MEK/ERK signalling in comparison to BRAF wild type (age at diagnosis and IGHV mutational status matched control) with or without stimulation (sCD40L-IL-4), and other proliferative signalling such as NF-κBP65 and P-AKT showed more expression with stimulation in mutated cells (figure 4.17). That indicates BRAF mutated cells might have more activated cancer growth pathways than malignant CLL cells counterparts without MAPK mutations.

MTS cell viability assay showed that P109 cells more sensitive to MAPK inhibitors vemurafenib, dabrafenib, and trametinib than P119 (figures 4.18-4.21). In addition, IC50 values of four inhibitors were lower in P109 in comparison to P119, and both (P109, P119) showed less IC50 than BRAF exon15 wild type CLL cells (figure 4.22). Western

blotting results showed more inhibition of MAPK and PARP cleavage in P109 (BRAFV600E, K601E) than P119 (BRAFK601N) (figure 4.23). Even less MAPK inhibition was observed in BRAF exon 15 wild type CLL cells (figure 4.24). We observed lower IC50 value for dabrafenib and vemurafenib in P109 (V600E). In wild type BRAF cancer cells, MAPK may not be the main proliferation signalling pathway, since RAF inhibitors are not very effective in inhibiting MAPK. However, in BRAF mutated cancer cells, selective inhibitors will inhibit BRAF activity and MAPK efficiently (Cox and Der, 2010). These data suggest that BRAFV600E point mutation in CLL could be targeted with MAPK inhibition as a target therapeutic option.

We were not able to confirm if CLL cells with BRAF mutations are a more aggressive form of CLL. However, the only 2 cases we have are U-CLL, a poor prognosis category of CLL. BRAFV600E mutation in thyroid cancer, especially in papillary thyroid carcinoma (PTC) is the main genetic alteration and is linked to poor outcomes (Yu *et al*, 2015).

# Chapter 5 Stratification of CLL patients according to their prognostic mutations and testing their sensitivity against targeted inhibitors.

New prognostic markers have been identified recently in CLL patients using NGS techniques (Quesada *et al*, 2011; Wang *et al*, 2011). A number of gene mutations that help to predict the prognosis of patients and to plan the treatment regimen accordingly. So far, TP53, ATM, NOTCH1, SF3B1, and MYD88 are implicated in management and prognosis of CLL patients. SF3B1 is a nuclear ribonucleoprotein, a subunit of the splicing machinery in eukaryotic cells.

SF3B1 mutations are approximately 10% in CLL patients and up to 17% in fludarabine refractory patients. The most recurrent mutation of SF3B1 in CLL is K700E. SF3B1 mutations lead to abnormal splicing of messenger RNA and cause introns retention. This will result in transcripts alterations and consequently will affect cell-cycle regulation, angiogenesis, apoptosis, etc., thus contributes to cancer (Amaya-Chanaga and Rassenti, 2016). It has been reported that SF3B1 mutations modify damage responses of DNA over upregulation of transcription factor Kruppel like factor 8 (KLF8), and NOTCH signalling via Dishevelled-2 (DVL2) different splicing (Wang *et al*, 2016). However, it has been suggested that SF3B1 mutation is not linked to other poor prognostic factors in CLL, such as IGHV mutational status.

NOTCH1 is a trans-membrane protein that contributes to haematopoietic cell development. The main mutation in NOTCH1 is a frameshift mutation due to CT deletion that affects C-terminus region (PEST domain, a peptide sequence that is rich in proline (P), glutamic acid (E), serine (S), and threonine (T)) of the protein (c.7541_7542delCT at exon 34). NOTCH1 mutations are associated with poor outcomes markers such as trisomy12+, unmutated IGHV, and their occurrence is increased in Richter syndrome transformed patients (Weissmann *et al*, 2013).

MYD88 is a cytosolic adaptor protein and is important in innate and adaptive immune responses in cells. MYD88 is vital signal transducer in the interleukin-1 and Toll-like receptor (TLR) signalling pathways, which regulates the activation of many pro-

inflammatory genes. MYD88 mutations occurs at low frequencies in CLL, and are linked to mutated IGHV, better prognosis and younger age patients (Amaya-Chanaga and Rassenti, 2016).

Our aim was to analyse 148 CLL patients from our cohort for the mutational status of SF3B1, MYD88, and NOTCH1. As treated patients would harbour more mutations than naïve, we selected all of CLL samples from treated patients. We also analysed available 7 HCL/and VHCL, MZL and T-cell lymphoma samples for the same 3 mutations as these samples were available to for comparison.

All patients DNA samples were screened using Sanger sequencing for SF3B1 mutations at exons 14-15, NOTCH1 mutations at exon 34, and MYD88 mutations at exon 5. The reference sequence of SF3B1 exons 14-15 was NM_012433, for NOTCH1 exon 34 was NG_007458.1 and for MYD88 exon 5 was NM_001172569. The BLAST program (http://www.ncbi.nlm.nih.gov/BLAST/) was used to analyse the nucleotide sequences and the (Ensemble gene browser) was used to confirm mutations and variations. Figure 5.1 shows the cytogenetic locations of each mutation (yellow arrows).

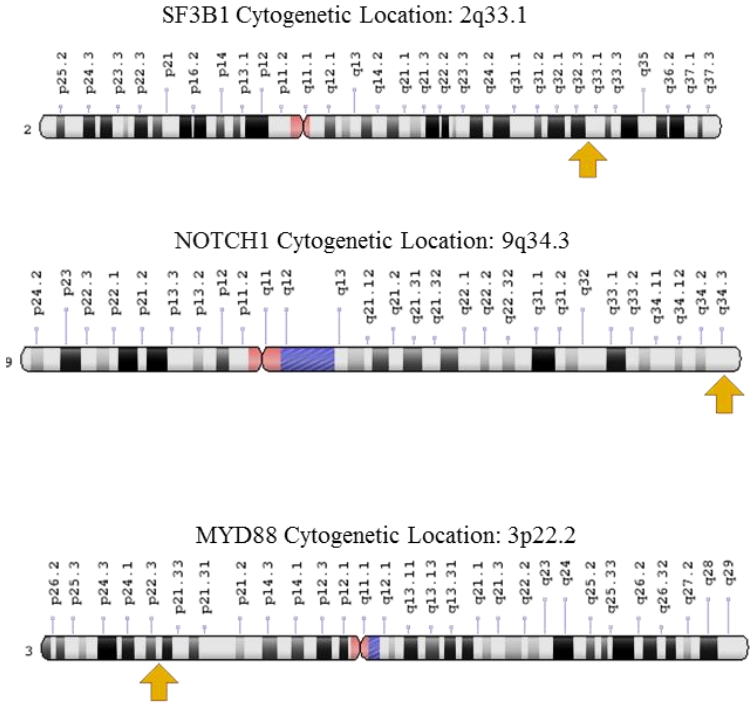


**Figure 5.1 Cytogenetic locations (yellow arrows) of three genes SF3B1 (2q33.1), NOTCH1 (9q34.3), and MYD88 (3p22.2).**

Three genes were sequenced in 148 CLL treated cohort. Adapted from genetic home reference https://ghr.nlm.nih.gov/gene/.

## 5.1 SF3B1, and NOTCH1 mutations had moderate frequency rates among the treated CLL cohort, whereas the MYD88 mutation had a very low frequency rate.

As can be seen in figure 5.2 and in table 5.1, the cohort of 148 CLL patients had a male to female ratio 1:0.59, IGHVM: IGHVU ratio of 1:0.56, and median age of diagnosis of 66 years. SF3B1 mutations were 16.21%. K700E was 5.4 %, and the new discovered non-reported intron mutations (non-coding) were 3.37% (figures 5.4, 5.5, 5.6, 5.7, and 5.8).

NOTCH1 mutations were 14.18%, 1.35% of them were in TAD P143 (c.6906_6943del38), and P36 with G insertion at (c.6877_6878insG), and all other mutations were in the PEST domain (figure 5.9).

The only 2 MYD88 mutated were from the M-CLL subset (figure 5.10).

SF3B1 were mostly M-CLL (13 out of total 20 known IGHV status). In contrast, NOTCH1 mutations were mostly U-CLL (13 out of 19 known IGHV status).

4 CLL samples had both SF3B1 and NOTCH1 mutations (figure 5.3) (table 5.1), 1 CLL sample with TP53 alterations and SF3B1, 2 CLL samples with TP53 alterations and NOTCH1. Due to limitation of TP53 (mutation/deletion) information of patients, TP53 result might not represent the overall percentage among the cohort (figure 5.3). Our results of mutations in the domains of Sf3b1, Notch1, and Myd88 proteins is illustrated in diagram 5.11.

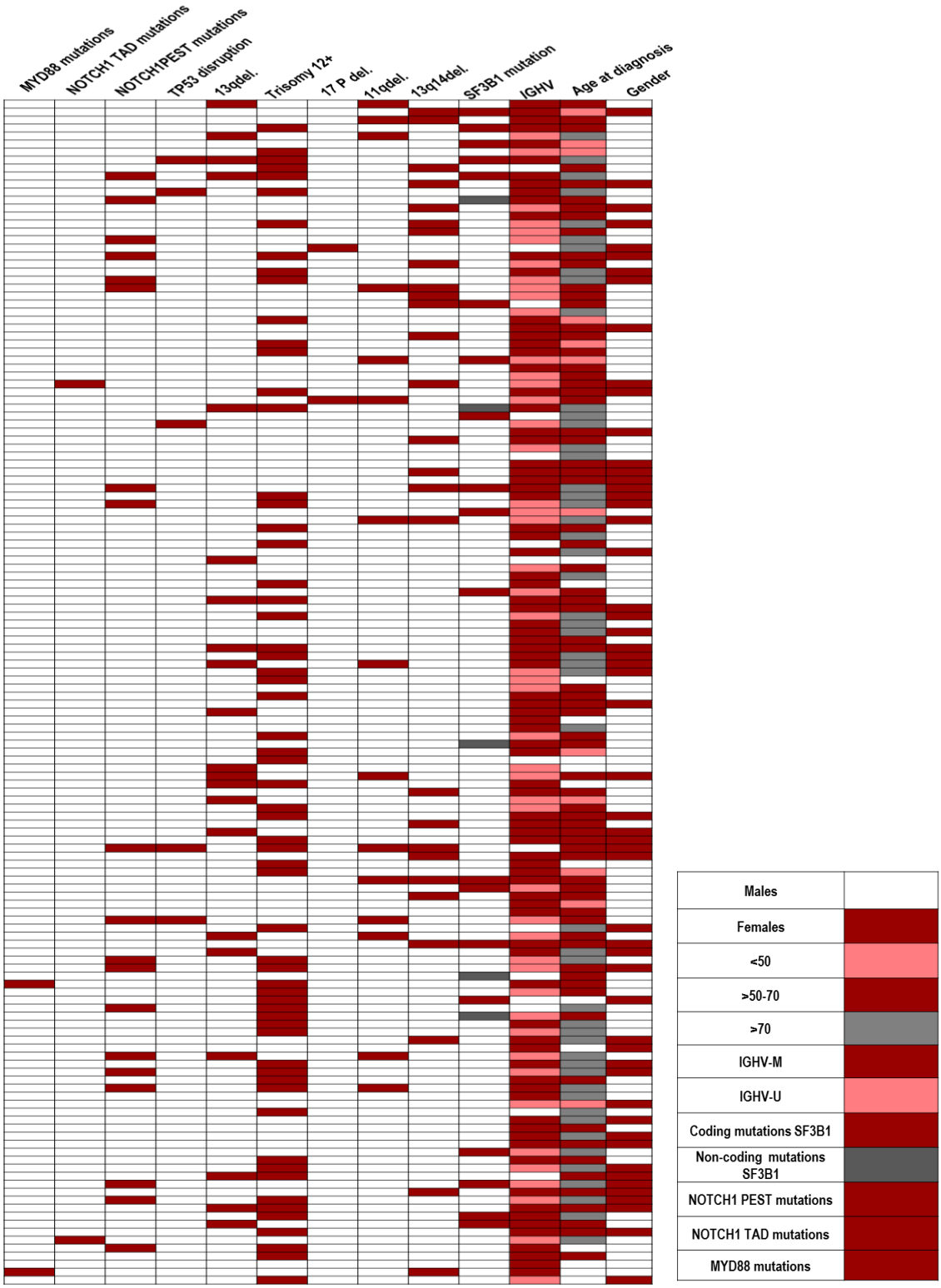


**Figure 5.2 Chart illustrating SF3B1, NOTCH1, and MYD88 mutations in our 148 CLL cohort.**

Gender divided into male (colourless boxes), and female (red boxes). Age at diagnosis divided into three groups of <50 yrs. (pink), >50 to 70yrs. (red), and >70yrs. (grey). IGHV-M (red), IGHV-U (pink). SF3B1 mutated in coding exons are in (red) boxes, and non-coding mutations are (grey) boxes. Colourless boxes in IGHV, age of diagnosis, and TP53 status were (not known).

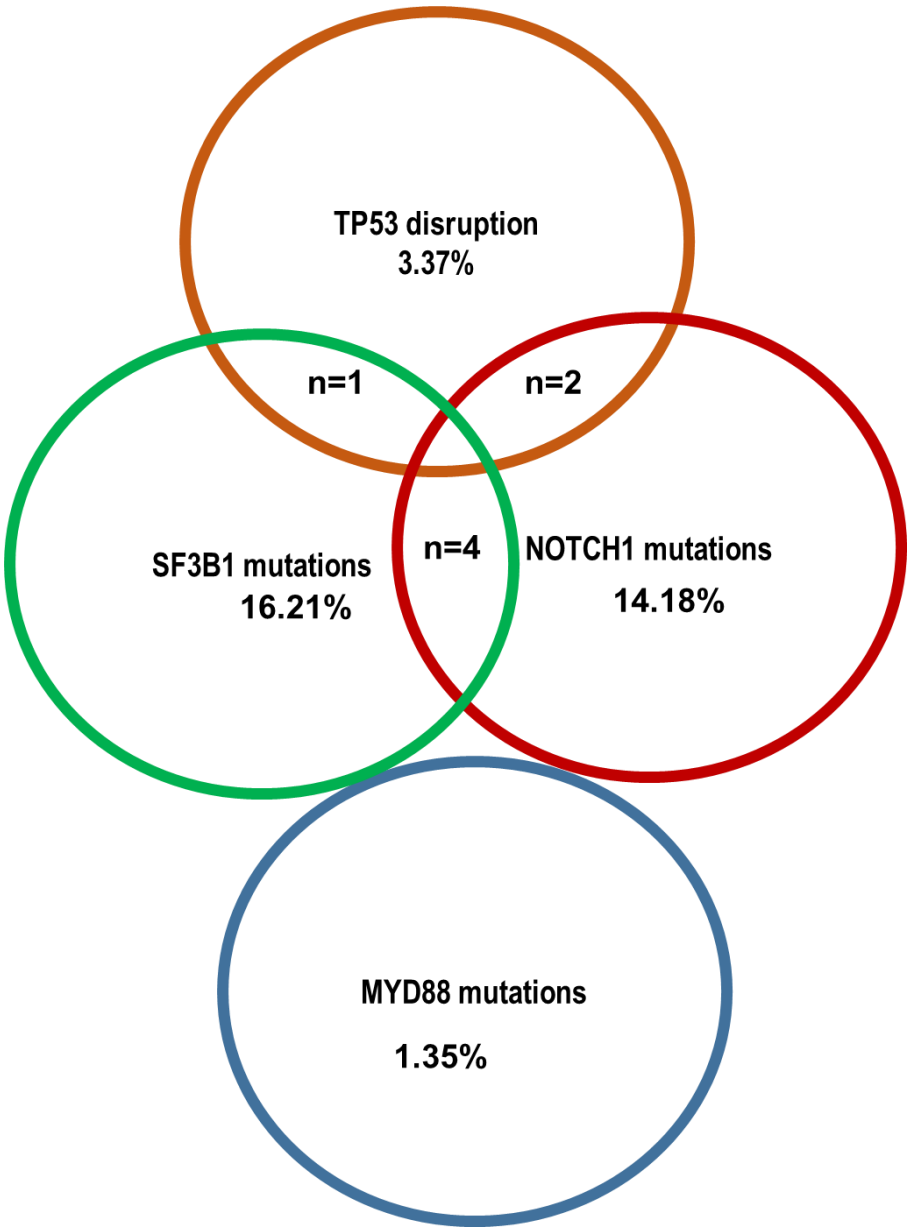


**Figure 5.3 Venn diagram (NOTCH1, SF3B1, TP53, and MYD88 mutations).**

Illustrating the overlap between NOTCH1 mutations and TP53 disruption by mutations, deletion, or both, and between SF3B1 mutations and TP53 alteration or both, and between SF3B1 and NOTCH1 mutations.

| | | |
|---|---|---|
| **<50yrs. age at diagnosis** | **12 of 148** | **8.1%** |
| **> 50-70yrs. age at diagnosis** | **71 of 148** | **47.97%%** |
| **>70yrs. age at diagnosis** | **50 of 148** | **33.78%** |
| **IGHVM** | **85 of 148** | **57.43%** |
| **IGHVU** | **48 0f 148** | **32.43%** |
| **M** | **93 0f 148** | **62.83%** |
| **F** | **55 of 148** | **37.16%** |
| **TP53mutation/deletion** | **5 of 148** | **3.37%** |
| **Trisomy 12** | **62 of 148** | **41.89%** |
| **13q14 deletion** | **27 of 148** | **18.24%** |
| **11q deletion** | **15 of 148** | **10.1%** |
| **17p deletion** | **2 of 148** | **1.35%** |
| **13q deletion** | **21 of 148** | **14.18%** |
| **SF3B1 mutation** | **24 of 148** | **16.21%** |
| **NOTCH1 mutations** | **21 of 148** | **14.18%** |
| **MYD88 mutations** | **2 of 148** | **1.35%** |

| **Number** | **P10** | **P13** | **P49** | **P136** |
|---|---|---|---|---|
| Gender | M | M | F | F |
| Age at diagnosis | 77 | 70 | 84 | 86 |
| IGHV | M | M | M | U |
| SF3B1 | p.K666T SF3B1 | non-coding SF3B1 mutation/variants | P.N626D FS3B1 | p.N621G SF3B1 |
| Cytogenetics | trisomy 12+ del13q | | del13q14 | |
| NOTCH1 | c.7541_7542delCT; p.Pro2514ArgfsTer4 | c.7541_7542delCT; p.Pro2514ArgfsTer4 | c.7541_7542delCT; p.Pro2514ArgfsTer4 | c.7541_7542delCT; p.Pro2514ArgfsTer4 |

**Table 5.1 SF3B1, NOTCH1, and MYD88 mutations in CLL.**

Top table: available information and mutations percentage of our 148CLL cohort for three main CLL mutations.
Lower table: 4 CLL patients have both NOTCH1 and SF3B1 mutations.

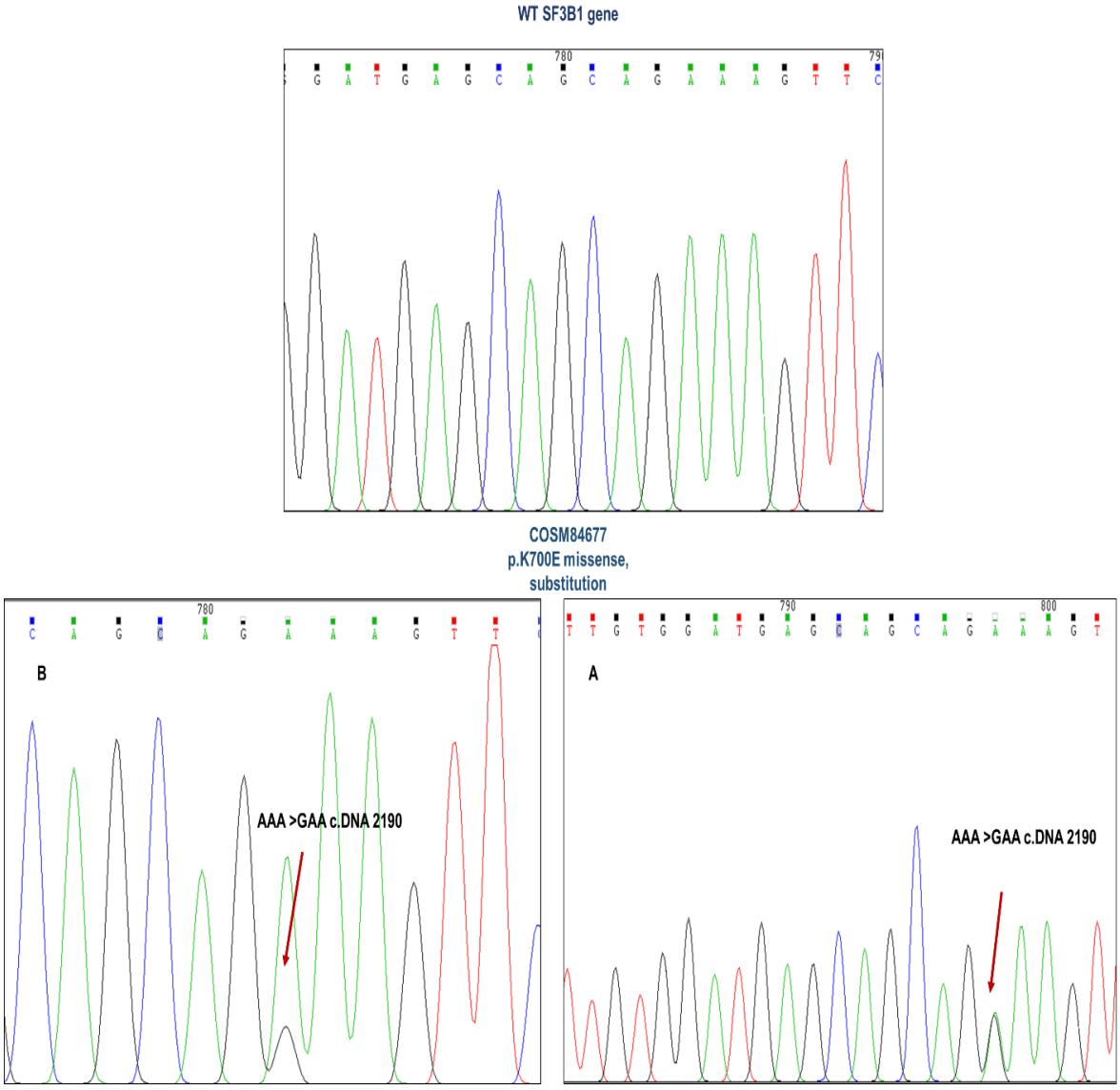


**Figure 5.4 SF3B1 K700E mutations were present in 5.4% of our cohort.**

Sanger sequencing results of mutated K700E patients either homozygous (A) or heterozygous (B) in comparison to unmutated wild type. c.2190 is cDNA position in which, lysine is substituted with glutamic acid. COSM84677 is cosmic mutation Id of p.K700E in the catalogue of somatic mutations in cancer.

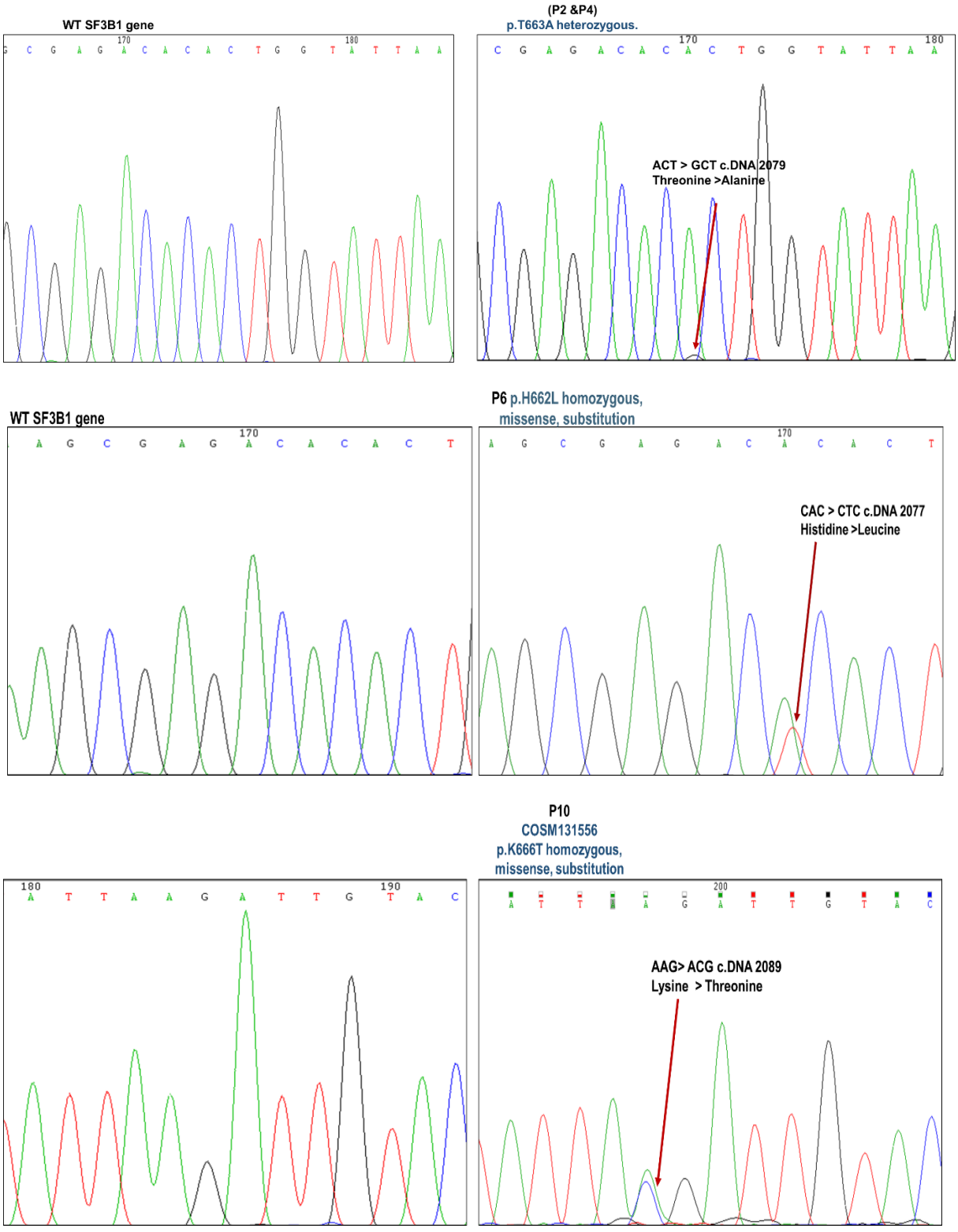


**Figure 5.5 SF3B1 mutations in comparison to wild type.**

Top: two patient primary cells, with heterozygous p.T663A missense substitution. Middle: one patient primary cell with H662L homozygous missense substitution. Lower: p.K666T homozygous missense substitution mutation.

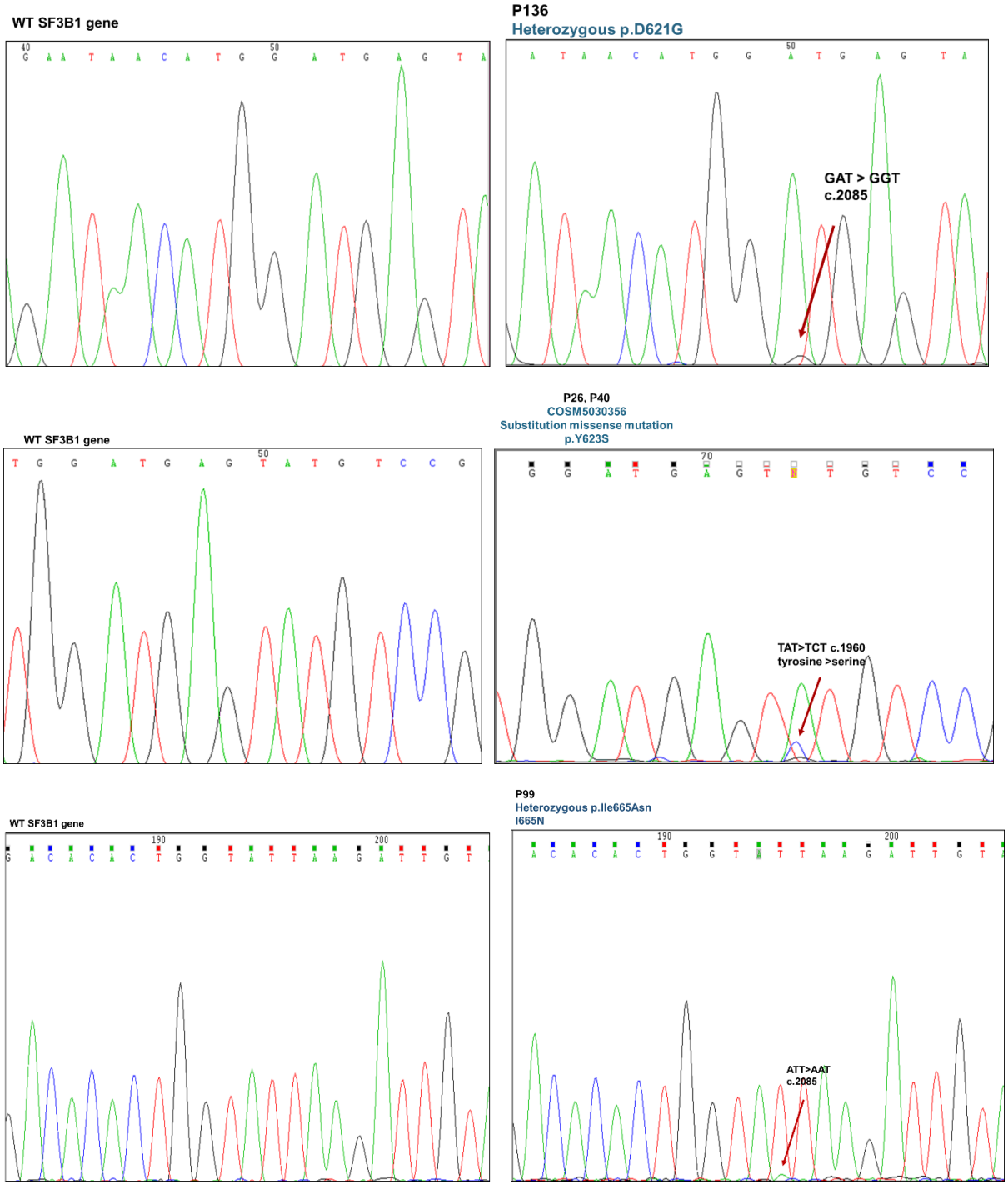


**Figure 5.6 SF3B1 mutations in comparison to wild type.**

Top: one patient primary cell with heterozygous p.D621G missense substitution. Middle: two patient primary cells with Y623S heterozygous missense substitution. Lower: one patient with p.I665N heterozygous missense substitution mutation.

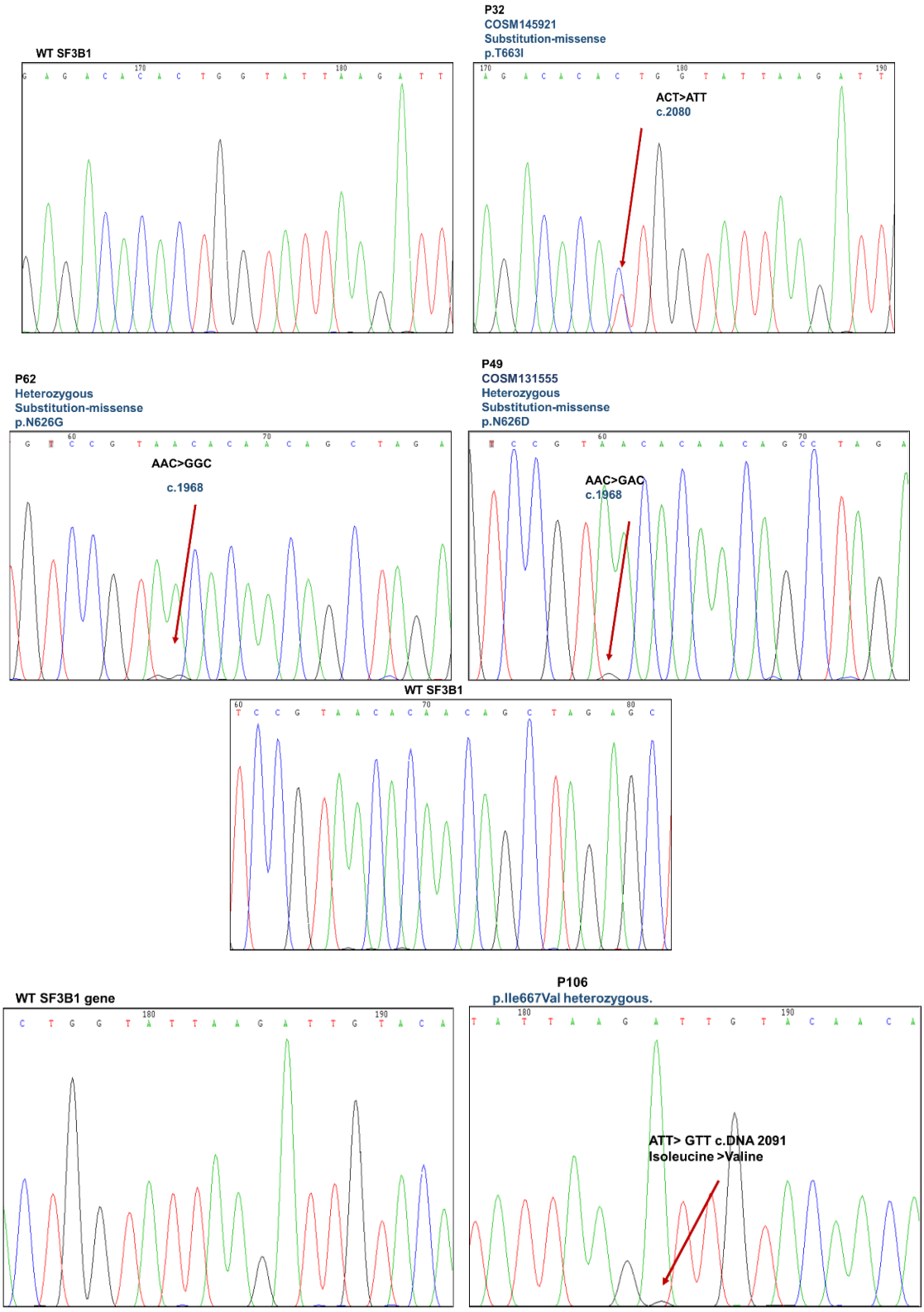


**Figure 5.7 SF3B1 mutations in comparison to wild type.**

Top: one patient primary cell with heterozygous p.T663I missense substitution. Middle: one with N626G, and one with N626D heterozygous missense substitution. Lower: one with heterozygous I667V substitution.

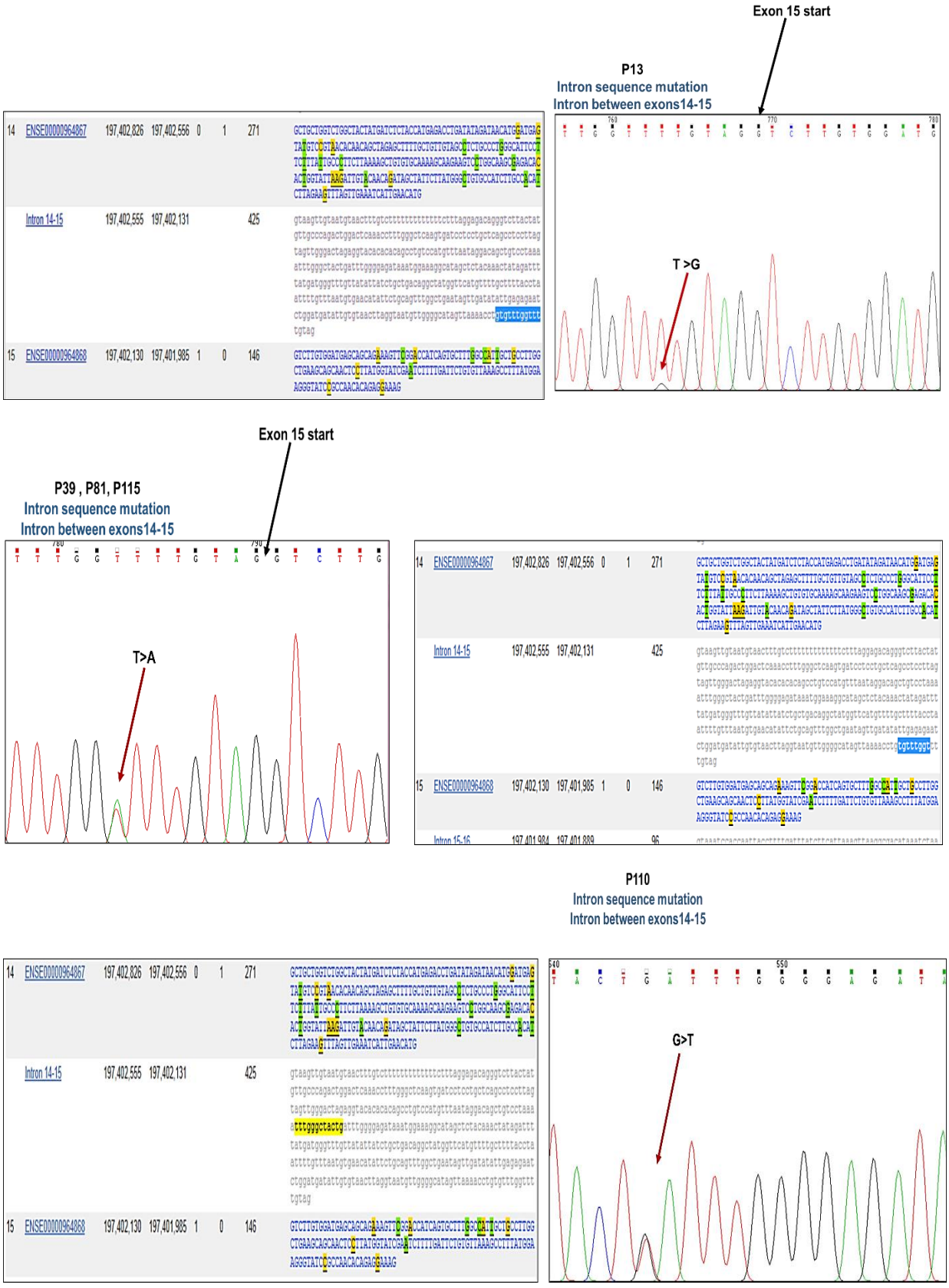


**Figure 5.8 SF3B1 (non-coding) mutations in comparison to wild type.**

Top: one patient primary cell with heterozygous T>G in the third T of 4 T sequence near splicing site. Middle: two with T>A homozygous in the first T of 4 T sequence near splicing site. Lower: G>A homozygous in the middle of intron sequence. Exons and intron positions according to ensemble genome browser.

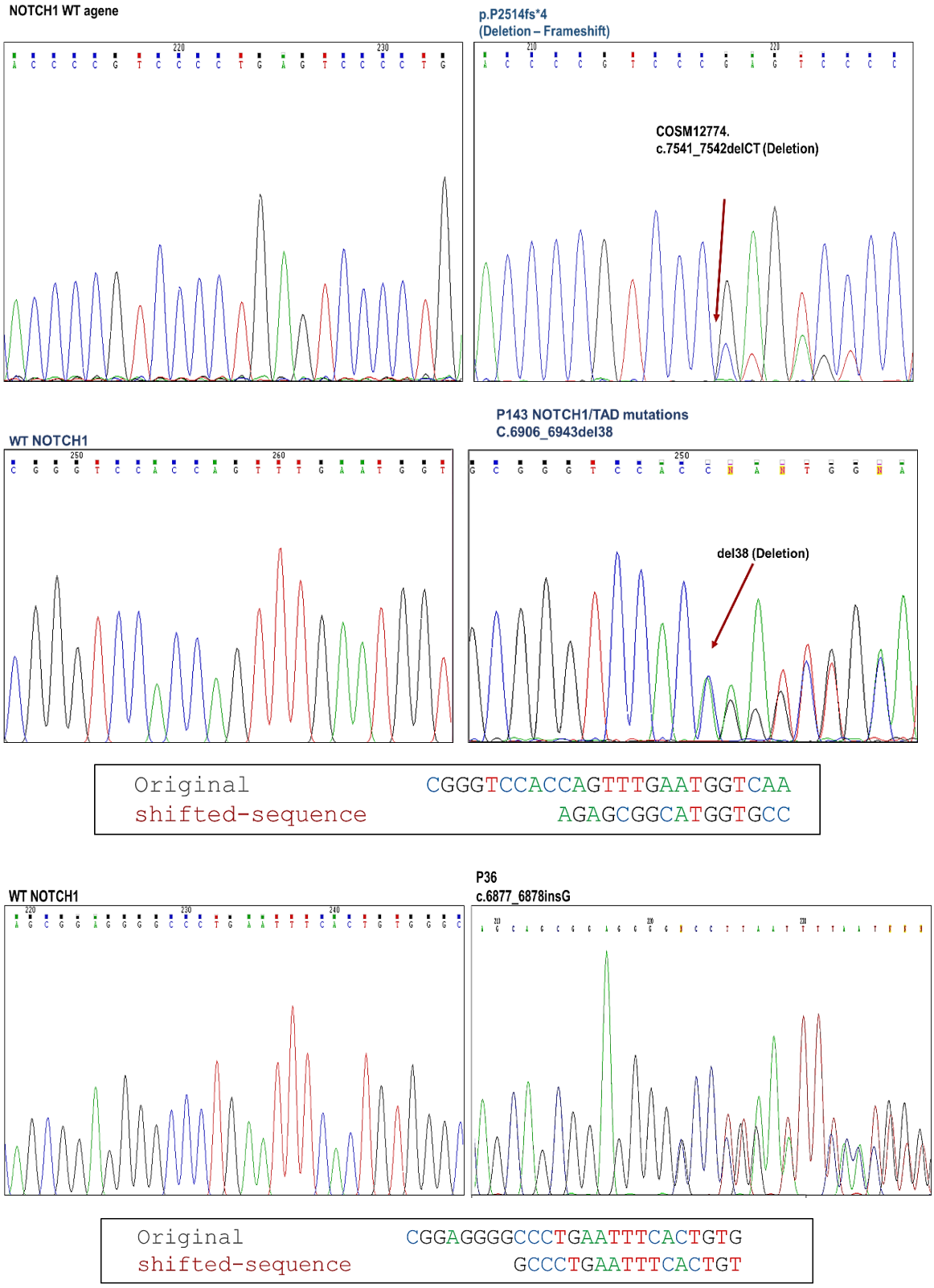


**Figure 5.9 NOTCH1 mutations in comparison to wild type.**

Top: most common mutation among our cohort of frameshift deletion of CT deletion at c.7541_7542delCT. Middle: TAD mutation P143: 38 base pair deletion (c.6906-6943del38), shifted sequence will begin at c.6944 (AGAGCGGCAT...) (delCAGTTTGAATGGTCAATGCGAGTGGCTGTCCCGGCTGC (38)). Lower: TAD domain mutation P36 of c.6877_6878insG will result in shifting the sequence (GCCCTGAA).

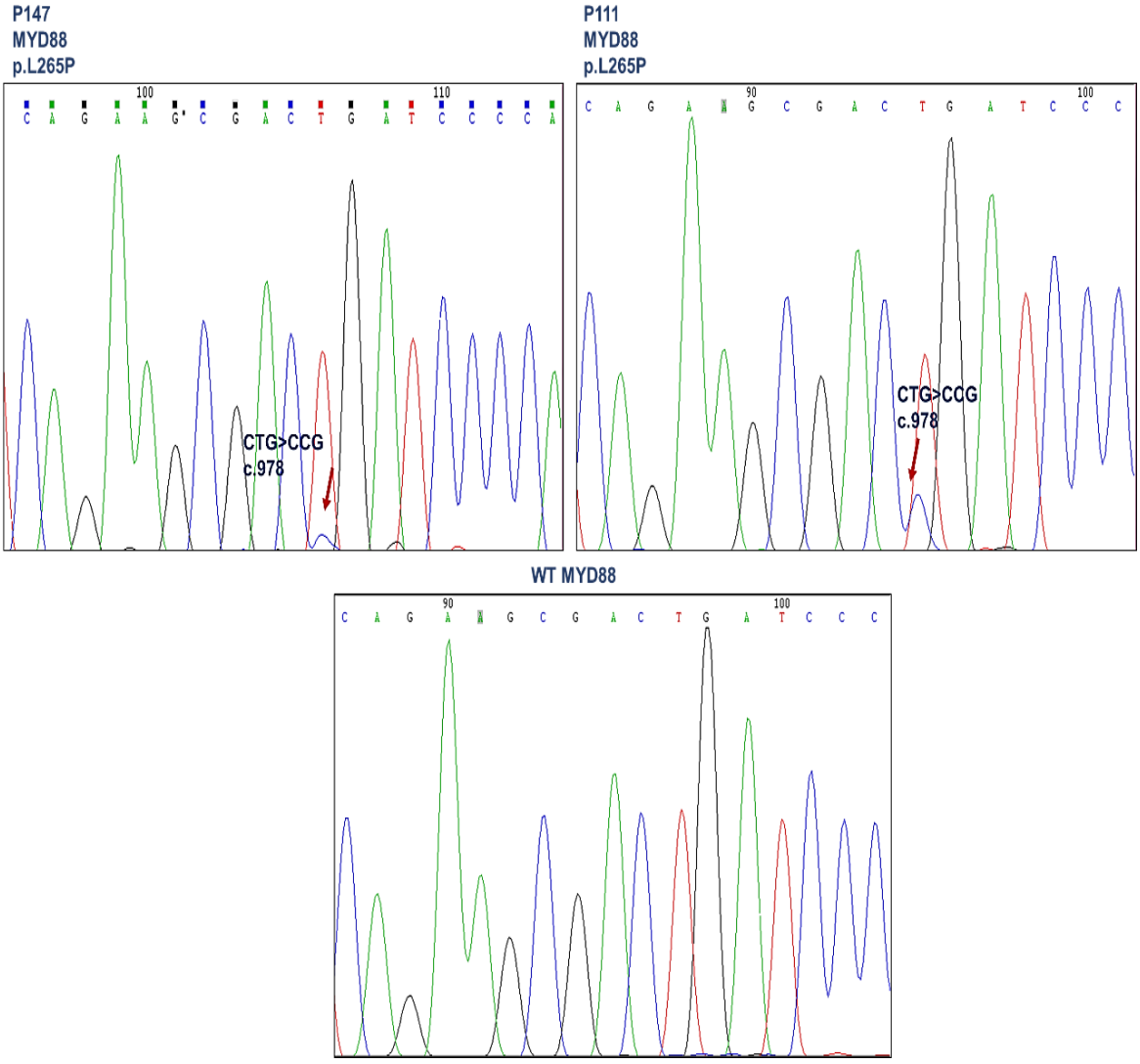


**Figure 5.10 MYD88 mutations in comparison to wild type.**

The only 2 patients (P147, and P111) mutated MYD88 both heterozygous of p.L265P.

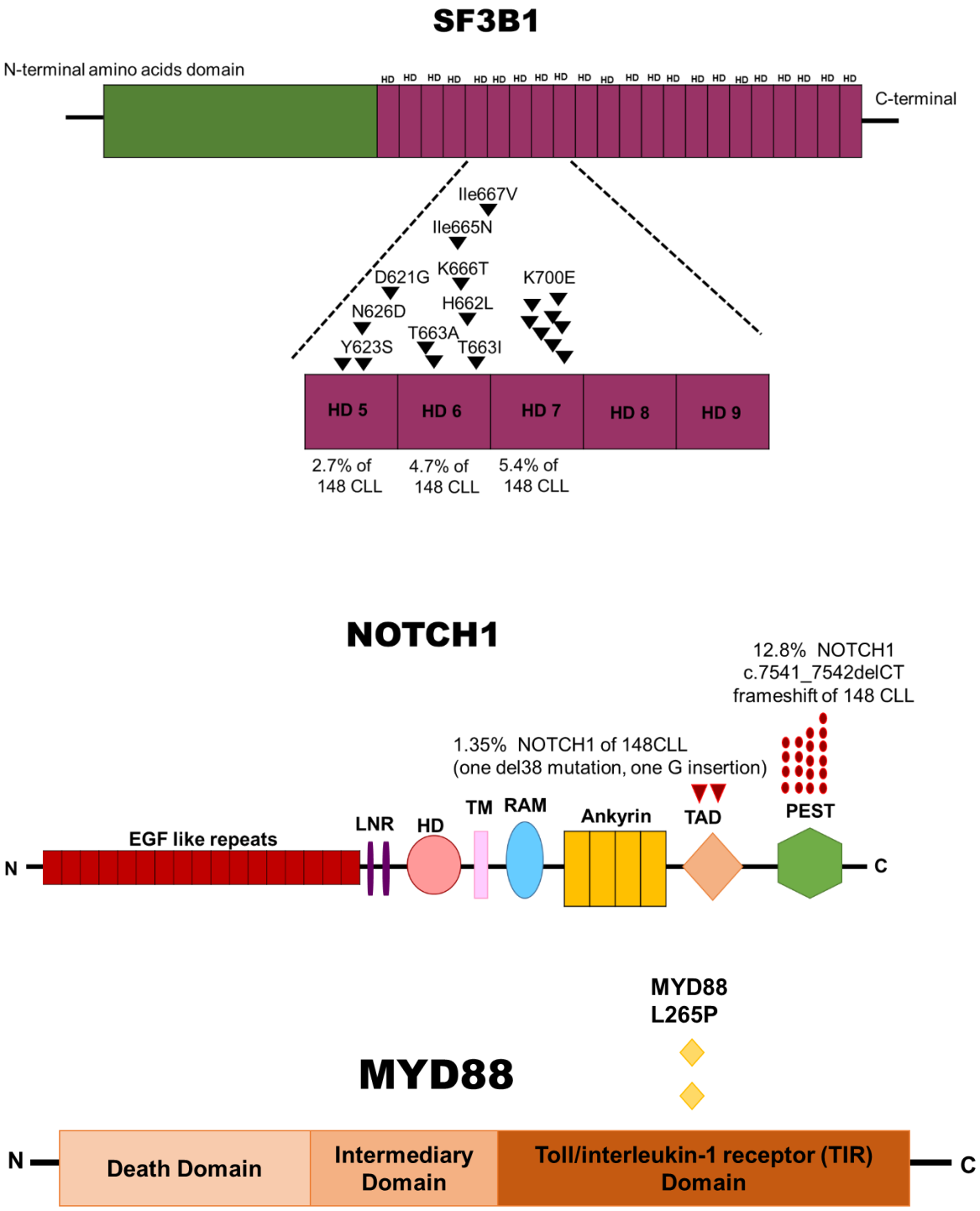


**Figure 5.11 Diagram illustrating mutations that have been found in our cohort**.

Top: SF3B1 domains and coding mutations of heat repeats. Middle: is NOTCH1 domains and mutations (EGF- like repeats and NRR (Negative Regulatory Region) in the extracellular domain, LIN-12-Notch repeats (LNRs) and a heterodimerization domain (HD),Transmembrane domain (TM), RAM (Rbp- Associated Molecule domain), ANK (Ankyrin) repeats and PEST region of the intracellular domain.). Bottom: MYd88 mutations in TIR domain.

In addition to our cohort of 148 CLL patients, SF3B1 mutations were checked in patients in the table below (figure 5.12). Heterozygous mutation at p.Y623S (missense substitution mutation) was detected in one hairy cell leukaemia patient. We believe it is the first time to report SF3B1 mutations in hairy cell leukaemia.

| | VHCL | VHCL | VHCL | VHCL | MZL | TCL | HCL |
|---|---|---|---|---|---|---|---|
| **Code** | BB | BDM | MAC | RES | GJE | SJA | DJO |
| **Gender** | F | F | F | F | F | F | M |
| **Age at diagnosis** | 79 | 62 | 85 | n/a | 76 | n/a | n/a |
| **FISH** | Trisomy 3q | Heterozygous deletion in 11q22~23 (ATM and FDX-gene locus) | del14q | | Loss of the CDK6 distal probe (95%) | n/a | 7q-deletion (36%) and three copies of MPO in 17q22 (26%) |
| **IGHVM/U** | U | M | n/a | M | U | n/a | M |
| **TP53 mutation/deletion** | | | | Heterozygous deletion of P53 (21%) | | | |
| **SF3B1 mutations** | WT | WT | WT | WT | WT | WT | (COSM5030356) p.Y623S (Substitution – Missense) Tyrosine>Serine DNA: c.1868A>C Substitution. |

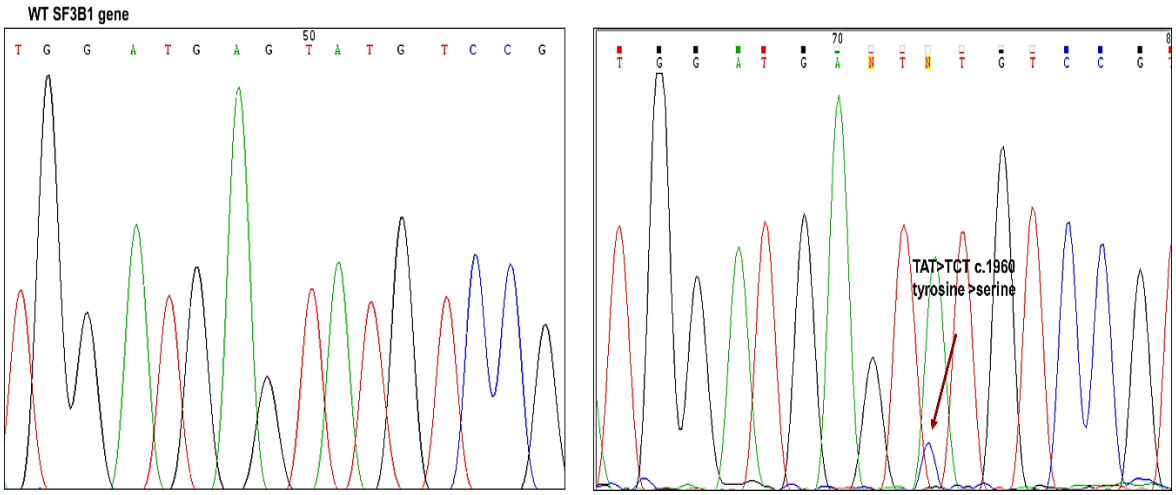


**Figure 5.12 SF3B1 screening results in non-CLL patients.**

One HCL patient cells were positive for SF3B1 mutation p.Y623S, (n/a not available).

## 5.2 Primary CLL cells exhibited different sensitivity to inhibitors depending on their mutations.

After the sequencing of key genes was done in our cohort, we seek to use this information to stratify patients and predict their sensitivity to six specific inhibitors (table 5.2). IRAK1/4 inhibitors that target Myd88/IRAK signalling, was chosen to observe the sensitivity of Myd88 mutated CLL cells and compare it to unmutated. MK-0752 gamma-secretase inhibitor for Notch1 signalling, was chosen to observe the sensitivity of Notch1 mutated CLL cells and compare it to unmutated. Pladienolide B is SF3B1, U2 inhibitor for splicing machinery, was chosen to observe the sensitivity of SF3B1 mutated CLL cells and compare it to unmutated. Dactolisib and PF- 04691502 are dual PI3K and mTOR inhibitors, and sotrastaurin, which is a protein kinase C inhibitor, were chosen to see their efficacy and compare it to other inhibitors. All primary cells were stimulated with sIL-4-CD40L, and treated for 48 hours with the six inhibitors independently. Experiments were done in technical duplicates and each experiment were done twice (biological duplicates). MYD88 mutated P111 primary cells were not available to test, therefore, we have tested only P147 with 6 inhibitors. Patient information (24 CLL cells) used in this study can be seen in table 5.4, and 5.5.

| Inhibitor | Target |
|---|---|
| Dactolisib (BEZ235, NVP-BEZ235) | is a dual ATP-competitive PI3K and mTOR inhibitor for p110α/γ/δ/β and mTOR(p70S6K) |
| PF- 04691502 | mTOR/PI3K dual inhibitor |
| Sotrastaurin (AEB071) | Protein kinase C inhibitor (PKC) (developed as immunosuppressant) |
| IRAK1/4 inhibitor | a potent inhibitor of interleukin-1 receptor-associated kinases 1/4 (IRAK 1/4) |
| MK-0752 | Is a moderately potent γ-secretase inhibitor. |
| Pladienolide B | mRNA splicing inhibitor; decreases splicing capacity up to 75% *in vitro*. Directly targets spliceosome-associated 130 (SAP130), inhibits splicing factor 3B subunit (SF3B1) and impairs U2 small nuclear ribonucleoprotein (U2 snRNP) interaction with pre-mRNA. Arrests cell cycle in $G_1$ and $G_{2/M}$ phases. |

**Table 5.2 Inhibitors used to stratify CLL cells sensitivity**.

| No. | Patient | M/F | Age at diagnosis | IGHV | FISH | TP53 | SF3B1/NOTCH1/MYD88 mutations |
|---|---|---|---|---|---|---|---|
| 1 | P148 | F | | U | BCL3 break (62%) 83% trisomy 12, | | |
| 2 | P145 | M | 56 | M | an IGH-BCL2-fusion (95%) and a (partial) trisomy 12 (8%), t(14;18) | | |
| 3 | P55 | M | 78 | M | Normal | | |
| 4 | P147 | M | | M | Heterozygous deletion in 13q14 (92%) and a reduced signal of IGH distal (17%) | | Heterozygous MYD88p.L265P |
| 5 | P2 | F | 40 | M | Homozygous deletion in 13q14 (99%) | | SF3B1 heterozygousp.T663A |
| 6 | P6 | M | 33 | M | t(2;4) with gain of the BCL11A/REL gene locus and add (13)(q14) | | SF3B1p.H662L missense substitution |
| 7 | P26 | M | 65 | mix | Heterozygous del13q14 | | SF3B1 p. Y623S |
| 8 | P106 | F | 63 | M | Heterozygous del13q14 (87%) | | SF3B1 p.Ile667V |
| 9 | P8 | M | 76 | M | del13q (89%) and three copies of the Myc-locus (16%). 93% trisomy 12+. | P53-deletion (34%) | SF3B1p.K700E |
| 10 | P62 | M | 64 | U | | | SF3B1p.K700E, heterozygous p.N626G |
| 11 | P141 | M | 59 | M | Heterozygous del13q (77%) | | SF3B1 p.K700E |
| 12 | P115 | M | 56 | U | 96% trisomy 12 IGH break (27%) and BCL3 break (32%) -> translocation t(14;19)(q32;q13) or IGH-BCL3 fusion and reduced signal of IGH distal (63%) | | non-coding intron mutation near splicing site intron14-15-exon15 |

**Table 5.3 Information of CLL patients used in this study.**

| No. | Patient | M/F | Age at diagnosis | IGHV | FISH | TP53 | SF3B1/NOTCH1/MYD88 mutations |
|---|---|---|---|---|---|---|---|
| 13 | P39 | M | 74 | M | trisomy 12, 13q del. | | SF3B1 non-coding mutation near splicing site (Intron14-15-exon15) |
| 14 | P110 | M | 70 | n/a | normal | | non-coding intron mutation faraway from splicing site intron14-15 |
| 15 | P24 | M | 54 | U | Heterozygous del.11q22~23 and del.13q14 | | NOTCH1 c.7541_7542delCT |
| 16 | P124 | M | 75 | M | 11q deletion 90% trisomy 12 | | NOTCH1 c.7541_7542delCT |
| 17 | P122 | F | 75 | U | reduced signal of IGH distal (61%)86% trisomy 12 | | NOTCH1 homozygous c.7541_7542delCT |
| 18 | P144 | M | | M | 72% trisomy 12 | | NOTCH1 c.7541_7542delCT |
| 19 | P143 | M | 77 | U | n/a | | NOTCH1 c.6906-6943del38 |
| 20 | P10 | M | 77 | M | Partial trisomy 12 (99%) 13q-deletion (23%) | | SF3B1p.K666T,NOTCH1 c.7541_7542delCT |
| 21 | P13 | M | 70 | M | n/a | | SF3B1 non-coding near splicing site mutation (Intron14-15-exon15) NOTCH1 c.7541_7542delCT |
| 22 | P36 | F | 60 | U | del13q14 | | NOTCH1 c.6877insG |
| 23 | P49 | F | 84 | M | Heterozygous del13q14 (98%) | | Heterozygous SF3B1 p.N626D, NOTCH1 c.7541_7542delCT |
| 24 | P136 | F | 86 | U | n/a | | SF3B1 p.D621G, NOTCH1 c.7541_7542delCT |

**Table 5.4 Information of CLL patients used in this study.**

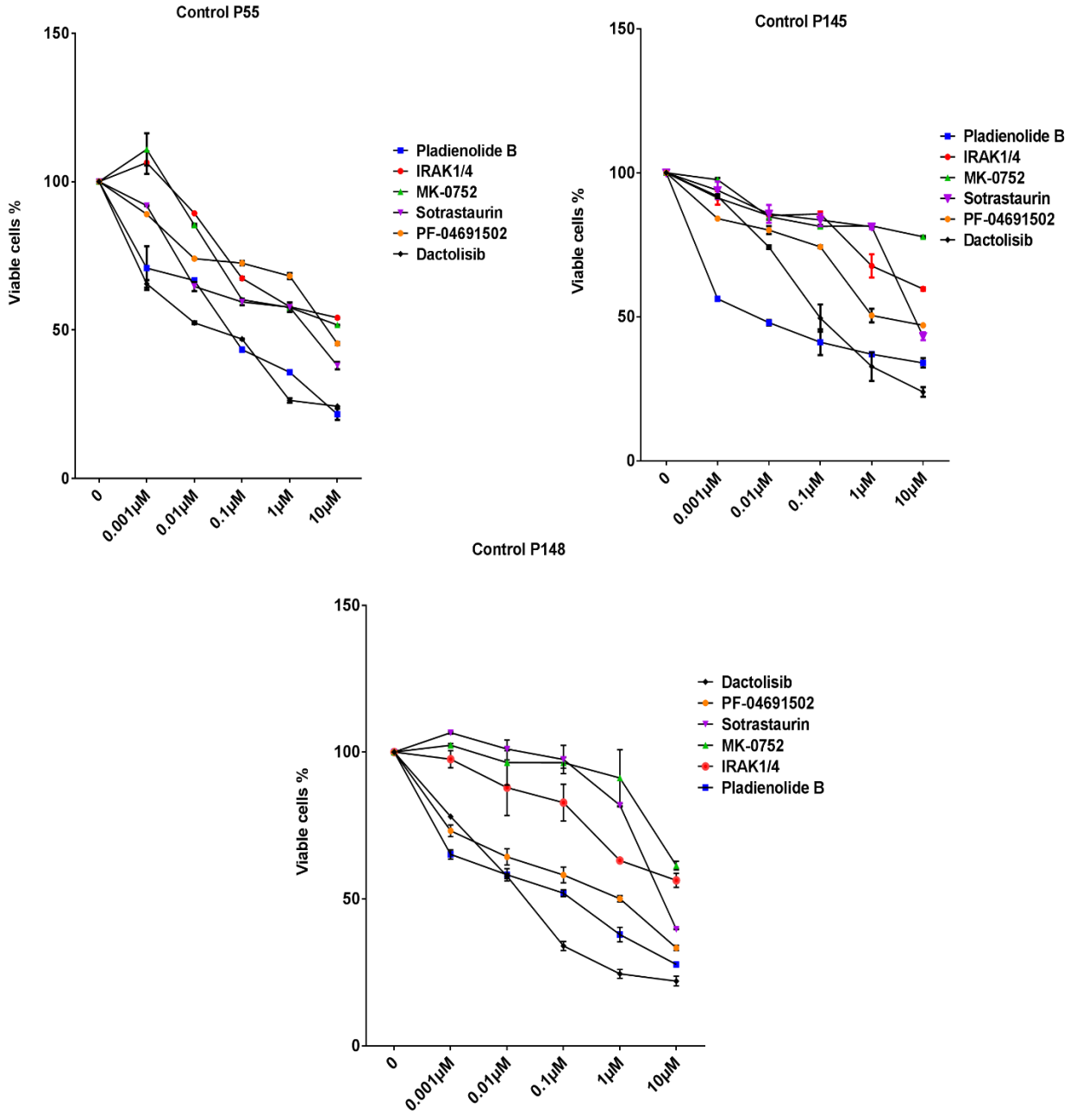


**Figure 5.13 Viability assay of 3 unmutated CLL samples.**

After stimulation to mimic microenvironment of CLL, cells were treated for 48 hours with five concentrations 10, 1, 0.1, 0.01, 0.001µM, MTS viability assay were performed and viable cells % were calculated after normalising DMSO control to 100%. DMSO was ~0.1% per well in 96 wells plates. All experiments were performed in technical and biological duplicates. All data are mean of viable cells percentage and error bars indicate SD.

As can be seen in figure 5.13 CLL cells that have no SF3B1, Notch1 or Myd88 mutations show fairly similar sensitivity to these inhibitors. In all three samples, CLL cells with IRAK1/4 and MK-0752 did not reach 50% inhibition. Dactolisib, sotrastaurin, and pladienolide B showed similar efficacies. PF-04691502 showed similar efficacy in P148 and P145, but less in P55.

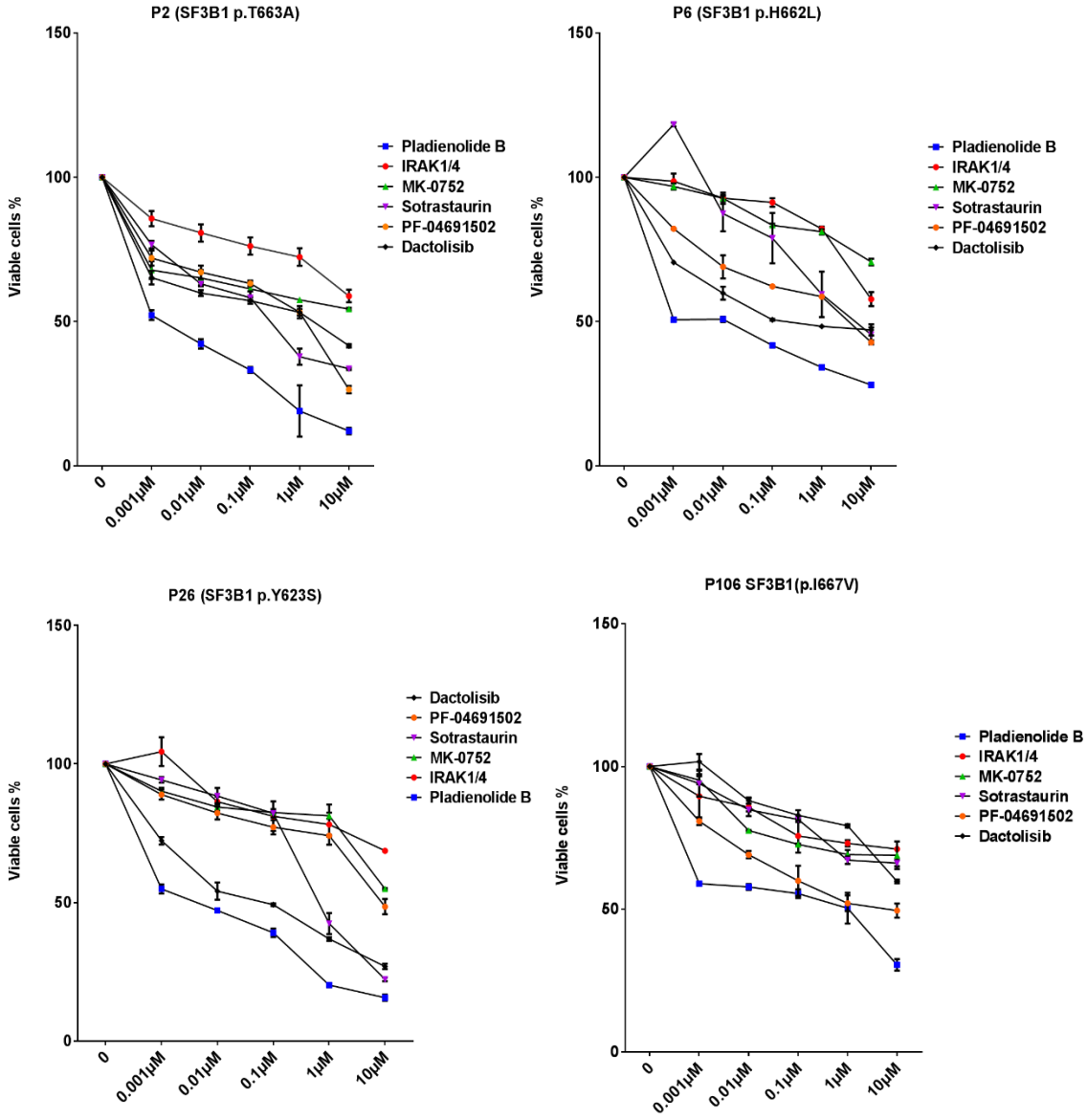


**Figure 5.14 Viability assay of SF3B1 mutated CLL samples after treatment.**

After stimulation to mimic microenvironment of CLL, cells were treated for 48 hours with five concentrations 10, 1, 0.1, 0.01, 0.001µM, MTS viability assay were performed and viable cells % were calculated after normalising DMSO control to 100%. DMSO was ~0.1% per well in 96 wells plates. All experiments were performed in technical and biological duplicates. All data are mean of viable cells percentage and error bars indicate SD.

P2, P6 and P26 showed similar sensitivity to pladienolide B. While, P106 showed slightly less sensitivity. IRAK1/4 and MK-0752 has no significant effects on cells viability. Sotrastaurin was effective in inhibiting cells viability in P26, and P2, moderate efficacy in P6 and not effective in P106. Dactolisib showed efficacy in P6, and P26, moderate efficacy in P2, and no efficacy in P106. P2, and P6 showed similar sensitivity to PF-04691502, but P106 showed more sensitivity. In contrast, P26 showed slight less sensitivity to PF-04691502.

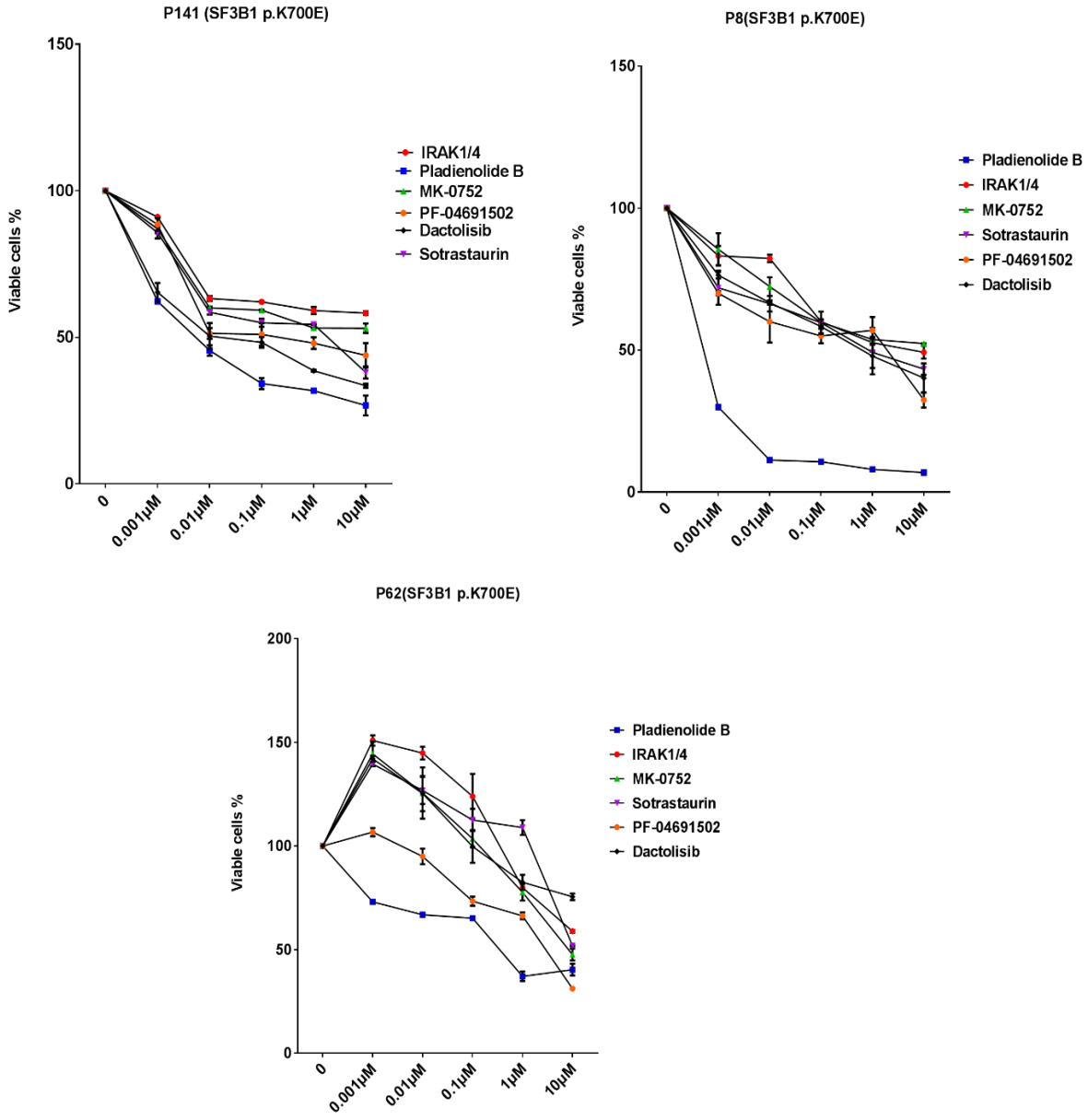


**Figure 5.15 Viability assay of SF3B1 (K700E) mutated CLL samples after treatment.**

After stimulation to mimic microenvironment of CLL, cells were treated for 48 hours with five concentrations 10, 1, 0.1, 0.01, 0.001µM, MTS viability assay were performed and viable cells % were calculated after normalising DMSO control to 100%. DMSO was ~0.1% per well in 96 wells plates. All experiments were performed in technical and biological duplicates. All data are mean of viable cells percentage and error bars indicate SD.

One patient (P8) showed great sensitivity to pladienolide B, other inhibitors showed slight different efficacy to each of K700E mutated patients. Surprisingly, P8 had P53 deletion, trisomy 12 and older age than P141 and P62 with same p.K700E mutation (table 5.3).

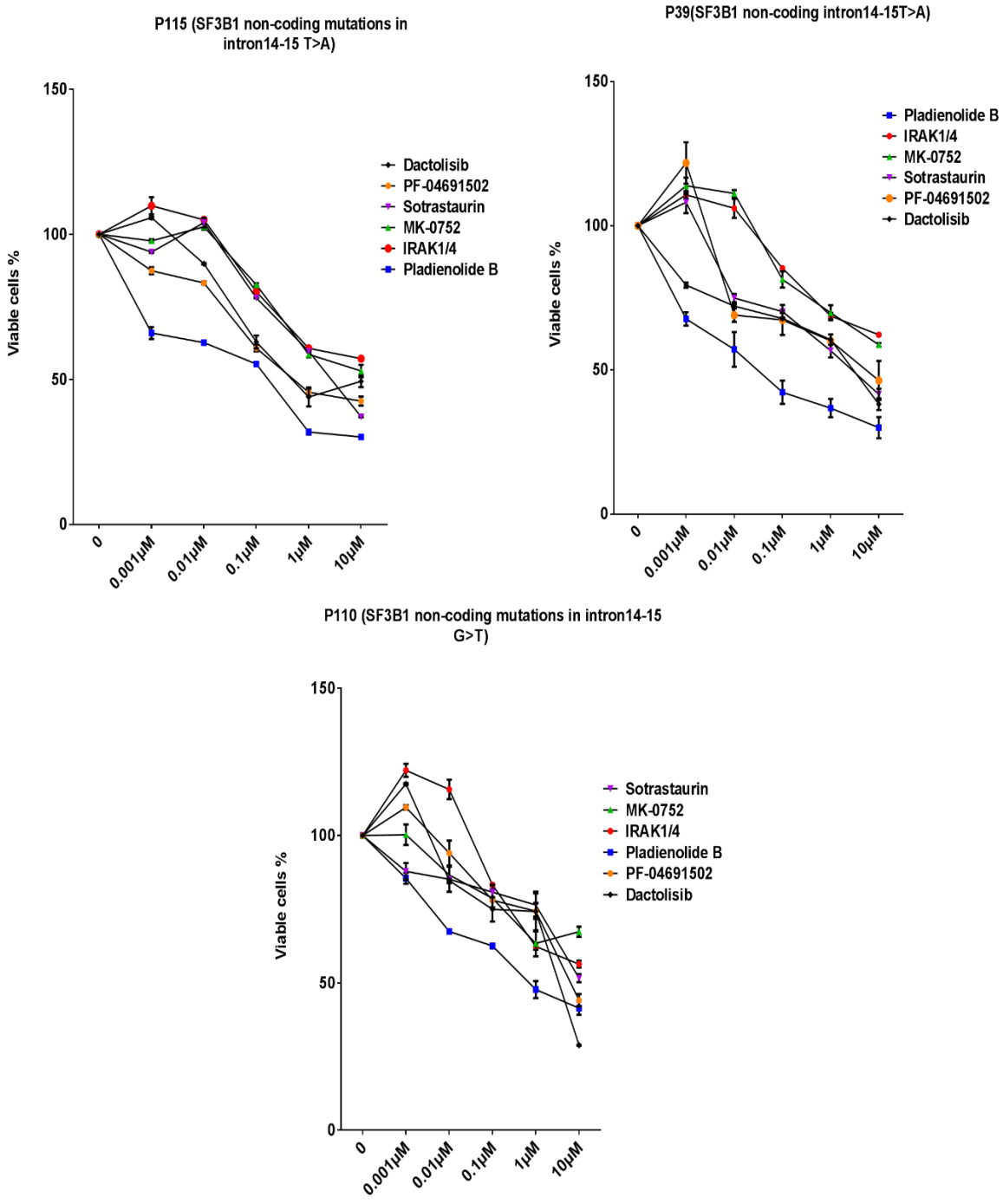


**Figure 5.16 Viability assay of SF3B1 (non-coding) mutated CLL samples after treatment.**

After stimulation to mimic microenvironment of CLL, cells were treated for 48 hours with five concentrations 10, 1, 0.1, 0.01, 0.001µM, MTS viability assay were performed and viable cells % were calculated after normalising DMSO control to 100%. DMSO was ~0.1% per well in 96 wells plates. All experiments were performed in technical and biological duplicates. All data are mean of viable cells percentage and error bars indicate SD.

Non-coding mutations/variants in SF3B1 showed slight difference in sensitivity to all inhibitors. Among all three patients no similar pattern of viability reduction could be noticed with splicing inhibitor pladienolide B. P115 and P39 both had non-coding SF3B1 mutations near splicing site. While P110 had mutation in the middle of intron sequence. P39 seems to be the most sensitive one to pladienolide B. IRAK1/4 and MK-0752 inhibitors showed no efficacy in reducing cells viability in all three patients. Sotrastaurin showed moderate efficacy in P39 and P115, but no efficacy in P110. Dactolisib and PF-04691502 showed similar efficacy in P39 and P115, and P110 was more sensitive to the highest concentration of dactolisib.

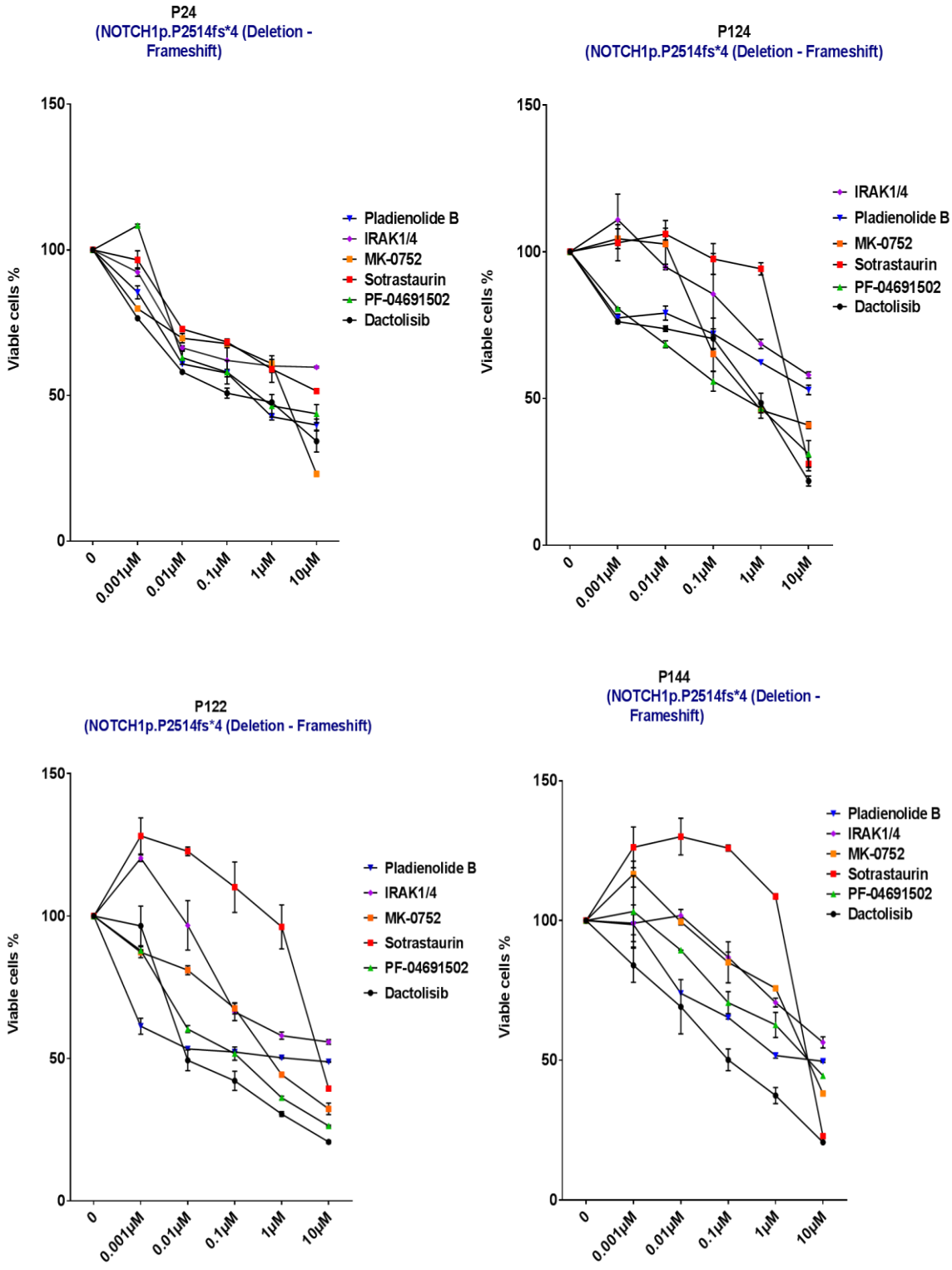


**Figure 5.17 Viability assay of NOTCH1 mutated (PEST region) mutated CLL samples after treatment.**

After stimulation to mimic microenvironment of CLL, cells were treated for 48 hours with five concentrations 10, 1, 0.1, 0.01, 0.001µM, MTS viability assay were performed and viable cells % were calculated after normalising DMSO control to 100%. DMSO was ~0.1% per well in 96 wells plates. All experiments were performed in technical and biological duplicates. All data are mean of viable cells percentage and error bars indicate SD.

All 4 Notch1 mutated patients showed moderate sensitivity to MK-0752 gamma secretase inhibitor. P144, P122, and P24 showed moderate sensitivity to pladienolide B, but P124 showed no reduction in viability. No reduction in viability of all 4 CLL cells with IRAK1/4 inhibitor. Dactolisib, sotrastaurin, and PF-04691502 showed moderate efficacy in all 4 Notch1 mutated CLL cells, P122, and P144 showed more sensitivity to dactolisib. P122 showed more sensitivity to PF-04691502.

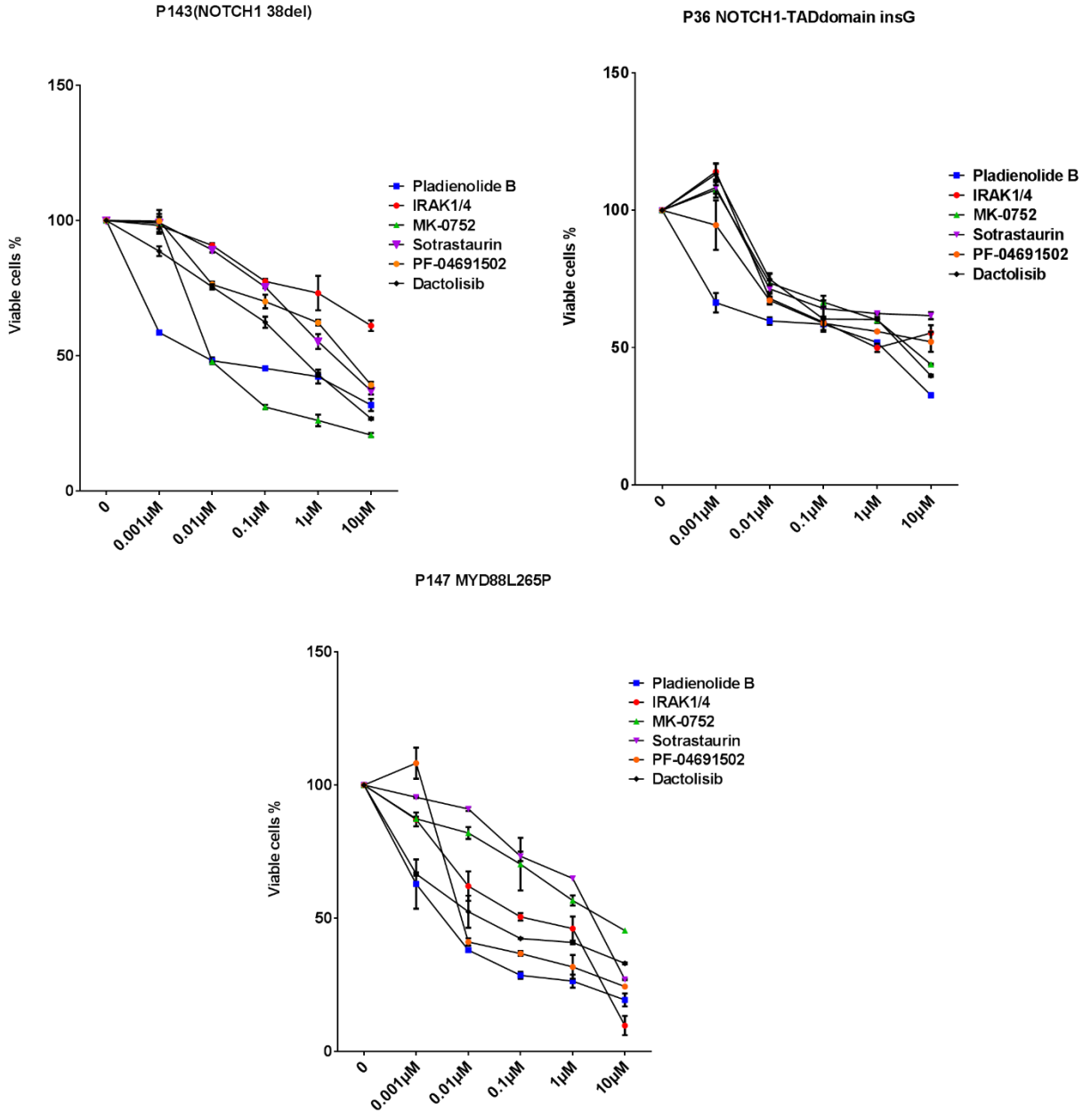


**Figure 5.18 Viability assay of two NOTCH1 mutated (TAD domain), and one MYD88 L265P mutated CLL samples after treatment.**

After stimulation to mimic microenvironment of CLL, cells were treated for 48 hours with five concentrations 10, 1, 0.1, 0.01, 0.001µM, MTS viability assay were performed and viable cells % were calculated after normalising DMSO control to 100%. DMSO was ~0.1% per well in 96 wells plates. All experiments were performed in technical and biological duplicates. All data are mean of viable cells percentage and error bars indicate SD.

P147 (Myd88p.L265P) and P143 (Notch138del. mutated) showed more sensitivity to pladienolide B than P36 (Notch1 insG. mutated). P143, and P36 showed sensitivity to MK-0752, though P143 (38delNotch1) was more sensitive than P36 (insGNotch1). Dactolisib, PF-04691502, and sotrastaurin showed moderate efficacy in P143 and P147 and less in P36. P147 with Myd88 mutation exhibited sensitivity to IRAK1/4 than P143 and P36.

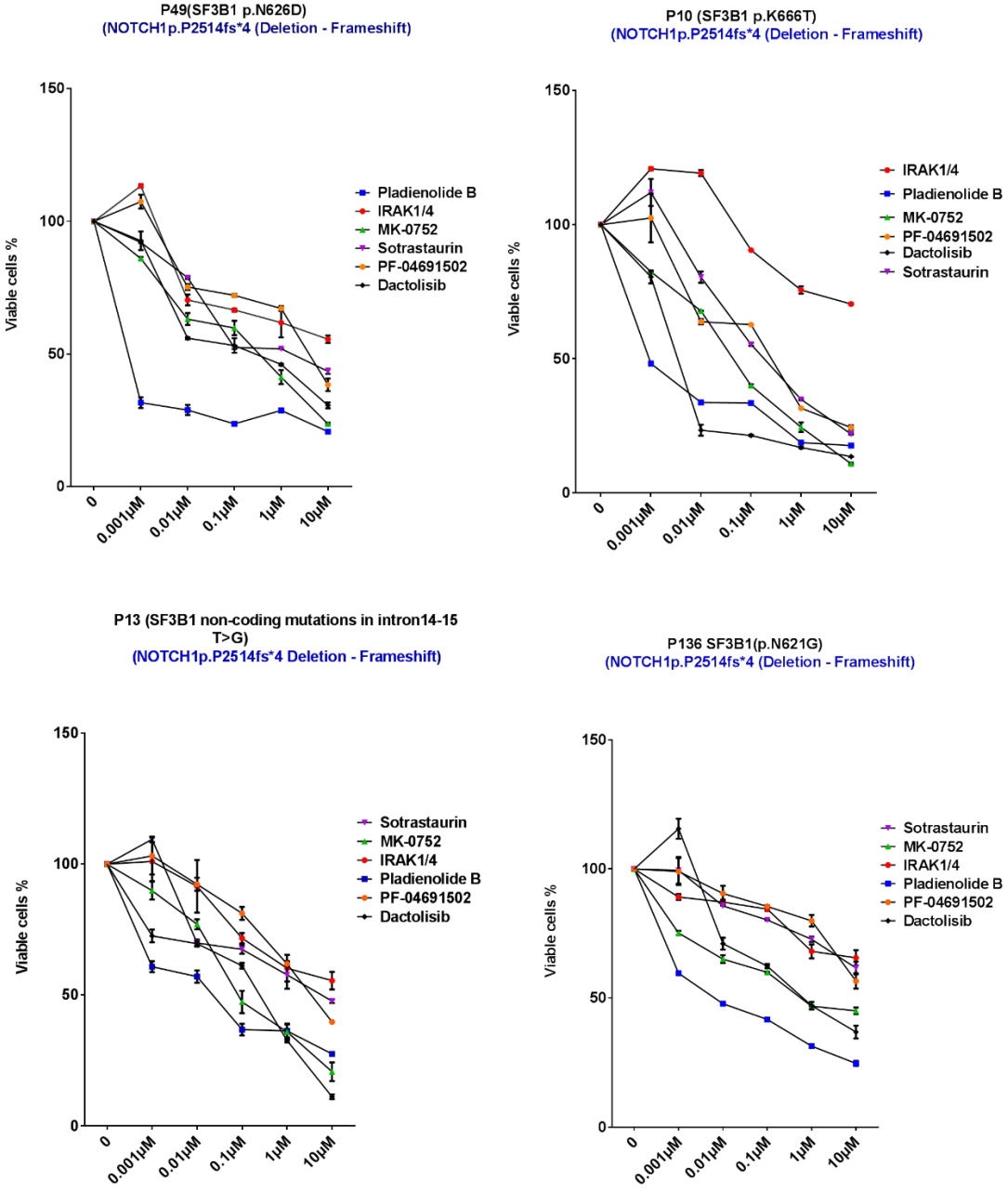


**Figure 5.19 Viability assay of both SF3B1 and NOTCH1 mutated CLL samples after treatment.**

After stimulation to mimic microenvironment of CLL, cells were treated for 48 hours with five concentrations 10, 1, 0.1, 0.01, 0.001µM, MTS viability assay were performed and viable cells % were calculated after normalising DMSO control to 100%. DMSO was ~0.1% per well in 96 wells plates. All experiments were performed in technical and biological duplicates. All data are mean of viable cells percentage and error bars indicate SD.

P10, P49, P136 and P13 (all both Notch1 (CT del.) and Sf3b1 mutated) cells viability was reduced by high concentration of MK-0752. Pladienolide B were effective in reducing cells viability at different concentrations in all 4 patients, particularly in P49 appears to be sensitive to all concentrations of pladienolide B. Thus, mutated patients showed sensitivity to target inhibitors. IRAK1/4 did not reduce cells viability below 50% in all 4 patients. Sotrastaurin and PF-04691502 seem to be effective in reducing cells viability in P49, P13, and P10, but not in P136. Dactolisib has moderate efficacy in all patients, except P10, which showed more sensitivity.

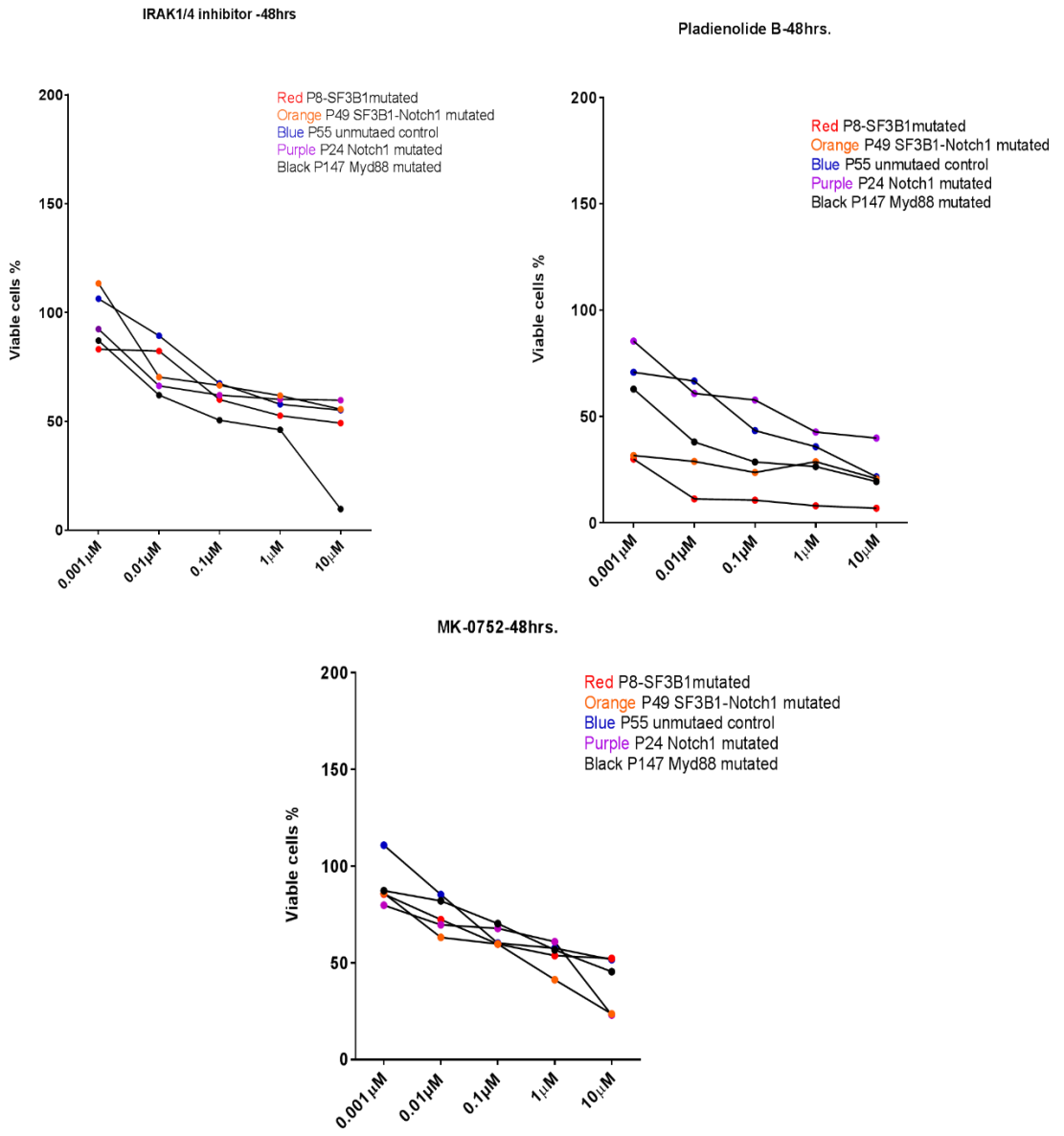


**Figure 5.20 Targeted inhibitors efficacy in mutated CLL cells in comparison to unmutated.**

IRAK1/4 inhibitor showed more efficacy in Myd88 mutated P147 (left top), pladienolide B inhibitor showed more efficacy in SF3B1 mutated P8 (top right), and MK-0752 inhibitor showed slight more efficacy in Notch1 mutated P24, and P49.

As can be seen in figure 5.20 that mutated CLL cells were sensitive to the inhibitor which target the mutated protein more than unmutated cells. P147 with p.L265P Myd88 mutation exhibited more sensitivity to IRAK1/4 inhibition. P8 with p.K700E SF3B1 mutation displayed more sensitivity to SF3B1 inhibitor pladienolide B than other patient cells. Both Notch1 mutated P24 and P49 showed sensitivity to gamma-secretase inhibitor MK-0752 at high concentration more than unmutated patient cells.

Next we calculated IC50 for each inhibitor as can be seen in figure 5.21.

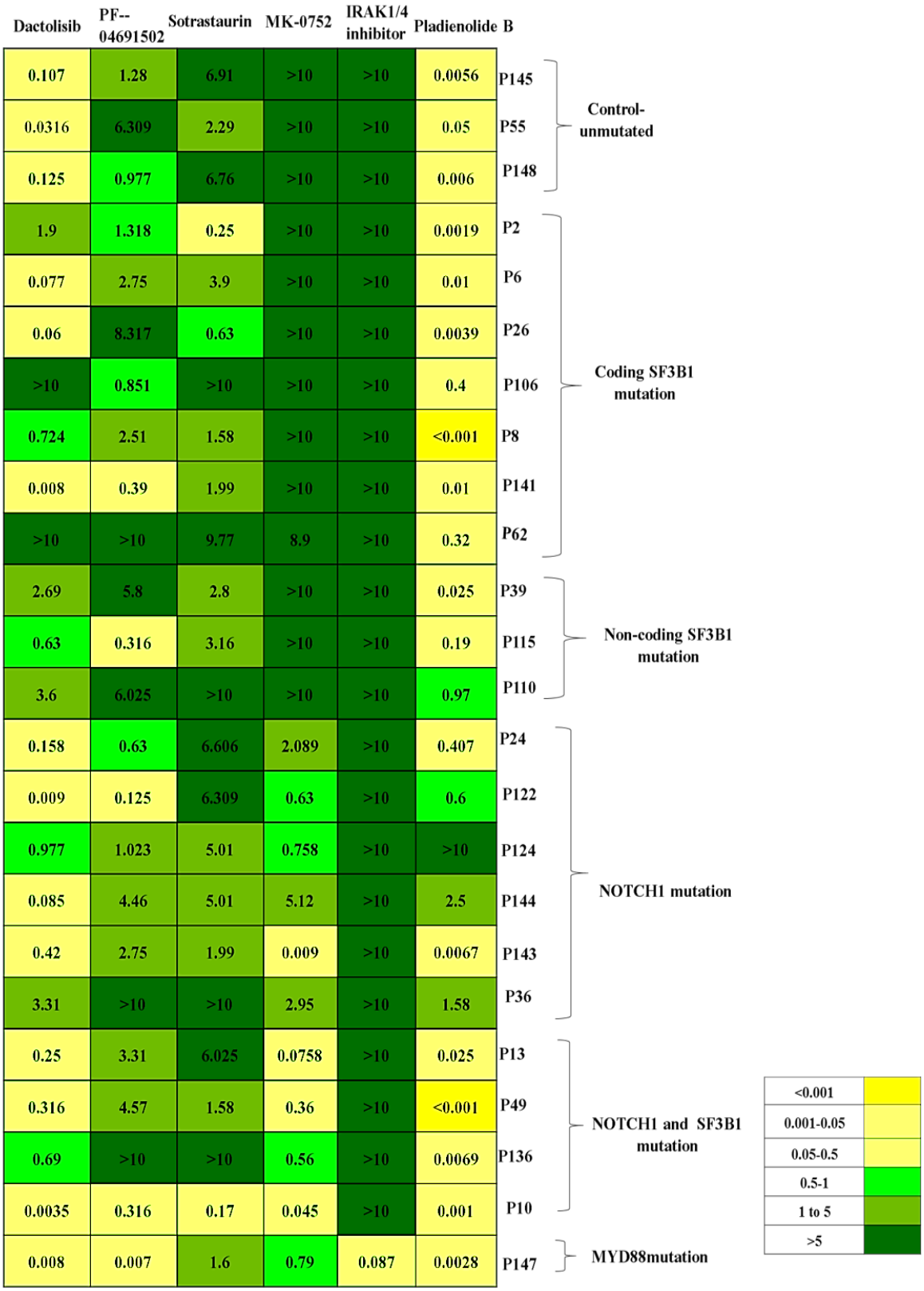


**Figure 5.21 Heat map of sensitivity of CLL (SF3B1, Notch1, or Myd88) mutated and unmutated (Control) cells to Pladienolide B, MK-0752, PF-04691502, Sotrastaurin, dactolisib and IRAK1/4 inhibitor (IC50 in µM concentrations).**

All experiments were in technical and biological duplicates. Prism software was used to calculate IC50, as described previously.

Figure 5.21 shows IC50 in µM concentrations. First row from right is splicing inhibitor pladienolide B. Among control samples, 2 out of three, P145 and P148, showed IC50 in nM concentrations of ~ 6nM. Among SF3B1 mutants (coding region mutations), in three out of 7 samples showed IC50 values in nanomolar concentrations, IC50 less than 1nM (P8), ~4nM (P26), and ~2nM (P2). Amongst Notch1 mutants, 1 out of 6 samples (P143) showed ~7nM IC50. Of 4 Notch1 and SF3B1 mutants, 3 showed IC50 in nanomolar concentrations: P49 less than 1nM, P10 1nM, and P136 ~7nM. The MYD88 mutant showed IC50 of ~3nM.

The second row from right is IRAK1/ 4 inhibitor IC50 value was more than 5µM for all samples except Myd88 mutant (0.087µM).

In third row from right (MK-0752 gamma secretase inhibitor), 1 out of 6 patient samples showed 9nM IC50 (P143) and low IC50 values among Notch1 mutated patients.

Fourth row from right is sotrastaurin (PKC inhibitor) had medium IC50 values. In fifth row from right is PF-04961502 (PI3K/mTOR inhibitor), only P147 MYD88 mutant showed low IC50 of ~7nM. Finally, dactolisib which showed ~ 8nM in SF3B1 mutant P141, ~9nM in P141 NOTCH1 mutant, ~4nM in NOTCH1/SF3B1 mutant P10, and ~8nM in MYD88 mutant P147.

In summary, we found that Myd88 mutant patient cells exhibited specific sensitivity to IRAK1/4 inhibitor. Also had remarkable sensitivity to PI3K/mTOR inhibitors dactolisib and PF-04691502. SF3B1 mutant had distinct sensitivity to pladienolide B with IC50 values less than 1µM among all SF3B1 mutant patients and in nanomolar concentration in number of them. NOTCH1 mutated patients cells displayed sensitivity to MK-0752 more than other patient cells. In addition, it seems that Notch1 mutants show resistance to pladienolide B.

The above results suggests that Myd88, Notch1, and SF3B1 mutations could be useful tools to stratify patients and provide the rationale to propose novel targeted therapies.

## 5.3 SF3B1 non-coding mutation near splicing site between intron-exon does not affect splicing.

We believe that it is the first time that intron mutations in SF3B1 have been reported. Intron mutations near the splicing site were of interest to us, as they can lead to reading frame disruption or loss of specificity of splicing.

Removal of introns in pre-mRNA is essential biological process in all eukaryotic cells. Interrupting such an essential process might lead to congenital disease or cancer. The spliceosome complex (SF3B1 is one of its subunits) is the main cellular machinery of splicing out intronic sequences from pre m-RNA and link exons to mature mRNA. Therefore, we aimed to investigate if there are any effects on splicing of intron14-15-exon 15 in SF3B1 due to these mutations.

Figure 5.22 and 5.23 shows all non-coding mutations/variants that we have detected near to splicing sites between (intron 14-15-exon 15).

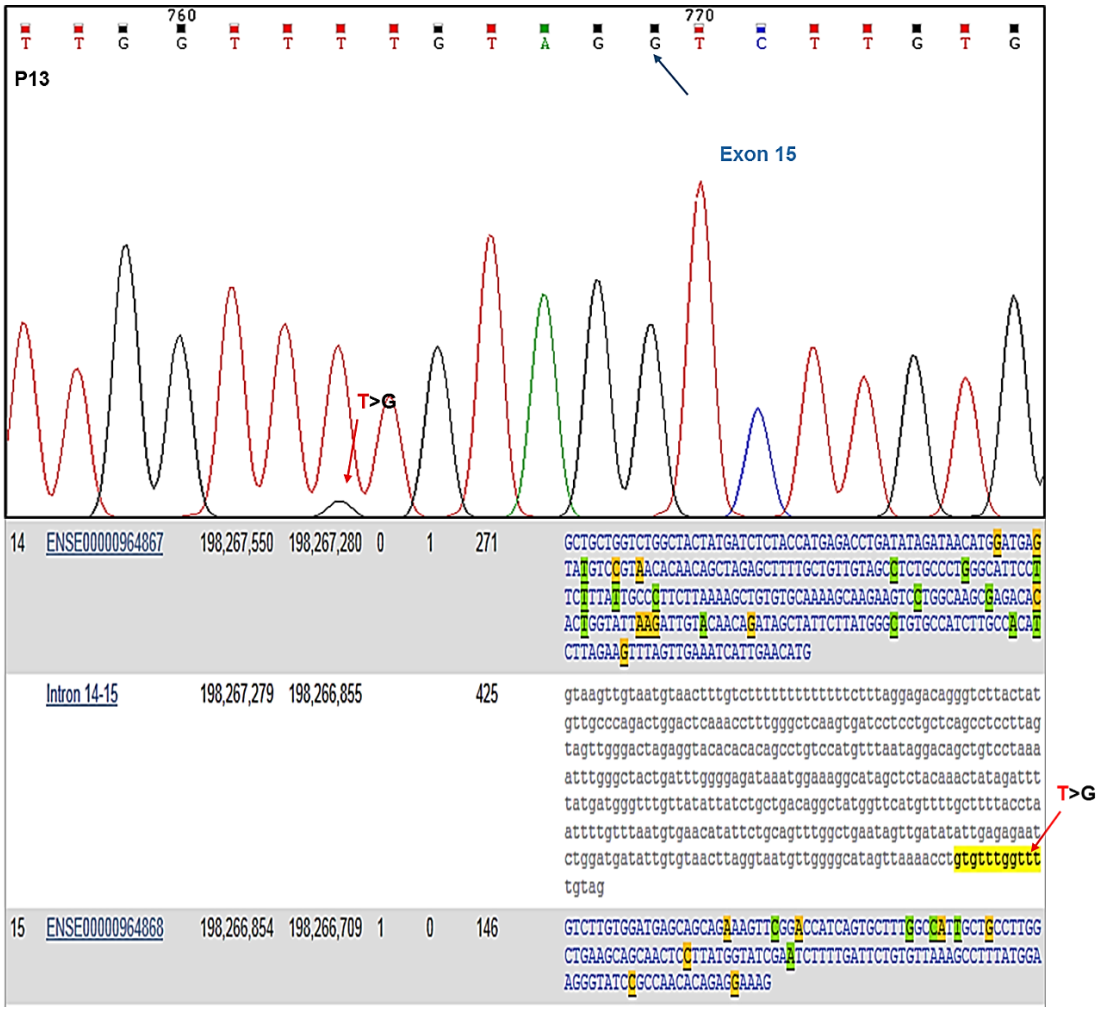

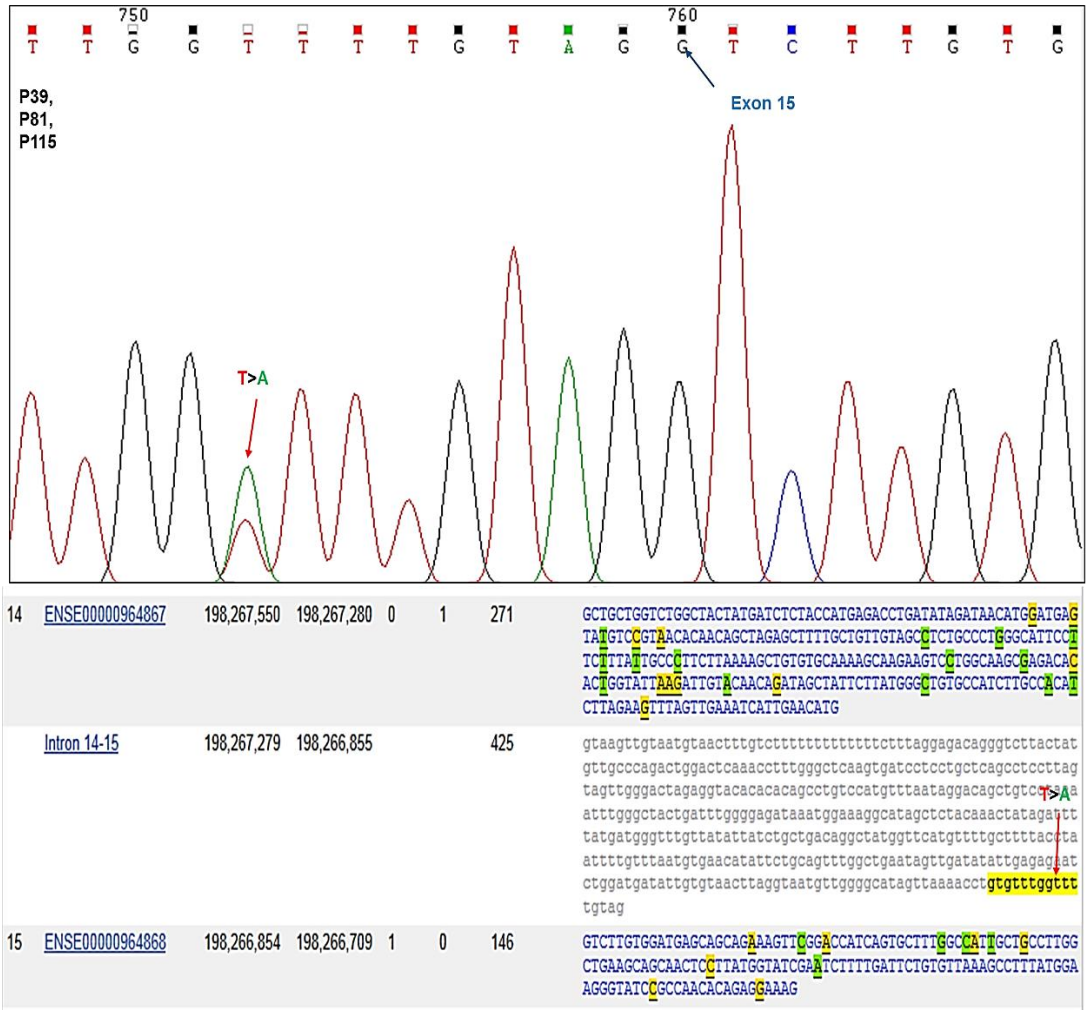


**Figure 5.22 First detected intron mutation/variant in SF3B1.**

6bp from splicing site between intron 14-15and exon 15 (P13) or 8bp from splicing site between intron 14-15 and exon15 (P39, P115, and P81).

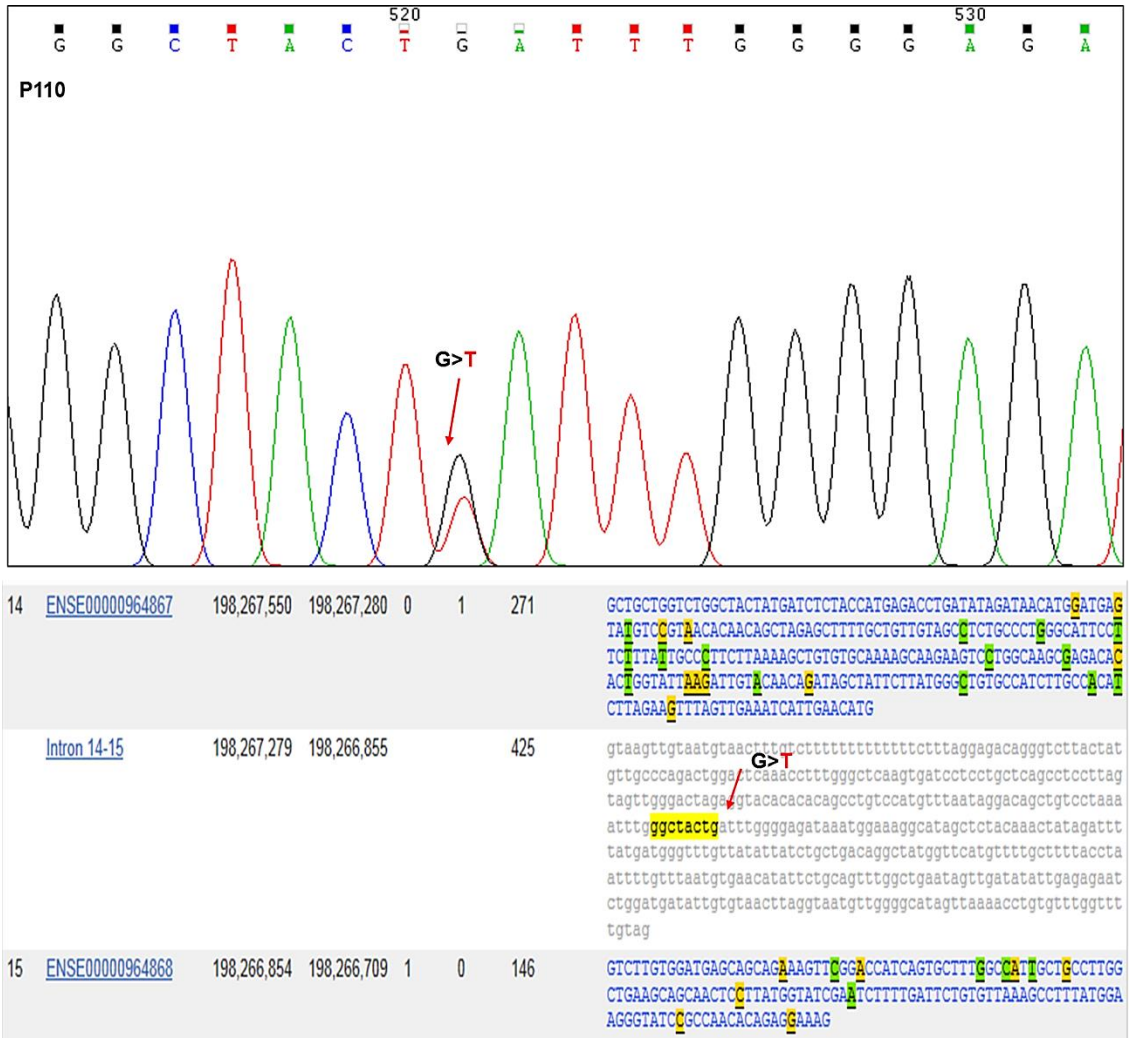


**Figure 5.23 Intron mutation/variant in SF3B1.**

P 110 non-coding mutations in middle of intron sequence far away from splicing site between intron 14-15and exon15.

RNA was extracted from P13, P39, P81, P115, and P110 and from unmutated control sample P55 (Control) to run a nested PCR (using internal and external primers to cover exon14-15 region). The resulting cDNA was sequenced to look at the effects on exons assembly.

As shown in (figures 5.24 and, 5.25) cDNA samples exon 14-exon 15 were assembled normally and sequences were not affected in all mutated near or faraway of intron-exon junction, and unmutated control.

We predicted that intron splicing would be affected as the mutated T was just 6bp (P13) and 8bp (P39, 115, 81) from Intron-Exon splicing site.

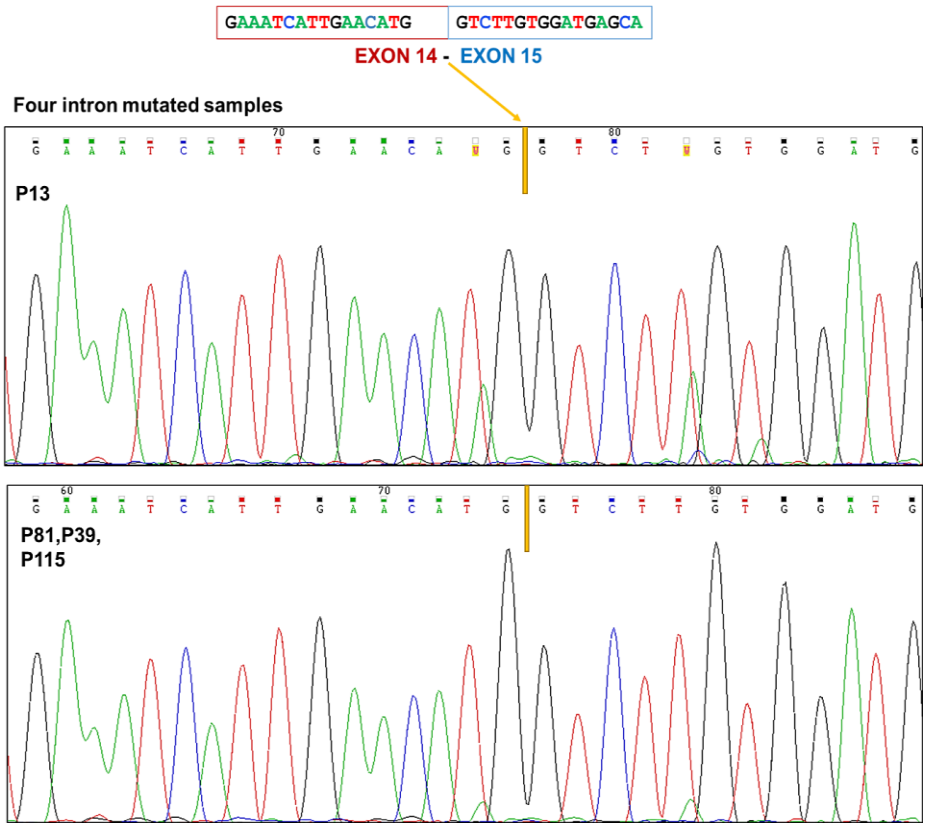


**Figure 5.24 Intron mutation does not affect the frame of exons 14-15.**

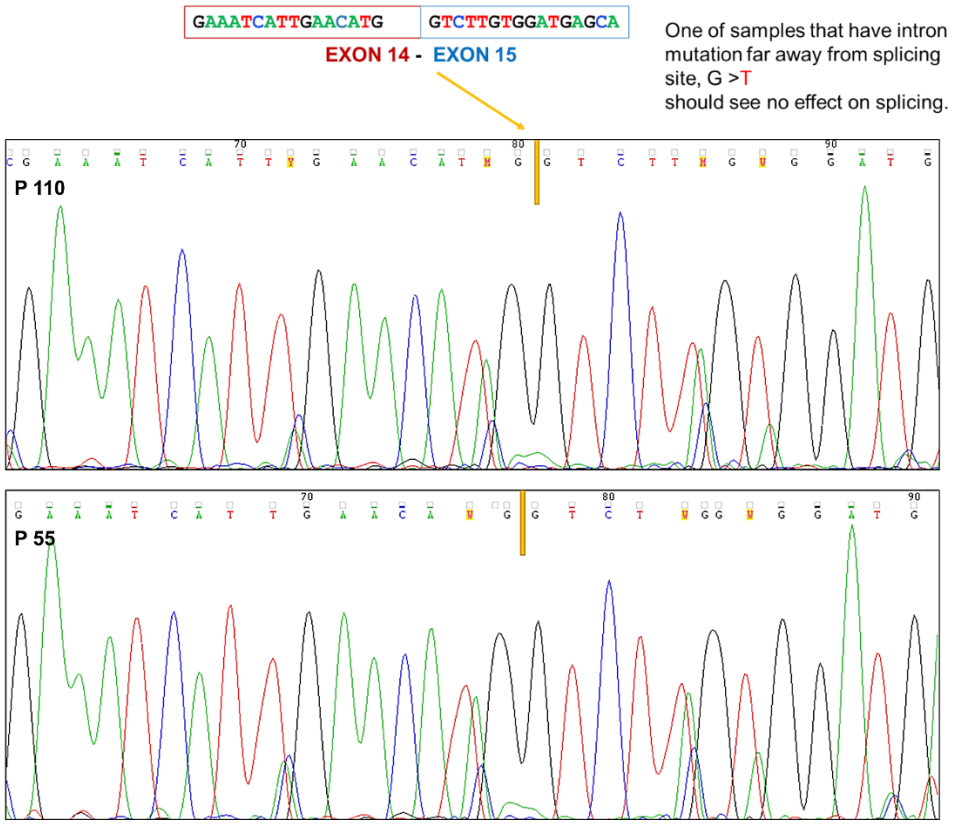


**Figure 5.25 Control sample (unmutated) and P110 mutated in middle of intron sequence.**

No effect on splicing as predicted.one mutation P110 is far away from intron-exon splicing site and other sample is unmutated control sample P55.

According to our results, we have seen no effect of the new SF3B1 non-coding mutations on exon alignment (figure 5.26).

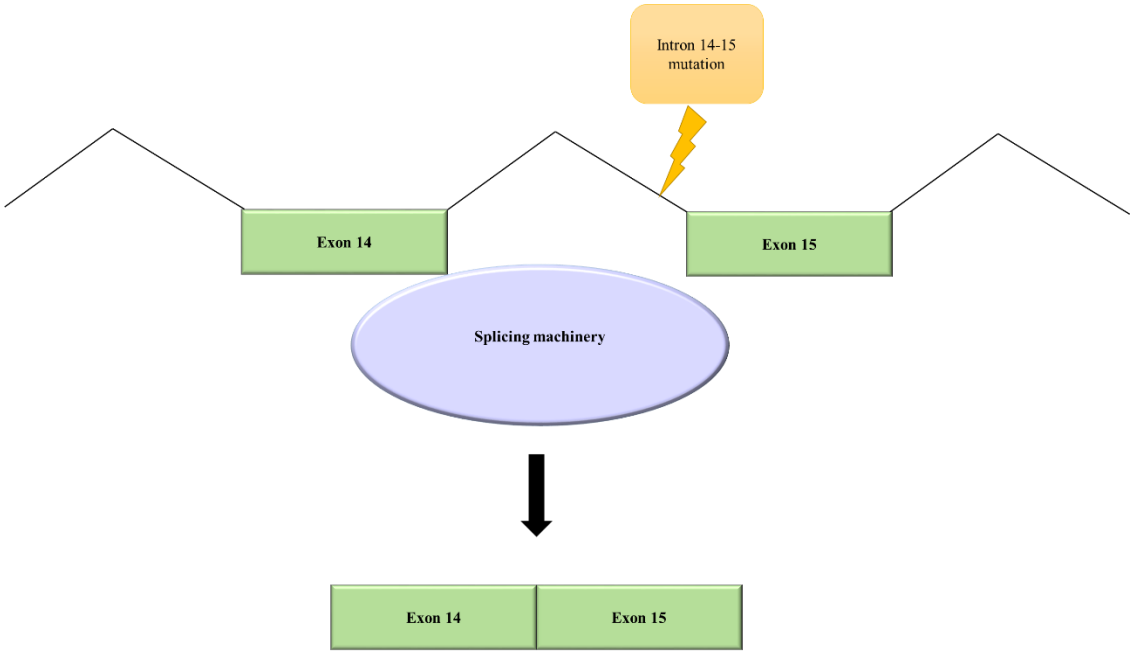


**Figure 5.26 SF3B1 intron sequence mutations (intron 14-15 –exon 15) did not affect the exons 14-15 assembly.**

## 5.4 Discussion

In a cohort study of untreated CLL patients using Sanger sequencing and NGS techniques, it has been found that Notch1 mutations (associated with trisomy 12), SF3B1 mutations (associated with 11q), and TP53 mutations were the most frequent mutations and more correlated to U-CLL (Jeromin *et al*, 2014). On the other hand, Myd88 mutations were correlated with M-CLL with low frequency. Mutations that adversely affect time to treatment and overall survival were SF3B1 and Notch1 and rarely co-occur.

We aimed in our cohort of 148 treated CLL patients to screen Myd88, Notch1, and SF3B1 mutations frequency and then to assess mutated cell sensitivity to targeted inhibition (for each specific mutation). Notch1 mutations in exon 34 were 14.18% and mostly (90.47%) in the PEST domain frameshift deletion of c.7541_7542delCT. Most Notch1 mutants were U-CLL, and trisomy12 was 57.1%. TAD domain mutations were 9.5% of all Notch1 mutated cases (figure 5.9). The first identified Notch1 mutations were in T-ALL (Ellisen *et al*, 1991). Notch1 activation mutation were identified in CLL using NGS with other

novel CLL mutations (Wang *et al*, 2011). Notch1 mutations were reported to be linked with U-CLL, trisomy 12, and poor prognosis (Oscier *et al*, 2013; Willander *et al*, 2013).

SF3B1 mutations in exons 14-15 were in high frequency (16.21%) and K700E were 33.3% of all mutated cases. The first reported non-coding mutations of SF3B1 were 20.8% (figures 5.4 -5.8). Interestingly, in our treated CLL cohort, SF3B1 mutations were mostly associated with M-CLL. Somatic SF3B1 mutations were first reported in myelodysplasia with ring sideroblasts which is a group of haematological malignancies (Papaemmanuil *et al*, 2011). SF3B1 mutations were highest frequency in myelodysplastic syndrome (MDS) (Malcovati *et al*, 2015) and were linked to favourable clinical outcomes (Malcovati *et al*, 2011). SF3B1 mutations were reported in CLL and were associated with 11q deletion (Rossi *et al*, 2011; Wang *et al*, 2011; Quesada *et al*, 2011).

Myd88 p.L265P substitution mutation in exon 5 had a low frequency (1.35%) and occurred in M-CLL category (figure 5.10). Myd88 mutations suggested to constitutive activate NF-κB activity and subsequently increase cancer proliferation (Baliakas *et al*, 2015b). It has been found that high frequency of Myd88 mutations in Waldenström's macroglobulinemia (WM) results in NF-κB pathway activation, which is stimulated through BTK, suggesting targeted therapy of those mutated cases with ibrutinib (Treon *et al*, 2012). Oncogenic p.L265P mutations in Myd88 in ABC-DLBCL leads to enhancement of JAK/STAT and NF-κB pathways through phosphorylated IRAK1 (Ngo *et al*, 2011). Higher frequency of Myd88 mutations was observed in young median age CLL patients (Martínez-Trillos *et al*, 2016).

Although Notch1 and SF3B1 mutations are unlikely to co-occur (Oscier *et al*, 2013), 4 of our 148 CLL of our patients harbour both SF3B1 and Notch1 mutations. 2 of them were males and 2 were females, and all were of old age at diagnosis. 3 of them were M-CLL. Finally, one of the SF3B1 mutants was in the non-coding region (intron sequences) (table 5.1, figure 5.3).

We are the first to report the first hairy cell leukaemia patient with SF3B1 heterozygous p.Y623S substitution mutation (figure 5.12). Hairy cell leukaemia is a rare type of B-lymphoid malignancy that is characterised by BRAFV600E in 100% of cases of the classical form, and that this mutation mediates constitutively active BRAF/MEK/ERK pathway (Falini, Martelli and Tiacci, 2016). We have found no reports regarding this mutation in HCL. We have found one case heterozygous, and due to insufficient samples

of HCL that we can have access to, we could not continue testing more samples to show relationships with age group, other related mutations or any relevant information.

Aiming for a stratified medicine approach, we tested our mutated samples with targeted inhibitors; for example we used gamma-secretase inhibitor (MK-0752) to observe its effects on Notch1 mutated and unmutated samples, IRAK1/4 inhibitor for its effects on Myd88 mutated and unmutated samples, and splicing inhibitor (Pladienolide-B) in our inhibitors panel to look at their effects on SF3B1 mutated and unmutated samples. We also tested newly emerging dual pan-PI3K/mTOR inhibitors Dactolisib (BEZ235) and (PF-04691502), and sotrastaurin (PKC inhibitor) to observe their effects on our samples in general.

Dactolisib (BEZ235) showed efficacy in PI3K activity inhibition in MEC-1 cells (Kern *et al*, 2015). Also, it showed dose-dependent inhibition of phosphorylation of AKT at S473 and apoptosis in glioblastoma cancer cells *in vitro.* However, in an *in vivo* orthotopic xenograft model of glioblastoma, it has shown neither tumour growth inhibition nor survival benefits accompanied with sever adverse effects (Netland *et al*, 2016). In addition, in a phase II clinical trial (#NCT01658436) in patients with everolimus-resistant pancreatic neuroendocrine tumours, it was poorly tolerated at 400-300mg two times a day doses and the study did not continue to the next stage (Fazio *et al*, 2016). Furthermore, using 300-400mg dose two times a day of BEZ-235 in advanced renal carcinoma patients resulted in dose limiting toxicity and discontinuation of the study (Carlo *et al*, 2016). Therefore, considering the efficacy of dactolisib in MEC-1 cells (Kern *et al*, 2015), the dose needed for solid cancers could possibly be higher than the dose needed for blood cancers. Thus, the toxicity limits might not be reached with lower less frequent doses.

The other dual pan-PI3K/mTOR inhibitor, PF-04691502, showed anti-tumour effects by PI3K and mTOR activity inhibition, and cell cycle arrest induction in G1 in cancer cell lines (Yuan *et al*, 2011). PF-04691502 was tolerable in a dose of 8mg per day and decreased phosphorylation of tumour pathways but it displayed dose limiting toxicities in advanced cancer phase I study (Britten *et al*, 2014). PF-04691502 showed apoptosis induction in CLL *in vitro*, anti-cancer efficacy in transient lymphocytosis and reduction in cancer cells in blood in the *in vivo* Eμ-TCL1 models of CLL (Blunt *et al*, 2015).

Protein kinase C-β is downstream target of BTK down to BCR signalling mediating NF-κB stimulation. PKC is also involved in malignant proliferation and invasiveness.

Sotrastaurin (AEB071) is a PKC-β inhibitor that showed preclinical anti-tumour activity in CLL cells *in vitro* and *in vivo* (El-Gamal *et al*, 2014). Sotrastaurin induced reduction of P-AKT and P-ERK1/2 and cell death at clinical relevant concentration in REC-1 mantle cell lymphoma cell lines, but the responses in primary MCL cells were heterogeneous (Rauert-Wunderlich *et al*, 2016). On the other hand, clinical trials with sotrastaurin as an immunosuppressant showed efficacy in inhibiting allo-reactivity *in vitro* but did not show same efficacy *in vivo* in kidney transplant patients (Weerd *et al*, 2014).

γ-Secretase is an aspartic protease that triggers Notch receptor by cleaving the Notch ligand/receptor complex. MK-0752 is a γ-secretase inhibitor that exhibited clinical activity as a single agent in high grade glioma patients and its dose limiting toxicities were diarrhoea and fatigue. In a phase I clinical trial, combination of MK-0752 with ridaforolimus (mTOR inhibitor) (#NCT01295632) showed clinical activity in head and neck squamous cell carcinoma (HNSCC). However, the study was discontinued after issues with tolerability (Piha-Paul *et al*, 2015). Additionally, in a phase I/II clinical trial, advanced breast cancer patients were treated with MK-0752 combined with chemotherapy, which showed efficacy and manageable toxicity (Schott *et al*, 2013). In a clinical trial of paediatric brain tumour MK-0752, inhibition of Notch signalling in 6 of 7 available tissues from patients was shown and was well tolerated among patients (Hoffman *et al*, 2015). Gamma-secretase inhibition has been shown to reduce cancer stem cells population and their self-renewal ability in head and neck squamous cell carcinoma *in vivo* and *in vitro* (Zhao *et al*, 2016).

It has been reported that Myd88/IRAK1/4 signalling is important pathway primary T cells, and that this pathway plays a significant role in T-cell acute lymphoblastic leukaemia (T-ALL) pathogenesis and disease progression. IRAK inhibition enhanced the effects of chemotherapeutic agents in T-ALL (Li *et al*, 2015b). It has been shown that IRAK1 inhibitor is an effective drug in Myelodysplastic syndromes (MDs), and combination with Bcl2 antagonists increased its efficacy (Rhyasen *et al*, 2013). It has been found that IRAK1 inhibition in triple-negative breast cancer metastasis and paclitaxel-resistant breast cancer cells stimulated apoptosis through inhibition of NF-κB and P38-Mcl1 signalling as a therapeutic target (Wee *et al*, 2015).

Of seven naturally occurring compounds, pladienolide B has the highest activity *in vivo* (Lee and Abdel-wahab, 2016). Recently, it has been shown that pladienolide B inhibited the growth of all tested small cell lung cancer cell lines *in vitro* at low nanomolar concentrations independent of Myc gene amplification status (Suda *et al*, 2017). Pladienolide is natural compound that exerts its anti-tumour effects through binding to SF3B1 and inhibit spliceosome complex formation and mRNA splicing, but R1074H mutation in SF3B1 impairs pladienolide binding (Yokoi *et al*, 2011). Intron-retention (spliceosome modulation) is found to be induced with pladienolide B in CLL cells (Kashyap *et al*, 2015). Pladienolide B induced expression of an alternatively spliced short pro-apoptotic Mcl-1 and Bcl-x isoforms at low nanomolar concentration, and its pro-apoptotic effects are independent from prognostic markers such as (17pdel), or (TP53, or SF3B1) mutations or microenvironment protection in CLL.

Dactolisib, and pladienolide B seem to be generally effective in reducing cell viability. While IRAK1/4 inhibitor and MK-0752 showed no efficacy in reducing cells viability in control cells. PF-04691502 and sotrastaurin showed moderate efficacies (Fig.5.13). Three out of four SF3B1 mutated CLL samples showed sensitivity to pladienolideB inhibitor in different concentrations, while the fourth was sensitive to high concentration only. MK-0752 and IRAK1/4 inhibitors had no effect in all 4 SF3B1 mutated CLL cells (Fig. 5.14). K700E mutant cells showed more sensitivity to pladienolideB than to other inhibitors (Fig.5.15), and SF3B1 intron mutant cells showed more reduced viability with splicing inhibitor pladienolide B (Fig.5.16). Notch1 (PEST domain mutant (delCT) CLL cells showed reduced viability at high concentrations of MK-0752 (Fig.5.17). While, Notch1 TAD domain mutants acted differently. (38del) mutant showed greater sensitivity to MK-0752 inhibitor than (insG) mutant cells (figure 5.18). Myd88 mutant showed more sensitivity than all other CLL cells to IRAK1/4 inhibitor (figure5.18). SF3B1 and Notch1 mutant showed great sensitivity to high concentrations of both MK-0752 and pladienolide B (figure 5.19). Notch1 mutants confer some resistance to pladienolide B. Myd88 mutant is the most sensitive to IRAK1/4 inhibitor. SF3B1 mutant showed more sensitivity to pladienolideB. In addition, Myd88 and Notch1 mutant cells showed more sensitivity to MK-0752 (figures 5.20, 5.21). Stratification of sensitivity of primary cells to selective inhibitors could be a potential therapy to be used in the future to tackle heterogeneous diseases such as CLL. Our last finding was of interest as was finding of intron mutation/variant in SF3B1 only 8bp (in three patients of 148) and 6bp (in one patient of

148) form splicing site in intron 14-15 and exon 15 (figure 5.22). One patient showed mutation in the middle of intron 14-15 ~50bp from splicing site between intron14-15 and exon15.

Having found intron mutations near a splicing site between intron14-15 to exon15 it was of huge interest to us, because they possibly affect the splicing of the splicing factor SF3B1. Unfortunately, our results showed no effect on exons 14-15 assembly in transcripts (figures 5.24, 5.25) 15% of disease causing mutations are due to mutations that affect pre-mRNA splicing. Therefore, these mutations needed further confirmatory experiments such as using different primers in nested-PCR to cover wider exons (e.g. exons 14-16) in the first primer set might show different results, as we only covered 14-15 exons in our experiment.

# Chapter 6 Final Discussion

CLL is one of the common slow-developing B-cell malignancy and it is characterised by highly variable clinical course. To add more complexity to the disease management, the microenvironment is playing a vital role in CLL cell proliferation. CLL cells in their cell microenvironment show activation of the main growth and anti-apoptotic signalling pathways, among them MAPK, PI3K and NF-κB pathways. Over the recent years there have been new drugs approved for CLL such as ibrutinib. In addition, in recent years the feasibility of NGS techniques and large-sized cohort studies has provided new stratification factors of the progression of the disease.

The aim of this study was to assess the sensitivity of leukaemia cell lines and primary CLL cells to specific inhibitors, particularly to MAPK signalling inhibitors, as well as combination treatments. Also, to evaluate the potential stratification factors in CLL: firstly, BRAF exon 15 mutations and their sensitivity to BRAF/MEK/ERK inhibitors; secondly, the frequency rate of SF3B1 (exon 14-15), Notch1 (exon 34), and Myd88 (exon5) mutations, to check their sensitivity to target inhibitors as a precision medicine approach.

## 6.1 Importance of the MAPK pathway in malignant B-cells: Therapeutic options.

The microenvironment of CLL cells is essential in CLL disease course and progression (Burger and Gribben, 2014). MAPK has been shown to be constitutively active in a subset of CLL patients (Muzio *et al*, 2008). This suggests that MAPK signalling is essential for CLL cells proliferation. Other survival pathways are also induced by the microenvironment. For instance, PI3K/AKT has been shown to be activated with CD40L-IL4 stimulation in CLL cells through miR-22 (Palacios *et al*, 2015). NF-κB P65 is also significantly increased sCD40L-IL4 CLL cells stimulation *in vitro*. All leukaemic primary cells used in this study had elevated P-ERK, P-AKT and NF-κB p65 expression, despite having different IGHV mutational status, which suggests that CLL cells rely on proliferative anti-apoptotic signalling that are induced in their tumour milieu. Because of this, microenvironment modelling is a very important approach in preclinical drug testing in cancer cells, as depend on their microenvironment to proliferate and metastasize.

The variation in sensitivity to MAPK inhibition among five cell lines, represents the heterogeneity of B-cell malignancy and suggests that monotherapies based on inhibiting this pathway may only benefit a subset of patients.

RAF inhibition of BRAF mutant dimers is not effective, because inhibitor binding to one site in mutant dimers would reduce its affinity to bind to the other site. Consequently, cancers of BRAF mutations, except BRAFV600E, would be insensitive to RAF inhibitors. In addition, BRAFV600E dimers formation after treatment could be the cause of drug-resistance to vemurafenib (Yao *et al*, 2015). This study exactly confirms our results that JVM-3 with BRAFK601N activation mutation is less sensitive to RAF inhibition in comparison to SIG-M5 BRAF V600E, which was the most sensitive cell line to all RAF inhibitors.

Sorafenib showed significant inhibition effect on cell viability among cell lines cells. Sorafenib was approved by FDA in 2013, for the treatment of progressive differentiated thyroid carcinoma refractory to radioactive iodine treatment. Sorafenib was previously approved for treatment of hepatocellular carcinoma in 2007, and of renal cell carcinoma in 2005. Clinically, it has been suggested that sorafenib works through inhibition of proliferation and angiogenesis of thyroid cancer cells (Worden, 2014). In a study of relapsed and refractory (FMS-like tyrosine kinase-3) FLT3- (internal tandem duplication) ITD-mutant acute myeloid leukaemia (AML), a number of patients have been treated with sorafenib as a pre-phase treatment and then followed by salvage chemotherapy, and it has been suggested as effective tolerable treatment plan (Cummins *et al*, 2014). In a phase 2 study of adding sorafenib to chemotherapy in treatment for FLT3-ITD AML has improved survival in old patients with FLT3-mutation (Uy *et al*, 2016). Our AML BRAFV600E mutated cell line SIG-M5 showed the lowest IC50 to sorafenib in nanomolar concentration, suggesting that BRAF mutant cells may have alternative survival pathways activated that can bypass downstream MAPK inhibition. As proteins in pathways cross-activate or inhibit each other, this could be potential cause behind this issue.

Trametinib had no effects on MEK1/2 phosphorylation in cell lines (JVM-3 and MEC-1) western blotting. Trametinib treatment has been used in a study for 58 multiple myeloma patients as a single agent, and complete responses were observed. Trametinib has shown encouraging clinical activity and responses in a phase I/II study and most of its complete

responses were seen in patients with refractory myeloid malignancies characterized by somatic RAS mutations (Borthakur *et al*, 2012). In our lab we found that MEK inhibitors paradoxically increased P-MEK in BRAF wild type CLL cells, and this is likely to be dependent on RAF reactivation. However, no increase in CRAF-BRAF dimer was observed. But downregulation of negative regulators of MAPK cascade (SPRY/DUSP) with increase in CRAF phosphorylation was noticed (Chen *et al*, 2017).

To sum up, BRAF V600E mutated cells are more sensitive to MAPK inhibition, though BRAF mutations are very low in CLL (Jebaraj *et al*, 2013). BRAFV600E and BRAFK601N mutations behave differently to MAPK inhibition, although both are BRAF activation mutations. It has been reported that BRAFK601N mutants are not sensitive to RAF inhibitors, while BRAFV600E mutants are effectively inhibited by them (Yao *et al*, 2015). We propose to stratify CLL patients according to their BRAF mutational status, as we have observed that BRAFV600E are more sensitive to MAPK inhibition. Further analysis is needed to confirm our finding in malignant B-cells such as gene expression analysis of MPAK signalling after treatment, and cell death assays such as propidium iodide staining after treatment with MAPK inhibitors.

## 6.2 MAPK signalling as a therapeutic target in BRAFV600E mutated CLL

Assessing the sensitivity of CLL primary cells to MAPK and kinase inhibitors showed that MAPK inhibitors seem to be not potent as a single agents in reducing viability of BRAF exon15 wild type CLL primary cells. In addition, modelling the microenvironment of CLL is essential in drug-sensitivity testing and studies, as the drug efficacy appears to be affected by CLL stimulation representing the complexity of the disease. BRAF exon 15 mutations showed low frequency (1.052%) in CLL in our 190 cohort. BRAFV600E mutated primary cells showed greater sensitivity to MAPK inhibitors, and both mutated primary cells P109 and P119 showed more sensitivity to MAPK inhibitors than wild type cells.

Clinically it has been reported that in patients with BRAFV600E melanoma, dabrafenib and vemurafenib caused substantial cancer shrinkage (Hauschild *et al*, 2012). It has also been found that dabrafenib and vemurafenib do cross the blood brain barrier and prevent melanoma brain metastasis (Long *et al*, 2012). In our lab it have been found that

vemurafenib (BRAFV600E inhibitor) caused complete clinical remission in HCL patient with complete reduction of leukaemic cells viability during treatment (Samuel, Macip and Dyer, 2014).

To conclude, CLL primary cells were not sensitive to MAPK inhibition *in vitro*. This indicates that the complexity of CLL disease course, and its genetic heterogeneity of cytogenetic mutations such as trisomy 12 or 13q14 deletions, IGHV mutations, and other prognostic mutations such as p53.

BRAFV600E mutated CLL cells displayed more sensitivity to MAPK inhibition than BRAFK601N mutated and both exhibit more sensitivity than wild type BRAF CLL primary cells. Our preclinical data of approved MAPK inhibitors could be suggested for clinical trials after stratifying patients according to IGHV, cytogenetic abnormalities, TP53 disruptions, and the new prognostic mutations such as Notch1 with the help of the new genetic sequencing approaches.

## 6.3 Synergistic Combination of kinase inhibitors as a therapeutic approach in CLL.

Our findings showed that CLL primary cells showed string to very strong synergism to (CUDC-907 and sorafenib) combination. This indicates that potentially these two inhibitors could potentially be used for CLL patients in the future, and that the nanomolar concentration of CUDC-907 possibly sensitises cells to sorafenib effects.

Sorafenib is currently used for treatment of hepatocellular carcinoma and renal cell cancer twice daily in a dose of 400mg. A dose limiting toxicity involves hypertension, diarrhoea, and hand-foot skin reaction (Pécuchet *et al*, 2012). Sorafenib is primarily metabolised through the liver (Walko and Grande, 2014). In a CUDC-907 phase I clinical trial in refractory/relapsed lymphoma or multiple myeloma patients, doses were given once daily, twice weekly, or three times weekly. The maximum tolerated dose was 150mg, and 84% discontinued the study as a consequence of progressive disease. Grade 3 or adverse events happened in 43% including thrombocytopenia, neutropenia and hyperglycaemia. The recommended dose of CUDC-907 was the 60 mg daily for 5 days followed by a 2 days break dosing schedule as single agent or combined with other therapeutic agents (Younes *et al*, 2016). In our preclinical combination of CUDC-907 and sorafenib is

effective in low nanomolar concentrations, and CUDC-907 adverse effects could be lowered with low doses of CUDC-907 in sorafenib-CUDC-907 combination.

*In vivo* studies are necessary to develop combination dosage that would be optimal for CLL treatment in future. Low concentrations of CUDC-907 in our combination pave the way to reduce CUDC-907 doses and avoid toxicity or sever adverse effects once they have been tested in clinical trials. Potent inhibitors such as CUDC-907, and dinacilcib showed more inhibition of CLL cells viability, which could be used in combination to enhance other inhibitors efficacy as a combination approach in CLL.

## 6.4 Potential stratification factors for CLL.

Mutations in Notch1 are oncogenic, such as in T-ALL and CLL malignancies. Activation mutations of Notch1 mostly are the frame shift mutation (delCT), which is suggested to prevent its degradation. On the other hand, Notch1 mutations work as a tumour suppressor in skin and hepatocellular cancers by inhibiting Wnt and Sonic–hedgehog pathways. Also, Notch1 signalling inhibition in both cancers leads to cancer proliferation (Lobry, Oh and Aifantis, 2011). In CLL, Notch1 mutations stabilizes the Notch1 pathway through a truncated PEST domain, which leads to constitutive upregulation of canonical and non-canonical Notch1 signalling (Arruga *et al*, 2014). Truncated PEST domain (due to delCT mutations) lacks the ubiquitination site, hence it continues to be transcriptionally active for a longer time in the nucleus (Arruga *et al*, 2016). Notch1 mutations have been reported to constitutively activate NF-κB pathway and GSI (gamma-secretase inhibitors) treatment of Notch1 mutants results in NF-κB pathway inhibition and apoptosis (Xu *et al*, 2015).

SF3B1 mutations occur relatively in high frequency in CLL, more frequently at hot spot K700E (Wang *et al*, 2011) and in higher frequency in fludarabine-refractory cases (Saez, Walter and Graubert, 2016). They are also related to poor clinical prognosis in CLL (Mansouri *et al*, 2013). SF3B1 mutations were linked to ATM and DNA damage response defects (te Raa *et al*, 2015). SF3B1 mutations have been found to be promoters of CLL progression, rather than initiators (Wan and Wu, 2013). Myd88 mutations was observed in high frequency in young median age CLL patients (Martínez-Trillos *et al*, 2016). Our 148 treated CLL patient cells cohort showed low frequency of Myd88p.L265P mutations and medium frequency NOTCH1 and SF3B1 mutations. Aiming for a stratified medicine approach, we tested our mutated samples with targeted inhibitors. To sum up,

Myd88p.L265P mutant was the only one that showed sensitivity and reduced viability to IRAK1/4 inhibitor. MK-0752 showed moderate efficacy in Notch1 mutant cells, which notably conferred some resistant to pladienolide B inhibitor, and less than 1nM IC50 was noted in SF3B1 mutant cells with pladienolide B inhibitor. These results suggest that future therapy regimens should put into account mutations that could be targeted in patients and could help in reduction of cancer proliferation either as single agents in relapsed or refractory patients or in combination with current therapeutic agents.

In view of all this, we propose the use of selective inhibitors for mutated CLL patients; vemurafenib, and dabrafenib for BRAFV600E mutants. IRAK1/4 inhibitor for Myd88 mutants. MK-0752 can be used for Notch1 mutants, and pladienolide B for SF3B1 mutants. We suggest that stratification of CLL patients is important to propose new therapeutic methods depending on these mutations.

# Conclusion

In this thesis, firstly we have demonstrated that modelling microenvironment stimulation in CLL cells results in significant expression of P-ERK, more than stimulated normal human B-cells. This highlights the importance of MAPK in CLL disease course.

Secondly, we have shown that B-cell leukaemia cell lines displayed miscellaneous sensitivity to several kinase inhibitors, and exhibited no considerable sensitivity to BRAF/MEK/ERK inhibitors. An, exception to that is BRAFV600E SIG-M5, which showed greatest sensitivity to MAPK inhibition. Interestingly, other BRAF mutated BRAFK601N cell line, JVM-3, showed less sensitivity to MAPK inhibition. In addition, we observed that 48 hours was the best time of IC50 calculation and drug-sensitivity in MTS cell viability assay. This finding was confirmed by Western blotting that showed more protein inhibition was achieved at 48 hours treatment. Moreover, sorafenib was the most efficacious agent among RAF/MEK inhibitors that we have tested.

U-CLL cells showed more resistance than M-CLL cells to different inhibitors, which was confirmed in our Western blotting. Also, stimulated cells (sCD40-IL-4) showed more resistance to inhibitors than unstimulated cells, as expected. Potent inhibitors such as CUDC-907, dinacilcib and MG-132 showed significant viability inhibition of CLL cells

and could be used in combination to enhance other inhibitors efficacy as a combination approach in CLL. Stratifying patients of a 190 CLL cohort for exon 15 BRAF mutations showed low mutation frequency of 1.052%. BRAFV600E mutated primary cells demonstrated more sensitivity to MAPK inhibition than BTRAFK601N mutated cells. This could be used in clinical trials, suggesting that the beneficial treatment regimen that can be used for BRAFV600E mutated CLL patients.

Combination of sorafenib and CUDC-907 showed very strong *in vitro* effects in 11 CLL primary cells. *In vivo* studies are necessary to develop combination dosage that would be optimal for CLL treatment in future. Low concentrations of CUDC-907 in our combination pave the way to reduce CUDC-907 doses and avoid toxicity or sever adverse effects if it has been tested in clinical trials. We discovered that Myd88p.L265P mutant was the only CLL cells that showed sensitivity and reduced viability to IRAK1/4 inhibitor. MK-0752 showed efficacy in Notch1 mutant cells, which notably conferred some resistant to pladienolide B inhibitor. Low nanomolar concentrations of pladienolide B was sufficient to inhibit SF3B1 mutant cells. These very important results confirm that future therapy regimens should explore mutations that could be targeted in patients and could help in reduction of cancer proliferation either as single agents or in combination with current therapeutic agents.

We have also found that one of hairy cell leukaemia primary cells showed a SF3B1 mutations that we believe we are the first ones to report. Finally, we believe that we are the first to report intron (non-coding) mutations/variants in near splicing site between introns-exons in the region between intron 14-15 and exon 15 in SF3B1 gene. In attempts to validate their effects on splicing of SF3B1 we have found out that there was no effect on the resulted transcript assembly. An understanding of the mechanisms of these mutations in CLL is fundamental for targeting them as a therapeutic potential. This can be achieved through introducing these mutations into CLL cells *in vitro*. Alternatively, selective inhibitors activity can be studied further by other methods such as RT-PCR, to show the effects on targeted gene expression. Larger cohort is also important to confirm sensitivity of mutated CLL to target inhibitors. Also, an *in vivo* model of CLL is essential to determine the efficacy and possible toxicity of these targeted inhibitors. This may subsequently help to determine their potential as new therapeutic targets for CLL.

# Appendices

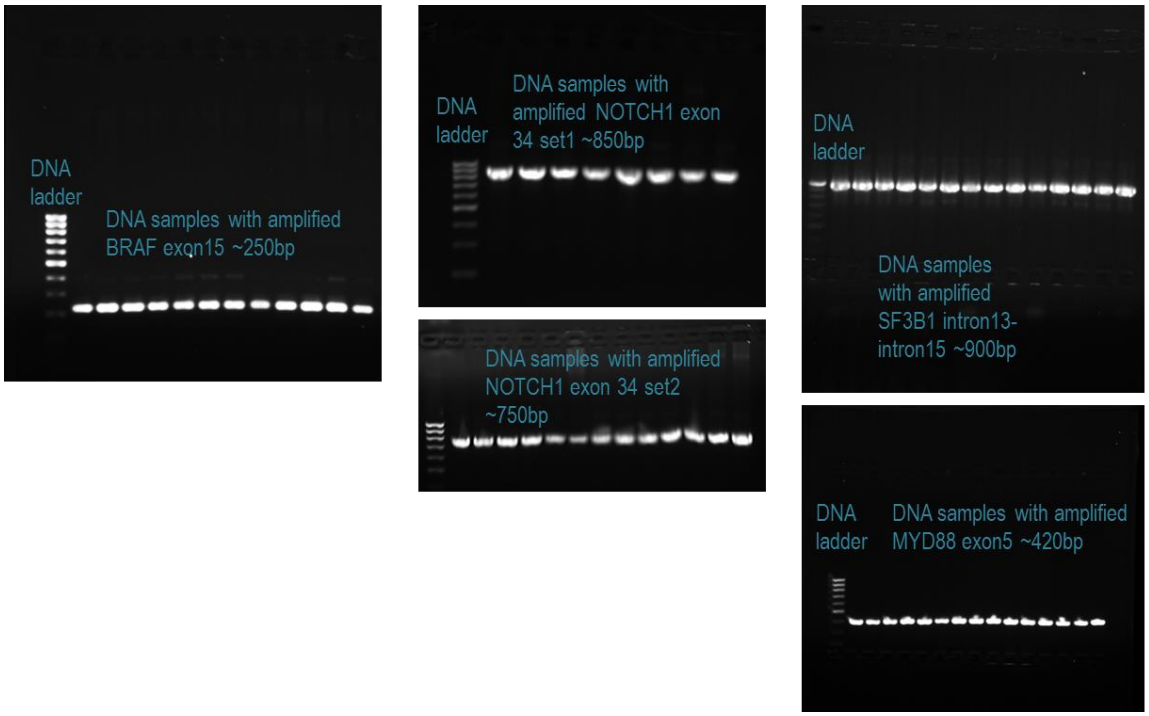


**Figure 1** Agarose gel electrophoresis to ensure the amplification of exons of MYD88, SF3B1, NOTCH1 and BRAF.

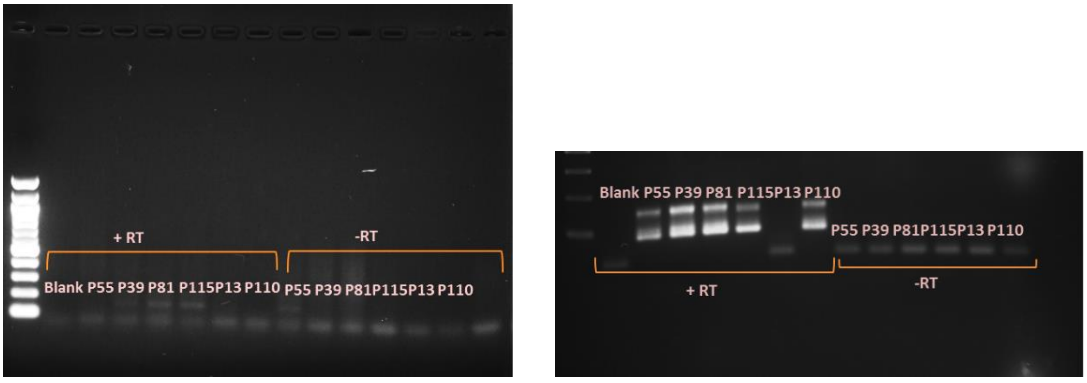


**Figure 2** Reverse Transcriptase results of 6 samples, P55 control, P39, 81, and 115 (8bp from ss) and P13 (6bp from ss) are intron mutated near splicing site (ss) (intron-exon junction), P110 intron mutated faraway from splicing site. The agarose gel on left is the external primers PCR results, and agarose gel in right are internal primers nested PCR.

**Table 1 CLL cohort 190 for screening BRAF exon 15 mutation**.

| | Code | Age at Diagnosis | IGHV | M/F | TP53 | FISH | BRAF Exon 15 mutation |
|---|---|---|---|---|---|---|---|
| **P1** | GMJ | | M | M | Heterozygous P53-deletion (71%) | Heterozygous P53-deletion (71%) | |
| **P2** | NRO | | | M | fail several times | Heterozygous (22%) and homozygous (66%) 13q14-deletion and a reduced signal of IGH distal (80%) | |
| **P3** | SPC | 70 | U | M | | Normal | |
| **P4** | SEJ | 78 | M | F | | | |
| **P5** | AMU | | M | F | | 13q-deletion (42%) | |
| **P6** | GIJ | | U | F | | Normal | |
| **P7** | AGD | | M | M | | Not done | |
| **P8** | PDM | | M | M | | Not done | |
| **P9** | UBI | 43 | U | F | | | |
| **P10** | MDM | | M | F | | t (14;18)-positive (100%) | |
| **P11** | HIP | 63 | MIX | F | | 11q- (66%) and 13q- (69%) deletions | |
| **P12** | WJP | | U | M | homR72 | Heterozygous13q, 17p deletions, trisomy12 | |
| **P13** | WJR | | M | M | | | |
| **P14** | ANS | | U | M | | Heterozygous deletion of 13q14 (50%) and a reduced signal of the IGH distal probe (47%) | |
| **P15** | JAB | 53 | M | F | | 6q-deletion (87%) and trisomy 3 (72%) and trisomy18 (74%) | |
| **P16** | FAP | | M | M | | 13q-deletion (16%) | |
| **P17** | DR | 48 | M | | | Heterozygous 13q-deletion (98%) and a reduced signal of IGH distal (63%). In a smaller percentage it showed three copies of the MYC locus (14%) | |
| **P18** | VIJ | | M | F | | Heterozygous 13q14-deletion (91%) and a reduced signal of the IGH distal probe (85%) | |
| **P19** | SSM | | M | F | | Not known | |
| **P20** | CPI | | M | M | | 13q deletion | |
| **P21** | CPS | | Mix | M | | 11q-deletion (58%) | |
| **P22** | NJW | | M | M | Heterozygous P53-deletion (80%) | Heterozygous P53-deletion (80%) and shows a reduced | |

| | | | | | | | |
|---|---|---|---|---|---|---|---|
| | | | | | | signal of IGH distal (73%) | |
| **P23** | BSA | | M | F | | Normal | |
| **P24** | GBR | | M | M | | Heterozygous deletion 13q (91%) | |
| **P25** | FJO | | M | F | | | |
| **P26** | EVD | | M | M | | Heterozygous 13q-deletion (49%) | |
| **P27** | STO | | M | M | | Normal | |
| **P28** | BAM | | M | M | | Normal | |
| **P29** | BVM | | No band | F | | Normal | |
| **P30** | GMI | | M | M | | | |
| **P31** | BJ | 59 | M | M | | Heterozygous 13q-deletion (15%) and a reduced signal of IGH distal (56%) | |
| **P32** | BPH | | M | F | | Heterozygous 13q-deletion (68%) | |
| **P33** | WMW | | M | M | | Heterozygous 13q-deletion (96%) | |
| **P34** | BOH | 73 | U | F | | | |
| **P35** | BDS | 60 | Partial | M | | | |
| **P36** | GAK | | U | M | | Normal | |
| **P37** | HFR | | M | M | | Normal | |
| **P38** | WOM | | U | F | | Aberrant clone with (partial) trisomy 12 (82%) and BCL3 break (62%) | |
| **P39** | BJN | | Mix | F | Q100Q heterozygous-deletion P53 (95%) | Heterozygous deletions of 6q (94%) | |
| **P40** | JCO | | M | M | | IGH-BCL2-fusion a trisomy 12 (91%) and a homozygous and a heterozygous deletion in 13q14 (77%) | |
| **P41** | ROF | | U | M | | Partial trisomy 12 (96%), an IGH-break (27%) and a BCL3-break (32%) deducing a translocation t(14;19)(q32;q13) | |
| **P42** | LTH | | U | M | | Heterozygous (51%) and homozygous (28%) 13q deletion | |
| **P43** | WAC | | U | M | P53-deletion (10%) | Heterozygous 13q-deletion (89%), a P53-deletion (10%) and a reduced signal of IGH distal (96%) | |
| **P44** | BJO | | U | M | | IGH break (67%) with unknown partner, a heterozygous deletion of 11q (86%) and | |

| | | | | | | | |
|---|---|---|---|---|---|---|---|
| | | | | | | three copies of the Myc-gene (66%) | |
| **P45** | KRN | | M | F | | Heterozygous deletion of 13q14 (92%) | |
| **P46** | HN | 59 | U | | | 13q14- deletion | |
| **P47** | CRT | | U | M | | Homozygous deletion in chromosomal region 13q14 (92%) | |
| **P48** | INJ | | M | F | Heterozygous P53-deletion (72 %) | Heterozygous P53-deletion (72 %) and a reduced signal of IGH distal (74 %) as well as a small clone with three copies of Myc (11%). | |
| **P49** | YSC | | U | F | | IGH- (43 %) and BCL3-break (44 %) indicating a t(14;19)(q32;q13) | |
| **P50** | BNS | 61 | M | M | | Heterozygous 13q-deletion (66%) | |
| **P51** | MRO | | M | F | Heterozygous deletions of P53 (94%) | 11q22~23 (94%) and 13q14 (99%), a (partial) trisomy 12 (66%) an additional copy of the Myc-gene (81%) and a reduced signal of IGH distal (83%). | |
| **P52** | JDA | | U | M | | Reduced signal of IGH distal (63 %) | |
| **P53** | SIM | 75 | M | M | | 11 q deletion 90% | |
| **P54** | BJR | 73 | M | M | | Homozygous 13 q deletion | |
| **P55** | CD | 57 | U | F | | Heterozygous deletion in 13q14 (66%) | |
| **P56** | LAN | | M | F | | normal | |
| **P57** | BAT | | M | M | | Homozygous deletion (95%) | |
| **P58** | HJC | 60 | U | F | | 11q-deletion (95%) | |
| **P59** | PTL | | M | F | | Heterozygous deletion in 13q14 (68%) | |
| **P60** | KGC | | U | M | | Reduced signal of IGH distal (87%) | |
| **P61** | SWT | | U | M | S215G-heterozygous P53-deletion (81% | Three copies of the Myc-locus (70%) | |
| **P62** | BHA | 76 | | M | p53del (95%) | Monosomy 17, 94% Trisomy 12. | |
| **P63** | SMF | 82 | | M | | reduced signal of IGH distal (68%) 80% trisomy 12 | |

| | | | | | | | |
|---|---|---|---|---|---|---|---|
| **P64** | SDA | | U | M | | Homozygous (79%) and heterozygous (15%) 13q-deletion | |
| **P65** | PT | | M | M | | Heterozygous deletion in 13q14 (89%) | |
| **P66** | RRO | 78 | M | M | homR72 | 11q-deletion (50%), homozygous (51 %) and heterozygous (24%) 13q14-deletion and a reduced signal of IGH distal (81%) | |
| **P67** | NF | 48 | U | M | | Heterozygous deletion in 11q22~23 (ATM-gene locus) (70%) | |
| **P68** | SJQ | | M | F | | not available | |
| **P69** | WMG | | U | M | | Heterozygous deletion in 13q14 (92%) and a reduced signal of IGH distal (17%) | |
| **P70** | WLD | 56 | M | M | | IGH-BCL2-fusion (95%) and a (partial) trisomy 12 (8%). | |
| **P71** | SMO | | M | F | Not done | | |
| **P72** | LJR | 52 | U | M | | 13q-deletion (97%) | |
| **P73** | SRC | | M | M | | Not done | |
| **P74** | PM | 63 | U | M | | deletions in 2p, 11q, 13q and an insertion in chr.13, karyotype | |
| **P75** | VP | 86 | U | F | homP72 | Not done | |
| **P76** | PGL | 67 | M | M | | IGH-BCL2-fusion (92%) and a BCL6-break (63%) | |
| **P77** | WHR | 59 | M | M | | Heterozygous deletion 13q (77%) | |
| **P78** | WAB | 58 | M | F | homR72 | Heterozygous deletion in 13q14 | |
| **P79** | DCR | | M | F | | Not done | |
| **P80** | MC | 47 | U | M | | Heterozygous deletion 13q (72%) | |
| **P81** | HOE | 78 | M | F | | Heterozygous deletions in 11q and 13q Karyotype | |
| **P82** | PC | 64 | U | M | | Heterozygous 6q-deletion (79%) | |
| **P83** | HDM | | M | M | | Not done | |
| **P84** | DHA | | | M | | Not done | |
| **P85** | WIJ | | U | M | | Not done | |
| **P86** | LLG | 60 | U | F | | 11q-deletion (84%), 13q-deletion (19%) | |
| **P87** | JEW | | M | F | | Normal | |
| **P88** | JOM | | M | M | | Normal | |
| **P89** | CGM | 65 | mix | M | | Heterozygous deletion in 13q14 | |

| | | | | | | | |
|---|---|---|---|---|---|---|---|
| **P90** | SBJ | | M | F | | Not done | |
| **P91** | PCR | | M | M | | bad cell quality | |
| **P92** | RRK | | M | M | | Trisomy 12 (74%) | |
| **P93** | SLE | | U | F | | Reduced signal of IGH distal (90%) | |
| **P94** | GBT | | M | M | | Reduced signal of IGH distal (59%) | |
| **P95** | BFM | | M | M | | Trisomy 12 (99%) and a smaller clone with 13q-deletion (23%) | |
| **P96** | JOC | | M | M | | Not done | |
| **P97** | MJM | | M | M | | Heterozygous deletion in 13q14 (20%) | |
| **P98** | AGW | 61 | M | M | | Partial trisomy 12 | |
| **P99** | AKH | 33 | M | M | | t(2;4) with gain of the BCL11A/REL gene locus and add (13)(q14) | |
| **P100** | BI | 70 | M | M | | Not done | |
| **P101** | BR | 59 | U | M | | Homozygous deletion in 13q14 | |
| **P102** | BRA | 77 | U | M | | Normal | |
| **P103** | BRC | 77 | | F | | 17p del. | |
| **P104** | BUP | 56 | U | M | | Heterozygous deletion in 13q14 | |
| **P105** | C | 82 | M | F | | Trisomy 12 | |
| **P106** | CAP | 77 | U | F | | Trisomy 12 (87%) | |
| **P107** | CB | 54 | U | M | | 90% heterozygous deletions in 11q22~23 (ATM gene locus) and 13q14 (D13S319 and D13S25). | |
| **P108** | CG | 58 | U | M | | 88% heterozygous deletion in 13q14 (D13S319 and D13S25) | |
| **P109** | CHR | 74 | U | M | | Normal | Heterozygous BRAFV600E, BRAFK601E |
| **P110** | CJE | 65 | M | F | | Normal | |
| **P111** | CK | 57 | M | M | | 74% homozygous deletion of 13q14 | |
| **P112** | CLF | 48 | M | M | | Trisomy 12 (77%) | |
| **P113** | CNG | 58 | M | M | | Trisomy 12 (57%) | |
| **P114** | CPA | 47 | U | M | | 11q deletion in 69% | |
| **P115** | CR | 68 | | M | | Not done | |
| **P116** | CT | 59 | U | M | | Normal | |
| **P117** | DAM | 60 | U | F | | 96% deletion in 13q14 | |
| **P118** | DE | 74 | M | M | | Trisomy 12, 13q del. | |

| | | | | | | | |
|---|---|---|---|---|---|---|---|
| **P119** | DN | 75 | U | M | | Not done | Homozygous BRAFK601N |
| **P120** | DN2 | 53 | M | F | | Not done | |
| **P121** | DT | 72 | U | M | | Not done | |
| **P122** | DW | 62 | M | F | | Not done | |
| **P123** | EJ | 57 | M | F | | 95% deletion in 11q22~23 and a deletion in 13q14 | |
| **P124** | FIR | 42 | U | M | | normal | |
| **P125** | FL | 80 | U | F | | 97% deletions in 11q22~23 (ATM and FDX gene) and 13q14 (D13S319 and D13S25) | |
| **P126** | GD | 80 | M | F | | Not done | |
| **P127** | GL | 73 | M | M | | Not done | |
| **P128** | GN | 64 | U | M | | 95% deletion in 13q14 | |
| **P129** | HA | 54 | M | F | | An atypical translocation t(14;18)(q32;q21) involving IGH and BCL2 | |
| **P130** | ADB | | M | F | | Homozygous deletion in 13q14 (99%) | |
| **P131** | FAS | 77 | U | F | | Trisomy 12 (98%) | |
| **P132** | MRT | | M | F | | Heterozygous deletion in 13q14 (28%) | |
| **P133** | SBI | | M | F | | Homozygous loss in 13q14 (69%) | |
| **P134** | SJE | 76 | M | M | | Trisomy 12 | |
| **P135** | PCH | | M | M | | Heterozygous deletion in 13q14 (97%) | |
| **P136** | SUT | 68 | M | F | | Normal | |
| **P137** | TEK | | U | M | | Not done | |
| **P138** | DTO | | | M | | Normal | |
| **P139** | PME | | M | F | | Heterozygous deletion in 13q14 (87%) and loss of the IGH distal signal (87%) | |
| **P140** | SHA | | U | F | | Trisomy 12 (86%) and a reduced signal of IGH distal (61%) | |
| **P141** | GIR | | mix | M | | 13q-deletion (73%) | |
| **P142** | JRG | 58 | M | M | TP53 deletion (47%)-two p53 mutations. | Heterozygous 13q deletion (78%). suspicious for 6q21 deletion (16%). | |
| **P143** | SDE | 83 | U | M | | 11q del. 15%; 13q del. 92%; IGH dim, Myc x3. 13%, | |
| **P144** | EMP | | M | F | | Heterozygous deletion of 13q14 (98%) | |

| | | | | | | | |
|---|---|---|---|---|---|---|---|
| **P145** | BCS | | M | M | P53-deletion (34%) | 13q-deletion (89%) and three copies of the Myc-locus (16%) | |
| **P146** | STJ | | M | F | | Not done | |
| **P147** | HEJ | | M | F | | Not done | |
| **P148** | AHU | | U | M | | Not done | |
| **P149** | GKI | | U | M | | Heterozygous deletion of IGH distal (97%) | |
| **P150** | PGR | 54 | U | M | homR72, C176Y. P53-deletion (81%), | 11q-deletion (21%) and a strongly reduced signal of IGH distal (93%) | |
| **P151** | PMR | | M | F | | Homozygous 13q-deletion (95%) | |
| **P152** | AAL | | M | M | | Not done | |
| **P153** | MOA | | M | F | | 13q-deletion (79%) | |
| **P154** | HTG | | U | M | | reduced signal of IGH distal | |
| **P155** | RDJ | | | M | | normal | |
| **P156** | JMH | | M | M | | Heterozygous 13q-deletion (29%) and a heterozygous deletion of 6q21 (33%) | |
| **P157** | HIF | | M | M | | Not done | |
| **P158** | MCJ | 65 | U | M | | Partial trisomy 12 (74%) and an IGH-break (70%) as well as an BCL3-break (74%) deducing a translocation t(14;19)(q32;q13) or IGH-BCL3-fusion | |
| **P159** | AED | | M | M | | Heterozygous deletions in 11q (98%) and 13q14 (96%) as well as a gain of the Myc-gene (68%) | |
| **P160** | WMD | | M | M | | Normal | |
| **P161** | EGS | | M | F | | Heterozygous (45%) but also with homozygous (38%) deletion in 13q14 | |
| **P162** | NDK | 62 | M | M | | Homozygous 13q14-deletion (85%) and also with deletion in 11q (71%) | |
| **P163** | DRS | 56 | M | M | | 99% heterozygous deletion in 13q14 | |
| **P164** | MBA | | M | M | | Heterozygous deletion in 13q14 (95%) | |
| **P165** | BGL | | M | F | | Homozygous deletion in 13q14 (94%) and a loss or a very tiny signal of the distal IGH probe (92%) | |

| | | | | | | | |
|---|---|---|---|---|---|---|---|
| **P166** | BJE | 60 | U | F | | Heterozygous deletion in 13q14 in all of the cells counted (100%) | |
| **P167** | SAA | 56 | M | M | Not available | Not available | |
| **P168** | MOP | | M | F | | Not known | |
| **P169** | APP | | M | M | | Normal | |
| **P170** | SHC | 57 | M | F | | Normal | |
| **P171** | HOL | 76 | U | F | homR72 | 81% 17p del. and 39% (partial) trisomy 12. | |
| **P172** | MJF | 52 | M | M | | Heterozygous deletion in 13q14 (80%) | |
| **P173** | KP | 65 | M | F | | Not available | |
| **P174** | STD | 74 | U | M | | Normal | |
| **P175** | WGE | 65 | M | M | | Heterozygous 13q deletion 60% | |
| **P176** | SNW | 76 | M | M | | Heterozygous deletion in 13q14 (16%) | |
| **P177** | BKJ | | M | F | | Heterozygous 13q-deletion (10%) and homozygous 13q-deletion (68%) | |
| **P178** | PSH | | M | M | Not available | Not available | |
| **P179** | GWL | 69 | U | F | | Not available | |
| **P180** | PMG | | M | F | R72P TP53 deletion 35% | Trisomy 12 93% TP53 deletion 35% | |
| **P181** | GPN | | No band | M | | Normal | |
| **P182** | HOD | | U | M | | Not available | |
| **P183** | HIL | 68 | M | F | | Heterozygous 13q deletion (93%) | |
| **P184** | PAJ | | M | M | | Heterozygous deletion in 13q14 (95%) | |
| **P185** | KHU | | U | M | | 72% of cells with reduced signal of IGH distal | |
| **P186** | CBA | | U | F | | 59% trisomy 12 | |
| **P187** | HNE | | M | M | | Homozygous deletion in 13q14 (79%), heterozygous deletion in 13q14 (18%) | |
| **P188** | BOR | | U | M | | Not available | |
| **P189** | TCH | | U | M | | Heterozygous 13 q deletion 88%, a clonal IGHV rearrangement to a terminal V-segment 49%. | |
| **P190** | BKI | | U | F | TP53 deletion (96%) | Homozygous 13q - deletion (98%) | |

**Table 2 CLL cohort 148 for screening SF3B1, MYD88, and NOTCH1 mutations.**

| | Code | M/F | Age at diagnosis | IGHV | FISH | TP53 | SF3B1/NOTCH1/MYD88 mutations |
|---|---|---|---|---|---|---|---|
| **P1** | AAL | M | 65 | M | del13q; del11q | | |
| **P2** | ADB | F | 40 | M | Homozygous deletion in 13q14 (99%) | | SF3B1 heterozygousp.T663A |
| **P3** | AED | M | 66 | M | Heterozygous deletions in 11q (98%), 13q14 (96%), gain of the Myc-gene (68%) | | |
| **P4** | AGW | M | 61 | M | partial trisomy 12 | | SF3B1 heterozygous p.T663A |
| **P5** | AHU | M | 73 | U | del13q; del11q | | |
| **P6** | AKH | M | 33 | M | t(2;4) with gain of the BCL11A/REL gene locus and add (13)(q14) | | SF3B1p.H662L missense substitution |
| **P7** | BAX | M | 52 | U | 40% trisomy 12 | | |
| **P8** | BCS | M | 76 | M | del13q (89%) and and three copies of the Myc-locus (16%) 93% trisomy 12 | P53-deletion (34%) | SF3B1p.K700E |
| **P9** | BDS | M | 60 | Partial | 13q14 deletion (5%) + extra copy of DDIT3 93%trisomy 12 | | |
| **P10** | BFM | M | 77 | M | Partial trisomy 12 (99%) 13q-deletion (23%) | | SF3B1p.K666T,NOTCH1 c.7541_7542delCT |
| **P11** | BGL | F | 66 | M | 13q14 deletion (94%) | | |
| **P12** | BHA | M | 76 | M | Monosomy 17p, trisomy 12 (94%) | P53del (95%) | |
| **P13** | BI | M | 70 | M | n/a | | SF3B1 non-coding near splicing site mutation (Intron14-15-exon15) NOTCH1 c.7541_7542delCT |
| **P14** | BJE | F | 60 | U | Heterozygous deletion in13q14 (100%) | | |
| **P15** | BM | M | 59 | M | +t(14;18) | | |
| **P16** | BOH | F | 73 | U | 13q14 deletion 99%, trisomy 12 | | |

| | | | | | | | |
|---|---|---|---|---|---|---|---|
| **P17** | BR | M | 59 | U | Homozygous deletion in 13q14 | | NOTCH1 c.7541_7542delCT |
| **P18** | BRA | M | 77 | U | Normal | | |
| **P19** | BRC | F | 77 | n/a | 17p deletion | | |
| **P20** | BS | F | 68 | M | 99% trisomy 12 | | NOTCH1 c.7541_7542delCT |
| **P21** | BUP | M | 56 | U | Heterozygous deletion in 13q14 | | |
| **P22** | C | F | 82 | M | trisomy 12 | | |
| **P23** | CAP | F | 77 | U | Trisomy 12 (87%) | | NOTCH1 c.7541_7542delCT |
| **P24** | CB | M | 54 | U | Heterozygous del.11q22~23 and del.13q14 | | NOTCH1 c.7541_7542delCT |
| **P25** | CG | M | 58 | U | heterozygous del13q14 | | |
| **P26** | CGM | M | 65 | mix | Heterozygous del13q14 | | SF3B1 p. Y623S |
| **P27** | CHR | M | 74 | U | normal | | |
| **P28** | CHT | M | 42 | M | 42% trisomy 12 | | |
| **P29** | CJE | F | 65 | M | normal | | |
| **P30** | CK | M | 57 | M | 74% homozygous deletion of 13q14 | | |
| **P31** | CLF | M | 48 | M | Trisomy 12 (77%) | | |
| **P32** | CPA | M | 47 | U | del11q (69%) | | SF3B1 p. T663I |
| **P33** | CNG | M | 58 | M | Trisomy 12 (57%) | | |
| **P34** | CR | M | 68 | M | n/a | | |
| **P35** | CT | M | 59 | U | normal | | |
| **P36** | DAM | F | 60 | U | del13q14 | | NOTCH1 c.6877insG |
| **P37** | DCR | F | 66 | M | Trisomy 12 (69%) | | |
| **P38** | DD | M | 62 | U | Heterozygous deletions in 11q22~23 (ATM gene locus) and in 17p13 (P53 gene locus) (90%) | p53 exon 6 mutation | |
| **P39** | DE | M | 74 | M | trisomy 12, 13q del. | | SF3B1 non-coding mutation near splicing site (Intron14-15-exon15) |
| **P40** | DHA | M | 77 | mix | n/a | | SF3B1 p. Y623S |
| **P41** | DN | M | 75 | U | n/a | | n/a |
| **P42** | DN2 | F | 53 | M | n/a | | |
| **P43** | DRS | M | 56 | M | Heterozygous dele13q14 | | |
| **P44** | DT | M | 72 | U | n/a | | |
| **P45** | DTO | M | 78 | n/a | Normal | | |

| | | | | | | | |
|---|---|---|---|---|---|---|---|
| **P46** | DW | F | 62 | M | n/a | | |
| **P47** | EGS | F | 54 | M | Heterozygous (45%) and homozygous (38%) del13q14 | | |
| **P48** | EJ | F | 57 | M | del11q22~23 and a del13q14 | | |
| **P49** | EMP | F | 84 | M | Heterozygous del13q14 (98%) | | Hetrozygous SF3B1 p.N626D, NOTCH1 c.7541_7542delCT |
| **P50** | FA | F | 74 | M | Trisomy 12 (37%) | | |
| **P51** | FAS | F | 77 | U | 98% trisomy 12 | | NOTCH1 c.7541_7542delCT |
| **P52** | FIR | M | 42 | U | Normal | | SF3B1 p.K700E |
| **P53** | FL | F | 80 | U | delet11q22~23 and 13q14 (D13S319 and D13S25) | | |
| **P54** | FLA | M | 65 | M | 90% trisomy 12 | | |
| **P55** | GBT | M | 78 | M | Normal | | |
| **P56** | GCH | M | 52 | n/a | Trisomy 12 (23%) | | |
| **P57** | GD | F | 80 | M | n/a | | |
| **P58** | GIR | M | n/a | mix | del13q (73%) | | |
| **P59** | GKI | M | 66 | U | Normal | | |
| **P60** | GL | M | 73 | M | n.d. | | |
| **P61** | GMI | M | | M | 20%trisomy 12 | | |
| **P62** | GN | M | 64 | U | | | SF3B1p.K700E, heterozygous p.N626G |
| **P63** | GTR | M | 59 | M | 13q deletion 50% trisomy 12 | | |
| **P64** | HA | F | 54 | M | t(14;18)(q32;q21) involving IGH and BCL2 | | |
| **P65** | HB | F | 75 | U | 78% trisomy 12 | | |
| **P66** | HDM | M | 75 | M | n.d. | | |
| **P67** | HEJ | F | 92 | M | n.d. | | |
| **P68** | HIF | M | 65 | M | n.d. | | |
| **P69** | HJT | F | 54 | M | 13q deletion (63%) trisomy 12 (79%) | | |
| **P70** | HMC | F | 77 | M | 94% trisomy12 | | |
| **P71** | HOE | F | 78 | M | heterozygous del.11q and del.13q | | |
| **P72** | HOL | F | 76 | U | 40% trisomy 12 +17q | | |
| **P73** | HT | M | | U | 34% trisomy 12 | | |
| **P74** | HTG | M | 58 | U | normal | | |
| **P75** | JB | M | 61 | M | 85% trisomy 12 | | |
| **P76** | JEW | F | 64 | M | normal | | |

| | | | | | | | |
|---|---|---|---|---|---|---|---|
| **P77** | JMH | M | 63 | M | Heterozygous 13q-deletion (29%) and a heterozygous deletion of 6q21 (33%) | | |
| **P78** | JOC | M | | M | n.d. | | |
| **P79** | JOM | M | 75 | M | normal | | |
| **P80** | JP | M | 56 | U | 66% Trisomy 12 | | |
| **P81** | JRG | M | 58 | M | n/a | | SF3B1 non-coding intron mutation(intron14-15-exon15) |
| **P82** | LAW | M | 42 | M | 62% trisomy 12 | | |
| **P83** | LJA | M | | n/a | 47% trisomy 12 | | |
| **P84** | LJR | M | 52 | U | del13q (97%) | | |
| **P85** | LLG | F | 60 | U | 11q-deletion (84%), 13q-deletion (19%) | | |
| **P86** | MA | M | | M | 13q deletion 60% trisomy 12 | | |
| **P87** | MBA | M | 69 | M | Heterozygous del13q14 (95%) | | |
| **P88** | MC | M | 47 | U | Heterozygous del13q (72%) | | |
| **P89** | MCJ | M | 65 | U | trisomy 12 (74%), t(14;19)(q32;q13) or IGH-BCL3-fusion | | |
| **P90** | MCY | F | 69 | M | 30% trisomy 12 | | |
| **P91** | MJM | M | 55 | M | Heterozygous del13q14 (20%) | | |
| **P92** | MOA | F | 57 | M | del13q (79%) | | |
| **P93** | MOR | F | 66 | M | 80% trisomy 12 | | |
| **P94** | MRO | F | 67 | n/a | 66% trisomy 12 heterozygous 11q22~23(94%), 13q14 (99%), additional copy of MYC gene (81%), reduced signal of IGH distal (83%) | Heterozygous p53 del (94%), | NOTCH1 c.7541_7542delCT |
| **P95** | MRT | F | 58 | M | Heterozygous del.13q14 (28%) | | |
| **P96** | MST | M | | M | 76% trisomy 12 | | |
| **P97** | NB | M | 46 | M | 97% trisomy 12 | | |
| **P98** | NDK | M | 62 | M | Homozygous del13q14 (85%) and del11q (71%) | | heterozygous SF3B1 p.K700E |
| **P99** | PC | M | 64 | U | Heterozygous del6q (79%) | | SF3B1 p.Ile665N |
| **P100** | PCH | M | 62 | M | Heterozygous del13q14 (97%) | | |
| **P101** | PCR | M | 44 | M | n/a | | |

| | | | | | | | |
|---|---|---|---|---|---|---|---|
| **P102** | PGL | M | 67 | M | IGH-BCL2-fusion (92%) and a BCL6-break (63%) | | |
| **P103** | PGR | M | 54 | U | del11q (21%) | P53-deletion (81%) | NOTCH1 c.7541_7542delCT |
| **P104** | PI | F | 93 | n/a | 81% trisomy 12 | | |
| **P105** | PM | M | 63 | U | deletions in 2p, 11q, 13q and an insertion in chromosome 13 | | |
| **P106** | PME | F | 63 | M | Heterozygous del13q14 (87%) | | SF3B1 p.Ile667V |
| **P107** | PMR | F | 80 | M | Homozygous 13q-deletion (95%) | | |
| **P108** | PRW | M | 78 | U | 72% trisomy 12 | | NOTCH1 c.7541_7542delCT |
| **P109** | PTJ | F | 61 | U | 85% trisomy 12 IGH-BCL2 fusion (30%) -> +BCL2 | | NOTCH1 c.7541_7542delCT |
| **P110** | RDJ | M | 70 | n/a | normal | | non-coding intron mutation faraway from splicing site intron14-15 |
| **P111** | RI | M | 69 | M | 46% trisomy 12 | | Heterozygous mutation MYD88 p.L265P |
| **P112** | RIJ | M | 58 | U | 76% trisomy 12 | | |
| **P113** | RJM | F | | n/a | 90% trisomy 12 | | SF3B1 p.K700E |
| **P114** | RL | M | 84 | n/a | 96% trisomy 12 | | NOTCH1 c.7541_7542delCT |
| **P115** | ROF | M | 56 | U | 96% trisomy 12 IGH break (27%) and BCL3 break (32%) -> translocation t(14;19)(q32;q13) or IGH-BCL3 fusion and reduced signal of IGH distal (63%) | | non-coding intron mutation near splicing site intron14-15-exon15 |
| **P116** | RRK | M | 72 | M | 74% trisomy 12 | | |
| **P117** | SA | M | 74 | U | 60% trisomy 12 | | |
| **P118** | SBI | F | 81 | M | Homozygous loss in 13q14 (69%) | | |
| **P119** | SBJ | F | n/a | M | n/a | | |
| **P120** | SDE | M | 83 | U | del11q (15%), del13q (92%), Mycx3 (13%) | | NOTCH1 c.7541_7542delCT |
| **P121** | SEJ | F | 78 | M | Extra copy of DDIT3, 90% trisomy 12 | | |
| **P122** | SHA | F | 75 | U | reduced signal of IGH distal (61%)86% trisomy 12 | | NOTCH1 homozygous c.7541_7542delCT |

| | | | | | | | |
|---|---|---|---|---|---|---|---|
| **P123** | SI | M | 59 | M | 21% trisomy 12 | | |
| **P124** | SIM | M | 75 | M | 11q deletion 90% trisomy 12 | | NOTCH1 c.7541_7542delCT |
| **P125** | SJE | M | 76 | M | Normal | | |
| **P126** | SLE | F | 44 | U | Normal | | |
| **P127** | SMF | M | 82 | n/a | Reduced signal of IGH distal (68%) trisomy 12(80%) | | |
| **P128** | SMO | F | 76 | M | n/a | | |
| **P129** | SRC | M | 66 | M | n/a | | |
| **P130** | STJ | F | 78 | M | n/a | | |
| **P131** | SUT | F | 68 | M | normal | | |
| **P132** | TEK | M | 84 | U | n/a | | SF3B1 p.K700E |
| **P133** | TP | M | 68 | M | 63% trisomy 12 | | |
| **P134** | VB | F | 82 | U | 86% trisomy 12 | | |
| **P135** | VM | F | 66 | n/a | 70 % trisomy 12 13q deletion (75%), reduced signal of IGH distal (72%), MYC x 3 copies (16%) | | |
| **P136** | VP | F | 86 | U | n/a | | SF3B1 p.D621G, NOTCH1 c.7541_7542delCT |
| **P137** | WAB | F | 58 | M | heterozygous del13q14 | | |
| **P138** | WDG | F | 76 | U | trisomy 12 90% + igh | | NOTCH1 c.7541_7542delCT |
| **P139** | WEC | F | 52 | M | 13q deletion 84 % trisomy 12 | | |
| **P140** | WF | M | 80 | M | 66% trisomy 12 | | SF3B1 p.K700E |
| **P141** | WHR | M | 59 | M | Heterozygous del13q (77%) | | SF3B1 p.K700E |
| **P142** | WIH | F | 63 | M | 70% trisomy 12 | | |
| **P143** | WIJ | M | 77 | U | n/a | | NOTCH1 c.6906-6943del38 |
| **P144** | WJR | M | | M | 72% trisomy 12 | | NOTCH1 c.7541_7542delCT |
| **P145** | WLD | M | 56 | M | an IGH-BCL2-fusion (95%) and a (partial) trisomy 12 (8%), t(14;18) | | |
| **P146** | WMD | M | | M | normal | | |
| **P147** | WMG | M | | M | Heterozygous deletion in 13q14 (92%) and a reduced signal of IGH distal (17%) | | Heterozygous MYD88p.L265P |
| **P148** | WOM | F | | U | BCL3 break (62%) 83% trisomy 12, | | |

# Bibliography


http://www.cancerresearchuk.org/about-cancer/type/cll/about/chronic-lymphocytic-leukaemia (Accessed: April/2017).

https://www.cancer.gov/publications/dictionaries/cancer-terms (Accessed: June/2017).

https://cansar.icr.ac.uk/cansar/cell-lines (Accessed: June/2017).

http://www.cancerrxgene.org/ (accessed:July:2017).

Abel, E.V., Kim, E.J., Wu, J., Hynes, M., Bednar, F., Proctor, E., Wang, L., Dziubinski, M.L. and Simeone, D.M. (2014) 'The Notch pathway is important in maintaining the cancer stem cell population in pancreatic cancer', *PloS one,* 9(3), pp. e91983.

Aguilar-Hernandez, M.M., Blunt, M.D., Dobson, R., Yeomans, A., Thirdborough, S., Larrayoz, M., Smith, L.D., Linley, A., Strefford, J.C., Davies, A., Johnson, P.M.W., Savelyeva, N., Cragg, M.S., Forconi, F., Packham, G., Stevenson, F.K. and Steele, A.J. (2016) 'IL-4 enhances expression and function of surface IgM in CLL cells', *Blood,* 127(24), pp. 3015-3025.

Ahearne, M.J., Willimott, S., Piñon, L., Kennedy, D.B., Miall, F., Dyer, M.J.S. and Wagner, S.D. (2013) 'Enhancement of CD154/IL4 proliferation by the T follicular helper (Tfh) cytokine, IL21 and increased numbers of circulating cells resembling Tfh cells in chronic lymphocytic leukaemia', *British Journal of Haematology,* 162(3), pp. 360-370.

Alsafadi, S., Houy, A., Battistella, A., Popova, T., Wassef, M., Henry, E., Tirode, F., Constantinou, A., Piperno-neumann, S., Roman-roman, S., Dutertre, M. and Stern, M. (2016) 'Cancer-associated SF3B1 mutations affect alternative splicing by promoting alternative branchpoint usage', *Nature communications,* 7, pp. 10615.

Amaya-Chanaga, C.I. and Rassenti, L.Z. (2016) 'Biomarkers in chronic lymphocytic leukemia: Clinical applications and prognostic markers', *Best Practice & Research Clinical Haematology,* 29(1), pp. 79-89.

Amigo-Jiménez, I., Elvira Bailón, Estefanía Ugarte-Berzal, Noemí Aguilera-Montilla, José A García-Marco and Angeles García-Pardo (2014) 'Matrix Metalloproteinase-9 Is Involved in Chronic Lymphocytic Leukemia Cell Response to Fludarabine and Arsenic Trioxide', *PLoS One,* 9(6).

Andersson, E.R. and Lendahl, U. (2014) 'Therapeutic modulation of Notch signalling--are we there yet?', *Nature reviews. Drug discovery,* 13(5), pp. 357.

Apollonio, B., Scielzo, C., Bertilaccio, M.T.S., Ten Hacken, E., Scarfò, L., Ranghetti, P., Stevenson, F., Packham, G., Ghia, P., Muzio, M. and Caligaris-Cappio, F. (2013) 'Targeting B-cell anergy in chronic lymphocytic leukemia', *Blood,* 121(19), pp. 3879.

Arruga, F., Gizdic, B., Bologna, C., Cignetto, S., Buonincontri, R., Serra, S., Vaisitti, T., Gizzi, K., Vitale, N., Garaffo, G., Mereu, E., Diop, F., Neri, F., Incarnato, D., Coscia, M., Allan, J., Piva, R., Oliviero, S., Furman, R.R., Rossi, D., Gaidano, G. and Deaglio, S. (2016) 'Mutations in NOTCH1 PEST-domain orchestrate CCL19-driven homing of Chronic Lymphocytic Leukemia cells by modulating the tumor suppressor gene DUSP22', *Leukemia,* .

Arruga, F., Gizdic, B., Serra, S., Vaisitti, T., Ciardullo, C., Coscia, M., Laurenti, L., D'arena, G., Jaksic, O., Inghirami, G., Rossi, D., Gaidano, G. and Deaglio, S. (2014) 'Functional impact of NOTCH1 mutations in chronic lymphocytic leukemia', *Leukemia,* 28(5), pp. 1060-1070.

Ascierto, P.A., Kirkwood, J.M., Grob, J., Simeone, E., Grimaldi, A.M., Maio, M., Palmieri, G., Testori, A., Marincola, F.M. and Mozzillo, N. (2012) 'The role of BRAF V600 mutation in melanoma', *Journal of Translational Medicine,* 10(1), pp. 85.

Atilla, E., Atilla, P.A., Bozdag, S.C., Toprak, S.K., Topcuoglu, P., Ilhan, O., Ozcan, M. and Arslan, O. (2016) 'Does Hypogammaglobulinemia at Diagosis Effects Survival and Infection Risk in Chronic Lymphocytic Leukemia (CLL)?', *Blood,* 128, pp. 5577.

Badoux, X.C., Keating, M.J., Wang, X., O'Brien, S.M., Ferrajoli, A., Faderl, S., Burger, J., Koller, C., Lerner, S., Kantarjian, H. and Wierda, W.G. (2011a) 'Fludarabine, cyclophosphamide, and rituximab chemoimmunotherapy is highly effective treatment for relapsed patients with CLL', *Blood,* 117(11), pp. 3016-3024.

Badoux, X., Bueso-Ramos, C., Harris, D., Li, P., Liu, Z., Burger, J., O'Brien, S., Ferrajoli, A., Keating, M.J. and Estrov, Z. (2011b) 'Cross-talk between chronic lymphocytic leukemia cells and bone marrow endothelial cells: role of signal transducer and activator of transcription 3', *Human Pathology,* 42(12), pp. 1989-2000.

Baliakas, P., Hadzidimitriou, A., Sutton, L., Rossi, D., Minga, E., Villamor, N., Larrayoz, M., Kminkova, J., Agathangelidis, A., Davis, Z., Tausch, E., Stalika, E., Kantorova, B., Mansouri, L., Scarfo, L., Cortese, D., Navrkalova, V., Rose-Zerilli, M.J.J., Smedby, K.E., Juliusson, G., Anagnostopoulos, A., Makris, A.M., Navarro, A., Delgado, J., Oscier, D., Belessi, C., Stilgenbauer, S., Ghia, P., Pospisilova, S., Gaidano, G., Campo, E., Strefford, J.C., Stamatopoulos, K. and Rosenquist, R. (2015a) 'Recurrent mutations refine prognosis in chronic lymphocytic leukemia', *Leukemia,* 29(2), pp. 329-336.

Baliakas, P., Hadzidimitriou, A., Agathangelidis, A., Rossi, D., Sutton, L., Kminkova, J., Scarfo, L., Pospisilova, S., Gaidano, G., Stamatopoulos, K., Ghia, P. and Rosenquist, R. (2015b) 'Prognostic relevance of MYD88 mutations in CLL: the jury is still out', *Blood,* 126(8), pp. 1043-1044.

Baliakas, P., Iskas, M., Gardiner, A., Davis, Z., Plevova, K., Nguyen-Khac, F., Malcikova, J., Anagnostopoulos, A., Glide, S., Mould, S., Stepanovska, K., Brejcha, M., Belessi, C., Davi, F., Pospisilova, S., Athanasiadou, A., Stamatopoulos, K. and Oscier, D. (2014) 'Chromosomal translocations and karyotype complexity in chronic lymphocytic leukemia: A systematic reappraisal of classic cytogenetic data', *American Journal of Hematology,* 89(3), pp. 249-255.

Balmanno, K., Chell, S.D., Gillings, A.S., Hayat, S. and Cook, S.J. (2009) 'Intrinsic resistance to the MEK1/2 inhibitor AZD6244 (ARRY-142886) is associated with weak ERK1/2 signalling and/or strong PI3K signalling in colorectal cancer cell lines', *International Journal of Cancer,* 125(10), pp. 2332-2341.

Banzi, M., De Blasio, S., Lallas, A., Longo, C., Moscarella, E., Alfano, R. and Argenziano, G. (2016) 'Dabrafenib: a new opportunity for the treatment of BRAF V600-positive melanoma', *OncoTargets and therapy,* 9, pp. 2725.

Baou, M., Kohlhaas, L.S., Butterworth, M., Vogler, M., Dinsdale, D., Walewska, R., Majid, A., Eldering, E., Dyer, S.J.M. and Cohen, M.G. (2010) 'Role of NOXA and its ubiquitination in proteasome inhibitor-induced apoptosis in chronic lymphocytic leukemia cells', *Haematologica,* 95(9), pp. 1510-1518.

Bayat, M.R., Homayouni, T.S., Baluch, N., Morgatskaya, E., Kumar, S., Das, B. and Yeger, H. (2017) 'Combination therapy in combating cancer', *Oncotarget,* 8(23), pp. 38022-38043.

Best, O.G., . Crassini, K., Stevenson, W.S., Mulligan, S.P. and FRCPA (2013) 'MAPK-Erk1/2 Pathway Activation and Survival Of Chronic Lymphocytic Leukemia (CLL) Cells Is Induced By In Vitro Modeling Of The Tumor Microenvironment and Can Be Effectively Inhibited Using The MEK1 Inhibitor MEK162.', *Blood,* 122, pp. 4192;.

Bhattacharya, N., Diener, S., Idler, I.S., Rauen, J., Häbe, S., Busch, H., Habermann, A., Zenz, T., Döhner, H., Stilgenbauer, S. and Mertens, D. (2011) 'Nurse-like cells show deregulated expression of genes involved in immunocompetence', *British Journal of Haematology,* 154(3), pp. 349-356.

Bhattacharya, N., Reichenzeller, M., Caudron-Herger, M., Haebe, S., Brady, N., Diener, S., Nothing, M., Döhner, H., Stilgenbauer, S., Rippe, K. and Mertens, D. (2015) 'Loss of cooperativity of secreted CD40L and increased dose–response to IL4 on CLL cell viability correlates with enhanced activation of NF-kB and STAT6', *International Journal of Cancer,* 136(1), pp. 65-73.

Billard, C. (2014) 'Apoptosis inducers in chronic lymphocytic leukemia', *Oncotarget,* 5(2), pp. 309-325.

Bilous, N.I., Abramenko, I.V., Chumak, A.A., Dyagil, I.S. and Martina, Z.V. (2016) 'Detection of NOTCH1 c.7541_7542delCT mutation in chronic lymphocytic leukemia using conventional and real-time polymerase chain reaction', *Experimental oncology,* 38(2), pp. 112.

Binder, M., Léchenne, B., Ummanni, R., Scharf, C., Balabanov, S., Trusch, M., Schlüter, H., Braren, I., Spillner, E. and Trepel, M. (2010) 'Stereotypical chronic lymphocytic leukemia B-cell receptors recognize survival promoting antigens on stromal cells', *PloS one,* 5(12), pp. e15992.

Binet, J.L., Auquier, A., Dighiero, G., Chastang, C., Piguet, H., Goasguen, J., Vaugier, G., Potron, G., Colona, P., Oberling, F., Thomas, M., Tchernia, G., Jacquillat, C., Boivin, P., Lesty, C. and Duault, M. (1981) 'A New Prognostic Classification of Chronic LymphocyticLeukemia Derived from a Multivariate Survival Analysis.  ', *cancer,* 48, pp. 198-206.

Blunt, M.D., Carter, M.J., Larrayoz, M., Smith, L.D., Aguilar-Hernandez, M., Cox, K.L., Tipton, T., Reynolds, M., Murphy, S., Lemm, E., Dias, S., Duncombe, A., Strefford, J.C., Johnson, P.W.M., Forconi, F., Stevenson, F.K., Packham, G., Cragg, M.S. and Steele, A.J. (2015) 'The PI3K/mTOR inhibitor PF-04691502 induces apoptosis and inhibits microenvironmental signaling in CLL and the Eμ-TCL1 mouse model', *Blood,* 125(26), pp. 4032.

Bojarczuk, K., Sasi, B.K., Gobessi, S., Innocenti, I., Pozzato, G., Laurenti, L. and Efremov, D.G. (2016) 'BCR signaling inhibitors differ in their ability to overcome Mcl-1-mediated resistance of CLL B cells to ABT-199', *Blood,* 127(25), pp. 3192-3201.

Bojarska-Junak, A., Hus, I., Chocholska, S., Wąsik-Szczepanek, E., Sieklucka, M., Dmoszyńska, A. and Roliński, J. (2009) 'BAFF and APRIL expression in B-cell chronic lymphocytic leukemia: Correlation with biological and clinical features', *Leukemia Research,* 33(10), pp. 1319-1327.

Borthakur et al (2012) 'Phase I/II Trial of the MEK1/2 Inhibitor Trametinib (GSK1120212) in Relapsed/Refractory Myeloid Malignancies: Evidence of Activity in Patients with RAS Mutation-Positive Disease', *Blood*, 120, pp. 677;.

Böttcher, S., Ritgen, M., Fischer, K., Stilgenbauer, S., Busch, R.M., Fingerle-Rowson, G., Fink, A.M., Bühler, A., Zenz, T., Wenger, M.K., Mendila, M., Wendtner, C., Eichhorst, B.F., Döhner, H., Hallek, M.J. and Kneba, M. (2012) 'Minimal Residual Disease Quantification Is an Independent Predictor of Progression-Free and Overall Survival in Chronic Lymphocytic Leukemia: A Multivariate Analysis From the Randomized GCLLSG CLL8 Trial', *Journal of Clinical Oncology*, 30(9), pp. 980-988.

Brennan, K. and Clarke, R.B. (eds.) (2013) *Combining Notch inhibition with current therapies for breast cancer treatment.* London, England: SAGE Publications.

Brian, J.A., McPherson, P.A., O'Brien, K., Czaicki, N.L., DeStefino, V., Osman, S., Li, M., Day, B.W., Grabowski, P.J., Moore, M.J., Vogt, A. and Koide, K. (2009) 'Meayamycin inhibits pre–messenger RNA splicing and exhibits picomolar activity against multidrug-resistant cells', *Molecular Cancer Therapeutics*, 8(8), pp. 2308-2318.

Britten, C., Adjei, A., Millham, R., Houk, B., Borzillo, G., Pierce, K., Wainberg, Z. and LoRusso, P. (2014) 'Phase I study of PF-04691502, a small-molecule, oral, dual inhibitor of PI3K and mTOR, in patients with advanced cancer', *Investigational New Drugs*, 32(3), pp. 510-517.

Buckley, G.M., Ceska, T.A., Fraser, J.L., Gowers, L., Groom, C.R., Higueruelo, A.P., Jenkins, K., Mack, S.R., Morgan, T., Parry, D.M., Pitt, W.R., Rausch, O., Richard, M.D. and Sabin, V. (2008) 'IRAK-4 inhibitors. Part II: A structure-based assessment of imidazo[1,2-a]pyridine binding', *Bioorganic & Medicinal Chemistry Letters*, 18(11), pp. 3291-3295.

Burger, J.A., Burger, M. and Kipps, T.J. (1999) 'Chronic lymphocytic leukemia B cells express functional CXCR4 chemokine receptors that mediate spontaneous migration beneath bone marrow stromal cells', *Blood*, 94(11), pp. 3658.

Burger, J.A., Tsukada, N., Burger, M., Zvaifler, N.J., Dell'Aquila, M. and Kipps, T.J. (2000) 'Blood-derived nurse-like cells protect chronic lymphocytic leukemia B cells from spontaneous apoptosis through stromal cell-derived factor-1', *Blood*, 96(8), pp. 2655.

Burger, J.A. and Gribben, J.G. (2014) 'The microenvironment in chronic lymphocytic leukemia (CLL) and other B cell malignancies: insight into disease biology and new targeted therapies', *Seminars in cancer biology*, 24, pp. 71-81.

Burger, J.A. and Montserrat, E. (2013) 'Coming full circle: 70 years of chronic lymphocytic leukemia cell redistribution, from glucocorticoids to inhibitors of B-cell receptor signaling', *Blood*, 121(9), pp. 1501-1509.

Burger, J.A., Quiroga, M.P., Hartmann, E., Bürkle, A., Wierda, W.G., Keating, M.J. and Rosenwald, A. (2009) 'High-level expression of the T-cell chemokines CCL3 and CCL4 by chronic lymphocytic leukemia B cells in nurselike cell cocultures and after BCR stimulation', *Blood*, 113(13), pp. 3050-3058.

Buske, C., Gogowski, G., Schreiber, K., Rave-Fränk, M., Hiddemann, W. and Wörmann, B. (1997) 'Stimulation of B-chronic lymphocytic leukemia cells by murine fibroblasts, IL-4, anti-CD40 antibodies, and the soluble CD40 ligand', *Experimental hematology*, 25(4), pp. 329.

Bystry, R.S., Betz, A.G., Kallikourdis, M., Welch, K.A. and Aluvihare, V. (2001) 'B cells and professional APCs recruit regulatory T cells via CCL4', *Nature Immunology,* 2(12), pp. 1126-1132.

Caligaris-Cappio, F. (2003) 'Role of the microenvironment in chronic lymphocytic leukaemia', *British Journal of Haematology,* 123(3), pp. 380-388.

Caligaris-Cappio, F. (2015) 'Directing CLL-cell traffic', *Blood,* 126(11), pp. 1267.

Calissano, C., Damle, R.N., Hayes, G., Murphy, E.J., Hellerstein, M.K., Moreno, C., Sison, C., Kaufman, M.S., Kolitz, J.E., Allen, S.L., Rai, K.R. and Chiorazzi, N. (2009) 'In vivo intraclonal and interclonal kinetic heterogeneity in B-cell chronic lymphocytic leukemia', *Blood,* 114(23), pp. 4832-4842.

Calpe, E., Codony, C., Baptista, M.J., Abrisqueta, P., Carpio, C., Purroy, N., Bosch, F. and Crespo, M. (2011) 'ZAP-70 enhances migration of malignant B lymphocytes toward CCL21 by inducing CCR7 expression via IgM-ERK1/2 activation', *Blood,* 118(16), pp. 4401-4410.

Cantwell-Dorris, E.R., O'Leary, J.J. and Sheils, O.M. (2011) 'BRAFV600E: implications for carcinogenesis and molecular therapy', *Molecular cancer therapeutics,* 10(3), pp. 385-394.

Capalbo, S., Trerotoli, P., Ciancio, A., Battista, C., Serio, G. and Liso, V. (2000) 'Increased risk of lymphoproliferative disorders in relatives of patients with B-cell chronic lymphocytic leukemia: relevance of the degree of familial linkage', *European journal of haematology,* 65(2), pp. 114.

Carlo, M.I., Molina, A.M., Lakhman, Y., Patil, S., Woo, K., DeLuca, J., Lee, C., Hsieh, J.J., Feldman, D.R., Motzer, R.J. and Voss, M.H. (2016) 'A Phase Ib Study of BEZ235, a Dual Inhibitor of Phosphatidylinositol 3-Kinase (PI3K) and Mammalian Target of Rapamycin (mTOR), in Patients With Advanced Renal Cell Carcinoma', *The oncologist,* 21(7), pp. 787-788.

Carvalho, T., Martins, S., Rino, J., Marinho, S. and Carmo-Fonseca, M. (2017) 'Pharmacological inhibition of the spliceosome subunit SF3b triggers EJC-independent NMD', *J Cell Sci,* 9(0021-9533), pp. 1519-1531.

Catovsky, D., Müller-Hermelink, H.K., Montserrat, E. and Harris, N.L. (2001) *B-cell prolymphocytic leukaemia. In: Jaffe ES, Harris NL, Stein H, Vardiman JW, editors. World Health Organization Classification of Tumours: Pathology and Genetics of Tumours of Haematopoietic and Lymphoid Tissues.* Lyon, France: IARC Press.

Cazzola, M., Rossi, M. and Malcovati, L. (2013) 'Biologic and clinical significance of somatic mutations of SF3B1 in myeloid and lymphoid neoplasms', *Blood,* 121(2), pp. 260.

Cerhan, J.R. and Slager, S.L. (2015) 'Familial predisposition and genetic risk factors for lymphoma', *Blood,* 126(20), pp. 2265-2273.

Chaudhary, D., Wood, N., Romero, D.L., Robinson, S.D., Greenwood, J.R., Shelley, M., Morin, M., Kapeller, R. and Westlin, W.F. (2013) 'Synergistic Blockade Of Activated B Cell-Like DLBCL Proliferation With a Selective Inhibitor Of IRAK4 In Combination With Inhibition Of The B-Cell Receptor Signaling Network', *Blood,* 128, pp. 3833.

Chen, L.S., Balakrishnan, K. and Gandhi, V. (2010) 'Inflammation and survival pathways: Chronic lymphocytic leukemia as a model system', *Biochemical Pharmacology,* 80(12), pp. 1936-1945.

Chen, Y., Germano, S., Clements, C., Samuel, J., Shelmani, G., Jayne, S., Dyer, M.J.S. and Macip, S. (2016) 'Pro-survival signal inhibition by CDK inhibitor dinaciclib in Chronic Lymphocytic Leukaemia', *British Journal of Haematology*, 175(4), pp. 641-651.

Chiorazzi, N. and Ferrarini, M. (2011) 'Cellular origin(s) of chronic lymphocytic leukemia: cautionary notes and additional considerations and possibilities', *Blood*, 117(6), pp. 1781-1791.

Choudhary, G.S., Al-harbi, S., Mazumder, S., Hill, B.T., Smith, M.R., Bodo, J., Hsi, E.D. and Almasan, A. (2015) 'MCL-1 and BCL-xL-dependent resistance to the BCL-2 inhibitor ABT-199 can be overcome by preventing PI3K/AKT/mTOR activation in lymphoid malignancies', *Cell Death and Disease*, 6(1), pp. e1593.

Cols, M., Barra, C.M., He, B., Puga, I., Xu, W., Chiu, A., Tam, W., Knowles, D.M., Dillon, S.R., Leonard, J.P., Furman, R.R., Chen, K. and Cerutti, A. (2012) 'Stromal Endothelial Cells Establish a Bidirectional Crosstalk with Chronic Lymphocytic Leukemia Cells through the TNF-Related Factors BAFF, APRIL, and CD40L', *Journal of Immunology*, 188(12), pp. 6071-6083.

Cox, A.D. and Der, C.J. (2010) 'The Raf Inhibitor Paradox: Unexpected Consequences of Targeted Drugs', *Cancer Cell*, 17(3), pp. 221-223.

Crassini, K., Shen, Y., Mulligan, S. and Giles Best, O. (2017) 'Modeling the chronic lymphocytic leukemia microenvironment in vitro', *Leukemia & Lymphoma*, 58(2), pp. 266-279.

Cseh, B., Doma, E. and Baccarini, M. (2014) '"RAF" neighborhood: Protein–protein interaction in the Raf/Mek/Erk pathway', *FEBS Letters*, 588(15), pp. 2398-2406.

Cummins, K.D., Jane, S.M., Nikovic, S., Bazargan, A., Filshie, R., Sutrave, G., Hertzberg, M., Scott, A., Lane, S., Yannakou, C.K., Ritchie, D., D'Rozario, J., Black, J., Bavishi, K. and Wei, A. (2014) 'Sorafenib priming may augment salvage chemotherapy in relapsed and refractory FLT3-ITD-positive acute myeloid leukemia', *Blood Cancer Journal*, 4(8), pp. e237.

Damle, R.N., Wasil, T., Fais, F., Ghiotto, F., Valetto, A., Allen, S.L., Buchbinder, A., Budman, D., Dittmar, K., Kolitz, J., Lichtman, S.M., Schulman, P., Vinciguerra, V.P., Rai, K.R., Ferrarini, M. and Chiorazzi, N. (1999) 'Ig V gene mutation status and CD38 expression as novel prognostic indicators in chronic lymphocytic leukemia', *Blood*, 94(6), pp. 1840.

Damm, F., Mylonas, E., Cosson, A., Yoshida, K., Della Valle, V., Mouly, E., Diop, M., Scourzic, L., Shiraishi, Y., Chiba, K., Tanaka, H., Miyano, S., Kikushige, Y., Davi, F., Lambert, J., Gautheret, D., Merle-Béral, H., Sutton, L., Dessen, P., Solary, E., Akashi, K., Vainchenker, W., Mercher, T., Droin, N., Ogawa, S., Nguyen-Khac, F. and Bernard, O.A. (2014) 'Acquired initiating mutations in early hematopoietic cells of CLL patients', *Cancer discovery*, 4(9), pp. 1088-1101.

Davids, M. and Burger, J.A. (2012) 'Cell Trafficking in Chronic Lymphocytic Leukemia', *Open Journal of Hematology*, 3.

Davies, H., Bognell, G.R., Cox, C., Stephens, P., Edkins, S., Clegg, S., Teague, J., Woffendin, H., Garnett, M.J., Bottomley, W., Davis, N., Dicks, E., Ewing, R., Floyd, R., Gray, K., Hall, S., Hawes, R., Hughes, J., Kosmidou, V., Menzies, A., Mould, C., Parker, A., Stevens, C., Stephen, W., Jayatilake, H., Gusterson, B.A., Steven, H., Wilson, R., Cooper, C., Shipley, J., Hargrave, D.R., Pritchard-Jones, C., Maitland, N., Chenevix-Trench, G., Reggins, G.J., Bigner, D.D., Palmieri, G., Cossu, A., Flanagan, A., Nicholson, A., Ho, J.W.C., Leung, Y.S.,

Yuen, S.T., Weber, B.L., Seigler, H.F., Darrow, T.L., Paterson, H., Marais, R., Marshall, C.J., Wooster, R., Stratton, M.R. and Futreal, P.A. (2002) 'Mutations of the BRAF gene in human cancer', *Nature*, 417(6892), pp. 949-954.

D'Avola, A., Yeomans, A., Drennan, S., Rose-Zerilli, M., Strefford, J.C., Stevenson, F.K., Steele, A.J., Packham, G. and Forconi, F. (2016) 'Global and MYC-Specific Translation Is Enhanced in Activated Chronic Lymphocytic Leukemia Cells Carrying NOTCH1 C.7541_7542delct Mutations', *Blood*, 128, pp. 970.

De La Garza, A., Cameron, R.C., Nik, S., Payne, S.G. and Bowman, T.V. (2016) 'Spliceosomal component Sf3b1 is essential for hematopoietic differentiation in zebrafish', *Experimental hematology*, 44(9), pp. 826.

de Rooij, M., Kuil, A., Kater, A.P., Kersten, M.J., Pals, S.T. and Spaargaren, M. (2015) 'Ibrutinib and idelalisib synergistically target BCR-controlled adhesion in MCL and CLL: a rationale for combination therapy', *Blood*, 125(14), pp. 2306.

Deaglio, S., Aydin, S., Grand, M.M., Vaisitti, T., Bergui, L., D'Arena, G., Chiorino, G. and Malavasi, F. (2010) 'CD38/CD31 interactions activate genetic pathways leading to proliferation and migration in chronic lymphocytic leukemia cells', *Molecular medicine (Cambridge, Mass.)*, 16(3-4), pp. 87.

Dearden, C. (2008) 'Disease-specific complications of chronic lymphocytic leukemia', *Hematology / the Education Program of the American Society of Hematology. American Society of Hematology. Education Program*, 2008(1), pp. 450-456.

DeBoever, C., Ghia, E.M., Shepard, P.J., Rassenti, L., Barrett, C.L., Jepsen, K., Jamieson, C.H.M., Carson, D., Kipps, T.J. and Frazer, K.A. (2015) 'Transcriptome sequencing reveals potential mechanism of cryptic 3' splice site selection in SF3B1-mutated cancers', *PLoS computational biology*, 11(3), pp. e1004105.

Decker, S., Zirlik, K., Djebatchie, L., Hartmann, D., Ihorst, G., Schmitt-Graeff, A., Herchenbach, D., Jumaa, H., Warmuth, M., Veelken, H. and Dierks, C. (2012) 'Trisomy 12 and elevated GLI1 and PTCH1 transcript levels are biomarkers for Hedgehog-inhibitor responsiveness in CLL', *Blood*, 119(4), pp. 997-1007.

Del Giudice, I., Rossi, D., Chiaretti, S., Marinelli, M., Tavolaro, S., Gabrielli, S., Laurenti, L., Marasca, R., Rasi, S., Fangazi, M., Guarini, A., Gaidano, G. and Foà, R. (2012) 'NOTCH1 mutations in +12 chronic lymphocytic leukemia (CLL) confer an unfavorable prognosis, induce a distinctive transcriptional profiling and refine the intermediate prognosis of +12 CLL', *Haematologica*, 97(3), pp. 437-441.

delaFuente, M., Casanova, B., Moyano, J.V., Garcia-Gila, M., Sanz, L., Garcia-Marco, J., Silva, A. and Garcia-Pardo, A. (2002) 'Engagement of alpha4beta1 integrin by fibronectin induces in vitro resistance of B chronic lymphocytic leukemia cells to fludarabine', *Journal of leukocyte biology*, 71(3), pp. 495.

Dighiero, G. (2003) 'Unsolved issues in CLL biology and management', *Leukemia*, 17(12), pp. 2385-2391.

Dighiero, G. and Binet, J. (2000) 'When and How to Treat Chronic Lymphocytic Leukemia', *The New England Journal of Medicine*, 343(24), pp. 1799-1801.

Dohner, H., Stilgenbauer, S., Benner, A., Leupolt, E., Krober, A., Bullinger, L., Dohner, K., Bentz, M. and Lichter, P. (2000) 'Genomic Aberrations and Survival in Chronic Lymphocytic Leukemia', *The New England Journal of Medicine*, 343(26), pp. 1910-1916.

Dreger, P., Schetelig, J., Andersen, N., Corradini, P., van Gelder, M., Gribben, J., Kimby, E., Michallet, M., Moreno, C., Stilgenbauer, S. and Montserrat, E. (2014) 'Managing high-risk CLL during transition to a new treatment era: stem cell transplantation or novel agents?', *Blood,* 124(26), pp. 3841-3849.

Duechler, M., Shehata, M., Schwarzmeier, J.D., Hoelbl, A., Hilgarth, M. and Hubmann, R. (2005) 'Induction of apoptosis by proteasome inhibitors in B-CLL cells is associated with downregulation of CD23 and inactivation of Notch2', *Leukemia,* 19(2), pp. 260-267.

Dühren-von Marcus, Rudolf Übelhart, Dunja Schneider, Thomas Wossning, Martina P Bach, Maike Buchner, Daniel Hofmann, Elena Surova, Marie Follo, Fabian Köhler, Hedda Wardemann, Katja Zirlik, Hendrik Veelken and Hassan Jumaa (2012) 'Chronic lymphocytic leukaemia is driven by antigen-independent cell-autonomous signalling', *Nature,* 489(7415), pp. 309-312.

Dvinge, H., Kim, E., Abdel-Wahab, O. and Bradley, R.K. (2016) 'RNA splicing factors as oncoproteins and tumour suppressors', *Nature Reviews: Cancer,* 16(7), pp. 413-430.

Dyer, M.J., Zani, V.J., Lu, W.Z., O'Byrne, A., Mould, S., Chapman, R., Heward, J.M., Kayano, H., Jadayel, D. and Matutes, E. (1994) 'BCL2 translocations in leukemias of mature B cells', *Blood,* 83(12), pp. 3682.

Dyer, M.J.S., Vogler, M., Samuel, J., Jayne, S., Wagner, S., Pritchard, C. and Macip, S. (2013) 'Precision medicines for B-cell leukaemias and lymphomas; progress and potential pitfalls', *British Journal of Haematology,* 160(6), pp. 725-733.

Effenberger, K.A., Urabe, V.K., Prichard, B.E., Ghosh, A.K. and Jurica, M.S. (2016) 'Interchangeable SF3B1 inhibitors interfere with pre-mRNA splicing at multiple stages', *RNA (New York, N.Y.),* 22(3), pp. 350.

Eichhorst, B., Robak, T., Montserrat, E., Ghia, P., Hillmen, P., Hallek, M. and Buske, C. (2015) 'Chronic lymphocytic leukaemia: ESMO Clinical Practice Guidelines for diagnosis, treatment and follow-up', *Annals of oncology : official journal of the European Society for Medical Oncology / ESMO,* 26 Suppl 5(suppl 5), pp. v84.

Eichhorst, B., Fink, A.M., Busch, R., Kovacs, G., Maurer, C., Lange, E., Köppler, H., G Kiehl, M., Soekler, M., Schlag, R., Vehling-Kaiser, U., R. A. Köchling, G., Plöger, C., Gregor, M., Plesner, T., Trneny, M., Fischer, K., Döhner, H., Kneba, M., Wendtner, C., Klapper, W., Kreuzer, K.A., Stilgenbauer, S., Böttcher, S. and Hallek, M. (2014) 'Frontline chemoimmunotherapy with fludarabine (F), cyclophosphamide (C), and rituximab (R) (FCR) shows superior efficacy in comparison to bendamustine (B) and rituximab (BR) in previously untreated and physically fit patients ( pts) with advanced chronic lymphocytic leukemia (CLL): final analysis of an international, randomized study of the German CLL Study Group (GCLLSG) (CLL10 Study).', *Blood,* 124, pp. abstract 19.

El-Gamal, D., Williams, K., LaFollette, T.D., Cannon, M., Blachly, J.S., Zhong, Y., Woyach, J.A., Williams, E., Awan, F.T., Jones, J., Andritsos, L., Maddocks, K., Wu, C.H., Chen, C.S., Lehman, A., Zhang, X., Lapalombella, R. and Byrd, J.C. (2014) 'PKC-b as a therapeutic target in CLL: PKC inhibitor AEB071 demonstrates preclinical activity in CLL', *Blood,* 124(9), pp. 1481-1491.

Elgueta, R., Benson, M.J., de Vries, V.C., Wasiuk, A., Guo, Y. and Noelle, R.J. (eds.) (2009) *Molecular mechanism and function of CD40-CD40L engagement in the immune system.* Denmark: Wiley Subscription Services, Inc.

Ellisen, L.W., Bird, J., West, D.C., Soreng, A.L., Reynolds, T.C., Smith, S.D. and Sklar, J. (1991) 'TAN-1, the human homolog of the Drosophila Notch gene, is broken by chromosomal translocations in T lymphoblastic neoplasms', *Cell*, 66(4), pp. 649-661.

Fabbri, G. and Dalla-Favera, R. (2016) 'The molecular pathogenesis of chronic lymphocytic leukaemia', *Nature Reviews: Cancer*, 16(3), pp. 145-162.

Fabbri, G., Rasi, S., Rossi, D., Trifonov, V., Khiabanian, H., Ma, J., Grunn, A., Fangazio, M., Capello, D., Monti, S., Cresta, S., Gargiulo, E., Forconi, F., Guarini, A., Arcaini, L., Paulli, M., Laurenti, L., Larocca, L.M., Marasca, R., Gattei, V., Oscier, D., Bertoni, F., Mullighan, C.G., Foa, R., Pasqualucci, L., Rabadan, R., Dalla-Favera, R. and Gaidano, G. (2011) 'Analysis of the chronic lymphocytic leukemia coding genome: role of NOTCH1 mutational activation', *Journal of Experimental Medicine*, 208(7), pp. 1389-1401.

Falchi, L., Baron, J.M., Orlikowski, C.A. and Ferrajoli, A. (2016) 'BCR Signaling Inhibitors: an Overview of Toxicities Associated with Ibrutinib and Idelalisib in Patients with Chronic Lymphocytic Leukemia', *Mediterr J Hematol Infect Dis*, 8, pp. 1-12.

Falini, B., Martelli, M.P. and Tiacci, E. (2016) 'BRAF V600E mutation in hairy cell leukemia: from bench to bedside', *Blood*, 128(15), pp. 1918-1927.

Foà, R., Del Giudice, I., Guarini, A., Rossi, D. and Gaidano, G. (2013) 'Clinical implications of the molecular genetics of chronic lymphocytic leukemia', *Haematologica*, 98(5), pp. 675-685.

Fazio, N., Buzzoni, R., Baudin, E., Antonuzzo, L., Hubner, R.A., Lahner, H., DE Herder, W.W., Raderer, M., Teulé, A., Capdevila, J., Libutti, S.K., Kulke, M.H., Shah, M., Dey, D., Turri, S., Aimone, P., Massacesi, C. and Verslype, C. (2016) 'A Phase II Study of BEZ235 in Patients with Everolimus-resistant, Advanced Pancreatic Neuroendocrine Tumours', *Anticancer research*, 36(2), pp. 713.

Fender, A.W., Nutter, J.M., Fitzgerald, T.L., Bertrand, F.E. and Sigounas, G. (2015) 'Notch-1 Promotes Stemness and Epithelial to Mesenchymal Transition in Colorectal Cancer', *Journal of Cellular Biochemistry*, 116(11), pp. 2517-2527.

Ferrer, G., Bosch, R., Hodgson, K., Tejero, R., Roué, G., Colomer, D., Montserrat, E. and Moreno, C. (2014) 'B cell activation through CD40 and IL4R ligation modulates the response of chronic lymphocytic leukaemia cells to BAFF and APRIL', *British Journal of Haematology*, 164(4), pp. 570-578.

Fischer, K., Bahlo, J., Fink, A.M., Goede, V., Herling, C.D., Cramer, P., Langerbeins, P., von Tresckow, J., Engelke, A., Maurer, C., Kovacs, G., Herling, M., Tausch, E., Kreuzer, K., Eichhorst, B., Böttcher, S., Seymour, J.F., Ghia, P., Marlton, P., Kneba, M., Wendtner, C., Döhner, H., Stilgenbauer, S. and Hallek, M. (2016) 'Long-term remissions after FCR chemoimmunotherapy in previously untreated patients with CLL: updated results of the CLL8 trial', *Blood*, 127(2), pp. 208-215.

Flynn, J., Jones, J., Johnson, A.J., Andritsos, L., Maddocks, K., Jaglowski, S., Hessler, J., Grever, M.R., Im, E., Zhou, H., Zhu, Y., Zhang, D., Small, K., Bannerji, R. and Byrd, J.C. (2015) 'Dinaciclib is a novel cyclin-dependent kinase inhibitor with significant clinical activity in relapsed and refractory chronic lymphocytic leukemia', *Leukemia*, 29(7), pp. 1524-1529.

Foà, R., Del Giudice, I., Guarini, A., Rossi, D. and Gaidano, G. (2013) 'Clinical implications of the molecular genetics of chronic lymphocytic leukemia', *Haematologica*, 98(5), pp. 675-685.

Forconi, F. (2015) 'Three years of ibrutinib in CLL', *Blood*, 125(16), pp. 2455-2456.

Forconi, F., Potter, K.N., Wheatley, I., Darzentas, N., Sozzi, E., Stamatopoulos, K., Mockridge, C.I., Packham, G. and Stevenson, F.K. (2010) 'The normal IGHV1-69-derived B-cell repertoire contains stereotypic patterns characteristic of unmutated CLL', *Blood*, 115(1), pp. 71-77.

Freeman, A.K., Ritt, D.A. and Morrison, D.K. (2013) 'Effects of Raf dimerization and its inhibition on normal and disease-associated Raf signaling', *Molecular cell*, 49(4), pp. 751.

Frei, E., Karon, M., Levin, R.H., Freireich, E.J., Taylor, R.J., Hananian, J., Selawry, O., Holland, J.F., Hoogstraten, B., Wolman, I.J., Abir, E., Sawitsky, A., Lee, S., Mills, S.D., Burgert, E.O., Spurr, C.L., Patterson, R.B., Ebaugh, F.G., James, G.W. and Moon, J.H. (1965) 'The effectiveness of combinations of antileukemic agents in inducing and maintaining remission in children with acute leukemia', *Blood*, 26(5), pp. 642-656.

Furman, R.R., Asgary, Z., Mascarenhas, J.O., Liou, H. and Schattner, E.J. (2000) 'Modulation of NF- Kappa B Activity and Apoptosis in Chronic Lymphocytic Leukemia B Cells', *Journal of Immunology*, 164(4), pp. 2200-2206.

Furman, R.R., Sharman, J.P., Coutre, S.E., Cheson, B.D., Pagel, J.M., Hillmen, P., Barrientos, J.C., Zelenetz, A.D., Kipps, T.J., Flinn, I., Ghia, P., Eradat, H., Ervin, T., Lamanna, N., Coiffier, B., Pettitt, A.R., Ma, S., Stilgenbauer, S., Cramer, P., Aiello, M., Johnson, D.M., Miller, L.L., Li, D., Jahn, T.M., Dansey, R.D., Hallek, M. and O'Brien, S.M. (2014) 'Idelalisib and rituximab in relapsed chronic lymphocytic leukemia', *The New England journal of medicine*, 370(11), pp. 997.

Gamberale, R., Geffner, J., Arrosagaray, G., Scolnik, M., Salamone, G., Trevani, A., Vermeulen, M. and Giordano, M. (2001) 'Non-malignant leukocytes delay spontaneous B-CLL cell apoptosis', *Leukemia*, 15(12), pp. 1860-1867.

Gentile, M., Zirlik, K., Ciolli, S., Mauro, F.R., Di Renzo, N., Mastrullo, L., Angrilli, F., Molica, S., Tripepi, G., Giordano, A., Di Raimondo, F., Selleri, C., Coscia, M., Musso, M., Orsucci, L., Mannina, D., Rago, A., Giannotta, A., Ferrara, F., Herishanu, Y., Shvidel, L., Tadmor, T., Scortechini, I., Ilariucci, F., Murru, R., Guarini, A., Musuraca, G., Mineo, G., Vincelli, I., Arcari, A., Tarantini, G., Caparrotti, G., Chiarenza, A., Levato, L., Villa, M.R., De Paolis, M.R., Zinzani, P.L., Polliack, A. and Morabito, F. (2016) 'Combination of bendamustine and rituximab as front-line therapy for patients with chronic lymphocytic leukaemia: multicenter, retrospective clinical practice experience with 279 cases outside of controlled clinical trials', *European Journal of Cancer*, 60, pp. 154-165.

Ghia, P., Ferreri, A.M. and Caligaris-Cappio, F. (2007) 'Chronic lymphocytic leukemia', *Critical Reviews in Oncology/Hematology*, 64(3), pp. 234–246.

Girbl, T., Hinterseer, E., Grössinger, E.M., Asslaber, D., Oberascher, K., Weiss, L., Hauser-Kronberger, C., Neureiter, D., Kerschbaum, H., Naor, D., Alon, R., Greil, R. and Hartmann, T.N. (2013) 'CD40-mediated activation of chronic lymphocytic leukemia cells promotes their CD44-dependent adhesion to hyaluronan and restricts CCL21-induced motility', *Cancer research*, 73(2), pp. 561-570.

Goede, V., Fischer, K., Busch, R., Engelke, A., Eichhorst, B., Wendtner, C.M., Chagorova, T., de la Serna, J., Dilhuydy, M., Illmer, T., Opat, S., Owen, C.J., Samoylova, O., Kreuzer, K., Stilgenbauer, S., Döhner, H., Langerak, A.W., Ritgen, M., Kneba, M., Asikanius, E., Humphrey, K., Wenger, M. and Hallek, M. (2014) 'Obinutuzumab plus chlorambucil in patients with CLL and coexisting conditions', *The New England journal of medicine*, 370(12), pp. 1101.

Gonzalez-Rodriguez, A.P., Contesti, J., Huergo-Zapico, L., Lopez-Soto, A., Fernández-Guizán, A., Acebes-Huerta, A., Gonzalez-Huerta, A.J., Gonzalez, E., Fernandez-Alvarez, C. and Gonzalez, S. (2010) 'Prognostic significance of CD8 and CD4 T cells in chronic lymphocytic leukemia', *Leukemia & Lymphoma,* 51(10), pp. 1829-1836.

Granziero, L., Ghia, P., Circosta, P., Gottardi, D., Strola, G., Geuna, M., Montagna, L., Piccoli, P., Chilosi, M. and Caligaris-Cappio, F. (2001) 'Survivin is expressed on CD40 stimulation and interfaces proliferation and apoptosis in B-cell chronic lymphocytic leukemia', *Blood,* 97(9), pp. 2777-2783.

Grdisa, M. (2003) 'Influence of CD40 ligation on survival and apoptosis of B-CLL cells in vitro', *Leukemia Research,* 27(10), pp. 951-956.

Guièze, R. and Wu, C.J. (2015) 'Genomic and epigenomic heterogeneity in chronic lymphocytic leukemia', *Blood,* 126(4), pp. 445-453.

Guo, B., Zhang, L., Chiorazzi, N. and Rothstein, T.L. (2016) 'IL-4 rescues surface IgM expression in chronic lymphocytic leukemia', *Blood,* 128(4), pp. 553.

Haerzschel, A., Catusse, J., Hutterer, E., Paunovic, M., Zirlik, K., Eibel, H., Krenn, P., Hartmann, T. and Burger, M. (2016) 'BCR and chemokine responses upon anti-IgM and anti-IgD stimulation in chronic lymphocytic leukaemia', *Annals of Hematology,* 95(12), pp. 1979-1988.

Hallaert, H.Y.D., Schmidlin, H., Eldering, E. and Van Oers, M H J (2007) 'GSI-1, a Putative Notch Inhibitor, Induces Apoptosis in B-CLL Cells Via Proteasomal Inhibition and Noxa Upregulation.', *Blood,* 110, pp. 3113.

Hallek, M., Cheson, B.D., Catovsky, D., Caligaris-Cappio, F., Dighireo, G., Döhner, H., Hillmen, P., Keating, M.J., Montserrat, E., Rai, K.R. and Kipps, T.J. (2008a) 'Guidelines for the diagnosis and treatment of chronic lymphocytic leukemia: a report from the International Workshop on Chronic Lymphocytic Leukemia updating the National Cancer Institute–Working Group 1996 guidelines.', *Blood,* 111, pp. 5446-5456.

Hallek, M. (2015) 'CME Information: Chronic lymphocytic leukemia: 2015 Update on diagnosis, risk stratification, and treatment.', *American Journal of Hematology,* 90, pp. 446-460.

Hallek, M., Cheson, B.D., Catovsky, D., Caligaris-Cappio, F., Dighiero, G., Döhner, H., Hillmen, P., Keating, M.J., Montserrat, E., Rai, K.R. and Kipps, T.J. (2008b) 'Guidelines for the diagnosis and treatment of chronic lymphocytic leukemia: a report from the International Workshop on Chronic Lymphocytic Leukemia updating the National Cancer Institute-Working Group 1996 guidelines', *Blood,* 111(12), pp. 5446-5456.

Hamblin, T.J., Davis, Z., Gardiner, A., Oscier, D.G. and Stevenson, F.K. (1999) 'Unmutated Ig V(H) genes are associated with a more aggressive form of chronic lymphocytic leukemia', *Blood,* 94(6), pp. 1848.

Hamblin, T.J. (2006) 'Autoimmune Complications of Chronic Lymphocytic Leukemia', *Seminars in Oncology,* 33(2), pp. 230-239.

Hamblin, T.J. and Oscier, D.G. (1997) 'Chronic lymphocytic leukaemia: the nature of the leukaemic cell', *Blood Reviews,* 11(3), pp. 119-128.

Hanahan, D. and Weinberg, R. (2011) 'Hallmarks of Cancer: The Next Generation', *Cell,* 144(5), pp. 646-674.

Hanahan, D. and Weinberg, R.A. (2000) 'The Hallmarks of Cancer', *Cell,* 100.

Hardy, R.R. and Hayakawa, K. (1986) 'Development and physiology of Ly-1 B and its human homolog, Leu-1 B', *Immunological reviews*, 93(1), pp. 53-80.

Hartmann, T.N., Grabovsky, V., Wang, W., Desch, P., Rubenzer, G., Wollner, S., Binsky, I., Vallon-Eberhard, A., Sapoznikov, A., Burger, M., Shachar, I., Haran, M., Honczarenko, M., Greil, R. and Alon, R. (2009) 'Circulating B-Cell Chronic Lymphocytic Leukemia Cells Display Impaired Migration to Lymph Nodes and Bone Marrow', *Cancer Research*, 69(7), pp. 3121-3130.

Harvey, W., Srour, E.F., Turner, R., Carey, R., Maze, R., Starrett, B., Kanagala, R., Pereira, D., Merchant, P., Taylor, M. and Jansen, J. (1991) 'Characterization of a new cell line (ESKOL) resembling hairy-cell leukemia: A model for oncogene regulation and late B-cell differentiation', *Leukemia Research*, 15(8), pp. 733-744.

Hauschild, A., Grob, J., Demidov, V.L., Jouary, T., Gutzmer, R., Millward, M., Rutkowski, P., Blank, U.C., Miller Jr, H.W., Kaempgen, E., Martín-Algarra, S., Karaszewska, B., Mauch, C., Chiarion-Sileni, V., Martin, A., Swann, Z., Haney, P., Mirakhur, B., Guckert, E.M., Goodman, V. and Chapman, B.P. (2012) 'Dabrafenib in BRAF-mutated metastatic melanoma: a multicentre, open-label, phase 3 randomised controlled trial', *The Lancet*, 380(9839), pp. 358-365.

He, B., Lu, C., Zheng, G., He, X., Wang, M., Chen, G., Zhang, G. and Lu, A. (2016) 'Combination therapeutics in complex diseases', .

He, C., Dong, X., Zhai, B., Jiang, X., Dong, D., Li, B., Jiang, H., Xu, S. and Sun, X. (2015) 'MiR-21 mediates sorafenib resistance of hepatocellular carcinoma cells by inhibiting autophagy via the PTEN/Akt pathway', *Oncotarget*, 6(30), pp. 28867.

Heidorn, S.J., Milagre, C., Whittaker, S., Nourry, A., Niculescu-Duvas, I., Dhomen, N., Hussain, J., Reis-Filho, J.S., Springer, C.J., Pritchard, C. and Marais, R. (2010) 'Kinase-Dead BRAF and Oncogenic RAS Cooperate to Drive Tumor Progression through CRAF', *Cell*, 140(2), pp. 209-221.

Heinig, K., Gätjen, M., Grau, M., Stache, V., Anagnostopoulos, I., Gerlach, K., Niesner, R.A., Cseresnyes, Z., Hauser, A.E., Lenz, P., Hehlgans, T., Brink, R., Westermann, J., Dörken, B., Lipp, M., Lenz, G., Rehm, A. and Höpken, U.E. (2014) 'Access to follicular dendritic cells is a pivotal step in murine chronic lymphocytic leukemia B-cell activation and proliferation', *Cancer discovery*, 4(12), pp. 1448-1465.

Herishanu, Y., Katz, B., Lipsky, A. and Wiestner, A. (2013) 'Biology of chronic lymphocytic leukemia in different microenvironments: clinical and therapeutic implications', *Hematology/oncology clinics of North America*, 27(2), pp. 173.

Herman, S.E.M. and Wiestner, A. (2016) 'Pre-clinical modeling of novel therapeutics in chronic lymphocytic leukemia: the tools of the trade', *Semin Oncol.*, 43, pp. 222-232.

Hernandez, T.F.N., Galvez, S.J.R. and Zweidler-McKay, P.A. (2014) 'The challenge of targeting notch in hematologic malignancies', *Frontiers in pediatrics*, 2, pp. 54.

Hernandez-Davies, J.E., Tran, T.Q., Reid, M.A., Rosales, K.R., Lowman, X.H., Pan, M., Moriceau, G., Yang, Y., Wu, J., Lo, R.S. and Kong, M. (2015) 'Vemurafenib resistance reprograms melanoma cells towards glutamine dependence', *Journal of Translational Medicine*, 13(1), pp. 210.

Heuck, C.J., Jethava, Y., Khan, R., van Rhee, F., Zangari, M., Chavan, S., Robbins, K., Miller, S.E., Matin, A., Mohan, M., Ali, S.M., Stephens, P.J., Ross, J.S., Miller, V.A., Davies, F.,

Barlogie, B. and Morgan, G. (2016) 'Inhibiting MEK in MAPK pathway-activated myeloma', *Leukemia,* 30(4), pp. 976-980.

Hewamana, S., Alghazal, S., Lin, T.T., Clement, M., Jenkins, C., Guzman, M., Jordan, C., Neelakantan, S., Crooks, P., Burnett, A.K., Pratt, G., Fegan, C., Rowntree, C., Brennan, P. and Pepper, C. (2008) 'The NF-κB subunit Rel A is associated with in vitro survival and clinical disease progression in chronic lymphocytic leukemia and represents a promising therapeutic target', 111(Blood), pp. 4681-4689.

Higgins, B., Glenn, K., Walz, A., Tovar, C., Filipovic, Z., Hussain, S., Lee, E., Kolinsky, K., Tannu, S., Adames, V., Garrido, R., Linn, M., Meille, C., Heimbrook, D., Vassilev, L. and Packman, K. (2014) 'Preclinical optimization of MDM2 antagonist scheduling for cancer treatment by using a model-based approach', *Clinical cancer research : an official journal of the American Association for Cancer Research,* 20(14), pp. 3742.

Higgins, M.J., Serrano, A., Kofi, B.Y., Parsons, V., Phuong, T., Seifert, A., Ricca, M.J., Tucker, K.C., Eidelman, S.A., Carey, M.A. and Kurt, R.A. (2016) 'A Multifaceted Role for Myd88-Dependent Signaling in Progression of Murine Mammary Carcinoma', *Breast Cancer: Basic and Clinical Research,* 2016(10), pp. 157-167.

Hilpert, J., Grosse-Hovest, L., Gruenebach, F., Buechele, C., Nuebling, T., Raum, T., Steinle, A. and Salih, H.R. (2012) 'Comprehensive Analysis of NKG2D Ligand Expression and Release in Leukemia: Implications for NKG2D-Mediated NK Cell Responses', *Journal of Immunology,* 189(3), pp. 1360-1371.

Hoffman, L., Fouladi, M., Olson, J., Daryani, V., Stewart, C., Wetmore, C., Kocak, M., Onar-Thomas, A., Wagner, L., Gururangan, S., Packer, R., Blaney, S., Gajjar, A., Kun, L., Boyett, J. and Gilbertson, R. (2015) 'Phase I trial of weekly MK-0752 in children with refractory central nervous system malignancies: a pediatric brain tumor consortium study', *Child's Nervous System,* 31(8), pp. 1283-1289.

Holderfield, M., Deuker, M.M., McCormick, F. and McMahon, M. (2014) 'Targeting RAF kinases for cancer therapy: BRAF-mutated melanoma and beyond', *Nature Reviews: Cancer,* 14(7), pp. 455-467.

Hong, D., Kurzrock, R., Naing, A., Wheler, J., Falchook, G., Schiffman, J., Faulkner, N., Pilat, M., O'Brien, J. and LoRusso, P. (2014) 'A phase I, open-label, single-arm, dose-escalation study of E7107, a precursor messenger ribonucleic acid (pre-mRNA) splicesome inhibitor administered intravenously on days 1 and 8 every 21 days to patients with solid tumors', *Investigational New Drugs,* 32(3), pp. 436-444.

Honjo, A., Nakano, N., Yamazaki, S., Hara, M., Uchida, K., Kitaura, J., Nishiyama, C., Yagita, H., Ohtsuka, Y., Ogawa, H., Okumura, K. and Shimizu, T. (2017) 'Pharmacologic inhibition of Notch signaling suppresses food antigen-induced mucosal mast cell hyperplasia', *Journal of Allergy and Clinical Immunology,* 139(3), pp. 996.e10.

Houlston, R.S., Catovsky, D. and Yuille, M.R. (2002) 'Genetic susceptibility to chronic lymphocytic leukemia', *Leukemia,* 16, pp. 1008–1014.

Hsu, T., Simon, L.M., Neill, N.J., Marcotte, R., Sayad, A., Bland, C.S., Echeverria, G.V., Sun, T., Kurley, S.J., Tyagi, S., Karlin, K.L., Dominguez-Vidaña, R., Hartman, J.D., Renwick, A., Scorsone, K., Bernardi, R.J., Skinner, S.O., Jain, A., Orellana, M., Lagisetti, C., Golding, I., Jung, S.Y., Neilson, J.R., Zhang, X.F., Cooper, T.A., Webb, T.R., Neel, B.J., Shaw, C.A. and Westbrook, T.F. (2015) 'The spliceosome is a therapeutic vulnerability in MYC-driven cancer', *Nature,* 525(7569), pp. 384-388.

Hutter et al, (2013) 'High Efficiency Of the PDPK1-Inhibitor, BX912, In MCL', *Blood*, 122, pp. 3077;.

Insuasti-Beltran, G., Gale, J.M., Wilson, C.S., Foucar, K. and Czuchlewski, D.R. (2015) 'Significance of MYD88 L265P Mutation Status in the Subclassification of Low-Grade B-Cell Lymphoma/Leukemia', *Archives of pathology & laboratory medicine*, 139(8), pp. 1035.

Jain, N., Curran, E., Iyengar, N.M., Diaz-Flores, E., Kunnavakkam, R., Popplewell, L., Kirschbaum, M.H., Karrison, T., Erba, H.P., Green, M., Poire, X., Koval, G., Shannon, K., Reddy, P.L., Joseph, L., Atallah, E.L., Dy, P., Thomas, S.P., Smith, S.E., Doyle, L.A., Stadler, W.M., Larson, R.A., Stock, W. and Odenike, O. (2014) 'Phase II Study of the Oral MEK Inhibitor Selumetinib in Advanced Acute Myelogenous Leukemia: A University of Chicago Phase II Consortium Trial', *Clinical Cancer Research*, 20(2), pp. 490-498.

Jain, N. and O'Brien, S. (2015) 'Initial treatment of CLL: integrating biology and functional status', *Blood*, 126(4), pp. 463-470.

Jain, P. and O'Brien, S. (2012) 'Richter's transformation in chronic lymphocytic leukemia', *Oncology (Williston Park, N.Y.)*, 26(12), pp. 1146.

Jebaraj, B.M.C., Kienle, D., Bühler, A., Winkler, D., Döhner, H., Stilgenbauer, S. and Zenz, T. (2013) 'BRAF mutations in chronic lymphocytic leukemia', *Leukemia & Lymphoma*, 54(6), pp. 1177-1182.

Jeromin, S., Weissmann, S., Haferlach, C., Dicker, F., Bayer, K., Grossmann, V., Alpermann, T., Roller, A., Kohlmann, A., Haferlach, T., Kern, W. and Schnittger, S. (2014) 'SF3B1 mutations correlated to cytogenetics and mutations in NOTCH1, FBXW7, MYD88, XPO1 and TP53 in 1160 untreated CLL patients', *Leukemia*, 28(1), pp. 108-117.

Jia, L., Clear, A., Liu, F., Matthews, J., Uddin, N., McCarthy, A., Hoxha, E., Durance, C., Iqbal, S. and Gribben, J.G. (2014) 'Extracellular HMGB1 promotes differentiation of nurse-like cells in chronic lymphocytic leukemia', *Blood*, 123(11), pp. 1709.

Jitschin, R., Braun, M., Qorraj, M., Saul, D., Le Blanc, K., Zenz, T. and Mougiakakos, D. (2015) 'Stromal cell-mediated glycolytic switch in CLL cells involves Notch-c-Myc signaling', *Blood*, 125(22), pp. 3432-3436.

Joh, E., Lee, I., Jung, I. and Kim, D. (2011) 'Ginsenoside Rb1 and its metabolite compound K inhibit IRAK-1 activation—The key step of inflammation', *Biochemical Pharmacology*, 82(3), pp. 278-286.

Johannessen, C.M., Boehm, J.S., Kim, S.Y., Thomas, S.R., Wardwell, L., Johnson, L.A., Emery, C.M., Stransky, N., Cogdill, A.P., Barretina, J., Caponigro, G., Hieronymus, H., Murray, R.R., Salehi-Ashtiani, K., Hill, D.E., Vidal, M., Zhao, J.J., Yang, X., Alkan, O., Harris, J.L., Wilson, C.J., Myer, V.E., Finan, P.M., Root, D.E., Roberts, T.M., Golub, T., Flaherty, K.T., Dummer, R., Weber, B.L., Sellers, W.R., Schlegel, R., Wargo, J.A., Hahn, W.C. and Garraway, L.A. (2010) 'COT drives resistance to RAF inhibition through MAP kinase pathway reactivation', *Nature*, 468(7326), pp. 968-972.

Kashyap, M.K., Kumar, D., Villa, R., La Clair, J.J., Benner, C., Sasik, R., Jones, H., Ghia, E.M., Rassenti, L.Z., Kipps, T.J., Burkart, M.D. and Castro, J.E. (2015) 'Targeting the spliceosome in chronic lymphocytic leukemia with the macrolides FD-895 and pladienolide-B', *Haematologica*, 100(7), pp. 945-954.

Keating, M.J., Kantarjian, H., Talpaz, M., Redman, J., Koller, C., Barlogie, B., Velasquez, W., Plunkett, W., Freireich, J.E. and McCredie, K.B. (1989) 'Fludarabine: a new agent with major activity against chronic lymphocytic leukemia', *Blood*, 74(1), pp. 19-25.

Kelly, P.N., Romero, D.L., Yang, Y., Shaffer, A.L., Chaudhary, D., Robinson, S., Miao, W., Rui, L., Westlin, W.F., Kapeller, R. and Staudt, L.M. (2015) 'Selective interleukin-1 receptor-associated kinase 4 inhibitors for the treatment of autoimmune disorders and lymphoid malignancy', *Journal of Experimental Medicine*, 212(13), pp. 2189-2201.

Kern, C., Cornuel, J., Billard, C., Tang, R., Rouillard, D., Stenou, V., Defrance, T., Ajchenbaum-Cymbalista, F., Simonin, P., Feldblum, S. and Kolb, J. (2004) 'Involvement of BAFF and APRIL in the resistance to apoptosis of B-CLL through an autocrine pathway', *Blood*, 103(2), pp. 679-688.

Kern, D., Regl, G., Hofbauer, S.W., Altenhofer, P., Achatz, G., Dlugosz, A., Schnidar, H., Greil, R., Hartmann, T.N. and Aberger, F. (2015) 'Hedgehog/GLI and PI3K signaling in the initiation and maintenance of chronic lymphocytic leukemia', *Oncogene*, 34(42), pp. 5341-5351.

Kesarwani, A.K., Ramirez, O., Gupta, A.K., Yang, X., Murthy, T., Minella, A.C. and Pillai, M.M. (2017) 'Cancer-associated SF3B1 mutants recognize otherwise inaccessible cryptic 3′ splice sites within RNA secondary structures', *Oncogene*, 36(8), pp. 1123-1133.

Kikushige, Y., Ishikawa, F., Miyamoto, T., Shima, T., Urata, S., Yoshimoto, G., Mori, Y., Iino, T., Yamauchi, T., Eto, T., Niiro, H., Iwasaki, H., Takenaka, K. and Akashi, K. (2011) 'Self-Renewing Hematopoietic Stem Cell Is the Primary Target in Pathogenesis of Human Chronic Lymphocytic Leukemia', *Cancer Cell*, 20(2), pp. 246-259.

Kim, S., Lee, J., Jeon, M., Lee, J. and Nam, S. (2016) 'MEK-dependent IL-8 induction regulates the invasiveness of triple-negative breast cancer cells', *Tumor Biology*, 37(4), pp. 4991-4999.

Kitada, S., Zapata, J.M., Andreeff, M. and Reed, J.C. (1999a) 'Bryostatin and CD40-ligand enhance apoptosis resistance and induce expression of cell survival genes in B-cell chronic lymphocytic leukaemia', *British Journal of Haematology*, 106(4), pp. 995-1004.

Kitada, S., Zapata, J.M., Andreeff, M. and Reed, J.C. (1999b) 'Bryostatin and CD40-ligand enhance apoptosis resistance and induce expression of cell survival genes in B-cell chronic lymphocytic leukaemia', *British Journal of Haematology*, 106(4), pp. 995-1004.

Klein, U., Tu, Y., Stolovitzky, G.A., Mattioli, M., Cattoretti, G., Husson, H., Freedman, A., Inghirami, G., Cro, L., Baldini, L., Neri, A., Califano, A. and Dalla-Favera, R. (2001) 'Gene Expression Profiling of B Cell Chronic Lymphocytic Leukemia Reveals a Homogeneous Phenotype Related to Memory B Cells', *Journal of Experimental Medicine*, 194(11), pp. 1625-1638.

Komarova, N.L. and Boland, C.R. (2013) 'Cancer: calculated treatment', *Nature*, 499(7458), pp. 291.

Konopleva, M., Milella, M., Ruvolo, P., Watts, J.C., Ricciardi, M.R., Korchin, B., McQueen, T., Bornmann, W., Tsao, T., Bergamo, P., Mak, D.H., Chen, W., McCubrey, J., Tafuri, A. and Andreeff, M. (2012) 'MEK inhibition enhances ABT-737-induced leukemia cell apoptosis via prevention of ERK-activated MCL-1 induction and modulation of MCL-1/BIM complex', *Leukemia*, 26(4), pp. 778-787.

Korfi, K., Smith, M., Swan, J., Somervaille, T.C.P., Dhomen, N. and Marais, R. (2016) 'BIM mediates synergistic killing of B-cell acute lymphoblastic leukemia cells by BCL-2 and MEK inhibitors', *Cell death & disease*, 7, pp. e2177.

Kotake, Y., Sagane, K., Owa, T., Mimori-Kiyosue, Y., Shimizu, H., Mai, U., Yasushi, I., Masao, I. and Yoshiharu, M. (2007) 'Splicing factor SF3b as a target of the antitumor natural product pladienolide', *Nature Chemical Biology*, 3(9), pp. 570-575.

Krop, I., Demut, T., Guthrie, T., .Wen, P.Y., Mason, W.P., Chinnaiyan, P., Butowski, N., Groves, M.D., Kesari, S., Freedman, S.J., Blackman, S., Watters, J., Loboda, A., Podtelezhnikov, A., Lunceford, J., Chen, C., Giannotti, M., Hing, J., Beckman, R. and LoRusso, P. (2012) 'Phase I Pharmacologic and Pharmacodynamic Study of the Gamma Secretase (Notch) Inhibitor MK-0752 in Adult Patients With Advanced Solid Tumors', *Journal of Clinical Oncology*, 30(19), pp. 2307-2313.

Küppers, R. (2005) 'Mechanisms of B-cell lymphoma pathogenesis', *Nature Reviews Cancer*, 5(4), pp. 251-262.

Kurtova, A.V., Balakrishnan, K., Chen, R., Ding, W., Schnabl, S., Quiroga, M.P., Sivina, M., Wierda, W.G., Estrov, Z., Keating, M.J., Shehata, M., Jäger, U., Gandhi, V., Kay, N.E., Plunkett, W. and Burger, J.A. (2009) 'Diverse marrow stromal cells protect CLL cells from spontaneous and drug-induced apoptosis: development of a reliable and reproducible system to assess stromal cell adhesion-mediated drug resistance', *Blood*, 114(20), pp. 4441-4450.

Lafouresse, F., Bellard, E., Laurent, C., Moussion, C., Fournié, J., Ysebaert, L. and Girard, J. (2015) 'L-selectin controls trafficking of chronic lymphocytic leukemia cells in lymph node high endothelial venules in vivo', *Blood*, 126(11), pp. 1336.

Lagneaux, L., Delforge, A., Bron, D., De Bruyn, C. and Stryckmans, P. (1998) 'Chronic lymphocytic leukemic B cells but not normal B cells are rescued from apoptosis by contact with normal bone marrow stromal cells', *Blood*, 91(7), pp. 2387.

Landau, D.A., Tausch, E., Taylor-Weiner, A.N., Stewart, C., Reiter, J.G., Bahlo, J., Kluth, S., Bozic, I., Lawrence, M., Böttcher, S., Carter, S.L., Cibulskis, K., Mertens, D., Sougnez, C.L., Rosenberg, M., Hess, J.M., Edelmann, J., Kless, S., Kneba, M., Ritgen, M., Fink, A., Fischer, K., Gabriel, S., Lander, E.S., Nowak, M.A., Döhner, H., Hallek, M., Neuberg, D., Getz, G., Stilgenbauer, S. and Wu, C.J. (2015) 'Mutations driving CLL and their evolution in progression and relapse', *Nature*, 526(7574), pp. 525-530.

Langabeer, S.E., Quinn, F., O'Brien, D., McElligott, A.M., Kelly, J., Browne, P.V. and Vandenberghe, E. (2012) 'Incidence of the BRAF V600E mutation in chronic lymphocytic leukaemia and prolymphocytic leukaemia', *Leukemia Research*, 36(4), pp. 483-484.

Law, P J et al (2017) 'Genome-wide association analysis implicates dysregulation of immunity genes in chroniclymphocytic leukaemia', *Nature Communications*, 8(14175), pp. 1-12.

Lee, S.C. and Abdel-wahab, O. (2016) 'Therapeutic targeting of splicing in cancer', *Nature Medicine*, 22(9), pp. 976-986.

Lee, S.C., Dvinge, H., Kim, E., Cho, H., Micol, J., Chung, Y.R., Durham, B.H., Yoshimi, A., Kim, Y.J., Thomas, M., Lobry, C., Chen, C., Pastore, A., Taylor, J., Wang, X., Krivtsov, A., Armstrong, S.A., Palacino, J., Buonamici, S., Smith, P.G., Bradley, R.K. and Abdel-Wahab, O. (2016) 'Modulation of splicing catalysis for therapeutic targeting of leukemia with mutations in genes encoding spliceosomal proteins', *Nature Medicine*, 22(6), pp. 672-678.

Li, N., Jiang, J., Fu, J., Yu, T., Wang, B., Qin, W., Xu, A., Wu, M., Chen, Y. and Wang, H. (2016) 'Targeting interleukin-1 receptor-associated kinase 1 for human hepatocellular carcinoma', *Journal of experimental & clinical cancer research : CR,* 35(1), pp. 140.

Li, Y., Shi, Y., McCaw, L., Li, Y., Zhu, F., Gorczynski, R., Duncan, G.S., Yang, B., Ben-David, Y. and Spaner, D.E. (2015a) 'Microenvironmental interleukin-6 suppresses toll-like receptor signaling in human leukemia cells through miR-17/19A', *Blood,* 126(6), pp. 766.

Li, Z., Younger, K., Gartenhaus, R., Joseph, A.M., Hu, F., Baer, M.R., Brown, P. and Davila, E. (2015b) 'Inhibition of IRAK1/4 sensitizes T cell acute lymphoblastic leukemia to chemotherapies', *Journal of Clinical Investigation,* 125(3), pp. 1081-1097.

Little, A.S., Balmanno, K., Sale, M.J., Smith, P.D. and Cook, S.J. (2012) 'Tumour cell responses to MEK1/2 inhibitors: acquired resistance and pathway remodelling', *Biochemical Society transactions,* 40(1), pp. 73.

Liu, F., Jia, L., Wang, P., Wang, H., Farren, T.W. and Agrawal, S.G. (2016) 'STAT3 and NF-κB cooperatively control in vitro spontaneous apoptosis and poor chemo-responsiveness in patients with chronic lymphocytic leukemia', *Oncotarget,* 7(22), pp. 32031.

Lobry, C., Oh, P. and Aifantis, I. (2011) 'Oncogenic and tumor suppressor functions of Notch in cancer: it's NOTCH what you think', *Journal of Experimental Medicine,* 208(10), pp. 1931-1935.

Long, G.V., Trefzer, U., Davies, M.A., Kefford, R.F., Ascierto, P.A., Chapman, P.B., Puzanov, I., Hauschild, A., Robert, C., Algazi, A., Mortier, L., Tawbi, H., Wilhelm, T., Zimmer, L., Switzky, J., Swann, S., Martin, A., Guckert, M., Goodman, V., Streit, M., Kirkwood, J.M. and Schadendorf, D. (2012) 'Dabrafenib in patients with Val600Glu or Val600Lys BRAF-mutant melanoma metastatic to the brain (BREAK-MB): a multicentre, open-label, phase 2 trial', *Lancet Oncology,* 13(11), pp. 1087-1095.

Lopez-Guerra, M., Xargay-Torrent, S., Rosich, L., Montraveta, A., Roldan, J., Matas-Cespedes, A., Villamor, N., Aymerich, M., Lopez-Otin, C., Perez-Galan, P., Roue, G., Campo, E. and Colomer, D. (2015) 'The gamma -secretase inhibitor PF-03084014 combined with fludarabine antagonizes migration, invasion and angiogenesis in NOTCH1-mutated CLL cells', *Leukemia,* 29(1), pp. 96-106.

Lortholary, P., Boiron, M., Ripault, P., Levy, J.P., Manus, A. and Bernard, J. (1964) 'Chronic lymphoid leukemia secondarily associated with a malignant reticulopathy: Richter'ssyndrome', *Nouv Rev Fr Hematol,* 4, pp. 621-644.

Lutzny, G.T., Kocher, M., Schmidt-Supprian, M., Rudelius, L. and Klein-Hitpass, A.J. (2013) 'Protein kinase c-beta-dependent activation of NF-kappaB in stromal cells is indispensable for the survival of chronic lymphocytic leukemia B cells in vivo      ', *Cancer Cell,* 23, pp. 77-92.

Machnicki, M.M. and Stoklosa, T. (2014) 'BRAF--a new player in hematological neoplasms', *Blood cells, molecules & diseases,* 53(1-2), pp. 77-83.

Maffei, R., Bulgarelli, J., Fiorcari, S., Martinelli, S., Castelli, I., Valenti, V., Rossi, D., Bonacorsi, G., Zucchini, P., Potenza, L., Vallisa, D., Gattei, V., Del Poeta, G., Forconi, F., Gaidano, G., Narni, F., Luppi, M. and Marasca, R. (2014) 'Endothelin-1 promotes survival and chemoresistance in chronic lymphocytic leukemia B cells through ETA receptor', *PloS one,* 9(6), pp. e98818.

Maffei, R., Fiorcari, S., Bulgarelli, J., Martinelli, S., Castelli, I., Deaglio, S., Debbia, G., Fontana, M., Coluccio, V., Bonacorsi, G., Zucchini, P., Narni, F., Torelli, G., Luppi, M. and Marasca, R. (2012) 'Physical contact with endothelial cells through β1- and β2- integrins rescues chronic lymphocytic leukemia cells from spontaneous and drug-induced apoptosis and induces a peculiar gene expression profile in leukemic cells', *Haematologica*, 97(6), pp. 952.

Maguire, S.L., Leonidou, A., Wai, P., Marchiò, C., Ng, C.K., Sapino, A., Salomon, A., Reis-Filho, J.S., Weigelt, B. and Natrajan, R.C. (2015) 'SF3B1 mutations constitute a novel therapeutic target in breast cancer', *The Journal of Pathology*, 235(4), pp. 571-580.

Malcovati, L., Karimi, M., Papaemmanuil, E., Ambaglio, I., Jädersten, M., Jansson, M., Elena, C., Gallì, A., Walldin, G., Della Porta, M.G., Raaschou-Jensen, K., Travaglino, E., Kallenbach, K., Pietra, D., Ljungström, V., Conte, S., Boveri, E., Invernizzi, R., Rosenquist, R., Campbell, P.J., Cazzola, M. and Hellström Lindberg, E. (2015) 'SF3B1 mutation identifies a distinct subset of myelodysplastic syndrome with ring sideroblasts', *Blood*, 126(2), pp. 233-241.

Malcovati, L., Papaemmanuil, E., Bowen, D.T., Boultwood, J., Della Porta, M.G., Pascutto, C., Travaglino, E., Groves, M.J., Godfrey, A.L., Ambaglio, I., Gallì, A., Da Vià, M.C., Conte, S., Tauro, S., Keenan, N., Hyslop, A., Hinton, J., Mudie, L.J., Wainscoat, J.S., Futreal, P.A., Stratton, M.R., Campbell, P.J., Hellström-Lindberg, E. and Cazzola, M. (2011) 'Clinical significance of SF3B1 mutations in myelodysplastic syndromes and myelodysplastic/myeloproliferative neoplasms', *Blood*, 118(24), pp. 6239-6246.

Mansouri, L., Cahill, N., Gunnarsson, R., Smedby, K.E., Tjönnfjord, E., Hjalgrim, H., Juliusson, G., Geisler, C. and Rosenquist, R. (2013) 'NOTCH1 and SF3B1 mutations can be added to the hierarchical prognostic classification in chronic lymphocytic leukemia', *Leukemia*, 27(2), pp. 512-514.

Manzoni, D., Catallo, R., Chebel, A., Baseggio, L., Michallet, A., Roualdes, O., Magaud, J., Salles, G. and Ffrench, M. (2016) 'The ibrutinib B-cell proliferation inhibition is potentiated in vitro by dexamethasone: Application to chronic lymphocytic leukemia', *Leukemia Research*, 47, pp. 1-7.

Maraver, A., Fernandez-Marcos, P.J., Cash, T.P., Mendez-Pertuz, M., Duenas, M., Maietta, P., Martinelli, P., Munoz-Martin, M., Martinez-Fernandez, M., Canamero, M., Roncador, G., Martinez-Torrecuadrada, J.L., Grivas, D., de la Pompa, Jose Luis, Valencia, A., Paramio, J.M., Real, F.X. and Serrano, M. (2015) 'NOTCH pathway inactivation promotes bladder cancer progression', *Journal of Clinical Investigation*, 125(2), pp. 824.

Marinelli, M., Peragine, N., Di Maio, V., Chiaretti, S., De Propris, M.S., Raponi, S., Tavolaro, S., Mauro, F.R., Del Giudice, I., Guarini, A. and Foà, R. (2013) 'Identification of molecular and functional patterns of p53 alterations in chronic lymphocytic leukemia patients in different phases of the disease', *Haematologica*, 98(3), pp. 371.

Marquez, M., Hernández-Uzcátegui, O., Cornejo, A., Vargas, P. and Da Costa, O. (2015) 'Bone marrow stromal mesenchymal cells induce down regulation of CD20 expression on B-CLL: implications for rituximab resistance in CLL', *British Journal of Haematology*, 169(2), pp. 211-218.

Marti, G.E., Rawstron, A.C., Ghia, P., Hillmen, P., Houlston, R.S., Kay, N., Schleinitz, T.A. and Caporaso, N. (2005) 'Diagnostic criteria for monoclonal B-cell lymphocytosis', *British Journal of Haematology*, 130(3), pp. 325-332.

Martínez-Trillos, A., Navarro, A., Aymerich, M., Delgado, J., López-Guillermo, A., Campo, E. and Villamor, N. (2016) 'Clinical impact of MYD88 mutations in chronic lymphocytic leukemia', *Blood*, 127(12), pp. 1611.

Martinez-Trillos, A., Pinyol, M., Navarro, A., Aymerich, M., Jares, P., Juan, M., Rozman, M., Colomer, D., Delgado, J., Gine, E., Gonzalez-Diaz, M., Hernandez-Rivas, J.M., Colado, E., Rayon, C., Payer, A.R., Terol, M.J., Navarro, B., Quesada, V., Puente, X.S., Rozman, C., Lopez-Otin, C., Campo, E., Lopez-Guillermo, A. and Villamor, N. (2014) 'Mutations in TLR/MYD88 pathway identify a subset of young chronic lymphocytic leukemia patients with favorable outcome', *Blood*, 123(24), pp. 3790-3796.

Matera, A.G. and Wang, Z. (2014) 'A day in the life of the spliceosome', *Nature reviews. Molecular cell biology*, 15(2), pp. 108.

McClanahan, F., Hanna, B., Miller, S., Clear, A.J., Lichter, P., Gribben, J.G. and Seiffert, M. (2015) 'PD-L1 checkpoint blockade prevents immune dysfunction and leukemia development in a mouse model of chronic lymphocytic leukemia', *Blood*, 126(2), pp. 203-211.

Melo, J.V., Catovsky, D., Gregory, W.M. and Galton, D.A. (1987) 'The relationship between chronic lymphocytic leukaemia and prolymphocytic leukaemia. IV. Analysis of survival and prognostic features', *British journal of haematology*, 65(1), pp. 23-29.

Messmer, B.T., Messmer, D., Allen, S.L., Kolitz, J.E., Kudalkar, P., Cesar, D., Murphy, E.J., Koduru, P., Ferrarini, M., Zupo, S., Cutrona, G., Damle, R.N., Wasil, T., Rai, K.R., Hellerstein, M.K. and Chiorazzi, N. (2005) 'In vivo measurements document the dynamic cellular kinetics of chronic lymphocytic leukemia B cells', *The Journal of clinical investigation*, 115(3), pp. 755-764.

Montserrat, E., Bauman, T. and Delgado, J. (2016) 'Present and future of personalized medicine in CLL', *Best Practice & Research Clinical Haematology*, 29(1), pp. 100-110.

Moreno, C., Hodgson, K., Ferrer, G., Elena, M., Filella, X., Pereira, A., Baumann, T. and Montserrat, E. (2010) 'Autoimmune cytopenia in chronic lymphocytic leukemia: prevalence, clinical associations, and prognostic significance', *Blood*, 116(23), pp. 4771-4776.

Motta, M., Rassenti, L., Shelvin, B.J., Lerner, S., Kipps, T.J., Keating, M.J. and Wierda, W.G. (2005) 'Increased expression of CD152 (CTLA-4) by normal T lymphocytes in untreated patients with B-cell chronic lymphocytic leukemia', *Leukemia*, 19(10), pp. 1788-1793.

Müller-Hermelink, H.K., Montserrat, E., Catovsky, D. and Harris, N.L. (2001) *Chronic lymphocytic leukemia/small lymphocytic lymphoma.* Jaffe ES, Harris NL, Stein H, Vardiman JW edn. Lyon, France: IARC Press.

Muzio, M., Apollonio, B., Scielzo, C., Frenquelli, M., Vandoni, I., Boussiotis, V., Caligaris-Cappio, F. and Ghia, P. (2008) 'Constitutive activation of distinct BCR-signaling pathways in a subset of CLL patients: a molecular signature of anergy', *Blood*, 112(1), pp. 188-195.

Myint, H., J A Copplestone, J Orchard, V Craig, D Curtis, A G Prentice, M D Hamon, D G Oscier and T J Hamblin (1995) 'Fludarabine-related autoimmune haemolytic anaemia in patients with chronic lymphocytic leukaemia', *British journal of haematology*, 91(2), pp. 341-344.

Netland, I.A., Førde, H.E., Sleire, L., Leiss, L., Rahman, M.A., Skeie, B.S., Gjerde, C.H., Enger, P.Ø and Goplen, D. (2016) 'Dactolisib (NVP-BEZ235) toxicity in murine brain tumour models', *BMC cancer*, 16(1), pp. 657.

Ngo, V.N., Young, R.M., Schmitz, R., Jhavar, S., Xiao, W., Lim, K.H., Kohlhammer, H., Xu, W., Yang, Y., Zhao, H., Shaffer, A.L., Romesser, P., Wright, G., Powell, J., Rosenwald, A., Muller-Hermelink, H.K., Ott, G., Gascoyne, R.D., Connors, J.M., Rimsza, L.M., Campo, E., Jaffe, E.S., Delabie, J., Smeland, E.B., Fisher, R.I., Braziel, R.M., Tubbs, R.R., Cook, J.R., Weisenburger, D.D., Chan, W.C. and Staudt, L.M. (2011) 'Oncogenically active MYD88 mutations in human lymphoma', *Nature,* 470(7332), pp. 115-119.

Nguyen-Khac, F., Chapiro, E., Lesty, C., Grelier, A., Luquet, I., Radford-Weiss, I., Lefebvre, C., Fert-Ferrer, S., Callet-Bauchu, E., Lippert, E., Raggueneau, V., Michaux, L., Barin, C., Collonge-Rame, M., Mugneret, F., Eclache, V., Taviaux, S., Dastugue, N., Richebourg, S., Struski, S., Talmant, P., Baranger, L., Gachard, N., Gervais, C., Quilichini, B., Settegrana, C., Maloum, K., Davi, F. and Merle-Béral, H. (2011) 'Specific chromosomal IG translocations have different prognoses in chronic lymphocytic leukemia', *American journal of blood research,* 1(1), pp. 13.

Niemann, C.U., Herman, S.E.M., Maric, I., Gomez-Rodriguez, J., Biancotto, A., Chang, B.Y., Martyr, S., Stetler-Stevenson, M., Yuan, C.M., Calvo, K.R., Braylan, R.C., Valdez, J., Lee, Y.S., Wong, D.H., Jones, J., Sun, C., Marti, G.E., Farooqui, M.Z.H. and Wiestner, A. (2016) 'Disruption of in vivo Chronic Lymphocytic Leukemia Tumor-Microenvironment Interactions by Ibrutinib--Findings from an Investigator-Initiated Phase II Study', *Clinical cancer research : an official journal of the American Association for Cancer Research,* 22(7), pp. 1572-1582.

Nishio, M., Endo, T., Tsukada, N., Ohata, J., Kitada, S., Reed, J.C., Zvaifler, N.J. and Kipps, T.J. (2005) 'Nurselike cells express BAFF and APRIL, which can promote survival of chronic lymphocytic leukemia cells via a paracrine pathway distinct from that of SDF-1alpha', *Blood,* 106(3), pp. 1012.

Nunes, C., Wong, R., Mason, M., Fegan, C., Man, S. and Pepper, C. (2012) 'Expansion of a CD8+PD-1+ Replicative Senescence Phenotype in Early Stage CLL Patients Is Associated with Inverted CD4:CD8 Ratios and Disease Progression', *Clinical Cancer Research,* 18(3), pp. 678-687.

Ojha, J., Codd, V., Nelson, C.P., Samani, N.J., Smirnov, I.V., Madsen, N.R., Hansen, H.M., de Smith, A.J., Bracci, P.M., Wiencke, J.K., Wrensch, M.R., Wiemels, J.L. and Walsh, K.M. (2016) 'Genetic Variation Associated with Longer Telomere Length Increases Risk of Chronic Lymphocytic Leukemia', *Cancer Epidemiology, Biomarkers & Prevention,* 25(7), pp. 1043-1049.

Okimoto, Lin Luping, Olivas Victor, Chan Elton, Markegard Evan, Rymar Andrey, Neel Dana, Chen Xiao, Hemmati Golzar, Bollag Gideon and Bivona Trever, G. (2016) 'Preclinical efficacy of a RAF inhibitor that evades paradoxical MAPK pathway activation in protein kinase BRAF-mutant lung cancer', *Proceedings of the National Academy of Sciences of the United States of America,* 113(47), pp. 13456.

Osborne, B.A. and Minter, L.M. (2007) 'Notch signalling during peripheral T-cell activation and differentiation', *Nature Reviews Immunology,* 7(1), pp. 64-75.

Oscier, D., Fegan, C., Hillmen, P., Illidge, T., Johnson, S., Maguire, P., Matutes, E. and Milligan, D. (2004) 'Guidelines on the diagnosis and management of chronic lymphocytic leukaemia', *British Journal of Haematology,* 125(3), pp. 294-317.

Oscier, D.G., Rose-Zerilli, M.J.J., Winkelmann, N., Gonzalez de Castro, D., Gomez, B., Forster, J., Parker, H., Parker, A., Gardiner, A., Collins, A., Else, M., Cross, N.C.P., Catovsky, D.

and Strefford, J.C. (2013) 'The clinical significance of NOTCH1 and SF3B1 mutations in the UK LRF CLL4 trial', *Blood*, 121(3), pp. 468.

Packham, G. and Stevenson, F.K. (2005) 'Bodyguards and assassins: Bcl-2 family proteins and apoptosis control in chronic lymphocytic leukaemia', *Immunology*, 114(4), pp. 441-449.

Palacios, F., Abreu, C., Prieto, D., Morande, P., Ruiz, S., Fernández-calero, T., Naya, H., Libisch, G., Robello, C., Landoni, A.I., Gabus, R., Dighiero, G. and Oppezzo, P. (2015) 'Activation of the PI3K/AKT pathway by microRNA-22 results in CLL B-cell proliferation', *Leukemia*, 29(1), pp. 115-125.

Palamarchuk, A., Efanov, A., Nazaryan, N., Santanam, U., Alder, H., Rassenti, L., Kipps, T., Croce, C.M. and Pekarsky, Y. (2010) '13q14 deletions in CLL involve cooperating tumor suppressors', *Blood*, 115(19), pp. 3916-3922.

Papaemmanuil, E., Cazzola, M., Boultwood, J., Malcovati, L., Vyas, P., Bowen, D., Pellagatti, A., Wainscoat, J.S., Hellstrom-Lindberg, E., Gambacorti-Passerini, C., Godfrey, A.L., Rapado, I., Cvejic, A., Rance, R., McGee, C., Ellis, P., Mudie, L.J., Stephens, P.J., McLaren, S., Massie, C.E., Tarpey, P.S., Varela, I., Nik-Zainal, S., Davies, H.R., Shlien, A., Jones, D., Raine, K., Hinton, J., Butler, A.P., Teague, J.W., Baxter, E.J., Score, J., Galli, A., Della Porta, M.G., Travaglino, E., Groves, M., Tauro, S., Munshi, N.C., Anderson, K.C., El-Naggar, A., Fischer, A., Mustonen, V., Warren, A.J., Cross, N.C.P., Green, A.R., Futreal, P.A., Stratton, M.R. and Campbell, P.J. (2011) 'Somatic SF3B1 Mutation in Myelodysplasia with Ring Sideroblasts', *The New England Journal of Medicine*, 365(15), pp. 1384-1395.

Parikh, S.A., Kay, N.E. and Shanafelt, T.D. (2014) 'How we treat Richter syndrome', *Blood*, 123(11), pp. 1647.

Parikh, S.A., Leis, J.F., Chaffee, K.G., Call, T.G., Hanson, C.A., Ding, W., Chanan-Khan, A.A., Bowen, D., Conte, M., Schwager, S., Slager, S.L., Van Dyke, D.L., Jelinek, D.F., Kay, N.E. and Shanafelt, T.D. (2015) 'Hypogammaglobulinemia in newly diagnosed chronic lymphocytic leukemia: Natural history, clinical correlates, and outcomes', *Cancer*, 121(17), pp. 2883-2891.

Pascutti, M.F., Jak, M., Tromp, J.M., Derks, I.A.M., Remmerswaal, E.B.M., Thijssen, R., van Attekum, Martijn H A, van Bochove, G.G., Luijks, D.M., Pals, S.T., van Lier, René A W, Kater, A.P., van Oers, Marinus H J and Eldering, E. (2013) 'IL-21 and CD40L signals from autologous T cells can induce antigen-independent proliferation of CLL cells', *Blood*, 122(17), pp. 3010.

Pécuchet, N., Lebbe, C., Mir, O., Billemont, B., Blanchet, B., Franck, N., Viguier, M., Coriat, R., Tod, M., Avril, M. and Goldwasser, F. (2012) 'Sorafenib in advanced melanoma: a critical role for pharmacokinetics?', *British journal of cancer*, 107(3), pp. 455.

Pedersen, I.M., Kitada, S., Leoni, L.M., Zapata, J.M., Karras, J.G., Tsukada, N., Kipps, T.J., Choi, Y.S., Bennett, F. and Reed, J.C. (2002) 'Protection of CLL B cells by a follicular dendritic cell line is dependent on induction of Mcl-1', *Blood*, 100(5), pp. 1795.

Pekarsky, Y. and Croce, C.M. (2015) 'Role of miR-15/16 in CLL', *Cell death and differentiation*, 22(1), pp. 6-11.

Pflug, N., Bahlo, J., Shanafelt, T.D., Eichhorst, B.F., Bergmann, M.A., Elter, T., Bauer, K., Malchau, G., Rabe, K.G., Stilgenbauer, S., Döhner, H., Jäger, U., Eckart, M.J., Hopfinger, G., Busch, R., Fink, A., Wendtner, C., Fischer, K., Kay, N.E. and Hallek, M. (2014)

'Development of a comprehensive prognostic index for patients with chronic lymphocytic leukemia', *Blood,* 124(1), pp. 49-62.

Piha-Paul, S.A., Munster, P.N., Hollebecque, A., Argilés, G., Dajani, O., Cheng, J.D., Wang, R., Swift, A., Tosolini, A. and Gupta, S. (2015) 'Results of a phase 1 trial combining ridaforolimus and MK-0752 in patients with advanced solid tumours', *European journal of cancer (Oxford, England : 1990),* 51(14), pp. 1865-1873.

Pittenger, M.F., Mackay, A.M., Beck, S.C., Jaiswal, R.K., Douglas, R., . Mosca, J.D., Moorman, M.A., Simonetti, D.W., Craig, S. and Marshak, D.R. (1999) 'Multilineage Potential of Adult Human Mesenchymal Stem Cells', *Science,* 284(5411), pp. 143-147.

Plander, M., Seegers, S., Ugocsai, P., Diermeier-Daucher, S., Ivanyi, J., Schmitz, G., Hofstaedter, F., Schwarz, S., Orso, E., Knuechel, R. and Brockhoff, G. (2009) 'Different proliferative and survival capacity of CLL-cells in a newly established in vitro model for pseudofollicles', *Leukemia,* 23(11), pp. 2118-2128.

Planelles, L., Castillo-Gutierrez, S., Medema, J.P., Morales-Luque, A., Merle-Beral, H. and Hahne, M. (2007) 'APRIL but not BLyS serum levels are increased in chronic lymphocytic leukemia: prognostic relevance of APRIL for survival', *Haematologica,* 92(9), pp. 1284-1285.

Polak et al, (2015) 'MEK1 Inhibitor Selumetinib Sensitizes Precursor B-Cell Acute Lymphoblastic Leukemia Cells (B-ALL) to Dexamethasone through Modulation of mTOR Activity and Stimulation of Autophagy', *Blood,* 126(5), pp. 4917;.

Ponader, S., Chen, S., Buggy, J.J., Balakrishnan, K., Gandhi, V., Wierda, W.G., Keating, M.J., O'Brien, S., Chiorazzi, N. and Burger, J.A. (2012) 'The Bruton tyrosine kinase inhibitor PCI-32765 thwarts chronic lymphocytic leukemia cell survival and tissue homing in vitro and in vivo', *Blood,* 119(5), pp. 1182-1189.

Poulain, S., Roumier, C., Decambron, A., Renneville, A., Herbaux, C., Bertrand, E., Tricot, S., Daudignon, A., Galiègue-Zouitina, S., Soenen, V., Theisen, O., Grardel, N., Nibourel, O., Roche-Lestienne, C., Quesnel, B., Duthilleul, P., Preudhomme, C. and Leleu, X. (2013) 'MYD88 L265P mutation in Waldenstrom macroglobulinemia', *Blood,* 121(22), pp. 4504.

Poulikakos, P.I., Zhang, C., Bollag, G., Shokat, K.M. and Rosen, N. (2010) 'RAF inhibitors transactivate RAF dimers and ERK signalling in cells with wild-type BRAF', *Nature,* 464(7287), pp. 427-430.

Powers, J.P., Li, S., Jaen, J.C., Liu, J., Walker, N.P.C., Wang, Z. and Wesche, H. (2006) 'Discovery and initial SAR of inhibitors of interleukin-1 receptor-associated kinase-4', *Bioorganic & Medicinal Chemistry Letters,* 16(11), pp. 2842-2845.

Pozzo, F., Dal Bo, M., Peragine, N., Bomben, R., Zucchetto, A., Maria Rossi, F., Degan, M., Rossi, D., Chiarenza, A., Grossi, A., Di Raimondo, F., Zaja, F., Pozzato, G., Secchiero, P., Gaidano, G., Del Poeta, G., Zauli, G., Foà, R., Guarini, A. and Gattei, V. (2013a) 'Detection of TP53 dysfunction in chronic lymphocytic leukemia by an in vitro functional assay based on TP53 activation by the non-genotoxic drug Nutlin-3: a proposal for clinical application', *Journal of Hematology & Oncology,* 6, pp. 83.

Pozzo, F., Dal Bo, M., Peragine, N., Bomben, R., Zucchetto, A., Rossi, M.F., Degan, M., Rossi, D., Chiarenza, A., Grossi, A., Di Raimondo, F., Zaja, F., Pozzato, G., Secchiero, P., Gaidano, G., Del Poeta, G., Zauli, G., Foà, R., Guarini, A. and Gattei, V. (2013b) 'Detection of TP53 dysfunction in chronic lymphocytic leukemia by an in vitro functional assay based on TP53

activation by the non-genotoxic drug Nutlin-3: a proposal for clinical application', *Journal of Hematology & Oncology,* 6, pp. 83.

Pozzo, F., Dal Bo, M., Peragine, N., Bomben, R., Zucchetto, A., Rossi, F., Degan, M., Rossi, D., Chiarenza, A., Grossi, A., Di Raimondo, F., Zaja, F., Pozzato, G., Secchiero, P., Gaidano, G., Del Poeta, G., Zauli, G., Fo À, R., Guarini, A. and Gattei, V. (2013c) 'Detection of TP53 dysfunction in chronic lymphocytic leukemia by an in vitro functional assay based on TP53 activation by the non-genotoxic drug Nutlin-3: a proposal for clinical application', *Journal of hematology & oncology,* 6, pp. 83.

Pratilas, C.A. and Solit, D.B. (eds.) (2010) *Targeting the mitogen-activated protein kinase pathway: physiological feedback and drug response*. United States: .

Puente, X.S., Pinyol, M., Quesada, V., Conde, L., Ordonez, G.R., Villamor, N., Escaramis, G., Jares, P., Bea, S., Gonzalez-Diaz, M., Bassaganyas, L., Baumann, T., Juan, M., Lopez-Guerra, M., Colomer, D., Tubio, J.M., Lopez, C., Navarro, A., Tornador, C., Aymerich, M., Rozman, M., Hernandez, J.M., Puente, D.A., Freije, J.M., Velasco, G., Gutierrez-Fernandez, A., Costa, D., Carrio, A., Guijarro, S., Enjuanes, A., Hernandez, L., Yaguee, J., Nicolas, P., Romeo-Casabona, C.M., Himmelbauer, H., Castillo, E., Dohm, J.C., de Sanjose, S., Piris, M.A., de Alava, E., Miguel, J.S., Royo, R., Gelpi, J.L., Torrents, D., Orozco, M., Pisano, D.G., Valencia, A., Guigo, R., Bayes, M., Heath, S., Gut, M., Klatt, P., Marshall, J., Raine, K., Stebbings, L.A., Futreal, P., Stratton, M.R., Campbell, P.J., Gut, I., Lopez-Guillermo, A., Estivill, X., Montserrat, E., Lopez-Otin, C. and Campo, E. (2011) 'Whole-genome sequencing identifies recurrent mutations in chronic lymphocytic leukaemia', *Nature,* 475(7354), pp. 101-105.

Puiggros, A., Blanco, G. and Espinet, B. (2014) 'Genetic Abnormalities in Chronic Lymphocytic Leukemia: Where We Are and Where We Go', *BioMed Research International,* 2014, pp. 1-13.

Purroy, N., Abrisqueta, P., Carabia, J., Carpio, C., Palacio, C., Bosch, F. and Crespo, M. (2015) 'Co-culture of primary CLL cells with bone marrow mesenchymal cells, CD40 ligand and CpG ODN promotes proliferation of chemoresistant CLL cells phenotypically comparable to those proliferating in vivo', *Oncotarget,* 6(10), pp. 7632.

Quesada, V., Conde, L., Villamor, N., Ordonez, G.R., Jares, P., Bassaganyas, L., Ramsay, A.J., Bea, S., Pinyol, M., Martinez-Trillos, A., Lopez-Guerra, M., Colomer, D., Navarro, A., Baumann, T., Aymerich, M., Rozman, M., Delgado, J., Gine, E., Hernandez, J.M., Gonzalez-Diaz, M., Puente, D.A., Velasco, G., Freije, J.M.P., Tubio, J.M.C., Royo, R., Gelpi, J.L., Orozco, M., Pisano, D.G., Zamora, J., Vazquez, M., Valencia, A., Himmelbauer, H., Bayes, M., Heath, S., Gut, M., Gut, I., Estivill, X., Lopez-Guillermo, A., Puente, X.S., Campo, E. and Lopez-Otin, C. (2011) 'Exome sequencing identifies recurrent mutations of the splicing factor SF3B1 gene in chronic lymphocytic leukemia', *Nature Genetics,* 44(1), pp. 47-52.

Rai, K.R., Sawitsky, A., Cronkite, E.P., Chanana, A.D., Levy, R.N. and Pasternack, B.S. (1975) 'Clinical staging of chronic lymphocytic leukemia', *Blood,* 46(2), pp. 219.

Rai, K.R. and Jain, P. (2016) 'Chronic lymphocytic leukemia (CLL)-Then and now', *American Journal of Hematology,* 91(3), pp. 330-340.

Rakoff-Nahoum, S. and Medzhitov, R. (2009) 'Toll-like receptors and cancer.', *Nature Reviews Cancer,* 9, pp. 57-63.

Ramsay, A.G., Clear, A.J., Fatah, R. and Gribben, J.G. (2012) 'Multiple inhibitory ligands induce impaired T-cell immunologic synapse function in chronic lymphocytic leukemia that can be

blocked with lenalidomide: establishing a reversible immune evasion mechanism in human cancer', *Blood*, 120(7), pp. 1412-1421.

Ramsay, A.G., Johnson, A.J., Lee, A.M., Gorgün, G., Le Dieu, R., Blum, W., Byrd, J.C. and Gribben, J.G. (2008) 'Chronic lymphocytic leukemia T cells show impaired immunological synapse formation that can be reversed with an immunomodulating drug', *The Journal of clinical investigation*, 118(7), pp. 2427.

Ranheim, E.A. and Kipps, T.J. (1993) 'Activated T cells induce expression of B7/BB1 on normal or leukemic B cells through a CD40-dependent signal', *Journal of Experimental Medicine*, 177(4), pp. 925-935.

Rauert-Wunderlich, H., Rudelius, M., Ott, G. and Rosenwald, A. (2016) 'Targeting protein kinase C in mantle cell lymphoma', *British Journal of Haematology*, 173(3), pp. 394-403.

Rawstron, A.C., Yuille, M.R., Fuller, J., Cullen, M., Kennedy, B., Richards, S.J., Jack, A.S., Matutes, E., Catovsky, D., Hillmen, P. and Houlston, R.S. (2002) 'Inherited predisposition to CLL is detectable as subclinical monoclonal B-lymphocyte expansion', *Blood*, 100(7), pp. 2289-2290.

Redondo-Muñoz, J., Ugarte-Berzal, E., Terol, M.J., Van den Steen, Philippe E, Hernández del Cerro, M., Roderfeld, M., Roeb, E., Opdenakker, G., García-Marco, J.A. and García-Pardo, A. (2010) 'Matrix Metalloproteinase-9 Promotes Chronic Lymphocytic Leukemia B Cell Survival through Its Hemopexin Domain', *Cancer Cell*, 17(2), pp. 160-172.

Reiners, K.S., Topolar, D., Henke, A., Simhadri, V.R., Kessler, J., Sauer, M., Bessler, M., Hansen, H.P., Tawadros, S., Herling, M., Krönke, M., Hallek, M. and Pogge von Strandmann, E. (2013) 'Soluble ligands for NK cell receptors promote evasion of chronic lymphocytic leukemia cells from NK cell anti-tumor activity', *Blood*, 121(18), pp. 3658.

Reis, B., Jukofsky, L., Chen, G., Martinelli, G., Zhong, H., So, W.V., Dickinson, M.J., Drummond, M., Assouline, S., Hashemyan, M., Theron, M., Blotner, S., Lee, J., Kasner, M., Yoon, S., Rueger, R., Seiter, K., Middleton, S.A., Kelly, K.R., Vey, N., Yee, K., Nichols, G., Chen, L. and Pierceall, W.E. (2016) 'Acute myeloid leukemia patients' clinical response to idasanutlin (RG7388) is associated with pre-treatment MDM2 protein expression in leukemic blasts', *Haematologica*, 101(5), pp. e188.

Rhyasen, G.W. and Starczynowski, D.T. (2015) 'IRAK signalling in cancer', *British journal of cancer*, 112(2), pp. 232-237.

Rhyasen, G.W., Bolanos, L., Fang, J., Jerez, A., Wunderlich, M., Rigolino, C., Mathews, L., Ferrer, M., Southall, N., Guha, R., Keller, J., Thomas, C., Beverly, L.J., Cortelezzi, A., Oliva, E.N., Cuzzola, M., Maciejewski, J.P., Mulloy, J.C. and Starczynowski, D.T. (2013) 'Targeting IRAK1 as a Therapeutic Approach for Myelodysplastic Syndrome', *Cancer Cell*, 24(1), pp. 90-104.

Ricci, F., Tedeschi, A., Morra, E. and Montillo, M. (2009) 'Fludarabine in the treatment of chronic lymphocytic leukemia: a review', *Therapeutics and Clinical Risk Management*, 5(1), pp. 187-207.

Riches, J.C. and Gribben, J.G. (2013) 'Understanding the Immunodeficiency in Chronic Lymphocytic Leukemia Potential Clinical Implications', *Hematol Oncol Clin*, 27, pp. 207–235.

Riches, J.C., O'Donovan, C.J., Kingdon, S.J., McClanahan, F., Clear, A.J., Neuberg, D.S., Werner, L., Croce, C.M., Ramsay, A.G., Rassenti, L.Z., Kipps, T.J. and Gribben, J.G. (2014) 'Trisomy 12 chronic lymphocytic leukemia cells exhibit upregulation of integrin signaling that is modulated by NOTCH1 mutations', *Blood,* 123(26), pp. 4101-4110.

Rickert, R.C. (2013) 'New insights into pre-BCR and BCR signalling with relevance to B cell malignancies', *Nature Reviews. Immunology,* 13(8), pp. 578-591.

Rizzo, P., Osipo, C., Foreman, K., Golde, T., Osborne, B. and Miele, L. (2008) 'Rational targeting of Notch signaling in cancer', *Oncogene,* 27(38), pp. 5124-5131.

Rizzo, R., Audrito, V., Vacca, P., Rossi, D., Brusa, D., Stignani, M., Bortolotti, D., D'Arena, G., Coscia, M., Laurenti, L., Forconi, F., Gaidano, G., Mingari, M.C., Moretta, L., Malavasi, F. and Deaglio, S. (2014) 'HLA-G is a component of the chronic lymphocytic leukemia escape repertoire to generate immune suppression: impact of the HLA-G 14 base pair (rs66554220) polymorphism', *Haematologica,* 99(5), pp. 888-896.

Robertson, L.E. and Plunkett, W. (1993) 'Apoptotic Cell Death in Chronic Lymphocytic Leukemia', *L eukemia and Lymphoma,* 11, pp. 71-74.

Rodríguez, D., Bretones, G., Arango, J.R., Valdespino, V., Campo, E., Quesada, V. and López-Otín, C. (2015) 'Molecular pathogenesis of CLL and its evolution', *International journal of hematology,* 101(3), pp. 219-228.

Rogalińska, M. and Kiliańska, Z.M. (2015) 'Personalized therapy versus targeted therapy, differences
in the meaning', *GLOBAL JOURNAL FOR RESEARCH ANALYSIS,* 4, pp. 5-8.

Rogalińska, M., BŁOŃSKI, J.Z., GÓRALSKI, P., WAWRZYNIAK, E., HARTMAN, M., ROGALSKA, A., ROBAK, P., KOCEVA-CHYŁA, A., PIEKARSKI, H., ROBAK, T. and KILIAŃSKA, Z.M. (2015) 'Relationship between in vitro drug sensitivity and clinical response of patients to treatment in chronic lymphocytic leukemia', *International Journal of Oncology,* 46(3), pp. 1259-1267.

Rogalińska, M., Gï¿½ralski, P., Błoński, J., Robak, P., Barciszewski, J., Koceva-Chyła, A., Piekarski, H., Robak, T. and Kilianska, Z. (2017) 'Personalized therapy tests for the monitoring of chronic lymphocytic leukemia development', *Oncology Letters,* 13(4), pp. 2079.

Rogers, K.A., Ruppert, A.S., Bingman, A., Andritsos, L.A., Awan, F.T., Blum, K.A., Flynn, J.M., Jaglowski, S.M., Lozanski, G., Maddocks, K.J., Byrd, J.C., Woyach, J.A. and Jones, J.A. (2016) 'Incidence and description of autoimmune cytopenias during treatment with ibrutinib for chronic lymphocytic leukemia', *Leukemia,* 30(2), pp. 346-350.

Rosati, E., Sabatini, R., De Falco, F., Del Papa, B., Falzetti, F., Di Ianni, M., Cavalli, L., Fettucciari, K., Bartoli, A., Screpanti, I. and Marconi, P. (2013) 'γ-Secretase inhibitor I induces apoptosis in chronic lymphocytic leukemia cells by proteasome inhibition, endoplasmic reticulum stress increase and notch down-regulation', *International Journal of Cancer,* 132(8), pp. 1940-1953.

Rose-Zerilli, M.J.J., Forster, J., Parker, H., Parker, A., Rodríguez, A.E., Chaplin, T., Gardiner, A., Steele, A.J., Collins, A., Young, B.D., Skowronska, A., Catovsky, D., Stankovic, T., Oscier, D.G. and Strefford, J.C. (2014) 'ATM mutation rather than BIRC3 deletion and/or mutation predicts reduced survival in 11q-deleted chronic lymphocytic leukemia: data from the UK LRF CLL4 trial', *Haematologica,* 99(4), pp. 736.

Rossi, D., Bruscaggin, A., Spina, V., Rasi, S., Khiabanian, H., Messina, M., Fangazio, M., Vaisitti, T., Monti, S., Chiaretti, S., Guarini, A., Del Giudice, I., Cerri, M., Cresta, S., Deambrogi, C., Gargiulo, E., Gattei, V., Forconi, F., Bertoni, F., Deaglio, S., Rabadan, R., Pasqualucci, L., Foà, R., Dalla-Favera, R. and Gaidano, G. (2011) 'Mutations of the SF3B1 splicing factor in chronic lymphocytic leukemia: association with progression and fludarabine-refractoriness', *Blood,* 118(26), pp. 6904-6908.

Rossi, D., Cerri, M., Capello, D., Deambrogi, C., Rossi, F.M., Zucchetto, A., De Paoli, L., Cresta, S., Rasi, S., Spina, V., Franceschetti, S., Lunghi, M., Vendramin, C., Bomben, R., Ramponi, A., Monga, G., Conconi, A., Magnani, C., Gattei, V. and Gaidano, G. (2008) 'Biological and clinical risk factors of chronic lymphocytic leukaemia transformation to Richter syndrome', *British Journal of Haematology,* 142(2), pp. 202-215.

Rossi, D. and Gaidano, G. (2016) 'The clinical implications of gene mutations in chronic lymphocytic leukaemia', *The British Journal of Cancer,* 114(8), pp. 849-854.

Rossi, D., Rasi, S., Fabbri, G., Spina, V., Fangazio, M., Forconi, F., Marasca, R., Laurenti, L., Bruscaggin, A., Cerri, M., Monti, S., Cresta, S., Famà, R., De Paoli, L., Bulian, P., Gattei, V., Guarini, A., Deaglio, S., Capello, D., Rabadan, R., Pasqualucci, L., Dalla-Favera, R., Foà, R. and Gaidano, G. (2012) 'Mutations of NOTCH1 are an independent predictor of survival in chronic lymphocytic leukemia', *Blood,* 119(2), pp. 521-529.

Rossi, D., Rasi, S., Spina, V., Bruscaggin, A., Monti, S., Ciardullo, C., Deambrogi, C., Khiabanian, H., Serra, R., Bertoni, F., Forconi, F., Laurenti, L., Marasca, R., Dal-Bo, M., Rossi, F.M., Bulian, P., Nomdedeu, J., Del Poeta, G., Gattei, V., Pasqualucci, L., Rabadan, R., Foa, R., Dalla-Favera, R. and Gaidano, G. (2013a) 'Integrated mutational and cytogenetic analysis identifies new prognostic subgroups in chronic lymphocytic leukemia', *Blood,* 121(8), pp. 1403-1412.

Rossi, D., Spina, V., Bomben, R., Rasi, S., Dal-Bo, M., Bruscaggin, A., Rossi, F.M., Monti, S., Degan, M., Ciardullo, C., Serra, R., Zucchetto, A., Nomdedeu, J., Bulian, P., Grossi, A., Zaja, F., Pozzato, G., Laurenti, L., Efremov, D.G., Di-Raimondo, F., Marasca, R., Forconi, F., Del Poeta, G., Gaidano, G. and Gattei, V. (2013b) 'Association between molecular lesions and specific B-cell receptor subsets in chronic lymphocytic leukemia', *Blood,* 121(24), pp. 4902-4905.

Rozkova, D., Novotna, L., Pytlik, R., Hochova, I., Kozak, T., Bartunkova, J. and Spisek, R. (2010) 'Toll-like receptors on B-CLL cells: expression and functional consequences of their stimulation', *International Journal of Cancer,* 126(5), pp. 1132-1143.

Saez, B., Walter, M.J. and Graubert, T.A. (2016) 'Splicing factor gene mutations in hematologic malignancies', *Blood,* 129, pp. 1260-1269.

Salton, M., Kasprzak, W.K., Voss, T., Shapiro, B.A., Poulikakos, P.I. and Misteli, T. (2015) 'Inhibition of vemurafenib-resistant melanoma by interference with pre-mRNA splicing', *Nature Communications,* 6, pp. 7103.

Samuel, J., Macip, S. and Dyer, M.J.S. (2014) 'Efficacy of vemurafenib in hairy-cell leukemia', *The New England journal of medicine,* 370(3), pp. 286-288.

Saulep-Easton, D., Vincent, F.B., Quah, P.S., Wei, A., Ting, S.B., Croce, C.M., Tam, C. and Mackay, F. (2016) 'The BAFF receptor TACI controls IL-10 production by regulatory B cells and CLL B cells', *Leukemia,* 30(1), pp. 163-172.

Schmid, C. and Isaacson, P.G. (1994) 'Proliferation centres in B-cell malignant lymphoma, lymphocytic (B-CLL): an immunophenotypic study', *Histopathology,* 24(5), pp. 445-451.

Schmidt-Wolf, I.G.H., Plass, C., Byrd, J.C., Frevel, K., Pietsch, T. and Waha, A. (2016) 'Assessment of Promoter Methylation Identifies PTCH as a Putative Tumor-suppressor Gene in Human CLL', *Anticancer research,* 36(9), pp. 4515-4520.

Schott, A.F., Landis, M.D., Dontu, G., Griffith, K.A., Layman, R.M., Krop, I., Paskett, L.A., Wong, H., Dobrolecki, L.E., Lewis, M.T., Froehlich, A.M., Paranilam, J., Hayes, D.F., Wicha, M.S. and Chang, J.C. (2013) 'Preclinical and clinical studies of gamma secretase inhibitors with docetaxel on human breast tumors', *Clinical cancer research : an official journal of the American Association for Cancer Research,* 19(6), pp. 1512-1524.

Seiffert, M., Schulz, A., Ohl, S., Doehner, H., Stilgenbauer, S. and Lichter, P. (2010) 'Soluble CD14 is a novel monocyte-derived survival factor for chronic lymphocytic leukemia cells, which is induced by CLL cells in vitro and present at abnormally high levels in vivo', *Blood,* 116(20), pp. 4223-4230.

Sellar, R.S., Fend, F., Akarca, A.U., Agostinelli, C., Shende, V., Quintanilla-Martínez, L., Stein, H., Pileri, S.A., Linch, D. and Marafioti, T. (2015) 'BRAFV600E mutations are found in Richter syndrome and may allow targeted therapy in a subset of patients', *British Journal of Haematology,* 170(2), pp. 282-285.

Sethi, N. and Kang, Y. (2011) 'Notch signalling in cancer progression and bone metastasis', *British journal of cancer,* 105(12), pp. 1805.

Sgambati, M.T., Linet, M.S. & Devesa, S.S. (2001) Chronic lymphocytic leukemia. In: Chronic Lymphoid Leukemias (ed. by B. Cheson),pp. 33–62. Marcel Dekker Inc., New York.

Sharman, J., Hawkins, M., Kolibaba, K., Boxer, M., Klein, L., Wu, M., Hu, J., Abella, S. and Yasenchak, C. (2015) 'An open-label phase 2 trial of entospletinib (GS-9973), a selective spleen tyrosine kinase inhibitor, in chronic lymphocytic leukemia', *Blood,* 125(15), pp. 2336-2343.

Shukla, A., Shukla, V. and Joshi, S.S. (2017) 'Regulation of MAPK signaling and implications in chronic lymphocytic leukemia', *Leukemia & Lymphoma,* 7, pp. 1-9.

Sivina, M., Hartmann, E., Kipps, T.J., Rassenti, L., Krupnik, D., Lerner, S., LaPushin, R., Xiao, L., Huang, X., Werner, L., Neuberg, D., Kantarjian, H., O'Brien, S., Wierda, W.G., Keating, M.J., Rosenwald, A. and Burger, J.A. (2011) 'CCL3 (MIP-1 alpha ) plasma levels and the risk for disease progression in chronic lymphocytic leukemia', *Blood,* 117(5), pp. 1662-1669.

Smallwood, D.T., Apollonio, B., Willimott, S., Lezina, L., Alharthi, A., Ashley, R., Ambrose, A.R., De Rossi, G., Ramsay, A.G. and Wagner, S.D. (2016) 'Extracellular vesicles released by CD40/IL-4–stimulated CLL cells confer altered functional properties to CD41 T cells.', *Blood,* 128, pp. 542-552.

Sorigue, M., Maluquer, C. and Junca, J. (2017) 'Phenotypic characterization of trisomy 12 monoclonal B-cell lymphocytosis', *Cytometry Part B: Clinical Cytometry,* .

Speedy, H.E., Kinnersley, B., Chubb, D., Broderick, P., Law, P.J., Litchfield, K., Jayne, S., Dyer, M.J.S., Dearden, C., Follows, G.A., Catovsky, D. and Houlston, R.S. (2016) 'Germ line mutations in shelterin complex genes are associated with familial chronic lymphocytic leukemia', *Blood,* 128(19), pp. 2319-2326.

Srivastava, S., Tsongalis, G.J. and Kaur, P. (2016) 'Role of microRNAs in regulation of the TNF/TNFR gene superfamily in chronic lymphocytic leukemia', *Clinical Biochemistry,* 49(16-17), pp. 1307-1310.

Stevenson, F.K., Krysov, S., Davies, A.J., Steele, A.J. and Packham, G. (2011) 'B-cell receptor signaling in chronic lymphocytic leukemia', *Blood,* 118(16), pp. 4313-4320.

Stilgenbauer, S., Bullinger, L., Lichter, P. and Döhner, H. (2002) 'Genetics of chronic lymphocytic leukemia: genomic aberrations and VH gene mutation status in pathogenesis and clinical course', *Leukemia,* 16(6), pp. 993-1007.

Strati, P., Abruzzo, L.V., Wierda, W.G., O'Brien, S., Ferrajoli, A. and Keating, M.J. (2015) 'Second cancers and Richter transformation are the leading causes of death in patients with trisomy 12 chronic lymphocytic leukemia', *Clinical lymphoma, myeloma & leukemia,* 15(7), pp. 420-427.

Suda, K., Rozeboom, L., Yu, H., Ellison, K., Rivard, C.J., Mitsudomi, T. and Hirsch, F.R. (2017) 'Potential effect of spliceosome inhibition in small cell lung cancer irrespective of the MYC status', *PLoS One,* 12(2), pp. e0172209.

Sugiyama, T., Kohara, H., Noda, M. and Nagasawa, T. (2006) 'Maintenance of the Hematopoietic Stem Cell Pool by CXCL12-CXCR4 Chemokine Signaling in Bone Marrow Stromal Cell Niches', *Immunity,* 25(6), pp. 977-988.

Sutton, L., Young, E., Baliakas, P., Hadzidimitriou, A., Moysiadis, T., Plevova, K., Rossi, D., Kminkova, J., Stalika, E., Pedersen, L.B., Malcikova, J., Agathangelidis, A., Davis, Z., Mansouri, L., Scarfò, L., Boudjoghra, M., Navarro, A., Muggen, A.F., Yan, X., Nguyen-Khac, F., Larrayoz, M., Panagiotidis, P., Chiorazzi, N., Niemann, C.U., Belessi, C., Campo, E., Strefford, J.C., Langerak, A.W., Oscier, D., Gaidano, G., Pospisilova, S., Davi, F., Ghia, P., Stamatopoulos, K. and Rosenquist, R. (2016) 'Different spectra of recurrent gene mutations in subsets of chronic lymphocytic leukemia harboring stereotyped B-cell receptors', *Haematologica,* 101(8), pp. 959-967.

Tam, C.S., Otero-Palacios, J., Abruzzo, L.V., Jorgensen, J.L., Ferrajoli, A., Wierda, W.G., Lerner, S., OBrien, S. and Keating, M.J. (2008) 'Chronic lymphocytic leukaemia CD20 expression is dependent on the genetic subtype: a study of quantitative flow cytometry and fluorescent in-situ hybridization in 510 patients', *British Journal of Haematology,* 141(1), pp. 36-40.

Tannock, I.F. and Hickman, J.A. (2016) 'Limits to Personalized Cancer Medicine', *The New England journal of medicine,* 375(13), pp. 1289.

te Raa, G.D., Moerland, P.D., Leeksma, A.C., Derks, I.A., Yigittop, H., Laddach, N., Loden-van Straaten, M., Navrkalova, V., Trbusek, M., Luijks, D.M., Zenz, T., Skowronska, A., Hoogendoorn, M., Stankovic, T., van Oers, M.H., Eldering, E. and Kater, A.P. (2015) 'Assessment of p53 and ATM functionality in chronic lymphocytic leukemia by multiplex ligation-dependent probe amplification', *Cell Death and Disease,* 6, pp. e1852.

te Raa, G.D., Pascutti, M.F., García-Vallejo, J.J., Reinen, E., Remmerswaal, E.B.M., ten Berge, Ineke J M, van Lier, René A W, Eldering, E., van Oers, Marinus H J, Tonino, S.H. and Kater, A.P. (2014) 'CMV-specific CD8+ T-cell function is not impaired in chronic lymphocytic leukemia', *Blood,* 123(5), pp. 717.

te Raa, G.D. and Kater, A.P. (2016) 'TP53 dysfunction in CLL: Implications for prognosis and treatment', *Best Practice & Research Clinical Haematology,* 29(1), pp. 90-99.

ten Hacken, E. and Burger, J.A. (2016) 'Microenvironment interactions and B-cell receptor signaling in Chronic Lymphocytic Leukemia: Implications for disease pathogenesis and treatment', *Biochimica et Biophysica Acta (BBA) - Molecular Cell Research,* 1863(3), pp. 401-413.

Tesar, B., Chaudhary, D., Werner, L., Improgo, R., Pochet, N., Fernandes, S.M., Hoang, K., Vartanov, A.R., Romero, D.L., Robinson, S.D., Neuberg, D.S., Westlin, W.F. and Brown, J.R. (2013) 'Effect Of MYD88 Mutation In CLL On IRAK4 and BTK Inhibition In Vitro', *Blood,* 122, pp. 4132;.

Treon, S.P., Tsakmaklis, N., Meid, K., Yang, G., Chen, G.J., Liu, X., Chen, J., Demos, M., Patterson, C.J., Dubeau, T., Gustine, J., Castillo, J.J., Advani, R.H., Palomba, M.L., Xu, L. and Hunter, Z. (2016) 'Mutated MYD88 Zygosity and CXCR4 Mutation Status Are Important Determinants of Ibrutinib Response and Progression Free Survival in Waldenstrom's Macroglobulinemia.', *Blood,* 128, pp. 2984;.

Treon, S.P., Cao, Y., Xu, L., Yang, G., Liu, X. and Hunter, Z.R. (2014) 'Somatic mutations in MYD88 and CXCR4 are determinants of clinical presentation and overall survival in Waldenstrom macroglobulinemia', *Blood,* 123(18), pp. 2791-2796.

Treon, S.P., Xu, L. and Hunter, Z. (2015) 'MYD88 Mutations and Response to Ibrutinib in Waldenström's Macroglobulinemia', *The New England journal of medicine,* 373(6), pp. 584.

Treon, S.P., Xu, L., Yang, G., Zhou, Y., Liu, X., Cao, Y., Sheehy, P., Manning, R.J., Patterson, C.J., Tripsas, C., Arcaini, L., Pinkus, G.S., Rodig, S.J., Sohani, A.R., Harris, N.L., Laramie, J.M., Skifter, D.A., Lincoln, S.E. and Hunter, Z.R. (2012) 'MYD88 L265P somatic mutation in Waldenström's macroglobulinemia', *The New England journal of medicine,* 367(9), pp. 826.

Tsimberidou, A., Susan O'Brien, Issa Khouri, Francis J. Giles, Hagop M. Kantarjian, Richard Champlin, Sijin Wen, Kim-Anh Do, Susan C. Smith, Susan Lerner, Emil J. Freireich and Michael J. Keating (2006) 'Clinical Outcomes and Prognostic Factors in Patients With Richter's Syndrome Treated With Chemotherapy or Chemoimmunotherapy With or Without Stem-Cell Transplantation', *Journal of Clinical Oncology,* 24(15), pp. 2343-2351.

Uri, R., Harris, D., Li, P., Liu, Z., Grgurevic, S., Lerner, S., Martinez, M., Wierda, M.G., Keating, M. and Estrov, Z. (2012) 'Spontaneous Apoptosis of Chronic Lymphocytic Leukemia (CLL) Cells Correlates with Disease Burden and Inversely Correlates with Intracellular Levels of Signal Transducer and Activator of Transcription-3 (STAT3)', *Blood,* 120, pp. 3910.

Uy, G.L., Mandrekar, S.J., Laumann, K., Marcucci, G., Zhao, W., Levis, M.J., Klepin, H.D., Baer, M.R., Powell, B.L., Westervelt, P., DeAngelo, D.J., Stock, W., Sanford, B., Blum, W.G., Bloomfield, C.D., Stone, R.M. and Larson, R.A. (2016) 'A phase 2 study incorporating sorafenib into the chemotherapy for older adults with FLT3-mutated acute myeloid leukemia: CALGB 11001', *Blood advances,* 1, pp. 331-340.

van Attekum, M., Terpstra, S., Reinen, E., Kater, A.P. and Eldering, E. (2016) 'Macrophage-mediated chronic lymphocytic leukemia cell survival is independent of APRIL signaling', *Cell death discovery,* 2, pp. 16020.

Van Kooten, C. and Banchereau, J. (2000) 'CD40-CD40 ligand', *Journal of Leukocyte Biology,* 67(1), pp. 2-17.

Vergani, E., Di Guardo, L., Dugo, M., Rigoletto, S., Tragni, G., Ruggeri, R., Perrone, F., Tamborini, E., Gloghini, A., Arienti, F., Vergani, B., Deho, P., De Cecco, L., Vallacchi, V., Frati, P., Shahaj, E., Villa, A., Santinami, M., De Braud, F., Rivoltini, L. and Rodolfo, M. (2016) 'Overcoming melanoma resistance to vemurafenib by targeting CCL2-induced miR-34a, miR-100 and miR-125b', *Oncotarget,* 7(4), pp. 4428.

Veuillen, C., Aurran-Schleinitz, T., Castellano, R., Rey, J., Mallet, F., Orlanducci, F., Pouyet, L., Just-Landi, S., Coso, D., Ivanov, V., Carcopino, X., Bouabdallah, R., Collette, Y., Fauriat, C. and Olive, D. (2012) 'Primary B-CLL Resistance to NK Cell Cytotoxicity can be Overcome In Vitro and In Vivo by Priming NK Cells and Monoclonal Antibody Therapy', *Journal of Clinical Immunology,* 32(3), pp. 632-646.

Villamor, N., Conde, L., Martinez-Trillos, A., Cazorla, M., Navarro, A., Bea, S., Lopez, C., Colomer, D., Pinyol, M., Aymerich, M., Rozman, M., Abrisqueta, P., Baumann, T., Delgado, J., Gine, E., Gonzalez-Diaz, M., Hernandez, J.M., Colado, E., Payer, A.R., Rayon, C., Navarro, B., Jose Terol, M., Bosch, F., Quesada, V., Puente, X.S., Lopez-Otin, C., Jares, P., Pereira, A., Campo, E. and Lopez-Guillermo, A. (2013) 'NOTCH1 mutations identify a genetic subgroup of chronic lymphocytic leukemia patients with high risk of transformation and poor outcome', *Leukemia,* 27(5), pp. 1100-1106.

Visentin, A., Compagno, N., Cinetto, F., Imbergamo, S., Zambello, R., Piazza, F., Semenzato, G., Trentin, L. and Agostini, C. (2015) 'Clinical profile associated with infections in patients with chronic lymphocytic leukemia. Protective role of immunoglobulin replacement therapy', *Haematologica,* 100(12), pp. e515.

Walker et al, (2016) 'Interim Results of a Phase 1b/2 Study of Entospletinib (GS-9973) Monotherapy and in Combination with Chemotherapy in Patients with Acute Myeloid Leukemia', *Blood,* 128, pp. 2831;.

Walko, C.M. and Grande, C. (2014) 'Management ofCommonAdverseEventsinPatients Treated WithSorafenib:NurseandPharmacist Perspective', *Seminars inOncology,* 41, pp. S28.

Wan, P.T.C., Garnett, M.J., Roe, S.M., Lee, S., Niculescu-Duvaz, D., Good, V.M., Project, C.G., Jones, C.M., Marshall, C.J., Springer, C.J., Barford, D. and Marais, R. (2004) 'Mechanism of Activation of the RAF-ERK Signaling Pathway by Oncogenic Mutations of B-RAF', *Cell,* 116(6), pp. 855-867.

Wan, Y. and Wu, C.J. (2013) 'SF3B1 mutations in chronic lymphocytic leukemia', *Blood,* 121(23), pp. 4627-4634.

Wang, C., Sashida, G., Saraya, A., Ishiga, R., Koide, S., Oshima, M., Isono, K., Koseki, H. and Iwama, A. (2014a) 'Depletion of Sf3b1 impairs proliferative capacity of hematopoietic stem cells but is not sufficient to induce myelodysplasia', *Blood,* 123(21), pp. 3336-3343.

Wang, J., Pursell, N., Ma, A., Atoyan, R., Samson M, B.M., DellaRocca, S., Yin, L., Wang, D., Zifack, B., Xu, G. and Voi M, L.C. (2013) 'CUDC-907, a Dual HDAC and PI3K Inhibitor, Potentially Targets Cancer Cells and The Microenvironment In Hematological Malignancies', *Blood,* 122(21), pp. 4930.

Wang, J.Q., Jeelall, Y.S., Ferguson, L.L. and Horikawa, K. (2014b) 'Toll-Like Receptors and Cancer: MYD88 Mutation and Inflammation', *Frontiers in immunology,* 5, pp. 367.

Wang, L., Brooks, A.N., Fan, J., Wan, Y., Gambe, R., Li, S., Hergert, S., Yin, S., Freeman, S.S., Levin, J.Z., Fan, L., Seiler, M., Buonamici, S., Smith, P.G., Chau, K.F., Cibulskis, C.L.,

Zhang, W., Rassenti, L.Z., Ghia, E.M., Kipps, T.J., Fernandes, S., Bloch, D.B., Kotliar, D., Landau, D.A., Shukla, S.A., Aster, J.C., Reed, R., DeLuca, D.S., Brown, J.R., Neuberg, D., Getz, G., Livak, K.J., Meyerson, M.M., Kharchenko, P.V. and Wu, C.J. (2016) 'Transcriptomic Characterization of SF3B1 Mutation Reveals Its Pleiotropic Effects in Chronic Lymphocytic Leukemia', *Cancer Cell*, 30(5), pp. 750-763.

Wang, L., Lawrence, M.S., Wan, Y., Stojanov, P., Sougnez, C., Stevenson, K., Werner, L., Sivachenko, A., DeLuca, D.S., Zhang, L., Zhang, W., Vartanov, A.R., Fernandes, S.M., Goldstein, N.R., Folco, E.G., Cibulskis, K., Tesar, B., Sievers, Q.L., Shefler, E., Gabriel, S., Hacohen, N., Reed, R., Meyerson, M., Golub, T.R., Lander, E.S., Neuberg, D., Brown, J.R., Getz, G. and Wu, C.J. (2011) 'SF3B1 and other novel cancer genes in chronic lymphocytic leukemia', *The New England journal of medicine*, 365(26), pp. 2497.

Wang, Z., Liu, J., Sudom, A., Ayres, M., Li, S., Wesche, H., Powers, J.P. and Walker, N.P.C. (2006) 'Crystal Structures of IRAK-4 Kinase in Complex with Inhibitors: A Serine/Threonine Kinase with Tyrosine as a Gatekeeper', *Structure*, 14(12), pp. 1835-1844.

Wee, Z.N., Yatim, Siti Maryam J M, Kohlbauer, V.K., Feng, M., Goh, J.Y., Yi, B., Lee, P.L., Zhang, S., Wang, P.P., Lim, E., Tam, W.L., Cai, Y., Ditzel, H.J., Hoon, D.S.B., Tan, E.Y. and Yu, Q. (2015) 'IRAK1 is a therapeutic target that drives breast cancer metastasis and resistance to paclitaxel', *Nature Communications*, 6, pp. 8746.

Weerd, A., Kho, M., Kraaijeveld, R., Zuiderwijk, J., Weimar, W. and Baan, C. (2014) 'The protein kinase C inhibitor sotrastaurin allows regulatory T cell function', *Clinical & Experimental Immunology*, 175(2), pp. 296-304.

Weiss, N.S. (1979) 'Geographical variation in the incidence of the leukemias and lymphomas', *National Cancer Institute monograph*, (53), pp. 139.

Weiss, R.B., J Freiman, S L Kweder, L F Diehl and J C Byrd (1998) 'Hemolytic anemia after fludarabine therapy for chronic lymphocytic leukemia', *Journal of Clinical Oncology*, 16(5), pp. 1885-1889.

Weissmann, S., Roller, A., Jeromin, S., Hernandez, M., Abaigar, M., Hernandez-Rivas, J.M., Grossmann, V., Haferlach, C., Kern, W., Haferlach, T., Schnittger, S. and Kohlmann, A. (2013) 'Prognostic impact and landscape of NOTCH1 mutations in chronic lymphocytic leukemia (CLL): a study on 852 patients', *Leukemia*, 27(12), pp. 2393-2396.

Wellbrock, C., Karasarides, M. and Marais, R. (2004) 'The RAF proteins take centre stage', *Nature Reviews Molecular Cell Biology*, 5(11), pp. 875-885.

Weng, A.P., Ferrando, A.A., Lee, W., Morris, J.P., IV, Silverman, L.B., Sanchez-Irizarry, C., Blacklow, S.C., Look, A.T. and Aster, J.C. (2004) 'Activating Mutations of NOTCH1 in Human T Cell Acute Lymphoblastic Leukemia', *Science*, 306(5694), pp. 269-271.

Weston-Bell, N.J., Heniks, D., Sugiyarto, G., Bos, N.A., Kluin-Nelemans, H.C., Forconi, F. and Sahota, S.S. (2013) 'Hairy cell leukemia cell lines expressing annexin A1 and displaying B-cell receptor signals characteristic of primary tumor cells lack the signature BRAF mutation to reveal unrepresentative origins', *Leukemia*, 27(1), pp. 241-245.

Wild, J., Schmiedel, B.J., Maurer, A., Raab, S., Prokop, L., Stevanovic, S., Dorfel, D., Schneider, P. and Salih, H.R. (2015) 'Neutralization of (NK-cell-derived) B-cell activating factor by Belimumab restores sensitivity of chronic lymphoid leukemia cells to direct and Rituximab-induced NK lysis', *Leukemia*, 29(8), pp. 1676-1683.

Willander, K., Dutta, R.V., Ungerbäck, J., Gunnarsson, R., Juliusson, G., Fredrikson, M., Linderholm, M. and Söderkvist, P. (2013) 'NOTCH1 mutations influence survival in chronic lymphocytic leukemia patients', *BMC Cancer*, 13(1), pp. 274.

Willimott, S., Baou, M., Naresh, K. and Wagner, S.D. (2007) 'CD154 induces a switch in pro-survival Bcl-2 family members in chronic lymphocytic leukaemia', *British Journal of Haematology*, 138(6), pp. 721-732.

Wodarz, D., Garg, N., Komarova, N.L., Benjamini, O., Keating, M.J., Wierda, W.G., Kantarjian, H., James, D., O'Brien, S. and Burger, J.A. (2014) 'Kinetics of CLL cells in tissues and blood during therapy with the BTK inhibitor ibrutinib', *Blood*, 123(26), pp. 4132-4135.

Worden, F. (ed.) (2014) *Treatment strategies for radioactive iodine-refractory differentiated thyroid cancer*. London, England: SAGE Publications.

Xu, L., Hunter, Z.R., Yang, G., Zhou, Y., Cao, Y., Liu, X. and Morra, E. (2013) 'MYD88 L265P in Waldenstr¨om macroglobulinemia, immunoglobulin M monoclonal gammopathy, and other B-cell lymphoproliferative  disorders using conventional and quantitative allele-specific polymerase chain reaction', *Blood*, 121(11), pp. 2051-2058.

Xu, Z., ZHANG, J., ZHANG, J., WU, S., XIONG, D., CHEN, H., CHEN, Z. and ZHAN, R. (2015) 'Constitutive activation of NF-κB signaling by NOTCH1 mutations in chronic lymphocytic leukemia', *Oncology Reports*, 33(4), pp. 1609-1614.

Yao, Z., Torres, N.M., Tao, A., Gao, Y., Luo, L., Li, Q., de Stanchina, E., Abdel-Wahab, O., Solit, D.B., Poulikakos, P.I. and Rosen, N. (2015) 'BRAF Mutants Evade ERK-Dependent Feedback by Different Mechanisms that Determine Their Sensitivity to Pharmacologic Inhibition', *Cancer Cell*, 28(3), pp. 370-383.

Yeh, P., Hunter, T., Sinha, D., Ftouni, S., Wallach, E., Jiang, D., Chan, Y., Wong, S.Q., Silva, M.J., Vedururu, R., Doig, K., Lam, E., Arnau, G.M., Semple, T., Wall, M., Zivanovic, A., Agarwal, R., Petrone, P., Jones, K., Westerman, D., Blombery, P., Seymour, J.F., Papenfuss, A.T., Dawson, M.A., Tam, C.S. and Dawson, S. (2017) 'Circulating tumour DNA reflects treatment response and clonal evolution in chronic lymphocytic leukaemia', *Nature Communications*, 8, pp. 14756.

Yokoi, A., Kotake, Y., Takahashi, K., Kadowaki, T., Matsumoto, Y., Minoshima, Y., Sugi, N.H., Sagane, K., Hamaguchi, M., Iwata, M. and Mizui, Y. (2011) 'Biological validation that SF3b is a target of the antitumor macrolide pladienolide', *FEBS Journal*, 278(24), pp. 4870-4880.

Younes, A., Berdeja, J.G., Patel, M.R., Flinn, I., Gerecitano, J.F., Neelapu, S.S., Kelly, K.R., Copeland, A.R., Akins, A., Clancy, M.S., Gong, L., Wang, J., Ma, A., Viner, J.L. and Oki, Y. (2016) 'Safety, tolerability, and preliminary activity of CUDC-907, a first-in-class, oral, dual inhibitor of HDAC and PI3K, in patients with relapsed or refractory lymphoma or multiple myeloma: an open-label, dose-escalation, phase 1 trial', *The Lancet Oncology*, 17(5), pp. 622-631.

Yu, H., Jung, Y., Kim, H., Lee, J., Oh, C., Yoo, K.H., Sim, T. and Hah, J. (2010) '1,4-Dihydropyrazolo[4,3- d]imidazole phenyl derivatives: A novel type II Raf kinase inhibitors', *Bioorganic & Medicinal Chemistry Letters*, 20(12), pp. 3805-3808.

Yu, L., Ma, L., Tu, Q., Zhang, Y.I., Chen, Y., Yu, D. and Yang, S. (2015) 'Clinical significance of BRAF V600E mutation in 154 patients with thyroid nodules', *Oncology Letters*, 9(6), pp. 2633-2638.

Yuan, J., Mehta, P.P., Yin, M., Sun, S., Zou, A., Chen, J., Rafidi, K., Feng, Z., Nickel, J., Engebretsen, J., Hallin, J., Blasina, A., Zhang, E., Nguyen, L., Sun, M., Vogt, P.K., McHarg, A., Cheng, H., Christensen, J.G., Kan, J.L.C. and Bagrodia, S. (2011) 'PF-04691502, a potent and selective oral inhibitor of PI3K and mTOR kinases with antitumor activity', *Molecular cancer therapeutics*, 10(11), pp. 2189-2199.

Yuan, X., Wu, H., Xu, H., Xiong, H., Chu, Q., Yu, S., Wu, G.S. and Wu, K. (2015) 'Notch signaling: an emerging therapeutic target for cancer treatment', *Cancer letters*, 369(1), pp. 20-27.

Yuille, M.R., Matutes, E., Marossy, A., Hilditch, B. and Catovsky, D. (2000) 'Familial chronic lymphocytic leukaemia: a survey and review of published studies.', *Br J Haematol.*, 109, pp. 799.

Zhang, S. and Kipps, T.J. (2014) 'The Pathogenesis of Chronic Lymphocytic Leukemia', *Annual Review of Pathology: Mechanisms of Disease*, 9, pp. 103-118.

Zhao, Z., Zhang, L., Huang, C., Ma, S., Bu, L., Liu, J., Yu, G., Liu, B., Gutkind, J.S., Kulkarni, A.B., Zhang, W. and Sun, Z. (2016) 'NOTCH1 inhibition enhances the efficacy of conventional chemotherapeutic agents by targeting head neck cancer stem cell', *Scientific reports*, 6, pp. 24704.